Natural fibre composites

© Woodhead Publishing Limited, 2014

Related titles:

Residual stresses in composite materials
(ISBN 978-0-85709-270-0)

Environmentally friendly polymer nanocomposites
(ISBN 978-0-85709-777-4)

Advanced fibre-reinforced polymer (FRP) composites for structural applications
(ISBN 978-0-85709-418-6)

Details of these books and a complete list of titles from Woodhead Publishing can be obtained by:

- visiting our web site at www.woodheadpublishing.com
- contacting Customer Services (e-mail: sales@woodheadpublishing.com; fax: +44 (0) 1223 832819; tel.: +44 (0) 1223 499140 ext. 130; address: Woodhead Publishing Limited, 80, High Street, Sawston, Cambridge CB22 3HJ, UK)
- in North America, contacting our US office (e-mail: usmarketing@woodheadpublishing.com; tel.: (215) 928 9112; address: Woodhead Publishing, 1518 Walnut Street, Suite 1100, Philadelphia, PA 19102–3406, USA)

If you would like e-versions of our content, please visit our online platform: www.woodheadpublishingonline.com. Please recommend it to your librarian so that everyone in your institution can benefit from the wealth of content on the site.

We are always happy to receive suggestions for new books from potential editors. To enquire about contributing to our Composites Science and Engineering series, please send your name, contact address and details of the topic/s you are interested in to gwen.jones@woodheadpublishing.com. We look forward to hearing from you.

The team responsible for publishing this book:

Commissioning Editor: Francis Dodds
Publications Coordinator: Adam Davies
Project Editor: Kate Hardcastle
Editorial and Production Manager: Mary Campbell
Production Editor: Mandy Kingsmill
Project Manager: Newgen Knowledge Works Pvt Ltd
Copyeditor: Newgen Knowledge Works Pvt Ltd
Proofreader: Newgen Knowledge Works Pvt Ltd
Cover Designer: Terry Callanan

© Woodhead Publishing Limited, 2014

Woodhead Publishing Series in Composites Science and Engineering:
Number 47

Natural fibre composites

Materials, processes and properties

Edited by
Alma Hodzic and
Robert Shanks



Oxford Cambridge Philadelphia New Delhi

© Woodhead Publishing Limited, 2014

Published by Woodhead Publishing Limited,
80 High Street, Sawston, Cambridge CB22 3HJ, UK
www.woodheadpublishing.com
www.woodheadpublishingonline.com

Woodhead Publishing, 1518 Walnut Street, Suite 1100, Philadelphia,
PA 19102-3406, USA

Woodhead Publishing India Private Limited, 303 Vardaan House, 7/28 Ansari Road,
Daryaganj, New Delhi – 110002, India
www.woodheadpublishingindia.com

First published 2014, Woodhead Publishing Limited
© Woodhead Publishing Limited, 2014. The publisher has made every effort to ensure that permission for copyright material has been obtained by authors wishing to use such material. The authors and the publisher will be glad to hear from any copyright holder it has not been possible to contact.
The authors have asserted their moral rights.

This book contains information obtained from authentic and highly regarded sources. Reprinted material is quoted with permission, and sources are indicated. Reasonable efforts have been made to publish reliable data and information, but the authors and the publishers cannot assume responsibility for the validity of all materials. Neither the authors nor the publishers, nor anyone else associated with this publication, shall be liable for any loss, damage or liability directly or indirectly caused or alleged to be caused by this book.

Neither this book nor any part may be reproduced or transmitted in any form or by any means, electronic or mechanical, including photocopying, microfilming and recording, or by any information storage or retrieval system, without permission in writing from Woodhead Publishing Limited.

The consent of Woodhead Publishing Limited does not extend to copying for general distribution, for promotion, for creating new works, or for resale. Specific permission must be obtained in writing from Woodhead Publishing Limited for such copying.

Trademark notice: Product or corporate names may be trademarks or registered trademarks, and are used only for identification and explanation, without intent to infringe.

British Library Cataloguing in Publication Data
A catalogue record for this book is available from the British Library.

Library of Congress Control Number: 2013952413

ISBN 978-0-85709-524-4 (print)
ISBN 978-0-85709-922-8 (online)
ISSN 2052-5281 Woodhead Publishing Series in Composites Science and Engineering (print)
ISSN 2052-529X Woodhead Publishing Series in Composites Science and Engineering (online)

The publisher's policy is to use permanent paper from mills that operate a sustainable forestry policy, and which has been manufactured from pulp which is processed using acid-free and elemental chlorine-free practices. Furthermore, the publisher ensures that the text paper and cover board used have met acceptable environmental accreditation standards.

Typeset by Newgen Knowledge Works Pvt Ltd, India
Printed by Lightning Source

© Woodhead Publishing Limited, 2014

Contents

Contributor contact details *xi*
Woodhead Publishing Series in Composites Science and Engineering *xv*

Part I Natural fibre reinforcements 1

1 Wood fibres as reinforcements in natural fibre composites: structure, properties, processing and applications 3
D. Dai and M. Fan, Brunel University, UK

1.1 Introduction 3
1.2 Wood fibres: nature and behaviour 5
1.3 Modification of wood fibres for composites 15
1.4 Matrices (binders) of wood fibre composites 22
1.5 Process techniques of wood fibre composites 27
1.6 Properties of wood fibre composites 32
1.7 Applications of wood fibre composites 34
1.8 Future trends 41
1.9 References 43

2 Chemistry and structure of cellulosic fibres as reinforcements in natural fibre composites 66
R. A. Shanks, RMIT University, Australia

2.1 Introduction 66
2.2 Glucose monomer 67
2.3 Glucose biopolymerization 70
2.4 Cellulose structure 71
2.5 Chemical and solubility properties of cellulose 73
2.6 Sources of cellulose 75
2.7 Separation of cellulose 75

© Woodhead Publishing Limited, 2014

2.8 Purification of cellulose 76
2.9 Cellulose polymorphism 77
2.10 Chemical modification of cellulose 78
2.11 Preparation of nano-cellulose 79
2.12 Processing of cellulose 79
2.13 Applications of cellulose fibres 80
2.14 Conclusions 81
2.15 References 81
2.16 Appendix: abbreviations 83

3 Creating hierarchical structures in cellulosic fibre reinforced polymer composites for advanced performance 84
K.-Y. Lee and A. Bismarck, University of Vienna, Austria and Imperial College London, UK

3.1 Introduction 84
3.2 Creating hierarchical structures in (ligno)cellulosic fibre reinforced composite materials 86
3.3 Surface microfibrillation of (ligno)cellulosic fibres 87
3.4 Creating hierarchical structures in renewable composites by incorporating microfibrillated cellulose (MFC) into the matrix 90
3.5 Coating of (ligno)cellulosic fibres with bacterial cellulose 91
3.6 Conclusions and future trends 99
3.7 Acknowledgements 100
3.8 References 100

4 Recycled polymers in natural fibre-reinforced polymer composites 103
M. A. Al-Maadeed and S. Labidi, Qatar University, Qatar

4.1 Introduction 103
4.2 Fibre reinforcements in recycled composites 104
4.3 Processes for adding natural fibre reinforcements to composites 108
4.4 Improving the mechanical properties of recycled composites using natural fibre reinforcements 109
4.5 Applications of recycled polymer composites with natural fibre reinforcements 111
4.6 Conclusions and future trends 112

© Woodhead Publishing Limited, 2014

4.7 References 112
4.8 Appendix: abbreviations 114

5 Electrospun cellulosic fibre-reinforced composite materials 115
D. S. Le Corre, University of Canterbury, New Zealand, N. Tucker, The NZ Institute for Plant and Food Research Ltd, New Zealand and M. P. Staiger, University of Canterbury, New Zealand

5.1 Introduction 115
5.2 Electrospinning of non-derivatised and derivatised cellulosic fibres 118
5.3 Electrospun cellulosic fibres via polymer blends 135
5.4 Electrospun nanocomposite fibres 138
5.5 Mechanical properties of electrospun fibres and mats 146
5.6 Cellulose nanofibre-reinforced polymer composites 147
5.7 Future trends 149
5.8 References 150

Part II Processing of natural fibre composites 159

6 Ethical practices in the processing of green composites 161
C. Baillie, The University of Western Australia, Australia and E. Feinblatt, Waste for Life, USA

6.1 Introduction 161
6.2 Social impact and ethical practice 162
6.3 Case study: Waste for Life waste management model 164
6.4 Conclusions 172
6.5 References 173

7 Manufacturing methods for natural fibre composites 176
J. Summerscales and S. Grove, Plymouth University, UK

7.1 Introduction 176
7.2 Fibre reinforcements 177
7.3 Reinforcement forms 180
7.4 Bio-based polymer matrices 183
7.5 Composites manufacturing processes 187

© Woodhead Publishing Limited, 2014

7.6 Key parameters for successful processing of natural fibre composites 189
7.7 Manufacturing techniques for natural fibre-reinforced polymer matrix composites 201
7.8 Case studies: automotive, building and construction, and marine applications 204
7.9 Conclusions 205
7.10 References 205

8 Compression and injection molding techniques for natural fiber composites 216
Y. W. Leong, Institute of Materials Research and Engineering, Republic of Singapore and S. Thitithanasarn, K. Yamada and H. Hamada, Kyoto Institute of Technology, Japan

8.1 Introduction 216
8.2 Emerging compression and injection molding technologies in the production of natural fiber composites 218
8.3 Processing natural fiber composites at high temperatures 227
8.4 Conclusions 229
8.5 References 230

9 Thermoset matrix natural fibre-reinforced composites 233
A. Crosky and N. Soatthiyanon, University of New South Wales, Australia and Cooperative Research Centre for Advanced Composite Structures, Australia, D. Ruys, St Andrew's Cathedral School, Australia and S. Meatherall and S. Potter, Composites Innovation Centre, Canada

9.1 Introduction 233
9.2 Natural fibres used in thermoset matrix composites 234
9.3 Thermoset matrix types 234
9.4 Fabrication of thermoset matrix composites 238
9.5 Mechanical properties of synthetic resin composites 240
9.6 Bioderived resin composites 258
9.7 Applications of thermoset matrix natural fibre composites 263
9.8 Future trends 265
9.9 Sources of further information and advice 265
9.10 References 265

© Woodhead Publishing Limited, 2014

Part III Testing and properties 271

10 Non-destructive testing (NDT) of natural fibre composites: acoustic emission technique 273
F. Sarasini and C. Santulli, University of Rome 'La Sapienza', Italy

10.1 Introduction 273
10.2 Using the acoustic emission (AE) technique in practice 279
10.3 Assessing results 285
10.4 Applications of AE 287
10.5 Future trends 295
10.6 Conclusions 296
10.7 Sources of further information and advice 296
10.8 References 297

11 High strain rate testing of natural fiber composites 303
W. Kim and A. Argento, University of Michigan-Dearborn, USA

11.1 Introduction 303
11.2 Materials 305
11.3 Test methods 306
11.4 Results and discussion 308
11.5 Applications and future trends 314
11.6 Acknowledgments 317
11.7 References 318

12 Performance of natural fiber composites under dynamic loading 323
H. Md Akil and M. H. Zamri, Universiti Sains Malaysia (USM), Malaysia

12.1 Introduction 323
12.2 Natural fibers and natural fiber composites 325
12.3 Dynamic properties of natural fiber composites 326
12.4 Dynamic mechanical testing of natural fiber composites 327
12.5 Testing in practice: the example of pultruded natural fiber reinforced composites 330
12.6 Dynamic testing of composites 331
12.7 Performance of natural fiber reinforced composites under dynamic loading 335

© Woodhead Publishing Limited, 2014

12.8 Future trends 341
12.9 Acknowledgments 341
12.10 References 341

13 The response of natural fibre composites to impact damage: a case study 345
H. Ghasemnejad and A. Aboutorabi, Kingston University London, UK

13.1 Introduction 345
13.2 Mechanical characterization 348
13.3 Specimen preparation 349
13.4 Charpy impact test 353
13.5 Experimental results 354
13.6 Conclusion 362
13.7 References 363

14 Natural fibre composites in a marine environment 365
M. P. Ansell, University of Bath, UK

14.1 Introduction 365
14.2 Properties and environmental impact of natural versus synthetic fibres 366
14.3 Natural fibre composites (NFCs) and moisture uptake 369
14.4 Geometrical considerations for plant fibres in NFCs 370
14.5 Marine applications of plant fibre composites 371
14.6 Conclusions and future trends 372
14.7 Sources of further information and advice 372
14.8 References 373

Index *375*

© Woodhead Publishing Limited, 2014

Contributor contact details

(* = main contact)

Editors

A. Hodzic
Faculty of Engineering
The University of Sheffield
Mappin Street
Sheffield S1 3JD, UK

E-mail: a.hodzic@sheffield.ac.uk

R. A. Shanks
Applied Sciences
RMIT University
GPO Box 2476
Melbourne, VIC 3001, Australia

E-mail: robert.shanks@rmit.edu.au

Chapter 1

D. Dai and M. Fan*
Department of Civil Engineering
Brunel University
Uxbridge UB8 3PH, UK

E-mail: mizi.fan@brunel.ac.uk

Chapter 2

R. A. Shanks (retired)
Applied Sciences
RMIT University
GPO Box 2476
Melbourne, VIC 3001, Australia

E-mail: robert.shanks@rmit.edu.au

Chapter 3

K.-Y. Lee and A. Bismarck*
Institute of Materials Chemistry and Research
University of Vienna
Waehringerstr. 42
1090 Wien, Austria

and

Polymer and Composite Engineering (PaCE) Group
Department of Chemical Engineering
Imperial College London
South Kensington Campus
London SW7 2AZ, UK

E-mail: alexander.bismarck@univie.ac.at; a.bismarck@imperial.ac.uk

Chapter 4

M. A. Al-Maadeed* and S. Labidi
Center for Advanced Materials
Qatar University
P.O. Box 2713
Doha, Qatar

E-mail: m.alali@qu.edu.qa

© Woodhead Publishing Limited, 2014

Chapter 5

D. S. Le Corre and M.P Staiger*
Department of Mechanical Engineering
University of Canterbury
Private Bag 4800
Christchurch 8140, New Zealand

E-mail: mark.staiger@canterbury.ac.nz

N. Tucker
The NZ Institute for Plant and Food Research Ltd
Gerald Street, Lincoln
Private Bag 4704
Christchurch 8140, New Zealand

Chapter 6

C. Baillie*
Faculty of Engineering, Computing and Mathematics
The University of Western Australia
35 Stirling Highway
Crawley 6009
Perth, Australia

E-mail: caroline.baillie@uwa.edu.au

E. Feinblatt
Waste for Life
76 Winkler Rd
Hankins, NY 12741, USA

E-mail: eric@wasteforlife.org

Chapter 7

J. Summerscales* and S. Grove
Advanced Composites Manufacturing Centre
School of Marine Science and Engineering
Plymouth University
Plymouth PL4 8AA, UK

E-mail: J.Summerscales@plymouth.ac.uk

Chapter 8

Y. W. Leong*
Synthesis & Integration Capability Group
Institute of Materials Research and Engineering
3 Research Link
Singapore 117602, Republic of Singapore

E-mail: leongyw@imre.a-star.edu.sg

S. Thitithanasarn, K. Yamada and H. Hamada
Advanced Fibro Science
Kyoto Institute of Technology
Matsugasaki, Sakyo-ku
606-8585 Kyoto, Japan

Chapter 9

A. Crosky* and N. Soatthiyanon
School of Materials Science and Engineering
University of New South Wales
Sydney, NSW 2052, Australia

and

Cooperative Research Centre for Advanced Composite Structures
Moorebank, NSW 2170, Australia

E-mail: a.crosky@unsw.edu.au

© Woodhead Publishing Limited, 2014

D. Ruys
St Andrew's Cathedral School
Sydney, NSW 2000, Australia

S. Meatherall and
S. Potter
Composites Innovation Centre
Winnipeg, Manitoba, Canada
R3P 0Z6

Chapter 10

F. Sarasini* and
C. Santulli
Department of Chemical
Engineering Materials
Environment
University of Rome 'La Sapienza'
Via Eudossiana 18
00184 Rome, Italy

E-mail: fabrizio.sarasini@uniroma1.
it; carlosantulli141@gmail.com

Chapter 11

W. Kim and
A. Argento*
Department of Mechanical
Engineering
University of Michigan-Dearborn
Dearborn, MI 48128, USA

E-mail: aargento@umich.edu;
wskim@umich.edu

Chapter 12

H. Md Akil*
School of Materials and Mineral
Resources Engineering and
Cluster for Polymer Composites
(CPC), Science and Engineering
Research Centre (SERC)
Engineering Campus
Universiti Sains Malaysia (USM)
14300, Nibong Tebal
Penang, Malaysia

E-mail: hazizan@eng.usm.my

M. H. Zamri
School of Materials and Mineral
Resources Engineering
Engineering Campus
Universiti Sains Malaysia (USM)
14300, Nibong Tebal
Penang, Malaysia

Chapter 13

H. Ghasemnejad* and
A. Aboutorabi
Faculty of Science, Engineering and
Computing (SEC)
Kingston University London
Roehampton Vale
London SW15 3DW, UK

E-mail: Hessam.Ghasemnejad@
kingston.ac.uk; A.Aboutorabi@
kingston.ac.uk

Chapter 14

M. P. Ansell
BRE Centre for Innovative
Construction Materials
Department of Mechanical
Engineering
University of Bath
Bath BA2 7AY, UK

E-mail: m.p.ansell@bath.ac.uk

© Woodhead Publishing Limited, 2014

Woodhead Publishing Series in Composites Science and Engineering

1 **Thermoplastic aromatic polymer composites**
F. N. Cogswell
2 **Design and manufacture of composite structures**
G. C. Eckold
3 **Handbook of polymer composites for engineers**
Edited by L. C. Hollaway
4 **Optimisation of composite structures design**
A. Miravete
5 **Short-fibre polymer composites**
Edited by S. K. De and J. R. White
6 **Flow-induced alignment in composite materials**
Edited by T. D. Papthanasiou and D. C. Guell
7 **Thermoset resins for composites**
Compiled by Technolex
8 **Microstructural characterisation of fibre-reinforced composites**
Edited by J. Summerscales
9 **Composite materials**
F. L. Matthews and R. D. Rawlings
10 **3-D textile reinforcements in composite materials**
Edited by A. Miravete
11 **Pultrusion for engineers**
Edited by T. Starr
12 **Impact behaviour of fibre-reinforced composite materials and structures**
Edited by S. R. Reid and G. Zhou
13 **Finite element modelling of composite materials and structures**
F. L. Matthews, G. A. O. Davies, D. Hitchings and C. Soutis
14 **Mechanical testing of advanced fibre composites**
Edited by G. M. Hodgkinson
15 **Integrated design and manufacture using fibre-reinforced polymeric composites**
Edited by M. J. Owen and I. A. Jones

© Woodhead Publishing Limited, 2014

16 **Fatigue in composites**
Edited by B. Harris
17 **Green composites**
Edited by C. Baillie
18 **Multi-scale modelling of composite material systems**
Edited by C. Soutis and P. W. R. Beaumont
19 **Lightweight ballistic composites**
Edited by A. Bhatnagar
20 **Polymer nanocomposites**
Y-W. Mai and Z-Z. Yu
21 **Properties and performance of natural-fibre composite**
Edited by K. Pickering
22 **Ageing of composites**
Edited by R. Martin
23 **Tribology of natural fiber polymer composites**
N. Chand and M. Fahim
24 **Wood-polymer composites**
Edited by K. O. Niska and M. Sain
25 **Delamination behaviour of composites**
Edited by S. Sridharan
26 **Science and engineering of short fibre reinforced polymer composites**
S-Y. Fu, B. Lauke and Y-M. Mai
27 **Failure analysis and fractography of polymer composites**
E. S. Greenhalgh
28 **Management, recycling and reuse of waste composites**
Edited by V. Goodship
29 **Materials, design and manufacturing for lightweight vehicles**
Edited by P. K. Mallick
30 **Fatigue life prediction of composites and composite structures**
Edited by A. P. Vassilopoulos
31 **Physical properties and applications of polymer nanocomposites**
Edited by S. C. Tjong and Y-W. Mai
32 **Creep and fatigue in polymer matrix composites**
Edited by R. M. Guedes
33 **Interface engineering of natural fibre composites for maximum performance**
Edited by N. E. Zafeiropoulos
34 **Polymer-carbon nanotube composites**
Edited by T. McNally and P. Pötschke
35 **Non-crimp fabric composites: Manufacturing, properties and applications**
Edited by S. V. Lomov

© Woodhead Publishing Limited, 2014

36 **Composite reinforcements for optimum performance**
Edited by P. Boisse
37 **Polymer matrix composites and technology**
R. Wang, S. Zeng and Y. Zeng
38 **Composite joints and connections**
Edited by P. Camanho and L. Tong
39 **Machining technology for composite materials**
Edited by H. Hocheng
40 **Failure mechanisms in polymer matrix composites**
Edited by P. Robinson, E. S. Greenhalgh and S. Pinho
41 **Advances in polymer nanocomposites: Types and applications**
Edited by F. Gao
42 **Manufacturing techniques for polymer matrix composites (PMCs)**
Edited by S. Advani and K-T. Hsiao
43 **Non-destructive evaluation (NDE) of polymer matrix composites: Techniques and applications**
Edited by V. M. Karbhari
44 **Environmentally friendly polymer nanocomposites: Types, processing and properties**
S. S. Ray
45 **Advances in ceramic matrix composites**
Edited by I. M. Low
46 **Ceramic nanocomposites**
Edited by R. Banerjee and I. Manna
47 **Natural fibre composites: Materials, processes and properties**
Edited by A. Hodzic and R. Shanks
48 **Residual stresses in composite materials**
Edited by M. M. Shokrieh
49 **Health and environmental safety of nanomaterials: Polymer nanocomposites and other materials containing nanoparticles**
Edited by J. Njuguna, K. Pielichowski and H. Zhu

© Woodhead Publishing Limited, 2014

1

Wood fibres as reinforcements in natural fibre composites: structure, properties, processing and applications

D. DAI and M. FAN, Brunel University, UK

DOI: 10.1533/9780857099228.1.3

Abstract: Wood fibres are the most abundantly used cellulose fibre. They have been extensively used in the modern composite industry due to their specific characteristics. This chapter systematically describes the structure, properties, processing and applications of wood fibres as reinforcements in natural fibre composites: first, the nature and behaviour of wood fibres and the developed technologies for the modification of wood fibres to enhance physical and mechanical properties (e.g. surface functionality and tensile strength) are investigated; the matrices and processing techniques for the development of wood fibre composites are then discussed; and finally, the properties and applications of wood fibre composites in industrial sectors are presented.

Key words: wood fibres, structure, physical and mechanical properties, modification, process technique, wood fibre composites.

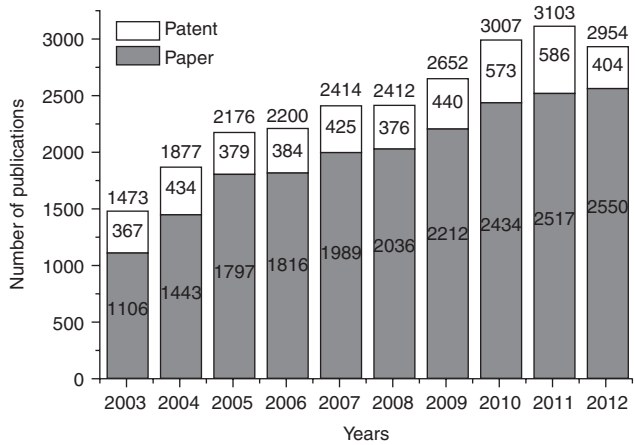
1.1 Introduction

Natural fibres are rich in cellulose, abundantly available and easy to handle and process. However, the application of natural fibres in composites came to a near-halt from the 1940s due to the low price and the steadily rising performance of technical and standard plastics.[1,2] In the 1990s, critical discussion about the preservation of natural resources and recycling had led to a renewed interest in natural renewable materials. With the recent increase in environmental awareness, exploiting natural fibres has raised great interest and become of importance. Among these natural fibres, wood fibres are the most abundantly used cellulose fibre having extensive use in the fibreboard, pulp and paper, and many other industrial sectors. Over 55% of paper and paperboard production[3] and 80% of natural fibre reinforced composites[4] are made from wood fibres. The use of wood composite materials dates from centuries ago.[5] In ancient China, wood, bamboo and straw were used to reinforce

© Woodhead Publishing Limited, 2014



1.1 Yuchang Lou in Fujian, China: a wood–clay composite building that is over 600 years old.



1.2 Number of publications on wood fibres and products.

clay for making walls, and many natural fibre-reinforced clay buildings are still in use, e.g. the 'Tulou', which dates from 1200 years ago, one of the oldest wood–clay buildings, can be observed in the south of China (Fig. 1.1).

To date, numerous publications have reported the applications of natural fibres, e.g. pulp,[6,7] ethanol[8] and composite.[9] Among these reports, more

© Woodhead Publishing Limited, 2014

than 85% focus on wood fibres. In addition, the growing importance of wood fibres can be evidenced from the increasing number of publications in the past 10 years (Fig. 1.2). It should be noted that these publications derive from the Google scholar database with the key word of wood fibre, and it is found that more than 75% of the publications are from journals or conferences, and about 70% of these reports focus on wood fibre composites.

The development of nanotechnology (NT) and biotechnology in the past 10 years has pushed the research and development of wood fibres a step further, and enlarged the role of wood fibres in many industrial sectors, such as pulp and paper, and material industries.

1.2 Wood fibres: nature and behaviour

1.2.1 Structure of wood fibres

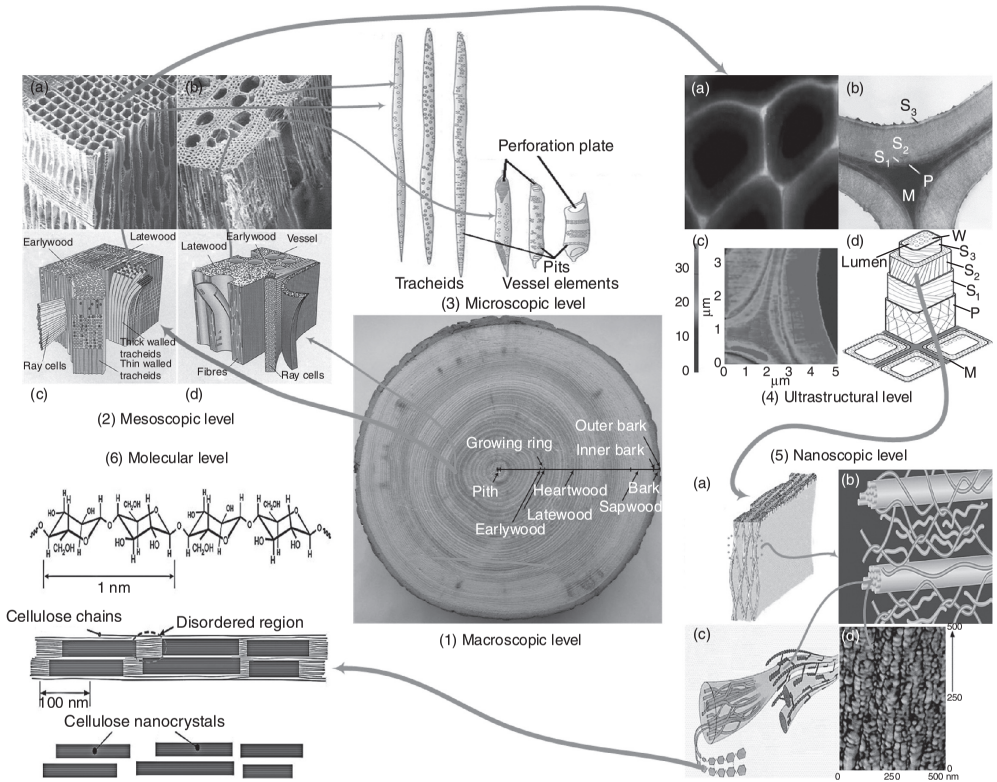
Wood fibres consist of both live and dead cells in the wood, depending on the location and the age of tree from which they are extracted. The hierarchical structure of wood fibres gives this fibrous material excellent performance properties, e.g. high strength to weight ratio. Wood fibres can be obtained from timber by chemical, mechanical, biological processes, and many combined processes.

At the macroscopic level (normally 0.1–1 m), wood fibres mainly exist within the layer of xylem in the wood[10] (Fig. 1.3(1)). The dark strip in the centre of the stem is the pith, which represents the tissues formed during the first year of growth. The inner part of the xylem layer consists of dark coloured heartwood. The lighter coloured outer part is sapwood, which conducts water from the roots to the foliage of the tree. Both inner and outer parts are organized with many concentric growth rings (annual increments), each of which is distinguished by earlywood, composed of large thin-walled cells produced during the spring when water is usually abundant, and the denser latewood, composed of small cells with thick walls (Fig. 1.3(2c)[11]). In addition, the inner bark layer comprises the tissues outside the vascular cambium, including secondary phloem, which transports the nutrients from photosynthesis in the leaves to the rest of the tree, cork cambium (cork-producing cells), and cork cells. The outer bark, composed of dead tissue, protects the inner region from injury, disease and desiccation. At the mesoscopic level (normally 1–10 mm), wood fibres form a continuum of cellular material.[12]

At the microscopic level (normally 0.01–6 mm), two kinds of wood cells with different hierarchical structures, namely tracheids (in softwoods and hardwoods) and vessels (only in hardwoods), can be easily distinguished[13] (Fig. 1.3(3)), and the dimensions of both wood fibres are shown in Table 1.1.[14–18]

© Woodhead Publishing Limited, 2014

© Woodhead Publishing Limited, 2014



1.3 Wood fibre from macroscopic to molecular levels: (1) macroscopic level; (2) mesoscopic level: 3D schematic of (a) softwood and (b) hardwood, scanning electron microscope (SEM) of (c) softwood and hardwood; (3) microscopic level; (4) ultrastructural level: (a) Raman image, (b) transmission electron microscope (TEM), (c) atomic force microscope (AFM) and (d) model of wood cell; (5) nanoscopic level: (a) schematic drawing of the cellulose aggregate structure in wood cell, (b) a schematic of cellulose fibrils laminated with hemicellulose and lignin, (c) AFM of a transverse section of the secondary wall of wood cell and (d) structure of cellulose in a wood cell wall; (6) molecular level.

Table 1.1 Dimensions of typical softwood and hardwood fibres

Types of fibres	Length (mm)	Width (μm)	Aspect ratio
Softwood	2–6	20–40	50–200
Hardwood	1–2	10–50	28–86

Tracheids constitute over 90% of the volume of most softwood[19] and 50% of the volume of hardwood.[15] Their average length is usually between 2 and 6 mm,[14,16,18] and their width is between 20 and 40 μm,[14,17] with a length to width ratio (aspect ratio) often in excess of 50–200. In hardwood, the length of tracheids, which is only 1–2 mm,[14,15] is considerably shorter than that of softwood tracheids, and the width is between 10 and 50 μm[14,15], with a narrow aspect ratio of 28:86.[14] In addition to tracheids, hardwoods have wider cells, namely vessel elements, which vary considerably in size and shape.[20] They are a series of broad and articulated cells (around 100 μm), which are long (many centimetres) and their function is to channel sap in almost straight lines. In some wood species, they may account for up to 50%–60% of the volumetric composition, but usually less than 10% by weight.[14] The wide vessel elements of the early wood are found to be 13%–47% shorter than those of the late wood.[21]

At the ultrastructural level (normally 1–25 μm), the wood fibres are built up of four layers (Fig. 1.3(4)).[22–25] These are middle lamella (M), primary wall (P), secondary wall (S), including the outer layer of the secondary wall (S_1), the middle layer of the secondary wall (S_2), the inner layer of the secondary wall (S_3), and the warty layer (W).[26,27] The middle lamella is located between the cells. This layer is highly rich in lignin; the concentration of lignin in this layer is about 70%–80%,[28] which is about twice that in secondary wall. The high concentration of lignin can cement the cells together very well, but in the processing of wood fibres, separation of the lignin remaining on the fibre surface can result in a decrease of inter-fibre bonding. The primary cell wall is a thin layer (0.1–0.2 μm) which surrounds the protoplast during cell division and subsequent enlargement.[14] It contains a randomly and loosely organized network of cellulose microfibrils. Due to the occurrence of pectin and protein, the properties of the primary wall layer differ from those of the secondary; in this layer strong interactions exist among the lignin, protein and pectin, as well as among the cellulose and hemicellulose. This obvious feature has a major influence on the separation of fibres. The secondary cell wall (1.2–5.4 μm) contains much more ordered microfibrils than the primary cell wall. It comprises a series of layers, namely S_1, S_2 and S_3. The warty layer (W) is comparable in thickness (0.1–0.3 μm) to the primary wall, and consists of four to six lamellae which spiral in opposite directions around the longitudinal axis

© Woodhead Publishing Limited, 2014

of the tracheid.[14] The outer secondary cell wall (S_1) has a crossed fibrillar structure. Although the S_1 layer has a large microfibril angle (MFA), about 50–70°,[29] this layer is considered to play an important role in determining the transverse mechanical properties and surface properties of fibres[30–32] as well as pulp fibre properties.[33] The main bulk of the secondary wall is contained in the middle secondary cell wall (S_2, 1–5 μm). The microfibrils in this layer spiral steeply about the axial direction at an angle of around 5–30°[29,34] and have a pronounced influence on the properties of fibres. The S_2 layer is the thickest cell wall layer and controls the strength of the entire fibre. The inner secondary wall (S_3, 0.1 μm), sometimes also known as the tertiary wall,[35] is at the lumen boundary and forms a barrier between the lumen and the rest of the cell wall. Compared with the other layers in the secondary wall, the S_3 layer contains the highest concentration of lignin, about 53%.[36] In this thin layer the microfibrils form a flat helix. The microfibrils in the S_3 layer are oriented almost perpendicularly to the microfibrils in the S_2 layer with MFA between 50° and 90°.[29] The innermost portion of the cell wall consists of the so-called warty layer, probably formed from protoplasmic debris. All softwoods have this segment in their cell wall; however, not all hardwoods do.[29]

At the nanoscopic level (Fig. 1.3(5)),[37–39] wood fibres have an important influence on the final performance of timbers. These influences include chemical reactions and physical effects. The wood fibres are built up by cellulose microfibrils (10–25 nm[26,40]), hemicelluloses and lignins due to the formation of lignin–carbohydrate complex (LCC) by covalent bonds.[41] Most of the microfibrils are not parallel to the cell axis and can form a particular angle, which is known as the MFA. The MFA was found to be a critical factor in determining the physical (e.g. shrinkage[42,43]) and mechanical properties (e.g. stiffness,[44] and tensile strength[45]) of wood fibres.

From the molecular point of view (Fig. 1.3(6)[46]), the main chemical components of wood fibres are cellulose, hemicellulose and lignin. As shown in Table 1.2,[47,48] the dominant component in wood fibres is cellulose. The

Table 1.2 Chemical compositions of hardwood and softwood fibres

Types of wood fibres	Cellulose (%)	Hemicellulose (%)	Lignin (%)	Extractives (%)
Original wood fibres				
Softwood	40–45	25–30	26–34	0–5
Hardwood	45–50	21–35	22–30	0–10
TMP wood fibres	37.07 ± 0.6	29.2 ± 0.1	13.8 ± 0.7	0.8 ± 0.6
Unbleached wood fibres				
Softwood	69.0 ± 2.5	22.0 ± 0.7	8.8 ± 1.8	0.2 ± 0.1
Hardwood	78 ± 0.5	19.3 ± 0.1	2.4 ± 0.4	0.3 ± 0.2
Bleached wood fibres				
Softwood	79.2 ± 0.2	20.0 ± 0.1	0.8 ± 0.1	0 ± 0
Hardwood	78 ± 0.2	20.3 ± 0.1	1.3 ± 0.1	0.5 ± 0.1

TMP, thermomechanical pulps.

© Woodhead Publishing Limited, 2014

cellulose of wood fibres is similar to other natural fibres, in that it consists of a linear chain of several hundred to over 10 000 $\beta(1\rightarrow4)$ linked D-glucose units[49] laid down in microfibrils in which there is extensive hydrogen bonding between cellulose chains, producing a strong crystalline structure in a crystalline region.[50,51] Combined with the amorphous region, the cellulose microfibrils aggregate into larger microfibrils.[51] The hydrogen bonds in the cellulose not only have a strong influence on the physical properties of the cellulose (e.g. solubility, hydroxyl reactivity) but also play an important role in its mechanical properties.[50]

1.2.2 Physical and mechanical properties of wood fibres

The surface property is one of the key properties of wood fibres; it can affect the interfacial adhesion of resin on the surface of fibres and the mechanical properties of fibre-based composite. This property is influenced by fibre morphology, chemical composition,[52] extractive chemicals and processing conditions.[53] Table 1.3 shows the surface properties of wood fibres in comparison with other natural fibres. Due to the high polar character of the surface, the fibres are less compatible with non-polar resin. Therefore, the combination of the inherent polar and hydrophilic features of wood fibres and the non-polar characteristics of resins gives rise to difficulties in compounding these materials, resulting in inefficient stress transfer of its composites under load. The use of different kinds of physical (i.e. corona discharge) and chemical surface treatment methods (i.e. coupling agents such as silanes) leads to changes in the surface structure of the fibres as well as to changes of surface properties.

The mechanical properties of wood fibres are of great importance for their use in the paper[67,68] and composite industries.[69] The mechanical properties of materials can be characterized from two methods, namely, macroscopic tests (e.g. tensile test) and indentation tests. The macroscopic tests focus on measuring the mechanical performance of the whole sample, while the indentation tests focus on measuring a local area of the sample.[70] In

Table 1.3 Surface properties of natural fibres

Fibres	Surface area (m^2/g)	γ^d (mJ/m^2)	$(\zeta_0-\zeta_\infty)/\zeta_0$ (mV)	$\zeta_{plateau}$ (mV)	References
Flax	0.31 ~ 0.79	23.85	0.88 ~ 0.95	–1.1 ~ –0.21	54–57
Hemp	0.75	31.6	0.91	–0.1	55, 57, 58
Sisal	1.63	32.90–48.35	0.76 ~ 0.88	–1.7 ~ –0.4	55–57, 59
Coir	0.48	45.05	0.22	–4.6 ~ –3.8	56, 59, 60
Softwood	0.97	31	–	–18.6 ± 5.0	61–63
Hardwood	1.34	32–47	–	–7.3	64–66

γ^d: dispersive surface energy; ζ_0: ζ-potential initial value; ζ_∞: ζ-potential final value; $\zeta_{plateau}$: ζ-potential plateau value.

© Woodhead Publishing Limited, 2014

the macroscopic tests, the parameters of mechanical properties generally include such items as tensile strength and modulus, elongation, compressive strength and modulus, impact strength, and flexible strength and modulus. Researchers traditionally use the elongation, tensile strength and Young's modulus[1,71] to evaluate the mechanical performance of wood fibres.

As aforementioned, the mechanical performance of wood fibres is influenced by their structure; in addition, the mechanical performance is influenced by the growing parameters, e.g. area of growth, climate, and the age of the plant.[72,73] Wood fibres generally display higher mechanical performance compared with other natural fibres (Table 1.4). However, due to wood source, growth conditions, and chemical and mechanical treatments, the strength of wood fibres varies considerably, which is one of the main drawbacks for all natural products. The range between minimum and maximum characteristic values of wood fibres is noticeably wider than that of synthetic fibres although the wood fibres display a good Weibull modulus (Table 1.5) which describes the variability of the failure strength.

The first report about the mechanical properties of wood fibres did not appear until the end of the 1950s.[91] The development of spectroscopic (especially X-ray diffraction (XRD) in 1912 and Raman spectroscopy in 1923) and microscopic (especially atomic force microscopy (AFM) in 1986) technologies enabled the characterization of mechanical properties on micro- or nano-scales for heterogeneous polymer or composites. These developed technologies have enlarged understanding of the mechanical properties of wood fibre (wood fibre itself is a polymeric composite) and the structure–property relationship,[92] and optimized the utilization of wood fibres as reinforcements in composites.[24] Nanoindentation and AFM techniques have been employed to investigate the micro- or nano-mechanical properties of

Table 1.4 Mechanical properties of natural fibres

Fibres	Density (g/cm^3)	Elongation (%)	Tensile strength (MPa)	Young's modulus (GPa)	References
Flax	1.5	1.2–3.2	345–2000	15–80	74–76
Hemp	1.48	1.6	550–900	26–80	72, 77, 78
Sisal	1.5	3.0–7.0	468–700	9.4–22	79
Coir	1.2	17–47	175	4.0–6.0	1,71
Softwood	1.5	–	600–1020	18–40	80, 81
Hardwood	1.2	–	–	37.9	82
E-glass	2.5	2.5	2000–3500	70	1
S-glass	2.5	2.8	4570	86	1
Aramid	1.4	3.3–3.7	3000–3150	63.0–67.0	1

© Woodhead Publishing Limited, 2014

Table 1.5 Weibull modulus of natural fibres

Natural fibre	Weibull modulus	Gauge length (mm)	References
Flax	2.6	10	83
Hemp	2.86	10	84
Sisal	4.6	10	85
Coir	3.1	8	86
Wood	3–5	–	87
E-glass	6.61	10	88
S-glass	20.5	–	89
Aramid	10.4	5	90

Table 1.6 Effect of wood species on the mechanical properties of wood fibres

Type of fibres	MFA (°)	Elastic modulus (GPa)	References
Softwood			
Spruce	–	13.49 (CV 43.00%, earlywood)	93
Scots pine	5	21.00 (CV 16.00%, latewood)	93
(pulp)	–	12.2 ± 1.6	94
Hardwood			
Oak	3 ± 3	18.27 ± 1.74 (earlywood: latewood = 1:1)	94
Eucalyptus (pulp)	–	9.10 ± 1.60	

wood fibres since the first report about the cell wall mechanics of softwood by using nanoindentation in 1997.[93]

By using these new techniques, researchers have revealed various novel properties of wood fibres. These findings support the selection of wood fibres as composites, and the understanding of the interaction mechanism between wood fibres and the matrices. For example: (i) the identification of different properties among wood species and across growing stages: at cell wall level, it seems that the elastic modulus of hardwood fibres is similar to that of softwood fibres; however, earlywood has a lower elastic modulus than latewood (Table 1.6); (ii) the anisotropic properties of wood fibres: Jäger *et al*.[96,97] employed the Vlassak model to evaluate the relationship between indentation modulus, indentation direction and elastic material constants of spruce cell wall material $M^{pred}(E_t, _{El}, G_{tl}, \upsilon_{tt}, \upsilon_{tl}, \delta_i)$, and then using an error minimization procedure to analyse the values of the elastic material constants – the values for the longitudinal elastic modulus, transverse modulus and shear modulus are reported as 26.3, 4.5 and 4.8 GPa, respectively; (iii) the interfacial compatibility between S_2 and S_3 layers: by using a nanoindentation-AFM technique the interfacial compatibility in the cell

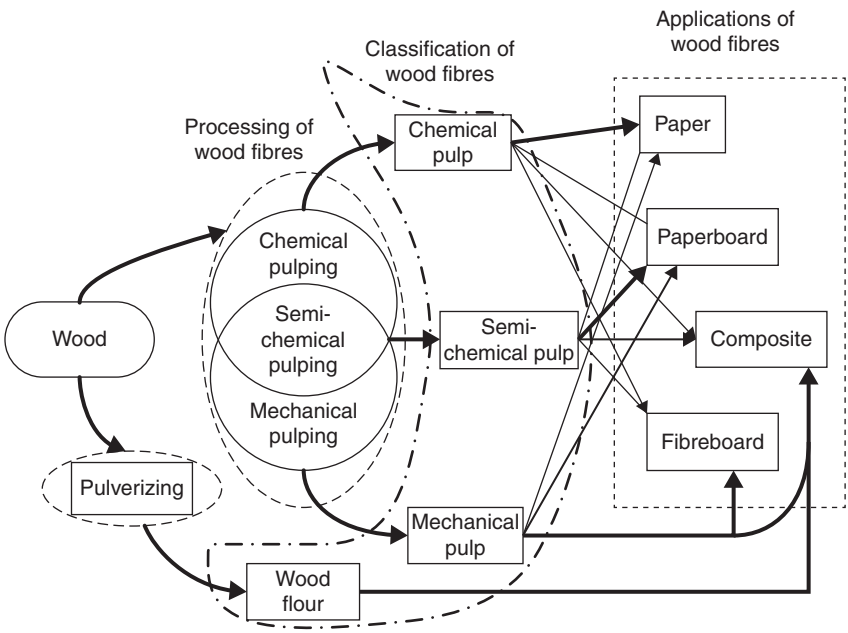
© Woodhead Publishing Limited, 2014

wall of spruce was further investigated[98] and it has been found that the S_3 layer has a less polar character than the S_2 layer; hence polyurethane (PUR) was found to have a better adhesion to the S_3 layer and poorer adhesion to the S_2 layer compared with urea formaldehyde (UF). It is proposed that differences in the polarity of the adhesives used and in the surface chemistry of the two cell wall surfaces examined account for the observed trends.

In addition, nanoindentation and AFM have been widely used to reveal much more detail about wood fibres, e.g. cell wall lignification,[99] melamine modification,[100] stiffness and hardness of wood fibres,[101] and conformability of wet wood fibres.[102]

1.2.3 Processing of wood fibres

The separation of wood fibres includes two methods (Fig. 1.4): a pulping process and a pulverizing process. Pulverizing is the process by which the wood is reduced into small particles (180–425 μm). It is the main step for the production of wood flour, which is mainly used as filler in plastics. For dry mechanical processing, the final products typically have low aspect ratios (only 1–5). These low aspect ratios allow wood flour to be more easily metered and fed than individual wood fibres, which tend to bridge. However, the low aspect ratio limits the reinforcing ability. Pulping is the process by



1.4 Processing and applications of wood fibre.

© Woodhead Publishing Limited, 2014

which the macroscopic structure of raw wood is reduced to a fibrous mass. It is achieved by rupturing bonds within the wood structure. It can be accomplished chemically, mechanically or by some combination of these treatments. These treatments are (i) chemical,[103–105] (ii) mechanical[106,107] and (iii) semi-chemical, which combines (i) and (ii) to separate wood fibres.[108–110]

The main commercial chemical treatment technique is the sulphate or kraft process; an acid sulfite process is also used. The chemical process involves the use of chemicals to degrade and dissolve lignin from the wood cell walls, releasing high cellulose content fibres. Chemical pulping processes yield pulps with higher strength compared with mechanical processes. However, these processes are low yield (40–55%)[111,112] (Table 1.7) and are very capital-intensive.[111] Products from the chemical treatment process (chemical pulp) are always used for paper (e.g. tissue), paperboard, etc.

Stone groundwood (SGW), pressure groundwood (PGW), refiner mechanical pulps (RMP) and thermomechanical pulps (TMP) are the main products of wet mechanical treatments. Wet mechanical treatment involves the use of mechanical force to separate the wood fibres. Mechanical defibration of wood and chips results in only small material losses and the gross composition of the resulting pulps differ only slightly from that of the original. However, the fibre structure is somewhat damaged. Mechanical treatment under wet conditions can obtain higher yield (Table 1.7), but these processes are electrical energy-intensive and produce paper with lower strength, higher pitch content, and higher colour reversion rate compared with chemical processes. Mechanically produced pulp has a higher proportion of broken cell fragments (called 'fines') among the fibres. The mechanical pulps can be used for paper (printing paper), paperboard, composite and fibreboard.

The semi-chemical techniques normally involve pretreatment of wood chips with a chemical method. There are several types of semi-chemical pulps in production, e.g. chemimechanical pulps (CMP), chemithermomechanical pulps (CTMP) and neutral sulfite semi-chemical (NSSC) pulps. NSSC is the most common product, made primarily from hardwood species and noted for its exceptional stiffness and high rigidity. The yield of semi-chemical pulping is 58.7–95%[129] (Table 1.7). Its primary use is for the production of paperboard as well as printing papers, greaseproof papers and bond papers. The semi-chemical pulps are still used for composite, but very much less for fibreboard.

1.2.4 Applications of wood fibres

As a result of a growing awareness of the interconnectivity of global environmental factors, the principles of sustainability, industrial ecology and ecoefficiency, and also green chemistry and engineering, are being integrated into the

© Woodhead Publishing Limited, 2014

Table 1.7 Pulp yield and relative strength achieved using various pulping methods

Classification	Process	Yield (%)	Strength			References
			Tensile index (Nm/g)	Tear index ($mN \cdot m^2/g$)	Burst index ($kPa \cdot m^2/g$)	
Chemical treatment	Kraft pulping	40–50	92.0–98.5	8.6	6.8–7.3	113,114
	Sulfite pulping	45–55	85–132.7	7.4–12.2	4.43–6.42	115, 116
	Soda pulping	45–55	69.9–83.6	3.2–9.2	4.2–7.34	117, 118
Mechanical treatment	Stone groundwood (SGW) pulping	90–98.5	28.2	2.2	0.86	119,120
	Pressure groundwood (PGW) pulping	95.5	18.4	2.8	0.90	119,120
	RMP	90–97.5	28.1	2.8	0.66	119–121
	TMP	91–95	27.6	3.2	1.10	120,122,123
Semi-chemical treatment	Chemimechanical pulping (CMP)	80–90	49–63	5.45–5.5	3.11	115,120,124
	Chemithermomechanical pulping (CTMP)	80–95	51.8	6.4	2.4	120,124,127
	NSSC	58.7–80	30.90–35.57	3.73–4.08	1.38–1.60	126–128

© Woodhead Publishing Limited, 2014

Table 1.8 Production of commercially important fibre sources during 2002–2011

Year	Production of wood fibres (t)	Production of cotton lint (t)	Production of flax (t)	Production of hemp (t)	Production of jute (t)	Production of sisal (t)	Fibre share of wood (%)
2002	167 257 547	18 885 577	781 762	78 110	2 863 037	284 355	87.96
2003	170 046 697	19 467 665	786 350	69 824	2 798 567	305 867	87.89
2004	174 785 477	24 530 832	1 013 105	72 793	2 562 784	325 679	85.98
2005	173 985 135	24 476 010	1 008 656	78 664	2 766 596	330 895	85.86
2006	175 826 129	24 449 953	661 958	113 270	2 870 460	366 497	86.07
2007	180 993 713	25 066 925	541 087	77 079	2 823 671	370 519	86.24
2008	177 469 786	22 487 098	527 851	71 336	2 691 315	370 786	87.16
2009	160 557 039	20 898 428	382 538	79 721	3 045 089	393 953	86.62
2010	170 871 722	23 717 040	315 583	81 048	2 828 533	363 558	86.22
2011	173 309 240	26 102 935	315 084	81 964	2 861 996	411 864	85.34

development of the next generation of materials, products and processes.[130] In 2003, the UK government established highly ambitious long-term goals relating to climate change, with the objective of moving towards a 'low carbon economy' and a target to cut carbon dioxide (CO_2) emissions by 60% by mid-twenty-first century. The White Paper states that this should be achieved without detriment to the UK's competitiveness or security. Then, to effectively reduce CO_2 emissions while keeping economic growth, different countries have begun to search for new development paths, among which low-carbon development has become widely advocated.[131] These actions have accelerated research in natural fibres for application in many industrial sectors.

Wood fibres are the most important source among the natural fibres, e.g. as shown in Table 1.8 (these data are arranged based on reference 132), showing a share of wood fibres of over 85%. Wood fibres are primarily used for the paper and paperboard industry (about 80.5%), representing over 55% of total paper and paperboard production.[3] Some 17.03% of wood fibres are used in composites, with wood-fibre-based composites making up over 80% of natural fibre reinforced composites.[4]

1.3 Modification of wood fibres for composites

The use of wood fibre to make low cost and eco-friendly composite materials is a subject of great importance. However, certain drawbacks of natural fibres (e.g. higher polar and hydrophilic) cause natural fibres to be poorly compatible with polymers, which results in the loss of mechanical properties upon atmospheric moisture adsorption.[65] Compared with glass fibres, natural fibres show lower mechanical properties. In order to improve the mechanical properties and the interfacial property of natural fibres, various modifications of the natural fibres have been investigated. These modifications are of three types: physical, chemical and NT.

© Woodhead Publishing Limited, 2014

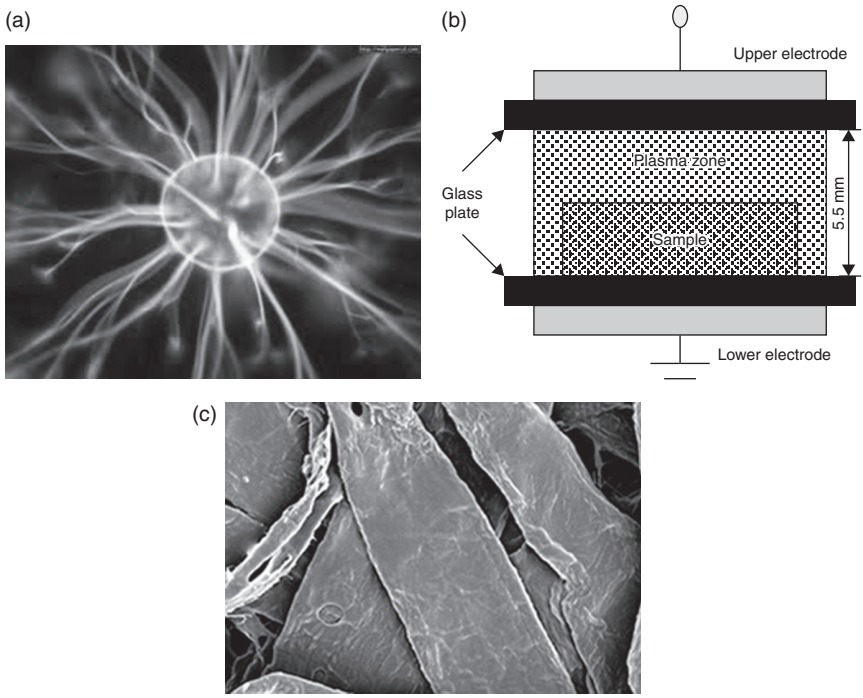
1.3.1 Physical modification

Physical modification has always been carried out by using instruments to change the structural and surface properties of the fibres, with the aim of increasing the strength of fibres and the interfacial compatibility between wood fibre and matrices. Traditional methods involve thermotreatment,[133,134] calendering[135,136] and stretching of these, thermotreatment is the most useful to modify natural fibres. When the fibres are subjected to heat treatment above the glass transition temperature of lignin, it is postulated that the lignin will be softened and migrate to the fibre surface. Kraft lignin has a glass transition temperature of 142°C.[134] Lignin begins to degrade at around 214°C; hence, heating the fibres to 200°C would be expected to cause some softening.[138] Thermal treatments can increase the crystallinity, dimensional stability, hydrophobicity of lignocellulosic fibres.

Thermal treatment is an efficient modification for forest products. The final properties of the products may significantly depend on the modification of hemicelluloses. This treatment can improve the moisture resistance of wood-based panels.[139,140] Hydrothermal treatment to modify wood flour can increase the storage modulus of poly(lactic acid) (PLA)–wood flour composites by up to 55.65% without any other chemical reagents.[141] Saturated steam under pressure at various temperatures above 100°C results in a decrease in the thickness swelling of the panels while mechanical properties, flexural properties, internal bond strength and screw withdrawal resistance, decrease.[142] Medium density fibreboard (MDF) panels made from thermally-treated wood fibres at 180°C for 30 min appear to be a practical choice for achieving a low thickness swelling of MDF products.

Surface modification by discharge treatment,[143,144] such as low-temperature plasma, sputtering and corona discharge, is of great interest in relation to the improvement in functional properties of natural fibres. This technique was found to be effective for the improvement of the compatibility between hydrophilic fibres and a hydrophobic matrix. Scientists in some industrialized countries, such as France, Japan and the United States, have carried out surface treatment of different fibres with various plasma techniques since the 1960s. To date, scientists in most countries have studied this topic to develop their own industrial projects. Plasma technology has been widely used as an effective method for surface modification of natural fibres such as flax,[145,146] sisal,[147] and keratin.[148] Plasma treatment (Fig. 1.5)[149–151] mainly causes chemical implantation, etching, polymerization, free radical formation and crystallization, whereas the sputter etching brings about mainly physical changes, such as surface roughness, and this leads to increase in adhesion.[145]

© Woodhead Publishing Limited, 2014



1.5 Schematic of plasma treatment: (a) plasma lamp; (b) plasma system and (c) wood fibre after discharge treatment.

The processing of wood fibres can result in various chemical compositions in the wood fibres, as shown in Table 1.2. The discharge treatment[152] (diffuse coplanar surface barrier discharge (DCSBD) plasma) of wood fibres can result in polar carbonyl groups (C=O) and a considerable increase of free surface energy to reduce the water uptake of wood. The discharge treatment (corona discharge) of wood fibres obtained by mechanical processing was reported to produce 2.4 carboxyl and 10.9 carbonyl functions per hundred C9 units of lignin.[153] The cold Ar plasma treatment can result in the generation of higher phenoxy radical concentration in CTMP,[154] the concentration of which was four times that of TMP. By using heteronuclear single quantum coherence (2D-HSQC) spectroscopy and nuclear magnetic resonance spectroscopy of carbon (^{13}C-NMR), it was found that the generation of phenoxy radicals can lead to cross-linkages of lignin monomeric units and formation of new inter-monomeric C–C and C–O bonds. In both fibres, the chemical structure of lignin was heavily modified by plasma treatment and the CTMP forms much more radicals than chemical pulp.[155]

In addition, a variety of surface modifications can be achieved depending on the type of discharge. Carlsson *et al*.[156,157] studied the effects of hydrogen

© Woodhead Publishing Limited, 2014

and oxygen plasma treatments on wood fibres and found that the hydrogen plasma treatment reduced the hydroxyl groups and the water absorption of the wood fibres. By contrast, the oxygen plasma treatment displayed an improvement of water wettability.

1.3.2 Chemical modification

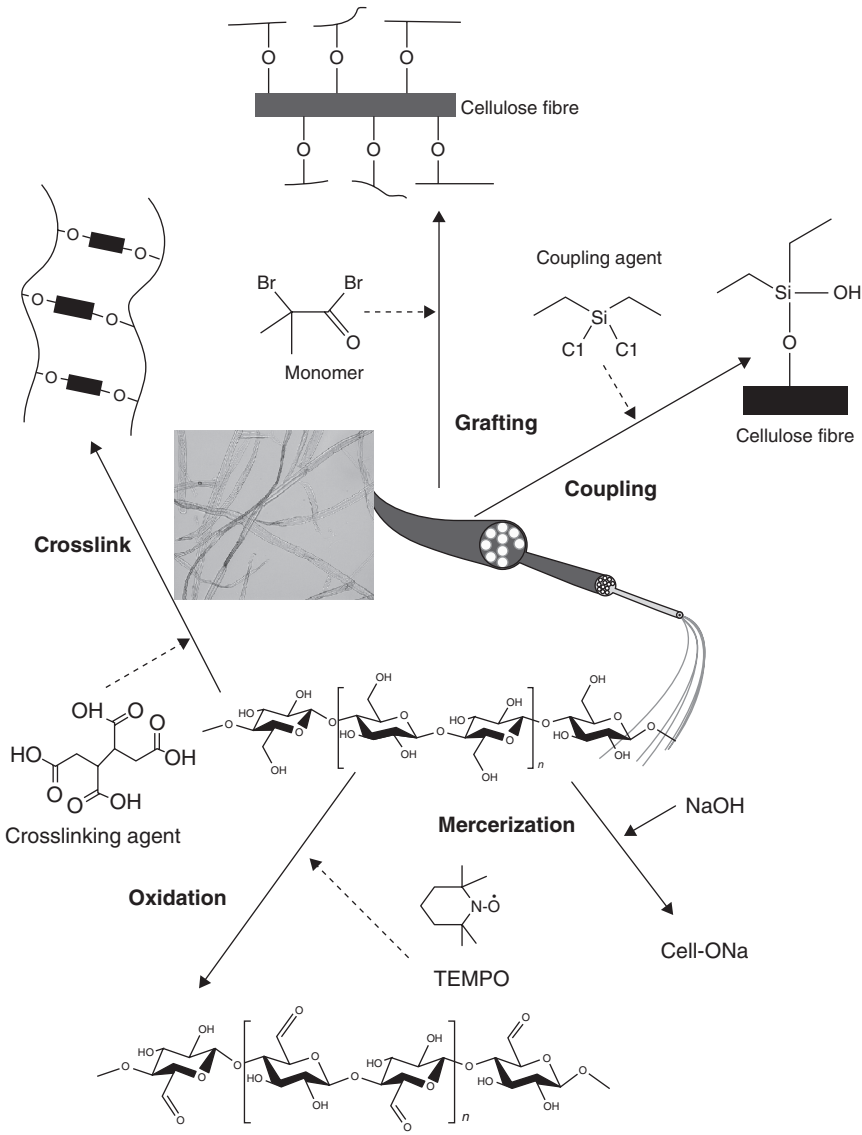
Chemical modifications utilize chemical agents to modify the surface of fibres or the whole fibre. They can modify the structure of wood fibres or introduce new hydrophobic functional groups into the surface of wood fibres to reduce the hydrophobicity of fibres. The modification can be classified into five methods: mercerization, oxidation, crosslink, grafting and coupling agent treatment (Fig. 1.6).

Mercerization

Mercerization is an old method of cellulose fibre modification, which is an alkaline treatment method for cellulose fibres. The process was devised in 1844 by John Mercer of Great Harwood, Lancashire, England, who treated cotton fibre with sodium hydroxide.[158] This treatment caused the fibres to swell; about 25% of hydrogen bonds are broken during the swelling process in the post-treatment (drying).[159] These bonds will re-bond and the consequent effects of the re-bond have been reported in the literature: including (i) decreasing the spiral angle of the microfibrils and increasing the molecular direction;[1] (ii) producing fibre fibrillation, i.e. axial splitting of the elementary fibres (or microfibres that constitute the elementary fibre).[160–162] This process leads to a decrease in fibre diameter, increasing the aspect ratio and the effective surface area available for wetting by a matrix in a composite; there is also an increase in fibre density as a consequence of the collapse of its cellular structure; and (iii) changing the fine structure of the native cellulose I to cellulose II.[163–166] These changes may result in an improvement in fibre strength and hence stronger composite materials.[161,167,168]

It was reported that after immersion in alkali for 48 h, the globular pultrusion presented in the untreated fibre disappeared, leading to the formation of a larger number of voids. Systematic investigations[159] have already revealed three important phenomena of cellulose swelling in aqueous alkali, i.e. (i) the passing of the swelling value through a maximum, depending on lye concentration; (ii) a qualitatively similar, but quantitatively different, behaviour of all the alkali hydroxides in aqueous solution from LiOH to CsOH on interaction with cellulose in an aqueous medium; and (iii) a phase transition within the region of crystalline order above a lye (alkaline) concentration of 12–15% due to a so-called intracrystalline swelling caused by inclusion of NaOH and H_2O into the crystallites.

© Woodhead Publishing Limited, 2014



1.6 Main chemical treatments and modification mechanism of natural fibre.

The mercerization process increases the number of hydroxyl groups on the wood fibres surface, which in turn favours water absorption,[169] therefore, wood fibres with mercerization should not be suitable for hydrophobic matrices. It was reported that the alkaline treated wood fibres incorporated in polypropylene (PP) can induce the hexagonal phase of iPP and the mechanical

© Woodhead Publishing Limited, 2014

performance of the wood-PP composite was increased.[170] Alberto *et al.*[171] modified wood fibres with (i) cold water, (ii) hot water and (iii) hot water with sodium hydroxide (1% concentration), and found that the third treatment could increase the compatibility factor significantly for the fibres from *Jambire* and *Wimbe* with a compatibility factor of 84.77% and 83.77% respectively. The main mechanism of the reinforcement by alkaline treatment may be due to the degradation of hemicellulose and amorphous content, as the alkaline treatment products are more effective than the polar extractive treatment.[172]

Oxidation

Oxidation modification can be achieved under mild conditions. In this case carboxyl groups, aldehyde groups and ketone groups can be introduced into the cellulose chains by the selective oxidation of primary or secondary hydroxyl groups in the chains. In 1938, Yackel *et al.*[173] firstly employed NO_2 as oxidant to oxidate cellulose selectively. After that, various primary[174–181] and secondary[185–186] oxidative systems have been reported. Recently, due to the excellent selective oxidation, TEMPO-NaBr-NaClO and TEMPO-NaClO-$NaClO_2$ oxidative systems[181,187–197] have received much attention around the world. Potthast *et al.*[198] investigated the new functional groups on the surface of hemp fibres which were introduced by the TEMPO oxidation system. Results showed that the content of hydroxyl groups was influenced by the concentration of oxidant and the treatment time. Matsui *et al.*[199,200] investigated the influence of ozone oxidation pretreatment on the graft copolymerization of methyl methacrylate on the surface of hemp fibres and found that, with the increase of oxidation time, hydroperoxide (HPO) increased from 0 mol/cell. molecule to 160 mol/ cell. molecule, and the CI of the fibres decreased from 69.7% to 68.3%, but the degree of grafting increased significantly from 14% to 129%.

Crosslinking

Multifunctional compounds which have more than two functional groups have always been used as crosslink agents to crosslink the inter-chains of cellulose by reacting with the hydroxyl groups. The crosslink modification of cellulosic fibres has always been carried out by etherification[201] and esterification.[202] The crosslinking of cellulose has been found important for commercial application in textile finishing of cellulose-based fabrics with end-use properties, e.g. wrinkle resistance, permanent press and easy care properties. Wood fibres are the main contributor to the hygro-expansion (which is one of the drawbacks of wood fibres) of wood fibre-based composites. The crosslinking modification can reduce the transverse coefficient of hygro-expansion of the wood fibres[203] and result in the improvement of environment and dimension stability of wood fibre-based composite.[77,204]

© Woodhead Publishing Limited, 2014

Grafting

Chemical modification through graft copolymerization is an effective method that improves the compatibility of wood and other natural fibres with hydrophobic matrices. The technique involves the grafting of various monomers onto the surface of cellulosic fibres.[205,206] The reaction is usually initiated by free radicals of cellulose molecules. The cellulose is exposed to high-energy ionizing radiation. After treatment with the selected ions (transition metal ions), oxidative reagents (as initiating agents), initiate free radicals on cellulose.[207] The radical sites initiate the grafting of alkyl acrylates (such as methyl, ethyl, butyl and propyl), vinyl monomer (such as methyl methacrylate and acrylonitrile) to the cellulosic surface. Maleic anhydride (MA) grafting treatment has been reported to function efficiently for natural fibre-based composite. Among the grafting treatments, MA grafting is the main method[208–226] for the modification of wood fibres. The type and concentration of MA can influence the mechanical performance of the composite. It has been reported that MD411D displayed a better performance at 2% concentrations.[210] Compared with the other natural fibres (e.g. cotton), wood fibre-based composites display better mechanical performance under low fibre loading (<10%).[216] The length of fibres has a positive effect on the tensile modulus and modulus of elasticity (MOE).[220] In addition, the other additives (e.g. compatibilizer[210,212]) also affect the mechanical performance of composites. Other grafting methods, e.g. methyl methacrylate (MMA) grafting,[227–230] styrene grafting,[231–233] cetyl alcohol[234] grafting and polymer grafting[235,236] have also been reported.

Coupling

In wood fibre composite industries, the coupling modification is the most important method. Coupling agents can be defined as the substances that are used in small quantities to treat a surface so that bonding occurs between filler and matrix. Coupling agents can be subdivided into two broad categories: bonding agents and surfactants (also known as surface active agents). At present, over 40 coupling agents have been used in the production and research of natural fibre composites.[237] The most popular treatments include the use of silanes[238–251] and isocyanates.[236,248,252,253]

1.3.3 Nanotechnology (NT) modification

Nanotechnology (NT) is defined by the US National Nanotechnology Initiative as the understanding, manipulation and control of matter at dimensions around 1–100 nm. Currently, most major governments around the world are investing heavily in NT[254] and many see it as the fuel for the next Industrial Revolution. With the large amount of fundamental research

© Woodhead Publishing Limited, 2014

under government funding today, NT has applications across nearly all economic sectors and allows the development of new critical enabling science with broad commercial potential, such as nano-structured materials, nanoscale-based manufacturing processes and nano-electronics. It has been demonstrated in recent years that NT can be used to modify natural fibres to introduce new functions onto the surface of fibres and enhance the performance of the final fibre-based products. This modification has been used in the textile[255,256] and paper industries[257] successfully. It is believed that the application of NT to the modification of wood fibres offers high economic potential for the development of fibre-based industry.

Various approaches have been developed to immobilize nanoparticles on the surface of wood and other natural fibres, among which, layer-by-layer (LbL) deposition[258–261] and the sol-gel process[262–265] are the main approaches that have commonly been employed by researchers. Different kinds of nanoparticles (e.g. AgNPs,[258,266–269] TiO_2,[269,270] SiO_2,[271–273] ZnO[274,275]) have been developed to impart multifunctional properties (e.g. anti-bacteria, UV resistant, anti-wrinkle finishing, water repellent) to fibres.

A novel way of combining biological technology with NT was first reported by Juntaro *et al.*[276] in 2007. This green technique firstly employed bacteria *Gluconacetobacter xylinus* strain BPR 2001 to treat natural fibres (hemp and sisal), then fabricated the bacterial cellulose on the surface of natural fibres. These modified natural fibres were then incorporated into the renewable polymers cellulose acetate butyrate (CAB) and poly-L-lactic acid (PLLA). It was found that the modified sisal PLLA composites showed an increase in parallel strength of 44% and an increase in off-axis composite strength of 68%.

1.4 Matrices (binders) of wood fibre composites

Wood-based composites can be classified as follows, based on the form of their structural components:

(i) Fibrous composites (composed of fibres in a matrix), such as fibreboard, MDF and wood plastic composite (WPC);
(ii) Laminar composites (composed of layers of materials), such as plywood, woven and non-woven textile composite;
(iii) Particulate composites (composed of particles in a matrix), such as particle boards (PB).

In wood fibre composites, wood fibres are the dispersed phase. The matrix may be inorganic compound, natural polymer or synthetic resin. The composites' shape, surface appearance, environmental tolerance and overall durability are dominated by the matrix, while the fibrous reinforcement

© Woodhead Publishing Limited, 2014

carries most of the structural load, thus providing macroscopic stiffness and strength.[277]

1.4.1 Inorganic compounds

The inorganic compounds used for wood fibre composites are cement, clay and lime. In ancient Egypt and China, clay had first been used to make walls. In the early to mid-1940s, natural fibre–cement composite was first investigated in Australia.[278]

Wood fibre–inorganic compound composites are one of the most successful applications of wood fibres in the composite industry. They have been widely used as corrugated or flat roofing materials, cladding panels and water containers, in a large number of building and agriculture applications. One of the drawbacks associated with wood fibres in inorganic application is their dimensional instability when the composites are subjected to changing relative humidity (RH) atmosphere. This instability is promoted by: (i) the water sensitivity of cellulose fibres, (ii) the effects of carbonation, high alkali content of the cement matrix and the generation of incompatible stresses. However, the addition of wood fibre can bring three benefits: (i) improving the toughness, tensile strength and the cracking deformation of the composite; (ii) increasing the solids retention and (iii) capturing CO_2 and locking it up in buildings.

1.4.2 Natural polymers

Natural polymer matrices include natural polymers and synthetic natural polymers. The natural polymers typically include starch and rubber. The synthetic natural polymers include PLA and poly(hydroxy butyrate) (PHB), etc. which are made from natural products (e.g. sugar, vegetable oil) by various chemical polymerization methods.

The use of starch to produce biodegradable plastics began in the 1970s. Starch-based products have prevailed all over the market, from packaging to the toy industry.[279]

Starch has been considered as one of the most promising materials for biodegradable plastics because of its natural abundance and low cost. However, low water resistance and poor mechanical properties are the main drawbacks of starch-based plastics. Using wood fibre to reinforce thermoplastic starch did not gain attention until the end of the 1990s. In 2001, researchers[280,281] reported that (i) the addition of wood fibre could increase the modulus and the tensile strength of the composite by up to 156% and 120%, respectively, and reduce the water uptake of the composite,[281] and (ii) the addition of wood

© Woodhead Publishing Limited, 2014

flour could influence the rheological behaviour of the composite and result in a slight decrease of mechanical performance.

Wood flour has been used as filler for rubber matrix. The addition of wood flour could increase the modulus, hardness and tensile strength of rubber. Wood fibre–rubber composites can be processed by extrusion, injection moulding, calendering and milling. They can be used for automotive tyres, sheeting, metal braids, belts, diaphragms and gaskets, roofing and ship fenders.

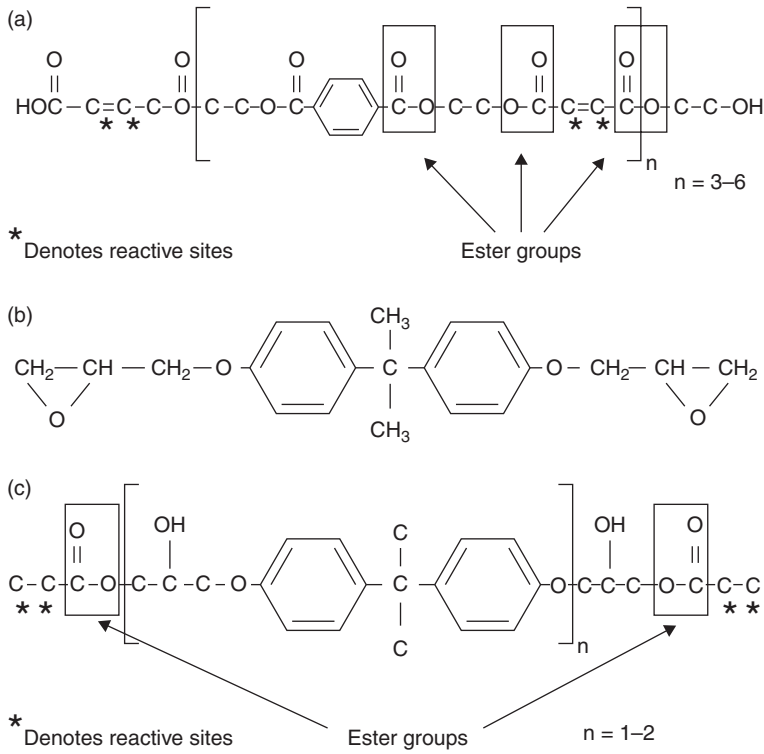
PLA is a versatile biopolymer made from renewable agricultural raw materials, and is fully biodegradable. It can be processed similarly to polyolefin. The final PLA-based products display good stiffness and strength. PLA–wood fibre composites can be processed by extrusion, injection moulding, film and sheet casting, and spinning, providing access to a wide range of materials. The main drawbacks of PLA-based products are low toughness and thermal stability. Due to their inferior interface,[282] the addition of wood fibres without any treatment has negative effects on the mechanical performance. In addition, the low aspect ratio of wood fibre will reduce the strength of composites.[282] Grafting[283] and coupling[284,285] treatments of wood fibres, as aforementioned, have been reported to improve the strength of the PLA–wood fibre composites significantly. In addition, the nanoscale wood fibres without treatment have been found to have a positive reinforcement effect on the PLA matrix.[286]

1.4.3 Synthetic polymers

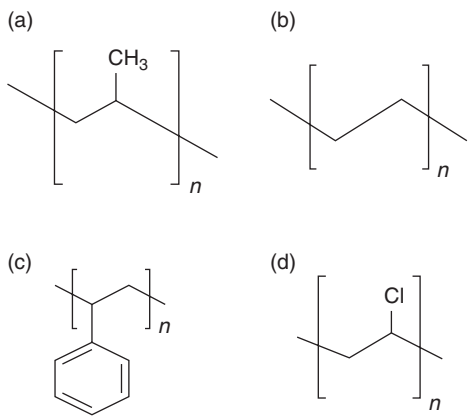
The synthetic polymers that are used as the matrix for wood fibres include thermoplastics and thermosets. Extensive research has reported the incorporation of wood fibre with various synthetic polymers. Wood–synthetic polymer composites, namely, WPCs, can be dated back to as early as 1900. Over the past 110 years, the matrices used for WPC have shifted from thermosets to thermoplastic. Currently, the raw materials for WPCs consist of a broad range of materials, from those manufactured from waste to those consisting of pulped wood and engineering resins. Formulating for the desired outcome is key for wood fibre–based composites outperforming conventional filled or reinforced products. The main applications of WPCs are decking, consumer goods, car interior parts, house-wares, construction, etc. WPCs have many inherent benefits, including consistent material quality and attractive visual appearance.

PP,[250,287–299] polyethylene (PE),[289] polystyrene (PS)[300–303] and poly(vinyl chloride) (PVC)[304–307] are the most commonly used thermoplastic matrices. The use of thermoplastic composites is diverse, ranging from automotive applications where they serve as door panels and gearshift knobs, to

© Woodhead Publishing Limited, 2014



1.7 Chemical structure of thermoset matrices: (a) polyester; (b) epoxy; (c) vinyl ester.



1.8 Chemical structure of thermoplastic matrices: (a) polypropylene; (b) polyethylene; (c) polystyrene; (d) poly(vinyl chloride).

© Woodhead Publishing Limited, 2014

Table 1.9 Advantages and disadvantages of synthetic matrices

Resin	Advantages	Disadvantages
Polyester	Tough and rigid; processed by thermoplastic operations; recycled into useful products as basis of resins in such applications as sailboats	Subject to attack by acids and bases; low thermal resistance, poor solvent resistance
Epoxy	High mechanical and thermal properties; high water resistance; long working times available; temperature resistance; low cure shrinkage	More expensive than vinylesters, critical mixing, corrosive handling
Vinyl ester	Very high chemical and environmental resistance; higher mechanical properties than polyester	Postcure generally required for high properties; high styrene content, higher cost than polyester; high cure shrinkage
Polypropylene	Low cost, low coefficient of friction; excellent flexural, impact strength; excellent moisture fatigue and chemical resistance	High thermal expansion; UV degradation; poor weathering resistance; flammable
Polyethylene	Lightweight; resistance to stain and organic solvents; low moisture absorption; resistance to electrolytic attack; good fatigue and wear resistance; excellent stress and crack resistance	High thermal expansion; poor weathering resistance; subject to stress cracking; difficult to bond; flammable; poor temperature capability; low strength/ stiffness
Polystyrene	Low cost; non-hygroscopic; good optical clarity; easily processed; good thermal stability; good property retention; good creep resistance; easily decorated; easily bonded; good toughness	Thick sooty smoke Poor weatherability Highly flammable Highly notch sensitive Poor resistance to petroleum solvents
poly(vinyl chloride)	Relatively inexpensive; very compatible with additive and plasticizers; good weatherability can be made to be extremely flexible; easy to decorate; excellent abrasion, cut through, and solder resistance; heat shrinkable; flame retardant; lightweight compared with steel alternatives; good insulator	Hydrochloric gas can be formed when burned; not good for food packaging because of; plasticizer leakage; non-biodegradable; unable to use in Europe (banned); can be highly reactive when mixed with acetal

© Woodhead Publishing Limited, 2014

building materials where they have been successfully used as decking and window framing. Polyester,[308–310] epoxy[82] and vinyl esters (VE)[311] are used as the thermoset matrices. The main chemical structures, advantages and disadvantages of each of these matrices are given in Figs 1.7, 1.8 and Table 1.9 respectively. The thermoset matrix-based composites include furniture, housing panels, doors and windows, ceilings, flooring, household articles, containers, mechanical components and corrugated boards.

1.5 Process techniques of wood fibre composites

The processing of wood fibre composites has a crucial influence on the properties of the final products. Generally, the selection of process techniques is based on the matrices, the feed form of the raw ingredients, final product (e.g. form, application) and costs.

The processes of compression,[45,312–316] extrusion[289,293,294,296,306,317–319] and injection moulding[291,313,315,320–322] have been used for the inorganic compound, natural high polymer, thermoplastic matrices. These methods are also the most popular processes within the wood–fibre composite industries. The sheet moulding compound (SMC)[323] and resin transfer moulding (RTM)[315,324–326] are suitable for thermoset matrices.

Moisture control, along with the specific mechanical energy (SME) generated during processing, plays an important role in establishing the final composite properties. Maintaining the desired pressure and temperature throughout the component over the required period of time is the basic requirement of all composite manufacturing processes.[327] The feature of low thermal stability limits the process temperature and the matrices for natural fibre-based composites. Maintaining the critical aspect ratio of the wood fibres is essential in order to obtain the reinforcing characteristic of the fibre.

Compounding is the process of blending wood fibre with matrices. It is a critical step for the manufacture of wood fibre composites. The purpose of a compounding operation is to produce a pelletized feed stock that can be processed further, such as by injection moulding, extrusion or thermoforming. There are several types of compounding processes, including extrusion, kneading, and high-shear mixers. Manufacturing processes can be divided into open mould and closed mould. The open mould process comprises wet lay-up, bag moulding and autoclave moulding. The closed mould process comprises transfer moulding, compression moulding and injection moulding.

Another main stream of wood fibre composites is to use resins as binder for the composites, such as MDF, PB, and oriented strand boards (OSB) and hardboard (HB). The composites generally consist of over 90% wood fibre or particles, and less than 10% of resin binding systems. Random distribution

© Woodhead Publishing Limited, 2014

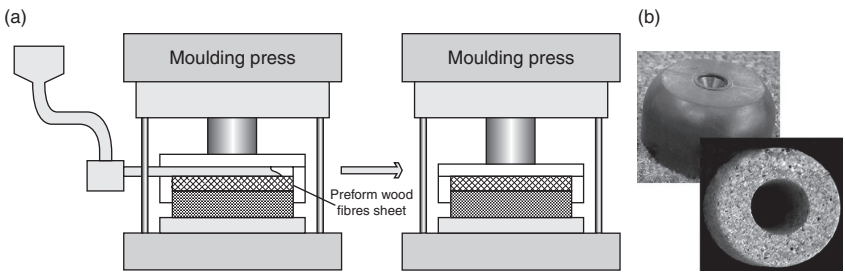
of resin over the surface of the fibre or particles governs the properties of final products. Hardboard, one of the fibreboards, can also be manufactured without any binder, using water as a medium.

1.5.1 Compression

Compression (Fig. 1.9) is a method of moulding in which the moulded material, generally preheated, is first placed in an open, heated mould cavity.[328] The compression moulding technique has proved suitable for the production of profiles with any thermoplastic and thermoset composites. The mechanical properties and dimensional stability of compression moulded composites are influenced by the design of the mould cavity, location of the charge and processing parameters, e.g. compound temperature, mould cooling or heating rate, closing speeds and the filler loading.[329] The compression method is common, popular in the manufacture of WPC. It can be connected with other processes (e.g. extrusion,[150,330,331] injection[314]) to form a new process. It also can be used as one component of the manufacturing process (e.g. SMC, bulk moulding compound (BMC)).

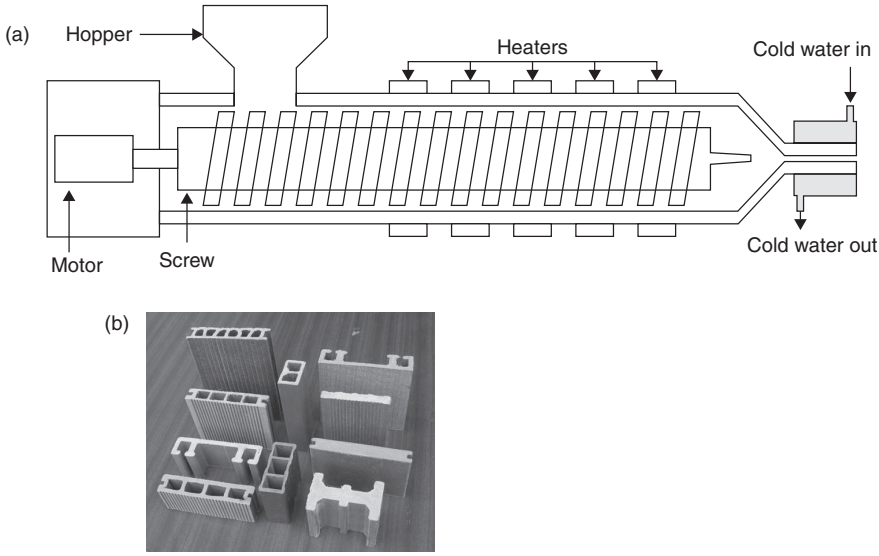
1.5.2 Extrusion

Extrusion (Fig. 1.10) is by far the most important processing method for WPC. Non-synthetic polymers, e.g. cement,[317,332] starch[289,333] and PLA,[334] can be used as the matrices in this process. It involves two types of extruders: single-screw and twin-screw. Due to the modular character[335] and other advantages (e.g. excellent compounding capability, good functional versatility) over single-screw extruders, twin-screw extruders dominate today's market for the manufacture of wood fibre composites. A suitable combination of processing variables including screw speed, screw configuration, throughput



1.9 Schematic of compression moulding (a) and compression moulded wood fibre composite products (b).

© Woodhead Publishing Limited, 2014



1.10 Schematic of extrusion moulding (a) and extrusion moulded wood fibre composite products (b).

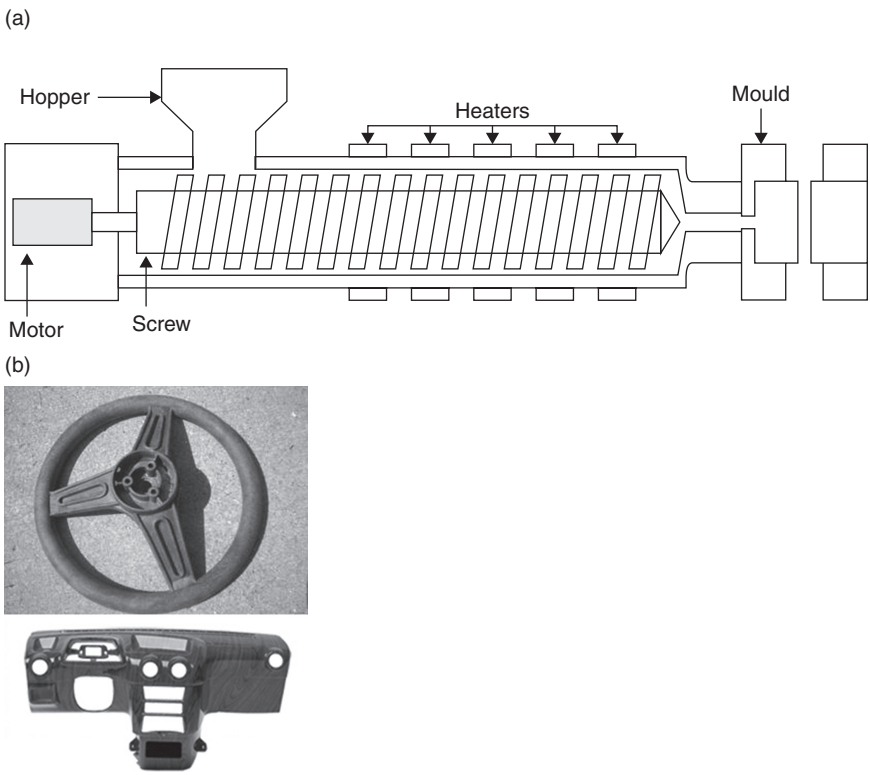
rate and barrel temperatures is necessary to limit thermal degradation and darkening of the filler.

Extrusion has overcome the shortcomings of Hatschek and other conventional processing systems of wood fibre cement, and has improved the mechanical performance. The extruded wood fibre cement products offer advantages in terms of the versatility of section profiles, end product performance characteristics, and production throughput. Wood fibres offer a desirable balance of performance and cost in this composite. A comparison between the extruded and cast fibreboard[336] reveals that the extruded products are better in terms of strength, stiffness, toughness, fibre distribution, fibre orientation, and bond of fibre with matrix, even in the presence of a higher percentage of air voids.

1.5.3 Injection moulding

Injection moulding is a versatile process accounting for nearly one-third of polymeric materials processed, particularly where intricate shapes are needed in cyclic, high volume production. The benefits include excellent dimensional tolerance and short cycle times coupled with few post-processing operations (Fig. 1.11). One of the challenges posed by injection moulding wood fire composites is to produce pellets of a consistent quality. Injection moulding requires a polymer with a low molecular weight to

© Woodhead Publishing Limited, 2014



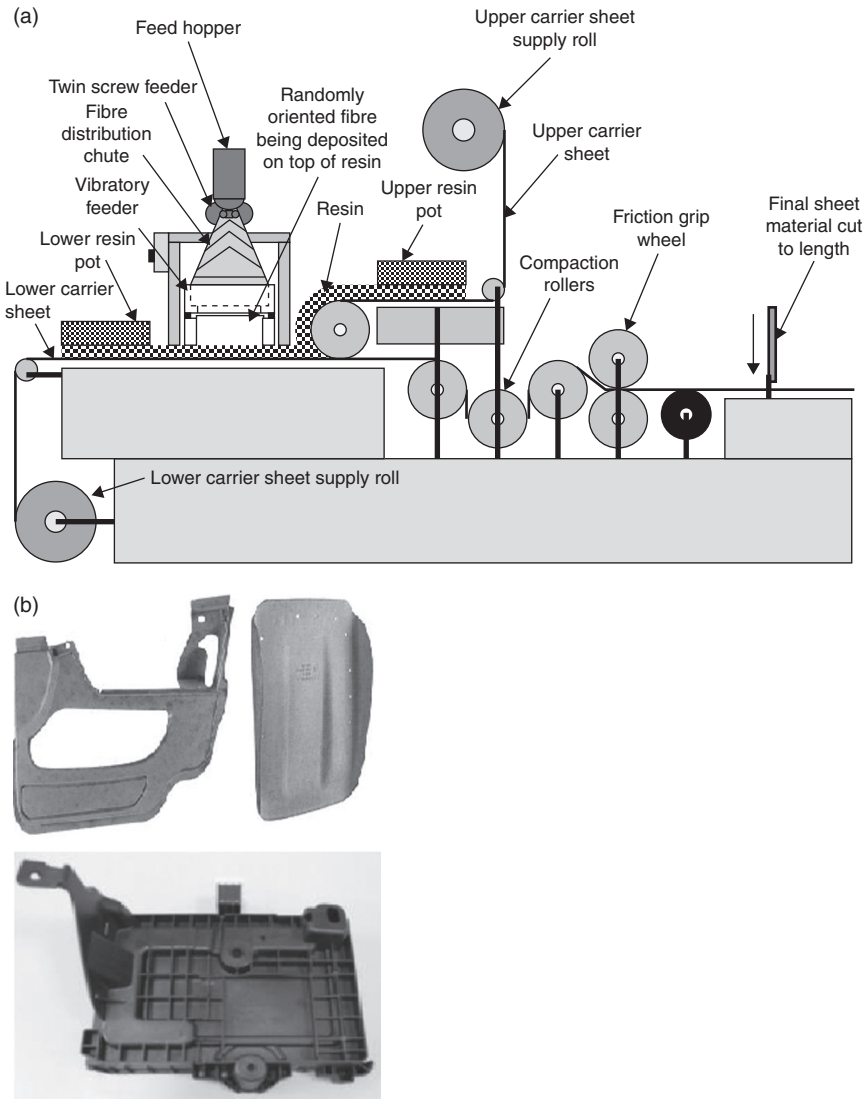
1.11 Schematic of injection moulding (a) and injection moulded wood fibre composite products (b).

maintain low viscosity. The process temperature[337] and the fibre length[338] have little influence on the mechanical properties of the composite. It has been reported that wood fibre reinforced PP composites manufactured by the injection moulding process showed better performance than those from the compression moulding process[339–342]

1.5.4 Sheet moulding compound (SMC)

SMC is produced in a two-step production process[343,344] (Fig. 1.12), which is normally used for short fibre reinforced thermoset composite. The first step is the preparation of the so-called prepreg. The prepreg must remain in a homogeneous state during flow to the extremities of the mould. The second step is the compression. The processing parameters affect the properties of the end product and are critical to ensure the uniformity of mat weight, short wood fibre content and final sheet viscosity.

© Woodhead Publishing Limited, 2014

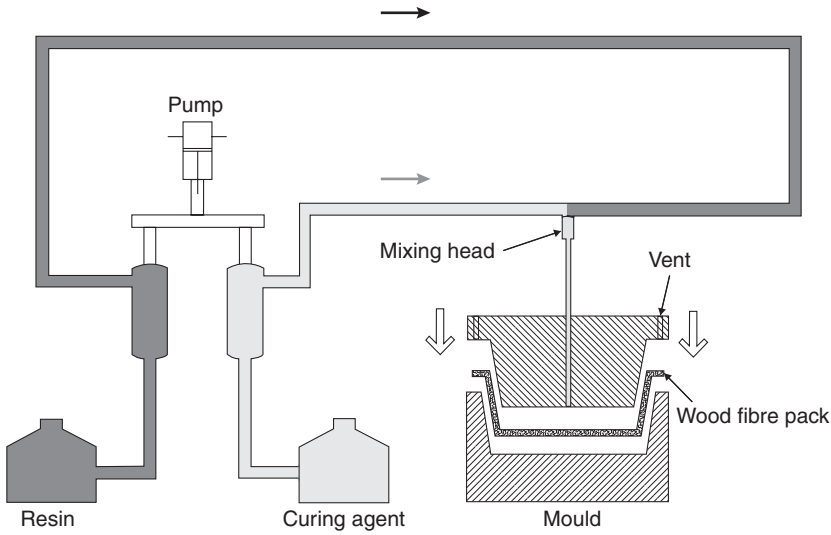


1.12 Schematic of SMC (a) and SMC moulded wood fibre composite products (b).

1.5.5 Resin transfer moulding (RTM)

RTM is a low pressure and low-temperature method of transferring a liquid thermoset resin into a closed mould, which offers a dimensionally accurate and high quality of surface finish of composite. RTM is applicable to various forms of fibre reinforcement (Fig. 1.13). RTM of natural fibre composite

© Woodhead Publishing Limited, 2014



1.13 Schematic of RTM.

could provide additional technological, economical, ecological and environmental benefits; however, there are additional influencing factors, including fibre washing, edge flow and fibre concentrations.[345] The utilization of wood fibre as a glass fibre replacement to make fibre reinforced composite under the RTM process has been reported to have a positive contribution to stiffness and strength of composites.[346]

1.6 Properties of wood fibre composites

1.6.1 Mechanical properties

Among the mechanical properties, the tensile, impact and flexural strength are the most important parameters for evaluating the performance of wood fibre composites. Various factors are found to have effects on the mechanical properties of wood fibre composite. Some of the important factors are listed in Table 1.10. The list of factors as given in Table 1.10 is not exhaustive but emphasizes the complexity of the subject. All the factors are almost equally important in influencing the properties of wood fibre composites.

1.6.2 Physical properties

One drawback of wood fibre composites, compared with other conventional inorganic fibres for composites, is the inherent susceptibility of cellulosie

© Woodhead Publishing Limited, 2014

Table 1.10 Factors affecting properties of natural fibre reinforced concretes

Factors	Constituents	Results	References
Fibre types	1. Softwood, hardwood	Softwood > hardwood	82, 347, 348
	2. Wood flour *vs* sisal	Sisal > wood flour	349
	3. TMP *vs* hemp	Hemp > TMP	350
Fibre geometry	Length (30, 300 μm)	300 μm > 30 μm	333
Processing of fibre	TMP, CTMP	TMP < CTMP	82
Fibre orientation	Isotropy, anisotropy	Isotropy > anisotropy	82
Fibre modification	1. Various coupling agents: (i) pyromellitic dianhydride (PMDA); (ii) benzophenone-3,3′,4,4′-tetracarboxylicdianhydride (BPDA); (iii) 1,4-phenylene diisocyanate (PPDI); (iv) methylene-bis-diphenyl diisocyanate (MDI); (v) γ-mercaptopropyltriethoxysilane (MRPS); (vi) γ-methacrylopropyltriethoxysilane (MPS)	(i) In CAB matrix PMDA and BPDA are the best; (ii) in rubber matrix MPS is the best	248
	2. Coupling, surfactants, benzylation	Benzylation > surfactants > coupling	351
Processing	1. Compounding (extrusion *vs* mechanical blending	Extrusion > mechanical blending	352
	2. Injection moulding *vs* compression moulding	Injection moulding > compression moulding	231, 339

fibres to moisture expansion. Due to the abundance of hydroxyl groups,[353] mainly in the amorphous regions of hemicellulose in the cell wall of the wood fibres, the fibres will swell in the presence of moisture or water. As a consequence, mechanical properties, such as stiffness and strength, are negatively influenced.[354] Lignocellulosic-fibre reinforced plastics also tend to swell considerably on water uptake, both in the plane of the composite panel and in the thickness direction, and therefore reduce the dimensional stability of the composite.[355,356] This drawback limits the application of natural fibres, and results in extra energy consumption for the fibre drying. By using chemical treatment or physical treatment, this negative influence could be reduced significantly. Another limitation of using wood fibre in fibre composite applications is its low thermal resistance and thermal degradation initiating around 200°C.[357] Therefore, most polymers used for wood fibre composites have relatively low melting temperatures. The degradation is determined by the wood species and composition.

© Woodhead Publishing Limited, 2014

Table 1.11 Comparison of the thermal insulativity of natural fibre-based materials and cement-based concrete

Material	K-value (W/mK)
Fibreglass	0.033–0.40
Sheep wool batts	0.038–0.043
Wood fibre batts	0.038–0.044
Cotton batts	0.038–0.045
Flax batts	0.042
Hemp batts	0.043
Wood fibre board	0.08
Hempcrete	0.12–0.13
Cement based concrete	0.3178

Table 1.12 Embodied energy and carbon of fibreglass, timber and wood fibre-based board

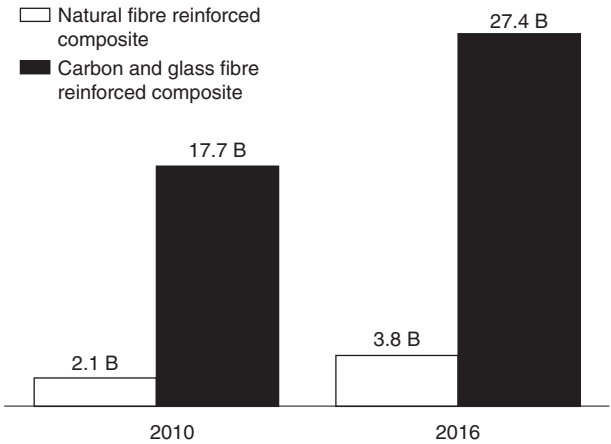
Material	Embodied energy (MJ/kg)	Embodied carbon (kgC/kg)
Fibreglass	28	0.417
Timber	8.5	0.125
Particle board	9.5	0.139
Medium fibreboard	11	0.161

However, wood fibre also displays some positive effects on the composites due to its pronounced characteristics. The fibrous shape can dissipate wave energy and convert sound energy into heat.[358,359] Wood fibre-based composites display a higher sound absorption coefficient over other fibre-based composites.[358] The excellent characteristics of low thermal conductivity and climate friendliness of wood fibres are other advantages worthy of attention for developing functional composites for specific requirements (Tables 1.11 and 1.12).[360–362]

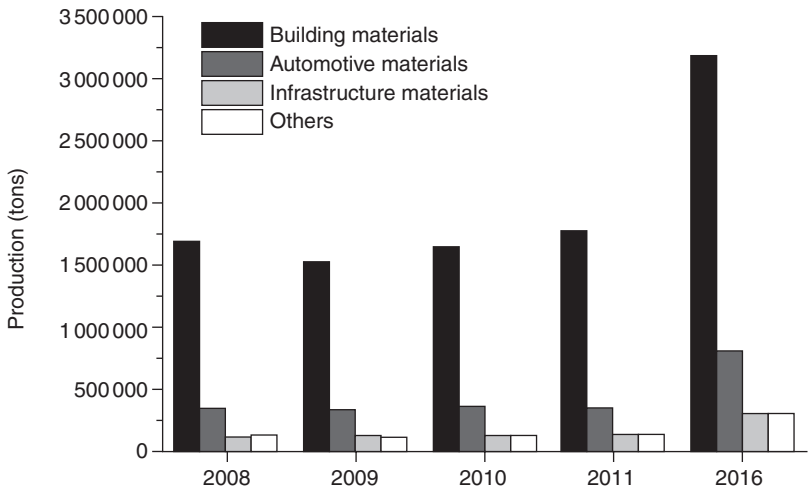
1.7 Applications of wood fibre composites

The use of wood and other natural fibres in composites is predicted to grow in future due especially to their sustainability, renewability and environmental factors. In 2010, the global natural fibre composite market reached US$2.1 B[363] (Fig. 1.14). It is estimated that the market for natural fibre composite will reach US$27.4 B in 2016.[364] It should be noted that these data exclude the wood fibreboard market, which has reached US$8.5 B.[132] Wood fibre composites have been exploited extensively in the previous century. These oldest resources are still being widely used in a large number of applications, and this is showing a robust growth rate (Fig. 1.15). Among these products, the building and automotive sectors are the main users of these materials, sharing 70.8% and 12.5% of the natural fibre composite market

© Woodhead Publishing Limited, 2014



1.14 Comparison of composite market of natural and synthetic composites (US$ billions).



1.15 Application of natural fibre composites.

respectively. As one of the natural fibres, wood fibre composites overall possess 80% of the market share of natural fibre composites (Table 1.13).

1.7.1 Wood fibre composites in building applications

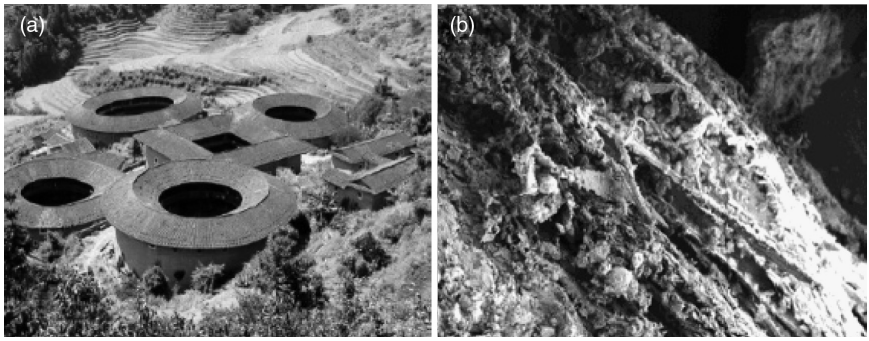
Using wood fibre composites in building has the longest history. One of the most successful examples is the Tulou building (Fig. 1.16a). Tulou buildings, built with wood fibre–clay composite, are a unique type of rural dwelling

© Woodhead Publishing Limited, 2014

© Woodhead Publishing Limited, 2014

Table 1.13 Wood fibre composites products

	Sector			
	Building	Automotive	Industrial/infrastructure	Other
End market application	Cladding; doorframes and components, ducting; fascia, soffits and barge boards; pre-finished floorboards; roofline products; shingles; stairs; window frames and components; balustrades; blinds; coving; dado rails; decorative profiles; interior panels; interior panels; kitchen cabinets; laminate flooring; sound proofing; shelving; skirting boards	Door and head liners; ducting; interior panels; rear shelves; spare tyre covers; truck floors	Handrails; industrial packaging; marine pilings/bulkheads; pallets/crates totes; piles/docks; railings; railway sleepers; rubbish bins; signage	Black piano keys, hot tubs



1.16 Wood fibre–clay composite in building: (a) Tulou; (b) scanning electron microscope (SEM) morphology of Tulou.[370]



1.17 Wood fibre–cement composites in building: (a) wall; (b) sound wall; (c) cladding; (d) house.

in south China. This wood–clay composite building has displayed excellent mechanical durability. After 1240 years, the compressive strength of walls in some Tulou still reaches up to 30.17 MPa,[365,366] due to the reinforcement of wood fibres (Fig. 1.16b). It also displays excellent environmental performance, e.g. the annual household energy consumption for this kind of building is only

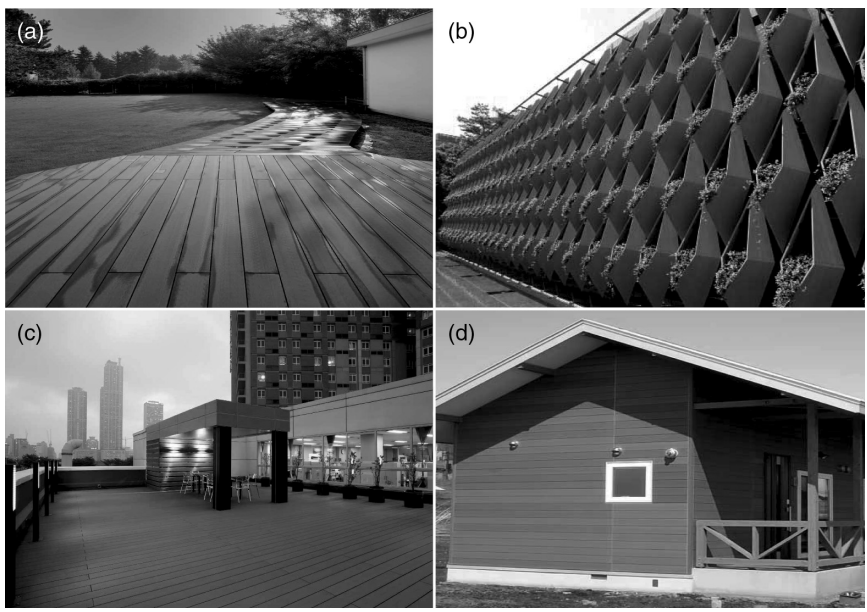
© Woodhead Publishing Limited, 2014

2.43×10^4 MJ/y, which is far lower than for other rural buildings in this region. Compared with modern building (cement building), this kind of building can make residents feel thermally comfortable.[367]

The second form of wood fibre composites is the wood fibre–cement composite, which has been used to manufacture a wide variety of products primarily for the construction industry, such as for insulating concrete forms, noise barriers, cladding and house-building (Fig. 1.17). This kind of composite is dimensionally stable when subjected to water soaking, as compared with common synthetic binder–wood fibre composites. In addition, this kind of composite presents excellent fire resistance.

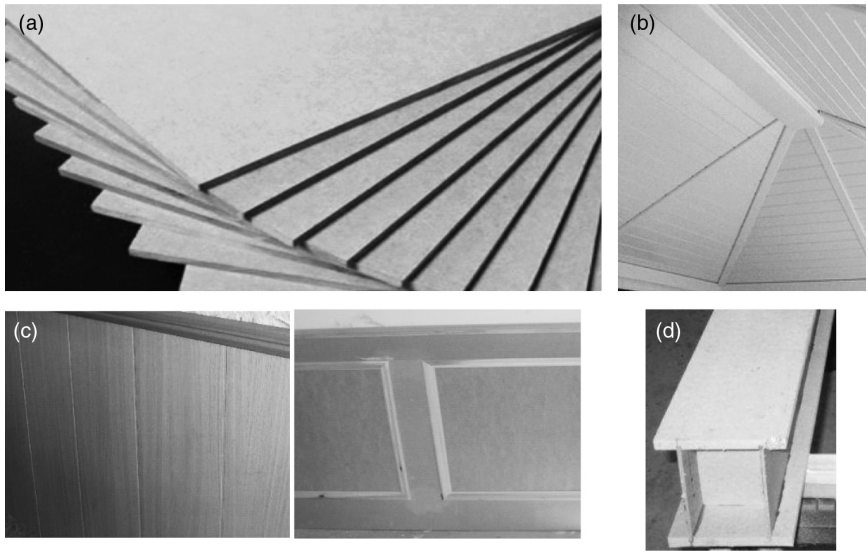
The third form of wood fibre composite is wood fibre–plastic composite. This kind of composite has the perfect natural look and feel of wood. It is generally lightweight but offers similar levels of strength and structural support as solid wood. The development of wood fibre–plastic composites exceeds that of other plastic industries since its emergence in the late 1980s. Wood fibre composites are currently undergoing a significant market expansion as a replacement for solid wood, mainly in building applications such as steps, trellises, flooring and cladding (Fig. 1.18).

The fourth type of wood fibre composite includes MDF and HB. This group of wood fibreboards is the engineered wood products formed by the



1.18 Wood fibre–plastic composites in building: (a) steps; (b) trellises; (c) wood flooring; (d) cladding.[372]

© Woodhead Publishing Limited, 2014



1.19 MDF in building construction: (a) MDF raw material; (b) roofing; (c) wall panels; (d) box beam.

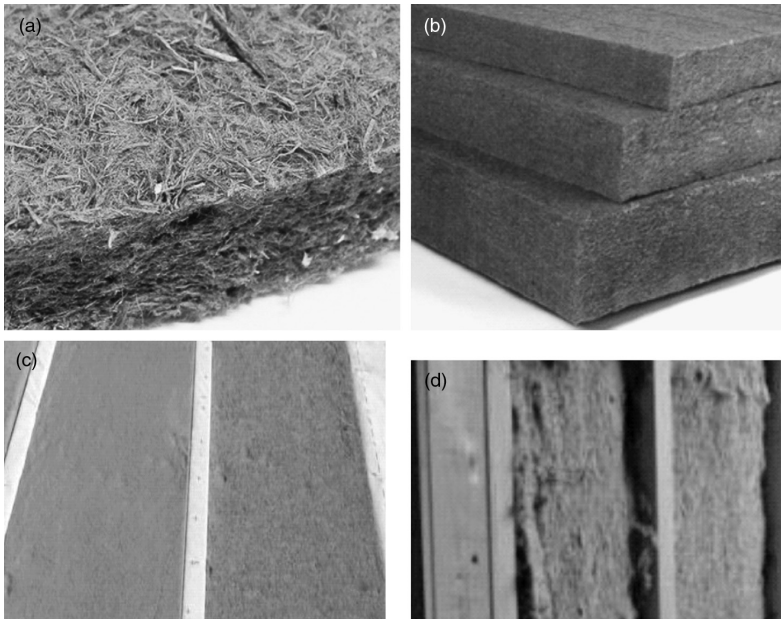
separated fibres but can be used as building materials. It is normally stronger and denser than PB. MDF has been used for building and construction over the last several decades (Fig. 1.19). MDF is ideal as a wall covering, offering better resilience to wear and tear and temperature changes than PB, plastic wall and solid wood panels. MDF may also be used for door panels, such as creating door skins which may be laminated to the whole surface and edge of an MDF board.

The fifth type of wood fibre composite is the wood fibre insulation board. These products are generally without, or with a very small amount, of resin binder added during their production. Wood fibre fabrics as insulation materials are normally loosely formatted and non-woven (Fig. 1.20). They can also sometimes be loose-filled or wet-sprayed on site. These green products can be produced by using 80% recycled newspaper, cardboard and paperboard. The products may also be treated with chemicals to obtain fire resistance or other properties. It has excellent acoustic properties and similar thermal resistance to other insulation materials, such as fibreglass.

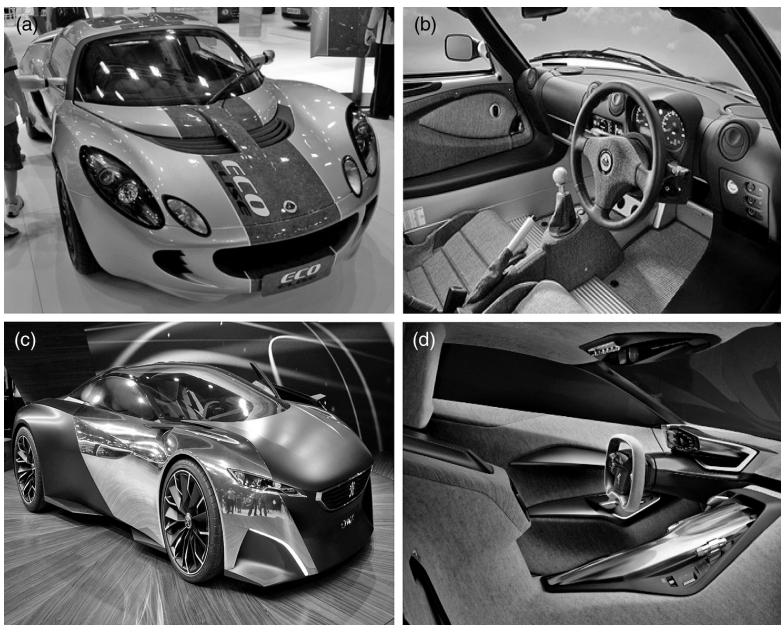
1.7.2 Wood fibre composites in automotive applications

The application of natural fibre composite can be traced back to the 1940s. In 1942, Henry Ford developed the first prototype composite car made from hemp fibre.[369] In the 1950s, the body of the East German Trabant was built

© Woodhead Publishing Limited, 2014



1.20 Wood fibre board as insulation: (a) non-woven mat; (b) softboard; (c) roofing; (d) loose wall insulation.



1.21 Natural fibre composites in automotive applications: (a) outside of hemp car; (b) inside of hemp car; (c) outside of wood car; (d) inside of wood car.

© Woodhead Publishing Limited, 2014

from composites containing natural fibres. However, owing to the development of petrochemical-based polymer, this green technology was not economical and lost its place in the automotive industry. In the 1970s, the first oil crisis revived natural fibre composites in the automotive industry. WPC was born at that time in Italy. In the 1980s, automotive door panels made from all-bio composite natural fibre and bioresin was developed. In the 1990s, Daimler-Benz pioneered the use of natural fibre in commercial vehicles as part of the 'Belem' project based in the Amazon delta in South America.[370] This application not only improved the quality of life for the individuals involved in this new application, but it also became a commercial success and ensured its continuation. At the end of 2000s, the natural fibre composite for the automotive industry had become a fashionable concept in advanced automotive design (Fig. 1.21).[371] The well-established applications of natural fibres in the automotive sector are summarized in Table 1.14.

1.7.3 Wood fibre composites in aerospace applications

Natural fibre composite is the precursor of aerospace materials. As early as the 1920s, Messrs Caldwell and Clay had employed natural fabric composite to make airscrews. In the 1930s De Bruyne developed a material known as 'Gordon-Aerolite', a composite of paper and unidirectional, unbleached flax yarn impregnated with phenolic resin and hot pressed. This material was used experimentally to produce a full-scale main wing spar for the 'Bristol Blenheim' light bomber, and for the fuselage of the 'Supermarine Spitfire' fighter aircraft.[372] After the World War II, the application of natural fibre composite in aerospace material came to a near-halt. However, at the end of the 1990s, aerospace manufacturers started to look for a lightweight and sustainable aircraft material, and as might be expected natural fibre-based composites attracted their consideration. In 2005, the resurgence of the global automotive market and the interest of leading players in the aerospace industries for sourcing natural fibre reinforced composite products and technology sparked a project on natural fibre reinforced composites, called the AMTS programme, in South Africa, to address the research problems and aiming to fulfil the technical need for structural and exterior components.[373] In 2006, researchers at the State University of New York first made real progress by using NT to create wood-based cellulose that was strong enough to strengthen plastics for aerospace application. A wood-and-sisal reinforced honeycomb core has also been developed with high mechanical performance and other functional properties for aerospace application.

1.8 Future trends

Wood fibres are low cost, lightweight, very tough and environmentally friendly compared with other traditional reinforcing materials, such as

© Woodhead Publishing Limited, 2014

Table 1.14 Vehicle manufacturers and use of natural fibre composites

Automotive manufacturer	Size	Model applications
Audi	A2, A3, A4 (and Avant), A6, A8,	Roadster, coupe, seat backs, side and back door panels, boot lining, hat rack, spare tyre lining
BMW	3, 5, 7 Series	Door panels, headliner panel, boot lining, seat backs, noise insulation panels, moulded foot well linings
Citroen	C5	Interior door panelling
Daimler-Chrysler	A, C, E and S-class models, EvoBus (exterior)	Door panels, windshield, dashboard, business table, pillar cover panel
Ford	Mondeo CD 162, Focus	Door panels, B-pillar, boot liner
Lotus	Eco Elise (July 2008)	Body panels, spoiler, seats, interior carpets
Mercedes-Benz	Trucks	Internal engine cover, engine insulation, sun visor, interior insulation, bumper, wheelbox, roof cover
Peugeot	406	Seat backs, parcel shelf
Renault	Clio, Twingo	Rear parcel shelf
Rover	2000 and others	Insulation, rear storage shelf/panel
Toyota	Brevis, Harrier, Celsior, Raum	Door panels, seat backs, Spare tyre cover
Vauxhall	Corsa, Astra, Vectra, Zafira	Headliner panel, interior door panels, pillar cover panel, instrument panel
Volkswagen	Golf, Passat, Bora	Door panel, seat back, boot lid finish panel, boot liner
Volvo	C70, V70	Seat padding, natural foams, cargo floor tray

glass fibres. Scientific work and technical application in combining wood fibres with various matrices over the previous century has culminated in the growth of new markets and industries. The major market for wood fibre composite is in building construction, and this will continue and control the building material market. The increasing acceptance in the automobile

© Woodhead Publishing Limited, 2014

industry indicates that the wood fibre reinforced composites are becoming more mature materials, and attention has been drawn to the use of wood fibre composites in aerospace materials. The main drawback of wood fibres is their weak mechanical performance when compared with glass fibre or carbon fibre. This drawback limits the application of wood fibre composite in hi-tech engineering materials, but much research has been initiated to develop enhanced products.

The science and technology of the interface betweenth wood fibre and matrix has always been an interesting and important research topic. Various modifications, such as alkali treatment, oxidation, crosslinking, grafting and coupling treatment, have been assessed and continue to be optimized.

The development of NT seems to be capable of bringing wood fibre composites to their full potential in the near future. Wood-derived nanocellulose could reach higher tensile strengths than carbon fibre. Since the first report on the superior performance of nanocellulose composite in 1995, the application of nanocellulose has been pushed into a new era and there has emerged extensive research in the application of nanocellulose. Most major governments around the world are investing heavily in nano- cellulose. In 2002, the European Commission underpinned the 'NANOFOREST' project to develop a research and development roadmap, and to recognize the newly emerging development in NT and related areas suitable for practical application in the forest products sector. In 2004, the US initiated 'NT for the Forest Products Industry – Vision and Technology Roadmap'. In 2011, Innventia opened the world's first pilot plant for the production of nanocellulose, which has a capacity of 100 kg/day. This facility makes it possible to produce nanocellulose on a large scale, which is an important step towards the industrialization of the technology, promoting the application of nanocellulose in composites and boosting the exploitation of wood resources. In 2012, Forest Product Laboratory (FPL) USA opened a pilot plant for the production of wood-derived cellulosic nanomaterials. Although the large scale production of wood nanocellulose is still on its way, a boost from a new generation of wood fibre composites will come in the next decades. It is predicted that this new material would create jobs and contribute $600B to the economy by 2020.

1.9 References

1. Bledzki AK and Gassan J. Composites reinforced with cellulose based fibres. *Progress in Polymer Science*. (1999); **24**: 221–274.
2. Mohanty AK, Misra M and Drzal LT. Natural fibers, biopolymers, and biocomposites: an introduction. In: Mohanty AK, Misra M, Drzal LT, Selke SE, Harte BR and Hinrichsen G, editors. *Natural Fibers, Biopolymers, and Biocomposites*. Boca Raton: CRC (2005). p. 3.

© Woodhead Publishing Limited, 2014

3. Lundmark R. Investment behaviour in the European pulp and paper industry. *Scandinavian Journal of Forest Research*. (2003); **18**: 184–192.
4. Shah DU, Schubel PJ, Clifford MJ and Licence P. Fatigue life evaluation of aligned plant fibre composites through S–N curves and constant-life diagrams. *Composites Science and Technology*. (2013); **74**: 139–149.
5. Bledzki AK, Sperber VE and Faruk O. *Natural and Wood Fibre Reinforcement in Polymers*. Shropshire: Smart Publications, Rapra Technology Ltd (2002).
6. Gutiérrez A and del Río JC. Chemical characterization of pitch deposits produced in the manufacturing of high-quality paper pulps from hemp fibers. *Bioresource Technology*. (2005); **96**: 1445–1450.
7. Lachenal D. Paper boards. High technicity fibrous materials. *Actualite Chimique*. (2002); **8**: 32–35.
8. Kreuger E, Sipos B, Zacchi G, Svensson S-E and Björnsson L. Bioconversion of industrial hemp to ethanol and methane: the benefits of steam pretreatment and co-production. *Bioresource Technology*. (2011); **102**: 3457–3465.
9. Ramires EC, Megiatto Jr JD, Gardrat C, Castellan A and Frollini E. Biobased composites from glyoxal–phenolic resins and sisal fibers. *Bioresource Technology*. (2010); **101**: 1998–2006.
10. http://kids.britannica.com/elementary/art-66141/Cross-section-of-a-tree-trunk.
11. http://alternative11.livejournal.com/33423.html.
12. Bigorgne L, Brunet M, Maigre H, Simon P and Chaudet P. Investigation of softwood fracture criteria at the mesoscopic scale. *International Journal of Fracture*. (2011); **172**: 65–76.
13. http://www.studyblue.com/notes/note/n/plant-phys-studying/deck/1022265.
14. Roberts JC. The chemistry of paper: Royal Society of chemistry (1996).
15. Kopač J and Šali S. Wood: an important material in manufacturing technology. *Journal of Materials Processing Technology*. (2003); **133**: 134–142.
16. Lebow ST. Interactions of ammoniacal copper zinc arsenate (ACZA) wood preservative with Douglas-fir: Oregon State University (1992).
17. Krahmer RL. Anatomical features of permeable and refractory Douglas-fir. *For Prod J*. (1961); **11**: 439–441.
18. Pulkkinen I, Ala-Kaila K and Aittamaa J. Characterization of wood fibers using fiber property distributions. *Chemical Engineering and Processing*. (2006); **45**: 546–554.
19. Panshin AJ and Zeeuw C. *Textbook of Wood Technology*. New York: McGraw-Hill Book Co. (1980).
20. Lersten NR, Krueger L and Curtis JD. Tracheoid variation among Bignoniaceae seed wings, with emphasis on Campsis radicans. *International Journal of Plant Sciences*. (2002); **163**: 369–378.
21. Kitin P, Funada R, Sano Y, Beeckman H and Ohtani J. Variations in the lengths of fusiform cambial cells and vessel elements in Kalopanax pictus. *Annals of Botany*. (1999); **84**: 621–632.
22. Gierlinger N and Schwanninger M. Chemical imaging of poplar wood cell walls by confocal Raman microscopy. *Plant Physiology*. (2006); **140**: 1246–1254.
23. Kim JS, Singh AP, Wi SG, Koch G and Kim YS. Ultrastructural characteristics of cell wall disintegration of *Pinus spp*. in the windows of an old Buddhist temple exposed to natural weathering. *International Biodeterioration & Biodegradation*. (2008); **61**: 194–198.

© Woodhead Publishing Limited, 2014

24. Nair SS, Wang S and Hurley DC. Nanoscale characterization of natural fibers and their composites using contact-resonance force microscopy. *Composites Part A-Applied Science and Manufacturing*. (2010); **41**: 624–631.
25. Fratzl P and Weinkamer R. Nature's hierarchical materials. *Progress in Materials Science*. (2007); **52**: 1263–1334.
26. Sjöström E. *Wood Chemistry: Fundamentals and Applications*. California: Academic Press (1993).
27. Hildén L, Daniel G and Johansson G. Use of a fluorescence labelled, carbohydrate-binding module from Phanerochaete chrysosporium Cel7D for studying wood cell wall ultrastructure. *Biotechnology Letters*. (2003); **25**: 553–558.
28. Scheepers GC. *Liquid Water Flow and Discolouration of Wood During Kiln Drying*. Stellenbosch: University of Stellenbosch (2006).
29. Stevanic Srndovic J. *Ultrastructure of the Primary Cell Wall of Softwood Fibres Studied Using Dynamic FT-IR Spectroscopy*: KTH, Stockholm (2008).
30. Bergander A and Salmén L. Variations in transverse fibre wall properties: relations between elastic properties and structure. *Holzforschung*. (2000); **54**: 654–660.
31. Bergander A, Brändström J, Daniel G and Sahnen L. Fibril angle variability in earlywood of Norway spruce using soft rot cavities and polarization confocal microscopy. *Journal of Wood Science*. (2002); **48**: 255–263.
32. Bardage S, Donaldson LA, Tokoh C and Daniel G. Ultrastructure of the cell wall of unbeaten Norway spruce pulp fibre surfaces: implication for pulp and paper properties. *Nordic Pulp and Paper Research Journal*. (2003); **19**: 448–452.
33. Jordan BD and O'Neill MA. The birefringence of softwood mechanical pulp fines. *Journal of Pulp and Paper Science*. (1994); **20**: J172–J174.
34. Donaldson L. Microfibril angle: measurement, variation and relationships – A review. *Iawa Journal*. (2008); **29**: 345.
35. Meier H. Chemical and morphological aspects of the fine structure of wood. *Pure and Applied Chemistry*. (1962); **5**: 37–52.
36. Donaldson LA. S3 lignin concentration in radiata pine tracheids. *Wood Science and Technology*. (1987); **21**: 227–234.
37. Salmén L. Micromechanical understanding of the cell-wall structure. *Comptes Rendus Biologies*. (2004); **327**: 873–880.
38. http://www.scidacreview.org/0905/html/biofuel.html.
39. http://www.emc.maricopa.edu/faculty/farabee/biobk/biobookchem2.html.
40. Fahlen J and Salmen L. Cross-sectional structure of the secondary wall of wood fibers as affected by processing. *Journal of Materials Science*. (2003); **38**: 119–126.
41. Whitmore FW. Lignin-carbohydrate complex formed in isolated cell walls of callus. *Phytochemistry*. (1978); **17**: 421–425.
42. Harris JM and Meylan BA. The influence of microfibril angle on longitudinal and tangential shrinkage in Pinus radiata. *Holzforschung-International Journal of the Biology, Chemistry, Physics and Technology of Wood*. (1965); **19**: 144–153.
43. Meylan BA. The influence of microfibril angle on the longitudinal shrinkage-moisture content relationship. *Wood Science and Technology*. (1972); **6**: 293–301.
44. Cave ID and Walker JCF. Stiffness of wood in fast-grown plantation softwoods: the influence of microfibril angle. *Forest Products Journal and Index*. (1994); **44**: 43–48.

© Woodhead Publishing Limited, 2014

45. Burgert I, Keckes J, Frühmann K, Fratzl P and Tschegg SE. A comparison of two techniques for wood fibre isolation – evaluation by tensile tests on single fibres with different microfibril angle. *Plant Biology*. (2002); **4**: 9–12.
46. Lahiji RR, Xu X, Reifenberger R, Raman A, Rudie A and Moon RJ. Atomic force microscopy characterization of cellulose nanocrystals. *Langmuir*. (2010); **26**: 4480–4488.
47. Dányádi L. Interfacial interactions in fiber reinforced thermoplastic composites: Phd dissertation, Budapest University of Technology and Economics (2009).
48. Spence KL, Venditti RA, Habibi Y, Rojas OJ and Pawlak JJ. The effect of chemical composition on microfibrillar cellulose films from wood pulps: mechanical processing and physical properties. *Bioresource Technology*. (2010); **101**: 5961–5968.
49. Fratzl P. Cellulose and collagen: from fibres to tissues. *Current Opinion in Colloid & Interface Science*. (2003); **8**: 32–39.
50. Fan M, Dai D and Huang B. Fourier transform infrared spectroscopy for natural fibres. In: Salih MS, editor. *Fourier Transform–Materials Analysis*: *InTech*, Rijeka, Croatia (2012). p. 45.
51. Beck-Candanedo S, Roman M and Gray DG. Effect of reaction conditions on the properties and behavior of wood cellulose nanocrystal suspensions. *Biomacromolecules*. (2005); **6**: 1048–1054.
52. Liu FP, Rials TG and Simonsen J. Relationship of wood surface energy to surface composition. *Langmuir*. (1998); **14**: 536–541.
53. Li K, Lei X, Lu L and Camm C. Surface characterization and surface modification of mechanical pulp fibers. *Pulp & Paper Canada*. (2010); **111**: 28.
54. Stamboulis A, Baillie CA and Peijs T. Effects of environmental conditions on mechanical and physical properties of flax fibers. *Composites Part A: Applied Science and Manufacturing*. (2001); **32**: 1105–1115.
55. Bismarck A, Aranberri-Askargorta I, Springer J, Lampke T, Wielage B, Stamboulis, A Shenderovich I and Limbach HH. Surface characterization of flax, hemp and cellulose fibers; Surface properties and the water uptake behavior. *Polymer Composites*. (2002); **23**: 872–894.
56. Arbelaiz A, Cantero G, Fernandez B, Mondragon I, Ganan P and Kenny JM. Flax fiber surface modifications: effects on fiber physico mechanical and flax/polypropylene interface properties. *Polymer Composites*. (2005); **26**: 324–332.
57. Baltazar-y-Jimenez A and Bismarck A. Wetting behaviour, moisture up-take and electrokinetic properties of lignocellulosic fibres. *Cellulose*. (2007); **14**: 115–127.
58. Park J-M, Quang ST, Hwang B-S and DeVries KL. Interfacial evaluation of modified Jute and Hemp fibers/polypropylene (PP)-maleic anhydride polypropylene copolymers (PP-MAPP) composites using micromechanical technique and nondestructive acoustic emission. *Composites Science and Technology*. (2006); **66**: 2686–2699.
59. Cordeiro N, Gouveia C, Moraes AGO and Amico SC. Natural fibers characterization by inverse gas chromatography. *Carbohydrate Polymers*. (2011); **84**: 110–117.
60. Bismarck A, Mohanty AK, Aranberri-Askargorta I, Czapla S, Misra M, Hinrichsen G and Springer J. Surface characterization of natural fibers; surface properties and the water up-take behavior of modified sisal and coir fibers. *Green Chemistry*. (2001); **3**: 100–107.
61. Jacob PN and Berg JC. Acid-base surface energy characterization of microcrystalline cellulose and two wood pulp fiber types using inverse gas chromatography. *Langmuir*. (1994); **10**: 3086–3093.

© Woodhead Publishing Limited, 2014

62. Di Risio S and Yan N. Adsorption and inactivation behavior of horseradish peroxidase on cellulosic fiber surfaces. *Journal of Colloid and Interface Science*. (2009); **338**: 410–419.
63. Coupas AC, Gauthier H and Gauthier R. Inverse gas chromatography as a tool to characterize ligno cellulosic fibers modified for composite applications. *Polymer Composites*. (2004); **19**: 280–286.
64. Carrasco F, Mutjé P and Pèlach MA. Refining of bleached cellulosic pulps: characterization by application of the colloidal titration technique. *Wood Science and Technology*. (1996); **30**: 227–236.
65. Belgacem MN and Gandini A. The surface modification of cellulose fibres for use as reinforcing elements in composite materials. *Composite Interfaces*. (2005); **12**: 41–75.
66. Carvalho MG, Santos JMRCA, Martins AA and Figueiredo MM. The effects of beating, web forming and sizing on the surface energy of eucalyptus globulus kraft fibres evaluated by inverse gas chromatography. *Cellulose*. (2005); **12**: 371–383.
67. Åkerholm M and Salmén L. Interactions between wood polymers studied by dynamic FT-IR spectroscopy. *Polymer*. (2001); **42**: 963–969.
68. Selig B, Hendriks C, Bardage S and Borgefors G. Segmentation of highly lignified zones in wood fiber cross-sections. *Image Analysis*. (2009); 5575: 369–378.
69. Robin JJ and Breton Y. Reinforcement of recycled polyethylene with wood fibers heat treated. *Journal of Reinforced Plastics and Composites*. (2001); **20**: 1253–1262.
70. Tranchida D, Piccarolo S, Loos J and Alexeev A. Mechanical characterization of polymers on a nanometer scale through nanoindentation. A study on pile-up and viscoelasticity. *Macromolecules*. (2007); **40**:1259–67.
72. Keller A, Leupin M, Mediavilla V and Wintermantel E. Influence of the growth stage of industrial hemp on chemical and physical properties of the fibres. *Industrial Crops and Products*. (2001); **13**: 35–48.
73. Mediavilla V, Leupin M and Keller A. Influence of the growth stage of industrial hemp on the yield formation in relation to certain fibre quality traits. *Industrial Crops and Products*. (2001); **13**: 49–56.
74. Sridhar MK, Basavarajappa G, Kasturi SG and Balasubramanian N. Evaluation of jute as a reinforcement in composites. *Indian Journal of Fibre Textile Research* (1982); **7**: 87–92.
75. Mohanty AK, Misra M and Hinrichsen G. Biofibres, biodegradable polymers and biocomposites: an overview. *Macromolecular Materials and Engineering*. (2000); **276–277**: 1–24.
76. Charlet K, Jernot J-P, Breard J and Gomina M. Scattering of morphological and mechanical properties of flax fibres. *Industrial Crops and Products*. (2010); **32**: 220–224.
77. Wambua P, Ivens J and Verpoest I. Natural fibres: can they replace glass in fibre reinforced plastics? *Composites Science and Technology*. (2003); **63**: 1259–1264.
78. Korte S. *Processing-Property Relationships of Hemp Fibre*. University of Canterbury, Canterbury (2006).
79. Mohanty AK, Misra M and Drzal LT. *Natural Fibers, Biopolymers, and Biocomposites*: CRC Press Taylor & Francis Group, Boca Roton (2005).
80. Neagu R, Gamstedt E and Lindström M. Characterization methods for elastic properties of wood fibers from mats for composite materials. *Wood and Fiber Science*. (2006); **38**: 95–111.

© Woodhead Publishing Limited, 2014

81. Mott L, Groom L and Shaler S. Mechanical properties of individual southern pine fibers. Part II. Comparison of earlywood and latewood fibers with respect to tree height and juvenility. *Wood and Fiber Science*. (2002); **34**: 221–237.
82. Neagu RC, Gamstedt EK and Berthold F. Stiffness contribution of various wood fibers to composite materials. *Journal of Composite Materials*. (2006); **40**: 663–699.
83. Biagiotti J, Puglia D, Torre L, Kenny JM, Arbelaiz A, Cantero G, Marieta C, Llano-Ponte R and Mondragon I. A systematic investigation on the influence of the chemical treatment of natural fibers on the properties of their polymer matrix composites. *Polymer Composites*. (2004); **25**: 470–479.
84. Placet V. Characterization of the thermo-mechanical behaviour of Hemp fibres intended for the manufacturing of high performance composites. *Composites Part A: Applied Science and Manufacturing*. (2009); **40**: 1111–1118.
85. Silva FdA, Chawla N and de Toledo Filho RD. Tensile behavior of high performance natural (sisal) fibers. *Composites Science and Technology*. (2008); **68**: 3438–3443.
86. Kulkarni AG, Satyanarayana KG and Rohatgi PK. Weibull analysis of strengths of coir fibres. *Fibre Science and Technology*. (1983); **19**:59–76.
87. Travitzky N, Windsheimer H, Fey T and Greil P. Preceramic paper-derived ceramics. *Journal of the American Ceramic Society*. (2008); **91**: 3477–3492.
88. Gurvich MR, Dibenedetto AT and Pegoretti A. Evaluation of the statistical parameters of a Weibull distribution. *Journal of Materials Science*. (1997); **32**: 3711–3716.
89. Sglavo VM, Prezzi A and Zandonella T. Engineered stress-profile silicate glass: high strength material insensitive to surface defects and fatigue. *Advanced Engineering Materials*. (2004); **6**: 344–349.
90. Wagner HD, Phoenix SL and Schwartz P. A study of statistical variability in the strength of single aramid filaments. *Journal of Composite Materials*. (1984); **18**: 312–338.
91. Eder M, Arnould O, Dunlop JWC, Hornatowska J and Salmén L. Experimental micromechanical characterisation of wood cell walls. *Wood Science and Technology*. (2012); **47**: 1–20.
92. Jayne BA. Mechanical properties of wood fibers. *Tappi*. (1959); **42**: 461–467.
93. Wimmer R, Lucas BN, Oliver WC and Tsui TY. Longitudinal hardness and Young's modulus of spruce tracheid secondary walls using nanoindentation technique. *Wood Science and Technology*. (1997); **31**: 131–141.
94. Adusumalli R-B, Mook W, Passas R, Schwaller P and Michler J. Nanoindentation of single pulp fibre cell walls. *Journal of Materials Science*. (2010); **45**: 2558–2563.
95. de Borst K, Bader TK and Wikete C. Microstructure–stiffness relationships of ten European and tropical hardwood species. *Journal of Structural Biology*. (2012); **177**: 532–542.
96. Jäger A, Bader T, Hofstetter K and Eberhardsteiner J. The relation between indentation modulus, microfibril angle, and elastic properties of wood cell walls. *Composites Part A: Applied Science and Manufacturing*. (2011); **42**: 677–685.
97. Jäger A, Hofstetter K, Buksnowitz C, Gindl-Altmutter W and Konnerth J. Identification of stiffness tensor components of wood cell walls by means of nanoindentation. *Composites Part A: Applied Science and Manufacturing*. (2011); **42**: 2101–2109.

© Woodhead Publishing Limited, 2014

98. Obersriebnig M, Konnerth J and Gindl-Altmutter W. Evaluating fundamental position-dependent differences in wood cell wall adhesion using nanoindentation. *International Journal of Adhesion and Adhesives*. (2013); **40**: 129–134.
99. Gindl W, Gupta HS and Grünwald C. Lignification of spruce tracheid secondary cell walls related to longitudinal hardness and modulus of elasticity using nano-indentation. *Canadian Journal of Botany*. (2002); **80**: 1029–1033.
100. Gindl W and Gupta HS. Cell-wall hardness and Young's modulus of melamine-modified spruce wood by nano-indentation. *Composites Part A: Applied Science and Manufacturing*. (2002); **33**: 1141–1145.
101. Tze WTY, Wang S, Rials TG, Pharr GM and Kelley SS. Nanoindentation of wood cell walls: continuous stiffness and hardness measurements. *Composites Part A: Applied Science and Manufacturing*. (2007); **38**: 945–953.
102. Yan D and Li K. Conformability of wood fiber surface determined by AFM indentation. *Journal of Materials Science*. (2013); **48**: 322–331.
103. Nimz HH and Casten R. Chemical processing of lignocellulosics. *European Journal of Wood and Wood Products*. (1986); **44**: 207–212.
104. Tanbda H, Nakano J, Hosoya S and Chang HM. Stability of α-ether type model compounds during chemical pulping processes. *Journal of Wood Chemistry and Technology*. (1987); **7**: 485–497.
105. Fardim P and Duran N. Surface chemistry of eucalyptus wood pulp fibres: effects of chemical pulping. *Holzforschung*. (2002); **56**: 615–622.
106. Rudie AW, Morra J, St Laurent JM and Hickey KL. The influence of wood and fiber properties in mechanical pulping. *Tappi Journal* (1993); **77**: 86–90.
107. Ekman R and Holmbom B. Analysis by gas chromatography of the wood extractives in pulp and water samples from mechanical pulping of spruce. *Nordic Pulp and Paper Research Journal*. (1989); **4**: 16–24.
108. Michell AJ, Chin CWJ and Nelson PJ. Bleaching and yellowing of eucalypt chemimechanical pulps. Diffuse reflectance spectra of oxygen bleached pulps. *Appita*. (1991); **44**: 333–336.
109. Stationwala MI. Production of high quality and low energy chemithermomechanical pulp. *Tappi Journal*;(United States). (1994); **77:** 113–119.
110. Myers GC, Barbour RJ and AbuBakr SM. *Small-diameter trees used for chemithermomechanical pulps*. US Department of Agriculture, Forest Service, Forest Products Laboratory, 2003.
111. Akhtar M, Scott GM, Swaney RE and Kirk TK. Overview of biomechanical and biochemical pulping research. In: Karl-Erik LE and Artur CP (eds). "*Enzyme Applications in Fiber Processing*" ACS Publications, Washington (1998). pp. 15–26.
112. Alén R. Basic chemistry of wood delignification. *Forest Products Chemistry*. (2000): 59–104.
113. Lisboa SA, Evtuguin DV, Neto CP and Goodfellow BJ. Isolation and structural characterization of polysaccharides dissolved in *Eucalyptus globulus* kraft black liquors. *Carbohydrate Polymers*. (2005); **60**: 77–85.
114. Ibarra D, Camarero S, Romero J, Martínez MJ and Martínez AT. Integrating laccase–mediator treatment into an industrial-type sequence for totally chlorine-free bleaching of eucalypt kraft pulp. *Journal of Chemical Technology & Biotechnology*. (2006); **81**: 1159–1165.
115. Ristolainen M and Alén R. Carbohydrates from chemical pulps: characterization by capillary zone electrophoresis. *Encyclopedia of Analytical Chemistry*. (2006).

© Woodhead Publishing Limited, 2014

116. Naithani V, Lindström M, Kirkman H and Jameel H. Effect of sulfite, sulfide and hydroxide concentrations in mini sulfide sulfite AQ pulping. Tappi engineering, pulping, and environmental conference (2007).
117. Hemmasi AH. Manufacturing paper sheets from olive wood by soda, sulphite and kraft pulping. *World Applied Sciences Journal*. (2012); **18**: 510–513.
118. SÁNchez R, Rodríguez A, Requejo A, García A and Jiménez L. Chemical and thermogravimetric analysis and soda and organosolv pulping of Hesperaloe funifera. (2010).
119. Axelsson A. Fibre based models for predicting tensile strength of paper: Master's Thesis. Lulea (Sweden): Lulea University of Technology (2009).
120. McGovern JN and Wegner TH. Papermaking properties of aspen ultrahigh-yield mechanical pulps. *Tappi Journal*. (1991); **74**: 157–161.
121. Scott GM and Akhtar M. Biotechnological Applications of Lignin-Degrading Fungi (White-Rot Fungi). Biopolymers Online. (2001).
122. http://www.fao.org/docrep/005/V9933E/V9933E03.htm.
123. Chandra RP. *Improving the brightness and bleachability of douglas-fir mechanical pulps using white-rot fungi and laccase enzymes*. Columbia: University of British (1999).
124. Sabourin MJ and Hart PW. Enhanced fiber quality of black spruce (Picea mariana) thermomechanical pulp fiber through selective enzyme application. *Industrial & Engineering Chemistry Research*. (2010); **49**: 5945–5951.
125. Walter K. Influence of acid hydrogen peroxide treatment on refining energy and TMP properties: Mid Sweden University (2009).
126. Area MC, Felissia FE, Venica AD and Valade JL. NSSC process optimization: II. Spent liquors. Tappi pulping conference: TAPPI PRESS; (1998). pp. 683–690.
127. Ahmadi M, Latibari AJ, Faezipour M and Hedjazi S. Neutral sulfite semi-chemical pulping of rapeseed residues. *Turkish J Agric Forest*. (2010); **34**: 11–16.
128. Area MC, Felissia FE, Venica A and Valade JL. NSSC process optimization: I. Pulps quality. Tappi pulping conference: TAPPI PRESS; (1998). pp. 671–682.
129. Badar S and Farooqi IH. Pulp and Paper Industry—Manufacturing Process, Wastewater Generation and Treatment. Environmental Protection Strategies for Sustainable Development. (2012): 397–436.
130. Mohanty AK, Misra M and Drzal LT. Natural fibers, biopolymers, and biocomposites: an introduction. In: Mohanty AK, Misra M, Drzal LT, Selke SE, Harte BR and Hinrichsen G, editors. *Natural Fibers, Biopolymers, and Biocomposites*. CRC: Boca Raton (2005). p. 1.
131. Yuan H, Zhou P and Zhou D. What is low-carbon development? A conceptual analysis. *Energy Procedia*. (2011); **5**: 1706–1712.
132. http://faostat3.fao.org/home/index.html#SEARCH_DATA.
133. Ray PK, Chakravarty AC and Bandyopadhaya SB. Fine structure and mechanical properties of jute differently dried after retting. *Journal of Applied Polymer Science*. (1976); **20**: 1765–1767.
134. Da Cunha C, Deffieux A and Fontanille M. Synthesis and polymerization of lignin-based macromonomers. III. Radical copolymerization of lignin-based macromonomers with methyl methacrylate. *Journal of Applied Polymer Science*. (1993); **48**: 819–831.
135. Semsarzadeh MA. Fiber matrix interactions in jute reinforced polyester resin. *Polymer Composites*. (1986); **7**: 23–25.

© Woodhead Publishing Limited, 2014

136. Bisanda ETN and Ansell MP. The effect of silane treatment on the mechanical and physical properties of sisal-epoxy composites. *Composites Science and Technology*. (1991); **41**: 165–178.
137. Haig Zeronian S, Kawabata H and Alger KW. Factors affecting the tensile properties of nonmercerized and mercerized cotton fibers. *Textile Research Journal*. (1990); **60**: 179–183.
138. Brett CT and Waldron K. *Physiology and Biochemistry of Plant Cell Walls*. London: Chapman & Hall (1996).
139. Tomek A. Heat Treatment of Wood Chips, a New Process for Making Particle Board Water Repellent. Holz Technology. (1966); **7**: 157–160.
140. Garcia RA, Cloutier A and Riedl B. Dimensional stability of MDF panels produced from heat-treated fibres. *Holzforschung*. (2006); **60**: 278–284.
141. Gregorova A, Hrabalova M, Kovalcik R and Wimmer R. Surface modification of spruce wood flour and effects on the dynamic fragility of PLA/wood composites. *Polymer Engineering and Science*. (2011); **51**: 143–150.
142. Ayrilmis N, Jarusombuti S, Fueangvivat V and Bauchongkol P. Effect of thermal treatment of rubberwood fibres on physical and mechanical properties of medium density fibreboard. *Journal of Tropical Forest Science*. (2011); **23**: 10–16.
143. Belgacem MN, Bataille P and Sapieha S. Effect of corona modification on the mechanical properties of polypropylene/cellulose composites. *Journal of Applied Polymer Science*. (1994); **53**: 379–385.
144. Wakida T and Tokino S. Surface modification of fibre and polymeric materials by discharge treatment and its application to textile processing. *Indian Journal of Fibre and Textile Research*. (1996); **21**: 69–78.
145. Wong KK, Tao XM, Yuen CWM and Yeung KW. Topographical study of low temperature plasma treated flax fibers. *Textile Research Journal*. (2000); **70**: 886–893.
146. Lee SG, Choi SS, Park WH and Cho DW. Characterization of surface modified flax fibers and their biocomposites with PHB. *Macromolecular Symposia*. (2003); **197**: 89–99.
147. Martin AR, Manolache S, Denes FS and Mattoso LHC. Functionalization of sisal fibers and high-density polyethylene by cold plasma treatment. *Journal of Applied Polymer Science*. (2002); **85**: 2145–2154.
148. Molina R, Jovančić P, Jocić D, Bertran E and Erra P. Surface characterization of keratin fibres treated by water vapour plasma. *Surface and Interface Analysis*. (2003); **35**: 128–135.
149. http://onlyhdwallpapers.com/abstract/plasma-ball-desktop-hd-wallpaper-23751/.
150. Ragoubi M, Bienaimé D, Molina S, George B and Merlin A. Impact of corona treated hemp fibres onto mechanical properties of polypropylene composites made thereof. *Industrial Crops and Products*. (2010); **31**: 344–349.
151. Song Z, Tang J, Li J and Xiao H. Plasma-induced polymerization for enhancing paper hydrophobicity. *Carbohydrate Polymers*. (2013); **92**: 928–933.
152. Odrášková M, Ráhel' J, Zahoranová A, Tiňo R and Černák M. Plasma activation of wood surface by diffuse coplanar surface barrier discharge. *Plasma Chemistry and Plasma Processing*. (2008); **28**: 203–211.
153. Sawatari A and Nakamura H. Analysis of the functional groups formed on the corona-treated cellulose fibre sheet surface by means of chemical modification in liquid phase-ESCA technique. *Sen'i Gakkaishi*. (1993); **49**: 279–286.

© Woodhead Publishing Limited, 2014

154. Zanini S, Canevali C, Orlandi M, Tolppa E-L, Zoia L, Riccardi C *et al*. Radical formation on CTMP fibers by argon plasma treatments and related lignin chemical changes. *Bioresources*. (2008); **3**: 995–1009.
155. Zanini S, Riccardi C, Canevali C, Orlandi M, Zoia L and Tolppa EL. Modifications of lignocellulosic fibers by Ar plasma treatments in comparison with biological treatments. *Surface and Coatings Technology*. (2005); **200**: 556–560.
156. Carlsson G, Ström G and Annergren G. Waters sorption and surface composition of untreated or oxygen plasma-treated chemical pulps [manuscripts dedicated to Professor Lennart Stockman-75 years]. *Nordic Pulp and Paper Research Journal*. (1995); **10**.
157. Carlsson CMG and Stroem G. *Reduction and oxidation of cellulose surfaces by means of cold plasma. Langmuir*. (1991); **7**: 2492–2497.
158. http://en.wikipedia.org/wiki/Mercerization.
159. Klemm D and Heinze T. *Comprehensive cellulose chemistry: Fundamental and Analytical Methods, Volume 1*. Weinheim: Wiley-VCH (1998).
160. Ganan P, Garbizu S, Llano-Ponte R and Mondragon I. Surface modification of sisal fibers: effects on the mechanical and thermal properties of their epoxy composites. *Polymer Composites*. (2005); **26**: 121–127.
161. Ray D, Sarkar BK and Bose NR. Impact fatigue behaviour of vinylester resin matrix composites reinforced with alkali treated jute fibres. *Composites Part A: Applied Science and Manufacturing*. (2002); **33**: 233–241.
162. de Albuquerque AC, Joseph K, Hecker de Carvalho L and d'Almeida JRM. Effect of wettability and ageing conditions on the physical and mechanical properties of uniaxially oriented jute-roving-reinforced polyester composites. *Composites Science and Technology*. (2000); **60**: 833–844.
163. Okano T and Sarko A. Mercerization of cellulose. I. X-ray diffraction evidence for intermediate structures. *Journal of Applied Polymer Science*. (1984); **29**: 4175–4182.
164. Okano T and Sarko A. Mercerization of cellulose. II. Alkali–cellulose intermediates and a possible mercerization mechanism. *Journal of Applied Polymer Science*. (1985); **30**: 325–332.
165. Nishimura H and Sarko A. Mercerization of cellulose. III. Changes in crystallite sizes. *Journal of Applied Polymer Science*. (1987); **33**: 855–866.
166. Oh SY, Yoo DI, Shin Y, Kim HC, Kim HY, Chung YS, Park WH and Youk JH. Crystalline structure analysis of cellulose treated with sodium hydroxide and carbon dioxide by means of X-ray diffraction and FTIR spectroscopy. *Carbohydrate Research*. (2005); **340**: 2376–2391.
167. Rodriguez ES, Stefani PM and Vazquez A. Effects of fibers' alkali treatment on the resin transfer molding processing and mechanical properties of jute—vinylester composites. *Journal of Composite Materials*. (2007); **41**: 1729–1741.
168. Saha P, Manna S, Chowdhury SR, Sen R, Roy D and Adhikari B. Enhancement of tensile strength of lignocellulosic jute fibers by alkali-steam treatment. *Bioresource Technology*. (2010); **101**: 3182–3187.
169. Ichazo MN, Albano C, Gonzalez J, Perera R and Candal MV. Polypropylene/wood flour composites: treatments and properties. *Composite Structures*. (2001); **54**: 207–214.
170. Borysiak S. Supermolecular structure of wood/polypropylene composites: I. The influence of processing parameters and chemical treatment of the filler. *Polymer Bulletin*. (2010); **64**: 275–290.

© Woodhead Publishing Limited, 2014

171. Alberto MM, Mougel E and Zoulalian A. Compatibility of some tropical hardwoods species with Portland cement using isothermal calorimetry. *Forest Products Journal*. (2000); **50**: 83–88.
172. Govin A, Peschard A, Fredon E and Guyonnet R. New insights into wood and cement interaction. *Holzforschung*. (2005); **59**: 330–335.
173. Yackel EC and Kenyon WO. Preparation of oxycellulose. US1941.
174. Nabar GM and Padmanabhan CV. Studies in oxycellulose. Part III. Oxidation of cellulose with a mixture of nitrogen dioxide and oxygen. *Proceedings Mathematical Sciences*. (1950); **32**: 212–231.
175. Colvin JR. Oxidation of cellulose microfibril segments by alkaline silver nitrate and its relation to the fine structure of cellulose. *Journal of Applied Polymer Science*. (1964); **8**: 2763–2774.
176. Shenai VA and Singh OP. Studies in accelerated oxidation of cellulose. I – Hypochlorite oxidation of cellulose in presence of manganous hydroxide. *Journal of the Society of Dyers and Colourists*. (1971); **87**: 228–231.
177. Arendt JH, Carrière JP, Bouchez P and Sachetto JP. Oxidation of cellulose by acid-sodium nitrite systems. *Journal of Polymer Science: Polymer Symposia*. (1973); **42**: 1521–1529.
178. Heinze T, Klemm D, Loth F and Nehls I. Sphärische ionotrope gele carboxygruppenhaltiger cellulosederivate als trägermaterialien für biologische wirkstoffe, IV. Synthese von carboxycellulose und ionotrope gelbildung mit calciumionen. *Die Angewandte Makromolekulare Chemie*. (1990); **178**: 95–107.
179. Schnabelrauch M, Heinze T, Klemm D, Nehis I and Kötz J. Investigations on synthesis and characterization of carboxy-groups containing cellulose sulfates. *Polymer Bulletin*. (1991); **27**: 147–153.
180. Isogai A and Kato Y. Preparation of polyuronic acid from cellulose by TEMPO-mediated oxidation. *Cellulose*. (1998); **5**: 153–164.
181. Hirota M, Tamura N, Saito T and Isogai A. Surface carboxylation of porous regenerated cellulose beads by 4-acetamide-TEMPO/NaClO/$NaClO_2$ system. *Cellulose*. (2009); **16**: 841–851.
182. Toda T. Graft copolymerization to cellulose by sodium periodate. *Journal of Polymer Science*. (1962); **58**: 411–427.
183. Sihtola H. Chemical properties of modified celluloses. *Die Makromolekulare Chemie*. (1960); **35**: 250–265.
184. Rowland SP and Cousins ER. Periodate oxidative decrystallization of cotton cellulose. *Journal of Polymer Science Part A-1: Polymer Chemistry*. (1966); **4**: 793–799.
185. Kangle PJ and Nabar GM. Studies in chemically modified celluloses. I. Oxidative susceptibility of chemically, modified cellulose. *Journal of Applied Polymer Science*. (1969); **13**: 323–336.
186. Morooka T, Norimoto M and Yamada T. Periodate oxidation of cellulose by homogeneous reaction. *Journal of Applied Polymer Science*. (1989); **38**: 849–858.
187. Shibata I, Yanagisawa M, Saito T and Isogai A. SEC-MALS analysis of cellouronic acid prepared from regenerated cellulose by TEMPO-mediated oxidation. *Cellulose*. (2006); **13**: 73–80.
188. Saito T and Isogai A. Introduction of aldehyde groups on surfaces of native cellulose fibers by TEMPO-mediated oxidation. *Colloids and Surfaces A: Physicochemical and Engineering Aspects*. (2006; **289**: 219–225.

© Woodhead Publishing Limited, 2014

189. Saito T, Okita Y, Nge TT, Sugiyama J and Isogai A. TEMPO-mediated oxidation of native cellulose: microscopic analysis of fibrous fractions in the oxidized products. *Carbohydrate Polymers*. (2006); **65**: 435–440.
190. DiFlavio J-L, Pelton R, Leduc M, Champ S, Essig M and Frechen T. The role of mild TEMPO–NaBr–NaClO oxidation on the wet adhesion of regenerated cellulose membranes with polyvinylamine. *Cellulose*. (2007); **14**: 257–268.
191. Isogai T, Yanagisawa M and Isogai A. Degrees of polymerization (DP) and DP distribution of cellouronic acids prepared from alkali-treated celluloses and ball-milled native celluloses by TEMPO-mediated oxidation. *Cellulose*. (2009); **16**: 117–127.
192. Johnson R, Zink-Sharp A, Renneckar S and Glasser W. A new bio-based nanocomposite: fibrillated TEMPO-oxidized celluloses in hydroxypropylcellulose matrix. *Cellulose*. (2009); **16**: 227–238.
193. Fujisawa S, Isogai T and Isogai A. Temperature and pH stability of cellouronic acid. *Cellulose*. (2010); **17**: 607–615.
194. Hirota M, Tamura N, Saito T and Isogai A. Oxidation of regenerated cellulose with NaClO2 catalyzed by TEMPO and NaClO under acid-neutral conditions. *Carbohydrate Polymers*. (2009); **78**: 330–335.
195. Praskalo J, Kostic M, Potthast A, Popov G, Pejic B and Skundric P. Sorption properties of TEMPO-oxidized natural and man-made cellulose fibers. *Carbohydrate Polymers*. (2009); **77**: 791–798.
196. Xhanari K, Syverud K, Chinga-Carrasco G, Paso K and Stenius P. Reduction of water wettability of nanofibrillated cellulose by adsorption of cationic surfactants. *Cellulose*. (2011); **18**: 257–270.
197. Fukuzumi H, Saito T, Okita Y and Isogai A. Thermal stabilization of TEMPO-oxidized cellulose. *Polymer Degradation and Stability*. (2010); **95**: 1502–1508.
198. Potthast A, Kostic M and Schiehser S. Studies on oxidative modifications of cellulose by the TEMPO and periodate oxidation system. *Proceedings of Italic 4, Science and Technology of Biomass: Advances and Challenges*. Rome, May 8–10 (2007).
199. Matsui T and Yamaoka A. Ozone-oxidation of hemp and graft copolymerization of mathyl mechacrylate onto it. *Research memoirs of the Kobe Technical College* (1997); **36**: 51–55.
200. Matsui T and Yamaoka A. Graft-copolymerization of methylmethacrylate onto hamp oxidized with ozone II: effects of the graft-copolymerization on fine structures, mechanical properties and chemical resistances. *Research Memoirs of the Kobe Technical College*. (1998); **38**: 21–24.
201. Jones EW and Rayburn JA. Crosslinking of cotton cellulose with diglycidyl ether. *Journal of Applied Polymer Science*. (1961); **5**: 714–720.
202. Clingman AL and Schwenker RF. The alkane dithioether and the polysulfide crosslinking of cellulose. *Journal of Polymer Science Part C: Polymer Symposia*. (1965); **11**: 107–118.
203. Almgren KM, Gamstedt EK and Varna J. Contribution of wood fiber hygroexpansion to moisture induced thickness swelling of composite plates. *Polymer Composites*. (2010); **31**: 762–771.
204. Almgren KM, Gamstedt EK, Berthold F and Lindstrom M. Moisture uptake and hygroexpansion of wood fiber composite materials with polylactide and polypropylene matrix materials. *Polymer Composites*. (2009); **30**: 1809–1816.
205. Gupta KC, Sahoo S and Khandekar K. Graft copolymerization of ethyl acrylate onto cellulose using ceric ammonium nitrate as initiator in aqueous medium. *Biomacromolecules*. (2002); **3**: 1087–1094.

© Woodhead Publishing Limited, 2014

206. Nayak PL, Lenka S and Pati NC. Grafting vinyl monomers onto silk fibers. II. Graft copolymerization of methyl methacrylate onto silk by hexavalent chromium ion. *Journal of Applied Polymer Science.* (1979); **23**: 1345–1354.
207. Mishra S, Misra M, Tripathy SS, Nayak SK and Mohanty AK. Graft copolymerization of acrylonitrile on chemically modified sisal fibers. *Macromolecular Materials and Engineering*. (2001); **286**: 107–113.
208. Sameni JK, Ahmad SH and Zakaria S. Performance of rubberwood fiber-thermoplastic natural rubber composites. *Polymer-Plastics Technology and Engineering*. (2003); **42**: 139–152.
209. Geng Y, Li K and Simonsen J. Effects of a new compatibilizer system on the flexural properties of wood-polyethylene composites. *Journal of Applied Polymer Science*. (2004); **91**: 3667–3672.
210. Sombatsompop N, Yotinwattanakumtorn C and Thongpin C. Influence of type and concentration of maleic anhydride grafted polypropylene and impact modifiers on mechanical properties of PP/wood sawdust composites. *Journal of Applied Polymer Science*. (2005); **97**: 475–484.
211. Guo CG and Wang QW. Compatibilizing effect of maleic anhydride grafted styrene-ethylene-butylene-styrene (MAH-g-SEBS) on the polypropylene and wood fiber composites. *Journal of Reinforced Plastics and Composites*. (2007); **26**: 1743–1752.
212. Karmarkar A, Chauhan SS, Modak JM and Chanda M. Mechanical properties of wood-fiber reinforced polypropylene composites: effect of a novel compatibilizer with isocyanate functional group. *Composites Part A-Applied Science and Manufacturing*. (2007); **38**: 227–233.
213. Mendez JA, Vilaseca F, Pelach MA, Lopez JP, Barbera L, Turon X, Girones J and Mutje P. Evaluation of the reinforcing effect of ground wood pulp in the preparation of polypropylene-based composites coupled with maleic anhydride grafted polypropylene. *Journal of Applied Polymer Science*. (2007); **105**: 3588–3596.
214. Gao H, Song Y-m, Wang Q-w, Han Z and Zhang M-L. Rheological and mechanical properties of wood fiber-PP/PE blend composites. *Journal of Forestry Research* (Harbin). (2008); **19**: 315–318.
215. Jiang L, Huang J, Qian J, Chen F, Zhang J, Wolcott MP and Zhu Y. Study of poly(3-hydroxybutyrate-co-3-hydroxyvalerate) (PHBV)/bamboo pulp fiber composites: effects of nucleation agent and compatibilizer. *Journal of Polymers and the Environment*. (2008); **16**: 83–93.
216. Kim S-J, Moon J-B, Kim G-H and Ha C-S. Mechanical properties of polypropylene/natural fiber composites: comparison of wood fiber and cotton fiber. *Polymer Testing*. (2008; **27**: 801–806.
217. Nygard P, Tanem BS, Karlsen T, Brachet P and Leinsvang B. Extrusion-based wood fibre-PP composites: wood powder and pelletized wood fibres – a comparative study. *Composites Science and Technology*. (2008); **68**: 3418–3424.
218. Yuan Q, Wu D, Gotama J and Bateman S. Wood fiber reinforced polyethylene and polypropylene composites with high modulus and impact strength. *Journal of Thermoplastic Composite Materials*. (2008); **21**: 195–208.
219. Lee S, Shupe TF, Groom LH and Hse CY. Maleated polypropylene film and wood fiber handsheet laminates. *Polymer Composites*. (2009); **30**: 1864–1872.
220. Basiji F, Safdari V, Nourbakhsh A and Pilla S. The effects of fiber length and fiber loading on the mechanical properties of wood-plastic (polypropylene) composites. *Turkish Journal of Agriculture and Forestry*. (2010); **34**: 191–196.

© Woodhead Publishing Limited, 2014

221. Gu R and Kokta BV. Mechanical properties of PP composites reinforced with BCTMP aspen fiber. *Journal of Thermoplastic Composite Materials*. (2010); **23**: 513–542.
222. Zabihzadeh SM, Dastoorian F and Ebrahimi G. Tensile properties and thermal analysis of chemimechanical pulp-reinforced HDPE composites. *Journal of Reinforced Plastics and Composites*. (2010); **29**: 1814–1819.
223. Ayrilmis N and Jarusombuti S. Flat-pressed wood plastic composite as an alternative to conventional wood-based panels. *Journal of Composite Materials*. (2011); **45**: 103–112.
224. Jarusombuti S and Ayrilmis N. Surface characteristics and overlaying properties of flat-pressed wood plastic composites. *European Journal of Wood and Wood Products*. (2011); **69**: 375–382.
225. Sailaja RRN and Deepthi MV. Mechanical and thermal properties of compatibilized composites of LDPE and esterified unbleached wood pulp. *Polymer Composites*. (2011); **32**: 199–209.
226. Ayrilmis N, Akbulut T, Dundar T, White RH, Mengeloglu F, Buyuksari U, Candan Z and Avci E. Effect of boron and phosphate compounds on physical, mechanical, and fire properties of wood–polypropylene composites. *Construction and Building Materials*. (2012); **33**: 63–69.
227. Abu-Ilaiwi FA, Ahmad MB, Ibrahim NA, Rahman MZA, Dahlan KZM and Yunus W. Graft copolymerization of methyl methacrylate onto rubber-wood fiber using H_2O_2 and Fe^{2+} as an initiator system. *Journal of Applied Polymer Science*. (2003); **88**: 2499–2503.
228. Kamdem DP, Riedl B, Adnot A and Kaliaguine S. ESCA spectroscopy of poly (methyl methacrylate) grafted onto wood fibers. *Journal of Applied Polymer Science*. (2003); **43**: 1901–1912.
229. Sailaja RRN. Mechanical and thermal properties of bleached kraft pulp-LDPE composites: effect of epoxy functionalized compatibilizer. *Composites Science and Technology*. (2006); **66**: 2039–2048.
230. Zhang Hh, Cui Y and Zhang Z. Chemical treatment of wood fiber and its reinforced unsaturated polyester composites. *Journal of Vinyl and Additive Technology*. (2013); **19**: 18–24.
231. Cai XL, Riedl B and Bouaziz M. Lignocellulosic composites with grafted polystyrene interfaces. *Composite Interfaces*. (2005); **12**: 25–39.
232. Nassar MA, Abdelwahab NA and Elhalawany NR. Contributions of polystyrene to the mechanical properties of blended mixture of old newspaper and wood pulp. *Carbohydrate Polymers*. (2009); **76**: 417–421.
233. Tastet D, Save M, Charrier F, Charrier B, Ledeuil J-B, Dupin J-C and Billon L. Functional biohybrid materials synthesized via surface-initiated MADIX/RAFT polymerization from renewable natural wood fiber: grafting of polymer as non leaching preservative. *Polymer*. (2011); **52**: 606–616.
234. Gardea-Hernandez G, Ibarra-Gomez R, Flores-Gallardo SG, Hernandez-Escobar CA, Perez-Romo P and Zaragoza-Contreras EA. Fast wood fiber esterification. I. Reaction with oxalic acid and cetyl alcohol. *Carbohydrate Polymers*. (2008); **71**: 1–8.
235. Zampano G, Bertoldo M and Bronco S. Poly(ethyl acrylate) surface-initiated ATRP grafting from wood pulp cellulose fibers. *Carbohydrate Polymers*. (2009); **75**: 22–31.

© Woodhead Publishing Limited, 2014

236. Ly EHB, Bras J, Sadocco P, Belgacem MN, Dufresne A and Thielemans W. Surface functionalization of cellulose by grafting oligoether chains. *Materials Chemistry and Physics*. (2010); **120**: 438–445.
237. Lu JZ, Wu Q and McNabb HS. Chemical coupling in wood fiber and polymer composites: a review of coupling agents and treatments. *Wood and Fiber Science*. (2000); **32**: 88–104.
238. Lu JZ, Wu QL and McNabb HS. Chemical coupling in wood fiber and polymer composites: a review of coupling agents and treatments. *Wood and Fiber Science*. (2000); **32**:88–104.
239. Garcia-Hernandez E, Licea-Claverie A, Zizumbo A, Alvarez-Castillo A and Herrera-Franco PJ. Improvement of the interfacial compatibility between sugar cane bagasse fibers and polystyrene for composites. *Polymer Composites*. (2004); **25**: 134–145.
240. Bengtsson M, Gatenholm P and Oksman K. The effect of crosslinking on the properties of polyethylene/wood flour composites. *Composites Science and Technology*. (2005); **65**: 1468–1479.
241. Bengtsson M, Oksman K and Stark NM. Profile extrusion and mechanical properties of crosslinked wood-thermoplastic composites. *Polymer Composites*. (2006); **27**: 184–194.
242. Kuan C-F, Kuan H-C, Ma C-CM and Huang C-M. Mechanical, thermal and morphological properties of water-crosslinked wood flour reinforced linear low-density polyethylene composites. *Composites Part A-Applied Science and Manufacturing*. (2006); **37**: 1696–1707.
243. Kuan C-F, Ma C-CM, Kuan H-C, Wu H-L and Liao Y-M. Preparation and characterization of the novel water-crosslinked cellulose reinforced poly(butylene succinate) composites. *Composites Science and Technology*. (2006); **66**: 2231–2241.
244. Mansour SH, El-Nashar DE and Abd-El-Messieh SL. Effect of chemical treatment of wood flour on the properties of styrene butadiene rubber/polystyrene composites. *Journal of Applied Polymer Science*. (2006); **102**: 5861–5870.
245. Sombatsompop N, Kantala C and Wimolmala E. Wood sawdust fibres as a secondary filler in carbon black filled NR vulcanizates. *Polymers & Polymer Composites*. (2006); **14**: 331–347.
246. Nachtigall SMB, Cerveira GS and Rosa SML. New polymeric-coupling agent for polypropylene/wood-flour composites. *Polymer Testing*. (2007); **26**: 619–628.
247. Love KT, Nicholson BK, Lloyd JA, Franich RA, Kibblewhite RP and Mansfield SD. Modification of Kraft wood pulp fibre with silica for surface functionalisation. *Composites Part A-Applied Science and Manufacturing*. (2008); **39**: 1815–1821.
248. Ly B, Thielemans W, Dufresne A, Chaussy D and Belgacem MN. Surface functionalization of cellulose fibres and their incorporation in renewable polymeric matrices. *Composites Science and Technology*. (2008); **68**: 3193–3201.
249. Bettini SHP, Bonse BC, Melo EA and Munoz PAR. Effect of sawdust surface treatment and compatibilizer addition on mechanical behavior, morphology, and moisture uptake of polypropylene/sawdust composites. *Polymer Engineering and Science*. (2010); **50**: 978–985.
250. Ghasemi I and Farsi M. Interfacial behaviour of wood plastic composite: effect of chemical treatment on wood fibres. *Iranian Polymer Journal*. (2010); **19**: 811–818.

© Woodhead Publishing Limited, 2014

251. Xie Y, Hill CAS, Xiao Z, Militz H and Mai C. Silane coupling agents used for natural fiber/polymer composites: a review. *Composites Part A-Applied Science and Manufacturing*. (2010); **41**: 806–819.
252. Rozman HD, Tay GS, Abubakar A and Kumar RN. Tensile properties of oil palm empty fruit bunch-polyurethane composites. *European Polymer Journal*. (2001); **37**: 1759–1765.
253. Chauhan SS, Karmarkar A and Aggarwal P. Evaluation of dynamic elastic properties of wood-filled polypropylene composites. *Journal of Applied Polymer Science*. (2006); **102**: 1706–1711.
254. http://www.observatorynano.eu/project/filesystem/files/PublicFundingofNanotechnologies_March2012.pdf.
255. Sawhney APS, Condon B, Singh KV, Pang SS, Li G and Hui D. Modern applications of nanotechnology in textiles. *Textile Research Journal*. (2008); **78**: 731–739.
256. Xue C-H, Jia S-T, Zhang J and Tian L-Q. Superhydrophobic surfaces on cotton textiles by complex coating of silica nanoparticles and hydrophobization. *Thin Solid Films*. (2009); **517**: 4593–4598.
257. Ngo YH, Li D, Simon GP and Garnier G. Paper surfaces functionalized by nanoparticles. *Advances in Colloid and Interface Science*. (2011); **163**: 23–38.
258. Dubas ST, Kumlangdudsana P and Potiyaraj P. Layer-by-layer deposition of antimicrobial silver nanoparticles on textile fibers. *Colloids and Surfaces A: Physicochemical and Engineering Aspects*. (2006); **289**: 105–109.
259. Wang Q and Hauser PJ. Developing a novel UV protection process for cotton based on layer-by-layer self-assembly. *Carbohydrate Polymers*. (2010); **81**: 491–496.
260. Strydom SJ, Otto DP, Liebenberg W, Lvov YM and de Villiers MM. Preparation and characterization of directly compactible layer-by-layer nanocoated cellulose. *International Journal of Pharmaceutics*. (2011); **404**: 57–65.
261. Uğur ŞS, Sarıışık M and Aktaş AH. Nano-Al_2O_3 multilayer film deposition on cotton fabrics by layer-by-layer deposition method. *Materials Research Bulletin*. (2011); **46**: 1202–1206.
262. Wang CX and Chen SL. Surface treatment of cotton using β-cyclodextrins sol–gel method. *Applied Surface Science*. (2006; **252**: 6348–6352.
263. Li F-Y, Xing Y-J and Ding X. Immobilization of papain on cotton fabric by sol–gel method. *Enzyme and Microbial Technology*. (2007); **40**: 1692–1697.
264. Alongi J, Ciobanu M and Malucelli G. Novel flame retardant finishing systems for cotton fabrics based on phosphorus-containing compounds and silica derived from sol–gel processes. *Carbohydrate Polymers*. (2011); **85**: 599–608.
265. Brancatelli G, Colleoni C, Massafra MR and Rosace G. Effect of hybrid phosphorus-doped silica thin films produced by sol-gel method on the thermal behavior of cotton fabrics. *Polymer Degradation and Stability*. (2011); **96**: 483–490.
266. Chen C-Y and Chiang C-L. Preparation of cotton fibers with antibacterial silver nanoparticles. *Materials Letters*. (2008); **62**: 3607–3609.
267. Zhang F, Wu X, Chen Y and Lin H. Application of silver nanoparticles to cotton fabric as an antibacterial textile finish. *Fibers and Polymers*. (2009); **10**: 496–501.
268. Ravindra S, Murali Mohan Y, Narayana Reddy N and Mohana Raju K. Fabrication of antibacterial cotton fibres loaded with silver nanoparticles via

© Woodhead Publishing Limited, 2014

'Green Approach'. *Colloids and Surfaces A: Physicochemical and Engineering Aspects*. (2010); **367**: 31–40.
269. Onar N, Ebeoglugil MF, Kayatekin I and Celik E. Low-temperature, sol–gel-synthesized, silver-doped titanium oxide coatings to improve ultraviolet-blocking properties for cotton fabrics. *Journal of Applied Polymer Science*. (2007); **106**: 514–525.
270. Zheng C, Chen G and Qi Z. Ultraviolet resistant/antiwrinkle finishing of cotton fabrics by sol-gel method. *Journal of Applied Polymer Science*. (2011); **122**: 2090–2098.
271. Schmidt H, Jonschker G, Goedicke S and Mennig M. The sol-gel process as a basic technology for nanoparticle-dispersed inorganic-organic composites. *Journal of Sol-Gel Science and Technology*. (2000); **19**: 39–51.
272. Yeh J-T, Chen C-L and Huang K-S. Preparation and application of fluorocarbon polymer/SiO2 hybrid materials, part 1: preparation and properties of hybrid materials. *Journal of Applied Polymer Science*. (2007); **103**: 1140–1145.
273. Yeh J-T, Chen C-L and Huang K-S. Preparation and application of fluorocarbon polymer/SiO2 hybrid materials, Part 2: water and oil repellent processing for cotton fabrics by sol–gel method. *Journal of Applied Polymer Science*. (2007); **103**: 3019–3024.
274. Yadav A, Prasad V, Kathe A, Raj S, Yadav D, Sundaramoorthy C and Vigneshwaran N. Functional finishing in cotton fabrics using zinc oxide nanoparticles. *Bulletin of Materials Science*. (2006); **29**: 641–645.
275. Becheri A, Dürr M, Lo Nostro P and Baglioni P. Synthesis and characterization of zinc oxide nanoparticles: application to textiles as UV-absorbers. *Journal of Nanoparticle Research*. (2008); **10**: 679–689.
276. Juntaro J, Pommet M, Mantalaris A, Shaffer M and Bismarck A. Nanocellulose enhanced interfaces in truly green unidirectional fibre reinforced composites. *Composite Interfaces*. (2007); **14**: 753–762.
277. Faruk O, Bledzki AK, Fink H-P and Sain M. Biocomposites reinforced with natural fibers: 2000–2010. *Progress in Polymer Science*. (2012); **37**: 1552–1596.
278. Coutts RSP. A review of Australian research into natural fibre cement composites. *Cement & Concrete Composites*. (2005); **27**: 518–526.
279. Han Y, Manolach SO, Denes F and Rowell RM. Cold plasma treatment on starch foam reinforced with wood fiber for its surface hydrophobicity. *Carbohydrate Polymers*. (2011); **86**: 1031–1037.
280. Cunha AM, Liu ZQ, Feng Y, Yi XS and Bernardo CA. Preparation, processing and characterization of biodegradable wood flour/starch-cellulose acetate compounds. *Journal of Materials Science*. (2001); **36**: 4903–4909.
281. Curvelo AAS, de Carvalho AJF and Agnelli JAM. Thermoplastic starch-cellulosic fibers composites: preliminary results. *Carbohydrate Polymers*. (2001); **45**: 183–188.
282. Mathew AP, Oksman K and Sain M. Mechanical properties of biodegradable composites from poly lactic acid (PLA) and microcrystalline cellulose (MCC). *Journal of Applied Polymer Science*. (2005); **97**: 2014–2025.
283. Huda MS, Drzal LT, Misra M and Mohanty AK. Wood-fiber-reinforced poly(lactic acid) composites: evaluation of the physicomechanical and morphological properties. *Journal of Applied Polymer Science*. (2006); **102**: 4856–4869.
284. Gregorova A, Hrabalova M, Wimmer R, Saake B and Altaner C. Poly(lactide acid) composites reinforced with fibers obtained from different tissue types of picea sitchensis. *Journal of Applied Polymer Science*. (2009); **114**: 2616–2623.

© Woodhead Publishing Limited, 2014

285. Petinakis E, Yu L, Edward G, Dean K, Liu H and Scully AD. Effect of matrix-particle interfacial adhesion on the mechanical properties of poly(lactic acid)/wood-flour micro-composites. *Journal of Polymers and the Environment*. (2009); **17**: 83–94.
286. Suryanegara L, Nakagaito AN and Yano H. Thermo-mechanical properties of microfibrillated cellulose-reinforced partially crystallized PLA composites. *Cellulose*. (2010); **17**: 771–778.
287. Bledzki AK and Faruk O. Wood fibre reinforced polypropylene composites: effect of fibre geometry and coupling agent on physico-mechanical properties. *Applied Composite Materials*. (2003); **10**: 365–379.
288. Bledzki AK and Faruk O. Creep and impact properties of wood fibre-polypropylene composites: influence of temperature and moisture content. *Composites Science and Technology*. (2004); **64**: 693–700.
289. Beg MDH, Pickering KL and Weal SJ. Corn gluten meal as a biodegradable matrix material in wood fibre reinforced composites. *Materials Science and Engineering A-Structural Materials Properties Microstructure and Processing*. (2005); **412**: 7–11.
290. Bledzki AK, Letman M, Viksne A and Rence L. A comparison of compounding processes and wood type for wood fibre – PP composites. *Composites Part A-Applied Science and Manufacturing*. (2005); **36**: 789–797.
291. Bledzki AK, Zhang WY and Faruk O. Microfoaming of flax and wood fibre reinforced polypropylene composites. *Holz Als Roh-Und Werkstoff*. (2005); **63**: 30–37.
292. Bledzki AK and Faruk O. Injection moulded microcellular wood fibre-polypropylene composites. *Composites Part A-Applied Science and Manufacturing*. (2006); **37**: 1358–1367.
293. Beg MDH and Pickering KL. Accelerated weathering of unbleached and bleached Kraft wood fibre reinforced polypropylene composites. *Polymer Degradation and Stability*. (2008); **93**: 1939–1946.
294. Beg MDH and Pickering KL. Reprocessing of wood fibre reinforced polypropylene composites. Part II: hygrothermal ageing and its effects. *Composites Part A-Applied Science and Manufacturing*. (2008); **39**: 1565–1571.
295. Beg MDH and Pickering KL. Reprocessing of wood fibre reinforced polypropylene composites. Part I: effects on physical and mechanical properties. *Composites Part A-Applied Science and Manufacturing*. (2008); **39**: 1091–1100.
296. Schirp A and Stender J. Properties of extruded wood-plastic composites based on refiner wood fibres (TMP fibres) and hemp fibres. *European Journal of Wood and Wood Products*. (2010); **68**: 219–231.
297. Shen M, Touchard F, Bezine G and Brillaud J. Direct numerical simulation of fracture behaviour for random short wood fibres reinforced composites, comparison with digital image correlation experiments. In: Bremand F, editor. Icem 14: 14th International Conference on Experimental Mechanics, Vol 62010.
298. Ayrilmis N, Jarusombuti S, Fueangvivat V and Bauchongkol P. Effect of thermal-treatment of wood fibres on properties of flat-pressed wood plastic composites. *Polymer Degradation and Stability*. (2011); **96**: 818–822.
299. Butylina S, Martikka O and Karki T. Properties of wood fibre-polypropylene composites: effect of wood fibre source. *Applied Composite Materials*. (2011); **18**: 101–111.

© Woodhead Publishing Limited, 2014

300. Xu B, Simonsen J and Rochefort WE. Creep resistance of wood-filled polystyrene/high-density polyethylene blends. *Journal of Applied Polymer Science*. (2001); **79**: 418–425.
301. Rizvi G, Matuana LM and Park CB. Foaming of PS/wood fiber composites using moisture as a blowing agent. *Polymer Engineering and Science*. (2000); **40**: 2124–2132.
302. Romero-Balderrama L, Mendoza-Duarte ME, Gaspar-Rosas A, Flores-Gallardo SG and Ibarra-Gomez R. Composites of polystyrene/wood fiber, processing effect to creep resistance. In: Co A, Leal LG, Colby RH and Giacomin AJ, editors. XVth International Congress on Rheology – the Society of Rheology 80th Annual Meeting, Pts 1 and 2 (2008). pp. 135–137.
303. Obataya E, Osawa K and Yamauchi H. Mechanical properties of acetylated wood fiber-polystyrene composites. *Mokuzai Gakkaishi*. (2011); **57**: 88–93.
304. Mengeloglu F, Matuana LM and King JA. Effects of impact modifiers on the properties of rigid PVC/wood-fiber composites. *Journal of Vinyl & Additive Technology*. (2000); **6**: 153–157.
305. Matuana LM, Kamdem DP and Zhang J. Photoaging and stabilization of rigid PVC/wood-fiber composites. *Journal of Applied Polymer Science*. (2001); **80**: 1943–1950.
306. Augier L, Sperone G, Vaca-Garcia C and Borredon M-E. Influence of the wood fibre filler on the internal recycling of poly(vinyl chloride)-based composites. *Polymer Degradation and Stability*. (2007); **92**: 1169–1176.
307. Cheng R-X, Li Y, Wang Q-W and Zhang L. Bonding properties of poly(vinyl chloride)-based wood-plastic composites bonded with epoxy adhesive. *Journal of Applied Polymer Science*. (2012); **125**: 175–179.
308. van Dyk H, Peralta P, Peszlen I and Banks-Lee P. An innovative wood-fiber composite incorporating nonwoven textile technologies. *Forest Products Journal*. (2009); **59**: 11–17.
309. Lv X, Ma D, Song Y and Gao Z. Impacts of molding pressure on performances of Kraft fiber reinforced unsaturated polyester composites. In: Shi YG and Zuo JL, editors. *Environmental Biotechnology and Materials Engineering*, Pts 1–3 (2011). pp. 2173–2177.
310. Gregorova A, Wimmer R, Hrabalova M, Koller M, Ters T and Mundigler N. Effect of surface modification of beech wood flour on mechanical and thermal properties of poly (3-hydroxybutyrate)/wood flour composites. *Holzforschung*. (2009); **63**: 565–570.
311. Meekum U. Experimental design on multi layers of LVL fiber reinforced wood composite using bagasse as core structure 2010. In: Lieping Y, Peng F and Qingrui Y, editors. *Proceeding of the 5th International Conference on FRP Composite in Civil Engineering*. (2010); **5**: 135–138.
312. Brandstrom J. Ultrastructure of compression wood fibres in fractions of a thermomechanical pulp. *Nordic Pulp & Paper Research Journal*. (2004); **19**: 13–17.
313. Bledzki AK and Faruk O. Microcellular wood fibre reinforced PP composites – A comparative study between extrusion, injection moulding and compression moulding. *International Polymer Processing*. (2006); **21**: 256–262.
314. Umer R, Bickerton S and Fernyhough A. Characterising wood fibre mats as reinforcements for liquid composite moulding processes. *Composites Part A-Applied Science and Manufacturing*. (2007); **38**: 434–448.

© Woodhead Publishing Limited, 2014

315. Umer R, Bickerton S and Fernyhough A. Modelling the application of wood fibre reinforcements within liquid composite moulding processes. *Composites Part A-Applied Science and Manufacturing*. (2008); **39**: 624–639.
316. Panthapulakkal S and Sain M. Preparation and characterization of cellulose nanofibril films from wood fibre and their thermoplastic polycarbonate composites. *International Journal of Polymer Science*. (2012); **2012**: 1–6.
317. Shao YX, Moras S, Ulkem N and Kubes G. Wood fibre – cement composites by extrusion. *Canadian Journal of Civil Engineering*. (2000); **27**: 543–552.
318. Bledzki AK and Faruk O. Extrusion and injection moulded microcellular wood fibre reinforced polypropylene composites. *Cellular Polymers*. (2004); **23**: 211–227.
319. Hietala M, Samuelsson E, Niinimäki J and Oksman K. The effect of pre-softened wood chips on wood fibre aspect ratio and mechanical properties of wood–polymer composites. *Composites Part A: Applied Science and Manufacturing*. (2011); **42**: 2110–2116.
320. Frisk H and Schwendemann D. Injection moulding: compounding wood fibres with plastic. *Kunststoffe-Plast Europe*. (2004); **94**: 76–80.
321. Bledzki AK and Faruk O. Influence of different endothermic foaming agents on microcellular injection moulded wood fibre reinforced PP composites. *Cellular Polymers*. (2006); **25**: 143–158.
322. Peltola H, Laatikainen E and Jetsu P. Effects of physical treatment of wood fibres on fibre morphology and biocomposite properties. *Plastics Rubber and Composites*. (2011); **40**: 86–92.
323. Mehta G, Mohanty AK, Drzal LT, Kamdem DP and Misra M. Effect of accelerated weathering on biocomposites processed by SMC and compression molding. *Journal of Polymers and the Environment*. (2006); **14**: 359–368.
324. Ulven CA and Vaidya UK. Impact response of fire damaged polymer-based composite materials. *Composites Part B-Engineering*. (2008); **39**: 92–107.
325. Oksman K, Wallstrom L, Berglund LA and Toledo RD. Morphology and mechanical properties of unidirectional sisal-epoxy composites. *Journal of Applied Polymer Science*. (2002); **84**: 2358–2365.
326. Wienhold PD, Lennon AM, Roberts JC, Rooney M, Kercher AK, Nagle DC *et al*. Characterization of carbonized wood core for use in FRP sandwich ship structures 2000.
327. Astrom BT. *Manufacturing of Polymer Composites*. CRC: Boca Raton (1997).
328. Khosravani MR. Composite materials manufacturing processes. *Applied Mechanics and Materials*. (2012); **110**: 1361–1367.
329. Davis BA. *Compression Molding*. Hanser Gardner Publications Inc; Kempten (2003).
330. Nechwatal A, Mieck K-P and Reußmann T. Developments in the characterization of natural fibre properties and in the use of natural fibres for composites. *Composites Science and Technology*. (2003); **63**: 1273–1279.
331. Nechwatal A, Reußmann T, Böhm S and Richter E. The dependence between the process technologies and the effect of MAH-PP-adhesives in natural fibre reinforced thermoplastic composites. *Advanced Engineering Materials*. (2005); **7**:68–73.
332. Soroushian P, Elzafraney M, Nossoni A and Chowdhury H. Evaluation of normal-weight and light-weight fillers in extruded cellulose fiber cement products. *Cement & Concrete Composites*. (2006); **28**: 69–76.

© Woodhead Publishing Limited, 2014

333. Averous L and Boquillon N. Biocomposites based on plasticized starch: thermal and mechanical behaviours. *Carbohydrate Polymers*. (2004); **56**: 111–122.
334. Jonoobi M, Harun J, Mathew AP and Oksman K. Mechanical properties of cellulose nanofiber (CNF) reinforced polylactic acid (PLA) prepared by twin screw extrusion. *Composites Science and Technology*. (2010); **70**: 1742–1747.
335. Cartier H and Hu GH. Morphology development of in situ compatibilized semicrystalline polymer blends in a co-rotating twin-screw extruder. *Polymer Engineering & Science*. (1999); **39**: 996–1013.
336. Shao Y, Marikunte S and Shah SP. Extruded fiber reinforced composites. *Concrete International-Design and Construction*. (1995); **17**: 48–53.
337. Bledzki AK and Faruk O. Influence of processing temperature on microcellular injection-moulded wood-polypropylene composites. *Macromolecular Materials and Engineering*. (2006); **291**: 1226–1232.
338. Thumm A and Dickson AR. The influence of fibre length and damage on the mechanical performance of polypropylene/wood pulp composites. *Composites Part A: Applied Science and Manufacturing*. (2013); **46**: 45–52.
339. Bledzki AK and Faruk O. Wood fiber reinforced polypropylene composites: compression and injection molding process. *Polymer-Plastics Technology and Engineering*. (2004); **43**: 871–888.
340. Bourmaud A, Ausias G, Lebrun G, Tachon ML and Baley C. Observation of the structure of a composite polypropylene/flax and damage mechanisms under stress. *Industrial Crops and Products*. (2013); **43**: 225–236.
341. El-Sabbagh A, Steuernagel L and Ziegmann G. Characterisation of flax polypropylene composites using ultrasonic longitudinal sound wave technique. *Composites Part B: Engineering*. (2013); **45**: 1164–1172.
342. Fung KL, Xing XS, Li RKY, Tjong SC and Mai YW. An investigation on the processing of sisal fibre reinforced polypropylene composites. *Composites Science and Technology*. (2003); **63**: 1255–1258.
343. Sawallisch K. Compounding of sheet molding compound. *Polymer-Plastics Technology and Engineering*. (1984); **23**: 1–36.
344. van Voorn B, Smit HHG, Sinke RJ and de Klerk B. Natural fibre reinforced sheet moulding compound. *Composites Part A: Applied Science and Manufacturing*. (2001); **32**: 1271–1279.
345. Sèbe G, Cetin N, Hill CS and Hughes M. RTM hemp fibre-reinforced polyester composites. *Applied Composite Materials*. (2000); **7**: 341–349.
346. Almgren KM, Gamstedt EK, Nygard P, Malmberg F, Lindblad J and Lindstrom M. Role of fibre-fibre and fibre-matrix adhesion in stress transfer in composites made from resin-impregnated paper sheets. *International Journal of Adhesion and Adhesives*. (2009); **29**: 551–557.
347. Bledzki AK, Letman M, Viksne A and Rence L. A comparison of compounding processes and wood type for wood fibre – PP composites. *Composites Part A: Applied Science and Manufacturing*. (2005); **36**: 789–797.
348. Aranguren MI, Marcovich NE and Reboredo MM. Composites made from lignocellulosics and thermoset polymers. *Molecular Crystals and Liquid Crystals*. (2000); **353**: 95–108.
349. Albano C, Ichazo M, Gonzalez J, Delgado M and Poleo R. Effects of filler treatments on the mechanical and morphological behavior of PP plus wood flour and PP plus sisal fiber. *Materials Research Innovations*. (2001); **4**: 284–293.

© Woodhead Publishing Limited, 2014

350. Schirp A and Stender J. Properties of extruded wood-plastic composites based on refiner wood fibres (TMP fibres) and hemp fibers. *Eur J Wood Pr*. (2010); **68**: 219–231.
351. Danyadi L, Moczo J and Pukanszky B. Effect of various surface modifications of wood flour on the properties of PP/wood composites. *Composites Part A-Applied Science and Manufacturing*. (2010); **41**: 199–206.
352. Balasuriya PW, Ye L and Mai YW. Mechanical properties of wood flake-polyethylene composites. Part I: effects of processing methods and matrix melt flow behaviour. *Composites Part A-Applied Science and Manufacturing*. (2001); **32**: 619–629.
353. Hill C and Hughes M. Natural fibre reinforced composites opportunities and challenges. *Journal of Biobased Materials and Bioenergy*. (2010); **4**: 148–158.
354. Hua L, Zadorecki P and Flodin P. Cellulose fiber-polyester composites with reduced water sensitivity (1) – chemical treatment and mechanical properties. *Polymer Composites*. (1987); **8**: 199–202.
355. Neagu RC, Gamstedt EK and Lindstrom M. Influence of wood-fibre hygroexpansion on the dimensional instability of fibre mats and composites. *Composites Part A-Applied Science and Manufacturing*. (2005); **36**: 772–788.
356. Adhikary KB, Pang S and Staiger MP. Dimensional stability and mechanical behaviour of wood-plastic composites based on recycled and virgin high-density polyethylene (HDPE). *Composites Part B-Engineering*. (2008); **39**: 807–815.
357. Sliwa F, El Bounia N-e, Marin G, Charrier F and Malet F. A new generation of wood polymer composite with improved thermal stability. *Polymer Degradation and Stability*. (2012); **97**: 496–503.
358. Liu DT, Xia KF, Yang RD, Li J, Chen KF and Nazhad MM. Manufacturing of a biocomposite with both thermal and acoustic properties. *Journal of Composite Materials*. (2012); **46**: 1011–1020.
359. FH O, MR B, MD R and BP L. Development of cork-gypsum biocomposites for building applications. *Construction Building Materials*. (1999); **13**: 179–186.
360. http://www.superhomes.org.uk/resources/whats-best-insulation-material/.
361. Demirboğa R and Gül R. The effects of expanded perlite aggregate, silica fume and fly ash on the thermal conductivity of lightweight concrete. *Cement and Concrete Research*. (2003); **33**: 723–727.
362. Hammond GP and Jones CI. Embodied energy and carbon in construction materials. *Proceedings of the Institution of Civil Engineers-Energy*. (2008); **161**:87–98.
363. http://www.lucintel.com/LucintelBrief/PotentialofNaturalfibercomposites-Final.pdf.
364. http://www.lucintel.com/LucintelBrief/OpportunitiesinGlobalCompositesMarket-Final.pdf.
365. Wang S-S, Li S-Y and Liao S-J. The genes of tulou: a study on the preservation and sustainable development of tulou. *Sustainability*. (2012); **4**: 3377–3386.
366. Liang R, Stanislawski D and Hota G. Structural responses of Hakka rammed earth buildings under earthquake loads. Proceedings of International Workshop on Rammed Earth Materials and Sustainable Structures 2011. pp. 28–31.

© Woodhead Publishing Limited, 2014

367. Li Q, Sun X, Chen C and Yang X. Characterizing the household energy consumption in heritage Nanjing Tulou buildings, China: a comparative field survey study. *Energy and Buildings*. (2012); **49**: 317–326.
368. http://www.greentins.com/doc/EINWOOD%20Catalog.pdf.
369. Rusu D and Boyer SAE. Bioplastics for automotive applications. *Handbook of Bioplastics and Biocomposites Engineering Applications*. (2011); **81**: 397.
370. Suddell BC. Industrial fibres: recent and current developments. In: *Symposium on Natural Fibres*, Rome, October 20, 2008.
371. http://greenupgrader.com/2448/lotus-eco-elise-taking-sustainability-up-a-notch
372. McMullen P. Fibre/resin composites for aircraft primary structures: a short history, 1936–1984. *Composites*. (1984); **15**: 222–230.
373. Haupt P and Parker K. Acumen in advanced aerospace materials expertise. *CSIR Science Scope*. (2006); **1** (5): 12–13.

© Woodhead Publishing Limited, 2014

2

Chemistry and structure of cellulosic fibres as reinforcements in natural fibre composites

R. A. SHANKS, RMIT University, Australia

DOI: 10.1533/9780857099228.1.66

Abstract: Cellulose fibres, derivatives and regenerated compositions have traditionally been applied in many materials for structural, decorative and disposable products. Cellulose structure–property–performance begins with glucose covalent bonding, and properties extend to supramolecular assemblies. Chirality dependent stereochemistry distinguishes cellulose from synthetic polymers. Cellulose fibre structure, separation and purification from plant materials are described. Processing dependent properties, enhanced performance, shaping into regenerated fibres, sheets or nano-fibres and crystals are reviewed. Cellulose chemistry extends into crystallinity, polymorphism, solubility and environmental dependent characteristics. Cellulose, as with all biopolymers, exhibits typical polymer characteristics expected from theory; however, its unique structural complexity gives cellulose an additional property set. Strongly hydrogen-bonding solvents including ionic liquids are adopted for processing. New cellulose technologies contribute value-added materials derived from trees and crops, with emphasis on nanostructured celluloses.

Key words: natural fibre, cellulose structure, cellulose solution, regenerated fibre, cellulose derivative.

2.1 Introduction

Cellulose is the most abundant organic chemical. Cellulose is a polymer with complex monomeric units that have a precise stereochemistry arising from a group of chiral carbons arranged in a six-membered ring. This complex monomer and its reproducible attachments along cellulose chains provide a set of structural levels that each contribute to the formation of cellulose crystals, the chemical properties and consequential physical and mechanical properties. The complexity and order within cellulose needs to be developed from the primary covalent bonded monomer to perceive the many contributions of stereochemistry and intra-/intermolecular interactions that constitute the cellulose fibre structure and properties. Within each of the

© Woodhead Publishing Limited, 2014

levels of structure from primary bonding in the monomer, stereochemistry, polymer chain linkages, macromolecular conformation and supramolecular assembly, cellulose is a chemical marvel. The stereochemical complexity brought about from four chiral carbon atoms plus a fifth chiral carbon arising from cyclic structure and interchain link ensures the selective conformation and consistent molecular arrangement within cellulose structures.

Cellulose is the structural material of plants, algae and bacterial species. It is a resource derived from trees, plant stalks and agricultural waste. Formation of cellulose by photosynthesis utilizes atmospheric carbon dioxide, and this carbon capture secures the carbon within plants and any products derived from them. Cellulose fibre composites are used in many durable materials for building, transport and furnishings where carbon contained in the cellulose is removed from the atmosphere. Because cellulose is a natural structural material, cellulose sources are already available with suitable properties for application after separation, purification, shaping, where applicable. In many cases minor modification is required to meet an application. More processed forms have been developed for specialized use, such as treated timber, reconstituted fibres and paper making. Cellulose is combined with other substances in plants, therefore to utilize cellulose fibres directly they must first be separated and purified. A further step is to disassemble the structure of native cellulose through solution processes and then reconstitute it into new forms such as textile cellulose fibres, films and moulded shapes.

The aim of this chapter is to review the structure, chemistry and properties of cellulose based on chemical structure, stereochemistry and supramolecular structures, through to bulk properties such as lower critical solution properties, ionic solvents, solution characteristics, nano-cellulose and high performance materials. This review will provide a context for inclusion of cellulose fibres from natural fibres, regenerated fibres, modified fibres and nanostructured fibres, in composite materials. Other composites utilize cellulose and derivatives as a matrix phase in fibre and inorganic particle containing composites, where typically one of the reinforcements will be a type of cellulose fibres. Microcrystalline cellulose (MCC) and nano-forms of cellulose including cellulose nano-fibres (CNF) and cellulose nano-crystals (CNC) are included.

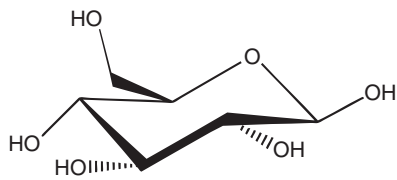
2.2 Glucose monomer

Glucose is the monomer that forms cellulose via a biological-enzyme catalysed step-growth or condensation polymerization. The repeat unit is β-1,4-anhydroglucopyranose. This chapter will briefly consider the mechanism of glucose biopolymerization; however, emphasis is on the structure and properties. Glucose is a hexose, 6-carbon sugar, a diastereoisomer of 2,3,4,5,6-pentahydroxyhexanal, where each of carbons 2, 3, 4, 5 are chiral, giving 16 possible configurations comprising diastereoisomers and enantiomers

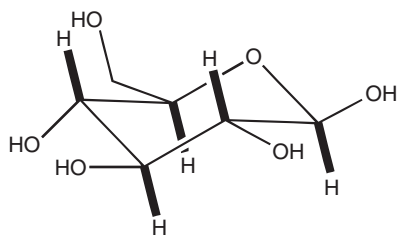
© Woodhead Publishing Limited, 2014

(a special case of being mirror image structures). The 5-hydroxy combines with the aldehyde to form a six-membered cyclic hemiacetal called the pyroanose form of glucose, shown in Fig. 2.1.

The cyclic structure is not planar and, in the case of glucose only, all of the hydroxyl groups pendent to the cyclic structure are in the most stable conformation, being approximately planar (equatorial) to the puckered ring. The hemiacetal hydroxy on carbon 1 on the right in Fig. 2.1 is a new chiral centre, giving a total of 32 diastereoisomers and enantiomers. The conformation is called *β*-glucopyranoside and is the conformation that occurs in cellulose. The opposite conformation is called *α*-glucopyranoside, which creates the more bent link that occurs in starch. The difference between cellulose and starch (amylose and amylopectin) is the chirality about carbon 1. In glucose the *α*-anomer is more stable than the *β*-anomer by about 2:1 even though the *α*-hydroxy is in a normally less stable axial configuration. This reversal of stability is called the anomeric effect, which is brought about by interaction of the dipole from the non-bonding electrons on the adjacent hemiacetal-ring oxygen aligning with the hemiacetal hydroxyl on C1. The planar structure of cellulose suits it to regular close-packing and crystal formation. The bent conformation of starch makes it suitable to form loose coils that crystallize with space for water and other complexed molecules within the coils. Each carbon in the glucopyranose structure has a pendant hydroxy or $-CH_2OH$ (carbon 5) and hydrogen, where the small hydrogen atoms are directed out of the cyclic plane, because since hydrogens are small they are less crowded in this conformation than if the hydroxyls were the non-planar (axial) groups. This is illustrated in the more complete structure of *β*-glucopyranose in Fig. 2.2. The in-plane groups are called equatorial, while



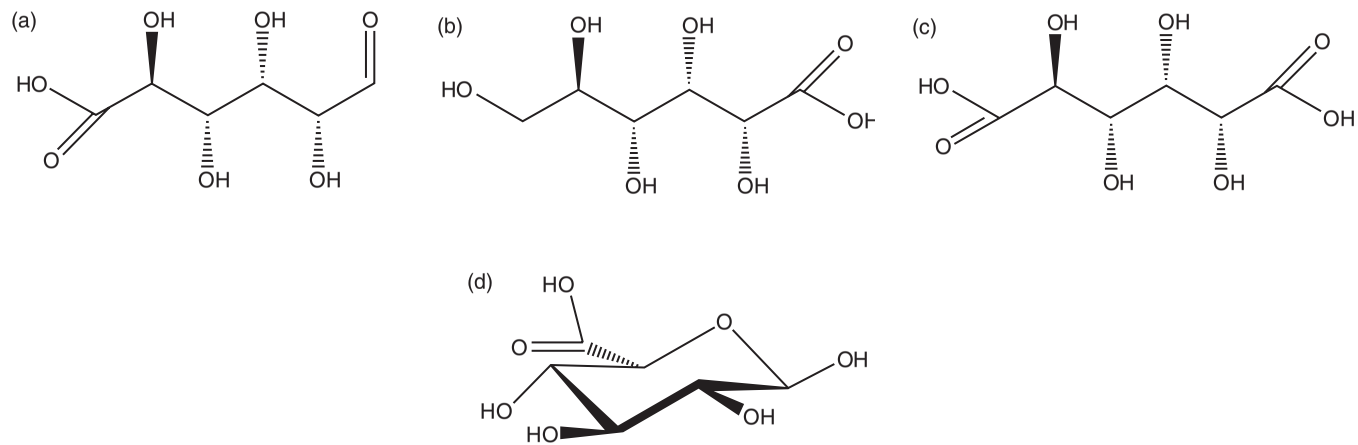
2.1 *β*-Glucopyranose.



2.2 β-Glucopyranose showing out of plane hydrogen atoms.

© Woodhead Publishing Limited, 2014

© Woodhead Publishing Limited, 2014



2.3 (a) Glucuronic acid, (b) gluconic acid, (c) glutaric acid, (d) cyclic form β-glucuronic acid.

the out-of-plane groups are called axial, the descriptions approximating to the actual directional orientation of the pendant groups.

The hydroxyl groups of cellulose appear to be typical alcohol functional groups; however, each hydroxyl has other hydroxyls in proximity including the hemiacetal ether type oxygen. Attraction of electrons by oxygens renders each hydroxyl group more acidic than a typical alcohol. The hydroxyl groups form salts with strong bases such as sodium hydroxide, and lithium or potassium homologues. The salts form in low concentration even in strong base because the hydroxyl groups are only marginally acidic. The acidic nature of cellulose hydroxyls is utilized for swelling, partial dissolving, polymorphic transitions, dyeing and derivatization reactions. The cyclic structure of glucose is oxidized at the C6 hydroxyl to form an aldehyde or carboxylic acid, generally a carboxylic acid with many mild oxidizing agents such as sodium perborate. The carboxylic acid, glucuronic acid, shown in Fig. 2.3 can form salts the same as any carboxylic acid; however, in carbohydrate structures gluconic acid and other carboxylic acids from isomeric hexapyranoses convert these materials into gels, viscose solutions, or with divalent metal ions such as calcium, magnesium or zinc, ionic crosslinking takes place. Figure 2.3 shows gluconic acid formed by oxidation of the aldehyde at carbon 1 in open chain form, and oxidation of both carbon 1 and 6 to form open chain glutaric acid. Glucuronic acid is the carboxylic acid form found in polysaccharides since carbon 6 can be oxidized to carboxylic acid without preventing or disrupting polymer formation.

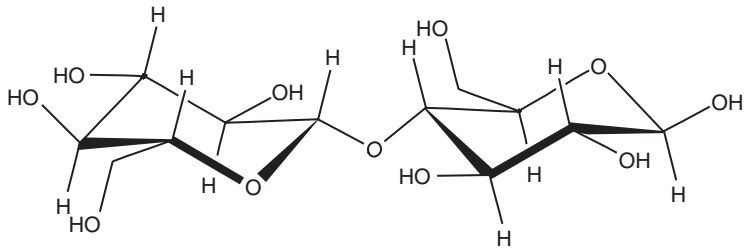
Other hexoses are found in polysaccharides often as copolymers, such as hemicelluloses, pectins and gums (Kaplan, 1998). Common alternative hexoses to glucose are galactose, mannose, fructose and shorter chain aldoses such as xylose, rhamnose and arabinose. However, in cellulose, amylose and amylopectin only glucose is present. Cellulose in particular must have a highly regular structure for it to form close-packed crystals, combining into fibres where modulus and strength are maximized.

2.3 Glucose biopolymerization

Biopolymerization of glucose to form poly(β-1,4-glucopyranosyl) or cellulose creates a regular polymer in which each adjacent glucose is inverted without changing any of its stereochemistry. Thus the repeat unit of a cellulose chain consists of two glucose units, the disaccharide cellobiose shown in Fig. 2.4. Biopolymerization progressively links glucose units with alignment of neighbouring chains of cellulose simultaneously forming cellulose(I) crystal morphology, called native cellulose.

Enzymatic hydrolysis of cellulose can form glucose, cellobiose or short chain glucans. Acid hydrolysis of cellulose is indiscriminate and forms glucose as the product of complete hydrolysis. Consistency of cellulose structure

© Woodhead Publishing Limited, 2014



2.4 Cellobiose, the stereochemical repeat unit of cellulose.

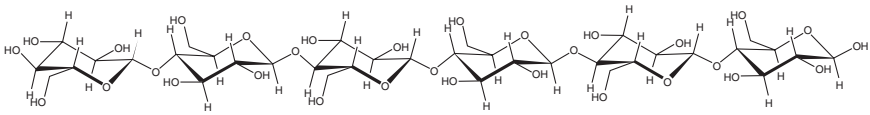
involves synthetic complexity and supramolecular assembly. Synthesis is controlled by the enzyme, cellulose synthase. Cellulose microfibrils are visualized as requiring a multi-step synthetic process. The assembly of cellulose chains into microfibrils is a spontaneous process requiring assembly from the synthesizing sites. Studies on mutants and herbicide-treated plants have assisted in interpreting polymerization and crystallization during cellulose biosynthesis. Most biosynthesis results in crystalline cellulose type I, while some few produce crystalline cellulose type II. A complete understanding of the process will require further investigation (Saxena and Brown, 2005).

Cellulose is synthesized within membrane-bound enzyme complexes. The individual enzymatic subunits are spatially separated. The synthesis mechanism in plants occurs in hexagonal structures in the plasma membrane, giving a complex network of microfibrils, though the assembly of individual chains is poorly understood. Cellulose synthase polymerizes β-(1–4)-glucopyranose chains from uracil diphosphate-glucose, where the phosphate groups activate glucose (Guerriero *et al*., 2010). The precise arrangement and association of cellulose synthase units controls extracellular chain assembly as well as the morphology and width of cellulose fibril deposition (Ross *et al*., 1991). The morphology formed during synthesis and assembly is metastable cellulose I, which upon being given the chance by swelling or solubilization rearranges into cellulose II morphology. The gene that encodes a cotton cellulose synthase motivated research exploration for genes that encode cell wall polysaccharide synthesis. About 2500 genes, control synthesis, dynamic architecture, sensing functions, and metabolism of plant cell walls (Carpita, 2011).

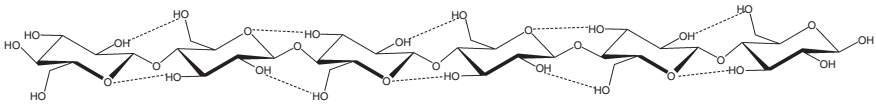
2.4 Cellulose structure

Cellulose is bio-polymerized with high degree of polymerization, typically 300–1000 (to as high as 10 000–15 000) glucose units in each molecule, giving a molar mass range of 540 000–1 800 000 g/mol. Figure 2.5 illustrates a segment of cellulose with six glucose residues presented in a conformational

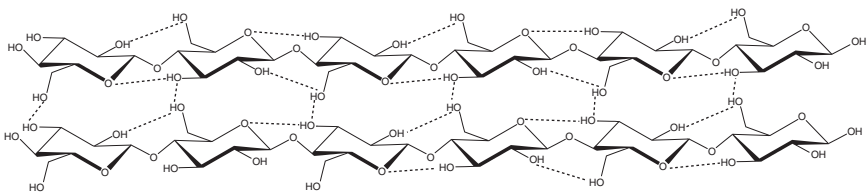
© Woodhead Publishing Limited, 2014



2.5 Cellulose chain segment showing relatively planar structure.



2.6 Cellulose chain segment showing intramolecular hydrogen bonding.



2.7 Parallel cellulose chain segments showing intra- and intermolecular hydrogen bonding.

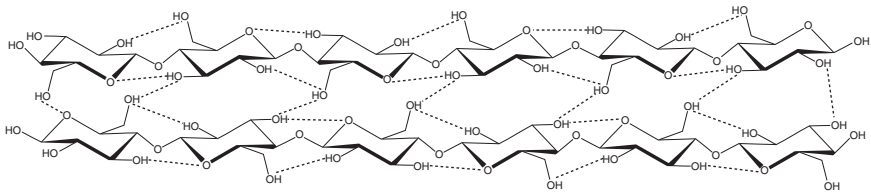
view showing the relatively planar configuration and conformation. The complex interweaving of bonding and stereochemistry with many possible isomers has been naturally selected to form a relatively rigid planar structure with many hydroxyl groups for potential hydrogen bonding. The molecule is rigid apart from the –O– acetal links between glucose units.

Cellulose thus consists of high molar mass, planar, β-1,4-, cellobiose repeat units, with potential for intramolecular hydrogen bonding, hindrance to rotation within a chain; potential for intermolecular hydrogen bonding, assembling chains into regular arrays, crystals and microfibrils.

Intramolecular hydrogen bonds can form within a cellulose molecule and due to the planar structure these hydrogen bonds are aligned along the chain axis (Fig. 2.6). Orientation of hydroxyl groups within each glucose unit, due to chirality in the carbon chain structure, predetermines the proximity and alignment of hydroxyl groups and monomer units.

Assemblies of cellulose chains, each confined to a fixed conformation by intramolecular hydrogen bonding, are formed due to the regularity and symmetry of individual chains and maintained by intermolecular hydrogen bonding as shown in Fig. 2.7. The structure shown in Fig. 2.7 has adjacent chains in parallel orientation, which is the structure of cellulose I crystals or native cellulose. This is the thermodynamically less stable crystalline

© Woodhead Publishing Limited, 2014



2.8 Anti-parallel cellulose chain segments showing intra- and inter molecular hydrogen bonding.

form of cellulose, although it is the most abundant form found natively. Cellulose II occurs after swelling and rearrangement or regeneration of cellulose, although there are instances of natural formation (Fidale *et al.*, 2008).

Figure 2.8 shows an assembly of two cellulose chains to illustrate the anti-parallel orientation found in cellulose type II crystals (textile cellulose). This is not the predominant conformation found in plants. Cellulose synthesis determines the orientation, even though it is not the most stable form. There are other variants of cellulose crystalline structure, some formed natively, others formed under special regeneration conditions. The transition of crystal structure has been examined as a function of permeation and swelling by ionic liquids and other components, such as lignin, contributed to the rate of transformation to cellulose II (Cheng *et al.*, 2011).

2.5 Chemical and solubility properties of cellulose

Cellulose monomers are linked by acetal groups that are inherently resistant to alkali, though hydrolysed by acid. Acids such as hydrochloric and sulphuric acid randomly hydrolyse cellulose leaving shorter chain length and ultimately glucose. Hydrolysis occurs more rapidly in amorphous and less perfect or smaller crystallites. This differential hydrolysis rate is used for selective hydrolysis to prepare nano-fibres and nano-crystals. Alkali promotes oxidation of cellulose when accompanied by oxidizing agents such as chlorine, sodium hypochlorite, sodium periodate, sodium perborate and redox metals such as cerium, copper and silver ions. Oxidation occurs at the hydroxyl on C6, giving a carboxylic acid (glucuronic acid), though depending on the oxidizing agent the bond between C2 and C3 can be disrupted since the two hydroxyls are a glycol formation. In biodegradation, the enzyme cellobiose sequentially hydrolyses the chain two glucose units in each step to give the disaccharide cellobiose as the final product.

Thermal degradation is studied using thermogravimetry (TGA) under either inert (nitrogen) or oxidizing (air) conditions. Thermal degradation of hemp was investigated after several treatments and TGA revealed

© Woodhead Publishing Limited, 2014

degradation steps due to pectins, hemicellulose, cellulose and lignin. TGA derivative (DTG) peaks for non-cellulose substances decreased after treatment with sodium hydroxide though the onset temperature decreased after treatment with sodium hydroxide, silane and ethanol–water extraction (Rachini *et al*., 2009). TGA was used to distinguish structural changes in cellulose during cotton fibre development. Differences were revealed between primary and secondary cell walls and of two cultivars, with chemical differences identified using Fourier transform infrared spectroscopy (Abidi *et al*., 2009). Sisal degradation has been studied using differential scanning calorimetry (DSC) and TGA where raw and defatted fibres and their chemical constituents (cellulose, hemicellulose and lignin) were examined under nitrogen and air. Raw sisal degraded at higher temperature than cellulose and hemicellulose, attributed to the lignin content of the sisal. Sisal results were compared with results for jute and hemp (Martin *et al*., 2010).

Cellulose swells in liquids such as water and organic liquids. Swelling of microcrystalline, native and Mercerized cotton and eucalyptus celluloses by 16 aprotic solvents was investigated. Swelling has been correlated with liquid molar volume, basicity, polarizability, as well as cellulose crystal size, surface area and whether chains are parallel or anti-parallel (Fidale *et al*., 2008).

Cellulose is soluble in strongly hydrogen-bonding liquids and solutions. Cellulose has been observed to exhibit lower critical solution temperature (LCST) phenomena, which is solubility promoted by cooling in successive freeze–thaw cycles. Sodium hydroxide solutions swell cellulose and, with suitable concentration and heating, cause change from type I to type II crystals in the mercerization process. However, upon cooling using a series of freeze–thaw cycles, cellulose dissolves in sodium hydroxide solution. Solubility is enhanced by adding urea to sodium hydroxide to increase hydrogen-bonding capacity. Dipolar aprotic solvents such as N,N-dimethylformamide (DMF), N,N-dimethylacetamide (DMAc) and dimethylsulfoxide (DMSO) are efficient solvents for cellulose when some lithium chloride is added to increase dielectric constant.

The zwitterionic solvent, N-methylmorpholine-N-oxide (NMMO) dissolves cellulose and allows purification by filtration. Pure NMMO is a solid at ambient temperatures, so solutions are made at elevated temperature with addition of some water. NMMO is non-volatile and can be regenerated after dilution with water to precipitate cellulose and then evaporation of water from the NMMO filtrate, allowing it to be recycled. NMMO solutions are injected into a precipitation bath to form regenerated cellulose fibres under the names Lyocel (Lenzing AG, Lenzing, Austria) and Tencel (Courtaulds Fibres UK, currently by Tencel Group). Ionic liquids are similar to NMMO except that they are cationic with a separate counter-anion. Examples of ionic liquids used to dissolve cellulose are 1-allyl-3-methylimidazolium

© Woodhead Publishing Limited, 2014

chloride (AmimCl) and 1-ethyl-3-methylimidazolium acetate (EmimAc), with the acetate derivative being preferred.

2.6 Sources of cellulose

Cellulose is the main cell wall or structural component of plants and is found in all plants, some bacteria and algae. A closely related polysaccharide, chitin (2-acetamidocellulose) constitutes the fabric of the cell walls of fungi, exoskeletons of crustaceans and insects, molluscs, and beaks and shells of squid and octopuses. A plant cell wall is a composite of cellulose, lignin, pectin and hemicelluloses that provides strength, rigidity, and prevents swelling of the cell. The main source of cellulose is wood. The composition of wood contains about 30–40% cellulose depending on species, with the remainder composed of lignin, hemicellulose and a complexity of minor components. Cellulose fibres for textiles are derived from cotton, a fibrous and relatively pure form of cellulose. Bamboo is a diverse source of cellulose for construction, furnishings and regenerated fibres. Another source of cellulose is bast fibres, such as the external stalk skeletal structures from flax (see Ghasemnejad and Aboutorabi in this volume, Chapter 13), kenaf, hemp, ramie (see Crosky *et al.*, Chapter 9) and jute (see Summerscales and Grove, Chapter 7). Fruit fibre residues, grains and husks (hierarchical polymeric materials) are waste material cellulose sources.

2.7 Separation of cellulose

Cellulose fibres co-exist with many other plant components that are necessary for functioning of the plant, but they do not contribute to mechanical properties and performance. These components are likely to detract from adhesion of fibres with a polymer matrix, they may discolour with heat or sunlight, and they conceal the flexibility and processability of cellulose fibres. There are many methods of separation, some partial, depending on the plant material and conditions. Retting is a natural process where the plant material, particularly bast fibres, is left in contact with stagnant water. Bast fibres have the cellulose fibres as an exoskeleton and microorganisms in the water biodegrade other components faster than they degrade the closely packed cellulose crystals in the fibres. Retting is used for flax, hemp, ramie and jute, for example. Retting is a partially selective natural purification step that makes the original plant material degraded sufficiently for further purification.

Decortication is a physical process where the plant materials are beaten or physically disrupted by passing through sets of rollers with roughened surface to shred the plants and release fibres. The fibres resist mechanical rupture more than the rest of the plant because they are stronger and more

© Woodhead Publishing Limited, 2014

flexible. The fibres are released from the complex composite structures of the plant material though all the components are still present. The fibres can be separated by blowing away degraded plant residues in a stream of air. Often further purification may follow; however, the mechanical process is an effective first stage.

Steam explosion physically disrupts fibres from within. Fibres in water are heated under pressure so that the water temperature is well above its atmospheric boiling temperature. The super-heated water penetrates the fibres swelling them. Sudden release of the pressure causes the water to rapidly boil, including the water within the plant material. The force of the rapidly boiling water within the plant materials causes physical disruption that releases the fibres. The fibres are not significantly damaged because of strength, crystal structure and limited water uptake compared with the rest of the material. Some cellulose fibre degradation may occur depending on the severity of treatment, that is, time and temperature. An indication of cellulose degradation is formation of 5-hydroxymethylfurfural (Jacquet *et al*., 2011). Steam processing has been used in conjunction with hydrogen-bonding solvent systems, such as aqueous alkali or lithium chloride–urea solutions at 120–130°C. These solutions enable less liquid to be used due to their enhanced swelling ability (Tatárová *et al*., 2012) (see Chapter 7 in this volume by Summerscales and Grove).

2.8 Purification of cellulose

A first step in cellulose purification is often organic solvent extraction with acetone or ethanol, to remove waxes. After acetone extraction the fibres have increased water absorptivity. Alkali extraction is then used to dissolve or partially dissolve lignin and pectins. Lignins, pectins and hemicelluloses possess acidic phenolic groups in the former and carboxyl groups in the latter two. Swelling of cellulose will occur during alkali treatment and this may be accompanied by crystal rearrangement from type I to type II, depending on alkali concentration, temperature and time. Purification of cellulose may include chemical procedures such as acid hydrolysis, chlorination, alkaline extraction, and bleaching (Morán *et al*., 2008). Acidic hydrolysis includes pectins, hemicellulose and some cellulose. Acid hydrolysis of cellulose occurs more rapidly with amorphous regions and then less perfect crystals, so while some cellulose is lost the remaining cellulose is more pure. More details of acid hydrolysis are given in the nano-cellulose section.

Oxidative alkaline extraction is used to bleach the product cellulose, however the treatment likely produces further carboxyl groups that are soluble in the concurrent alkali of the sodium hypochlorite and chlorite. A milder and selective form of hydrolysis of pectins is performed with the enzyme

© Woodhead Publishing Limited, 2014

pectinase. Pectinase is an active pectolytic enzyme preparation produced by a selected strain of *Aspergillus aculeatus* that contains mainly pectintranseliminase, polygalacturonase, and pectinesterase and small amounts of hemicellulases and cellulases. Pectinase hydrolyses pectin, which is a component of the cell wall. They may attack methyl-esterified pectin or de-esterified pectin. It is a source of pectinase activity, also containing cellulase and hemicellulase activities (P2611 from Sigma-Aldrich Chemical Company). Pectinase solution in a pH buffer at moderate temperature (38°C) is used to incubate raw cellulose and after the treatment and washing pectins will have been removed without harsh reagents and treatments previously described.

2.9 Cellulose polymorphism

Crystalline cellulose takes on several morphologies depending on source and treatment. Cellulose type I is native cellulose found in most plant cell walls and structures. Cellulose type II is textile cellulose obtained by heating with strong alkalis, such as 2 mol/L sodium hydroxide, a process called Mercerization. Cellulose III and IV are less widely found and occur in combination with types I and II depending on extend of treatment. Cellulose I crystallizes in monoclinic sphenodic structures with unit cell lattice parameters: $a = 0.835$ nm; $b = 1.03$ nm; $c = 0.79$ nm (Meyers *et al*., 2008). Cellulose crystals in sugarcane culms were assessed using wide-angle X-ray scattering (WAXS) and microfibril angles were greater for bundles from pith compared with bundles from intermediate regions and rind. Microfibril angles were similar for sugarcane cultivars, culm internodes, and ratoon cane. Scherrer analyses of diffraction peaks widths gave crystal size from equatorial [200] reflection and apparent crystal lengths from meridional [002] and [004] reflections that were similar to wood and bamboo (Driemeier *et al*., 2012; Ouajai and Shanks, 2006). WAXS detects crystal types, crystallinity and orientation, by comparison of coherent scattering or diffraction from repeating arrays of atoms in the regular crystal morphologies.

Small-angle X-ray scattering (SAXS) is used to characterize crystal dimensions and shape. SAXS was performed on flax fibre bundles to measure the cellulose microfibril structure. Microfibril misalignment depended on hydration level. A crystalline/non-crystalline repeat distance of 0.6–0.7 nm was found. Structure of the fibres differed between dry and wet states (Astley and Donald, 2001). Fibre symmetry of collagen or cellulose and synthetic polymers can be measured using SAXS and WAXS. WAXS allows determination of an orientational angle since fibres exhibit cylindrical rotational symmetry, resulting in a distribution of orientation angles known as orientation distribution function. Mathematical analysis of orientation from scattering patterns applies to both SAXS and WAXS (Burger *et al*., 2010).

© Woodhead Publishing Limited, 2014

2.10 Chemical modification of cellulose

Alkyl celluloses, such as methyl and ethyl cellulose, with varying degrees of substitution impart solubility. With low substitution methyl cellulose is soluble in water and used as a rheological agent. At high degrees of substitution methyl celluloses (MC) become soluble in organic solvents such as dichloromethane. Ethyl cellulose solutions in m-cresol exhibit lyotropic liquid crystalline solution behaviour accompanied by transient rheological behaviour. Transient viscosity in creep revealed that director tumbling occurred for ethyl cellulose solutions with large strain recoveries obtained in recoil (Lizaso *et al*., 1999).

Cellulose nitrate (NC), cellulose acetate (CA), cellulose propionate (CP), cellulose acetate propionate (CAP), cellulose acetate butyrate (CAB), MC, carboxymethyl cellulose (CMC), hydroxyethyl cellulose, hydroxypropyl cellulose and combinations of these derivatives are used to reduce free hydroxyl groups and hence hydrogen bonding, providing soluble forms of cellulose for conversion into fibres, film and coatings..

Cellulose-2,5-acetate was produced as a thermoplastic polysaccharide and used in reactive processing where cyclic lactones were grafted with choice of processing parameters such as temperature, feed ratio and screw speed determining molecular architecture, mechanical and thermal properties (Warth *et al*., 1997). Cellulose gels were formed by crosslinking cellulose with adipoyl chloride or 4-pentenyl chloride where a second functionality was the alkene bond. The gels exhibited liquid crystallinity and were swelled by DMF and acetone (Marsano *et al*., 1997). CAP and CAB are formed in addition to pure CA or higher carbon number esters. CP has been found to be more compatible or even miscible with synthetic polymers and biopolymers such as poly(3-hydroxybutyrate) (PHB) to form blends with a single glass transition temperature, improved tensile properties and ductility (Maekawa *et al*., 1998). Grafting with maleic anhydride, silane derivatives, allyl cellulose, allyl CMC and allyl hydroxypropyl cellulose has been used to prepare further functional derivatives.

Grafting into cellulose fibres has been performed using acrylonitrile (AN) initiated by azobisisobutyronitrile (AIBN). Sodium hydroxide pretreated fibres exhibited a decrease of crystallinity measured using Fourier transform infrared (FTIR) spectroscopy. Structural transformation of fibres from cellulose I to cellulose II was observed at high sodium hydroxide concentrations. The degree of grafting depended upon AIBN and monomer concentrations. AN grafted fibres showed no further transformation of crystal structure as observed after sodium hydroxide treatment. A change in X-ray measured crystallinity with grafting was observed. Moisture regain of pre-treated and grafted fibres depended on fibre structure and degree of grafting. Mechanical properties measured using a single fibre test were

© Woodhead Publishing Limited, 2014

determined by the cellulose structure, lateral crystallinity index and graft fraction. Scanning electron microscopy (SEM) was used to characterize surface morphologies of the treated fibres (Ouaja *et al.*, 2004).

2.11 Preparation of nano-cellulose

Several forms of cellulose are available where dimensions are small while internal structure is maintained. Examples are MCC, microfibrulated cellulose (MFC), CNF, CNC, bacterial cellulose, cellulose nanowhiskers (CNW); partial hydrolysis, separation from soluble by-products by dialysis (see Staiger, Chapter 15). Each form is prepared by partial and selective hydrolysis of purified cellulose. The cellulose is mixed with aqueous mineral acid, such as sulphuric acid and, after a set time which may involve warming, the suspension is diluted and neutralized. The remaining cellulose is that which has the most perfect crystal structure, since amorphous and semi-regular crystals are hydrolysed first due to facile diffusion of the acid into less tightly packed structures. MCC can be separated by filtration. CNF, CNC and CNW are too small to be seen in suspension or filtered from suspension, so the hydrolysis products (glucose and oligosaccharides) and salts from neutralization are separated using dialysis. The nano-dimensioned cellulose remains in suspension and can be isolated by freeze drying or evaporation of the water.

2.12 Processing of cellulose

Cellulose cannot be directly melted, so processing is performed via solution or derivatization. Solutions in solvents, previously discussed in Section 2.5, allow cellulose to be separated from insoluble impurities and then regenerated by injecting into a non-solvent. Fibres regenerated from solution are available under names such as Rayon, Lyocell and Tencel. Films are similarly formed, such as cellophane. NMMO is a recent commercial solvent, however ionic liquids dissolve cellulose and are being investigated as newer solvents. Solutions can be injected as fibres, cast as films, extruded and moulded with the distinction from thermoplastics that the solvent must be washed from the product since the solvents are non-volatile. The new solvents can be purified and recycled resulting in more environmentally friendly production.

Other processing using typically organic solvent can be performed when cellulose derivatives are used. Cellulose derivatives are soluble in a wide range of solvents from water, for methyl and ethyl celluloses and CMC, acetone and dichloromethane for highly substituted MC for example.

Cellulose was dissolved in NMMO to give a solution concentration of 12% w/v with low solution viscosity at 100°C. The solution was combined

© Woodhead Publishing Limited, 2014

with hemp fibres and at ambient temperature the solid mixtures compression moulded at 85°C to obtain a flat smooth-surfaced composite sheet of approximately 0.2 mm thickness. Cellulose was regenerated from NMMO solution with 50:50 water–ethanol that was used to wash NMMO from the composite. FTIR spectroscopy and wide-angle X-ray scattering were performed to investigate the structural change of cellulose from fibre (cellulose I) into partially regenerated composite (cellulose II), while the hemp fibres retained their original crystal structure. Composition and thermal stability of composites were investigated using TGA. A broadening of the diffraction peak of the main crystalline plane (0,0,2) and a depression of the degradation temperature of the fibres were observed. The mechanical properties of composites depended on fibre content, size, surface area, crystallinity and the structural swelling of fibres during NMMO treatment (Ouajai and Shanks, 2009).

2.13 Applications of cellulose fibres

Cellulose fibres are foremost used in textiles with cotton being a well-known example. Hemp was widely used for clothing and ship sails in the past. Flax, processed to provide linen, has a long history of application in household textiles. The fibres are combined into a yarn, which is then woven into cloth in most textiles. Many weave patterns are in use to provide the bulking, flexibility and feel of textiles. Non-woven textiles are formed by needle-punching or felting in which the fibres are tightly entangled into a dense mat that has characteristics of a textile. Non-woven textiles cost less to produce and are typically used for soft furnishings such as curtains. A significant property of textiles is thermal and sound insulation, as well as decoration. They are suitable for composite preparation due to low cost and ultimate binding by a matrix resin. In addition to textiles, cellulose fibres are woven into cords and rope, each a one dimensional type of textile.

Cellulose fibres present as wood are already in a suitable form for construction, since wood can be shaped and fastened. In addition to shaping by cutting, wood can be shaped by bending under water and heat. The wood or other cellulose fibres can be used in polymer composites in particulate (wood flour), fibrous (separated cellulose fibres) or laminates (wood veneers). The matrix resins used to bind cellulose reduce moisture susceptibility, increase dimensional stability and allow consistent and uniform size and shapes to be readily supplied.

In summary, cellulose finds many applications as fibres, insulation materials, textiles – both woven and non-woven (felted), rope and cords, building materials and composites, thickening additives in water and organic solvent, pharmaceutical carriers, reinforcement (see Lee and Bismarck, at Chapter 3), paper, paperboard, cellulose ester films and sheets, automotive

© Woodhead Publishing Limited, 2014

composites, many varieties of packaging materials, composite beams, decking, cladding and membranes.

2.14 Conclusions

Cellulose fibres are a readily available, renewable resource that requires separation and purification. The source and type of cellulose determines applications since structure is predetermined, though able to be modified. Cellulose is modified by transformation of crystal structure from type I to type II, derivatization and grafting. Cellulose has high modulus and strength, though it is humidity and moisture-immersion sensitive. Cellulose is hydrophilic, while most polymers are hydrophobic, therefore it requires compatibilization or coupling agents when combined with other polymers. Cellulose fibres are convertible into micro- and nano-forms for rheology control and high surface area, giving efficient enhancements at low concentration. Processing limitations occur due to temperature sensitivity, excessive loss of moisture causes embrittlement and high temperatures cause chemical dehydration followed by degradation. Solution processing has been expanded due to use of NMMO and ionic liquids as efficient solvents. With these and many more specific treatments and modifications cellulose is finding renewed interest as an advanced material and in nanomaterials.

2.15 References

Abidi, N., Cabrales, L. and Hequet, E. (2009), Thermogravimetric analysis of developing cotton fibers. *Thermochimica Acta*, **498**, 27–32.

Astley, O. M. and Donald, A. M. (2001), A small-angle x-ray scattering study of the effect of hydration on the microstructure of flax fibers. *Biomacromolecules*, **2**, 672–680.

Burger, C., Hsiao, B. S. and Chu, B. (2010), Preferred orientation in polymer fiber scattering. *Polymer Reviews*, **50**, 91–111.

Carpita, N. C. (2011), Update on mechanisms of plant cell wall biosynthesis: How plants make cellulose and other (1→4)-β-D-glycans. *Plant Physiology*, **155**, 171–184.

Cheng, G., Varanasi, P, Li, C., Liu, H., Melnichenko, Y. B., Simmons, B. A., Kent, M. S. and Singh, S. (2011), Transition of cellulose crystalline structure and surface morphology of biomass as a function of ionic liquid pretreatment and its relation to enzymatic hydrolysis. *Biomacromolecules,* **12**, 933–941.

Driemeier, C., Santos, W. D. and Buckeridge, M. S. (2012), Cellulose crystals in fibrovascular bundles of sugarcane culms: orientation, size, distortion, and variability. *Cellulose,* **19**, 1507–1515.

Fidale, L. C., Ruiz, N., Heinze, T. and Seoud, O. A. E. (2008), Cellulose swelling by aprotic and protic solvents: What are the similarities and differences? *Macromolecular Chemistry and Physics,* **209**, 1240–1254.

© Woodhead Publishing Limited, 2014

Guerriero, G., Fugelstad, J. and Bulone, V. (2010), What do we really know about cellulose biosynthesis in higher plants? *Journal of Integrative Plant Biology*, **52**, 161–175.

Jacquet, N., Quivy, N., Vanderghem, C., Janas, S., Blecker, C., Wathelet, B., Devaux, J. and Paquot, M. (2011), Influence of steam explosion on the thermal stability of cellulose fibres. *Polymer Degradation and Stability*, **96**, 1582–1588.

Kaplan, D. L. (1998), Introduction to biopolymers from renewable resources. In *Biopolymer Renewable Resources,* D. L. Kaplan (Ed.), pp. 1–29.

Lizaso, I., Munoz M. E. and Santamaria A. (1999), Transient rheological behavior of lyotropic solutions of ethyl cellulose in m-cresol. *Rheologica Acta*, **38**, 108–116.

Maekawa, M., Pearce, R. H., Marchessault, R. H. and R. S. J. Manley, R. S. J. (1998), Miscibility and tensile properties of poly(β-hydroxybutyrate)-cellulose propionate blends. *Polymer*, **40**. 1501–1505.

Marsano, E., Bianchi, E., Boero, E., Gastaldi, G. and Focher, B. (1997), Liquid crystalline polymer gels: preparation and swelling behavior of cellulose-based networks. *Polymers for Advanced Technologies,* **8**, 17–22.

Martin, A. R., Martins, M. A., da Silva, O. R. R. F. and Mattoso, L. H. C. (2010), Studies on the thermal properties of sisal fiber and its constituents. *Thermochimica Acta*, **506**, 14–19.

Meyers, M. A., Chen, P-Y., Lin, A. Y-M. and Seki, Y. (2008), Biological materials: Structure and mechanical properties. *Progress in Materials Science,* **53**, 1–206

Morán, J., Alvarez, V., Cyras, V. and Vázquez, A. (2008), Extraction of cellulose and preparation of nanocellulose from sisal fibers. *Cellulose*, **15**, 149–159.

Ouajai, S. and Shanks R. A. (2009), Preparation, structure and mechanical properties of all-hemp cellulose biocomposites. *Composites Science and Technology,* **69**, 2119–2126.

Ouajai, S. and Shanks, R. A. (2006), Solvent and enzyme induced recrystallization of mechanically degraded hemp cellulose. *Cellulose*, **13**, 31–44.

Ouajai, S., Hodzic, A. and Shanks, R. A. (2004), Morphological and grafting modification of natural cellulose fibers. *Journal of Applied Polymer Science*, **94**, 2456–2465.

Rachini, A., Troedec, M. L., Peyratout C. and Smith, A. (2009), Comparison of the thermal degradation of natural, alkali-treated and silane-treated hemp fibers under air and an inert atmosphere. *Journal of Applied Polymer Science*, **112**, 226–234.

Ross, P., Mayer, R. and Benziman, M. (1991), Cellulose biosynthesis and function in bacteria. *Microbiology Reviews*, **55**, 35–58.

Saxena, I. M and Brown, M. D. (2005), Cellulose biosynthesis: current views and evolving concepts. *Annals Botany*, **96**, 9–21.

Tatárová, I., MacNaughtan, W., Manian, A. P., Široká, B. and Bechtold, T. (2012), Steam processing of regenerated cellulose fabric in concentrated LiCl/urea solutions. *Macromolecular Materials and Engineering*, **297**, 540–549.

Warth, H., Mulhaupt, R. and Schatzle, J. (1997), Thermoplastic cellulose acetate and cellulose acetate compounds prepared by reactive processing. *Journal of Applied Polymer Science,* **64**, 231–242.

© Woodhead Publishing Limited, 2014

2.16 Appendix: abbreviations

AIBN	azobisisobutyronitrile
AN	acrylonitrile
CA	cellulose acetate
CAB	cellulose acetate butyrate
CAP	cellulose acetate propionate
CMC	carboxymethyl cellulose
CNC	cellulose nano-crystals
CNF	cellulose nano-fibres
CNW	cellulose nanowhiskers
CP	cellulose propionate
DMAc	N,N-dimethylacetamide
DMF	N,N-dimethylformamide
DMSO	dimethylsulfoxide
DSC	differential scanning calorimetry
DTG	derivative thermogravimetry
FTIR	Fourier transform infrared
LCST	lower critical solution temperature
MCC	microcrystalline cellulose
MFC	microfibrillated cellulose
NC	cellulose nitrate
NMMO	N-methylmorpholine-N-oxide
SAXS	small-angle X-ray scattering
SEM	scanning electron microscopy
TGA	thermogravimetry
WAXS	wide-angle X-ray scattering

© Woodhead Publishing Limited, 2014

3

Creating hierarchical structures in cellulosic fibre reinforced polymer composites for advanced performance

K.-Y. LEE and A. BISMARCK, University of Vienna, Austria and Imperial College London, UK

DOI: 10.1533/9780857099228.1.84

Abstract: Interest in greener materials has re-energised the utilisation of natural fibres, but now as reinforcement for renewable polymers. However, such bio-based composites often fail to deliver in terms of mechanical performance. This chapter discusses nature-inspired hierarchical composites and evaluates the potential of these materials to create a new generation of advanced renewable composite materials. Three strategies for creating hierarchical structures are explored: surface microfibrillation of (ligno)cellulosic fibres; dispersing microfibrillated cellulose within the matrix of conventional fibre reinforced composites; and attaching nano-sized bacterial cellulose onto natural fibres. The mechanical performance of the resulting hierarchical (nano)composites reported so far is discussed. By creating hierarchical structures within composites, we could potentially bridge the property performance gap between renewable and petroleum-derived materials for commercial use.

Key words: bacterial cellulose, hierarchical composites, short-fibre composites, binder, polymer matrix composites.

3.1 Introduction

Nature maximises the efficiency of structural materials by organising them hierarchically – the arrangement of the constituents at every level, from the molecular to macroscopic level (Blaker *et al*., 2011). These hierarchically structured materials, such as bone and nacre, attain good mechanical performance from weak constituents by arranging them across multiple length scales (Mayer, 2005; Fratzl and Weinkamer, 2007; Luz and Mano, 2010). Bone, for example, possesses brittle nano-minerals arranged in a staggered fashion within a soft protein matrix. By confining the brittle minerals at the nanoscale, these minerals can be made insensitive to crack-like flaws (Gao *et al*., 2003). The large aspect ratio (~30–40) of the minerals compensates for the softness in the matrix and the combination of staggered minerals

© Woodhead Publishing Limited, 2014

arrangement and the soft protein matrix provides the stiffness/toughness required of bones (Gao, 2006).

However, translating these architectural features found in nature at the micro- and nano-scales into engineering materials still remains a major challenge. This is attributed to the difference in the design strategies used by material scientists/engineers and nature (see Fig. 3.1). Material engineers have greater choices of elements to create structural materials compared with nature. Nevertheless, nature has managed to find ways to produce stiff materials, such as trees and bones, from its limited choices of elements (Wegst and Ashby, 2004). The materials manufacturing processes of engineers and nature are also vastly different. Biological materials are *grown* by biologically controlled processes, whereas engineering materials are *fabricated* based on exact designs optimised by engineers. Moreover, biological materials have the ability to adapt, model and remodel in response to the ever-changing chemical environment and mechanical load throughout their lifetime. Living biological materials can even heal themselves.

Therefore, it is our challenge to exploit the mechanisms and opportunities found in nature to engineering materials. Unlike biological materials, engineering materials are not limited by the choices of elements, physiological requirements and environmental constraints such as temperature and

BIOLOGICAL MATERIALS	ENGINEERING MATERIALS
Light elements dominate: C, N, O, H, Ca, P, ...	**Large variety** of elements: Fe, Cr, Ni, Al, Si, C, N, O, ...
Growth by biologically controlled self-assembly (approximate design)	**Fabrication** from melts, powders, solutions, etc. (exact design)
Hierarchical structuring at all size and levels	**Forming** (of the part) and **micro-structuring** (of the materials)
Adaptation of form and structure to the function	**Selection** of material according to function
Modelling and remodelling: capability of adaptation to changing environmental conditions	**Secure design** (considering possible maximum loads as well as fatigue)
Healing: capability of self-repair	

3.1 A comparison between the design strategies for biological and engineering materials. (*Source*: Redrawn from Fratzl and Weinkamer (2007) with kind permission from Elsevier.)

© Woodhead Publishing Limited, 2014

pH. This chapter discusses the progress towards the realisation of renewable nature-inspired hierarchical composite materials and evaluate the potential of these materials to create a new generation of advanced renewable composites. Interest is growing in the development of renewable composites due to substantial environmental legislations and public demand for more environmental friendly products. We hope to bridge the property performance gap between renewable and petroleum-derived materials for commercial applications by creating hierarchical structures in renewable composite materials (see also Chapter 9).

3.2 Creating hierarchical structures in (ligno)cellulosic fibre reinforced composite materials

Although much work has been done towards utilising (ligno)cellulosic fibres as reinforcement for composite materials, these renewable composites often fall short of expectation due to poor compatibility between the fibre and the matrix. Chemical surface modification is often needed to enhance the fibre–matrix interface. Surface modifications often applied to natural fibres include silylation (Valadez-Gonzalez *et al*., 1999; Ganan *et al*., 2005; Mehta *et al*., 2006; Pothan *et al*., 2006), acetylation (Tserki *et al*., 2005), benzoylation (Nair *et al*., 2001), maleated coupling agents (Mishra *et al*., 2000), isocyanate treatment (George *et al*., 1996) and grafting polymers to natural fibres (Kaith and Kalia, 2008). This adds extra cost to the production of natural fibre reinforced composites, making the chemical treatments less attractive as a viable solution for the production of greener materials.

Moreover, chemical treatments of natural fibres do not always result in improved composite performance. The main reason is the anisotropicity of natural fibres themselves. The transverse modulus of natural fibres is orders of magnitude lower than the axial modulus (Cichocki and Thomason, 2002; Baley *et al*., 2006). Cichocki and Thomason (2002) showed that the axial modulus of jute fibre is 38.4 GPa but its transverse modulus is only 5.5 GPa. Baley *et al*. (2006) also showed that the axial modulus of flax fibre is seven times larger than the transverse modulus (axial modulus: 59 GPa, transverse modulus: 8 GPa). In addition to this, Thomason (2009) attributed the failure of natural fibre to deliver good performance in composites to the high linear thermal coefficient of expansion (LTCE) of natural fibres. The interfacial shear stress between the fibre and the matrix is the product of residual compressive stress (σ_r) and the static friction coefficient at the fibre–matrix interface. Due to the high LTCE of natural fibres, σ_r is lowered, leading to poor interfacial shear strength between the fibre and the matrix. Therefore, chemical modification of natural fibres might not be the best solution. Instead, lessons can be learnt from nature by creating hierarchical structures

© Woodhead Publishing Limited, 2014

in renewable composites to bridge this gap due to the shrinkage of (ligno) cellulosic fibres.

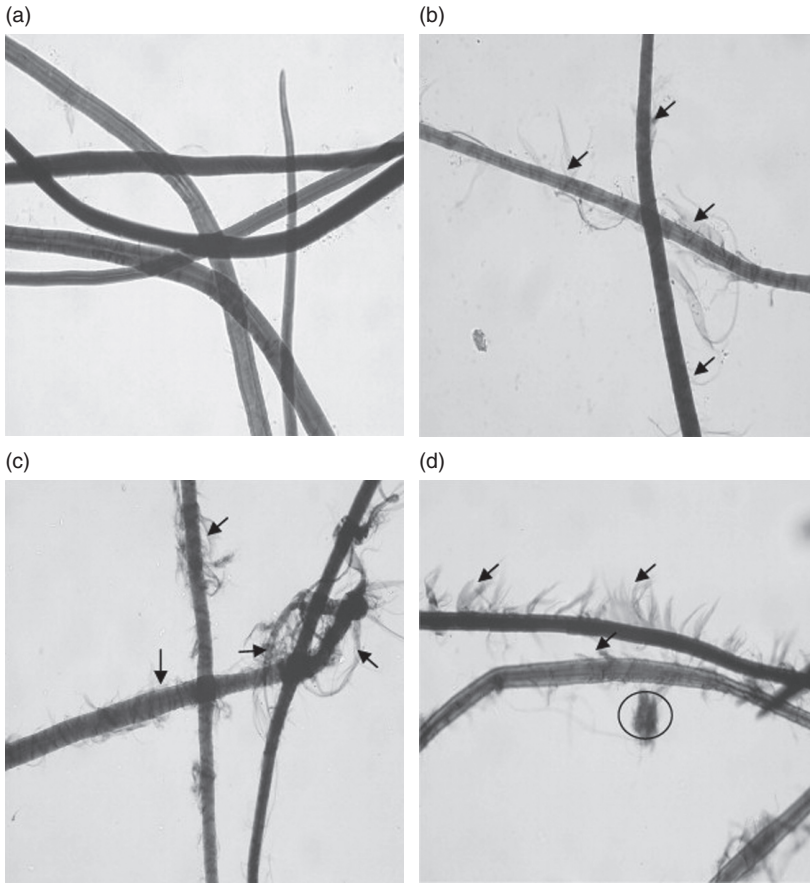
3.3 Surface microfibrillation of (ligno)cellulosic fibres

Hierarchical structures can be created by microfibrillating the surface of (ligno)cellulosic fibres. The surface microfibrillation can be conducted using a pulp refiner (Zhong *et al.*, 2011b) and the gap between the rotor and the stator discs of the refiner can be adjusted to achieve various degrees of surface microfibrillation (see Fig. 3.2). A plant cell wall is a multi-layered structure consisting predominantly of cellulose, hemicellulose and lignin Chapter 2; (Bismarck *et al.*, 2005). Through the use of the refiner, the microfibrils on the surface of the fibres can be liberated, producing 'hairy' fibres. The degree of microfibrillation was quantified using Schopper-Riegler (SR) values, which are used to quantify the drainability of fibre mats (Zhong *et al.*, 2011b). It can be seen from Fig. 3.2 that the SR values correlate well with the degree of microfibrillation observed using scanning electron microscopy. A larger degree of microfibrillation reduces the drainability of the fibre mat as a result of the liberated microfibrils reducing the porosity of the filter cake.

These 'hairy' fibres were used as reinforcement to produce hybrid phenolic resin composites. These composites contained 30 wt.% fibres, of which 80 wt.% of these fibres were 'hairy' sisal fibres and the rest were aramid fibres. The tensile modulus and strength of the 'hairy' sisal fibre reinforced hybrid composites increased by as much as 67% and 102%, respectively, compared with neat sisal fibre reinforced hybrid composites (see Table 3.1). Significant fibre pull-out from the composites was observed when neat sisal fibres were used. This led to the conclusion that the observed increment in the 'hairy' fibre reinforced hybrid composites was due to the enhanced fibre–matrix interface, possibly by mechanical interlocking due to the larger contact area provided by the liberated microfibrils (Zhong *et al.*, 2011b). In addition to hybrid composites, Zhong *et al.* (2011a) also produced 'hairy' sisal fibre reinforced phenolic resin, with 70 wt.% fibre loading. Both the tensile modulus and strength of the composites improved with increasing degree of microfibrillation (see Table 3.2). This improvement was attributed to enhanced mechanical interlocking and the extensive entanglement between the 'hairy' fibres.

A similar concept was also applied to regenerated cellulose fibres. Water is known as a swelling and fibrillating agent for Lyocell fibres (Marini, 1994). In order to determine the degree of fibrillation of Lyocell fibres, Marini (1994) developed the *shake test*. This test involves the immersion of the fibres in distilled water with shaking over a period of time, followed by drying and microscopic investigation. The influence of water and

© Woodhead Publishing Limited, 2014



3.2 Scanning electron micrographs of neat and surface microfibrillated sisal fibres. These images are taken at ×400 magnification. (a) Neat sisal fibres, (b) surface microfibrillated sisal fibres (18°SR), (c) surface microfibrillated sisal fibres (24°SR), and (d) surface microfibrillated sisal fibres (32°SR). The arrows indicate the microfibrils and the circle shows the detached microfibrils due to the severe microfibrillation of the fibres. (*Source*: Reprinted from Zhong *et al*. (2011b) with kind permission from Elsevier.)

mechanical stresses from the shaking motion results in the fibrillation of Lyocell fibres (Tomljenovic and Cunko, 2010). Instead of testing the fibrillation tendency of Lyocell fibres, Karlsson *et al*. (1996) used the method described in the s*hake test* to create hierarchical structures in the fibres by fibrillating them, producing 'hairy' fibres. The authors immersed Lyocell fibres in distilled water and mechanically treated them by shaking the vessel containing the fibres for either 3 or 9 h. It can be seen from Fig. 3.3 that the surface of the Lyocell fibres undergoes significant fibrillation,

© Woodhead Publishing Limited, 2014

Table 3.1 Tensile properties of hybrid phenolic resin composites reinforced with surface microfibrillated sisal fibres and neat aramid fibres

Types of sisal fibres	*E* (GPa)	σ (MPa)
Neat sisal	1.50	13.3
18°SR	2.50	25.1
24°SR	2.38	25.7
32°SR	2.25	26.9

The loading fraction of the sisal and aramid fibres is 30 wt.%.
The weight fraction of sisal fibres is 80 wt.% relative to the total mass of fibres used.
E and σ denote the tensile modulus and strength, respectively.

Source: Adapted from Zhong *et al*. (2011b).

Table 3.2 The tensile properties of sisal fibre reinforced phenolic resin composites with various degrees of microfibrillation

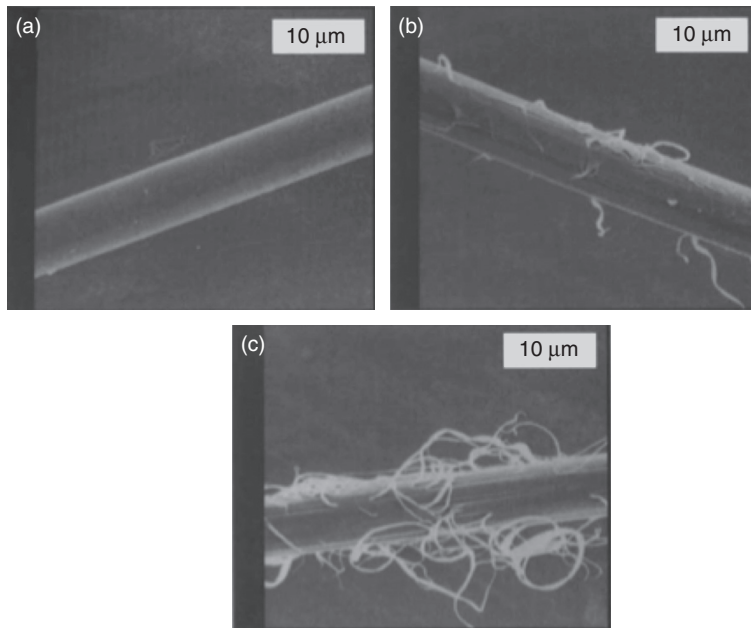
Degree of microfibrillation	*E* (GPa)	σ (MPa)
12°SR	0.74 ± 0.10	13.0 ± 1.5
14°SR	1.02 ± 0.11	18.0 ± 1.5
16°SR	1.24 ± 0.14	24.5 ± 2.2
21°SR	1.30 ± 0.13	24.3 ± 2.0
32°SR	1.46 ± 0.15	23.5 ± 2.0
46°SR	1.62 ± 0.14	22.8 ± 2.3

All the composites contain 70 wt.% sisal fibres. *E* and σ denote the tensile modulus and tensile strength of the composites, respectively.

Source: Adapted from Zhong *et al*. (2011a).

thereby creating 'hairy' fibres. The degree of fibrillation agrees well with the residence time of the fibres in water. No significant difference in the tensile strength was found between the neat and 9 h mechanically treated Lyocell fibres (~350 ± 70 MPa). Model composites of Lyocell fibres in low-density polyethylene (LDPE) were prepared by the authors to study the interfacial shear strength using single fibre fragmentation test (Table 3.3). An improved fibre–matrix interface was observed when 'hairy' Lyocell fibres were used in the matrix. The interfacial shear strength between the 'hairy' Lyocell fibres and LDPE increased by 75% when compared with neat Lyocell fibres. This improvement is attributed to the increased fibre roughness as a result of fibrillation, promoting anchoring sites for mechanical interlocking (Wu, 1982).

© Woodhead Publishing Limited, 2014



3.3 Scanning electron micrographs of Lyocell fibres at ×1000 magnification. (a) Neat Lyocell fibres, (b) Lyocell fibres shaken for 3 h and (c) Lyocell fibres shaken for 9 h in distilled water. (*Source*: Reprinted from Karlsson *et al*. (1996) with kind permission from John Wiley & Sons.)

Table 3.3 The critical length (l_c) and apparent interfacial shear strength (τ) of neat and mechanically treated Lyocell fibres in LDPE matrix

Types of fibres	l_c (mm)	τ (MPa)
Neat Lyocell fibres	0.75	4.8
3 h mechanically treated Lyocell fibres	0.57	6.6
9 h mechanically treated Lyocell fibres	0.53	8.4

Source: Adapted from Karlsson *et al*. (1996).

3.4 Creating hierarchical structures in renewable composites by incorporating microfibrillated cellulose (MFC) into the matrix

Hierarchical structures can also be created within composite materials by the addition of nano- or micro-sized cellulose into natural fibre reinforced polymer composites The addition of 10 wt.% microfibrillated cellulose (MFC) into the matrix of polylactide (PLLA) composites (containing 40 wt.% bamboo fibres) increased the 3-point bending strength by 14%

© Woodhead Publishing Limited, 2014

Table 3.4 Interfacial shear strength (τ_{IFSS}) and fracture toughness (G_{1C}) of bamboo fibres (with or without 10 wt.% MFC) dispersed in the matrix and polylactide

Composites	τ_{IFSS} (MPa)	G_{1C} (kJ m^{-2})
PLA-bamboo fibres (50:50 w/w)	5.0 ± 0.8	2.0 ± 0.8
PLA-MFC-bamboo fibres (50:10:40 w/w)	6.7 ± 0.9	3.8 ± 0.8

Source: Adapted from Okubo *et al.* (2005).

compared with 50 wt.% bamboo fibre reinforced PLLA composites without MFC dispersed in the matrix (Okubo *et al.*, 2005). The flexural modulus of the hierarchical composites also improved by 20% when compared with the composites without MFC dispersed in the matrix. This is attributed to the enhanced fibre–matrix interface as determined using micro-drop test. These results are tabulated in Table 3.4, along with the fracture toughness of the (hierarchical) composites. This could be a result of stiffening of the matrix due to the incorporation of stiff MFC.

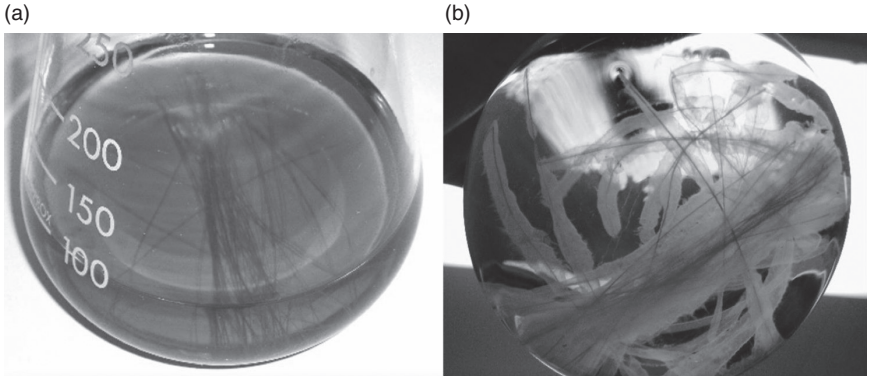
Okubo *et al.* (2005) also studied the crack propagation behaviour of the (hierarchical) composites. As soon as the crack reached the bamboo fibre when MFC was not dispersed in the matrix, the crack would propagate along the fibre–matrix interface, resulting in fibre pull-out. However, when MFC was dispersed in the PLLA matrix, the crack propagation behaviour was altered compared with composites without MFC dispersed in the matrix. It was observed that the crack would reach the fibre but fibre pull-out was not observed due to the enhanced fibre–matrix interface. Instead, fibre breakage was observed indicating that the maximum load of the fibres was utilised. In addition to this, the dispersion of MFC in the matrix was also found to be an important factor governing the crack propagation through the composites (Okubo *et al.*, 2009).

3.5 Coating of (ligno)cellulosic fibres with bacterial cellulose

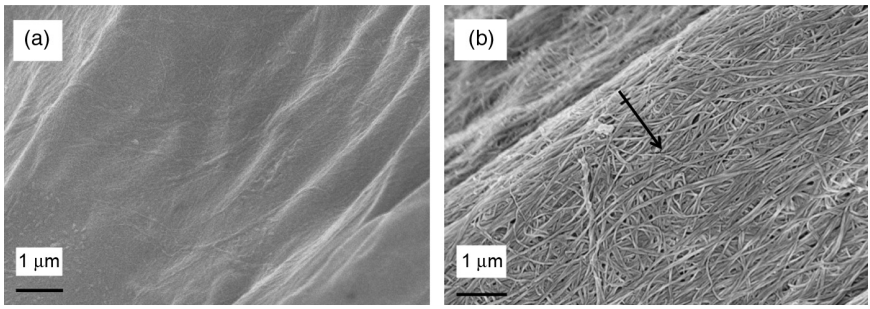
3.5.1 Culturing of bacterial cellulose in the presence of natural fibres

Cellulose can be synthesised by bacteria, such as from the *Acetobacter* species (Brown, 1886; Lee *et al.*, 2013). By culturing cellulose-producing bacteria in the presence of natural fibres in an appropriate culture medium, bacterial cellulose (BC) is preferentially deposited *in situ* onto the surface of natural fibres (Juntaro *et al.*, 2007, 2008; Pommet *et al.*, 2008; Juntaro, 2009). Figure 3.4 shows the images of the culture medium and natural fibres immersed in the culture medium before and two days after culturing (Pommet *et al.*, 2008).

© Woodhead Publishing Limited, 2014



3.4 Images showing (a) natural fibres immersed in a culture medium of *Gluconacetobacter xylinum* before bacteria culturing and (b) the culture medium after two days. (*Source*: Reprinted from Pommet *et al*. (2008) with kind permission from ACS Publications.)



3.5 Scanning electron micrographs showing (a) neat sisal fibre and (b) sisal fibre coated with bacterial cellulose. (*Source*: Reprinted from Pommet *et al*. (2008) with kind permission from ACS Publications.)

A layer of BC pellicles can be seen growing away from the surface of the natural fibres. After extraction from the culture medium and purification, a layer of BC nanofibrils can be seen attached onto the surface of sisal fibres under scanning electron microscopy (Fig. 3.5b). Simple weight gain measurements showed that approximately 5–6 wt.% of BC was deposited onto the surface of these natural fibres (Pommet *et al*., 2008). The introduction of BC onto natural fibres provides new means of controlling the interaction between natural fibres and polymer matrices. Utilising BC-coated natural fibres as reinforcement introduced nanocellulose into the composites at the interface between the fibres and the matrix, leading to increased stiffness of the matrix around the natural fibres. The coating of natural fibres with BC could also be a potential solution to the aforementioned shrinkage of

© Woodhead Publishing Limited, 2014

natural fibres during thermal processing of the composites. Due to the low thermal expansion of BC (0.1×10^{-6} K^{-1}) (Nishino *et al.*, 2004), the BC coating could potentially bridge the gap that forms between the fibres and the matrix due to the high linear coefficient of thermal expansion (LCTE) of natural fibres.

However, the mechanical properties of the natural fibres after BC modification depend on the type of natural fibres used. The modification process did not affect the mechanical properties of sisal fibres but the properties of hemp fibres decreased significantly (see Table 3.5). This might be due to a further separation of the bast fibres into smaller individual fibres making up the technical fibre as a result of the intrinsically non-cohesive structure of bast fibres. The interfacial shear strengths between sisal fibres and cellulose acetate butyrate (CAB) and PLLA increased by 46% and 21%, respectively, and the interfacial shear strength between hemp fibres and CAB increased by as much as 140% (Table 3.6). It should be noted that the increment seen in the interfacial shear strength between hemp fibres and CAB could also be due to the combined effect of BC coating and the disintegration of the fibres, resulting in significant fibre fibrillation. This improvement seen in the interfacial shear strengths indicates enhanced stress transfer between the fibres and the matrix, which is a direct result of improved interfacial adhesion due to the BC coating applied to natural fibres.

BC modified sisal and hemp fibres have also been used to produce unidirectional natural fibre reinforced CAB and PLLA model composites (Juntaro *et al.*, 2007, 2008). The mechanical properties of BC-coated sisal fibre reinforced polymers showed significant improvements over neat

Table 3.5 The mechanical properties of natural fibres modified with BC nanofibrils

Natural fibres	Young's modulus (GPa)	Tensile strength (MPa)	Elongation at break (%)
Neat sisal fibre	15.0 ± 1.2	342 ± 33	2.9 ± 0.1
BC modified sisal fibre	12.5 ± 1.0	324 ± 33	4.5 ± 0.4
BC modified sisal fibre with purification*	12.0 ± 0.9	310 ± 32	4.1 ± 0.5
Neat hemp fibre	21.4 ± 2.0	286 ± 31	2.0 ± 0.2
BC modified hemp fibre	8.8 ± 0.7	171 ± 11	2.9 ± 0.2
BC modified hemp fibre with purification*	8.0 ± 0.6	130 ± 12	2.9 ± 0.2

*Purification indicates the extraction of post-BC modified sisal fibres with NaOH at 80°C.

Source: Adapted from Pommet *et al.* (2008).

© Woodhead Publishing Limited, 2014

Table 3.6 Interfacial shear strengths between modified natural fibres and CAB or PLLA

Natural fibres	Interfacial shear strength to CAB (MPa)	Interfacial shear strength to PLLA (MPa)
Neat sisal fibre	1.02 ± 0.06	12.1 ± 0.5
BC modified sisal fibre	1.49 ± 0.03	14.6 ± 1.2
Neat hemp fibre	0.76 ± 0.06	–
BC modified hemp fibre	1.83 ± 0.12	–

Source: Adapted from Pommet *et al*. (2008) and Juntaro *et al*. (2008).

Table 3.7 Mechanical properties of BC modified hemp and sisal fibres reinforced CAB and PLLA composites

Composites	Neat fibre		Modified fibre		Improvements	
	σ (MPa)	E (GPa)	σ (MPa)	E (GPa)	σ (%)	E (%)
CAB/hemp*	98.1 ± 12.7	8.5 ± 1.3	86.7 ± 13.6	5.8 ± 0.5	–12	–35
PLLA/hemp*	110.5 ± 27.2	11.8 ± 4.2	104.8 ± 9.1	7.9 ± 1.2	–5	–33
CAB/sisal*	92.9 ± 9.3	5.5 ± 0.5	100.4 ± 7.0	8.8 ± 1.4	8	59
PLLA/sisal*	78.9 ± 14.7	7.9 ± 1.3	113.8 ± 14.0	11.2 ± 1.2	44	42
CAB/hemp†	15.8 ± 2.2	1.9 ± 0.1	13.4 ± 1.4	0.6 ± 0.2	–15	–69
PLLA/hemp†	13.4 ± 3.6	3.2 ± 0.2	13.3 ± 2.5	2.3 ± 0.3	–1	–28
CAB/sisal†	10.9 ± 1.7	1.6 ± 0.1	14.4 ± 3.7	1.8 ± 0.3	32	15
PLLA/sisal†	10.0 ± 3.1	2.1 ± 0.1	16.8 ± 4.1	3.1 ± 0.2	68	49

*The loading direction is parallel (0°) to the fibres.

†The loading direction is perpendicular (90°) to the fibres.

Source: Adapted from Juntaro *et al*. (2007).

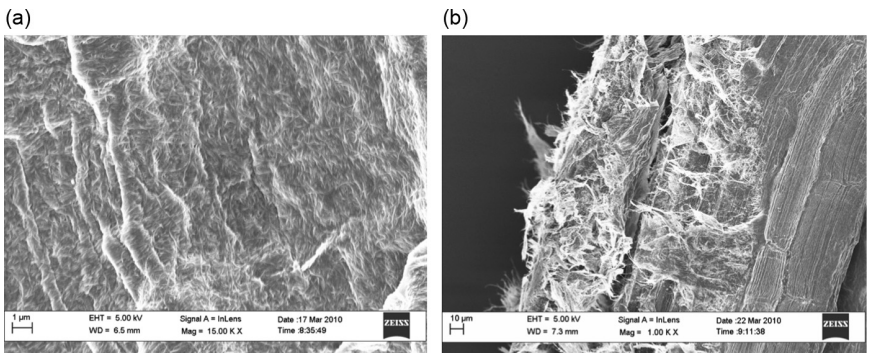
polymers (Table 3.7). The tensile strength and modulus for sisal/PLLA composites improved by as much as 68% and 49%, respectively. However, improvements were not observed for composites containing BC-coated hemp fibres. The tensile strength and modulus decreased by as much as 15% and 69%, respectively, for hemp–CAB composites. One should note that the fibres were damaged during bacteria culture and their tensile strength was only one third that of the original fibres. The use of BC-coated sisal fibres also led to some improvements in the tensile modulus and flexural properties of the randomly oriented short sisal fibre reinforced PLLA composites (Juntaro, 2009). However, the tensile strength of the composites did not show improvement over the neat polymer (see Table 3.8). The tensile strength of neat sisal fibre reinforced PLLA composites dropped to roughly half of pure polymer. The same trend was also observed for BC-coated sisal fibre reinforced PLLA composites. It was postulated that the lack of improvements in the hierarchical composites could be a result of fibre damage induced by

© Woodhead Publishing Limited, 2014

thermal processing. In addition to this, the relatively high cost associated with the culturing cellulose-producing bacterial in the presence of natural fibres limits the potential of this coating technique to be scaled up.

3.5.2 Coating the surface of natural fibres with bacterial cellulose using a slurry dipping method

A novel, simple and cost effective method based on slurry dipping to coat sisal fibres with nano-sized BC without the need of bioreactors was developed (Lee *et al*., 2012a). The morphology of BC-coated sisal fibres (see Fig. 3.6) resembles that of the BC-coated fibres obtained by culturing *Acetobacter* in the presence of sisal fibres in a bioreactor (Fig. 3.5). It was also possible to obtain true 'hairy' BC-coated sisal fibres by employing a different drying regime (Fig. 3.6b). The loading fraction of BC on sisal fibres obtained by this method was found to be 10 ± 1 wt.%. Natural fibres when immersed into dispersions of BC in water will absorb water into the fibres, drawing in the water and BC nanofibrils from the medium. BC nanofibrils are filtered against the surface sisal fibres, resulting in a BC coating of sisal fibres. The fast drying rate of the coated fibres under vacuum resulted in the collapse of BC nanofibrils onto the surface of sisal fibres (Fig. 3.6a). By pressing the wet BC-coated sisal fibres between filter papers, the fibres were partially dried. It is hypothesised that during this process, the water contained in the BC nanofibrils was drawn into the filter paper by capillary action. The combination of capillary action with the slow drying of the coated fibres (which prevents the collapse of the nanofibrils) results in a BC coating in which BC

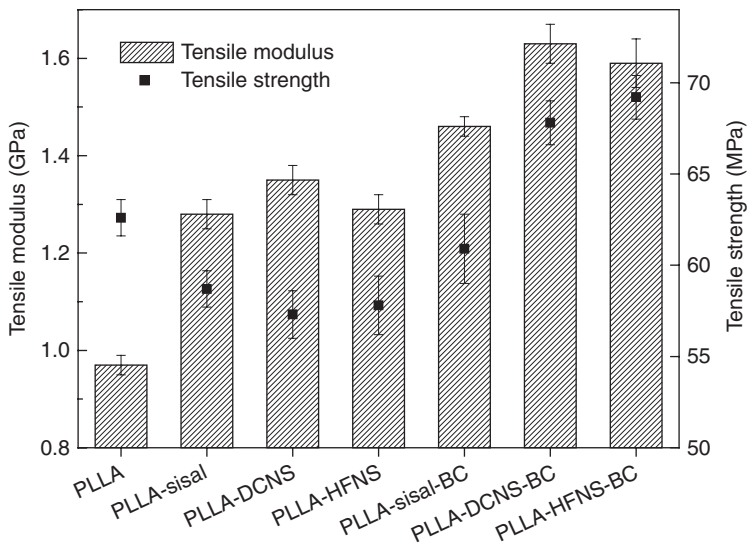


3.6 Scanning electron micrographs showing (a) sisal fibres coated with a dense layer of BC and (b) 'hairy' sisal fibres produced using a novel slurry dipping method. A dense layer of BC on sisal fibres was obtained by drying the slurry-dipped fibres under vacuum at 80°C. 'Hairy' sisal fibres were obtained by partially drying the slurry-dipped fibres between filter papers, followed drying in an air oven held at 40°C.

© Woodhead Publishing Limited, 2014

nanofibrils were oriented perpendicular to the sisal surface. The morphology resembles 'hairy fibres' (Fig. 3.6b).

The tensile properties of randomly oriented short (BC-coated) sisal fibre reinforced PLLA composites were studied by Lee *et al*. (2012a). Two different types of hierarchical composites were prepared; (i) BC-coated sisal fibre reinforced PLLA and (ii) BC-coated sisal fibre reinforced PLLA–BC nanocomposites. The former composites contained BC on the surface of sisal fibres only, and the latter composites contained BC both on the fibre surfaces and dispersed within the PLLA matrix. From the results summarised in Fig. 3.7, it can be seen that with (BC-coated) sisal fibres as reinforcement, the tensile moduli for all composites increased. The increase in the tensile modulus of the hierarchical composites was enhanced when BC was additionally dispersed in the matrix. This is thought to be due to the stiffening of the matrix by BC. It has been shown that a PLLA matrix can be stiffened by as much as 40% if BC is dispersed in the matrix at a loading fraction of 5 wt.% (Lee *et al*., 2009). With BC dispersed in the matrix and attached to the fibres, both the matrix and the fibre–matrix interface could be reinforced



3.7 Tensile properties of (hierarchical) sisal fibre reinforced PLLA (nano) composites. PLLA-sisal, PLLA-densely coated neat sisal (DCNS) and PLLA-hairy fibres, neat sisal (HFNS) denote PLLA (nano)composites reinforced with 20 wt.% neat sisal fibres, densely coated neat sisal fibres and 'hairy' fibres of neat sisal, respectively. PLLA-sisal-BC, PLLA-DCNS-BC and PLLA-HFNS-BC represent PLLA nanocomposites reinforced with 15 wt.% neat sisal fibres, densely coated neat sisal fibres and 'hairy' fibres of neat sisal, respectively, with 5 wt.% BC dispersed in the matrix. (*Source*: Adapted from Lee *et al*. (2012a).)

© Woodhead Publishing Limited, 2014

(or stiffened). The tensile strength of the hierarchical composites showed a slightly different trend compared with tensile modulus. A decrease in tensile strength was observed when PLLA is reinforced with (BC-coated) sisal fibres, with no BC dispersed in the matrix. This result is consistent with studies by Juntaro (2009) (see Table 3.8). When the hierarchical composites were reinforced with BC dispersed in the PLLA matrix, the tensile strength improved by as much as 11% when compared with neat PLLA, and 21% when compared with BC-coated sisal fibre reinforced PLLA composites without BC dispersed in the matrix. This could be due to enhanced interfacial adhesion between BC-coated fibres and BC reinforced PLLA matrix. With BC dispersed in the matrix, the matrix is stiffened.

The more interesting results came from the fractography analysis of the composites that failed in tension. In general, short-fibre composites exhibit a combination of failures, and fracture occurs along the weakest part of a composite (Greenhalgh, 2009). The overall fracture surface of BC-coated sisal fibre reinforced PLLA composite exhibited L-fibre fractured surface as the dominant mechanism (crack plane oriented parallel to fibre orientation – low fracture energy). This explained the poor tensile strengths of these composites, even though the fibre–matrix interface was enhanced through mechanical interlock. Through this mechanical interlock enhancement, the weakest region in the composite is no longer the fibre–matrix interface but the bulk of the polymer. This resulted in L-fibre fractured surface as the dominant failure mechanism. However, when BC was dispersed in the fibre reinforced PLLA composites, the overall fracture surface, and hence fracture mechanism, was modified. No significant fibre debonding or fibre pull-out could be observed in the composites. This was accompanied by the improved mechanical properties (both tensile strength and modulus) of hierarchical composites when compared with neat PLLA.

This slurry dipping method for creating hierarchical structures in composite materials can be extended to create non-woven natural fibre preforms using a paper making process (Lee *et al.*, 2012b). Instead of dipping the sisal

Table 3.8 The tensile strength (σ) of neat and BC-coated sisal fibre reinforced PLLA hierarchical composites

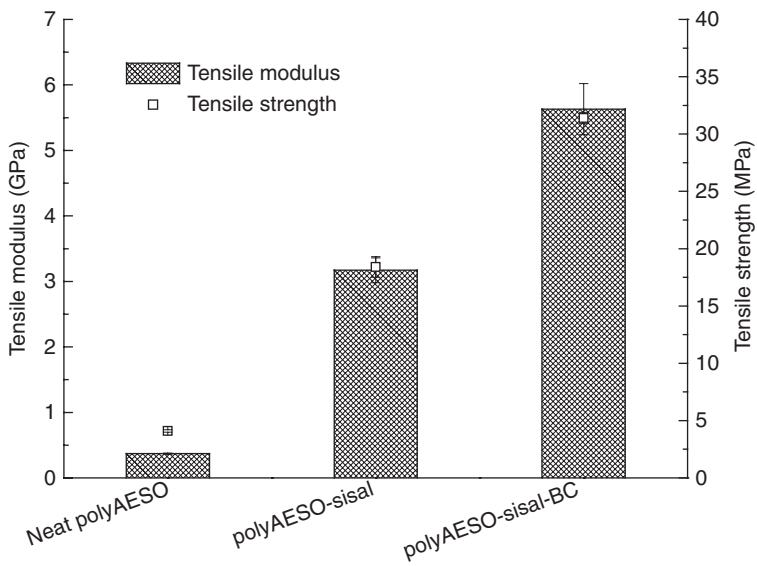
Content of fibres in PLLA (wt.%)	Neat sisal σ (MPa)	BC-coated sisal σ (MPa)
0	63.6 ± 1.8	63.6 ± 1.8
20	35.3 ± 0.6	38.7 ± 1.9
30	32.1 ± 1.3	37.8 ± 2.1
40	19.5 ± 0.9	35.8 ± 1.1

Source: Adapted from Juntaro *et al.* (2009).

© Woodhead Publishing Limited, 2014

fibres into a water dispersion of BC, the dispersion of sisal fibres–BC can be vacuum filtered, wet pressed and dried to produce rigid fibre preforms using BC as binder for the production of composite materials. With BC as the binder, a tensile strength (defined as the maximum load required to break the sample per unit width of the specimen as the cross-sectional area of the fibre mat) of 13.1 kN m^{-1} was achieved. However, the tensile strength of the neat sisal fibre preforms without BC binder was not measureable. This is due to the fact that these sisal fibres are loose and held together only by friction between the fibres, even after the wet pressing step to consolidate them into fibre preforms. The improved mechanical performance of BC–sisal fibre preforms can be attributed to the use of BC as the binder, which also promotes fibre–fibre stress transfer. The nano-sized BC holds the otherwise loose sisal fibres together due to hornification (irreversible hydrogen bonding between the nanocellulose) (Diniz *et al.*, 2004). The high tensile strength of the BC network, which formed in between the sisal fibres, provided the mechanical performance of the manufactured BC–sisal fibre preforms.

The natural fibre preforms were infused with acrylated epoxidised soybean oil (AESO) and polymerised to produce sisal fibre reinforced hierarchical composites (Lee *et al.*, 2012b). The tensile properties of neat polyAESO (polymerised AESO) and the (hierarchical) composites reinforced with



3.8 Tensile properties of neat polyAESO and sisal fibre preform reinforced polyAESO (hierarchical) composites. PolyAESO-sisal and polyAESO-sisal-BC indicate composites reinforced with neat sisal fibre preform and sisal fibre preform using BC as binder, respectively. (*Source*: Adapted from Lee *et al.* (2012b).)

© Woodhead Publishing Limited, 2014

sisal fibre preforms are shown in Fig. 3.8. The fibre volume fractions of sisal–polyAESO and BC–sisal–polyAESO is 40 vol.%. When sisal fibres were used as reinforcement for polyAESO, the tensile modulus improved from 0.4 GPa for neat polyAESO to 3.2 GPa for 40 vol.% sisal fibre reinforced polyAESO composites. A further improvement of the tensile modulus of the composites from 3.2 to 5.6 GPa was achieved when BC was used as the binder for the natural fibre preform. This is thought to be due to the stiffening of polymer matrix when the fibre preform contained a hornified network of BC.

A similar trend was observed for the tensile strength of the (hierarchical) composites. Neat polyAESO had a tensile strength of only 4.1 MPa. When neat polyAESO was reinforced with 40 vol.% sisal fibres the tensile strength increased to 18.4 MPa. A further improvement was achieved when 40 vol.% of BC and sisal fibres in the form of a preform were used as reinforcement. The tensile strength of BC–sisal–polyAESO increased by 71% and nearly 700% when compared with sisal–polyAESO and neat polyAESO, respectively. This significant improvement when BC–sisal fibre preforms were used to create hierarchical composites can be attributed to (i) the enhanced fibre–matrix interaction and (ii) enhanced fibre–fibre stress transfer. The use of BC as binder for the fibres resulted in the formation of a continuous but hornified BC network, encasing sisal fibres bonding them together. It is postulated that this enhances the fibre–fibre stress transfer compared with sisal fibre only preforms, where the fibres are mostly isolated. In addition to this, it has been shown that using BC as binder enhances the tensile properties of the BC–sisal fibre preforms compared with sisal fibre preforms. This translates to the improved tensile strength of the manufactured BC–sisal–polyAESO.

3.6 Conclusions and future trends

This chapter reports and demonstrates the potential to improve the mechanical performance of traditional (ligno)cellulosic fibre reinforced renewable composites by creating hierarchical structures either on the fibres or within the composites. The fibre–matrix interface can be improved via mechanical interlocking by fibrillating the surface of the fibres. With MFC dispersed in the matrix, the crack propagation behaviour can be altered, which ultimately improved the overall mechanical performance of the hierarchical composites. Nanocellulose can also be coated onto the surface of (ligno) cellulosic fibres by culturing cellulose-producing bacterial in the presence of (ligno)cellulosic fibres. Such BC coating on natural fibres can also be produced by dipping the fibres into a dispersion containing BC. This method can also be extended to produce robust natural fibre preforms for thermosetting matrices.

© Woodhead Publishing Limited, 2014

The use of hierarchical composites is still in its infancy, but we have shown in this chapter that it has great potential to replace traditional fibre reinforced composites. In order to fully utilise the potential of hierarchical composites, several fundamental issues need to be addressed. The ratio and alignment of the nanofiller in the matrix is important in determining the performance of the hierarchical composites. Furthermore, novel processing routes need to be developed to align the nanofillers in the fibre reinforced polymer matrix in a staggered fashion to fully utilise the potential of these materials. The cost of manufacturing these hierarchical composites plays an important role in the commercialisation of these materials. A cost versus benefit analysis needs to be performed in order to fully exploit the potential of hierarchical composites as replacement for conventional glass fibre reinforced plastics. Nonetheless, the promising results seen in hierarchical composites will spark new research interest to create truly renewable composite materials and possibly with triggered biodegradability.

3.7 Acknowledgements

The authors are grateful for the funding provided by the Knowledge Secondment Scheme (KTS) of Imperial College London and the Follow-on Grant (no.: EP/J013390/1) by the UK Engineering and Physical Sciences Research Council (EPSRC).

3.8 References

Baley C, Perrot Y, Busnel F, Guezenoc H and Davies P (2006) Transverse tensile behaviour of unidirectional plies reinforced with flax fibres. *Materials Letters*, **60** (24): 2984–2987.

Bismarck A, Mishra S and Lampke T (2005) Plant fibers as reinforcement for green composites. In: Mohanty AK, Misra M, Drzal LT (eds) *Natural Fibers, Biopolymers and Biocomposites*. 1st edn. CRC Press, Boca Raton.

Blaker JJ, Lee KY and Bismarck A (2011) Hierarchical composites made entirely from renewable resources. *Journal of Biobased Materials and Bioenergy*, **5**: 1–16.

Brown AJ (1886) The chemical action of pure cultivations of bacterium aceti. *Journal of the Chemical Society*, *Transations,* **49**: 172–187.

Cichocki FR and Thomason JL (2002) Thermoelastic anisotropy of a natural fiber. *Composites Science and Technology,* **62** (5): 669–678.

Diniz J, Gil MH and Castro J (2004) Hornification – its origin and interpretation in wood pulps. *Wood Science and Technology,* **37** (6): 489–494. doi:10.1007/s00226–003–0216–2.

Fratzl P and Weinkamer R (2007) Nature's hierarchical materials. *Progress in Materials Science,* **52** (8): 1263–1334. doi:10.1016/j.pmatsci.2007.06.001.

Ganan P, Garbizu S, Llano-Ponte R and Mondragon I (2005) Surface modification of sisal fibers: Effects on the mechanical and thermal properties of their epoxy composites. *Polymer Composite,* **26** (2): 121–127.

© Woodhead Publishing Limited, 2014

Gao HJ (2006) Application of fracture mechanics concepts to hierarchical biomechanics of bone and bone-like materials. *International Journal of Fracture,* **138** (1–4): 101–137. doi:10.1007/s10704–006–7156–4.

Gao HJ, Ji BH, Jager IL, Arzt E and Fratzl P (2003) Materials become insensitive to flaws at nanoscale: Lessons from nature. *Proceedings of the National Academy of Sciences of the United States of America,* **100** (10): 5597–5600. doi:10.1073/pnas.0631609100.

George J, Janardhan R, Anand JS, Bhagawan SS and Thomas S (1996) Melt rheological behaviour of short pineapple fibre reinforced low density polyethylene composites. *Polymer,* **37** (24): 5421–5431.

Greenhalgh ES (2009) *Failure Analysis and Fractography of Polymer Composites*. Woodhead Publishing Limited, Cambridge.

Juntaro J (2009) Environmentally friendly hierarchical composites. PhD Thesis, Imperial College London, London.

Juntaro J, Pommet M, Kalinka G, Mantalaris A, Shaffer MSP and Bismarck A (2008) Creating hierarchical structures in renewable composites by attaching bacterial cellulose onto sisal fibers. *Advanced Materials,* **20** (16): 3122–3126.

Juntaro J, Pommet M, Mantalaris A, Shaffer M and Bismarck A (2007) Nanocellulose enhanced interfaces in truly green unidirectional fibre reinforced composites. *Composite Interfaces,* **14** (7–9): 753–762. doi:10.1163/156855407782106573.

Kaith BS and Kalia S (2008) Graft copolymerization of MMA onto flax under different reaction conditions: a comparative study. *Express Polymer Letters,* **2** (2): 93–100.

Karlsson JO, Blachot JF, Peguy A and Gatenholm P (1996) Improvement of adhesion between polyethylene and regenerated cellulose fibers by surface fibrillation. *Polymer Composites,* **17** (2): 300–304. doi:10.1002/pc.10614.

Lee K-Y, Bharadia P, Blaker JJ and Bismarck A (2012a) Short sisal fibre reinforced bacterial cellulose polylactide nanocomposites using hairy sisal fibres as reinforcement. *Composites Part A – Applied Sciencce and Manufacturing,* **43** (11): 2065–2074.

Lee, K-Y, Buldum, G, Mantalaris, A and Bismarck, A (2013) More than meets the eye in bacterial cellulose: biosynthesis, bioprocessing, and applications in advanced fiber composites. *Macromolecular Bioscience*, 10.1002/mabi.201300298.

Lee K-Y, Blaker JJ and Bismarck A (2009) Surface functionalisation of bacterial cellulose as the route to produce green polylactide nanocomposites with improved properties. *Composites Science and Technology,* **69** (15–16): 2724–2733.

Lee K-Y, Ho KKC, Schlufter K and Bismarck A (2012b) Hierarchical composites reinforced with robust short sisal fibre preforms utilising bacterial cellulose as binder. *Composites Science and Technology,* **72** (13): 1479–1486.

Luz GM and Mano JF (2010) Mineralized structures in nature: Examples and inspirations for the design of new composite materials and biomaterials. *Composites Science and Technology,* **70** (13): 1777–1788. doi:10.1016/j.compscitech.2010.05.013.

Marini I (1994) Lenzing Lyocell fibers. In: *Man-Made Fiber Year Book*. International Business Press, Frankfurt, pp. 22–26.

Mayer G (2005) Rigid biological systems as models for synthetic composites. *Science,* **310** (5751): 1144–1147. doi:10.1126/science.1116994.

Mehta G, Drzal LT, Mohanty AK and Misra M (2006) Effect of fiber surface treatment on the properties of biocomposites from nonwoven industrial hemp fiber

© Woodhead Publishing Limited, 2014

mats and unsaturated polyester resin. *Journal of Applied Polymer Science,* **99** (3): 1055–1068.

Mishra S, Naik JB and Patil YP (2000) The compatibilising effect of maleic anhydride on swelling and mechanical properties of plant-fiber-reinforced novolac composites. *Composites Science and Technology,* **60** (9): 1729–1735.

Nair KCM, Thomas S and Groeninckx G (2001) Thermal and dynamic mechanical analysis of polystyrene composites reinforced with short sisal fibres. *Composites Science and Technology,* **61** (16): 2519–2529.

Nishino T, Matsuda I and Hirao K (2004) All-cellulose composite. *Macromolecules,* **37** (20): 7683–7687.

Okubo K, Fujii T and Thostenson ET (2009) Multi-scale hybrid biocomposite: Processing and mechanical characterization of bamboo fiber reinforced PLA with microfibrillated cellulose. *Composites Part A – Applied Science and Manufacturing,* **40** (4): 469–475. doi:10.1016/j.compositesa.2009.01.012.

Okubo K, Fujii T and Yamashita N (2005) Improvement of interfacial adhesion in bamboo polymer composite enhanced with micro-fibrillated cellulose. *Jsme International Journal Series A – Solid Mechanics and Material Engineering,* **48** (4): 199–204. doi:10.1299/jsmea.48.199.

Pommet M, Juntaro J, Heng JYY, Mantalaris A, Lee AF, Wilson K, Kalinka G, Shaffer MSP and Bismarck A (2008) Surface modification of natural fibers using bacteria: Depositing bacterial cellulose onto natural fibers to create hierarchical fiber reinforced nanocomposites. *Biomacromolecules*, **9** (6): 1643–1651.

Pothan LA, Thomas S and Groeninckx G (2006) The role of fibre/matrix interactions on the dynamic mechanical properties of chemically modified banana fibre/polyester composites. *Composites Part A – Applied Science and Manufacturing,* **37** (9): 1260–1269.

Thomason JL (2009)Why are natural fibres failing to deliver on composite performance? In: Conference Proceedings of the 17th International Conference of Composite Materials, Edinburgh, 27–31 July 2009.

Tomljenovic A and Cunko R (2010) Reducing fibrillation tendency of man-made cellulose fibres employing ultrasound treatment. *Journal of the Textile Institute,* **95** (1–6): 327–339.

Tserki V, Zafeiropoulos NE, Simon F and Panayiotou C (2005) A study of the effect of acetylation and propionylation surface treatments on natural fibres. *Composites Part A – Applied Science and Manufacturing,* **36** (8): 1110–1118.

Valadez-Gonzalez A, Cervantes-Uc JM, Olayo R and Herrera-Franco PJ (1999) Chemical modification of henequen fibers with an organosilane coupling agent. *Composites Part B – Engineering,* **30** (3): 321–331.

Wegst UGK and Ashby MF (2004) The mechanical efficiency of natural materials. *Philosophical Magazine,* **84** (21): 2167–2181. doi:10.1080/14786430410001680935.

Wu S (1982) *Polymer Interface and Adhesion*. Marcel Dekker Inc., New York.

Zhong LX, Fu SY and Zhan HY (2011a) The effects of microfibrillation on the properties of hierarchical sisal fibres and its composites. *Journal of Biobased Materials and Bioenergy,* **5** (4): 491–499.

Zhong LX, Fu SY, Zhou XS and Zhan HY (2011b) Effect of surface microfibrillation of sisal fibre on the mechanical properties of sisal/aramid fibre hybrid composites. *Composites Part A – Applied Science and Manufacturing,* **42** (3): 244–252. doi:10.1016/j.compositesa.2010.11.010.

© Woodhead Publishing Limited, 2014

4

Recycled polymers in natural fibre-reinforced polymer composites

M. A. AL-MAADEED and S. LABIDI, Qatar University, Qatar

DOI: 10.1533/9780857099228.1.103

Abstract: This chapter discusses different types and classifications of natural fibres and their effect on recycled polymers. The improvement of environmental, physical and mechanical modification of the natural fibre reinforced recycled polymer composites are explained. The techniques used to improve the surface properties of these fibres and how to modify the adhesion between the filler and the polymer matrix are explained. Possible processing methods to change the polymers to composites are discussed. The chapter then explains the application of recycled polymer composites with natural fibre reinforcements, future trends and drawback.

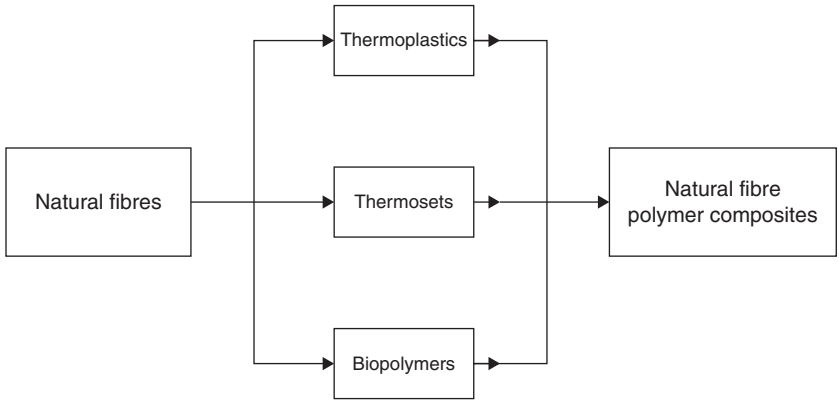
Key words: natural fibre, recycled polymers, mechanical properties, failure, applications.

4.1 Introduction

Plastic recycling is receiving increasing attention as a means of meeting ecological and environmental requirements. Waste consisting of recyclable materials such as plastic may be used as a raw material in many applications. The use of recycled materials also reduces waste, raw material consumption and the energy needed for manufacturing finished plastics. Plastic waste consists of a wide variety of polymer matrices. The largest fraction of waste is composed of polyolefin (60–70%), polystyrene (PS) (10–15%), poly(vinyl chloride) (PVC) (15%), and poly(ethylene terephthalate) (PET) (5%) (Malkapuram *et al.*, 2009). Plastic waste is an important component of solid waste in many countries. In Qatar it is about 16% of total waste. The main difficulties in polymer recycling are due to its degradation. It is necessary for reprocessing to produce recycled polymers with the required mechanical properties. The use of fillers is an important means of improving plastic waste (Li X. *et al.*, 2009). Different fillers may be introduced to polymer wastes to enhance their mechanical and physical properties.

A fibre-reinforced polymer is a composite material consisting of a polymer matrix containing high strength fibres. The purpose of incorporating fibres into a polymer matrix is to provide a reinforcing component which improves the properties when compared with those of the virgin components. Polymers

© Woodhead Publishing Limited, 2014



4.1 Different types of matrices used to make composites.

used in composites are classified as either thermoplastics or thermosets. Thermoplastic materials usually dominate in matrices for natural fibres, such as polypropylene (PP), polyethylene (PE), polyamide (PA), and PVC (Coutinho *et al*., 1997; George *et al*., 2001; Hornsby *et al*., 1997). However, for thermoset materials, phenolic, epoxy and polyester resins are the most commonly used matrices (Coutinho *et al*., 1997; George *et al*., 2001; Hornsby *et al*., 1997). The fibres most commonly used in traditional composites are carbon, glass and aramid with conventional matrices such as PP, epoxy resins (ER), unsaturated polyester resins (UP), and polyurethanes (PU).

Because of an increase in environmental legislation and the growing interest in green materials, biocomposites based on biopolymers and recycled composites have been developed. Examples include poly(α-hydroxyalkanoic acid)s, such as poly(lactic acid) (PLA), and poly(β-hydroxyalkanoate)s, such as poly(3-hydroxybutyrate) (PHB) (Wong and Shanks, 2009). Figure 4.1 shows the three types of polymers currently used to produce natural fibre recycled polymer composites.

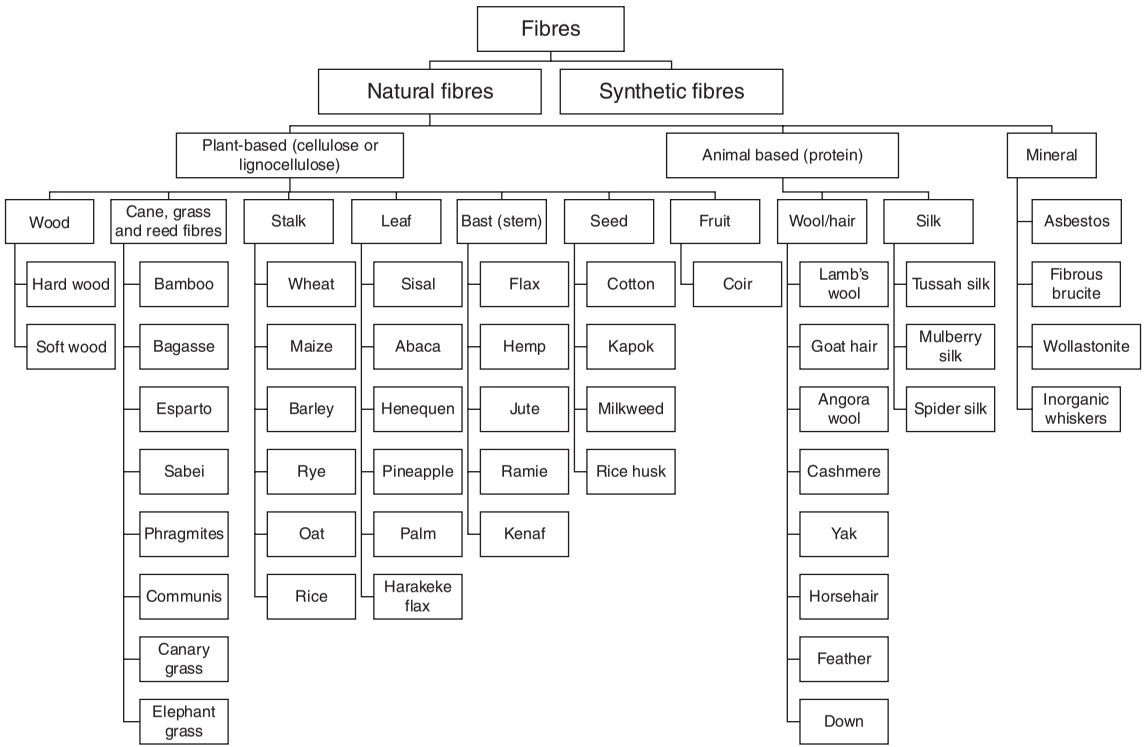
4.2 Fibre reinforcements in recycled composites

Natural fibres can be divided into different categories, based on their origin and derivation, and are detailed in Fig. 4.2 (Amar *et al*., 2005). Natural fibres are an abundant and renewable resource, so their cost is relatively low compared with other conventional fibres. They are eco-friendly and biodegradable, and reduce the problem of solid waste production when used to replace non-degradable fillers. Figure 4.3a shows date palm leaf waste, and Fig. 4.3b shows an example of the extracted fibres.

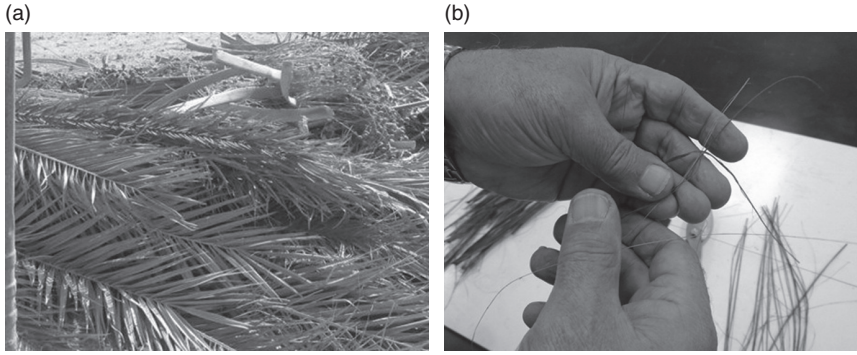
Due to their inherent properties, natural fibres are flexible. Because of their non-abrasive behaviour, the filler loading within the polymer matrix can be used in larger quantities than non-organic fillers as it is unlikely to cause

© Woodhead Publishing Limited, 2014

© Woodhead Publishing Limited, 2014



4.2 Classifications of natural fibres.



4.3 (a) Date palm leaf waste and (b) palm leaf fibres.

damage to machinery or health during manufacturing. Natural fibres possess many advantages, such as low density, and relatively high mechanical properties, such as specific modulus and specific strength (Xie *et al.*, 2010). The mechanical properties of natural and man-made fibres are summarized in Table 4.1.

Natural fibres have recently become more attractive to researchers as an alternative reinforcement for fibre-reinforced polymer. They are extracted from renewable sources and provide a new generation of reinforcements for polymer materials. These eco-efficient fibres have been used as substitutes for glass fibre and other synthetic polymer fibres in diverse applications.

Natural fibre composites help to preserve non-renewable resources, which are the main source for most materials used in current applications. Natural fibre based materials are produced in smaller quantities than petroleum-based products and their applications are directed towards different areas (John and Anandjiwala, 2008).

The main advantages of these fibres are their low cost, renewability, biodegradability, low specific gravity, abundance, high specific strength, and stiffness. A wide variety of agricultural species, such as oil-palm, banana, jute, bamboo, sisal, pineapple leaves and coir, have been used in the production of plant fibres (Idicula *et al.*, 2009).

Natural fibres have a low density and can provide reinforcement capable of imparting high specific mechanical properties to a composite when compared with many synthetic fibres such as glass, carbon and Kevlar in advanced applications (Wambua *et al.*, 2003). As natural fibres are derived from renewable natural resources, their production requires less energy. They also eliminate many of the problems related to environmental degradation, which means that the disposal of natural fibre composites (NFCs) is easier, safer and less expensive when compared with advanced fibre composites. NFCs also provide impressive acoustic absorption properties, which are useful in building construction. Energy consumption for the pre- and post-harvesting/cultivation facets of the natural fibre separation process,

© Woodhead Publishing Limited, 2014

Table 4.1 Mechanical properties of natural and industrial fibres

Fibre	Density (g/cm^3)	Elongation (%)	Tensile strength (MPa)	Young's modulus (GPa)	References
Natural fibre					
Cotton	1.5–1.6	7.0–8.0	287–597	5.5–12.6	Ahmad *et al.*, 2006; Mohanty *et al.*, 2000
Jute	1.3	1.5–1.8	393–773	26.5	Ahmad *et al.*, 2006
Flax	1.5	2.7–3.2	500–1500	27.6	Saheb and Jog, 1999
Hemp	1.47	2.0–4.0	690	70	Saheb and Jog, 1999
Ramie	–	3.6–3.8	400–938	61.4–128	Holbery and Houston, 2006
Sisal	1.5	2.0–2.5	511–635	9.4–22	Holbery and Houston, 2006
Coir	1.2	30	175	04-June	Hargitai *et al.*, 2008
Soft wood kraft	1.5	4.4			
Kenaf	1.45	1.6	930	53	Saheb and Jog, 1999
Pineapple		2.4	170–1627	60–82	Zahn *et al.*, 1980
Banna		3	529–914	27–32	Zahn *et al.*, 1980
Industrial fibres					
E-glass	2.5	0.5	2000–3500	70	Hargitai *et al.*, 2008
S-glass	2.5	2.8	4570	86	Hargitai *et al.*, 2008
Aramid	1.4	3.3–3.7	3000–3150	63–67	Hargitai *et al.*, 2008
Carbon	1.4	1.4–1.8	4000	230–240	Hargitai *et al.*, 2008

is lower than that of synthetic fibre production processes (Almeida, 2001). The principal advantages of using natural fibres in composites are therefore lower cost, sustainability and low density.

The properties of natural fibres are determined by their architecture and the particular chemical composition and structural features of the fibre (Mukherjee and Satyanarayana, 1984). The orientation of cellulose in the form of micro-fibrils oriented at an angle to the fibre axis (micro-fibril angle) determines the stiffness of the fibres and the cellulose content contributes to the strength characteristics of the fibre. Several features may have a significant influence on the structure and chemical composition of the fibre, such as climatic conditions and processing procedures.

Natural plant fibre constituents can be divided into three groups, based on their chemical composition: cellulose, hemicellulose and lignin.

© Woodhead Publishing Limited, 2014

- Cellulose contains hydroxyl groups and is hydrophilic (Baillie, 2004). It has a highly crystalline structure containing around 80% crystalline regions. Cellulose microcrystalline structure is composed of highly ordered crystalline regions distributed throughout the fibre, and of lower order amorphous regions (Baillie, 2004). The equilibrium moisture content may reach 12.6% (Mohanty *et al*., 2000).
- Hemicellulose is composed of highly branched polysaccharides such as glucose, mannose, galactose and xylose. It is a highly branched polymer and has a degree of polymerization 10–1000 times lower than that of cellulose (Yao *et al*., 2008).
- Lignin is amorphous, highly complex and mainly aromatic (Yao *et al*., 2008). Because of its stiffness, lignin acts as a protective barrier for cellulose. During the synthesis of plant cell walls, lignin fills the spaces between the polysaccharide fibres and cements them together, so protecting the cell walls from chemical and physical damage (Mohanty *et al*., 2000).

Although conventional composites exhibit high strength and modulus, a major drawback is the difficulty of disposal after use. Synthetic composites are well interconnected and relatively stable and therefore separation for recycling is difficult.

4.3 Processes for adding natural fibre reinforcements to composites

Many factors, such as processing, temperature, screw speed, processing time, screw configuration, material flow and shear, can play a crucial role in dispersion of the filler and consequently on the mechanical properties of the composite. The apparatus used (extruder, internal mixer, compression moulder) can also affect the physical and mechanical properties. In the case of partial affinity between matrix and filler, process optimization is needed to improve the mechanical properties.

Processing techniques and conditions must therefore be chosen to permit the transformation of raw materials into the final composite without causing damage to the different components (matrix and/or natural fibre).

A variety of processes can be used to transform the raw materials into composites, including extrusion/injection moulding, compression moulding, thermoforming and resin transfer moulding (RTM). These depend on criteria which include the raw materials (thermosets/thermoplastics/recycled or virgin matrices/natural fibres/high or low viscosity), and processing features (temperature/screw speed).

The size of the fillers is the dominant factor in the choice of suitable manufacturing processes. Extrusion/injection and compression moulding are preferable for small and medium sized natural fibres due to ease and

© Woodhead Publishing Limited, 2014

speed. However, for long fibres, composites are typically manufactured by compression moulding and RTM.

The criteria for manufacturing NFCs differ from those used for traditional fibres. The length, orientation, diameter and content of natural fibre in relation to the processing features are important in determining the final properties of composites. Some manufacturing processes can affect the final properties of the composites. For example, it is well known that improved tensile strength can be achieved by increasing both the aspect ratio and the fibre volume fraction.

Extrusion/injection moulding processes have their limitations, such as:

- Possibility of fibre expansion after mixing with liquid forms of polymers.
- Fibre attrition. If the fibres are shorter than the expected length, their adhesion with the matrix may be altered.

Where the length of the fibres is reduced, they will be unable to carry their maximum load. Due to the fibre gathering around the gate and sprue, the amount of fibre within the polymer matrices after extrusion/injection will also be limited. During melting, material degradation may take place. Natural fibres are thermally less stable compared with some polymer matrices, especially in the case of technical polymers such as PET and polyimide (PI), which present a high processing temperature. Thermal degradation usually starts at 200°C (Yao *et al.*, 2008). This may limit the efficiency of the filler within the polymer matrix with a consequent decrease in the mechanical performance of the composites. Compression moulding can therefore replace the extrusion/injection methods for the manufacturing of composite products. Side feeders may also be used in the last stage of extrusion to reduce thermal degradation of the fibres.

Compression moulding or RTM methods may cause some weaknesses as these processes cannot provide a mechanical dispersion of natural fibres within the matrix. The formation of fibre agglomeration, due to inter-fibre hydrogen bonding, prevents the dispersion of fibres during the manufacturing process and results in poor mechanical strength (Kazayawoko *et al.*, 1999; Saheb and Jog, 1999).

4.4 Improving the mechanical properties of recycled composites using natural fibre reinforcements

A major problem encountered in polymer composites is the interface between hydrophilic natural fibres, which exhibit poor resistance to moisture, leading to high water absorption, and hydrophobic polymer matrices, which have a tendency to form agglomerates. Fibre surfaces also contain natural substances such as waxes, lignin or pectin, which create poor adhesion

© Woodhead Publishing Limited, 2014

with the matrices. This incompatibility lessens the adhesion between filler and polymer matrix and causes poor load transfer between them.

A semi-empirical equation developed for the quantitative description of composition dependence of tensile yield stress in heterogeneous polymer systems, allows the interfacial adhesion of fillers to be estimated (Baillie, 2004). The interface thickness and yield stress of composites are considered as the key parameters.

$$\frac{\sigma_{yc}}{\sigma_{ym}} = \frac{1-\varphi_f}{1+2.5\varphi_f}\exp\left(B_{\sigma y}\,\varphi_f\right) \qquad [4.1]$$

$$B_\sigma = \left(1+A_f\rho_f t\right)\ln\left(\frac{\sigma_{yi}}{\sigma_{ym}}\right) \qquad [4.2]$$

where φ_f is the volume fraction of the filler, σ_{yc} and σ_{ym} are the tensile yield stress of composite and matrix, A_f is the specific surface area of the filler, ρ_f is its density, t is the thickness of the interface and σ_{yi} is the strength of interaction. The first and second terms in Equation [4.1] are related to a decrease in the load bearing cross-section and the interfacial interaction between filler and matrix, respectively. The interphase and the strength of the interaction are shown in Equation [4.2].

In order to improve the adhesion of the natural fibres within the matrices and enhance the mechanical properties of the composite, it is necessary to increase the fibre hydrophobicity by surface treatment. Modification of the fibre surface is done by means of chemical treatments which improve the interfacial bonding between fibre and matrix (Ho *et al.*, 2011). Grafting and a variety of coupling agents can be employed. However, the choice of system will depend on the type of filler and matrix components.

Mercerisation is the most widely used chemical treatment for natural fibres Sodium hydroxide (NaOH) is used to impede the hydrogen bonding in the structure of the cellulosic fibres (Hargitai *et al.*, 2008). Acrylic acid treatment was also found to be effective for this kind of application (Ho *et al.*, 2011).

Chemical coupling is another effective method of improving interfacial adhesion. The fibre surface is treated with a compound that allows a reaction with the matrix (Ho *et al.*, 2011). For example, silane coupling agents significantly improve the mechanical properties of composites when cellulosic fibres are incorporated within matrices such as recycled high-density polyethylene (HDPE), PP, or low density polyethylene (LDPE) (Xie *et al.*, 2010). The most commonly used coupling agent is maleic anhydride (MA). The tensile strength and elongation at break have been improved when MA grafted polyethylene or polypropylene (PEgMA/PPgMA) are used as coupling agents (Kazayawoko *et al.*, 1999; Saheb and Jog, 1999).

© Woodhead Publishing Limited, 2014

Poor interfacial adhesion with polar matrices and difficulties in mixing due to ineffective wetting of the fibre with the matrix will cause a weak interface. Fibre bundles reduce the stress transfer which results in impaired properties. The fibre–matrix interface in the fibre-reinforced composites transfers an externally applied load to the fibres. A load applied directly to the matrix at the surface of the composite is transferred to the fibres via the matrix and the interface. If the interface is weak, effective load distribution is not achieved and the mechanical properties of the composites will be impaired. A strong interface enables the composite to bear a load even if several fibres break, because the load can be transferred to the intact portion of the fibres. Thus, adhesion between the fibre and matrix is an important factor (John and Anandjiwala, 2008).

Plant fibres become more ductile if micro-fibrils are spirally oriented to the fibre axis. The degree of cellulose polymerization, orientation and crystallinity are also influenced by conditions prevailing during plant growth, as well as by the fibre extraction method used. The mechanical properties of natural fibres are therefore functions of the cellulose content (Bledzki, 1999).

As may be seen from the above, the chemical composition and physical structure of plant fibres are complex, and the plant fibre itself may be considered to be a natural composite material. Almost all ligno-cellulosic natural fibres have poor fire resistance and low durability. They are hydrophilic and polar in nature, mainly as a consequence of their chemical constituents and structure (Karmaker, 1997).

Water absorption is another limiting factor. Natural fibres absorb water from the air and through direct contact with their environment. This is due to the hydroxyl and oxygen containing groups, and moisture is attracted through hydrogen bonding. This absorption deforms the surface of the composites by swelling and creating voids. These deformations reduce the strength and increase the mass with a consequent degradation of mechanical and physical properties.

4.5 Applications of recycled polymer composites with natural fibre reinforcements

There are many current and future possible applications of recycled polymer composites in the construction industry, including walling and roofing, outdoor furniture and timbers. These composites can be moulded into sheets, gratings, frames, pellets, and a variety of shapes. They can be used as substitutes for wood, metals and other expensive materials in flooring, fences, railings, facades, decking, and false ceilings. Their use in buildings is controlled by international standards. ASTM E 119–05 is one of the most important test methods for fire resistance in building construction and materials subject to different conditions and loading.

There are several advantages to the use of these materials. They are environmentally friendly, lightweight, low cost and durable. Photo degradation

© Woodhead Publishing Limited, 2014

caused by ultraviolet (UV) radiation is a major disadvantage but may be overcome by the addition of UV stabilizers.

High quality recycled polymers combined with reinforced natural fibres can be used for non-structural parts in the automotive industry, such as car headliners, door panels and covers. At present, only virgin polymers reinforced with natural fibres are used in cars.

Cellulose fibres from paper coated with LDPE have been produced as laminated paper since 1976 (Michell *et al*., 1976). Thin, low cost composites are widely used around the world for packaging.

4.6 Conclusions and future trends

The widespread availability of natural fibres and waste plastics offers advantages for the future as the industrial recycling of plastics and use of fibre waste can produce high quality materials at a low cost. The drawbacks and limitations of natural fibres may be circumvented by a variety of approaches and techniques for the production of fibres with a homogenized composition and a near equalization of properties throughout their length. These include fibre separation procedures, appropriate sizing and coating of fibres, chemical modification or fibre surface treatments, grafting, thermal treatment and coupling (Michell *et al*., 1976; Sawpan *et al*., 2011; Sipiao *et al*., 2011). The treatment of fibres is an area of research which is currently receiving significant attention.

Recycled polymers reinforced by natural fibres have recently attracted considerable attention from both academics and industry due to their renewability, low specific gravity and high mechanical properties. The low cost of these materials eliminates the increasing cost of using petroleum-based materials.

There is a need to close the gap between research and the industrial application of natural fibre/polymer composites, particularly in fibre extraction technology, modification of fibre interfaces and processing techniques. The physical and mechanical properties of the final product depend on the aspect ratio of the fibres and more information about this is required. Modelling techniques can be used for analysis and evaluation of these parameters.

4.7 References

Ahmad, I., Baharum, A. and Abdullah, I. (2006). Effect of extrusion rate and fibre loading on mechanical properties of twaron fibre-thermoplastic natural rubber (TPNR) composites. *Journal of Reinforced Plastics and Composites,* **25**, 957–965.

Almeida, J. R. M. (2001). Analysis of cost and flexural strength performance of natural fibre–polyester composites. *Polymer-Plastics Technology and Engineering,* **40,** 205–215.

Baillie, C. *Green Composites – Polymer Composites and the Environment*. Woodhead Publishing.

Bledzki, A. (1999). Composites reinforced with cellulose based fibres. *Progress in Polymer Science,* **24,** 221–274.

© Woodhead Publishing Limited, 2014

Coutinho, F. M. B., Costa, T. H. S. and Carvalho, D. L. (1997). Polypropylene–wood fibre composites: Effect of treatment and mixing conditions on mechanical properties. *Journal of Applied Polymer Science,* **65,** 1227–1235.

George, J., Sreekala, M. S. and Thomas, S. (2001). A review on interface modification and characterization of natural fibre reinforced plastic composites. *Polymer Engineering & Science,* **41,** 1471–1485.

Hargitai, H., Rácz, I. and Anandjiwala, R. D. (2008). Development of HEMP fibre Reinforced Polypropylene Composites. *Journal of Thermoplastic Composite Materials,* **21,** 165–174.

Ho, M.-P., Wang, H., Lee, J.-H., Ho, C.-K., Lau, K.-T., Leng, J. and Hui, D. (2011). Critical factors on manufacturing processes of natural fibre composites. *Composites Part B: Engineering*.

Holbery, J. and Houston, D. (2006). Natural-fibre-reinforced polymer composites in automotive applications. *JOM Journal of the Minerals, Metals and Materials Society,* **58,** 80–86.

Hornsby, P., Hinrichsen, E. and Tarverdi, K. (1997). Preparation and properties of polypropylene composites reinforced with wheat and flax straw fibres: Part II Analysis of composite microstructure and mechanical properties. *Journal of Materials Science,* **32,** 1009–1015.

Idicula, M., Sreekumar, P. A., Joseph, K. and Thomas, S. (2009). Natural fibre hybrid composites—A comparison between compression molding and resin transfer molding. *Polymer Composites,* **30,** 1417–1425.

John, M. J. and Anandjiwala, R. D. (2008). Recent developments in chemical modification and characterization of natural fibre-reinforced composites. *Polymer Composites,* **29,** 187–207.

Karmaker, A. (1997). Effect of water absorption on dimensional stability and impact energy of jute fibre reinforced polypropylene. *Journal of Materials Science Letters,* **16,** 462–464.

Kazayawoko, M., Balatinecz, J. J. and Matuana, L. M. (1999). Surface modification and adhesion mechanisms in woodfibre-polypropylene composites. *Journal of Materials Science,* **34,** 6189–6199.

Kushwaha, P. K. and Kumar, R. (2010). Influence of chemical treatments on the mechanical and water absorption properties of bamboo fibre composites. *Journal of Reinforced Plastics and Composites*. **30**, 73–85, 2011

Li, X., Tabil, L. G., Panigrahi, S. and Crerar, W. J. (2009). The influence of fibre content on properties of injection molded flax fibre-HDPE biocomposites. *Biosystems Engineering,* **8,** 1–10.

Malkapuram, R., Kumar, V. and YUVRAJ SINGH NEGI (2009). Recent Development in Natural fibre Reinforced Polypropylene Composites. *Journal of Reinforced Plastics and Composites,* **28,** 1169–1189.

Michell, A. J., Vaughan, J. E. and Willis, D. (1976). Wood fibre-synthetic polymer composites. I. Laminates of paper and polyethylene. *Journal of Polymer Science: Polymer Symposia,* **55,** 143–154.

Mohanty, A. M., Misra, M., Dizal, L. T., Sclke, S. E., Harte, B. R. and Hinrichsen, G. (2005). Natural fibres, biopolymers, and biocomposites: an introduction. In *Natural Fibres, Biopolymers, and Biocomposites* (Eds. A. K. Mohanty, M. Misra and L. T. Drzal). CRC Press London.

Mohanty, A. K., Misra, M. and Hinrichsen, G. (2000). Biofibres, biodegradable polymers and biocomposites: an overview. *Macromolecular Materials and Engineering,* **276–277,** 1–24.

© Woodhead Publishing Limited, 2014

Mukherjee, P. S. and Satyanarayana, K. G. (1984). Structure and properties of some vegetable fibres. *Journal of Materials Science,* **19,** 3925–3934.

Saheb, D. N. and Jog, J. P. (1999). Natural fibre polymer composites: a review. *Advances in Polymer Technology,* **18,** 351–363.

Sawpan, M. A., Pickering, K. L. and Fernyhough, A. (2011). Effect of various chemical treatments on the fibre structure and tensile properties of industrial hemp fibres. *Composites Part A: Applied Science and Manufacturing,* **42,** 888–895.

Sipiao, B. L. S., Paiva, R. L. M., Goulart, S. A. S. and Mulinari, D. R. (2011). Effect of chemical modification on mechanical behaviour of polypropylene reinforced pineapple crown fibres composites. *Procedia Engineering,* **10,** 2028–2033.

Wambua, P., Ivens, J. and Verpoest, I. (2003). Natural fibres: can they replace glass in fibre reinforced plastics? *Composites Science and Technology,* **63,** 1259–1264.

Wong, S. and Shanks, R. (2009). Biocomposites of natural fibres and poly(3-hydroxybutyrate) and copolymers: improved mechanical properties through compatibilization at the interface. *Biodegradable Polymer Blends and Composites from Renewable Resources.* John Wiley & Sons, Inc.

Xie, Y., Hill, C. A. S., Xiao, Z., Militz, H. and Mai, C. (2010). Silane coupling agents used for natural fibre/polymer composites: a review. *Composites Part A: Applied Science and Manufacturing,* **41,** 806–819.

Yao, F., Wu, Q., Lei, Y., Guo, W. and Xu, Y. (2008). Thermal decomposition kinetics of natural fibres: Activation energy with dynamic thermogravimetric analysis. *Polymer Degradation and Stability,* **93,** 90–98.

Zahn, H., Föhles, J., Nlenhaus, M., Schwan, A. and Spel, M. (1980). Wool as a Biological Composite Structure. *Industrial & Engineering Chemistry Product Research and Development,* **19,** 496–501.

4.8 Appendix: abbreviations

LDPE	low density polyethylene
MA	maleic anhydride
NFC	natural fibre composites
PA	polyamide
PE	polyethylene
PEgMA/PPgMA	maleic anhydride grafted polyethylene or polypropylene high-density polyethylene
PET	polyethylene terephthalate
PHB	poly(3-hydroxybutyrate)
PI	polyimide
PLA	poly(lactic acid)
PP	polypropylene
PS	polystyrene
PVC, PVC	polyvinyl chloride
RTM	resin transfer melding

© Woodhead Publishing Limited, 2014

5

Electrospun cellulosic fibre-reinforced composite materials

D. S. LE CORRE, University of Canterbury, New Zealand, N. TUCKER, The NZ Institute for Plant and Food Research Ltd, New Zealand and M. P. STAIGER, University of Canterbury, New Zealand

DOI: 10.1533/9780857099228.1.115

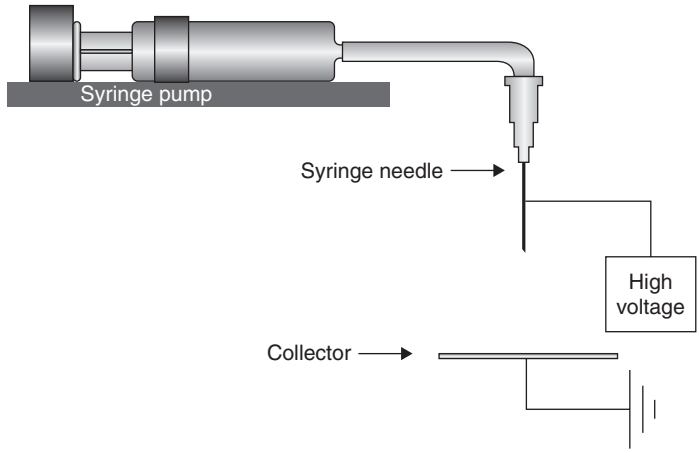
Abstract: Cellulose in the nanometric form has tremendous potential as a component in bionanocomposites. Methods are being developed for the production of nanometric cellulose via incorporation of cellulose into electrospun fibres or electrospinning the material itself. Electrospun cellulosic (native and derivatised) fibres, solution blending to incorporate cellulosics, use of cellulose nanofibres and nanocomposites based on cellulose nanofibres are reviewed, and electrospun cellulose nanofibres as reinforcing material are compared with other polymers. This chapter gives a broad overview of activities related to electrospinning and cellulose and examines future trends in terms of cellulose-based nanocomposites and the role of electrospinning in their development.

Key words: electrospinning, cellulose, regeneration, nanocrystals, composites.

5.1 Introduction

The processing of materials at the submicron to nanometer scale is becoming an increasingly important industrial application (Geraci, 2011). Nanomaterials may exhibit enhanced properties in themselves or enhance the properties of bulk materials even at low levels of addition. Thus, there is much interest in the possibility of creating nano-forms from a range of both synthetic and natural materials to exploit the unusual characteristics of nanomaterials. Electrospinning is an appealing method with a long history (Tucker *et al.*, 2012) for synthesising submicron or nanoscale materials in the form of a fibre, especially polymeric materials. An electrospun polymeric fibre is normally characterised as being a continuous fibre that exhibits a fine diameter (typically in the range of 10–700 nm) and, thus, a large surface area per unit volume. Electrospinning is a term derived from 'electrostatic spinning'. Electrospinning differs from conventional fibre spinning

© Woodhead Publishing Limited, 2014



5.1 Typical electrospinning apparatus. (*Source*: After Stanger *et al.,* 2009.)

processes in that the polymer solution (or melt) is *drawn* from an electrically charged spinneret rather than being mechanically *pushed* through the spinneret. Thus, electrospinning relies on electrostatic forces to drive the process rather than mechanical (e.g. extrusion) or gravitational (e.g. cotton candy) forces. A high voltage (typically in the order of 15 kV) is applied to a droplet of polymer solution or melt supplied to the tip of a spinneret as seen in Fig. 5.1. The droplet may stretch into a jet and form a thin filament as the mutual repulsion of charge within the droplet overcomes the surface tension of the polymer. The filament or fibre is drawn toward any grounded surface where it will discharge. Ideally, the electrospun fibre will lose solvent through evaporation (for solutions) or freezing (for melts) during its flight, leaving a solid phase polymer fibre at the grounded surface.

The use of submicron to nanometer scale fibres for the mechanical enhancement of polymers and conventional composite materials is widely reported in the literature. Much research has focussed on the use of technical nanoscaled reinforcements such as carbon nanotubes (CNTs) (Coleman *et al*., 2006; Lau and Hui, 2002; Lau *et al*., 2006) and graphene (Kuilla *et al*., 2010) to reinforce polymers or to modify the properties of the polymer matrix in conventional composite materials (e.g. carbon fibre–epoxy). Less attention has been given to the use of fibres produced via electrospinning for the modification of polymeric or composite materials. Recently, Zucchelli *et al.* (2011) discussed the benefits of using electrospun fibres for enhancing the structural performance of engineered composite materials. It was concluded that several practical issues need to be resolved before the application of electrospun fibres as a reinforcing phase in polymers or composites including (i) improvement of mechanical properties of single nanofibres;

© Woodhead Publishing Limited, 2014

(ii) optimisation of the fibre-matrix interaction; and (iii) improved control over fibre orientation. Further, it was suggested that the mechanical properties of electrospun fibres could be improved by (i) processing polymers with inherently high mechanical properties; (ii) selecting polymers suitable for post-processing and/or (iii) using fibres based on polymer blends or nanocomposites.

The electrospinning of synthetically derived polymers has been the subject of much research. However, there is increasing interest in exploiting natural polymeric materials (e.g. polysaccharides, polypeptides, polylactates, etc.) as an eco-friendly alternative to the synthetic petrochemically-derived polymers. Unsurprisingly, there has been an exciting merging of the biopolymers and electrospinning fields to explore the possibilities of fabricating 'natural' electrospun fibres. Note that the adjective 'natural' can imply the synthesis of materials having a native structure that is variously based on microfibrils, nanofibres and/or rod-like nanocrystals (or whiskers). However, it is often necessary to disrupt the native structure prior to electrospinning to make the material amenable to electrospinning (e.g. dissolution in a solvent). The term *regenerated* is used to describe electrospun material where there is no opportunity for the polymer fibre to self-assemble back into its native structure during electrospinning. Examples of molecular structure regeneration occur following electrospinning of proteins (e.g. collagen (Zhang *et al.*, 2006)) and polysaccharides (e.g. cellulose (Kim *et al.*, 2006)). It should be noted that the regenerated structure may have quite different physicochemical properties to the native biopolymer structure, and that this can be a distinct disadvantage where biomimicry is an objective. Hence, some emphasis has been placed on control over the final structure of the nanofibre and development methods for replicating the native structure (Hofman *et al.*, 2012; Kim *et al.*, 2006).

Submicron electrospun fibres based on cellulose and its derivatives have attracted the attention of materials scientists primarily due to their abundance, low cost (<1 €/kg) and potential for low environmental impact of cellulose. Furthermore, cellulose has the potential to form fibres with intrinsically high mechanical properties due to extensive inter- and intra-molecular hydrogen bonding. For instance, the elastic moduli of regenerated cellulose fibre, native cellulose fibre, and cellulose nanocrystals (CNCs) are reported to be as high as ~20 GPa (Adusumali *et al.*, 2006), 30 GPa and 140 GPa (Eichhorn *et al.*, 2010), respectively. Cellulose also has the added advantage of presenting numerous reactive groups for potential crosslinking and interaction with the other polymers and nanofillers. Finally, cellulose has relatively high thermal stability and chemical resistance (Han *et al.*, 2008b) compared with other biopolymers, further increasing its range of potential applications. However, non-derivatised cellulose does not exhibit a melting temperature as a consequence of the extensive hydrogen bonding. Thus, non-derivatised cellulose

© Woodhead Publishing Limited, 2014

only becomes amenable to electrospinning following dissolution of the solid phase in an appropriate solvent. Electrospun cellulose is envisaged to be a useful component in novel polymer composite materials systems due to its high mechanical properties, as well as in regenerative medicine (Lee *et al.*, 2009b) due to its compatibility with biological systems.

In spite of the appealing physicochemical properties of cellulose, there are complications involved in the electrospinning of cellulose that arise from the poor solubility of cellulose in most conventional solvents. Cellulose-solvent solutions also tend to be highly viscous, further complicating the electrospinning process. The first regenerated cellulose fibre was named 'viscose' because of this. For these reasons, it is less problematic to electrospin chemical derivatives of cellulose or non-derivatised cellulose blended with other polymers that act as 'carriers'.

In this overview, the various approaches to obtaining submicron cellulosic fibres via electrospinning are presented, including those based on (i) non-derivatised or derivatised cellulosic fibres; (ii) cellulosic-polymer blends and (iii) nanocomposite cellulosic fibres. The use of electrospun cellulose fibres as a reinforcement in novel composite material systems is explored and compared with other polymer fibre types. Finally, future trends and some recommendations for further research in this emerging field are presented.

5.2 Electrospinning of non-derivatised and derivatised cellulosic fibres

5.2.1 Non-derivatised cellulose

Non-derivatised cellulose presents some difficulties in terms of processing due to strong inter- and intra-molecular hydrogen bonding. Consequently, the production of manmade regenerated cellulose is still largely based on the century-old technology of viscose production that produces cellulose (type II) in the form of fibres (rayon) or films (cellophane). However, the viscose process significantly reduces the molecular weight of cellulose, induces several side reactions, requires extra-purification steps and is not environmentally-friendly. Recently, alternative solvents for non-derivatised cellulose have been developed.

In the early 1990s, amine oxides were developed as an alternative solvent system for the production of cellulose fibres, also known commercially as Lyocell. Several research groups have used the N-methylmorpholine oxide (NMMO)–water (H_2O) solvent system to electrospin cellulose (Table 5.1). Kulpinski was first to report the preparation of electrospun cellulose fibres of up to 500 nm in diameter from mercerised cellulose and raw cellulose using NMMO (Kulpinski, 2005). The optimum cellulose concentration was found to be 2 wt.% at temperatures in the range of 90–100°C, since at 4 wt.% the

© Woodhead Publishing Limited, 2014

solutions were too viscous to electrospin, even at temperatures up to 130°C. Kim *et al*. (2006) electrospun submicron cellulose fibres using NMMO as the solvent and H_2O as the regeneration medium. This work investigated the effect of solvent system (NMMO vs lithium chloride–N,N-dimethylacetamide (LiCl–DMAc)), degree of polymerisation of the cellulose source, processing conditions and post-spinning treatment on the structural properties of the cellulose fibre. Interestingly, the degree of crystallinity was varied between 42% and 66% by alteration of the process parameters. The fibres were later investigated for their potential use in pulp and paper (Yeoh *et al*., 2009) and composite materials (Han *et al*., 2008a). Yeoh *et al.* (2009) reported that the electrospun cellulose fibres were stronger and more thermally stable than the as-received Kraft pulp. Han *et al.* (2008a) utilised electrospun cellulose fibres as a reinforcement in poly(butylene succinate) (PBS), greatly improving the storage modulus of the neat PBS in spite of the low crystallinity of the electrospun cellulose. There have been no further reports on the use of NMMO–H_2O as a solvent system for the electrospinning of cellulose; presumably, this is due to the (i) solutions requiring elevated temperatures for successful electrospinning, and (ii) limited cellulose concentration range in NMMO (Table 5.1). There is only a small region within the cellulose–NMMO–water phase diagram for which cellulose is completely dissolved (Fig. 5.2). The formation of highly viscous solutions further restricts this processing window for the electrospinning of cellulose from cellulose–NMMO solutions. The use of diluents such as N-methyl pyrrolidinone (NMP) can enhance the electrospinnability of cellulose–NMMO solutions by reducing the solution viscosity (Johnson, 1970). Further, Uppal and Ramaswamy (2011) successfully used the NMMO–NMP–water solvent system for electrospinning cellulose fibres with reduced diameters (200–250 nm) compared with the standard solvent system.

LiCl–DMAc was first discovered to dissolve polyamides and chitin in 1972 (Huglin, 1972). The presence of LiCl has since been proven to be necessary to bridge the electrostatic interaction between DMAc and cellulose (McCormick *et al*., 1985). The LiCl–DMAc solvent system has been a popular direct solvent for cellulose in recent years due to rapid dissolution rates and reproducibility compared with derivatisation (Dupont, 2003). Moreover, LiCl–DMAc dissolves cellulose with molecular weights greater than 10^6 g/mol under ambient conditions without severe degradation or undesirable side reactions (Matsumoto *et al*., 2002). Kim *et al*. (2005) used LiCl–DMAc to electrospin cellulose solutions of varying concentrations. The cellulose-LiCl–DMAc solution was found to be highly elastic and viscous at cellulose concentrations as low as 3 wt.%. The use of a heated collector and water coagulation post-electrospinning were required to obtain submicron-scaled fibres. Kim *et al*. (2006) also showed that electrospinning of cellulose from a cellulose-LiCl–DMAc solution results in fibres with an amorphous

© Woodhead Publishing Limited, 2014

Table 5.1 Non-derivatised cellulose electrospinning

Solvent	Coagulant	Cellulose type	DP/MW	Concentration*	Voltage (kV)	Diameter (nm)	References
NMMO							
NMMO–H_2O (50%)	Water	Raw and mercerised α-cellulose from spruce	700, 800	1–4 wt.% (2)	9–10	200–500	Kulpinski, 2005
NMMO–H_2O (85–/15 w/w)	Water 10°C – rotating collector	Cotton	210, 1140	9 wt.%, 1.5–2.5 wt.% (2.5) resp	10—80	250–750	Kim *et al.*, 2006
NMMO–H_2O (85–15 w/w)	None	NA	700	3–9 wt.% (7)	25–30	450–1080	Han *et al.*, 2008
NMMO–H_2O (85–15 w/w)	Water 20°C – bath	Kraft pulp	1200	1–3 wt.%	5–10	NA	Yeoh *et al.*, 2009
NMMO–NMP–H_2O	None	α-cellulose	NA	1.25–4.3 wt.%	25–28	200–250	Uppal and Ramaswamy, 2011
DMAc–LiCl							
LiCl–DMAc	Water – heated rotating collector	Cotton linters and battings	1070, 1140	1–3 wt.% (3)	10–80	150–500	Kim *et al.*, 2005
LiCl–DMAc	Water – heated rotating collector	Cotton	1140	1–3 wt.%	15–25	250–750	Kim *et al.*, 2006
LiCl (8 wt%)–DMAc	Rotating collector	Pulp (non-specified)	NA	2 wt.%	15	NA	Lee *et al.*, 2009
LiCl (8.5 %w–v)–DMAc	Plate and rotating collector – water washed	Cotton linters	12000	1–1.35 wt.% (1.15)	12–18	50–400	Li *et al.*, 2011

© Woodhead Publishing Limited, 2014

TFA based							
Pure TFA	None	Cotton, wood pulp	36, 40 kDa	2–5 wt.% (4.5)	15	30–50	Ohkawa *et al.*, 2009
Pure TFA, TFA–H_2O, TFA/AA	None	Wheat straw	NA	4–5.5 wt.% (4)	12–20	270	Montaño-Leyva *et al.*, 2011
NaOH–urea–water							
7 wt% NaOH–12 wt% urea	None but binder	Cotton linters	500	0.9–4.5 wt.%	25	400	Qi *et al.*, 2010
6 wt% NaOH–4 wt% urea	None	A-cellulose	NA	Could not dissolve	–	–	Uppal and Ramaswamy, 2011
IL-based							
[bmIm][Cl] for cellulose	Ethanol	NA	5800 kDa	10% w/v	15–20	500	Viswanathan *et al.*, 2006
[AmIm][Cl]–DMSO							Xu, 2011
[BmIm][Cl]–DMSO	Still distilled water bath	Cellulose powder (hydrosung)	194.4 kDa	1.5–5 wt.%	NA	500–800	Quan *et al.*, 2010
[EmIm][Ac]–MWCT gel	Water–ethanol	Cellionic™ (5 wt.% cellulose in [EmIm][Ac])	1100	1.5 wt.%	18–22	100–1000	Miyauchi *et al.*, 2010
[EmIm][Ac]	Agitated (rotary shaker 50 rpm) distilled water bath	Microgranular cellulose, beechwood xylan, Kraft lignin	NA	Cellulose/xylan/lignin/P3OT (0.5/0.3/0.2/0.1 wt.%)	30	NA	Park *et al.*, 2011b
[EmIm][Ac]	NA	NA	NA	0.5 wt.% (with 0.25 wt.% chitosan)	NA	NA	Park *et al.*, 2011a
[EmIm][OAc]	Plate in water or water–ethanol bath	Cellionic™ (5 wt% cellulose in [EmIm][Ac])	1100	1.75 wt.%	18–19	100	Miyauchi *et al.*, 2011

(*Continued*)

© Woodhead Publishing Limited, 2014

Table 5.1 Continued

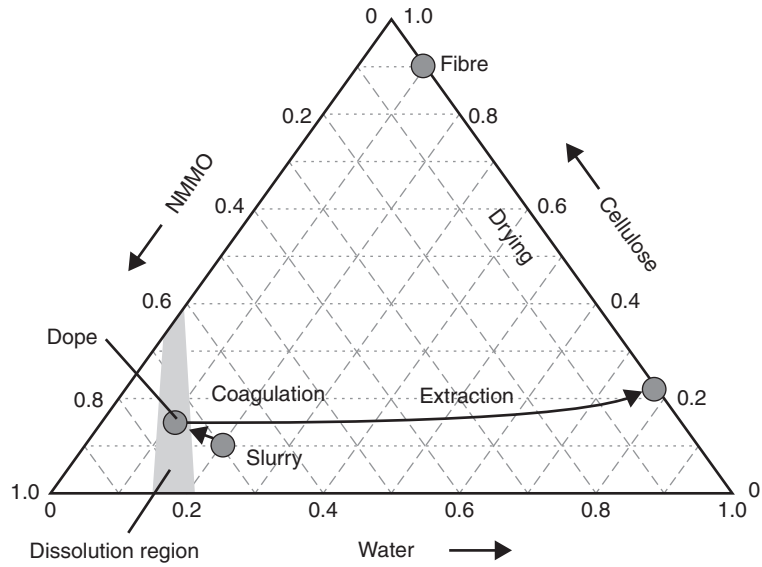
Solvent	Coagulant	Cellulose type	DP/MW	Concentration	Voltage (kV)	Diameter (nm)	References
[Emim][Ac] with[C10mIm]Cl	Agitated water bath	Raw cellulose fibres	53 kDa	8 wt.%	20	120	Freire *et al.*, 2011
[EmIm][Ac]–DMSO or DMAc or DMF	Water–rotating collector	Dissolving pulp from Domjso AB	750	2.5 wt.%	10–50	NA	Härdelin *et al.*, 2012
[EmIm][OAc]–DMF	Ethanol 4°C	Alkali treated hemp (lignocellulosic)	NA	14 wt.%	35 kV/15 cm	200–900	Ahn *et al.*, 2012b
[EmIm][OAc]–DMF or DMAc	Ethanol 4°C	NA	NA	6–8.3 wt.%	30 kV/15 cm	100–200 and 200–400	Ahn *et al.*, 2012a

Abbreviations:

DP, degree of polymerisation; MW, molecular weight; IL, ionic liquid; NMMO, N-methyl-morpholine N-oxide; LiCl, lithium chloride; NMP, N-methyl pyrrolidinone; TFA, trifluoroacetic acid; DMAc, dimethyl acetamide; TAA, acetic acid; DMSO, dimethyl sulfoxide.

* Values in parentheses indicate optimal concentrations.

© Woodhead Publishing Limited, 2014



5.2 Phase diagram of cellulose–NMMO–water. (*Source*: After Fink *et al.,* 2001.)

structure that is expected to reduce the potential mechanical properties of the cellulose. More recently, the LiCl–DMAc system has been used to dissolve native cellulose with the objective of targeting biomedical applications including an electroactive paper actuator (Lee *et al*., 2009a) and tissue engineering scaffolds (Li *et al*., 2011). These studies observed that there is a need to both heat the pathway between the tip of the needle and collector and to stretch the electrospun fibres, presumably to encourage the formation of crystalline cellulose (i.e. cellulose II). Lee *et al*. (2009a) applied heated air (~80°C) to a rotating drum-type collector and subsequently applied a 10% strain to the electrospun mat. Similarly, Li *et al*. (2011) used a 275 W infrared lamp to heat the collector and increased the rotational speed of the drum collector to orientate the fibres as they are collected. The ethylene diamide–potassium thiocyanate solvent system (ED–KSCN), a similar volatile solvent /salt system, has also been used to electrospin high molecular weight cellulose sourced from cotton. An 8 wt.% cellulose-ED–KSCN solution resulted in electrospinning of very fine cellulose segments with intermittent beads (Frey and Song, 2003; Frey *et al*., 2003).

The research group of Ohkawa empirically identified three important characteristics in the selection of an ideal solvent for electrospinning of polysaccharides: (i) semiconductive with moderate charge capacity; (ii) high volatility for rapid solidification of the solution jet; and (iii) an ability to dissolve polysaccharides with minimal intermolecular interaction (Ohkawa

© Woodhead Publishing Limited, 2014

et al., 2009). Trifluoroacetic acid (TFA) was found to satisfy all of these requirements and does not require elevated temperatures, concentrated salt, high voltage or pre- or post-treatment (e.g. oxidation). TFA was first identified as a direct solvent for chitosan. Chitosan-TFA solutions were successfully electrospun (Ohkawa *et al*., 2004) with fibre diameters in the range of 60–100 nm (Ohkawa *et al*., 2006). Ohkawa *et al*. (2009) also found that cellulose–TFA solutions were electrospinnable and exhibited lower viscosity than LiCl–DMAc- or NMMO-based ones. In fact, cellulose concentrations above 4 wt.% were necessary for successful electrospinning. The resulting cellulose fibres were found to be suitable as controlled drug release carriers. A drawback of the cellulose–TFA solutions is the amorphous state of the resulting cellulose fibres. However, an amorphous structure is also viewed as advantageous in terms of biodegradation. On the contrary, Montaño-Leyva *et al*. (2011) report highly crystalline electrospun fibres based on cellulose isolated from wheat straw using a TFA solvent system. The crystallinity of the as-received wheat straw was 37%, whilst that of the extracted cellulose and the electrospun fibres was 52% and 62%, respectively.

A small number of studies have reported the electrospinning of cellulose using sodium hydroxide and urea (NaOH–urea) since it was found to be a non-derivatising solvent system (Zhou *et al*., 2004) suitable for preparing regenerated-material. Qi *et al*. (2010) observed that electrospraying of a cellulose-NaOH–urea solution was possible with particle diameters in the range of 100–300 nm. Electrospinning of cellulose fibres was possible by blending the solution with high molecular weight poly(ethylene glycol) or poly(vinyl alcohol). Uppal and Ramaswamy (2011) also observed the NaOH–urea system was not able to dissolve high molecular weight cellulose, which severely limits the use of this solvent system for electrospinning.

The term ionic liquids (IL) was introduced in the 1990s (Endres and Zein El Abedin, 2006) to define liquids that consist solely of cations and anions and with a melting temperature of up to 100°C. Room temperature ionic liquids (RTIL) are a subcategory of ILs that melt at ambient temperature due to large molecular ions that often possess some level of asymmetry and charge delocalisation resulting in low lattice energy (Krossing *et al*., 2006). RTILs have attracted increasing attention as they facilitate safer and more sustainable reactions and separations, mostly due to their properties of low volatility and flammability, high thermal stability, electric conductivity and solvent power. ILs have been thoroughly investigated as direct solvents for cellulose (Pinkert *et al*., 2009), and other biopolymers in the electrospinning process (Meli *et al*., 2010). The effectiveness of ILs as direct solvents for cellulose is attributed to the formation of hydrogen bonds with hydroxyl groups (Ding *et al*., 2012). However, the solvency of cellulose in ILs has also been attributed to weakened hydrophobic interactions (Medronho *et al*., 2012). ILs are often referred to as ‘designer solvents’ since in principle

© Woodhead Publishing Limited, 2014

the combination of various cationic base, alkyl chains and anions permit tuneable properties and are thought to be able to generate up to 10^{18} (Endres and Zein El Abedin, 2006) (or even limitless amounts (Ohno, 2006)) different ILs with varying properties. However, the potential of ILs appears relatively untapped since virtually all investigations of cellulose dissolution since 2002 have used imidazolium-type ILs (denoted as [mIm]) and preferably [BmIm][Cl] as it was reported to solubilise cellulose concentrations of up to 25 wt.% via microwave heating) (Swatloski *et al.*, 2002). The use of ILs as solvents has also been applied in the preparation of cellulose for electrospinning (Table 5.1). The ILs are normally mIm-based with alkyl chains of butyl ([C4mIm] or [BmIm]), allyl ([AmIm]) or ethyl ([C2mIm] or [EmIm]), whilst [Ac] and [Cl] are commonly selected anions.

Viswanathan *et al.* (2006) were first to report the electrospinning of 10 wt.% cellulose fibres using RTILs ([BmIm][Cl]). The fibres were regenerated by electrospinning into a bath of ethanol that acted as the anti-solvent for cellulose (precipitation) and is miscible with [BmIm][Cl] (washing); the process is referred to as 'dry-jet wet-electrospinning' in reference to wet-spinning. Such a process is found to be simpler than regeneration via alkaline hydrolysis (Miyauchi *et al.*, 2010, 2011; Viswanathan *et al.*, 2006). However, the cellulose fibres produced by this method results in micron-sized diameters due to the high viscosity of the cellulose-IL solution and low volatility of [BmIm][Cl]. Quan *et al.* (2010) investigated the effect of using DMSO as co-solvent for reducing the solution viscosity, achieving lower cellulose concentrations and using water as the anti-solvent. It was observed that the presence of small quantities of DMSO in a 4 wt.% cellulose solution in [BmIm][Cl] encouraged the production of smooth cellulose fibres with a reduced diameter although, at higher cellulose concentrations (e.g. 5 wt.%), the DMSO has limited influence on the solution viscosity. [EmIm][Ac] has also been used successfully as a cellulose solvent (Miyauchi *et al.*, 2010) with the added advantage of lower viscosity and higher conductivity compared with [BmIm][Cl] for a given cellulose concentration. In a more complex system, a 1.5 wt.% cellulose-[EmIm][Ac] solution was used successfully in coaxial electrospinning wherein the solution was used as a sheath material to help carry a gel core consisting of CNTs and [EmIm][Ac]; the gel alone was not amenable to electrospinning. A bath of ethanol and water (to reduce flammability) was used as the regeneration medium and resulted in regeneration without problems. Indeed, the electrospun fibres exhibited a ribbon morphology with pure water as the coagulant, whereas cylindrical fibres were obtained with a 1:1 water–ethanol mixture. The same system was then used to prepare affinity separation membranes using a slightly more concentrated solution (1.75 wt.%) (Miyauchi M *et al.*, 2011). Group-specific affinity ligands were immobilised on the as-electrospun nanofibres, which were then packed into a column to investigate bovine serum albumin (BSA)

© Woodhead Publishing Limited, 2014

adsorption/desorption properties. The resulting membranes were found to be a promising packing material for affinity chromatography. Subsequently, Freire *et al*. (2011) tailored the surface tension of a cellulose/[EmIm][Ac] electrospinning dope using a surface active IL, namely 1-decyl-3-methylimidazolium chloride ([C10mIm][Cl]) in a mole fraction ratio of 0.10 with respect to the [EmIm][Ac] content to reduce surface tension. A higher cellulose concentration of 8 wt.% was used since the molecular weight of the cellulose was lower than in previous studies. The average diameter of the electrospun fibres was 120 nm with [C10mIm][Cl] and 470 nm without, which is thought to contribute to enhanced thermal stability in comparison to thicker fibres obtained (500–800 nm) by Quan *et al*. (2010). The thermal degradation temperature of the finer cellulose was only ~10 K lower than the as-received cellulose but higher than regenerated films. Similarly, Härdelin *et al*. (2012) investigated the use of DMAc, dimethyl formamide (DMF) and DMSO as viscosity and surface tension modifying co-solvents on the electrospinnability of a 2.5 wt.% cellulose/[EmIm][Ac] solution. The study established that a high viscosity, high surface tension, and some degree of shear-thinning were important for the electrospinnability of cellulose, regardless of the selected co-solvent. The DMSO-modified system exhibited the greatest viscosity and shear-thinning, surface tension was least affected, and fibre formation was unsurpassed. Recently, low viscosity co-solvent systems including [EmIm][Ac]/DMF and [EmIm][Ac]/DMAc were successfully used to prepare lignocellulosic (Ahn *et al*., 2012b) and cellulosic (Ahn *et al*., 2012a) fibres. The lignocellulosic system demonstrated successful electrospinning of fibres when the lignin content was less than 6 wt.%. The fibre diameter and crystallinity were decreased and the thermal stability of the cellulosic fibres increased with increasing content of co-solvent, regardless of which co-solvent was selected.

Despite the advances in the preparation methods for the electrospinning of non-derivatised cellulose fibres, there are very few systematic studies of the thermal and mechanical properties of the resulting fibres. Moreover, a lack of knowledge of electrospun cellulose fibre properties, particularly mechanical properties, presents an obstacle in assessing the reinforcement potential of such fibres in new types of biocomposite materials.

5.2.2 Derivatised cellulose

The majority of studies on electrospun cellulose fibres are based on the use of cellulose derivatives. A survey of the literature shows that 70% of investigations into electrospinning of cellulosic materials are focussed on the use of cellulose derivatives, with around 75% of these based on cellulose acetate (CA). A major advantage of using derivatised cellulose in the production of electrospun fibres is elimination of the difficulties associated with

© Woodhead Publishing Limited, 2014

the dissolution step that precedes the electrospinning of non-derivatised cellulose. For example, CA is easy to dissolve in many common solvents. Furthermore, the solidification of the CA-solvent dope occurs more easily by evaporation during electrospinning. Often, binary mixtures that consist of a low volatility solvent or a diluent (e.g. DMAc, acetic acid or water) and relatively higher volatility solvent (e.g. acetone) are used in order to tune the evaporation rate and avoid clogging of the spinneret during electrospinning (Table 5.2) (Frey, 2008; Celebioglu and Uyar, 2011).

Liu and Hsieh (2002) investigated the use of acetone, acetic acid, DMAc and mixtures thereof as solvents for the preparation of CA for electrospinning. A mixture of acetone and DMAc produced optimal results for the stable formation of uniform electrospun CA fibres, whilst acetic acid/DMAc and acetic acid/acetone blends resulted in beaded CA fibres. In contrast, electrospinning of the CA dope into fibres was not possible by using the individual solvents. Several studies have reported the successful preparation of submicron CA fibres using acetone–DMAc (Ding *et al.*, 2006; Nista *et al.*, 2012; Tang and Liu, 2008; Tungprapa *et al.*, 2007; Wang and Hsieh, 2004). Son *et al.* made extensive use of the acetone–water solvent system (Son, 2004a, 2004b; Son *et al.*, 2003, 2004, 2006) since it was found to increase the evaporation rate during electrospinning. However, in most studies, reported nanofibre diameters are larger than for acetone–DMAc solvent systems (Nista *et al.*, 2012; Son, 2004b, Son *et al.*, 2003, 2004, 2006; Xiang *et al.*, 2007). Mixtures of acetone and ethanol were also used successfully to electrospin a CA mat for the development of an ultrathin and flexible monolithic structure to be used in a bio-battery (Baptista *et al.*, 2011).Thin metal film electrodes are deposited onto the faces of the CA membranes. Instead of forming a continuous film at the surface, the metal penetrates the layers and the fibres are thus covered by a conductive layer, forming a light weight monolithic structure.

Another ternary system (acetone–DMF–TFE) has been reported earlier by Ma *et al.* (2005) to prepare affinity membranes from a 5 wt.% CA solution. The obtained mat had only poor mechanical strength (about 1 MPa) said to be like that of 'sticky and fluffy cotton', because the fibres did not adhere to each other. This is in the same order of magnitude (strength of 2.8 MPa and Young Modulus of 14.7 GPa) as electrospun 20 wt.% CA in acetone–DMAc mat used as reinforcement in a soy protein isolate matrix (Tang and Liu, 2008). When the fluffy mat was heat treated (208°C between T_g and T_m), some fusing between the fibres occurred improving the mat strength by five times.

Tungprapa *et al.* (2007) explored the use of solvents normally used to prepare plant extracts such as hexane, dichloromethane (DCM), ethyl acetate (EA), ethanol, methanol (MeOH), formic acid and pyridine, to broaden the selection of appropriate solvent systems for the electrospinning of CA nanofibres. The

© Woodhead Publishing Limited, 2014

Table 5.2 Binary and ternary solvent systems used to electrospin CA

Solvents	CA	Processing	Fibre diameters	References
Acetone/DMAc				
2:1	DS 2.45/Mn 30 kDa/C = 12.5 wt%	12–15 kV/6–10 in	100 nm–1 μm	Liu and Hsieh, 2002
2:2	DS 2.45/Mn 30 kDa/C = 12.5 wt%	10 kV/7 in	500 nm	Wang and Hsieh, 2004
2:1	Mn 40 kDa/C = 8–10 wt%	30 kV/15 cm	183 nm	Ding *et al.*, 2006
2:2	DS 2.4/MW 30 kDa/C = 12–20 wt%	NA	140–370 nm	Tungprapa *et al.*, 2007
2:1 (v/v)	39.8% Ac/MW 30 kDa/C = 20 wt%	8 kV/cm	200–940 nm	Chen and Liu, 2008
2:1	39.8% Ac/MW 30 kDa/C = 20 wt%	8 kV/15 cm	120–210 nm	Tang and Liu, 2008
2:1 (w/w)	DS 40%/Mn 29 kDa/C = 17–19 wt%	15–25 kV/7–10 cm	295 nm–1 μm	Nista *et al.*, 2012
Acetone/water				
85–15	39.8% Ac/MW 30 kDa/C = 17–21 wt%	12 kV/8 cm	3–4 μm	Son *et al.*, 2003
80–20	39.8% Ac/MW 30 kDa/C = 10 wt%	17 kV/10 cm	610 nm–1.9 μm	Son, 2004b
85–15	39.8% Ac/MW 30 kDa/C = 17 wt %	12 kV/8 cm	3–4 μm	Son, 2004a
80–20	39.8% Ac/MW 30 kDa/C = 10 wt%	17 kV/10 cm	610 nm	Son *et al.*, 2006
85–15	29.8% Ac/Mn 30 kDa/C = 17 wt%	NA	500 nm–2 μm	Xiang *et al.*, 2007
85–15	DS 40%/Mn 29 kDa/C = 17–19 wt%	15–25 kV/7–10 cm	1.7–3.6 μm	Nista *et al.*, 2012
Acetone/ethanol				
70/30	40% Ac/MW 61 kDa/C = 15–21 wt%	15–30 kV/10–25 cm	–	Baptista *et al.*, 2011
DCM–MeOH				
1:9, 1:4, 3:7, 2:3, 1:1	DS 2.4/MW 30 kDa/C = 5 wt%	15–25 kV/7–10 cm	670 nm–1.06 μm	Tungprapa *et al.*, 2007

© Woodhead Publishing Limited, 2014

MeOH–chloroform 1:4, 3:7, 2:3, 1:1	DS 2.4/MW 30 kDa/C = 5 wt%	15–25 kV/7–10 cm	790 nm–1.09 μm beaded	Tungprapa *et al.*, 2007
Acetone–DCM 1:1, 1:2, 1:3, 9:1 (v/v)	MW 30 kDa/C = 5, 7.5, 10 wt%	15 kV/10 cm	300 nm–7 μm	Celebioglu and Uyar, 2011
Acetic acid–water 3:1 (w/w)	DS 40%/Mn 29 kDa/C = 13–18 wt%	15–25 kV/7–10 cm	60–190 nm	Nista *et al.*, 2012
Acetone–DMF–TFE 3:1:1	Mr 29 kDa/40% Ac/C = 16% (wt/v)	25 kV/15 cm	200 nm–1 μm	Ma *et al.*, 2005
Acetone–DMAc–water 63:32:5 (w/w)	DS 40%/Mn 29 kDa/C = 14–17 wt%	15–25 kV/7–10 cm	310–605 nm	Nista *et al.*, 2012

DS = degree of substitution; MW = molecular weight; Mn = number average molecular weight; Mr = rheological molecular weight; C = concentration; Ac = acetyl content.

© Woodhead Publishing Limited, 2014

mixed solvent systems were based on acetone–DMAc, chloroform–MeOH and DCM–MeOH. Whilst the use of single solvents resulted in discrete beads or beaded short fibres (in the case of acetone), the MeOH mixed systems produced both beaded and smooth long fibres depending on solvent ratios, although with larger diameters than for acetone–DMAc.

A new binary solvent system composed of two highly volatile solvents, acetone and DCM, was investigated by Celebioglu and Uyar (2011). Bead-free CA fibres could be electrospun by increasing the proportion of DCM and decreasing the polymer concentration of the solutions, although this high viscosity spinning mixture produced relatively thick fibres. Nista *et al.* (2012) investigated acetone–water, acetone–DMAc, acetic acid–water and water–acetone–DMAc solvent systems, demonstrating that acetone–DMAc (either with or without water) were the optimal solvent systems in terms of CA fibre diameter.

Oxidised cellulose (OC) is completely bioresorbable under physiological conditions (Son, 2004b). Due to its use in biomedical applications, OC mats have been prepared as non-woven adhesion barriers, porous film implants for tissue engineering with reduced post-surgical adhesions (Khil *et al.*, 2005; Son, 2004b). However, OC mats cannot be directly prepared by electrospinning due to the poor solubility of OC. They are obtained by deacetylation and subsequent oxidation of an electrospun CA mat. OC mats have also been used as a metal ion chelator in environmental applications (Han *et al.*, 2009). The carboxyl groups of the OC are postulated to act as binding sites for heavy metal ions such as U^{6+}, Ce^{3+} and Eu^{3+}.

There are several reports on the use of cellulose derivatives (other than CA) as the base material for the electrospinning of cellulosic fibres. Table 5.3 presents a wide range of derivatives that have been investigated for their electrospinnability including cellulose esters such as cellulose triacetate (CTA) (Abitbol *et al.*, 2010; Han *et al.*, 2005; Yoon *et al.*, 2009), cellulose acetate butyrate (CAB), cellulose nitrate (CN) (Nartker and Drzal, 2010; Nartker *et al.*, 2011); and cellulose ethers such as ethyl cellulose (EC) (Park, 2007; Wu *et al.*, 2005), ethyl-cyanoethyl cellulose ((E-CE)C) (Zhao *et al.*, 2003, 2004), hydroxypropyl cellulose (HPC) (Shukla, 2007; Shukla *et al.*, 2005), hydroxyethyl cellulose (HEC) (Rosic *et al.*, 2011), carboxymethyl cellulose (CMC) (Kessick and Tepper, 2003), methyl cellulose (Frenot *et al.*, 2007), hydroxypropylmethyl cellulose (HPMC) (Frenot *et al.*, 2007; Verreck *et al.*, 2003), hydroxypropylmethyl cellulose phthalate (HPMCP) (Wang *et al.*, 2007), and acetoxypropyl cellulose (APC) (Godinho *et al.*, 2010). The majority of these investigations are focussed on the electrospinning mechanism or biomedical application of these cellulose derivatives.

CTA fibres have been prepared from solutions in which CTA is dissolved in a binary solvent system composed of methylene chloride (MC) and up to

© Woodhead Publishing Limited, 2014

Table 5.3 Cellulose derivate electrospun nanofibres

Cellulose derivates	Concentration (%)	Solvent	Processing	Fibre diameter	References
Cellulose esters					
Cellulose triacetate (CTA)	5 wt	Methylene chloride (MC) and MC/ethanol (90/10–-80/20)	15 kV/10 cm	#1 μm (pores 50–100 nm and 200–500 nm)	Han *et al.*, 2005
	3–9 wt	MC/ethanol (80/20)	10 kV/10 cm	200 nm–3.4 μm	Yoon *et al.*, 2009
	20 v/v	Methanol/MC (10 and 20 v/v%)	15 kV/10 cm	0.3–300 μm and 400–700 nm	Abitbol *et al.*, 2010
CAB	12–15 wt	Acetone/DMAc (2:1 v/v)	1 kV/cm (14–20 cm)	# 500 nm	Huang *et al.*, 2011a
CN	6–10 wt	EtOH/acetone (70/30 wt) and THF/DMF (60/40 wt)	10 kV/10 cm	100–1200 nm	Nartker *et al.*, 2011, Nartker and Drzal, 2010
Cellulose ethers					
Ethyl cellulose (EC)	13 wt	THF/DMAc (20/80–80/20)	0–100 kV/1–40 cm	200–500 nm	Wu *et al.*, 2005
	15 w/v	THF/DMAc (20/80–80/20)	10–20 kV/10 cm	1100–500 nm	Park, 2007
	6–12 wt	THF	10–25 kV/5–11 cm	~100 nm	Lim *et al.*, 2010
Ethyl-cyanoethyl cellulose (E-CE)	17 wt	THF	20–50 kV/5–20 cm	Av. 1.9–10.7 μm (lowest 200 nm)	Zhao *et al.*, 2003
	17 wt	THF	30 kV/15 cm	Av. 6.2 μm (lowest 250 nm)	Zhao *et al.*, 2003
Hydroxypropyl cellulose (HPC)	15 wt	Anhydrous ethanol and 2-propanol	10–30 kV/10–15 cm	80–300 nm and 150–1000 nm	Shukla, 2007, Shukla *et al.*, 2005

(*Continued*)

© Woodhead Publishing Limited, 2014

Table 5.3 Continued

Cellulose derivates	Concentration (%)	Solvent	Processing	Fibre diameter	References
Hydroxyethyl cellulose (HEC)	0.25–2.0 wt	Water	35–40 kV/10–25 cm	30–200 nm	Rosic *et al.*, 2011
Carboxymethyl cellulose (CMC)	0.01 wt	Water/methanol	~4 kV/cm	NA	Kessick and Tepper, 2003
Carboxymethyl cellulose (CMC) with PEO later extracted with ethanol	6–8 wt (1:1 CMC:PEO)	Water	35 kV/20 cm	200–250 nm	Frenot *et al.*, 2007
Methyl cellulose	2.86 wt	H_2O/EtOH (1:1)	40 kV/20 cm	NA	Frenot *et al.*, 2007
Hydroxypropyl methyl cellulose (HPMC)	2.14, 2.86 wt	H_2O/EtOH (1:1)	35 kV/20 cm	~130 nm	Frenot *et al.*, 2007
Hydroxypropyl methyl cellulose (HPMC) together with itraconazole (drug)	5 wt (with 10 wt drug)	Ethanol/methylene chloride (40/60 w)	16 and 24 kV/13 cm	1–4 μm and 300–500 nm	Verreck *et al.*, 2003
Hydroxypropyl methyl cellulose phthalate (HPMCP) with drug (erythromycin 1:9 HPMCP)	10–14 wt	Ethanol/acetone (1:1 v)	30 kV/10 cm	250–1000 nm	Wang *et al.*, 2007
Cellulose ethers esters					
APC	60 wt	Water/DMAc	15 kV/15 cm	25–50 μm	Godinho *et al.*, 2010

© Woodhead Publishing Limited, 2014

20% of an alcohol, typically ethanol (Han *et al*., 2005; Lim *et al*., 2010) or methanol (Abitbol *et al*., 2010). CTA fibres exhibit a higher porosity and BET surface area (14.47 m^2/g) as the relative content of MC in the solvent system is increased. Highly porous CTA fibres are suited to applications in nanofiltration or fibre templates (e.g. cell growth) (Han *et al*., 2005). Yoon *et al*. (2009) also applied a CF_4 plasma treatment to electrospun CTA mats to increase their hydrophobicity, obtaining water contact angles of up to 153° after 60 s of plasma treatment. CTA fibre has also been electrospun from MC–methanol solution to prepare fluorescent fibres. The fluorescence of the CTA fibres was derived from the colloidal CdSe/ZnS core/shell quantum dots that were added to the electrospinning solution. As was previously reported for ethanol, reducing the amount of methanol increases the porosity of the fibre. It is believed that at higher MC contents, phase separation occurs, whereas at higher alcohol contents the solidification of the polymer becomes dominant (Han *et al*., 2005). Huang *et al*. (2011) investigated the preparation of aligned cellulose acetate butyrate (CAB) fibres with the aim of producing a tissue engineering substrate that enhances cell growth. CN was electrospun into fibres with diameters in the range of 100–1200 nm (Nartker and Drzal, 2010). Two solvent systems (acetone–ethanol and tetrahydrofuran (THF)–DMF) and two types of collectors (a void gap and a steel drum) were investigated. Poly(vinylidene chloride) (PVDC) was utilised as a substrate material on the rotating collector to reduce damage to the CN fibres during deposition and the void gap produced aligned fibres. The electrospun CN mats could be incorporated into a biosensor device (as capture pad) to take advantage of the surface chemistry, enhanced capillary flow and surface area, and structural integrity.

EC has been electrospun from THF and THF–DMAc solvent systems with varying THF to DMAc ratios (20:80–80:20). Increasing the content of DMAc relative to THF increases the conductivity of the solution (Park, 2007), and reduces the viscosity, surface tension and fibre diameter (Park, 2007; Wu *et al*., 2005). The majority of these studies have focussed on assessing the effect of solvent composition on diameter and surface morphology of the electrospun fibres, with little work focussed on measuring the properties of the final fibres. (E-CE)C has been electrospun from a THF solution to produce porous fibres. The diameter of (E-CE)C fibres was as low as 200 nm. The crystallinity of electrospun (E-CE)C fibres varied with the applied voltage, reaching a maximum at 50 kV (Zhao *et al*., 2003, 2004). They proposed that for a given set up there is an optimum voltage at which electrostatic forces are high enough to promote molecular orientation if the flight time is long enough to allow for crystallisation.

Shukla *et al.* established the electrospinning characteristics of HPC with the final objective of obtaining ceramic oxide fibres using a HPC fibre template (Shukla, 2007; Shukla *et al*., 2005). HPC was dissolved in anhydrous ethanol

© Woodhead Publishing Limited, 2014

or anhydrous 2-propanol. The resulting solutions were electrospun at applied voltages between 10 and 30 kV using a spinneret-to-collector distance of either 100 or 300 mm. Beaded HPC fibres were observed, particularly when using ethanol as the solvent. The number of beads increased with increasing voltage and this was attributed to the combined effect of multiple jet formation and splaying due to a reduction in surface charge. The addition of Sn^{2+} and Cl^- ions to the solution drastically reduced bead formation in electrospun HPC.

Electrospun HEC fibres were investigated for their potential as a wound dressing material (Rosic *et al.*, 2011). Electrospun HEC fibres were produced with a diameter of 30–200 nm. The use of modified collectors (e.g. metal wire netting) dramatically reduced the number of beads and allowed orientated deposition of the fibres.

CMC was electrospun by Kessick and Tepper (2003) to demonstrate a micro-scaled version of electrospinning that requires lower electric potential to drive the process. CMC was also electrospun after blending with polyethylene oxide (PEO) (Frenot *et al.*, 2007). The PEO is subsequently removed by dissolution to yield CMC fibres with diameters between 200 and 250 nm. In the same study (Frenot *et al.*, 2007), MC and HPMC were electrospun from a water–ethanol solvent system to produce uniform fibres of 130 nm. A higher voltage was required to initiate electrospinning of MC (40 kV) compared to that of HPMC (35 kV), suggesting that the hydroxypropyl content influences the electrospinnability of the system. HPMC and HPMCP were also successfully electrospun in combination with medically active compounds (itraconazole and erythromycin respectively) for controlled drug delivery applications (Verreck *et al.*, 2003; Wang *et al.*, 2007). The 11% erythromycin-containing HPMCP fibre mat was observed to have a breaking stress and strain of 38.4 MPa and 15.7%, respectively, which was adequate in the drug carrier application.

APC was electrospun to study the physical mechanisms responsible for the helical and spiral conformations which can be found in biological systems (e.g. plant tendrils, curled hair or snails shells) (Godinho *et al.*, 2010). Indeed, such conformations are also observed in liquid-crystalline cellulosic fibres obtained by electrospinning. The fibres had large diameters (25–50 μm).

The electrospinning of cellulose fibres suffers from the poor solubility of cellulose in common solvents and high viscosity at low concentration. The use of poor solvents, low concentrations or derivatives results in regenerated fibres with limited structural integrity and crystallinity, which presumes for limited mechanical properties. Difficulties linked to the processing of cellulose can be overcome to some extent through the use of polymer blends. Improvements in the mechanical, as well as electrical or magnetic properties of electrospun fibres, can be achieved through the use of additives and fillers such as nanoparticles and nanotubes, leading to the formation of electrospun nanocomposite fibres. Of particular relevance in this chapter is

© Woodhead Publishing Limited, 2014

the recent use of CNC or whiskers as eco-friendly fillers to create nanobiocomposite fibres.

5.3 Electrospun cellulosic fibres via polymer blends

In general, electrospun cellulose blends have tended to be based on a mixture of CA with another hydrophilic polymer such as poly(ethylene glycol)–poly(ethylene oxide) (PEG–PEO) (Chen *et al.*, 2009a, 2009b, 2011a; Zhang and Hsieh, 2008), poly(vinylpyrrolidone) (PVP) (Castillo-Ortega *et al.*, 2010; Simons *et al.*, 2010; Uslu and Aytimur, 2012), or poly(vinyl alcohol) (PVA) (Jia *et al.*, 2011; Khatri *et al.*, 2012; Uslu and Aytimur, 2012). CA has also been blended with biopolymers that are difficult to process such as chitosan (Park *et al.*, 2011a), silk fibroin (SF) (Zhou *et al.*, 2011c), or egg albumen (Wongsasulak *et al.*, 2010). Polymer blends can consist of three different kinds of blends:

1. solution blending – two polymer solutions are mixed together before electrospinning
2. fibre blending – solutions are electrospun through separate nozzles but collected together as one mat
3. hybrid fibre – typically one polymer solution forms the core of the fibre and the other one the sheath.

The selection of one technique over another depends on the targeted application requirements (e.g. mechanical properties, functionalities) and/or the ability of finding a common solvent for the different polymers.

5.3.1 Solution blending

The aim of solution blending is to improve the electrospinnability of at least one of the polymers and/or exploit synergistic effects from combining different polymers with different properties. In general, solution blending is only possible if a common solvent is identified for all of the polymers to be blended.

Despite good mechanical properties, SF is brittle in the dry state, lacking in surface specificity, and has 'tedious' biodegradation rate control (Zhou *et al.*, 2011d). Generally, SF is difficult to electrospin in its native state due to difficulties with dissolution. Zhou *et al.* (Zhou *et al.*, 2011c, 2011b, 2011d) electrospun SF/CA fibres with a diameter of 50–300 nm from an SF/CA solution blend based on formic acid. Both the electrospinnability and mechanical properties of pure SF were improved by adding up to 10 wt.% CA such that the SF/CA blend produced fine, uniform fibres without beading. The tensile strength of the resulting SF/CA fibres was 2.5 times higher than SF (from 36–89 MPa), whilst the elongation at break was increased by 1.5 times (from 8% to 12.8%)

© Woodhead Publishing Limited, 2014

(Zhou *et al*., 2011d). Egg albumin is a low cost source of protein that can be used as a carrier for controlled release of active compounds, especially in the severe acidic conditions of the stomach. However, the globular molecular structure of egg albumin results in a low degree of molecular entanglement in solution, leading to difficulties in electrospinning. Wongsasulak *et al*. (2010) solution-blended egg albumin that was dissolved in 85% acetic acid with CA that was dissolved in 50% formic acid to produce electrospun edible egg albumin-based fibres with a diameter from 250 to 400 nm with potential applications in food packaging and controlled drug release.

Uslu and Aytimur (2012) combined *Aloe vera* as a carbohydrate-based active ingredient, HPMC as a water retention agent, PVA for high mechanical strength and flexibility, PEG for mechanical strength and high level of hydration, and PVP for its ability to bind iodine and thus resist bacteria to obtain the properties required for burn wound dressing materials. This complex mixture of materials was processed as an aqueous solution to electrospin fibres with diameters in the range of 100–900 nm. The resulting wound materials demonstrated controlled evaporative water loss, excellent oxygen permeability, good fluid drainage ability, and inhibition of exogenous microorganism invasion due to ultrafine pore size. Likewise, fibrillar-structured wound-healing gauzes have been developed to exploit the mechanical strength of cellulose and antibacterial and barrier properties of chitin. Du and Hsieh (2009) combined cellulose and chitin derivatives (CA and dibutyryl chitin (DBC)) as they have several common solvents including acetone, DMAc, DMF and acetic acid. A solution based on CA/DBC dissolved in acetone–acetic acid (1:1) was the most successful for electrospinning of CA/DBC fibres with diameters in the range of 30–350 nm. Park *et al*. (2011a) were able to solution blend native cellulose and chitosan using a common IL solvent ([EmIm][Ac]). The mechanical and insulating properties of cellulose have also been found to be useful in phase change materials (PCM) for thermal energy storage. For example, Chen *et al*. (2009b) reported the preparation of electrospun fibres based on a composite of PEG–CA, having diameters in the range of 1000–1750 nm. In this system, CA acts as a shielding matrix and PEG as the PCM. Cao *et al*. (2009) electrospun amphiphilic poly(styrene-co-(maleic sodium anhydride)) (SMA) that was solution-blended with CA. The resulting fibres were thermally crosslinked, giving a composite fibre that exploited the water stability of SMA and retained the mechanical strength of the CA. The electrospun SMA/CA fibres with diameters in the range of 300–400 nm were then hydrolysed to produce SMA–Na/cellulose hydrogel fibres that exhibited improved mechanical strength upon immersion in water and responsiveness to pH.

'Island in the sea' structures are commonly observed in polymer blends due to immiscibility and phase separation. For example, electrospun SF/PEO fibres can exhibit phase separation (Wang *et al*., 2004). The subsequent

© Woodhead Publishing Limited, 2014

selective removal of one of the phases or components can result in electrospun fibres with high surface area due to the formation of nanopores. The selective removal of a component is also exploited in the electrospinning of core-sheath fibres to obtain hollow fibres. In addition, co-continuous structures can be obtained by solution blending polymers that can interact with each other through molecular forces. Tang *et al.* (2008) prepared electrospun fibres with co-continuous structures by solution blending CA and polyurethane (PU) in a DMAc–acetone solvent system. It was possible to combine the dimensional stability and biocompatibility after regeneration of CA with the high tensile strength of PU to produce electrospun fibres that can exhibit mechanical properties superior to either of the individual components. The pure CA fibres exhibit a tensile strength, strain to failure and modulus of 0.98 MPa, 8% and 39 MPa, respectively; whilst pure PU has 8.98 MPa, 193% and 24 MPa, respectively; and in comparison the 40:60 CA/PU fibres have 3.20 MPa, 27% and 105 MPa, respectively.

Cellulose derivatives have also been used to increase the hydrophilicity of the electrospun system. For example, Zhang *et al.* (2009) combined the low density and flexibility of hydrophobic poly(acrylonitrile) (PAN) with the high hydrophilicity, processability, biocompatibility, and thermal resistance of HEC. The electrospun solution was crosslinked to yield smooth fibres with diameters in the range of 100–300 nm.

5.3.2 Fibre blending

Multi-jet electrospinning is sometimes preferred to solution blending since it can be problematic to identify a common solvent for the polymers to be combined during electrospinning. Using this strategy, the various polymers to be combined are electrospun independently of each other and combined at the collector as solid fibres. Although the ability to improve processability of the polymer solutions may be lost, the benefits of blending the electrospun fibres at the collector including tailoring of mechanical properties, functionalities and pore/fibre structure of the final electrospun mat, again creating synergies that are not achieved by using the components alone. Khatri *et al.* (2012) electrospun CA and PVA using a double spinneret to allow independent electrospinning. In this example of a hybrid mat, the wicking rate of the mat was tailored for biosensor or medical applications by varying the amount of electrospun PVA onto the target.

5.3.3 Hybrid fibres

The pharmaceutical and food industries are large consumers of cellulosic materials in a multitude of different applications. Hence, there has been interest in the coaxial electrospinning of core–shell type structures based on cellulosic materials for the design of new devices that accurately deliver

© Woodhead Publishing Limited, 2014

a controlled dosage of a substance. For example, Sakuldao *et al*. (2011) prepared hollow CA nanofibres with a diameter of 400 nm that were core-filled with a model protein for proof of concept. The electrospun CA-protein structure remained intact at a pH of 7.4 and temperature of 37°C and thus is expected to hold potential for the sustained release of proteinaceous compounds within the gastro-intestinal tract. Castillo-Ortega *et al*. (2011) exploited the water-solubility of PVP to prepare hollow nanotubes of CA with a diameter of 500 nm by coaxial electrospinning. The Young's modulus and breaking strength of the hollow nanotubes were 0.9 and 16.5 MPa, respectively, whilst that of the pure CA nanofibres was only 0.016 and 0.356 MPa, respectively. The membranes prepared with hollow CA fibres were loaded with drugs to examine the release behaviour. Amoxilicin time release was about 5 days, hence the material was found to have potential application in both oral and patch administration. CA nanofibres were also prepared using PVP as sheath. As-electrospun CA fibre had mechanical properties comparable to the hollow CA fibres.

5.4 Electrospun nanocomposite fibres

Electrospun fibres are regarded as promising candidates as reinforcements in polymer matrix composites due to their high specific surface. However, electrospun fibres must exhibit a higher strength and elastic modulus than the matrix in order to be termed reinforcement as opposed to filler. The electrospinning of *composite* fibres is one approach to improving the mechanical properties of electrospun fibres. Much of the published work until 2010 had focussed on the use of nanoclays (Marras *et al*., 2008) and carbon nanotubes (CNTs) (Chen *et al*., 2010; Chronakis, 2005; Lu and Hsieh, 2010; Miyauchi *et al*., 2010), especially in combination with synthetic polymer fibres. The addition of small quantities of synthetic single walled (SWCNT) and multiwalled nanotubes (MWCNT) to polymers are well known to greatly enhance the mechanical properties of the neat polymer. The high properties of CNTs are attributed to their intrinsic crystalline quality and straightness (Chronakis, 2005). Following from the surge in interest in nanosized reinforcement, there is also much interest in natural sources of nanostructured reinforcements. For example, cellulose in the form of nanocrystals (CNC or whiskers) has become recognised as a potential high performance biopolymer as highlighted in Table 5.4.

5.4.1 Electrospun carbon nanotube-reinforced cellulose fibres

Although the majority of work in the field has concentrated on using CNTs to reinforce electrospun petrochemically-derived polymers, there has been

© Woodhead Publishing Limited, 2014

Table 5.4 Nanocomposite fibres

Matrix polymer	Cellulose nanocrystals/whiskers			Voltage (kV)	Nanocrystals thickness x length (nm^2)	Diameter of electrospun fibres (nm)	References
	Cellulose type	Process	Concentration respective to matrix				
5.0 wt% PEO 900 kDa	Bacterial cellulose	65 wt% H_2SO_4, 40°C, 16 h	0.2, 0.4 wt%	12–24 kV/20 cm	11 ± 4 × 420 ± 190	250 ± 40 and 300 ± 40	Park *et al.*, 2007
10–30 wt% PS 230 kDa in THF + surfactant	Whatman cellulose	1.5 M HCl, 100°C, 4 h	6, 9 wt%	30–45 kV/16 cm	10–20 × 200	1.6–5.4 and 0.5–2 μm	Rojas 2009
1.5 wt% cellulose in NMMO/H_2O and DMSO	Pure cellulose (0.42, 3.28 wt%)	64 wt% H_2SO_4, 55°C, 2 h		20 kV/10 cm	–		Magalhães *et al.*, 2009
PLA in DMF			0,1,10 wt%				Xiang *et al.*, 2009
PCL (80 kDa) in DCM	Unmodified and PCL-grafted purified ramie cellulose	65 wt% H_2SO_4, 55°C, 45 min	2.5, 5, 7.5 wt%	10–15 kV (0.65–0.75 kV/cm)	3–10 × 100–250	~200	Zoppe *et al.*, 2009
4% PAA (450 kDa) in ethanol	Whatman cellulose	65 wt% H_2SO_4, 45°C, 60 min	0, 5, 10, 15, 20 wt%	30 kV/25 cm	–	69, 90, 141, 162, 349	Ping and You-Lo, 2009
7 wt % PVA (125,127 kDa; 98 DH; 2, 12 acetyl %)	Purified ramie cellulose	65 wt% H_2SO_4, 55°C, 45 min	0, 5, 10, 15 wt%	0–50 kV/15 cm	3–10 × 100–250	188–290	Peresin *et al.*, 2010b
PMMA (350 kDa) with DMF/THF	Bacterial cellulose	50 v/v% H_2SO_4, 60°C, 72 h	0, 1, 3.5, 7, 14, 20 wt%	12 kV/12 cm	15–20 × 0.8–8 μm (1.2 μm)	1415, 1802, 1306, 778, 237, 106	Olsson *et al.*, 2010
7 wt % PVA (125 kDa; 98 DH; 2 acetyl %)	Purified ramie cellulose	65 wt% H_2SO_4, 55°C, 45 min	0, 5, 10, 15 wt%	0–50 kV/15 cm	3–10 × 100–250	188–235	Peresin *et al.*, 2010a

(*Continued*)

© Woodhead Publishing Limited, 2014

Table 5.4 Continued

Matrix polymer	Cellulose nanocrystals/whiskers			Voltage (kV)	Nanocrystals thickness x length (nm^2)	Diameter of electrospun fibres (nm)	References
	Cellulose type	Process	Concentration respective to matrix				
5 wt% CA (50 kDa, 39.7% acetyl)	MCC	H_2SO_4 based	0–5 wt%	15 kV/3 cm	–	200–1048 at 5 wt%	Herrera *et al.*, 2011
Cellulose in NMMO with DMSO	Cotton fibres	H_2SO_4 based					Magalhaes, 2011
4.1, 4.6, 4.8, 5, 5.5% (w/v) EVOH (29 %mol ethylene) in 70/30 v/v propanol water	Bacterial cellulose	50 v/v% H_2SO_4, 50°C, 120 h	0, 5, 10, 15, 20, 25, 40 wt%	10–12 kV/12 cm	30 × –	200–400 range	Martínez-Sanz *et al.*, 2012
5, 7 wt% PEO (Mv 900 kDa)	MCC (Avicell)	64 wt% H_2SO_4	0, 5, 10, 20 wt%	30 kV/–	10 ± 3 × 112 ± 26	150–200 at 5 wt%; 230–270 at 7 wt%	Zhou *et al.*, 2011a
20 wt% degummed silk in formic acid	Mulbery branch bark	H_2SO_4 based	0–4 wt%	20 kV/12 cm	–	77–250	Huang *et al.*, 2011
8 wt% PVA (127 kDa, 99 DH)	Whatman cellulose	65 wt% H_2SO_4, 55°C, 45 min	0, 5, 10, 15 wt%	20 kV/20 cm	5–10 × 180–220	–	Lee and Deng, 2012
12 wt% PLA in THF	Bacterial cellulose	50 wt% H_2SO_4, 60°C, 4 h	2.5, 5.0, 7.5 wt%	8–10 kV/8 cm	20 × 500–1000	300	Liu *et al.*, 2012
5 wt% PEO (Mv 900 kDa)-UV crosslinked with PETA	Cotton	64 wt% H_2SO_4	0, 5, 10, 20 wt%	15 kV/20 cm	8.7 ± 1.7 × 70 ± 34	244 ± 45–183 ± 22	Zhou *et al.*, 2012

© Woodhead Publishing Limited, 2014

10 wt% CA (Mn = 30 kDa; 39.8% acetyl) in acetone/H_2O (8:2)	Silver nanoparticles ($AgNO_3$)		0.01–0.5 wt%	17 kV/10 cm		680–610	Son, 2004a
Bacterial cellulose dissolved in [amIm][Cl]/DMSO	MWCNT	H_2SO_4/HNO_3 (3:1)	0.02 wt%	25–30 kV/20 cm		200–500	Chen *et al.*, 2010
15 wt% CA (39.8 wt% Ac. 30 kDa) in 2:1 acetone/DMAc	MWCNT		0.11 and 0.55 wt%	14.25 kV/25cm	10–30 nm × 5–15 μm	200–300	Lu and Hsieh, 2010
1.5 wt% cellulose in [EmIm][Ac] (from Cellionic)	MWCNT		20–45 wt%	18–22 kV/9 cm			Miyauchi *et al.*, 2010

Abbreviations: PAA: poly(acrylic acid); EVOH: ethylene vinyl alcohol; PETA: pentaerythritol triacrylate.

© Woodhead Publishing Limited, 2014

some work to examine the use of CNTs to reinforce electrospun biopolymers including cellulose. Chen *et al*. (2010) examined the effect of adding MWCNTs to bacterial cellulose that was dissolved in an IL ([AmIm][Cl]) to make composites for medical, mechanical or electrical applications. The addition of 0.02 wt.% MWCNTs increased the crystallinity, conductivity, thermal and mechanical properties of the cellulose fibres. Specifically, the tensile strength and modulus of the electrospun cellulose was increased by 290% and 280%, respectively. MWCNTs have also been successfully incorporated into electrospun CA fibres. The addition of 0.55 wt.% MWCNTs increased the mechanical properties (Young's modulus and strength at break) by up to two times and decreased the average fibre diameter by 28% (Lu and Hsieh, 2010). Miyauchi *et al*. (2010) electrospun core-sheath MWCNTs/cellulose fibres via coaxial electrospinning such that the final structure consists of a conductive core and insulating sheath. However, the mechanical properties of the MWCNTs/cellulose fibres coaxial fibres were degraded with increasing content of MWCNTs since the MWCNTs within the core were not strongly bonded to each other.

5.4.2 Electrospun cellulose nanocrystal-reinforced biopolymer fibres

Cellulose nanocrystals (CNC), also known as cellulose whiskers, are a class of cellulosic material that exhibits high crystallinity and elastic modulus (~137–155 GPa). Understandably, CNCs have attracted considerable attention in bionanocomposite applications where they are potential alternatives to inorganic nanomaterials such as CNTs. Numerous publications have examined the electrospinning of eco-friendly polymers such as PEO, cellulose, PLA, PCL and PVA with cellulose nanocrystals as a reinforcement material. The mechanical properties of the resulting electrospun fibre mats are often difficult to compare across publications since a multitude of different combinations of CNCs and polymers from different sources have been used (Table 5.4). A summary of mechanical properties for different electrospun fibre mats are given in Table 5.5.

The filler content for nanoclay-reinforced nanocomposites is typically less than 5 wt.% (Marras *et al*., 2008). However, up to 15–20 wt.% of CNCs are commonly incorporated into the matrix material. The content of CNCs used is relatively high compared with other nanofillers. Indeed, it is expected that increasing the content of CNCs will increase the crystallinity and thermal stability of the composite fibre. However, the theoretical percolation threshold is estimated to be 2.5 wt.% for cotton and 5.9 wt.% for ramie whiskers (Siqueira *et al*., 2010). Thus, the addition of 20 wt.% cellulose whiskers may increase the viscosity of the solution and potentially lead

© Woodhead Publishing Limited, 2014

Table 5.5 Mechanical properties of nanocomposite electrospun fibres

Matrix	Fillers or whiskers	Specificity	Filler concentration (%)	Mechanical properties						References
				Young's modulus		Maximum stress		Strain at break		
				(MPa)	Relative value	(MPa)	Relative value	Value (%)	Relative value	
	Fillers									
Bacterial cellulose	MWCNT		0 wt.%	5.5 ± 0.3	1.00	93.6 ± 9.9	1.00	5.5 ± 0.9	1.00	Chen *et al.*, 2010
			0.02 wt.%	14.3 ± 0.9	2.60	247.4 ± 8.1	2.64	4.4 ± 1.5	0.80	
Cellionic	MWCNT	Core-sheath	0 wt.%	–	–	6.22 ± 0.06	1.00	7.5 ± 0.8	1.00	Miyauchi *et al.*, 2010
			20 wt.%	–	–	5.14 ± 0.41	0.83	5.5 ± 0.4	0.73	
			30 wt.%	–	–	4.23 ± 0.53	0.68	7.6 ± 0.8	1.01	
			40 wt.%	–	–	2.79 ± 0.18	0.45	8.9 ± 1.9	1.19	
			45 wt.%	–	–	2.54 ± 0.28	0.41	7.5 ± 0.8	1.00	
CA	MWCNT		0 wt.%	553 ± 39	1.00	21.9 ± 1.6	1.00	8.04 ± 0.27	1.00	Lu and Hsieh, 2010
			0.11 wt.%	937 ± 12	1.69	29.7 ± 1.2	1.36	9.04 ± 0.43	1.12	
			0.55 wt.%	1144 ± 37	2.07	40.7 ± 2.7	1.86	10.46 ± 0.33	1.30	
	Whiskers									
PEO	Bacterial	Mat	0 wt.%	32.7 ± 5.9	1.00	1.01 ± 0.15	1.00	176.4 ± 44.3	1.00	Park *et al.*, 2007
			0.2 wt.%	70.4 ± 8.7	2.15	1.45 ± 0.16	1.44	348.8 ± 80.3	1.98	
			0.4 wt.%	96.1 ± 10.7	2.94	1.74 ± 0.09	1.72	588.0 ± 102.5	3.33	
PCL	Ramie	Mat	0 wt.%	3.89 ± 0.10	1.00	1.10 ± 0.08	1.00	43.5 ± 10.4	1.00	Zoppe *et al.*, 2009

(*Continued*)

© Woodhead Publishing Limited, 2014

Table 5.5 Continued

Matrix	Fillers or whiskers	Specificity	Filler concentration (%)	Mechanical properties						References
				Young's modulus		Maximum stress		Strain at break		
				(MPa)	Relative value	(MPa)	Relative value	Value (%)	Relative value	
PCL	Ramie	Unmodified	2.5 wt.%	6.54 ± 0.26	1.68	1.51 ± 0.06	1.37	64.8 ± 2.4	1.49	
		Unmodified	5 wt.%	3.94 ± 0.58	1.01	0.86 ± 0.08	0.78	82.6 ± 8.2	1.90	
		Unmodified	7.5 wt.%	6.26 ± 0.73	1.61	1.32 ± 0.21	13.20	85.8 ± 14.4	1.97	
PAA	Whatman	Mat	0 wt.%	56	1.00	0.29	1.00	136 ± 7	1.00	Ping and You-Lo, 2009
			5 wt.%	188	3.36	0.68	2.34	126 ±6	0.93	
			10 wt.%	224	4.00	0.84	2.90	67 ± 4	0.49	
			15 wt.%	1192	21.29	3.26	11.24	60 ± 3	0.44	
			20 wt.%	1983	35.41	4.51	15.55	36 ± 2	0.26	
		Crosslinked	20 wt.%	4331	77.34	16.7	57.59	17 ± 1	0.13	
PVA	Ramie	10% RH	0 wt.%	1.5	1.00	–	–	0.57	1.00	Peresin *et al.*, 2010a
		70% RH	0 wt.%	0.4	1.00	–	–	2.63	1.00	
		80% RH	0 wt.%	0.2	1.00	–	–	3.7	1.00	
		10% RH	15 wt.%	2	1.33	–	–	0.33	0.58	
		70% RH	15 wt.%	0.8	2.00	–	–	1.26	0.48	
		80% RH	15 wt.%	0.3	1.50	–	–	2.85	0.77	
PEO	MCC	Mat 5 wt%	0 wt.%	2.50 ± 0.06	1.00	15.2 ± 0.3	1.00	200 ± 12	1.00	Zhou *et al.*, 2011a
			5 wt.%	5.08 ± 0.14	2.03	38.1 ± 0.7	2.51	122 ± 8	0.61	
			10 wt.%	5.96 ± 0.16	2.38	37.9 ± 0.6	2.49	103 ± 7	0.52	
			20 wt.%	7.04 ± 0.21	2.82	35.3 ± 0.5	2.32	166 ± 10	0.83	
		Mat 7 wt%	0 wt.%	4.00 ± 0.10	1.00	23.8 ± 0.9	1.00	168 ± 10	1.00	
			10 wt.%	6.68 ± 0.20	1.67	43.3 ± 1.5	1.82	141 ± 9	0.84	
			20 wt.%	8.52 ± 0.25	0.02	59.6 ± 3.8	3.92	125 ± 8	0.74	

© Woodhead Publishing Limited, 2014

Silk	Mulberry branch bark		0 wt.%	~300	1.00	12.5	1.00	10.8	1.00	Huang *et al.*, 2011b
			2 wt.%	621	2.07	22	1.76	7.6	0.70	
			4 wt.%	1237	4.12	38.5	3.08	4.8	0.44	
PVA	Whatman	Isotropic	0 wt.%	64.7	1.00	4.21	1.00	–	–	Lee and Deng, 2012
			15 wt.%	132.8	2.05	7.84	1.86	–	–	
		Aligned	0 wt.%	87.7	1.00	5.37	1.00	–	–	
			15 wt.%	19.05	0.22	10.5	1.96	–	–	
PEO	Cotton		0 wt.%	17.5 ± 1.1	1.00	6.74 ± 0.25	1.00	221 ± 16	1	Zhou *et al.*, 2012
			5 wt.%	31.3 ± 1.4	1.79	8.73 ± 0.30	1.30	201 ± 12	0.91	
			10 wt.%	39.8 ± 1.9	2.27	11.89 ± 0.57	1.76	163 ± 9	0.74	
			20 wt.%	36.3 ± 1.5	2.07	14.22 ± 0.78	2.11	167 ± 10	0.76	

© Woodhead Publishing Limited, 2014

to agglomeration of CNCs within the composite fibre, explaining the lower than expected mechanical properties. Nevertheless, Young's Modulus and tensile strength are easily doubled and sometimes tripled or quadrupled, whilst the strain to failure normally shows a reverse trend with increasing CNCs unless there is poor compatibility between the CNCs and matrix. The Young's modulus of the electrospun neat polymer fibre mat could be increased by between 35 (uncrosslinked matrix) and 77 (crosslinked) times in a 4 wt.% CNC-poly(acrylic acid) composite fibre. CNCs are known to act as nucleating agents in the crystallisation of polymers such as in the case of film casting of PCL (Habibi and Dufresne, 2008; Siqueira *et al*., 2008). Thus, an increase in the CNC content in electrospun materials is expected to increase the melting temperature and degree of crystallinity of electrospun fibre. However, the addition of CNCs in PCL, PVA, EVOH and PEO results in decreased crystallisation of the electrospun matrix material (Martínez-Sanz *et al*., 2012; Peresin *et al*., 2010b; Zhou *et al*., 2011a; Zoppe *et al*., 2009) (Table 5.5). Therefore, the observed increase in modulus in CNC-loaded PVA mats compared to neat PVA is thought to be a result of a percolation effect in which a hydrogen bonding network forms within the dispersed phase (Peresin *et al*., 2010b).

5.5 Mechanical properties of electrospun fibres and mats

Electrospun cellulose fibres are considered potential reinforcement materials for the development of new biocomposites due to the high mechanical properties that should be attainable. Tan and Lim (2006) reviewed the mechanical property characterisation of nanofibres and nanorods. The various characterisation techniques are divided into four categories of testing:

1. nano-tensile (using and atomic force microscope (AFM) cantilever or NanoBionix system),
2. nano-bend (AFM three-point bend test),
3. nanoindentation (mostly AFM-based),
4. resonance-based (cantilever induced and observed using transmission electron microscopy (TEM) or AFM).

Wang *et al*. (2004) used nanoindentation to assess the modulus of electrospun silk/PEO nanofibres treated with methanol and extracted with water. The lateral modulus was 8.00 ± 2.98 GPa. Gu *et al*. (2005) preferred the bend test method using AFM to measure the Young's modulus of an electrospun PAN fibre. Electrospun fibres obtained under a higher applied voltage exhibited an increased modulus (14.07–28.87 GPa at 22 kV compared to 3.79–6.88 GPa

© Woodhead Publishing Limited, 2014

at 18 kV). Yuya *et al.* (2007) obtained results of the same order of magnitude (26.8 GPa) as seen in Table 5.6. at lower voltage using a different technique (microcantilever vibration). The Young's modulus of electrospun PAN fibre could be doubled by using only 4 wt.% graphite nanoplatelets ((Mack *et al.*, 2005)). The highest measured modulus (140 GPa) was reported by Ko *et al.* (2003) for orientated electrospun 4 wt.% SWCNT-PAN fibres. The elastic modulus of electrospun PVA fibre before and after annealing at 135°C was found to be 4.4 ± 1.4 and 7.6 ± 2.3 GPa, using an AFM-based bend test (Wong *et al.*, 2010). Additionally, the mechanical properties of electrospun fibres will strongly depend on the diameter of the fibres. Lim *et al.* (2008) confirmed the effect of the diameter on the mechanical properties of electrospun PCL fibres. However, it was also pointed out that finer fibres are obtained from more dilute suspensions that yield more densely packed and stretched fibres. The Young's modulus was found to increase rapidly for diameters less than 500 nm from around 0.5 GPa up to 3 GPa, depending on the polymer concentration. The size effect increase in Young's modulus was also observed for very thin PVA nanofibres treated with plasma. The Young's modulus of the electrospun fibres deviated from the bulk material when the diameter decreased to 80 nm. For example, the mechanical property of a nanofibre with a diameter of 10 nm was 10 times higher (i.e. 500 GPa) compared to the bulk PVA. It is argued that dramatic increases in the Young's modulus are the direct result of fibre diameters less than 80 nm. Indeed, as reported earlier, highly drawn fibres show increased molecular organisation. It was proposed that the fibre diameter dominates the mechanical properties, overwhelming other changes in the surface morphology or polymer structure (Fu *et al.*, 2010).

5.6 Cellulose nanofibre-reinforced polymer composites

At this stage, the mechanical properties of single electrospun cellulose fibres have not been reported. However, it is expected that the mechanical properties of less ordered regenerated (i.e. electrospun) cellulose fibres will be lower compared with native cellulose nanofibrils (E = 150 GPa). The mechanical properties of single electrospun cellulosic fibres should be attainable in the future given the large number of experimental protocols being currently developed. In general, electrospun fibres are collected as a mat from which extracting a single fibre for characterisation without damage is experimentally challenging. Consequently, the mechanical properties of the electrospun mat are more frequently reported as shown in Table 5.6. The discrepancies in the mechanical properties are more likely to be attributable to variations in solvent systems, concentrations and post-spinning treatment. An order of magnitude difference in the Young's modulus of

© Woodhead Publishing Limited, 2014

Table 5.6 Mechanical properties of cellulose nanofibres, nanofibre mats and nanofibre filled composites

	Young's modulus *E*	Diameter (nm)	Measurements	References
Single nanofibre				
Nylon 6 20 wt%	901.65 GPa		Designed set up	Bazbouz and Stylios, 2010
PPA (polyamic acid)	13 ± 0.39 GPa	220–250	Microtension tester	Chen *et al.*, 2011b
PI (polyimide)	76 ± 12.6 GPa	220–280	Microtension tester	Chen *et al.*, 2011b
PAN 10 wt%	3.8–28.87 GPa	179–408	Bending test AFM	Gu *et al.*, 2005
PAN	26.8 GPa	200	Microcantilever vibration method	Yuya *et al.*, 2007
PAN with 1–4 wt% SWCNTs	60–140 GPa	300	AFM compression cantilever	Ko *et al.*, 2003
Silk/PEO 7.1 wt% (80/20)	8 GPa	800	Nanoindentation	Wang *et al.*, 2004
PVA	4.4 GPa	210	AFM bending test	Wong *et al.*, 2010
PVA annealed	7.6 GPa	190	AFM bending test	Wong *et al.*, 2010
Nanofibre mat				
Nylon 6	19.4 MPa			Bazbouz and Stylios, 2010
PEO	32.7 ± 5.9 MPa		Tensile test	Park *et al.*, 2007
	17.5 ± 1.1 MPa			Zhou *et al.*, 2012
	2.50 ± 0.06 MPa			Zhou *et al.*, 2011a
PVA	1.5 MPa			Peresin *et al.*, 2010a
	64.7 MPa			Lee and Deng, 2012
PAA	56 MPa			Ping and You-Lo, 2009
PCL	3.89 ± 0.10 MPa			Zoppe *et al.*, 2009
Silk	~300 MPa			Huang *et al.*, 2011b
Bacterial cellulose	5.5 ± 0.3 MPa			Chen *et al.*, 2010
CA	553 ± 39 MPa			Lu and Hsieh, 2010
Nanofibre filled composites				
SPI	30 MPa		Tensile test	Chen and Liu, 2008
SPI/20 wt% CA nanofibres	190 MPa			
Rubber	1.8 MPa			Kim and Reneker, 1999
Rubber/10 pph CA nanofibres	19.6 MPa			
PVA	350 MPa			Tang and Liu, 2008
PVA/40 wt% CA nanofibres	3900 MPa			

© Woodhead Publishing Limited, 2014

single high strength synthetic (100 GPa) and natural (10 GPa) fibres is not unusual, whilst variations in the mechanical properties of electrospun mats is less dramatic. Typical Young's moduli for both synthetic and natural electrospun fibre mats are in the range of 10–100 MPa in both cases. Hence, electrospun cellulose fibres are considered to be potentially useful components in composite material systems.

Typically, the mechanical properties of the neat polymer matrix are compared with the reinforced or filled matrix by tensile testing or dynamic mechanical analysis (DMA) in the development of novel composite materials. Han *et al*. confirmed the reinforcing efficiency of electrospun cellulose fibre mats in a PBS matrix, with increases in the storage modulus (E') by up to two decades (Han *et al*., 2008a). The Young's modulus of electrospun CA fibre-reinforced soybean protein isolate (SPI) (Chen and Liu, 2008) was determined to increase significantly from 30 MPa for the neat SPI film to 190 MPa for an electrospun 20 wt.% CA-SPI composite. Similarly, the Young's modulus of electrospun CA nanofibre-reinforced PVA was determined to increase by 11-fold from 0.35 GPa for the neat electrospun PVA mat to 3.9 GPa for an electrospun 40 wt.% cellulose nanofibre-PVA composite mat (Tang and Liu, 2008). Comparably, the level of reinforcement provided by ten parts per hundred (pph) electrospun polybenzimidazole (PBI) fibres in a rubber matrix was slightly lower than 11-fold (Kim and Reneker, 1999). Finally, the reinforcement of polymers nanocomposites by cellulose-whiskers-filled electrospun fibres is yet to be reported.

5.7 Future trends

Understandably the field is still grappling with the challenges of electrospinning cellulosic fibres and thus a large effort is being made to develop workable processes. However, there is an obvious lack of investigation of the mechanical properties of the resulting fibres, which is probably attributable to the experimental difficulty of measuring such properties. The thermal stability and crystallinity are usually presented in lieu of actual mechanical data to elucidate the effect of processing on the mechanical strength of an electrospun mat. Recent advances in the mechanical testing of single nanofibres will provide greater possibilities for measuring fibre properties. Recent strategies for the synthesis of electrospun hybrid fibres or cellulose nanocrystal-reinforced fibres with improved mechanical properties have been successful although the content of CNCs used is relatively high (~20 wt.%) compared with other nanofillers.

Current research covers a very broad area including applications in textile, energy storage, sensors, batteries, filtration, chelation, cables, tissue engineering, wound dressing, and drug delivery. Hence, there is a strong

© Woodhead Publishing Limited, 2014

need to develop characterisation techniques for a range of different physical properties. Further studies are required to systematically assess the physical properties of electrospun 'directly dissolved' cellulose fibres, cellulose derivatives, cellulose blends, reinforced cellulose and post-treated cellulose to fully understand the limitations of electrospun cellulose fibres. Furthermore, there is no research available that examines the incorporation of electrospun cellulosic fibres into bulk nanocomposites. Finally, the feasibility of the commercial development of specific products will probably require that cost effective processing methods are developed that permit the industrial scale production of electrospun cellulosic fibres.

5.8 References

Abitbol, T., Wilson, J. T. and Gray, D. G. (2010). Electrospinning of fluorescent fibers from cdse/zns quantum dots in cellulose triacetate. *Journal of Applied Polymer Science,* **119**, 803–810.

Adusumali, R.-B., Reifferscheid, M., Weber, H., Roeder, T., Sixta, H. and Gindl, W. (2006). Mechanical properties of regenerated cellulose fibres for composites. *Macromolecular Symposia,* **244**, 119–125.

Ahn, Y., Hu, D.-H., Hong, J. H., Lee, S. H., Kim, H. J. and Kim, H. (2012a). Effect of co-solvent on the spinnability and properties of electrospun cellulose nanofiber. *Carbohydrate Polymers,* **89**, 340–345.

Ahn, Y., Lee, S. H., Kim, H. J., Yang, Y.-H., Hong, J. H., Kim, Y.-H. and Kim, H. (2012b). Electrospinning of lignocellulosic biomass using ionic liquid. *Carbohydrate Polymers,* **88**, 395–398.

Baptista, A. C., Martins, J. I., Fortunato, E., Martins, R., Borges, J. P. and Ferreira, I. (2011). Thin and flexible bio-batteries made of electrospun cellulose-based membranes. *Biosensors and Bioelectronics,* **26**, 2742–2745.

Bazbouz, M.B. & Stylios, G.K (2010). The tensile properties of electrospun Nylon-6 single nanofibers. *Journal of Polymer Science Part B:* Polymer Physics, **48**, 1719–1731.

Cao, S., Hu, B. and Liu, H. (2009). Synthesis of ph-responsive crosslinked poly[styrene-co-(maleic sodium anhydride)] and cellulose composite hydrogel nanofibers by electrospinning. *Polymer International,* **58**, 545–551.

Castillo-Ortega, M. M., Najera-Luna, A., Rodriguez-Felix, D. E., Encinas, J. C., Rodriguez-Felix, F., Romero, J. and Herrera-Franco, P. J. (2011). Preparation, characterization and release of amoxicillin from cellulose acetate and poly(vinyl pyrrolidone) coaxial electrospun fibrous membranes. *Materials Science and Engineering, C,* **31**, 1772–1778.

Castillo-Ortega, M. M., Romero-Garcia, J., Rodriguez, F., Najera-Luna, A. and Herrera-Franco, P. J. (2010). Fibrous membranes of cellulose acetate and poly(vinyl pyrrolidone) by electrospinning method: Preparation and characterization. *Journal of Applied Polymer Science,* **116**, 1873–1878.

Celebioglu, A. and Uyar, T. (2011). Electrospun porous cellulose acetate fibers from volatile solvent mixture. *Materials Letters,* **65**, 2291–2294.

Chen, C.-Z., Wang, L.-E. and Huang, Y. (2011). Electrospun phase change fibers based on polyethylene glycol/cellulose acetate blends. *Applied Energy,* **88**, 3133–3139.

© Woodhead Publishing Limited, 2014

Chen, C., Wang, L. and Huang, Y. (2009a). Crosslinking of the electrospun polyethylene glycol/cellulose acetate composite fibers as shape-stabilized phase change materials. *Materials Letters,* **63**, 569–571.

Chen, C., Wang, L. and Huang, Y. (2009b). Role of M_n of PEG in the morphology and properties of electrospun PEG/CA composite fibers for thermal energy storage. *AIChE Journal,* **55**, 820–827.

Chen, G. and Liu, H. (2008). Electrospun cellulose nanofiber reinforced soybean protein isolate composite film. *Journal of Applied Polymer Science,* **110**, 641–646.

Chen, P., Yun, Y. S., Bak, H., Cho, S. Y. and Jin, H.-J. (2010). Multiwalled carbon nanotubes-embedded electrospun bacterial cellulose nanofibers. *Molecular Crystals and Liquid Crystals,* **519**, 169–178.

Chen, S., Han, D. & Hou, H.(2011b). High strength electrospun fibers. *Polymers for Advanced Technologies*, **22**, 295–303.

Chronakis, I. S. (2005). Novel nanocomposites and nanoceramics based on polymer nanofibers using electrospinning process – a review. *Journal of Materials Processing Technology,* **167**, 283–293.

Coleman, J. N., Khan, U., Blau, W. J. and Gun'ko, Y. K. (2006). Small but strong: A review of the mechanical properties of carbon nanotube–polymer composites. *Carbon,* **44**, 1624–1652.

Ding, B., Li, C. R., Hotta, Y., Kim, J. H., Kuwaki, O. and Shiratori, S. (2006). Conversion of an electrospun nanofibrous cellulose acetate mat from a super-hydrophilic to super-hydrophobic surface. *Nanotechnology,* **17**, 4332–4339.

Ding, Z.-D., Chi, Z., Gu, W.-X., Gu, S.-M., Liu, J.-H. and Wang, H.-J. (2012). Theoretical and experimental investigation on dissolution and regeneration of cellulose in ionic liquid. *Carbohydrate Polymers,* **89**, 7–16.

Du, J. and Hsieh, Y.-L. (2009). Cellulose/chitosan hybrid nanofibers from electrospinning of their ester derivatives. *Cellulose (Dordrecht, Netherlands),* **16**, 247–260.

Dupont, A.-L. (2003). Cellulose in lithium chloride/n,n-dimethylacetamide, optimisation of a dissolution method using paper substrates and stability of the solutions. *Polymer,* **44**, 4117–4126.

Eichhorn, S. J., Dufresne, A., Aranguren, M., Marcovich, N. E., Capadona, J. R., Rowan, S. J., Weder, C., Thielemans, W., Roman, M., Renneckar, S., Gindl, W., Veigel, S., Keckes, J., Yano, H., Abe, K., Nogi, M., Nakagaito, A. N., Mangalam, A., Simonsen, J., Benight, A. S., Bismarck, A., Berglund, L. A. and Peijs, T. (2010). Review: Current international research into cellulose nanofibres and nanocomposites. *Journal of Materials Science,* **45**, 1–33.

Endres, F. and Zein El Abedin, S. (2006). Air and water stable ionic liquids in physical chemistry. *Physical Chemistry Chemical Physics,* **8**, 2101–2116.

Fink, H. P., Weigel, P., Purz, H. J. and Ganster, J. (2001). Structure formation of regenerated cellulose materials from nmmo-solutions. *Progress in Polymer Science,* **26**, 1473–1524.

Freire, M. G., Teles, A. R. R., Ferreira, R. A. S., Carlos, L. D., Lopes-Da-Silva, J. A. and Coutinho, J. A. P. (2011). Electrospun nanosized cellulose fibers using ionic liquids at room temperature. *Green Chemistry,* **13**, 3173–3180.

Frenot, A., Henriksson, M. W. and Walkenström, P. (2007). Electrospinning of cellulose-based nanofibers. *Journal of Applied Polymer Science,* **103**, 1473–1482.

Frey, M. W. (2008). Electrospinning cellulose and cellulose derivatives. *Polymer Reviews,* **48**, 378–391.

© Woodhead Publishing Limited, 2014

Frey, M. W., Joo, Y. and Kim, C. (2003). New solvents for cellulose electrospinning and preliminary electrospinning results. *Abstracts of Papers of the American Chemical Society,* **226**, U404.

Frey, M. W. and Song, H. (2003). Cellulose fibers formed by electrospinning from solution. *Abstracts of Papers of the American Chemical Society,* **225**, U288.

Fu, Q., Jin, Y., Song, X., Gao, J., Han, X., Jiang, X., Zhao, Q. and Yu, D. (2010). Size-dependent mechanical properties of pva nanofibers reduced via air plasma treatment. *Nanotechnology,* **21**, 95703–95707.

Geraci, C. L. (2011). Nanotechnology research at niosh: Supporting safe development of the business. *2011 TAPPI Intl Conference on Nano for Renewable Materials.* Washington, USA.

Godinho, M. H., Canejo, J. P., Feio, G. and Terentjev, E. M. (2010). Self-winding of helices in plant tendrils and cellulose liquid crystal fibers. *Soft Matter,* **6**, 5965–5970.

Gu, S.-Y., Wu, Q.-L., Ren, J. and Vancso, G. J. (2005). Mechanical properties of a single electrospun fiber and its structures. *Macromolecular Rapid Communications,* **26**, 716–720.

Habibi, Y. and Dufresne, A. (2008). Highly filled bionanocomposites from functionalized polysaccharide nanocrystals. *Biomacromolecules,* **9**, 1974–1980.

Han, D., Halada Gary, P., Spalding, B. and Brooks Scott, C. (2009). Electrospun and oxidized cellulosic materials for environmental remediation of heavy metals in groundwater. *Model Cellulosic Surfaces.* Washington DC: American Chemical Society.

Han, S. O., Son, W. K., Youk, J. H., Lee, T. S. and Park, W. H. (2005). Ultrafine porous fibers electrospun from cellulose triacetate. *Materials Letters,* **59**, 2998–3001.

Han, S. O., Son, W. K., Youk, J. H. and Park, W. H. (2008a). Electrospinning of ultrafine cellulose fibers and fabrication of poly(butylene succinate) biocomposites reinforced by them. *Journal of Applied Polymer Science,* **107**, 1954–1959.

Han, S. O., Youk, J. H., Min, K. D., Kang, Y. O. and Park, W. H. (2008b). Electrospinning of cellulose acetate nanofibers using a mixed solvent of acetic acid/water: Effects of solvent composition on the fiber diameter. *Materials Letters,* **62**, 759–762.

Härdelin, L., Thunberg, J., Perzon, E., Westman, G., Walkenström, P. and Gatenholm, P. (2012). Electrospinning of cellulose nanofibers from ionic liquids: The effect of different cosolvents. *Journal of Applied Polymer Science,* **125**, 1901–1909.

Herrera, N. V., Mathew, A.P., Wang, L.Y. & Oksman, K. (2011). Randomly oriented and aligned cellulose fibres reinforced with cellulose nanowhiskers, prepared by electrospinning. *Plastics, Rubber and Composites*, **40**, 57–64.

Hofman, K., Tucker, N., Stanger, J., Staiger, M., Marshall, S. and Hall, B. (2012). Effects of the molecular format of collagen on characteristics of electrospun fibres. *Journal of Materials Science,* **47**, 1148–1155.

Huang, C., Tang, Y., Liu, X., Sutti, A., Ke, Q., Mo, X., Wang, X., Morsi, Y. and Lin, T. (2011a). Electrospinning of nanofibres with parallel line surface texture for improvement of nerve cell growth. *Soft Matter,* **7**, 10812–10817.

Huang, J., Liu, L. & Yao, J. (2011b). Electrospinning of *Bombyx mori* silk fibroin nanofiber mats reinforced by cellulose nanowhiskers. *Fibers and Polymers*, **12**, 1002–1006.

Huglin, M. B. (1972). *Lightscattering from Polymer Solutions,* London Academic Press.

© Woodhead Publishing Limited, 2014

Jia, B., Zhou, J. and Zhang, L. (2011). Electrospun nano-fiber mats containing cationic cellulose derivatives and poly (vinyl alcohol) with antibacterial activity. *Carbohydrates Research,* **346**, 1337–1341.

Johnson, D. L. (1970). Method of preparing polymers from a mixture of cyclic amine oxides and polymers. US patent application 3,508,941.

Kessick, R. and Tepper, G. (2003). Microscale electrospinning of polymer nanofiber interconnections. *Applied Physics Letters,* **83**, 557–559.

Khatri, Z., Wei, K., Kim, B.-S. and Kim, I.-S. (2012). Effect of deacetylation on wicking behavior of co-electrospun cellulose acetate/polyvinyl alcohol nanofibers blend. *Carbohydrate Polymers,* **87**, 2183–2188.

Khil, M., Kim, H., Kang, Y., Bang, H., Lee, D. and Doo, J. (2005). Preparation of electrospun oxidized cellulose mats and their *in vitro* degradation behavior. *Macromolecular Research,* **13**, 62–67.

Kim, C.-W., Kim, D.-S., Kang, S.-Y., Marquez, M. and Joo, Y. L. (2006). Structural studies of electrospun cellulose nanofibers. *Polymer,* **47**, 5097–5107.

Kim, C. W., Frey, M. W., Marquez, M. and Joo, Y. L. (2005). Preparation of submicron-scale, electrospun cellulose fibers via direct dissolution. *Journal of Polymer Science Part B: Polymer Physics,* **43,** 1673–1683.

Kim, J.-S. and Reneker, D. H. (1999). Mechanical properties of composites using ultrafine electrospun fibers. *Polymer Composites,* **20**, 124–131.

Ko, F., Gogotsi, Y., Ali, A., Naguib, N., Ye, H., Yang, G. L., Li, C. and Willis, P. (2003). Electrospinning of continuous carbon nanotube-filled nanofiber yarns. *Advanced Materials,* **15**, 1161–1165.

Krossing, I., Slattery, J. M., Daguenet, C., Dyson, P. J., Oleinikova, A. and Weingärtner, H. (2006). Why are ionic liquids liquid? A simple explanation based on lattice and solvation energies. *Journal of the American Chemical Society,* **128**, 13427–13434.

Kuilla, T., Bhadra, S., Yao, D., Kim, N. H., Bose, S. and Lee, J. H. (2010). Recent advances in graphene based polymer composites. *Progress in Polymer Science,* **35**, 1350–1375.

Kulpinski, P. (2005). Cellulose nanofibers prepared by the n-methylmorpholine-n-oxide method. *Journal of Applied Polymer Science,* **98**, 1855–1859.

Lau, A. K.-T. and Hui, D. (2002). The revolutionary creation of new advanced materials – carbon nanotube composites. *Composites Part B: Engineering,* **33**, 263–277.

Lau, K.-T., Gu, C. and Hui, D. (2006). A critical review on nanotube and nanotube/nanoclay related polymer composite materials. *Composites Part B: Engineering,* **37**, 425–436.

Lee, E.-H., Kim, H.-M., Lim, S.-K., Kim, K.-S. and Chin, I.-J. (2009a). Electro-active polymer actuator based on aligned cellulose nanofibrous membrane. *Molecular Crystals and Liquid Crystals,* **499**, 259/[581]–267/[589].

Lee, J. & Deng Y. (2012). Increases mechanical properties of aligned and isotropic electospun PVA nanofiber webs by cellulose nanowhisker reinforcement. *Macromolecular Research*, **20**, 76–83.

Lee, K. Y., Jeong, L., Kang, Y. O., Lee, S. J. and Park, W. H. (2009b). Electrospinning of polysaccharides for regenerative medicine. *Advanced Drug Delivery Reviews,* **61**, 1020–1032.

Li, C., Chen, R., Zhang, X., Xiong, J., Zheng, Y. and Dong, W. (2011). Fabrication and characterization of electrospun nanofibers of high dp natural cotton lines cellulose. *Fibers and Polymers,* **12**, 345–351.

© Woodhead Publishing Limited, 2014

Lim, C. T., Tan, E. P. S. and Ng, S. Y. (2008). Effects of crystalline morphology on the tensile properties of electrospun polymer nanofibers. *Applied Physics Letters,* **92**, 141908–141908–3.

Lim, Y.-M., Gwon, H.-J., Jeun, J. P. and Nho, Y.-C. (2010). Preparation of cellulose-based nanofibers using electrospinning. In Kumar, A. (ed.), *Nanofibers*. InTech, Chapter 9, 438pp. ISBN 978–953–7619–86–2 DOI: 10.5772/45660.

Liu, D., Yuan, X. & Bhattacharyya, D. (2012). The effects of cellulose nanowhiskers on electrospun poly(lactic acid) nanofibres. *Journal of materials Science*, **47**, 3159–3165.

Liu, H. and Hsieh, Y.-L. (2002). Ultrafine fibrous cellulose membranes from electrospinning of cellulose acetate. *Journal of Polymer Science Part B: Polymer Physics,* **40**, 2119–2129.

Lu, P. and Hsieh, Y.-L. (2010). Multiwalled carbon nanotube (mwcnt) reinforced cellulose fibers by electrospinning. *ACS Applied Materials & Interfaces,* **2**, 2413–2420.

Ma, Z., Kotaki, M. and Ramakrishna, S. (2005). Electrospun cellulose nanofiber as affinity membrane. *Journal of Membrane Science,* **265**, 115–123.

Mack, J. J., Viculis, L. M., Ali, A., Luoh, R., Yang, G., Hahn, H. T., Ko, F. K. and Kaner, R. B. (2005). Graphite nanoplatelet reinforcement of electrospun polyacrylonitrile nanofibers. *Advanced Materials,* **17**, 77–80.

Magalhaes, W.L.E. (2011). Novel all-cellulose composite displaying aligned cellulose nanofibers reinforced with cellulose nanocrystals. *Tappi journal*, **10**, 19.

Magalhães, W.L. E., Cao, X. & Lucia, L.A. (2009). Cellilose nanocrystals/cellilose core-in-shell nanocomposite assemblies. *Langmuir*, **25**, 13250–13257.

Marras, S. I., Kladi, K. P., Tsivintzelis, I., Zuburtikudis, I. and Panayiotou, C. (2008). Biodegradable polymer nanocomposites: The role of nanoclays on the thermomechanical characteristics and the electrospun fibrous structure. *Acta Biomaterialia,* **4**, 756–765.

Martínez-Sanz, M., Olsson, R. T., Lopez-Rubio, A. and Lagaron, J. M. (2012). Development of bacterial cellulose nanowhiskers reinforced evoh composites by electrospinning. *Journal of Applied Polymer Science,* **124**, 1398–1408.

Matsumoto, T., Tatsumi, D., Tamai, N. and Takaki, T. (2002). Solution properties of celluloses from different biological origins in licl – dmac. *Cellulose,* **8**, 275–282.

McCormick, C. L., Callais, P. A. and Hutchinson Jr, B. H. (1985). Solution studies of cellulose in lithium chloride and n,n-dimethylacetamide. *Macromolecules,* **18**, 2394–2401.

Medronho, B., Romano, A., Miguel, M., Stigsson, L. and Lindman, B. (2012). Rationalizing cellulose (in)solubility: Reviewing basic physicochemical aspects and role of hydrophobic interactions. *Cellulose,* **19**, 581–587.

Meli, L., Miao, J., Dordick, J. S. and Linhardt, R. J. (2010). Electrospinning from room temperature ionic liquids for biopolymer fiber formation. *Green Chemistry,* **12**, 1883–1892.

Miyauchi, M., Miao, J., Simmons, T.J., Dordick, J.S. and Linhardt, R.J. (2011). Flexible electrospun cellulose fibers as an affinity packing material for the separation of bovine serum albumin. *Journal of Chromatography & Separation Techniques,* **2**, 110.

Miyauchi, M., Miao, J., Simmons, T. J., Lee, J.-W., Doherty, T. V., Dordick, J. S. and Linhardt, R. J. (2010). Conductive cable fibers with insulating surface prepared by coaxial electrospinning of multiwalled nanotubes and cellulose. *Biomacromolecules,* **11**, 2440–2445.

© Woodhead Publishing Limited, 2014

Montaño-Leyva, B., Rodriguez-Felix, F., Torres-Chávez, P., Ramirez-Wong, B., López-Cervantes, J. and Sanchez-Machado, D. (2011). Preparation and characterization of durum wheat (triticum durum) straw cellulose nanofibers by electrospinning. *Journal of Agricultural and Food Chemistry,* **59**, 870–875.

Nartker, S., Askeland, P., Wiederoder, S. and Drzal, L. T. (2011). Surface chemistry of electrospun cellulose nitrate nanofiber membranes. *Journal of Nanoscience and Nanotechnology,* **11**, 1242–1247.

Nartker, S. and Drzal, L. T. (2010). Electrospun cellulose nitrate nanofibers. *Journal of Nanoscience and Nanotechnology,* **10**, 5810–5813.

Nista, S. V. G., Peres, L., D'ávila, M. A., Schmidt, F. L. and Innocentini Mei, L. H. (2012). Nanostructured membranes based on cellulose acetate obtained by electrospinning, part 1: Study of the best solvents and conditions by design of experiments. *Journal of Applied Polymer Science*, **126**(S1), E70–E78.

Ohkawa, K., Cha, D. I., Kim, H., Nishida, A. and Yamamoto, H. (2004). Electrospinning of chitosan. *Macromolecular Rapid Communications,* **25**, 1600–1605.

Ohkawa, K., Hayashi, S., Nishida, A., Yamamoto, H. and Ducreux, J. (2009). Preparation of pure cellulose nanofiber via electrospinning. *Textile Research Journal,* **79**, 1396–1401.

Ohkawa, K., Minato, K.-I., Kumagai, G., Hayashi, S. and Yamamoto, H. (2006). Chitosan nanofiber. *Biomacromolecules,* **7**, 3291–3294.

Ohno, H. (2006). Functional design of ionic liquids. *Bulletin of the Chemical Society of Japan,* **79**, 1665–1680.

Olsson, R. T., Kraemer, R., LóPez-Rubio, A., Torres-Giner, S., Ocio, M.a.J. & LagaróN, J. M. A. (2010). Extraction of microfibrils from bacterial cellulose networks for electrospinning of anisotropic biohybrid fiber yarns. *Macromolecules*, **43**, 4201–4209.

Park, J. (2007). Preparation of electrospun porous ethyl cellulose fiber by thf/dmac binary solvent system. *Journal of industrial and engineering chemistry (Seoul, Korea),* **13**, 1002.

Park, T.-J., Jung, Y. J., Choi, S.-W., Park, H., Kim, H., Kim, E., Lee, S. H. and Kim, J. H. (2011a). Native chitosan/cellulose composite fibers from an ionic liquid via electrospinning. *Macromolecular Research,* **19**, 213–215.

Park, T.-J., Jung, Y., Park, H., Choi, S.-W., Kim, E., Lee, S. & Kim, J. (2011b). Photoluminescent synthetic wood fibers from an ionic liquid via electrospinning. *Macromolecular Research*, **19**, 317–321.

Park, W.-I., Kang, M., Kim, H.-S. & Jin, H.-J. (2007). Electrospinning of poly(ethylene oxide) with bacterial cellulose whiskers. *Macromolecular Symposia*, 249–250, 289–294.

Persin, M. S., Habibi, Y., Vesterinen, A.-H., Rojas, O. J., Pawlak, J.J. & SeppaLä, J. V. (2010a). Effect of moisture on electrospun nanofiber composites of poly(vinyl alcohol) and cellulose nanocrystals. *Biomacromolecules*, **11**, 2471–2477.

Peresin, M. S., Habibi, Y., Zoppe, J. O., Pawlak, J. J. and Rojas, O. J. (2010b). Nanofiber composites of polyvinyl alcohol and cellulose nanocrystals: Manufacture and characterization. *Biomacromolecules,* **11**, 674–681.

Ping, L. & You-Lo, H. (2009). Cellulose nanocrystal-filled poly(acrylic acid) nanocomposite fibrous membranes, *Nanotechnology*, **20**, 415604

Pinkert, A., Marsh, K. N., Pang, S. and Staiger, M. P. (2009). Ionic liquids and their interaction with cellulose. *Chemical Reviews,* **109**, 6712–6728.

© Woodhead Publishing Limited, 2014

Qi, H., Sui, X., Yuan, J., Wei, Y. and Zhang, L. (2010). Electrospinning of cellulose-based fibers from naoh/urea aqueous system. *Macromolecular Materials and Engineering,* **295**, 695–700.

Quan, S.-L., Kang, S.-G. and Chin, I.-J. (2010). Characterization of cellulose fibers electrospun using ionic liquid. *Cellulose,* **17**, 223–230.

Rosic, R., Kocbek, P., Baumgartner, S. and Kristl, J. (2011). Electro-spun hydroxyethyl cellulose nanofibers: The relationship between structure and process. *Journal of Drug Delivery Science and Technology,* **21**, 229.

Sakuldao, S., Yoovidhya, T. and Wongsasulak, S. (2011). Coaxial electrospinning and sustained release properties of gelatin-cellulose acetate core-shell ultrafine fibres. *ScienceAsia,* **37**, 335–343.

Shukla, S. (2007). Polymer fiber assisted processing of ceramic oxide nano and submicron fibers. *Ceramic Engineering and Science Proceedings,* **27**, 57.

Shukla, S., Brinley, E., Cho, H. J. and Seal, S. (2005). Electrospinning of hydroxypropyl cellulose fibers and their application in synthesis of nano and submicron tin oxide fibers. *Polymer,* **46**, 12130–12145.

Simons, T. J., Miao, J., Miyauchi, M., Dordick, J. S. and Linhardt, R. J. (2010). Electrospun polyvinylpyrrolidone and cellulose fibers with magnetic nanoparticles for electromagnetic applications. PMSE Prepration, Washington DC, American Chemical Society, 102 pp.

Siqueira, G., Bras, J. and Dufresne, A. (2008). Cellulose whiskers versus microfibrils: Influence of the nature of the nanoparticle and its surface functionalization on the thermal and mechanical properties of nanocomposites. *Biomacromolecules,* **10**, 425–432.

Siqueira, G., Bras, J. and Dufresne, A. (2010). Cellulosic bionanocomposites: A review of preparation, properties and applications. *Polymers,* **2**, 728–765.

Son, W. K. (2004a). Preparation of antimicrobial ultrafine cellulose acetate fibers with silver nanoparticles. *Macromolecular Rapid Communications.,* **25**, 1632–1637.

Son, W. K. (2004b). Preparation of ultrafine oxidized cellulose mats via electrospinning. *Biomacromolecules,* **5**, 197–201.

Son, W. K., Youk, J. H., Lee, T. S. and Park, W. H. (2003). Electrospinning of ultrafine cellulose acetate fibers: Studies of a new solvent system and deacetylation of ultrafine cellulose acetate fibers. *Journal of Polymer Science Part B: Polymer Physics,* **42**, 5–11.

Son, W. K., Youk, J. H., Lee, T. S. and Park, W. H. (2004). Preparation of antimicrobial ultrafine cellulose acetate fibers with silver nanoparticles. *Macromolecular Rapid Communications,* **25**, 1632–1637.

Son, W. K., Youk, J. H. and Park, W. H. (2006). Antimicrobial cellulose acetate nanofibers containing silver nanoparticles. *Carbohydrate Polymers,* **65**, 430–434.

Stanger, J., Tucker, N., Wallace, A., Larsen, N., Staiger, M. and Reeves, R. (2009). The effect of electrode configuration and substrate material on the mass deposition rate of electrospinning. *Journal of Applied Polymer Science,* **112**, 1729–1737.

Swatloski, R. P., Spear, S. K., Holbrey, J. D. and Rogers, R. D. (2002). Dissolution of cellose with ionic liquids. *Journal of the American Chemical Society,* **124**, 4974–4975.

Tan, E. P. S. and Lim, C. T. (2006). Mechanical characterization of nanofibers – a review. *Composites Science and Technology,* **66**, 1102–1111.

Tang, C., Chen, P. and Liu, H. (2008). Cocontinuous cellulose acetate/polyurethane composite nanofiber fabricated through electrospinning. *Polymer Engineering & Science,* **48**, 1296–1303.

© Woodhead Publishing Limited, 2014

Tang, C. and Liu, H. (2008). Cellulose nanofiber reinforced poly(vinyl alcohol) composite film with high visible light transmittance. *Composites Part A: Applied Science and Manufacturing,* **39**, 1638–1643.

Tucker, N., Stanger, J. J., Staiger, M.P., Razzaq, H. and Hofman, K. (2012). The history of the science and technology of electrospinning from 1600 to 1995. *Journal of Engineered Fibers and Fabrics,***7**, 63–73.

Tungprapa, S., Puangparn, T., Weerasombut, M., Jangchud, I., Fakum, P., Semongkhol, S., Meechaisue, C. and Supaphol, P. (2007). Electrospun cellulose acetate fibers: Effect of solvent system on morphology and fiber diameter. *Cellulose,* **14**, 563–575.

Uppal, R. and Ramaswamy, G. N. (2011). Cellulose submicron fibers. *Journal of Engineered Fibers and Fabrics,* **6**, 39–45.

Uslu, İ. and Aytimur, A. (2012). Production and characterization of poly(vinyl alcohol)/poly(vinylpyrrolidone) iodine/poly(ethylene glycol) electrospun fibers with (hydroxypropyl)methyl cellulose and aloe vera as promising material for wound dressing. *Journal of Applied Polymer Science,* **124**, 3520–3524.

Verreck, G., Chun, I., Peeters, J., Rosenblatt, J. and Brewster, M. E. (2003). Preparation and characterization of nanofibers containing amorphous drug dispersions generated by electrostatic spinning. *Pharmaceutical Research,* **20**, 810–817.

Viswanathan, G., Murugesan, S., Pushparaj, V., Nalamasu, O., Ajayan, P. M. and Linhardt, R. J. (2006). Preparation of biopolymer fibers by electrospinning from room temperature ionic liquids. *Biomacromolecules,* **7**, 415–418.

Wang, M., Jin, H.-J., Kaplan, D. L. and Rutledge, G. C. (2004). Mechanical properties of electrospun silk fibers. *Macromolecules,* **37**, 6856–6864.

Wang, M., Wang, L. and Huang, Y. (2007). Electrospun hydroxypropyl methyl cellulose phthalate (hpmcp)/erythromycin fibers for targeted release in intestine. *Journal of Applied Polymer Science,* **106**, 2177–2184.

Wang, Y. and Hsieh, Y.-L. (2004). Enzyme immobilization to ultra-fine cellulose fibers via amphiphilic polyethylene glycol spacers. *Journal of Polymer Science Part A: Polymer Chemistry,* **42**, 4289–4299.

Wong, K., Zinke-Allmang, M. and Wan, W. (2010). Effect of annealing on aqueous stability and elastic modulus of electrospun poly(vinyl alcohol) fibers. *Journal of Materials Science,* **45**, 2456–2465.

Wongsasulak, S., Patapeejumruswong, M., Weiss, J., Supaphol, P. and Yoovidhya, T. (2010). Electrospinning of food-grade nanofibers from cellulose acetate and egg albumen blends. *Journal of Food Engineering,* **98**, 370–376.

Wu, X., Wang, L., Yu, H. and Huang, Y. (2005). Effect of solvent on morphology of electrospinning ethyl cellulose fibers. *Journal of Applied Polymer Science,* **97**, 1292–1297.

Xiang, C., Frey, M. W., Taylor, A. G. and Rebovich, M. E. (2007). Selective chemical absorbance in electrospun nonwovens. *Journal of Applied Polymer Science,* **106**, 2363–2370.

Xiang, C., Joo, Y.L. & Frey, M.W. (2009). Nanocomposites fibers electrospun from poly(latic acid)/cellulose nanocrystals. *Journal of Biobased Materials and Bioenergy*, **3**, 147–155.

Xu, Y. (2011). Functional inorganic-cellulose hybrid nanocomposites. *Huaxue Jinzhan*, **23**, 2183–2199.

Yeoh, S., Hamad, W. Y. and Ko, F. (2009). Structure and properties of electrospun cellulosic fibers from kraft pulp. 237th ACS National Meeting, 22–26 March 2009, Salt Lake City, UT, United States. American Chemical Society, CELL-178.

© Woodhead Publishing Limited, 2014

Yoon, Y. I., Moon, H. S., Lyoo, W. S., Lee, T. S. and Park, W. H. (2009). Superhydrophobicity of cellulose triacetate fibrous mats produced by electrospinning and plasma treatment. *Carbohydrate Polymers,* **75**, 246–250.

Yuya, P. A., Wen, Y., Turner, J. A., Dzenis, Y. A. and Li, Z. (2007). Determination of young's modulus of individual electrospun nanofibers by microcantilever vibration method. *Applied Physics Letters,* **90**, 111909–3.

Zhang, H., Nie, H., Li, S., White, C. J. B. and Zhu, L. (2009). Crosslinking of electrospun polyacrylonitrile/hydroxyethyl cellulose composite nanofibers. *Materials Letters,* **63**, 1199–1202.

Zhang, L. and Hsieh, Y.-L. (2008). Ultra-fine cellulose acetate/poly(ethylene oxide) bicomponent fibers. *Carbohydrates. Polymers,* **71**, 196–207.

Zhang, Y. Z., Venugopal, J., Huang, Z. M., Lim, C. T. and Ramakrishna, S. (2006). Crosslinking of the electrospun gelatin nanofibers. *Polymer,* **47**, 2911–2917.

Zhao, S., Wu, X., Wang, L. and Huang, Y. (2003). Electrostatically generated fibers of ethyl-cyanoethyl cellulose. *Cellulose,* **10**, 405–409.

Zhao, S., Wu, X., Wang, L. and Huang, Y. (2004). Electrospinning of ethyl–cyanoethyl cellulose/tetrahydrofuran solutions. *Journal of Applied Polymer Science,* **91**, 242–246.

Zhou, C., Chu, R., Wu, R. and Wu, Q. (2011a). Electrospun polyethylene oxide/cellulose nanocrystal composite nanofibrous mats with homogeneous and heterogeneous microstructures. *Biomacromolecules,* **12**, 2617–2625.

Zhou, C., Wang, Q. & Wu, Q. (2012). UV-initiated crosslinking of electrospun poly(ethylene oxide) nanofibers with pentaerythirtol triacrylate: Effect of irradiation time and incorporated cellulose nanocrystals. *Carbohydrate Polymers*, **87**, 1779–1786.

Zhou, J., Zhang, L. and Cai, J. (2004). Behavior of cellulose in naoh/urea aqueous solution characterized by light scattering and viscometry. *Journal of Polymer Science, Part B: Polymer Physics,* **42**, 347–353.

Zhou, W., He, J., Cui, S. and Gao, W. (2011b). Nanofibrous membrane of silk fibroin/cellulose acetate blend for heavy metal ion adsorption. *Advanced Material Research (Zuerich, Switzerland),* **148–149**, 1431–1435.

Zhou, W., He, J., Cui, S. and Gao, W. (2011c). Preparation of electrospun silk fibroin/cellulose acetate blend nanofibers and their applications to heavy metal ions adsorption. *Fibers and Polymers,* **12**, 431–437.

Zhou, W., He, J., Du, S., Cui, S. and Gao, W. (2011d). Electrospun silk fibroin/cellulose acetate blend nanofibres: Structure and properties. *Iranian Polymer Journal,* **20**, 389–397.

Zoppe, J. O., Peresin, M. S., Habibi, Y., Venditti, R. A. and Rojas, O. J. (2009). Reinforcing poly(ε-caprolactone) nanofibers with cellulose nanocrystals. *ACS Applied Materials & Interfaces,* **1**, 1996–2004.

Zucchelli, A., Focarete, M. L., Gualandi, C. and Ramakrishna, S. (2011). Electrospun nanofibers for enhancing structural performance of composite materials. *Polymers for Advanced Technologies,* **22**, 339–349.

© Woodhead Publishing Limited, 2014

6

Ethical practices in the processing of green composites

C. BAILLIE, The University of Western Australia, Australia
and E. FEINBLATT, Waste for Life, USA

DOI: 10.1533/9780857099228.2.161

Abstract: The majority of researchers and producers of 'green composites' would claim that 'sustainability' was one of their main objectives. Sustainability takes into consideration environmental, economic and social impacts. However, research in the area of green composites has focused on the environmental and economic sustainability issues but rarely is the social aspect considered. This chapter presents some ideas about the third leg of the sustainability stool. It starts by taking a fresh look at the idea of social impact, through the lens of ethical practice – a common concern for engineers – and then applies this to a case study of waste-based composite manufacture by the not-for-profit organization 'Waste for Life'.

Key words: green composites, natural fibre composites, recycling, development, plastic, sustainability, ethics, social impact.

6.1 Introduction

Green composites are attention grabbing because of their reduced environmental impact potential – especially in transport applications – where lighter/stronger materials equate to fuel savings. However, materials engineering is not immune to 'green washing'; it occurs there as it does in any other industry, which scurries to label its products 'green' without evidence that its production and usage result in a net reductive environmental footprint. Natural fibre composites that depend upon virgin plastics, or use fibres which are not waste products, or use thermosetting matrices that are not recyclable, are good examples of this. Claims of 'being green' conveniently sidestep the impacts of the above in final computations.

Increasing scrutiny of environmental impact statements and assessments has resulted in more complex, sophisticated analyses of what 'reduced impact' actually means, and a majority of researchers and producers of 'green composites' now tend to claim that 'sustainability' is, likewise, one

© Woodhead Publishing Limited, 2014

of their main objectives. The 1987 United Nations Brundtland Commission defined sustainable development as 'development that meets the needs of the present without compromising the ability of future generations to meet their own needs' (World Commission on Environment and Development, 1987) and, in so doing, inextricably linked environmental, economic and social impacts, which made it difficult to assess one without considering the others. Though green composite research has brought environmental and economic sustainability issues into focus, it pays scant consideration to the social impacts of composite production and use.

In order to address this, many industries have begun to embrace models of Corporate Social Responsibility that append social impact assessments to their bottom line matrices. Human Resources staff of some engineering companies (e.g. in mining) scour employment markets for persons with social relations expertise, and the resource industry is replete with employees having social sciences backgrounds who become community engagement experts. However, being one-step-removed from the application of their research, materials engineers are rarely asked to consider the social implications and impacts of their work.

This chapter presents some ideas about the third leg of the sustainability stool. It begins by taking a fresh look at the concept of social impact through the lens of ethical practice – a familiar concern for engineers – and then applies this to a case study of green composites – that of waste-based composite manufacturing. The main body of this chapter will be divided into two sections. *Social impact and Ethical Practice* will introduce contemporary thought about social impact and responsibility in the light of ethical practice. This will be followed by a *Case Study,* which focuses on an innovative model of waste management developed and disseminated by the not-for-profit organization Waste for Life (WFL) (http://wasteforlife.org). WFL depends upon the materials research from universities in their network to create composites from waste materials in different regions of the world and design products together with partners on the ground to enhance the livelihoods of people who scavenge waste as their sole economic activity. The chapter will conclude with some thoughts about the potential for green composites to be developed ethically for social and environmental benefit, and what changes might be needed in the industry for this to happen.

6.2 Social impact and ethical practice

There is increasing acceptance that ethics is, and should be, intrinsic to the profession of engineering, and there are several different sets of guiding principles behind our professional codes of ethics. These are drawn from various philosophical theories of ethics – most notably utilitarianism, Kantian ethics, virtue theory, ethics of care – (Catalano, 2008), which have

© Woodhead Publishing Limited, 2014

been supplemented and amplified, often didactically, with 'microethics' case studies of whistle-blowers and engineering disasters, in order to engender a sense of responsibility or 'duty of care' into engineers (e.g. Fledderman, 2004; Goreman *et al.*, 2000; Martin and Shinzinger, 2005; Whitbeck, 1998). Through the years, ethics committees have been instructed to produce industry-specific behavioural guidelines which are based upon members' interpretations of theory and its practical applicability. However, Baillie and Levine (2013) point out that the theories behind ethical guidelines are far from objectively neutral, being heavily influenced by contemporary political and social issues, and they demonstrate that one area consistently overlooked is of how to deal with the social impact of engineering – particularly on powerless populations. Franklin proposes an ethical framework that goes beyond the calculable benefits and costs of any particular engineering project, process or system. She asks that we focus not merely on 'doing no harm', of avoiding suffering and disaster, but that we should subject every project, system or product with the query: '*who* benefits and *who* pays' – if this is developed? (Franklin, 1999: 124). This recommendation is followed up by Riley and others who claim that what is needed is to focus on 'macro ethics' (Herkert, 2005) – 'the largely ignored body of ethical problems that involve collective action of engineers or society as a whole' (Riley, 2009: 9). Baillie and Levine note that ethics based on principles of justice, particularly as conceived by scholars such as Rawls (1971) and Sen (2009) will, to an extent, help us to frame our engineering development, processing, and systems in ways which are based on fairness and equity for all the people we serve as engineers.

So what does it mean to look at the broader social and ethical impacts of green composites in a just way? What kinds of impacts are these? Which are the social groups we refer to? How can we do anything about this as engineers? What does composite materials development have to do with social problems anyway? To help frame the discussion and give some practical data, the next section presents a case study of one not-for-profit organization, 'WFL', founded by the authors in 2007, and based upon Baillie's work on green composites over the past 16 years. The aim of WFL is to develop green composite materials and products with as much focus on the social as on the environmental impact of their production. It is not meant to be a shining example of what *should* be done – clearly the case given represents a very particular choice made by one of the authors (Baillie), a choice which may not be possible for all. That choice was to share her engineering knowledge about composites with a different 'client group' and work directly with marginalized communities as 'manufacturer' so that technology transfer of her laboratory work happened at street level, rather than in a production company. However, some of the principles involved will hopefully shed light on what is possible and what potential there is for green composites to make

© Woodhead Publishing Limited, 2014

a difference to people who would, because of their social and economic status, never have access to such science and technology. It will also guide our thinking in general about the choices we make, even when working in a first world context.

6.3 Case study: Waste for Life waste management model

6.3.1 Introduction

Natural fibre composite products made from waste-based materials offer great potential for waste management as well as poverty reduction, especially in developing communities where waste scavenging is common. This case study focuses on an innovative model of waste management developed and disseminated by the organization WFL (http://wasteforlife.org), which was set up by the authors, to act as a technology transfer organization for Baillie's research – but with a difference (Baillie and Feinblatt, 2010a, 2010b). WFL is a loosely joined network of academics, professional scientists, engineers, educators, designers and cooperatives that work internationally and inter-disciplinarily to develop poverty-reducing solutions to waste management. WFL's research and development activities are spread across the universities in its network, creating composites from waste materials in different regions of the world and designing products together with partners on the ground. They have worked with flax and hemp reinforced bale wrap (high density polyethylene, HDPE) in Canada; corn, wheat and agave reinforced plastic bags (low density polyethylene, LDPE) in Lesotho, Africa; and paper-, card- and textile-reinforced plastic PE film in Buenos Aires, Argentina (Aghedo *et al.*, 2008; Thamae and Baillie, 2007, 2008, 2009; Thamae *et al.*, 2008; 2009a, 2009b). The interdisciplinary support network allows the development of consistently produced strong and tough materials and creative product designs that are socially, economically, and politically appropriate for the local context. Materials and designs are *co-created* by the research team and the local communities. Production techniques are developed which suit the context and are tailored to specific communities, and WFL members design the means of production that can be locally manufactured and maintained. For example, WFL member and Professor at Queens University, Canada, Darko Matovic, has created a compression mould, a hotpress (The Kingston Press), which has been built using local labour and machinery in Buenos Aires, and is capable of manufacturing products that can be sold to augment the income of families associated with the local waste picker or *cartoneros* cooperatives (Baillie *et al.*, 2012; Matovic, in press). This case study briefly reports some of the technological development for the press, the materials, and products appropriate to the

© Woodhead Publishing Limited, 2014

cartoneros' context in Buenos Aires and we provide a template for waste management combined with poverty reduction through locally adjusted, grass-roots based social entrepreneurship.

6.3.2 The social context

In 2001, Argentina suffered an economic crisis that, overnight, created massive and widespread unemployment. Up to 100 000 people became *cartoneros* (literally, 'cardboard pickers'), scavenging the streets of Buenos Aires City for recyclable materials to sell (Schamber and Suarez, 2007). Even though, 11 years later, their numbers have diminished, there are still an estimated 6000–20 000 (numbers vary widely) cooperative, family, or individual cartoneros (often also referred to as 'urban recoverers') who collect, separate, sort, and sell waste as their sole economic activity. For the most part these unpaid informal workers live in outlying shantytowns but move through the city with their carts at all times of the day, collecting and recycling an estimated 90% of whatever Buenos Aires regurgitates and finally recycles. Most of the recycling waste that is collected is sold to agents or middlemen, though some more organized cooperatives separate, sort, and sell the materials directly to industry. But even such direct sales are barely profitable because the cooperatives are not marketing an end product that has wide commercial appeal.

WFL builds on the interdisciplinary knowledge of its members to develop such products from waste plastic and natural fibres – including paper and cardboard. In Buenos Aires the cartoneros collect waste paper and plastic, which can be used to make natural fibre composite material products that are far more useful and/or commercially valuable to them than the raw waste alone.

6.3.3 The material

Waste paper and plastic are widely available over most of the world. They comprise two of the largest sources of landfill waste in the Western world (Peltola, 2004). Paper is so commonly used that its annual production can be used to gauge a country's wealth. The wealthier the country, the more paper it uses. However, the widespread use of paper encourages deforestation on the one hand and pollution on the other, as waste paper mostly ends up in landfills. This problem has been addressed through paper recycling. However, conventional waster paper recycling directed towards new paper production may require sorting to avoid unclean waste, pulping, de-inking and bleaching, depending on the intended products. These processes can be costly and demanding in time, water and energy (Berglund and Söderholm,

© Woodhead Publishing Limited, 2014

2003). Expensive processes such as de-inking may produce toxic waste ink sludge containing both ink and various paper fillers. Other uses of waste paper include production of activated carbon but require specialized equipment and large energy expenditure. In view of these constraints, a very limited investigation in the use of waste paper in plastic composites has been done to date.

Several attempts to use waste paper in composites to date has led to use of water and chemical intensive pulping processes or energy intensive grinding of the paper followed by mixing with plastics in high shear mixers (Mehrabzadeh and Farahmand, 2009; Muehl *et al.*, 2004). Thus the fibres, which have already been weakened during papermaking and paper use processes, are further weakened in these steps. Also, ground or pulped waste paper tends to have high bulk density and agglomerates, making the composites hard to process (Mehrabzadeh and Farahmand, 2009). As a result, mechanical properties of these products have been modest compared to those of conventional wood-based ones.

By making composites from waste paper and plastic we can eliminate de-inking and pulping, but in addition WFL processes have been developed to avoid tough grinding and high speed shear mixing with the aim of preserving paper integrity. Taking advantage of the layer nature of most paper products (approximating laminates), the process involves using either paper layers intact or shredding paper into flakes and compression-moulding it with waste thermoplastics into composites. The objective of this latter is to make strong and rigid composites by using developing a particular packing arrangement of the flakes in a composite. Preserving the fibre integrity maintains inter-fibre hydrogen bonding within the paper. While simple, these methods result in composites with properties superior than those produced by following conventional approaches (Hwang, 2008). This is done using both waste paper, and waste HDPE and linear low density polyethylene (LLDPE) matrices, and manipulating a number of processing variables to improve results.

6.3.4 The materials production process

To properly understand the production process, it is necessary to locate the manufacturing process within its context. The composite materials in this context are made under very different conditions to those of Western industrial factories. The cooperatives with which WFL collaborates work in small sheds and warehouses in shantytowns. Making composites in warehouses in shantytowns with poor electrical supply presents key engineering challenges that require innovations of a different kind than are usual in our laboratories. The aim was to support the manufacture of composites from plastic and paper with a simple process, using heat and pressure only, adding

© Woodhead Publishing Limited, 2014

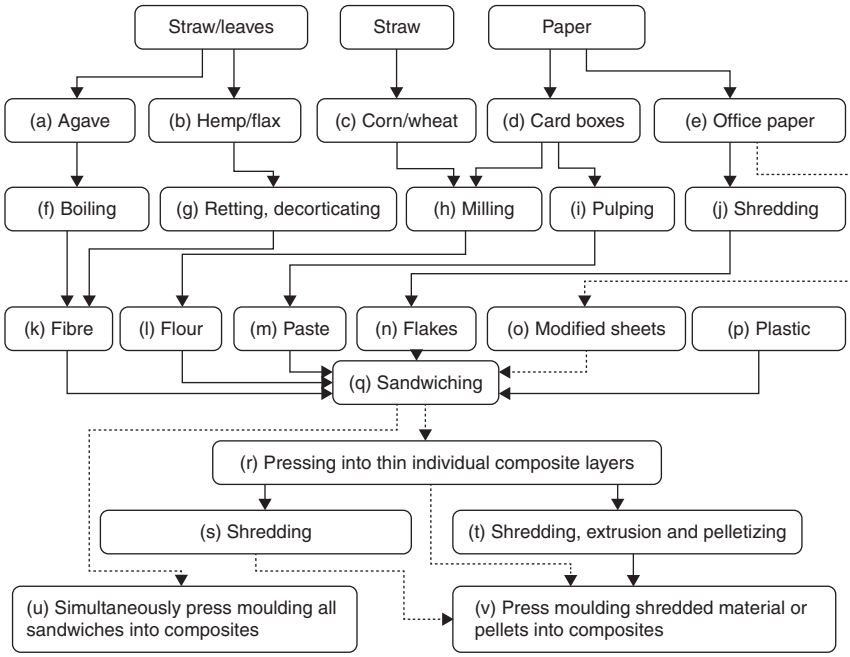
no chemicals which would contribute to environmental, health and safety concerns and cost.

Different pathways of fibre/plastics composite production, examined in our lab and published in Baillie *et al.* (2012), are shown in Fig. 6.1. Broadly, various processing stages can be classified into four layers: (a) selection of fibre material; (b) fibre material preparation; (c) primary fibre/plastics bonding; and (d) production of final products. The raw fibre sources are either dedicated fibre plants (agave, hemp, flax) or agricultural by-products (corn stover, wheat straw). Post-consumer sources are cardboard and office paper, generically grouped as 'paper' in the figure. Depending on the raw material type and realities of potential production environment, the fibre extraction method that we considered include boiling (for agave), retting and decortication for strongly bound fibres (hemp, flax) or milling for corn and wheat stalks. While cardboard requires either milling or pulping process, the office paper and newsprint can conveniently be shredded. Each of these processes produces different fibrous intermediaries: fibre, flour, paste, flakes or modified sheets. Once the fibrous material is adequately prepared, it is bonded to plastics, either by pressing it into thin layers and then shredding, or by extrusion and pelletization. Finally, the material with fibre/plastic bond established is subject to final press moulding to produce the end product.

Various routes examined are indicated by arrows in the figure (Baillie *et al.*, 2012). The pathways followed in the production of the composites in this study are identified by a dotted line in Fig. 6.1. Sections of thin LLDPE films were cut into approximately 200 mm square sheets. Office paper was also cut into 200 mm square sheets. A single square sheet of paper was placed in between a few square plastic films of LLDPE. The number of films depended on the desired paper weight fraction in the composite. These fractions varied from 0, 8, 15, 19 and 24. Each paper/LLDPE 'sandwich' was then hot-pressed in between two metal plates lined with Teflon sheets for 45 s, and then cooled to produce a thin composite film (Fig. 6.1, stages (q) and (r)) (Thamae *et al.*, 2008). The set point temperature of the heated plates was 150°C and the pressure was 3 MPa. A number of these thin composite films were created and placed within a 200 mm × 200 mm × 3.2 mm thick stainless steel mould and hot-pressed for 5 min under the same temperature and pressure.

All the composites followed the same processing route up to the point of the sandwiching stage. Therefore, the steps followed to make HDPE composites were the same as those mentioned for LLPDE composites before sandwiching, except for the following differences as shown by the designations in Fig. 6.1. Some composites made of HDPE went through stages (r) and (v) after sandwiching, and the final composite was pressed for 10 min. In others, the HDPE paper sheets were immediately pressed in a mould for 10 and 20 min respectively without being made into thin composite layers first. Others were either scissor or automatic machine shredded respectively

© Woodhead Publishing Limited, 2014



6.1 Different stages of processing followed by different fillers in our lab. The dotted line represents the path followed by the paper composites in Baillie *et al.* (2012).

at stage (s) and then finally pressed for 10 min. Due to the higher viscosity of HDPE compared to LLDPE, higher pressing times were necessary to improve plastic flow.

Table 6.1 shows a range of properties achieved by our own and other labs. Although the materials were not manufactured under the same conditions in each case, it is possible to make some broad generalizations. It is clear that for strength, layering and pressing, compared with shredding, mixing and pressing (with potential agglomeration and fibre breakage) can lead to higher values. It was also shown that reasonable properties could be produced without the use of chemical additives to improve interfacial adhesion (Baillie *et al.*, 2012). It was deemed that the properties produced were sufficient for a range of domestic and some non-structural building components.

6.3.5 Making the hot press

The second challenge necessary was to create a low cost hot press which could be manufactured locally. WFL proposed that acquiring such technology might enable cooperatives to remain independent and economically autonomous so long as it would be possible to locally create a piece of equipment

© Woodhead Publishing Limited, 2014

Table 6.1 Comparison of strength data for various paper/plastic composites

Composition, paper content (reference)	Tensile strength (MPa)	Flexural strength (MPa)	Tensile modulus (MPa)	Flexural modulus (MPa)
LLDPE/paper, layered, 48–72% w/w (Muehl *et al.*, 2004)	30–57	44.8–69		4197–7266
Polypropylene (PP)/HDPE/paper blend, 7/63/30 (Hwang, 2008)	17.7		1100	
LLDPE/paper layered, 0–24% w/w (Baillie *et al.*, 2012)	7–14	6–27	46–480	161–1918
HDPE/paper layered, 21% w/w (Baillie *et al.*, 2012)	19–23	28–40	550–900	1400–2100
HDPE/paper shredded/pressed, 21% w/w (Baillie *et al.*, 2012)	11–15	18–25	689	1140–1565

capable of delivering substantial pressure to the mould, while providing the required heating cycle, i.e. to compression mould or 'hotpress'.

As mentioned above, the press was designed at Queen's University in Kingston and is described in more detail in Matovic (in press) and Baillie *et al.* (2012). Key design parameters for the hot press were to allow moulds up to 60 × 60 cm size to be pressed, at pressures up to 6 MPa, maintaining temperature of up to 200°C with minimal deflection of the pressing pads (< 0.5 mm). The pressure and mould size translate into the requirement that the total force applied be up to approx. 2 MN (200 t). Industrial presses of these characteristics are typically priced in the $50 000–$100 000 range and require industrial type electrical circuitry to power electric motors of 5–10 kW. In contrast, the several presses built following our design were built locally, cost less than $3000 and use standard 220 V circuits for heating.

The design of the press core is shown in Fig. 6.2. It consists of the top and bottom lids, a series of links and leavers and a push mechanism powered by a 20 or 30 t hydraulic jack. Manufacturing the press does not require lathe, milling machine or other more specialized pieces of equipment – just machining and welding. Three 750 W strip heaters are mounted at the back surface of the pressing plates. The press prototype built at Queen's University is shown in Fig. 6.3. Its total mass is about 350 kg (770 lb).

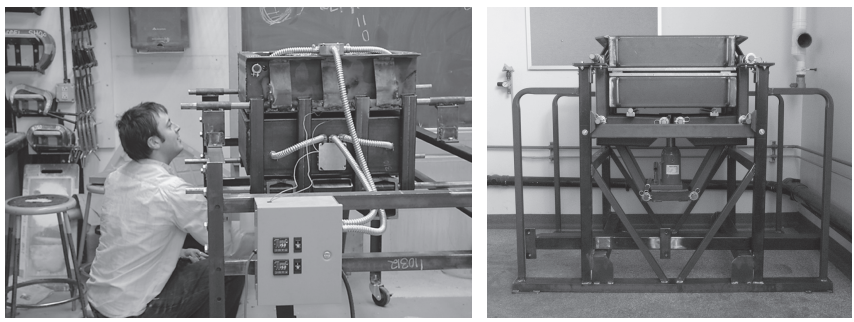
The Kingston hotpress was first prototyped in Buenos Aires (located at University Buenos Aires) and then in Canada for materials development (Queens University), for product design in the USA (Rhode Island School of Design), and for student projects to support WFL in the University of Western Australia. After 3 years of testing, in December 2010, the first production press was built specifically for the Nueve Mente cooperative in Buenos Aires, which after 1 year of usage has generated enough income to

© Woodhead Publishing Limited, 2014



6.2 Kingston hotpress computer aided design (CAD) (without the stand).

(a) (b)



6.3 (a) Kingston hotpress – Rhode Island School of Design (RISD) prototype (in the stand). (b) Kingston hotpress – UWA prototype (in the stand).

begin microloan repayments, which allowed the cooperative to initially purchase the press in March 2011.

There have been many problems with the hotpress along the way, and the design is still not perfect; however, many improvements have now been made. More details can be found on the WFL website (Waste for Life, 2012).

6.3.6 The product designs

It became clear very quickly that a good product design would be the key to an effective outcome. Industrial design students at the Rhode Island School of Design and the University of Buenos Aires, as well as engineering students at Queens University, Canada and UWA, Australia have been keeping

© Woodhead Publishing Limited, 2014

WFL supplied with a constant stream of designs as part of a range of different classes from first year design programmes to final year projects. The design criteria are simple: use only paper and plastic waste materials available with no additives; designs must be simple to make and consume as little energy as possible; aim for low skill levels, and be sure that any product is end-of-life recyclable; be certain to identify a realistic market. The last is the hardest to achieve, especially for at-a-distance designers. More details can be found in Baillie and Feinblatt (2010a). Some of the student designs are given in Fig. 6.4, although none of these has yet reached production stage. More examples are available at http://wasteforlife.org.

The most successful design to date, and the one currently in production, is an outdoor garbage bin, commissioned by the local municipality for use in a newly rehabilitated ecopark. This was designed by a local BsAs volunteer



6.4 Examples of the composite plastics products: wallets.



6.5 Nueva Mente group constructing Eco-Park Trashbin.

© Woodhead Publishing Limited, 2014

designer, Angeles Estrada Vigil, who happens to lead the project support for Cooperativa Nueve Mente. Recently the production team has announced that they will be producing interior recycling bins for the local neighbours, 4500 families from whom they collect recyclable waste door-to-door every week (the government does not do this). The ecopark bin design can be seen in Fig. 6.5, together with some of the cooperative members.

6.4 Conclusions

Increasingly we are seeing industry take note of the social dimension of developments. Sustainability is being seen as balanced only by applying the original *triple* bottom line – environmental, economic and social. The trend over the coming years will be for materials developments to include not only an economic appraisal and a life cycle assessment but a social impact assessment. This chapter provides insights as to how this is beginning to happen within the green composites business. This is seen through the lens of ethical practice and a particular case – that of the organization WFL, supporting waste picker cooperatives in Buenos Aires, in learning how to process waste into composite products to sell.

Adapting the composite plastics production to the context of waste pickers' cooperatives in Argentina presented challenges and opportunities that have the potential to substantially increase the value of their recycling work, while reducing the environmental impact of the entire consumption/disposal cycle. It is possible to see how the same technological principles can be adapted for use in totally different ways, and to different ends. This is a model that can be adapted and replicated throughout the world, demonstrating that it is possible to change the way one looks at composites and their potential to create not only environmental but also social benefits.

However, as we stated in the beginning, it is of course not possible for everyone to work directly with local dis-empowered communities, and only a few people reading this book (if any) are likely to drop what they are doing now, who they are working with, and start on a fresh path of imagining who might benefit from their skills and knowledge. However, there are many lessons that can be learnt from this case study, without necessarily reproducing it.

Throughout the chapter we have given many sources which may be followed up to support anyone interested in developing their thinking in this social dimension. Taking Franklin as inspiration we can ask ourselves: *who* will benefit from the research and development work I am doing on green composites? How do I know? Is it good enough for me to say 'everyone benefits' if the life cycle assessment score is lower than the materials they will replace, when I know nothing about the sourcing of the materials

© Woodhead Publishing Limited, 2014

themselves, under what conditions they will ultimately be manufactured and distributed, nor even who/how the final product will be used and what impact these variables might have? I could ask how the fibres will be grown, whether pesticides are used, and if the fibres are from genetically modified plants, which may ultimately reduce the variability and sustainability of crops, (Robin, 2008). Or I might question whether the fibres compete with food sources and render some areas of the world hungrier than before – as is being publically debated vis-à-vis the impact of biofuel, and corn, and soybean production (Oxfam, 2008). I might try to find out how the materials will be produced and under which conditions, what they will be used for, and where they will be used. Or I might decide that this is too much for me to bother with, it is not my responsibility nor my job or expertise, and I should leave it all to someone else to think about. One of the key challenges of materials development is that we are often so far removed from the end use that we feel none of this is our business. But if we believe that this should not be so, is it possible for us to at least begin to think about the ethical dimension of implementation of green composites?

6.5 References

Aghedo, S., Baillie, C., Offin, M., Vardy, S. and Macdougall, C. (2008). 'Alternative materials for Construction', UK *Institute for Civil Engineers Manual of Construction Materials.* Institute for Civil Engineers.

Baillie, C. (2004) (Ed). *Green Composites*. Cambridge: Woodhead Publishing Limited.

Baillie, C. (2012). 'Waste for life: Socially just materials research', in *Engineering and Social Justice: In the University and Beyond*. Morgan and Claypool, US: Purdue University Press, Chapter 4, pp. 87–107.

Baillie, C. and Levine, M. (2013). 'Engineering ethics from a justice perspective: A Critical Repositioning of what it means to be an engineer', *International Journal Engineering, Social Justice and Peace*, **2**(1), 10–20.

Baillie, C., Matovic, D., Thamae, T. and Vaja, S. (2011).'Waste based composites – Poverty reducing solutions to environmental problems', *Resources, Conservation and Recycling*, **55**(11), September 2011, 973–978.

Baillie, C. and Feinblatt, E. (2010a) *Needs and Feasiblity: A Guide for Engineers in Community Projects, the Case of Waste for Life*. Morgan and Claypool, US.

Baillie, C. and Feinblatt, E. (2010b) 'Recycling technologies and cooperativism: Waste-for-Life' in the new cooperativism special issue within affinities. *A Journal of Radical Theory, Culture*, **4**, 205–224.

Berglund, C. and Söderholm, P. (2003). 'An econometric analysis of global waste paper recovery and utilization', *Environmental and Resource Economics,* **26**, 429–456.

Catalano, G. (2006). *Engineering Ethics, Peace Justice and the Earth, Technology and Society*, Baillie, C. (Ed.). Morgan and Claypool, US.

Fledderman, C. (2004). *Engineering Ethics.* London: Pearson Education: Prentice Hall.

© Woodhead Publishing Limited, 2014

Franklin, U. (1999). *The Real World of Technology*. Toronto: House of Anansi Press.
Goreman, M., Mehalik, M. and Werhane, P.H. (2000). *Ethical and Environmental Challenges to Engineering*. NJ: Prentice Hall.
Herkert, J.R. (2005). 'Ways of thinking about and teaching ethical problem solving: Microethics and macroethics in engineering,' *Science and Engineering Ethics*, **11**, 373–385.
http://wasteforlife.org/wiki/index.php?title=Hotpress_Improvements: Accessed 30 March 2012.
Hwang, C.-Y. (2008). 'Feasibility of manufacturing paper-plastic laminates', *Taiwan Journal For Science*, **23**(1), 35–46.
Martin, M. and Schinzinger, R. (2005). *Ethics in Engineering*. New York: McGraw Hill.
Matovic, D (in press). 'Composite plastics production by locally made machines: A hotpress challenge', *International Journal of Engineering, Social Justice and Peace*.
Mehrabzadeh, M. and Farahmand, F. (2009). 'Recycling of commingled plastics waste containing polypropylene, polyethylene, and paper', *Journal of Applied Polymer Science*, **80**, 2573 –2577.
Muehl, H. J., Krzysik, A. M. and Chow, P. (2004). *Composite Panels Made with Biofiber or Office Wastepaper Bonded with Thermoplastic and/or Thermosetting Resin.* Madison: United States Department of Agriculture, Forest Service.
Oxfam International (2008). Another Inconvenient Truth: Biofuels are not the answer to climate or fuel crisis. Available from Oxfam.ca/news-and-publications Accessed 13 January 2012.
Peltola, P. (2004). 'Alternative fibre sources: Paper and wood fibres as reinforcement'. In Baillie C. (Ed.), *Green Composites* (pp. 81–98). Cambridge: Woodhead Publishing Limited.
Rawls, J. (1971). *A Theory of Justice.* Cambridge Mass.: Harvard University Press.
Riley, D. (2009). *Engineering and Social Justice*. Morgan and Claypool, US.
Robin, M.-M. (2008). *The World According to Monsanto: Pollution, Corruption and Control of the World's Food Supply*. The New Press.
Schamber, P.J. and Suarez, F.M. (2007). *Recicloscopio: Miradas sobre recuperadores urbanos de residuous de América Latina.* Buenos Aires: Prometeo Libros.
Sen, A. (1999). *Development as Freedom.* New York: Anchor Books.
Thamae, T. and Baillie, C. (2007). 'Influence of fibre extraction method, alkali and silane treatment on the interface of Agave americana waste HDPE composites as possible roof ceilings in Lesotho', *Composite Interfaces,* **14**(7–9), 821–836(16).
Thamae, T. and Baillie, C. (2008). 'A life cycle assessment of wood based composites: A case study', In Oksman, K. and Sain, M. (Eds), *Wood-Polymer Composites*. Cambridge: Woodhead Publishing Limited.
Thamae, T. and Baillie, C. (2009). *Natural Fibre Composites*: *Turning Waste into Useful Materials*. Saarbrücken, Germany: VDM Publishing House Ltd.
Thamae, T., Marian, R., Wu, C., Chong, L. and Baillie, C. (2008). 'Developing and characterizing new materials based on waste plastic and agro-fibre', *Journal of Materials Science*, **43(**12), 4057–4068.
Thamae, T., Aghedo, S., Baillie, C. and Matovic, D. (2009a) 'Tensile properties of hemp and agave fibres' in: Bunsell, A. and Schwartz, P. (eds), *Handbook of*

© Woodhead Publishing Limited, 2014

Tensile Properties of Textile and Technical Fibres. UK: Woodhead Publishing Limited.

Thamae, T., Vaja, S., Shangguan, Y., Finoro, C., Stefano, N. and Baillie, C. (2009b). 'Mechanical and moisture absorption of corn and wheat flour composites for developing countries', in Willems, F. and Moens, P. (Eds). *Green Composites: Properties, Design and Life Cycle*. NY: Nova Publishers.

Whitbeck, C. (1998). *Ethics in Engineering Practice and Research*. Cambridge: Cambridge University Press.

World Commission on Environment and Development (1987). Brundtland Report, 'Our Common Future', Oxford University Press.

© Woodhead Publishing Limited, 2014

7

Manufacturing methods for natural fibre composites

J. SUMMERSCALES and S. GROVE,
Plymouth University, UK

DOI: 10.1533/9780857099228.2.176

Abstract: In consideration of sustainable development, the Brundtland Commission Report demands that the world move to 'Meeting the needs of the present without compromising the ability of future generations to meet their own needs'. In response, there has been growing interest in the use of plant products as a replacement for industrial raw materials. This chapter considers the manufacturing methods that may permit the conversion of bast (stem) fibres into industrial products. The key constraints are the hydrophilic nature of the fibres (and hence moisture release in process) and the temperature sensitivity of the fibres that limits the time at temperature during processing. A moisture removal stage is considered an essential part of the manufacturing cycle. The processes that are most commonly used for engineered composites are compression moulding for both thermoplastics and thermosets and resin transfer moulding or resin infusion for thermosets.

Key words: bast fibres, bio-based materials, manufacture, moulding, natural fibres, plant fibres, processing.

7.1 Introduction

This chapter reviews key aspects of the manufacturing of natural fibre reinforced biocomposites. It first looks at natural fibre reinforcements, from cultivation and structure to reinforcement forms such as rovings, tows, yarns and fabrics. After reviewing bio-based polymer matrix materials, the chapter discusses process parameters which affect manufacturing and composite performance such as moisture, temperature and the effects of the rheological properties of the resin. The chapter then summarises key manufacturing techniques such as injection moulding for thermoplastic polymers and open, liquid composite and compression moulding for thermosetting resins, before considering machining, bonding and repair. The chapter concludes by looking at some applications of natural fibre composites in automotive, civil and marine engineering.

© Woodhead Publishing Limited, 2014

7.2 Fibre reinforcements

Natural fibres may be sourced from animals (e.g. hair, silk, wool), minerals (e.g. asbestos, basalt) or plants (e.g. leaf, seed, stem). The use of natural fibres as the reinforcement for polymer matrix composites has been reviewed by Summerscales *et al.* (2010a, 2010b, 2013), who list several other books and review papers within their texts. This chapter will focus on the use of plant fibres, as these are currently the subject of considerable interest because they are a renewable resource and hence are perceived to be a 'green' or 'sustainable' resource. Any claim for sustainability should be supported by a full Quantitative Life Cycle Analysis (QLCA) with reference to the ISO 14040 series of standards (ISO, 2000–2006) and BS8905 (BSI, 2011) in the context of the specific technical requirements of the product.

7.2.1 Fibre cultivation and production

Plant fibres can be categorised according to where they are located in the plant. The principal divisions are bast (from the stem, e.g. flax, hemp and nettle in temperate zones or jute and kenaf in tropical zones), leaf (e.g. abaca, pineapple or sisal), grasses (e.g. bamboo, miscanthus or wheat straw), seeds (e.g. coir or cotton) or wood fibres. All these fibres find application as the reinforcement for composites. The processes for growth, harvest and separation of the fibres from the source material vary, but for bast fibres the following sequence is normal and is described in greater detail in Summerscales *et al.* (2010a):

- Tillage to prepare the land for cropping by ploughing, harrowing or similar operations;
- Drilling (planting) the seed;
- Weed control: herbicides may be applied to control the growth of undesirable species;
- Plant growth (for flax this consists of a 45–60 day vegetative period, a 15–25 day flowering period, and a maturation period of 30–40 day);
- Dessication (drying) of the crop. This has numerous advantages over field retting (see below) including earlier harvesting, elimination of the need for swathing (lying after being cut), reduction in combine-harvester time, and less wear and tear on machinery;
- Harvest by either combine-harvester or pulling. This is normally in the autumn in temperate zones, with the consequent seasonal impact on the supply chain;

© Woodhead Publishing Limited, 2014

- Rippling to remove seed capsules (assuming the plant has not been dessicated at mid-point flowering and hence has no seed) by drawing stems through a coarse steel comb;
- Retting (controlled degradation) of the crop or deseeded straw using chemical or biological fermentation treatments to make the fibre bundles more easily separable from the woody part of the stem;
- Decortication (referred to as 'scutching' in the flax industry) by a manual operation, hammer mill, inclined plane/fluted rollers or willow to mechanically remove non-fibrous material from retted stalks or to extract the bast fibres from ribbons or strips of stem;
- Hackling (combing) the long (flax line) fibres to remove short fibres, to parallelise the remaining fibres and to remove any extraneous matter (shive);
- Carding to disentangle and align fibres by working them between two closely spaced, relatively moving surfaces clothed with pointed wire, pins, spikes or saw teeth. The product is known as sliver;
- Gilling (or pin drafting) is further combing of the sliver to decrease the mass per unit length;
- Spinning is the drafting and twisting of natural (or man-made) fibres to produce yarn (also known as filaments);
- Textile processes including weaving, braiding, knitting or felting to produce a fabric or preforms (see Section 7.3.2).

7.2.2 The structure of plant fibres

Plant fibres have a hierarchical structure with the following components:

- at the molecular level, the cell wall is usually (i) cellulose (structural fibres), (ii) hemi-cellulose (effectively the matrix), (iii) lignin (accumulates as the plant ages), and (iv) pectin (the binder acting as an adhesive at interfaces);
- individual cells (known as *microfibrils* or *ultimate fibres* in engineering or as *tracheids* in botany) with a hollow core (*lumen*);
- cellular arrays (*fibre bundles* or *technical fibres*).

Cellulose is normally the major component of reinforcement fibres. It is a linear polysaccharide with the empirical formula $(C_6H_{10}O_5)_n$ and is a carbohydrate (six carbons and five water molecules per repeating unit). The molecule is D-anhydro-glucopyranose (DAGP) joined by β-1.4-glucosidic linkages. Inter- and intra-molecular bonding can occur at the two primary (–OH) and one secondary ($–CH_2OH$) hydroxyl units on

© Woodhead Publishing Limited, 2014

each of the DAGP heterocyclic rings, and these alcohol groups are the most probable sites for chemical reactions with the matrix polymer.

7.2.3 Improving the fibre matrix interface

Manufacture of polymer matrix composites may bring together two materials that have inherent incompatibility. Raw natural fibres are hydrophilic, while matrix systems (especially olefinic polymers) may be hydrophobic. Surface treatment of the fibres can change the interfacial chemistry/physics of the fibres to enhance the system performance. Treatment of raw natural fibres or their textiles (Summerscales *et al.*, 2010a; Kabir *et al.*, 2012) may include:

- Acetylation (the process of introducing an acetyl radical into an organic molecule) to reduce the number of hydroxyl groups and hence confer a more hydrophobic character to the fibres;
- Biological treatments (Pickering *et al.*, 2007; Juntaro *et al.*, 2008) with bacteria or fungi;
- Bleaching (any procedure to decolour textile material other than scouring alone) to increase 'whiteness';
- Grafting (the incorporation of monomers (e.g. acrylation, cyanoethylation, maleation or treatment with isocyanates) or oligomers (short chain polymers) at the fibre surface by chemical reaction) to enhance compatibility with the chosen matrix polymer;
- Mercerisation (treatment of cellulosic textiles with a concentrated solution of caustic alkali [soda]) to swell the fibres and increase the strength and dye affinity while modifying their 'handle';
- Oxidation (reaction at the cellulose –OH group) by peroxide or permanganate treatment;
- Plasma treatment and corona discharge;
- Scouring (solvent treatment) to remove natural fats, waxes, proteins and other constituents, as well as dirt, oil and other impurities.

Pre-treatment of natural fibres to improve their effectiveness as reinforcements in polymer composites has recently been reviewed by George *et al.* (2001), Li *et al.* (2007), Kalia *et al.* (2009), Zafeiropoulos (2011) and Kabir *et al.* (2012). The fibre may also need the application of coupling agents (e.g. organometallic silanes, titanates or zirconates) to modify the wet-out and interfacial bonding (see Chapter 6).

It is normal practice to modify the matrix by use of a compatibiliser when hydrophilic fibres (e.g. cellulose) are to be used in combination with

© Woodhead Publishing Limited, 2014

hydrophobic polymers. This is commonly achieved by copolymerisation (e.g. maleic anhydride and polypropylene (MAPP)).

7.3 Reinforcement forms

7.3.1 Roving, tows and yarns

For textile processes, spray lamination, filament winding and pultrusion, the reinforcement fibre is required in a continuous form that may be classified as:

- roving: a bundle of continuous untwisted glass fibres, or
- tow: a large number of filaments collected into a loose strand or assemblage, substantially without twist, or
- yarn: a product of substantial length and relatively small cross-section with or without twist.

The use of spun short fibres will limit the tensile forces to which the reinforcement can be subjected, especially in comparison to continuous filament reinforcements. Spinning of short fibres to produce yarns or rovings is an energy intensive process and hence has high environmental (energy) costs. Dissanayake *et al.* (2009) have identified that the spinning of natural fibres to produce continuous fibre reinforcement (known as filaments, tows or yarns) constitutes a considerable proportion of the energy required for the production of the reinforcement. This may compromise the 'green' credentials of the natural fibre reinforcements and the use of aligned sliver may be a more sustainable route. Hybrid yarns (and fabrics) may commingle or overwrap natural fibres with a thermoplastic filament so that flow distances are minimised during component fabrication (e.g. Composites Evolution Biotex flax yarn and fabrics).

7.3.2 Fabrics

Spun fibres can be converted into a variety of forms:

- two-dimensional planar reinforcements produced by weaving or knitting;
- tubular reinforcements produced by braiding;
- non-crimp fabrics (NCF) produced by stitching single- or multiple-orientation unidirectional layers;
- three-dimensional (3D) fabrics and preforms using 3D weaving.

A key issue for all these formats is the mechanical properties, particularly drape and conformability of the textile. The terms 'drape' and

© Woodhead Publishing Limited, 2014

'conformability' are currently used interchangeably within the composites industry, with no clear definition for either term. The Textile Institute Terms and Definitions (Farnfield and Alvey, 1978) offers:

- drape: 'the ability of a fabric to hang in graceful folds, e.g. the sinusoidal-type of folds of a curtain or skirt';
- modelling: 'the direct application of a fabric to a stand, dummy or body and the manipulation or draping of the fabric to develop a design as a means of producing a pattern. Also known as "draping"'.

Table 7.1 proposes new definitions that might usefully be adopted by the reinforcements industry for drape and conformability respectively.

Standards exist for a variety of ways of testing drape/conformability:

- ASTM D1388–08 (ASTM, 2008a) is a pair of single directional tests. The Cantilever Test Option is simpler to perform and hence is the preferred procedure. However, it is not suitable for very limp fabrics or those that show a marked tendency to curl or twist at a cut edge. The Heart Loop Test Option is suitable for fabrics that show a tendency to curl or twist. Both options can provide a correlation with a subjective evaluation of a given fabric type as a higher number represents a stiffer fabric. In general, the procedures are more suitable for testing woven fabrics than knit fabrics.
- ASTM D5732–01 (ASTM, 2001) uses a cantilever bending test to measure the stiffness of nonwoven fabrics under their own weight. Bending length is measured and flexural rigidity calculated. This standard was withdrawn in July 2008 with no replacement because Committee D13 on Textiles D13 no longer had the appropriate technical expertise.
- BS 3356:1990 (BSI, 1990) measures the distance that a rectangular strip (200 mm long by 25 mm wide) on a horizontal surface must be extended to meet an inclined surface at 41.5° below the horizontal. The parameters determined are bending length and flexural rigidity of the fabric.

Table 7.1 Proposed definitions for drape and conformability

	Definitions
Conformability	The ability of a fabric to be shaped to closely follow a contoured surface with the assistance of an operator or of mechanical devices.
Drape	The natural ability of a fabric to conform to a double curvature surface without assistance.

© Woodhead Publishing Limited, 2014

- ASTM D4032–08 (ASTM, 2008b) uses a circular bend procedure to give a force value related to fabric stiffness while simultaneously averaging stiffness in all directions. 'The circular bend procedure is simple to perform and may be used for knitted, woven, or nonwoven fabrics, provided gage capacity is in keeping with fabric range tested'.
- BS5058:2007 (BSI, 2007) uses a circular fabric specimen held concentrically between smaller horizontal discs. An annular ring of fabric is allowed to drape into folds around the lower supporting disc. The shadow of the draped specimen is cast onto an annular ring of paper of the same size as the unsupported part of the fabric specimen. The outline of the shadow is traced onto the ring of paper, the mass of which is then determined. The paper is then cut along the trace of the shadow and the mass of the inner part representing the shadow is determined. The drape coefficient is calculated from the two masses.

Dominguez (1987) suggests that tape drapability is typically measured by the ease with which a prepreg can be formed around a small-radius rod. The pass/fail criterion requires forming without incurring fibre damage. This measurement indicates that fabrication personnel will be able to form the prepreg onto complex tools. Tapes are typically less drapable than fabric forms of prepreg.

Maha and Songa (2010) used 3D body scanning of 1000 mm diameter circular test specimens allowed to overhang around a 1200 mm tall and 220 mm diameter cylinder. A number of cross-sections were acquired along the length of the overhang. The data were compared to the drape coefficient for the fabrics calculated according to the BS 5058 test (BSI, 2007) using two 360-mm diameter circles and three replications for each specimen performed. Data were also compared to 2D stiffness results from the ASTM D1388 Cantilever Test Option (ASTM, 2008a) using four 200 × 25 mm specimens for each of the warp and weft directions for each fabric. Each specimen was tested with the face side either up or down and on both ends for a total of four measurements per specimen.

Gan *et al*. (2012) presented a novel (non-destructive) optical technique to quantify in-plane geometric variations (tow width, spacing and orientation and areal weight) within glass fibre reinforcement materials and found that areal weights were typically within 5% of the experimentally obtained mean values for one inch (25.4 mm) square samples. Comas-Cordona *et al.* (2011) and Zhang *et al.* (2012a,b) used the system to study E-glass chopped strand mat while Comas-Cordona *et al.* (2012) studied fabrics in the context of the FP5 TECABS project on virtual manufacturing. The effective permeability (see Section 7.6.6) was determined using the statistical properties in two different modelling approaches (Table 7.2) and was validated by mould-filling simulation. The inherent variation in the plant fibres may result in higher variations for natural fibre fabrics.

© Woodhead Publishing Limited, 2014

Table 7.2 Coefficients of variation in the principal in-plane permeabilities (K_1 = 0° and K_2 = 90°) and anisotropy ratios of reinforcements

Reinforcement	Areal weight (%)	K_1 or K_2 (%)	K_1/K_2 ratio (%)
Owens Corning M705450 457 gsm chopped strand mat (CSM)	5	Both 24	±10
Lintex WoviFab EWR800 822 gsm plain weave (PW) fabric	1	Both 17	27
Haining ChengruDan Reinforcement Fabrics LT800 875 gsm bidirectional stitched fabric	1	14 or 11	13

Source: Data from Comas-Cordona *et al.* (2011, 2012) and Zhang *et al.* (2012a, 2012b).

7.4 Bio-based polymer matrices

The key properties of some commercial bio-based thermoplastics are shown in Table 7.3. A range of polymers are attracting interest but it is not yet clear which of these might prove successful as the matrix for fibre-reinforced composites.

7.4.1 Bio-based thermoplastics

Polylactide aliphatic copolymer (CPLA) (Lenau, 2004a) is a biodegradable mixture of lactide and aliphatic polyesters. It can be either a hard plastic (similar to poly(styrene), PS) or a soft flexible one (similar to poly(propylene), PP) depending on the amount of aliphatic polyester present in the mixture. It is easy to process with stability up to 200°C. Possible applications include compost bags, cushioning materials, food wrapping materials, fishing nets, etc.

Polycaprolactone (PCL) (Lenau, 2004b; Anon, 2004a) is a biodegradable thermoplastic polymer made by polymerising ε-caprolactone and hence derived from the chemical synthesis of crude oil. Although not produced from renewable raw materials, it is fully biodegradable. It has good water, oil, solvent and chlorine resistance, a low melting temperature (58–60°C), low viscosity and it is easy to process. It is used mainly in thermoplastic polyurethanes, resins for surface coatings, adhesives, and synthetic leather and fabrics. It also serves to make fully biodegradable compostable bags, sutures, fibres and stiffeners for both shoes and orthopaedic splints. It is used as an additive for other resins to improve their processing characteristics and end-use properties, and acts as a polymeric plasticiser with poly(vinyl chloride) (PVC). PCL is compatible with most thermosetting and thermoplastic resins and elastomers. It increases impact resistance and aids mould release of thermosets.

© Woodhead Publishing Limited, 2014

Table 7.3 Key properties for some bio-based resins and thermoplastics

Polymer	Source	Density (kg/m^3)	HDT (°C)	T_g (°C)	T_m (°C)	T_p (°C)	Modulus (MPa)	Failure strain (%)	Strength (MPa)
Thermoplastics									
P(3HB) (Biomer® P240)	Wolf *et al.* (2005)	1170	53[v]				1000–1200	10–17	18–20
P(3HB) (Biomer® P226)	Wolf *et al.* (2005)	1250	96[v]				1700–2000	6–9	24–27
P(3HB-co-3HHx) (Kaneka Nodax®)	Wolf *et al.* (2005)	1070–1250	60–100					10–25	10–20
PGA (polyglycolic acid)	Maurus and Kaeding (2004)			35–40	225–230		12800		
PLA (Hycail® HM 1011)	Anon (2005b)	1240		60–63	150–175	190–240		3–5	56–62 (ISO 527)
PLA (NatureWorks®)	Wolf *et al.* (2005)	1250	40–45[a] 135[c]	55–65	120–170		350–450	10[a]–100[c]	53
PLLA (*via* Gupta *et al.*, 2007, Ref. 16)	Fambri *et al.* (1997)						7000–9200[f]	18–25[f]	410–870[f]
PLLA (*via* Gupta *et al.*, 2007, Ref. 26)	Yuan *et al.* (2001)			~62–66[f]	~168–178[f]	210–240[f]	1760–5220[f]	4.2–440[f]	51–535[f]
PTT (Dupont™ Sorona ® 3301 NC010	Anon (2012a)	1320	60–125		250–270		2400	5.5–15	60

© Woodhead Publishing Limited, 2014

Thermosets							
AOC EcoTek S905–70G multipurpose DCPD	Anon (2011)	138			4100	1.3	45
AOC EcoTek S404–60G PET for RTM/SMC	Anon (2011)	140			3500	2.4	68
Dilulin/DCPD (from 30:70 to 60:40 mix)	Henna *et al.* (2008)		21–76		0.91–525	35–156	0.5–29
Envirez® 70302 for pultrusion	Mannermaa (2011)	90			2500	4	73
Envirez® M 81502 INF-60 for infusion	Mannermaa (2011)	72			3800	2.6	64
Envirez® M 8600TA for HLU/spray	Mannermaa (2011)	70			3400	2.6	55
Envirez® SS 70419–09	Mannermaa (2011)	79			3600	3.7	79
Nov-I 35 w/o unreacted CNSL cardanol condensed with paraformaldehyde and oxalic acid	Campaner *et al.* (2009)		30–110	115	1700–2200	2.4–2.8	35–42
Nov-II 20 w/o unreacted CNSL cardanol condensed with paraformaldehyde and oxalic acid	Campaner *et al.* (2009)		96–116	115	1995–2487	3.2–4.0	36–49

Superscripts: a = amorphous, c = crystalline, f = mechanical properties from polymer fibre in tension, v = Vicat softening point.
HDT: heat deflection temperature. T_g, T_m and T_p: glass transition, crystalline melting and processing temperatures, respectively.

© Woodhead Publishing Limited, 2014

Poly(glycolic acid) (PGA) is a synthetic polymer of glycolic acid ($HOCH_2COOH$). As the monomer is terminated by a hydroxyl group at one end and a carboxyl group at the other, it can be polymerised by a condensation reaction to yield a polyester. The polymer degrades to natural metabolic waste products and finds use in biomedical applications.

Polyhydroxyalkanoate (PHA) (Lenau, 2004c) is a class of linear polyesters produced in nature by bacterial fermentation of sugar or lipids. More than 100 different monomers can be combined within this family to give materials with extremely different properties. They can be either thermoplastic or elastomeric materials, with melting temperatures in the range 40–180°C. The most common type of PHA is poly(3-hydroxybutyrate) (PHB). PHB has properties similar to those of PP, although it is stiffer and more brittle. More detail can be found on the AZoM site (Anon, 2004b). A PHB copolymer called poly(hydroxybutyrate-*co*-hydroxyvalerate) (PHBV) (Lenau, 2004c) is less stiff and tougher and finds use as packaging material. More detail can be found on the AZoM site (Anon, 2004c).

Polylactide (PLA) (Anon, 2004d; Lenau, 2004d; Lim *et al.*, 2008) is a biodegradable thermoplastic derived from lactic acid. It resembles clear polystyrene, provides good aesthetics (gloss and clarity), but it is stiff and brittle and needs modifications for most practical applications (i.e. plasticisers increase its flexibility). It can be processed like most thermoplastics into fibres or films and can be thermoformed or injection moulded. It is most commonly used for compost bags, plant pots, diapers and packaging. Cargill Dow NatureWorks PLA (Anon, 2006; Gupta, 2007) is derived from corn. Gupta *et al*. (2007) have reviewed the use of PLA as a fibre. Clark and Hardy (2004) have compared and contrasted the sustainability implications of the life cycle of PLA with that for conventional polymers. Ouagne *et al*. (2010) reported that the viscosity of poly(L-lactic acid) (PLLA) was 3500 (169°C = melting temperature), 1647 (179°C), 1011 (189°C) and 588 (199°C) Pa·s.

DuPont™ Sorona® (Anon, 2005a) is one member of a family of polymers based on Bio-PDO™ corn-derived chemical 1,3-propanediol: poly(trimethylene terephthalate).

There is some interest in the use of starch-based polymers as 'sustainable' materials for extrusion or injection moulding. However, processing these materials is more complex than using conventional polymers and involves multiple chemical and physical reactions, including water diffusion, granule expansion, gelatinisation, decomposition, melting and crystallisation. Starch-based resins can be made from corn, wheat, tapioca and potato (e.g. Cereplast Compostables® (Anon, 2006); Potatopak (Anon, 2009)). Hongsheng Liu *et al.* (2009) have reviewed the thermal processing of these materials. Xie *et al.* (2012) have reviewed the rheology of starch polymeric materials in order to understand and optimise their processibility, structures and properties.

© Woodhead Publishing Limited, 2014

7.4.2 Bio-based thermoset resin systems

The key properties of some bio-based thermosetting resins are shown in Table 7.3. A number of bio-based thermosetting resin systems are available from commercial suppliers, including:

- Advance Enterprises Limited rapeseed-oil derived resins;
- Ashland (Dublin, OH) Aropol™ Envirez 5000 acrylised epoxidised corn- and soybean-oil catalysed with Trigonox including a special formulation for resin transfer moulding (RTM) with 1 h gel time;
- Bio-Composites and more GmbH (Ipsheim, Germany) epoxidised linseed oil and polycarboxylic acid anhydrides;
- BioComposites Centre (Bangor, Wales) formaldehyde-free cashew nut shell liquid (CNSL) resin;
- Cargill Dilulin® partially norbornylised linseed oil;
- M/S. Golden Products (Pondicherry – India) CNSL including CNSL resin GP-002;
- Sustainable Composites Limited (Redruth, England) EcoComp® UV-L resins;
- TransFurans (Geel, Belgium) BioRez™ furan resin;
- UCB (Brussels, Belgium) Ebecryl acrylised epoxidised soybean oil resin.

7.5 Composites manufacturing processes

This section reviews the methods of manufacture used to create polymer matrix composites with synthetic (man-made) fibre reinforcement. The following section (Section 7.6) considers the process parameters appropriate for successful manufacture of natural fibre composites. The subsequent section (Section 7.7) considers the methods of manufacture as used to create polymer matrix composites with natural fibre reinforcement.

For the bulk manufacture of short fibre reinforced thermoplastics, the most successful processes are compounding or profile manufacture by extrusion (Incarnato and di Maio, 2012) and injection moulding (Ehrig, 2012).

The manufacture of continuous fibre reinforced composites has been reviewed by Åström (1997), Gutowski (1997), Davé and Loos (1999), Akovali (2001), Mazumdar (2002), Campbell (2003), Strong (2008), Hoa (2009) and Grove (2012). For low performance components, spray and hand lamination are often chosen because the raw materials are relatively inexpensive, the process can use relatively unskilled labour, and the mould tools do not need to be vacuum tight. However, these open mould processes produce composites with low fibre volume fractions and high levels of voids (porosity), For higher-performance composites, vacuum bagging of wet-lay-up or pre-impregnated

© Woodhead Publishing Limited, 2014

(prepreg) materials can add one bar of pressure for consolidation, while for the highest performance an autoclave can add further external pressure to the bag (Ciriscioli and Springer, 1990; Seferis, 2000; Noakes, 2008; McBeath and O'Rourke, 2009; Giordano *et al*., 2012; Louis and Ermanni, 2012).

High performance composites can also be produced using compression moulding in a (normally hydraulic) press between a matched (male and female) mould tool set with heated platens or integrally heated tooling (Revellino *et al.*, 2000; Wakeman and Rudd, 2000; Isayev, 2012). The moulds are usually of steel to withstand the high closing forces. For thermosetting matrix materials, the simplest form of the process involves loading the open mould cavity with a shaped arrangement of the reinforcement to be used. The preform may be assembled in the tool or more likely moulded or sprayed off-line. Liquid resin is added to the mould cavity, then the press is closed and the part cured under pressure. An alternative approach is the use of glass fibre reinforcement sheet moulding compound (SMC) or bulk moulding compound (BMC) materials, both based on catalysed polyester resins. Materials are formulated to give rapid cure, and moulding cycle times of a few minutes are possible at process temperatures of around 150°C

For thermoplastic composites, the usual commercial compression moulding route involves the preheating of a stack of pre-impregnated sheets outside the mould tool, typically in an oven or by infrared lamps. This process is sometimes referred to as 'stamping', and is widely used for the mass production of glass mat-reinforced thermoplastic parts for automotive applications. Pre-impregnation can be difficult and time consuming; as an alternative, thin sheets of reinforcement and polymer can be 'film stacked'. When softened, they are rapidly transferred to the matched mould tool, then simultaneously shaped and cooled. The process cycle time is determined not only by heat transfer rates, but also by the ability of the matrix to flow and achieve adequate impregnation and consolidation.

RTM (van Harten, 1993; Potter, 1997; Rudd *et al.*, 1997; Beckwith and Hyland, 1998; Kruckenberg and Paton, 1998; Benjamin and Beckwith, 1999; Advani, 2000; Parnas, 2000; Ermanni, 2012) is emerging as the most probable route to mass production for small-medium sized composite components of complex shape. In RTM, a mould is loaded with dry fibres then resin flows into the fabric stack before the resin cures to produce a solid component. While RTM is appropriate for relatively small components, the mould closure forces become excessive as component size increases.

One solution to this problem is to use only vacuum to drive long-range resin flow and enclose the laminate in a bag rather than in a matched pair of moulds. This technique is known by various names including resin infusion under flexible tooling (RIFT) (Abraham and McIlhagger, 1996; Williams *et al.*, 1996; Cripps *et al.*, 2000; Cocquyt, 2001; Summerscales and Searle, 2005; Beckwith, 2007; Summerscales, 2012), the Seeman Composites Resin Infusion Molding Process (SCRIMP™) (Anon, 2008) and Vacuum-Assisted Resin

© Woodhead Publishing Limited, 2014

Transfer Moulding (VARTM). Smith (1999) has reviewed the status of resin infusion in the context of its application for toughened aerospace structures.

Searle and Summerscales (2005) classified the resin infusion processes in four divisions:

- RIFT I: in-plane flow parallel to the layers of reinforcement;
- RIFT II: through-plane flow from a flow medium or scored core;
- RIFT III: resin film infusion (Marsh, 2002) (the use of un-reinforced B-staged resin film stacked with the dry reinforcement fabrics (for thermoplastic composites, the equivalent process is referred to as 'film stacking'); or
- RIFT IV: partially pre-impregnated reinforcement materials (referred to as 'semi-preg').

The latter two processes minimise the resin flow distance by utilising only through-thickness flow and use the resin in a form where the base/hardener mix ratio is set by the materials supplier. Commercial versions of the semi-preg process include Carboform (Cytec), HexFIT™ (Hexcel Composites), SPRINT™ (SP Systems) and ZPREG (Advanced Composites Group).

Automated processes include filament winding (Munro, 1988; Peters *et al.*, 1999; Koussios, 2004; Peters, 2011; Koussios and A Beukers, 2012), robot-assisted fibre placement (Newell *et al.*, 1996; Crosky *et al.*, 2012) and pultrusion and pulforming (Meyer, 1985; Starr, 2000; Goldsworthy, 2012; Vázquez and M Escobar, 2012). Machining of composites has been reviewed by various authors (Abrate and Walton, 1992a,b; Gordon and Hillery, 2003; Robinson *et al.*, 2007; Sharma *et al.*, 2008; Sadat, 2012; Sheikh-Ahmad and Paulo Davim, 2012). Methodologies for the care and repair of composites have been presented by Armstrong *et al.* (2005) and Baker (2012). Process monitoring techniques have been reviewed by Summerscales (2003) and process modelling has been reviewed by Advani and Sozer (2010) and Davé *et al.* (2012).

7.6 Key parameters for successful processing of natural fibre composites

The successful production of natural fibre reinforced polymer composites requires control of the several parameters as discussed below.

7.6.1 Moisture

Natural fibres are hygroscopic and thus absorb moisture from the surrounding environment. The extent of moisture absorption will depend on the relative humidity and the time that the fibres are exposed to the environment. It is essential that moisture levels are well controlled before and during manufacture of natural fibre reinforced polymer matrix composites. A cellulosic

© Woodhead Publishing Limited, 2014

paper sheet will absorb up to 7% moisture when exposed to 50% relative humidity if allowed to reach equilibrium (Anon, 2012b). For comparison, the equilibrium level of moisture content for Nomex® paper is equal to ~ 1/10 of the relative humidity of the environment to which the paper is exposed, so at 50% RH it will contain roughly 5% moisture (Anon, 2012b).

In respect of workshop conditions/temperature and humidity, ISO12215–4:2002 (ISO, 2002a) states:

> Where a conventional manual lay-up or spray-up process is used, the moulding shop temperature shall be maintained within the limits specified by the resin manufacturer during lay-up and curing periods. Should the temperature vary outside the specified limits, the boat builder shall establish with the resin manufacturer that the resulting laminate will meet the requirements upon which scantlings and design are based. The relative humidity in the moulding shop shall be maintained within the limit recommended by the material manufacturers. Materials shall be brought up to the workshop temperature prior to use. The temperature and humidity shall be monitored in appropriate locations, and records shall be kept

and for reinforcing and core materials:

> Reinforcing and core materials shall be stored in clean and dry conditions, in accordance with the material manufacturer's recommendations.

Armstrong and Barrett (1998) state that 'Nomex and other aramid honeycomb should be stored in a clean environment at approximately 20°C (68°F) and in a relative humidity not exceeding 65% and preferably lower. It should be dried for 16 h at 40°C (104°F) immediately prior to use. Alternative drying cycles are 1 h at 160°C (320°F) or 3 h at 100°C (212°F)' and 'Dried materials should be used within 1 h of drying, or a further drying process immediately before use will be necessary'. Davis (2009) has stated that Nomex core should be thoroughly dried before composite fabrication. Otherwise, the moisture may be liberated during the bonding process and then cause micro-voiding. He suggests that moisture control can be achieved by storing cores in a dedicated room maintained at 50°C and <10% RH. In the absence of other formal requirements for natural fibres, these conditions should be regarded as a minimum requirement for the fabrication of good natural fibre composites.

7.6.2 Thermal transition temperatures

The key criterion in the selection of a polymeric matrix for a natural fibre reinforced polymer is the transition temperatures. In ascending order, the major transition temperatures are normally:

© Woodhead Publishing Limited, 2014

- T_g = glass transition temperature
- T_c = peak crystallisation temperature (*not applicable to amorphous polymers)
- T_m = crystalline melting temperature – normally $T_m \approx T_g + 200 \pm 50°C$. (* there is no melting temperature for amorphous materials)
- T_p = processing temperature – normally $T_p \approx T_m + \sim 30°C$ for partially crystalline thermoplastic polymers – T_g is normally similar to the (post-) cure temperature for thermosetting resins
- T_d = degradation/decomposition temperature (range) – may limit T_p (especially for PVC)

These key temperatures do not necessarily occur in all cases (see asterisks above). As the temperature rises through the glass transition temperature short segments of the polymer backbone, that had had insufficient energy for movement other than atomic vibration, start to move as a group of atoms. On cooling through this temperature, it is normal to assume that all segmental motion has been frozen out. The mechanical properties of the polymer are then:

- below T_g: normally elastic and brittle (with good resistance to creep deformation);
- above T_g: normally viscoelastic and tough (however creep deformation can be a problem).

Polymers with a regular repeating structure can pack closely together to form crystalline structures. The fringed micelle theory suggests that each polymer molecule passes through several crystallites embedded in an amorphous matrix. More recently, the folded lamella theory suggests that the polymer molecules fold back on themselves at intervals of ~10 nm (100 Å). The close packing increases the material density and the secondary intermolecular forces with consequent increases in softening point, elastic modulus and strength (Brydson, 1999). The crystalline melting temperature (actually a narrow range of temperatures dependent on factors such molecular weight and extent of chain branching) is not applicable to amorphous polymers and is usually only important in thermoplastics.

Dry cellulose is variously reported to have glass transition temperatures (T_g) ranging from 84°C to 250°C with T_g decreasing with increasing water content (Table 7.4).

The T_g of cellulose is strongly dependent on the degree of crystallinity (Roig *et al.*, 2011). Colour changes are reported at 180°C and significant weight losses (~70%) occur between 220°C and 300°C (Szcześniak *et al.,* 2008). Cellulose normally decomposes in air before melting because of the extensive hydrogen bonding between the cellulose molecules. The ScienceLab MSDS (Anon, 2010) for cellulose gives a melting temperature of 500–518°C (presumably under inert gas or *in vacuo*).

© Woodhead Publishing Limited, 2014

Table 7.4 Glass transition temperatures reported for cellulose

Glass transition (°C)	Reference
200–250 (dry)	Kubát and Pattyranie (1967)
~230 (dry)	Back *et al.* (1969)
220 (dry)	Szcześniak *et al.* (2008)
84 ± 1 at 0% H_2O	Roig *et al.* (2011)
~79 at 1% H_2O	Roig *et al.* (2011)
~52 at 5% H_2O	Roig *et al.* (2011)

Given that cellulose degrades at ~200°C in air, it is difficult to find a thermoplastic matrix which can be used in a load-bearing application at ambient temperature (i.e. below T_g to avoid creep) yet processed without damage to the fibre structure (i.e. $T_p < 200$°C). A notable exception is poly(lactic acid) (see Section 7.4.1) with T_g = 55–65°C, T_m = 120–170°C and T_d just above 200°C so the polymer has a narrow process temperature window but can be stressed at ambient temperatures. The use of other polymer matrix systems might be possible by minimising the time at high temperature or by processing *in vacuo* or under an inert atmosphere (although the process costs will inevitably be higher).

7.6.3 Exotherm

For polymer systems where polymerisation or cross-linking (curing) is undertaken *in situ*, the progress of the reaction will normally generate heat (exotherm). The low thermal conductivity of the polymer will constrain the rate of heat loss, especially in thick sections. As the core of the moulding increases in temperature, the rate of reaction also increases. The high temperatures may result in discoloured resin and reduced matrix mechanical properties. In natural fibre composites, there may be also be thermal damage to the fibres. If not properly controlled, the exotherm may lead to a rapid temperature rise that could result in the material smoking or even ignition of fire. In polyester resins, increasing the styrene content will reduce the resin system viscosity (making the material easier to work) but will also increase the heat of reaction and hence the likelihood of exotherm issues.

7.6.4 Volatile components

For unsaturated polyester resins, Lundström *et al.* (1992, 1993) state that styrene must be subjected to 10 mbar absolute vacuum at 40°C for it to be evolved from the resin system. Elsewhere (Anon, 1994), the vapour pressure of styrene at 20°C is quoted as 6 mbar. Dreyer *et al.* (1955) give vapour

© Woodhead Publishing Limited, 2014

pressures of 8.2 and 13.7 torr (10.93 and 18.27 mbar respectively) at 29.9°C and 39.2°C respectively while Chaiyavech *et al.* (1959) give vapour pressures of 13.33 and 26.66 at 32.4°C and 45.6°C mbar respectively. Lundström *et al.* (1992, 1993) believe that porosity is not due to the 'boiling' of styrene but, in most cases, is due to poor mould sealing, which allows air to leak into the mould cavity, and they suggest that double seals should be used with a higher vacuum drawn between the seals than in the mould.

7.6.5 Rheology

Rheology can be defined as the science of flow and deformation of matter, while viscosity can be defined as the ability of a fluid to resist a change in the arrangement of the molecules when under an applied shear stress. Viscosity can then be divided into:

- **Dynamic viscosity**: the force required to overcome internal friction. The standard symbol for dynamic viscosity is the Greek symbol μ. The SI units are Pascal-second (Pa·s: identical to 1 $kg \cdot m^{-1} \cdot s^{-1}$) although the composites industry often uses cgs units: centiPoise (cP). There is a direct numerical equivalence between milliPascal-second and centiPoise (1 mPa.s = 1 cP).
- **Kinematic viscosity**: the ratio of the viscous force to the inertial force where the latter is a function of the fluid density (ρ). The standard symbol for kinematic viscosity is the Greek symbol η and the SI units are $m^{2} \cdot s^{-1}$. although the parameter is often given in centiStoke (cgs units: 1 centiStoke is 1 mm^2/s). Hence $\eta = \mu/\rho$.

Indicative viscosities for water and various polymeric systems or conditions are given in Table 7.5.

Effect of temperature on viscosity

As temperature rises, the motion of the atoms in a polymer chain increases and thus the polymer becomes more fluid. For a thermoplastic polymer, there is a direct and reversible relationship between temperature and viscosity (assuming no change in the molecular weight of the polymer due to further polymerisation or to degradation). For the individual components in a thermosetting resin there should also be a similar reversible relationship between temperature and viscosity, but this will not be true for the mixed materials. A typical relationship for the variation of viscosity with temperature would be:

$$\eta = \eta_o e^{a(T - T_o)} \qquad [7.1]$$

© Woodhead Publishing Limited, 2014

Table 7.5 Indicative viscosities for various materials or conditions

Dynamic viscosity (mPa.s)	Material or condition	Reference
1.0020	Water at 20°C	Kaye and Laby (2007)
<20	Cyclic butylene terephthalate (CBT) monomer at 180°C	Coll *et al.* (2004)
100–200	Initial viscosity for RTM/infusion resins	
800	Upper limit for viscosity in RTM	Becker (no date)
1000	Non-injection point (NIP) in RTM	Pearce *et al.* (1998)
7500–16500	Dwell-time window for wet-laid vacuum-bagged composites	Stringer (1989)
100 000–1000 000	Preferred (thermoplastic) melt viscosity range for most forming processes	Cogswell (1992)
300 000	Melt viscosity of PEEK	Cogswell (1992)

where η and T are the instantaneous viscosity and temperature respectively and η_o is the viscosity at temperature T_o. For a polyester resin, a typical value of a would be $-0.04°C^{-1}$, which would result in:

- a 33% fall in viscosity for a 10°C temperature rise,
- a 56% fall in viscosity for a 20°C temperature rise, and
- a 70% fall in viscosity for a 30°C temperature rise respectively (Potter, 1997).

Effect of cure on viscosity

Most thermosetting resins start out as a mixture of two low viscosity components that react to form a 3D cross-linked network. In consequence, the degree-of-cure and the viscosity increase with time after the mixing of the components. This is normally accompanied by the generation of heat that will act to accelerate the reaction. In the limit, the exotherm may result in smoke and/or fire.

The heat evolved during cross-linking (cure) can be assumed to be proportional to the degree-of-cure of the resin system with the equation to describe the reaction rate having the form: $\delta\alpha/\delta t = K(1 - \alpha)^n$ where K is based upon the Arrhenius equation: $K = K_o \cdot \exp(-E_a/RT)$ and where:

- K is the overall reaction rate,
- K_o is the pre-exponential constant (per second),

© Woodhead Publishing Limited, 2014

- E_a is the activation energy (J/mol),
- R is the universal gas constant (J/mol·s) and
- T is the absolute temperature (K).

For resin systems cured by an addition reaction (e.g. polyester and vinyl ester systems), the Kamal and Sourour (1973) model is often used. It incorporates both n-th order kinetics and an auto-catalytic term (Equation [7.2] (Rudd *et al.*, 1997)).

$$\frac{\mathrm{d}\alpha}{\mathrm{d}t} = \left(K_1 + K_2\alpha^m\right)(1-\alpha) \qquad [7.2]$$

where

$$\alpha(t) = \frac{\sum \Delta h}{H} \qquad [7.3]$$

$$K_1 = A_1 \exp\left(\frac{B_1}{RT}\right) \qquad [7.4]$$

$$K_2 = A_2 \exp\left(\frac{B_2}{RT}\right) \qquad [7.5]$$

- $\Sigma\Delta h$ is the cumulative specific heat release (J/kg),
- K_1 and K_2 are temperature dependent kinetic constants (per second),
- B_1 and B_2 are energy constants (J/mol),
- R is the universal gas constant (J/kg·K),
- T is the absolute temperature (K) and
- H is the specific enthalpy of reaction (J/kg).

For epoxy resin, White (1974) modelled the PR286 resin system with the following assumptions:

- the temperature of both the mould and the resin were equal,
- the problem could be simplified by considering it as a one-dimensional infinite plane problem,
- Equation [7.6] applies:

$$\log\left(\eta(T,t)\right) = \log\left(\eta_o(T) + K(T)t\right) \qquad [7.6]$$

© Woodhead Publishing Limited, 2014

where

- η is the viscosity at temperature T and time t,
- η_o is the viscosity at time zero and is solely a function of temperature,
- $\log_{10}(\eta_o) = 3850/T(K) - 8.93$ is the rate of viscosity rise calculated from the constant temperature experiments and
- $\log_{10}(K(T)) = -3930T(K) + 8.66$.

White (1974) further demonstrated that the profiles of the isothermal viscosity–time curves of an epoxy resin system were identical when plotted on logarithmic axes. The effect of temperature was a change in the position of the curve with respect to those axes. The application of an appropriate shift along the logarithmic time and logarithmic viscosity axes could bring any pair of curves into coincidence. By implication, it follows that any isothermal viscosity–time curve may be generated from any other by an appropriate scaling of the time and viscosity axes.

Roller (1975) presented experimental evidence for the determination of the viscosity of curing B-staged epoxy resins as a function of both time and temperature using Equation [7.7]:

$$\ln \eta(T,t) = \log \eta_x + \frac{\Delta E_\eta}{RT} + \int_0^t k_x \exp\left(\frac{\Delta E_k}{RT}\right) \mathrm{d}t \qquad [7.7]$$

where

- η is the time-dependent viscosity,
- η_o is the zero-time viscosity given by $\eta_o = \eta_x e\Delta E_\eta / RT$, although this expression may not hold near (i.e. within 50°C of T_g) the glass transition temperature,
- η_x is the calculated viscosity of the material at $T = \infty$,
- ΔE_η is the Arrhenius activation energy,
- k is the kinetic factor given by $k = k_x e\Delta E_k / RT$, where k_x and ΔE_k are the analogues of η and ΔE_η. The expression will not correctly model the kinetics if the reaction mechanism changes within the temperature range of interest,
- R is the gas constant and
- t is time.

7.6.6 Permeability

In the context of composites manufacture, permeability is a measurement of the ease with which a fluid can flow through the pore space in a reinforcement pack. Permeability is the constant of proportionality in the Darcy

© Woodhead Publishing Limited, 2014

(1856) equation (originally derived to predict the flow of water through aquifers supplying the town of Dijon and modified to account for the viscosity of different fluids) that should be expressed as a tensor for anisotropic material. The isotropic form of the equation is:

$$Q = \frac{KA\Delta P}{\mu L} \quad [7.8]$$

where Q is the volumetric flow rate of the fluid, K is the permeability of the reinforcement bed, A is the cross-sectional area of the bed, $\Delta P/L$ is the pressure drop over the length of the reinforcement bed and μ is the dynamic viscosity of the liquid. A reinforcement that constrains the flow has a low permeability. The units of permeability are m^2 in SI units with integer magnitudes typically expressed in $m^2 \times 10^{-12}$. An alternative unit is the darcy: a medium with a permeability of 1 darcy permits a flow of 1 cm^3/s of a fluid with viscosity of 1 centipoise (1 mPa.s in SI units) under a pressure gradient of 1 atmosphere/cm acting across an area of 1 cm^2. It is common practice to use 'ideal' fluids (i.e. systems without curing reactions) to measure permeability although this may change the physics and chemistry at the interface between the fibre and the polymer.

Kozeny (1927) and Carman (1937) developed an expression to relate the flow rate of fluid to the microscopical architecture of the reinforcement pack:

$$Q = \frac{\varepsilon A m^2 \Delta P}{\mu L} \quad [7.9]$$

where ε is the fractional free volume in the bed (porosity $= 1 - V_f$), m is the mean hydraulic radius of the bed (concept attributed to Blake (1922)) and k is the Kozeny constant. The mean hydraulic radius is defined as the cross-sectional area normal to the flow divided by the perimeter P presented to the fluid (or the volume divided by the wetted surface area S). Rearrangement of the above equations for constant area, pressure drop and viscosity (Griffin *et al.*, 1995) yields:

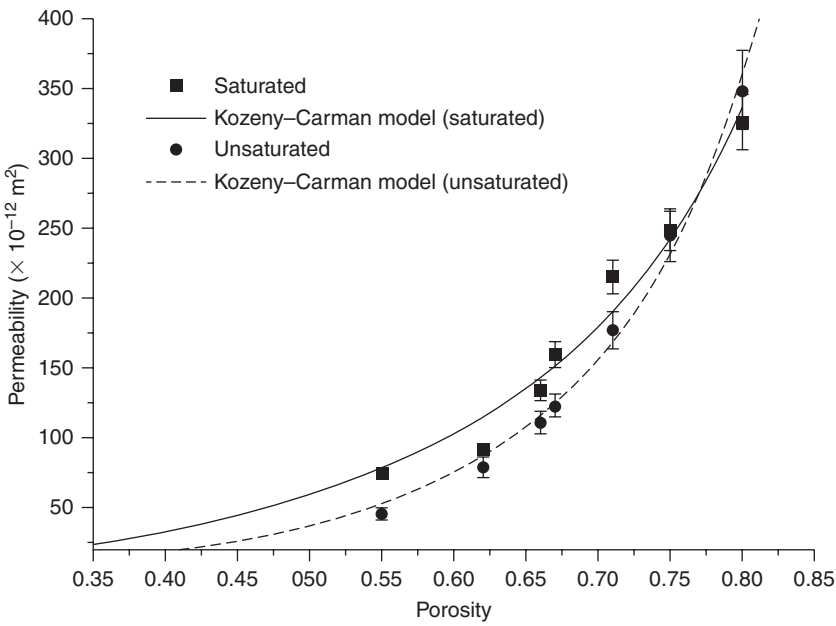
$$Q \propto \frac{\varepsilon^3}{S^2} \text{ or } Q \propto \frac{\varepsilon^3}{P^2} \quad [7.10]$$

so the flow rate at constant fibre volume fraction is inversely proportional to the square of the wetted circumference or the wetted area respectively.

Francucci *et al.* (2010) studied both the saturated and unsaturated permeabilities of bidirectional jute reinforcement fabrics during uniaxial flow of

© Woodhead Publishing Limited, 2014

water–glycerol mixtures. They found that the permeability increased with increasing porosity in both cases and thus confirmed that there is an inverse relationship to fibre volume fraction. The saturated permeability values were found to be higher than the unsaturated permeability values (Fig. 7.1) confirming the findings of other authors (Foley and Gutowski, 1991; Lundström *et al.*, 2000; Shojaei *et al.*, 2004). The difference in permeabilities tended to vanish for porosities above 75% (i.e. at low fibre volume fractions). The jute reinforcements were found to absorb fluid during the infusion process, unlike glass fibre reinforcements. The combination of the fibres acting as a sink for the permeant fluid and the consequent swelling reduced the permeability of the preform. Fibre swelling was also found to occur with commercial vinylester and phenolic resins. The authors suggest that flow simulation for natural fibre preforms should take into account the chemical and physical interaction of the test fluids or resins with the fibres. This supports the statement by Summerscales (2004) that there is 'a growing body of evidence to indicate that the measured permeability in unsaturated (wetting) flow differs from that in saturated (wetted) flow. This may be a function of contact angles or surface energies'.

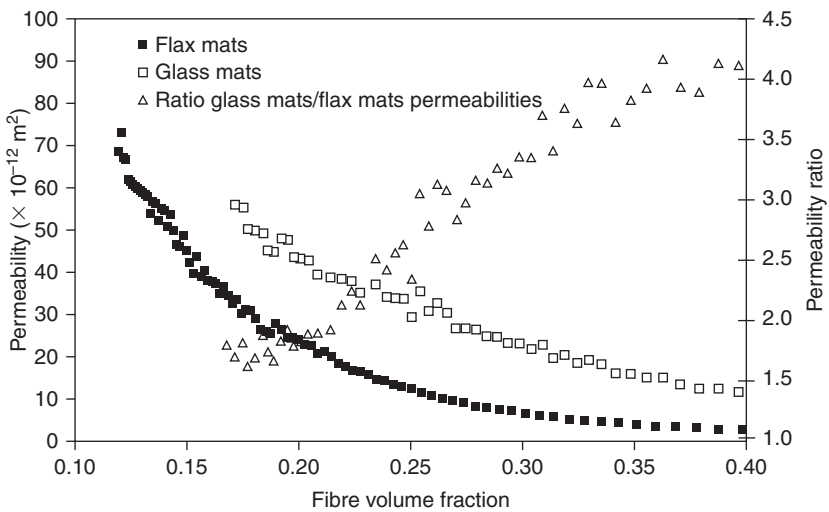


7.1 Saturated and unsaturated permeability values as a function of the porosity for bidirectional jute reinforcement fabrics. (*Source*: Reprinted from *Composites Part A: Applied Science and Manufacturing*, 41/1, G Francucci, ES Rodríguez and A Vázquez, Study of saturated and unsaturated permeability in natural fiber fabrics, 16–21, Copyright (2010), with permission from Elsevier and the authors.)

© Woodhead Publishing Limited, 2014

Bréard *et al.* (2006) studied flax and glass mats with areal weights of 220 g/m^2 at a fibre volume fraction of 24%. They found that the respective relative values of longitudinal permeabilities had ratio of four (4). The ratio for transverse permeabilities was around two (2) at volume fractions below 0.22, but at higher volume fractions the ratio could reach a value of 4.2. Ouagne *et al.* (2010) measured the through-thickness permeability of a stack of 20 layers of 100 mm diameter discs of 116 g/m^2 flax or 100 g/m^2 glass fibre mats as a function of the fibre volume fraction in continuous saturated flow using silicone oil with a viscosity of 100 mPa.s. Figure 7.2 shows that the permeability decreases with increasing fibre volume fraction as predicted by the Kozeny–Carman equation. The permeability is consistently higher for glass mats than for the flax that suggests the latter fibres have a higher wetted surface area per unit volume. The magnitude of transverse permeability for glass relative to flax mats is in the range 1.6–4.2 and appears to follow a linear relationship between 17% and 40% fibre volume fraction.

Masoodi and Pillai (2011) have suggested that there are two approaches for modelling the liquid composite moulding (LCM) process with natural fibre reinforcements: (i) using the conventional flow model and neglecting the fibre swelling, or (ii) modification of the governing equations to include the fibre-swelling phenomena due to liquid absorption by the reinforcement.



7.2 Transverse continuous saturated permeabilities of flax and glass mat preforms. (*Source*: Reprinted from *Journal of Composite Materials*, 44/(10), P. Ouagne, L. Bizet, C. Baley and J. Bréard, Analysis of the film-stacking processing parameters for PLLA/flax fiber biocomposites, 1201–1215. Copyright (2010), with permission from Sage under the STM Permissions Guidelines and from the authors.)

© Woodhead Publishing Limited, 2014

Their results indicate that the time-dependent permeability model yields more accurate solutions. The time-dependent porosity can be defined by Equation [7.11]:

$$\varepsilon(t) = 1 - (1 - \varepsilon_0)\left(\frac{D_f(t)}{D_{f0}}\right)^2 \quad [7.11]$$

and permeability as a function of time is given by Equation [7.12]:

$$K = K_0\left(\frac{\varepsilon_f}{\varepsilon_{f0}}\right)^3 \frac{(1 - \varepsilon_{f0})}{(1 - \varepsilon_f)} \quad [7.12]$$

where ε is the porosity, D_f is the fibre diameter, K is the permeability, and subscript 0 denotes the initial state.

7.6.7 Shrinkage

Many processes involve the use of elevated temperatures. In common with most materials, the polymer will shrink on cooling due to the coefficient of thermal expansion. For perfectly isotropic shrinkage, the total volumetric shrinkage rate of a material, S_v, can be related to the linear shrinkage rate S_l by Equation [7.13]:

$$S_l = 1 - (1 - S_v)^{1/3} \quad [7.13]$$

Table 7.6 Cure shrinkage of typical commercial resin systems

System	Shrinkage (%)	Source
Robnor PX439N epoxy encapsulating resin	0.3 (Volume)	Robnor resins technical data sheet
Gurit Prime™ 20LV infusion epoxy/extra slow hardener	1.5 (Linear)	Gurit manufacturers product data sheet
Gurit Prime™ 20LV infusion epoxy/fast hardener	1.8 (Linear)	Gurit manufacturers product data sheet
Crystic 491/491PA thixotropic isophthalic polyester resin	*2.6 (Linear)* 7.5 (Volume)	Scott Bader Technical Leaflet TL164. July 1987
Crystic 474PA thixotropic orthophthalic polyester resin (thixotropic pre-accelerated Crystic 198)	*2.8 (Linear)* 8.2 (Volume)	Scott Bader Technical Leaflet TL274, May 2000
Crystic 198 medium viscosity orthophthalic polyester resin	*2.8 (Linear)* 8.2 (Volume)	Scott Bader Technical Leaflet TL273, May 2000

Italicised values calculated using Equation [7.13].

© Woodhead Publishing Limited, 2014

This is often simplified by neglecting higher order terms in the binomial expansion to give $S_l \approx S_v/3$. Changes in volume may also occur due to loss of volatile components and/or crystallisation. For thermoplastic in-mould polymerisation systems, changes may arise due to the chemical reaction. For thermosetting systems, changes are due to the cross-linking (cure) reactions with typical values shown in Table 7.6.

The contractions arising from cure can result in thermal residual stresses, and hence distortion (springback or springforward), surface defects (e.g. sink marks) on the component or in extreme cases matrix cracking.

7.7 Manufacturing techniques for natural fibre-reinforced polymer matrix composites

With the exception of the work reported above, in most cases the manufacturing route used for natural fibre composites is merely incidental to the results obtained with minimal contribution to knowledge of processing.

7.7.1 Injection moulding of short fibre-reinforced thermoplastics

In injection moulding (and extrusion compounding) of fibre-reinforced polymers, the mechanical action of the screws causes significant damage to the fibres (Quijano-Solis *et al*., 2009; Ho *et al.*, 2012). Changes in fibre size and shape distribution arise from the interaction of the fibres with each other, with the polymer and with the machine. Moigne *et al*. (2011) have performed statistical analysis of natural (flax, sisal or wheat straw) fibres in polypropylene. Disaggregation of the fibres led to the presence of particles in all the studied composites. A major factor controlling the heterogeneity of the composites, and the consequent rheological and mechanical behaviour, was the origin of the fibres.

7.7.2 Open mould process (spray and hand lamination)

Spray lamination is unlikely to find application for natural fibre composites as the process is normally configured for continuous roving reinforcement and the costs implicit in spinning short fibres into yarn and the inherent low yarn strength will increase the difficulty of operating the process in a commercial context. Hand lamination has been used to produce natural fibre composites for academic studies. However, the low fibre volume fraction (and consequent resin-rich volumes) and high void fractions lead to low elastic moduli and seriously compromise material strengths.

© Woodhead Publishing Limited, 2014

7.7.3 Liquid composite moulding (LCM) processes

RTM and RIFT are often reported as the manufacturing route for natural fibre reinforced polymer (NFRP) composites (e.g. Table 7.7) but, with the exception of the work reported above, the process is often just incidental to the results obtained with minimal contribution to knowledge of processing.

7.7.4 Compression moulding, including film stacking

The short cycle times in compression moulding of thermoset parts makes the process suitable for low to medium-series automotive parts, such as body panels and doors. Natural fibre SMC materials have been under development for at least 10 years (van Voorn *et al.*, 2001; Lee *et al.*, 2005), but their commercial availability is limited. In such applications as door trim panels and headliners, the weight-saving potential of natural fibre–thermoplastic composites has long been recognised, and their use in commercial products dates from the 1980s. A wide range of fibres, including flax, jute and sisal are used in combination with PP and polyurethane (PU) (Suddell and Evans, 2005). Compression moulding is one of the standard manufacturing methods for laboratory studies of natural fibre composites (e.g. Torres and Cubillas, 2005). For thermoplastic matrices, the quality of the moulded composite depends crucially on the pre-impregnation (typically extrusion) or film stacking (Wambua *et al.*, 2003) stage as the ability of the matrix to flow in the mould tool

Table 7.7 Examples of composite systems reported to be manufactured by LCM processes

Reinforcement	Resin matrix	Process	Reference
Castanhal Textil 300 gsm bidirectional woven jute fabric	Ashland Derakane 411–350 vinylester or unspecified phenolic resin	RTM	Francucci *et al.* (2010)
Abaca, flax, hemp, kenaf and sisal fibres	Only specified as 'base resin'	RIFT II	Symington *et al.* (2008)
One layer of 880 gsm carded quasi-unidirectional technical jute fibres	Sicomin™ SR8100/ SD8822 (100:31 by weight) epoxy resin	RIFT II	Virk *et al.* (2012)
French 78 gsm balanced, degummed 2 × 2 twill-weave silk fabric or long unidirectional bamboo fibres	MC Technics standard novolac epoxy resin	RFI	van Vuure *et al.* (2009)

RFI = Resin Film Infusion (also known as RIFT III).

© Woodhead Publishing Limited, 2014

is limited. Zampaloni *et al.* (2007) achieved some success with a powder pre-impregnation process.

7.7.5 Automated processes

It is unlikely that natural fibre reinforced composites will be manufactured commercially by filament winding, fibre placement or pultrusion as the yarn tensions are likely to exceed the yarn strengths and hence fraying and fracture will add disproportionate cost to these 'low cost' composites. Hutchinson (2011) has reported that aligned hemp and flax fibres with 10% wool fibre have been formulated into yarns by wrap-spinning with poly(ethylene terephthalate) (PET) thread'.

Various authors (Table 7.8) have reported that pultrusion of natural fibre composites is feasible. Peng *et al.* (2012) observed that while the mechanical properties of the pultruded natural fibre composite were promising, scanning electron microscopy (SEM) revealed that the fibre/matrix adhesion was poor and fibres tended to concentrate in the centre of the rod. Hutchinson (2011) further reported that for use in pultrusion, it was necessary to increase the PET wrap density (data not given) and reduce the yarn weight to 1 ktex ('one fifth of the weight of glass roving'). Even so, it was stated: 'the technique needs refining as the greatly increased number of creels needed to feed the yarn into the pultrusion machine could have an adverse effect on product cost'. Mutnuri *et al.* (2010) found that pultrusion worked better with some glass fibres included in the reinforcement.

Table 7.8 Composite systems reported to be manufactured by pultrusion

Reinforcement	Resin matrix	Reference
Hybrids of unidirectional E-glass with either unidirectional hemp yarn or woven hemp fabric	Unsaturated polyester (UPE)	Lackey *et al.* (2008)
Twisted roving jute fibres	Crystic P9901 unsaturated polyester resin	Md Akil *et al.* (2009)
685 gsm flax fabric and hybrid flax/glass rovings	ENVIREZ resin	Mutnuri *et al.* (2010)
70 w/o jute or kenaf roving	Unsaturated polyester resins	Omar *et al.* (2010)
Aligned wool fibres were retained in the yarn by wrap-spinning with polyethylene terephthalate thread	Thermosetting polyester	Hutchinson (2011)
Hybrid 5% wool–30% hemp fibres wound into a strand	65% PU, UPE or vinyl ester (VE) resin	Peng *et al.* (2012)

© Woodhead Publishing Limited, 2014

7.7.6 Hierarchical composites and self-reinforcing cellulose

Nanocellulose coated natural fibres in hierarchical green composites are beyond the scope of this chapter, as are all-cellulose and cellulose whiskers nanocomposites.

7.7.7 Machining, bonding and repair

Special tools and techniques are appropriate for machining aramids (Pinzelli, 1990, 1991) and these may be more relevant for natural fibre composites than traditional machining routes. Techniques include a band saw with a fine tooth blade (550–866 teeth/m) with straight-set or raker-set teeth operated at high speed to stretch and shear the material. To minimise the production of fuzz and to keep the teeth from snagging fibres, the blade is run in reverse (teeth pointing upwards).

7.8 Case studies: automotive, building and construction, and marine applications

The following section briefly reviews the use of NFRP in automotive, building and construction, and marine applications.

7.8.1 Automotive

Ellison and McNaught (2000) undertook a comprehensive study to determine the status of knowledge and commercial usage of natural fibres in the pan-European automotive components industry, and to identify constraints and future market opportunities. In reaction to the European End of Life Vehicle (ELV) directive, the major car manufacturers in Germany have adopted NFRP for various internal components (e.g. polypropylene matrix composites for dashboards and door panels). Holbery and Houston (2006) and Brady and Brady (2007) have provided updates on the status of the use of NFRP in cars.

7.8.2 Infrastructure

Dittenber and GangaRao (2012) have reviewed the potential for use of natural composites in infrastructure and concluded that they have:

- 'impressive specific mechanical properties', but
- 'the main challenges [are] associated with moisture absorption, fire resistance, mechanical properties and durability, variability and manufacturing/processing'.

© Woodhead Publishing Limited, 2014

They believe that such systems would generate economic development in rural/agricultural regions, and that NFRP modular construction for housing could alleviate extreme poverty.

7.8.3 Marine

The Breton NavEcoMat collaboration have produced the 4 m 30 kg Naskapi demonstrator canoe entirely from flax fibre and PLA (polylactic acid) biocomposites using the vacuum-bagged film stacking technique (Anon, 2012b).

7.9 Conclusions

This chapter has reviewed the manufacturing process and associated constraints encountered in bringing together natural fibres and polymer matrices to make composite materials and structures. Many different fibres have been investigated in recent years, and, due to their 'natural' characteristics, there are many stages from growth through to harvest and processing at which variability in properties can be introduced. There is an inherent chemical incompatibility between natural (cellulose-based) fibres and the polymer matrix, and much effort has been devoted to the modification of both constituents to improve the interface and hence achievable mechanical properties.

Of the processes used for thermosetting polymers, compression moulding and LCM (e.g. RTM and resin infusion) are the most widely used for research and applications. The variability of natural fibres extends to their capability of absorbing resin and consequently swelling during processing, and this makes characterisation of permeability more problematic. Natural fibres are widely used, especially in automotive applications, in combination with thermoplastics – here, however, the choice of polymer is limited by the maximum processing temperature at which fibre degradation occurs. A moisture removal stage is considered an essential part of the manufacturing cycle.

7.10 References

D Abraham and R McIlhagger (1996), A review of liquid injection techniques for the manufacture of aerospace composite structures, *Polymers and Polymer Composites*, **4**(6), 437–444.

S Abrate and DA Walton (1992a), Machining of composite materials. Part 1: traditional methods, *Composites Manufacturing*, **3**(2), 75–83.

S Abrate and D Walton (1992b), Machining of composite materials. Part 2: non-traditional methods, *Composites Manufacturing*, **3**(2), 85–94.

S Advani (2000), Chapter 2.23: Liquid impregnation techniques, in R Talreja and J-A Månson (editors): *Comprehensive Composite Materials Encyclopædia, volume 2: Polymer Matrix Composites*, Elsevier, Oxford, pp. 807–844.

© Woodhead Publishing Limited, 2014

SG Advani and ME Sozer (2010), *Process Modeling in Composites Manufacturing*, second edition, CRC Press, Boca Raton, FL. ISBN 978–1-42009082–6.

HM Akil, LW Cheng, ZA Md Ishak, A Abu Bakar and MA Abd Rahman (2009), Water absorption study on pultruded jute fibre reinforced unsaturated polyester composites, *Composites Science and Technology*, **69**(11–12), 1942–1948.

G Akovali (2001), *Handbook of Composite Fabrication*, Woodhead Publishing, Cambridge. ISBN 978–1-85957–263–4.

Anon. (1994), UP Resin Handling Guide, European Organisation of Reinforced Plastics/Composite Materials.

Anon. (2002), Moisture effects and processing information for Nomex® paper, EI du Pont de Nemours and Company report H-52744 05/02, 2002, on-line version accessed 29 June 2012.

Anon. (2004a), Polycaprolactone, http://composite.about.com/library/glossary/p/bldef-p4071.htm, accessed Saturday 27 November 2004 12:26.

Anon. (2004b), Supplier data – polyhydroxybutyrate (PHB) biopolymer, http://www.azom.com/details.asp?ArticleID=1881, accessed Saturday 27 November 2004 12:16.

Anon. (2004c), Supplier data – polyhydroxybutyrate/polyhydroxyvalerate 8% (PHB92/PHV8) biopolymer, http://www.azom.com/details.asp?ArticleID=1954, accessed Saturday 27 November 2004 12:19.

Anon. (2004d), Plastics Produced from Renewable Sources Such as Corn Gaining in Popularity, http://www.azom.com/details.asp?ArticleID=2146, accessed Saturday 27 November 2004 12:21.

Anon. (2005a), DuPont™ Sorona® Technology Platform, http://www.dupont.com/sorona/technologyplatform.html, accessed 15:16 Friday 11 February 2005.

Anon. (2005b), Material Data Sheet Hycail® HM 1011, http://www.hycail.fi/chemicals/DatasheetHM1011.pdf, 06 June 2005, accessed on 10 August 2012.

Anon. (2006a), Natureworks LLC, http://www.natureworkspla.com/, accessed 15:20 on Monday 26 June 2006.

Anon. (2006b), Cereplast Incorporated, The renewable plastic, 2006, accessed 09:55 on 31 October 2009.

Anon. (2008), SCRIMP technology, http://www.tpicomposites.com/?id=9, accessed 13:25 on 10 May 2008.

Anon. (2009), Potatopak Limited, http://www.potatopak.org/home.html, accessed 10:00 on 31 October 2009.

Anon. (2010), Material Safety Data Sheet/Cellulose MSDS, ScienceLab.com, 11/01/2010 accessed at 13:45 on 25 April 2012.

Anon, (2011), EcoTek® Product selection Guide, AOC, Collierville TN, accessed 12:58 on 16 August 2012.

Anon. (2012a), Dupont™ Sorona® 3301 NC010 product information, Dupont, accessed 11:50 on 16 August 2012.

Anon. (2012b), First small watercraft that is compostable at end of life, *JEC Composites Magazine*, March 2012, (71), 24 (webpage requires registration).

KB Armstrong and RT Barrett (1998), *Care and Repair of Advanced Composites*, SAE International, Warrendale PA. ISBN 0–7680–0047–5.

KB Armstrong, G Bevan and WF Cole (2005), *Care and Repair of Advanced Composites* – second edition, SAE International, Warrendale PA. ISBN 0–7680–1062–4.

© Woodhead Publishing Limited, 2014

ASTM (2001), Standard test method for stiffness of nonwoven fabrics using the cantilever test, American Standard ASTM D5732–95(2001 – withdrawn 2008), ASTM International, West Conshohocken PA.

ASTM (2008a), Standard test method for stiffness of fabrics, American Standard ASTM D1388–08, ASTM International, West Conshohocken PA.

ASTM (2008b), Standard test method for stiffness of fabric by the circular bend procedure, American Standard ASTM D4032–08 (07.01), ASTM International, West Conshohocken PA.

BT Åström (1997), *Manufacturing of Polymer Composites*, Chapman & Hall, London. ISBN 0–412–81960–0.

EL Back, E Didriksson and E Inger (1969), Four secondary and the glass transition temperatures of cellulose evaluated by sonic pulse technique, Svenska Traforskningsinstitutet Stockholm report. DTIC AD0712148 <full report not available in the UK>.

A Baker (2012), Bonded repair of composite aircraft structures, *Encyclopedia of Composites* – second edition, John Wiley & Sons, Hoboken, NJ, USA, pp 121–127.

DW Becker (no date), *Tooling for Resin Transfer Moulding*, Wichita State University, Wichita – Kansas.

SW Beckwith (2007), Resin Infusion Technology * Part 1 – Industry highlights * Part 2 – Process definitions and industry variations * Part 3 – A detailed overview of RTM and VIP infusion processing, *SAMPE Journal*, **43**(1), **61** and **43**(3), **46** and **43**(4), 6 and 66–70.

SW Beckwith and CR Hyland (1998), Resin transfer molding: a decade of technology advances, *SAMPE Journal*, **34**(6), 7–19.

W P Benjamin and S W Beckwith (1999), Resin Transfer Moulding, SAMPE Monograph 3, Covina CA. ISBN 0–938–99483–2.

FC Blake (1922), The resistance of packing to fluid flow, Transactions of the American Institute of Chemical Engineers, 14, 415–421.

P Brady and Mike Brady (2007), Automotive composites: which way are we going?, *Reinforced Plastics*, **51**(10), 32–35.

J Bréard, L Bizet, N Montrelay and C Baley (2006), Comparaison des propriétés de composites mats verre/polyester et lin/polyester pour faisabilité par Procédé RTM, *Revue des Composites et des Matériaux Avancés*, **16**(1), 101–113.

JA Brydson (1999), *Plastics Materials* – seventh edition, Butterworth-Heinemann, Oxford. ISBN 0–7506–4132–0.

BSI (1973), Method for the assessment of the drape of fabrics, British Standard BS5058:1973, (confirmation date 1 November 2007), BSI Group, London. ISBN 0–580–07939–2.

BSI (1990), Method for the determination of bending length and flexural rigidity of fabrics, ISBN 0 580 19293 8 replaces Method for the determination of stiffness of cloth, British Standard BS3356 (1961) (1982), withdrawn, BSI Group, London.

BSI (2011), Framework for the assessment of the sustainable use of materials – guidance, British Standard BS8905:2011, BSI Group, London.

P Campaner, D D'Amico, L Longo, C Stifani and A Tarzia (2009), Cardanol-based novolac resins as curing agents of epoxy resins, *Journal of Applied Polymer Science*, **114**(6), 3585–3591.

© Woodhead Publishing Limited, 2014

F Campbell (2003), *Manufacturing Processes For Advanced Composites*, Elsevier, New York. ISBN 978–1-85617–415–2.

PC Carman (1937), Fluid flow through a granular bed, Transactions of the Institution of Chemical Engineers (London), 15, 150–166.

P Chaiyavech and M van Winkle (1959), Styrene-ethylbenzene vapor-liquid equilibria at reduced pressures, *Journal of Chemical and Engineering Data*, **4**(1), 53–56.

PR Ciriscioli and GS Springer (1990), *Smart Autoclave Cure of Composites*, Technomic Publishing, Lancaster PA. ISBN 0–87762–802–5.

JH Clark and JJE Hardy (2004), Towards sustainable chemical manufacturing: polylactic acid – a sustainable polymer?, Chapter 7 in A Azapagic, S Perdan and R Clift (editors), *Sustainable Development in Practice – Case Studies for Engineers and Scientists*, John Wiley & Sons. ISBN 0–470–85609–2.

A Cocquyt (2001), Infusion revisited, *Professional Boatbuilder*, **69**, 132–149.

FN Cogswell (1992), *Thermoplastic Aromatic Polymer Composites*, Butterworth-Heinemann, Oxford. ISBN 0–7506–1986–7. Now Woodhead Publishing, Cambridge. ISBN 978 1 85573 086 1.

S Coll, A Murtagh and C Ó Brádaigh (2004), Resin film infusion of cyclic PBT composites: consolidation analysis, Proceedings of the Eighth International Conference on Flow Processes in Composite Materials, New York (USA), pp 101–106.

S Comas-Cardona (2012), Manufacturing composite structures for automotive applications: robustness challenges, 11th International Conference on Flow Processes in Composite Materials, Auckland NZ, plenary talk.

S Comas-Cardona, F Zhang, S Bickerton, L Tourneier, JM Gan and C Binetruy (2011), Fiber reinforcements: correlating permeability and local spatial fibrous features, Proceedings of ICCM18: The 18th International Conference on Composite Materials, Jeju Island – Korea.

D Cripps, TJ Searle and J Summerscales (2000), Chapter 2.21: Open mould techniques for thermoset composites, In R Talreja and J-A Månson (editors): '*Comprehensive Composite Materials Encyclopædia, volume 2: Polymer Matrix Composites*', Elsevier Science, Oxford, pp 737–761. Set ISBN: 0–08–043720–6. Volume ISBN: 0–08–043725–7.

A Crosky, C Grant and D Kelly (2012), Fiber placements, *Encyclopedia of Composites* – second edition, John Wiley and Sons, pp 945–949.

HPG Darcy (1856), Les Fontaines Publiques de la Ville de Dijon, Damont, Paris.

RS Davé, M Henne, B Louis and P Ermanni (2012), Processing: autoclave modeling, *Encyclopedia of Composites* – second edition, John Wiley and Sons, pp 2443–2454.

RS Davé and AC Loos (1999), *Processing of Composites*, Hanser Publishers, Munich. ISBN 1–56990–226–7.

MJ Davis (2009), Managing micro-voiding of adhesive bonds, Adhesion Associates Pty. Ltd. Report, Redbank – Australia, on-line version accessed 29 June 2012.

NPJ Dissanayake, J Summerscales, SM Grove and MM Singh (2009), Energy use in the production of flax fiber for the reinforcement of composites, *Journal of Natural Fibers*, **6**(4), 331–346.

DB Dittenber and HVS GangaRao (2012), Critical review of recent publications on use of natural composites in infrastructure, *Composites Part A: Applied Science and Manufacturing*, **43**(8), 1419–1429.

F S Dominguez (1987), Unidirectional tape prepregs, In T J Reinhart (editor), '*Engineered Materials Handbook 1 – Composites*', ASM International, Metals Park OH, pp 143–145.

© Woodhead Publishing Limited, 2014

R Dreyer, W Martin and U von Weber (1955), Die sättigungsdampfdrucke von benzol, toluol, äthylbenzol, styrol, cumol und brombenzol zwischen 10 und 760 torr, *Journal für Praktische Chemie*, **1**(5–6), 324–328.

F Ehrig (2012), Molding: polymer injection, *Encyclopedia of Composites* – second edition, John Wiley and Sons, pp 1870–1883.

GC Ellison and R McNaught (2000), The use of natural fibres in nonwoven structures for applications as automotive component substrates, Ministry of Agriculture, Fisheries and Food Research and Development report NF 0309, accessed 10 August 2012 at 11:55.

P Ermanni, C di Fratta and F Trochu (2012), Molding: liquid composite molding (LCM), *Encyclopedia of Composites* – second edition, John Wiley and Sons, pp 1884–1893.

L Fambri, A Pegoretti, R Fenner, D Incardona S and C Migliaresi (1997), Biodegradable fibers of poly(L-lactic acid) produced by melt spinning, *Polymer*, **38**(1), 79–85.

CA Farnfield and PJ Alvey (1978), *Textile Terms and Definitions* – seventh edition, The Textile Institute, Manchester.

FM Foley and T Gutowski (1991), The effect of process variables on permeability in the flexible resin transfer molding (FRTM) process. In: Proceedings of the 23rd international SAMPE Technical Conference, Kiamesha Lake – USA, pp 326–339.

G Francucci, ES Rodríguez and A Vázquez (2010), Study of saturated and unsaturated permeability in natural fiber fabrics, *Composites Part A: Applied Science and Manufacturing*, **41**(1), 16–21.

JM Gan, S Bickerton and M Battley (2012), Quantifying variability within glass fibre reinforcements using an automated optical method, *Composites Part A: Applied Science and Manufacturing*, **43**(8), 1169–1176.

J George, MS Sreekala and S Thomas (2001), A review on interface modification and characterization of natural fiber reinforced plastic composites, *Polymer Engineering and Science*, **41**(9), 1471–1485.

M Giordano, V Antonucci and A Langella (2012), Processing: autoclave, *Encyclopedia of Composites* – second edition, John Wiley and Sons, pp 2437–2442.

WB Goldsworthy (2012), Pulforming, *Encyclopedia of Composites* – second edition, John Wiley and Sons, pp 2542–2544.

S Gordon and MT Hillery (2003), A review of the machining of composite materials, *Proceedings of IMechE Part L: Journal of Materials Design and Applications*, **L217**(1), 35–45.

PR Griffin, SM Grove, P Russell, D Short, J Summerscales, FJ Guild and E Taylor (1995), The effect of reinforcement architecture on the long-range flow in fibrous reinforcements, Appendix 1, *Composites Manufacturing*, **6**(3–4), 221–235.

S Grove (2012), Manufacture of polymer composites, *Encyclopedia of Composites* – second edition, John Wiley and Sons, pp 1506–1525.

B Gupta, N Revagade and J Hilborn (2007), Poly(lactic acid) fiber: an overview, *Progress in Polymer Science*, **32**(4), 455–482.

TG Gutowski (1997), *Advanced Composites Manufacturing*, John Wiley, New York. ISBN 0–471–15301-x.

PH Henna, MR Kessler and RC Larock (2008), Fabrication and properties of vegetable-oil-based glass fiber composites by ring-opening metathesis polymerization, *Macromolecular Materials and Engineering*, **293**(12), 979–990.

M-P Ho, H Wang, J-H Lee, C-K Ho, K-T Lau, J Leng and D Hui (2012), Critical factors on manufacturing processes of natural fibre composites, *Composites Part B: Engineering*, December 2012, **43**(8), 3549–3562.

© Woodhead Publishing Limited, 2014

SV Hoa (2009), *Principles of the Manufacturing of Composite Materials*, DesTech Publications, Lancaster PA, USA. ISBN 978–1-932078–26–8.

J Holbery and D Houston (2006), Natural-fiber-reinforced polymer composites in automotive applications, *JOM Journal of the Minerals, Metals and Materials Society*, **58**(11), 80–86.

J Hutchinson (2011), Building in natural strengths, *Materials World*, **19**(9), 27–29.

L Incarnato and L di Maio (2012), Polymeric extrusion, *Encyclopedia of Composites* – second edition, John Wiley and Sons, pp 2225–2243.

AI Isayev (2012), Molding: compression, *Encyclopedia of Composites* – second edition, John Wiley and Sons, pp 1853–1869.

ISO (2000), Environmental Management – Life Cycle Assessment – examples of applications of ISO 14041 to goal and scope definition and inventory analysis, Technical Report ISO/TR 14049:2000: International Organization for Standardization, Geneva. ISBN 0 580 36007 5. Replaced by Environmental management – Life cycle assessment – Illustrative examples on how to apply ISO 14044 to goal and scope definition and inventory analysis, Technical Report ISO/TR 14049:2012.

ISO (2002a), Small craft – Hull construction and scantlings – Part 4: Workshop and manufacturing, incorporating Corrigendum no. 1, International Standard BS EN ISO 12215–4:2002, International Organization for Standardization, Geneva. ISBN 0 580 39873 0.

ISO (2002b), Environmental Management – Life Cycle Assessment – data documentation format, International Standard ISO/TS 14048:2002, International Organization for Standardization, Geneva.

ISO (2003), Standard, Technical Report: Environmental Management – Life Cycle Assessment – examples of application of ISO 14042, Technical Report ISO/TR 14047:2003, International Organization for Standardization, Geneva. ISBN 0 580 43112 6. Replaced by Environmental management – Life cycle assessment – Illustrative examples on how to apply ISO 14044 to impact assessment situations, Technical Report ISO/TR14047:2012

ISO (2006a), Environmental Management – Life Cycle Assessment – principles and frameworks, International Standard ISO 14040:2006, International Organization for Standardization, Geneva.

ISO (2006b), Environmental Management – Life Cycle Assessment – requirements and guidelines, International Standard ISO 14044:2006, International Organization for Standardization, Geneva.

J Juntaro, M Pommet, G Kalinka, A Mantalaris, MSP Shaffer and A Bismarck (2008), Creating hierarchical structures in renewable composites by attaching bacterial cellulose onto sisal fibers, *Advanced Materials*, **20**(16), 3122–3126.

MM Kabir, H Wang, KT Lau and F Cardona (2012), Chemical treatments on plant-based natural fibre reinforced polymer composites: an overview, *Composites Part B: Engineering*, **43**(7), 2883–2892.

S Kalia, BS Kaith and I Kaur (2009), Pretreatments of natural fibers and their application as reinforcing material in polymer composites – a review. *Polymer Engineering and Science*, **49**(7), 1253–72.

MR Kamal and S Sourour (1973), Kinetics and thermal characterization of thermoset cure, *Polymer Engineering and Science*, **13**(1), 59–64.

Kaye and Laby Tables of Chemical and Physical Constants (2007), http://www.kayelaby.npl.co.uk/general_physics/2_2/2_2_3.html, accessed 15 November 2007.

© Woodhead Publishing Limited, 2014

S Koussios (2004), *Filament Winding: A Unified Approach*, IOS Press, Lansdale PA. ISBN 978–90–407–2551–7.

S Koussios and A Beukers (2012), Filament winding: design, materials, structures and manufacturing processes, *Encyclopedia of Composites* – second edition, John Wiley and Sons, pp 1011–1026.

J Kozeny (1927), Uber die kapillare Leitung des Wassers in Boden, Sitzungsberichte Akademie der Wissenschaft Wien Math-naturw, 136(kl.Abt.IIa), 271–306.

T M Kruckenberg and R Paton (editors) (1998), *Resin Transfer Moulding for Aerospace Structures*, Kluwer Academic Publishers, Dordrecht NL. ISBN 0–412–73150–9.

J Kubát and C Pattyranie (1967), Transition in cellulose in the vicinity of -30°C, *Nature*, **215**(5099), 390–391.

E Lackey, JG Vaughan, K Inamdar and B Hancock (2008), Statistical characterization of pultruded composites with natural fiber reinforcements – Part A: fabrication, *Journal of Natural Fibers*, **4**(4), 73–87.

EC Lee, CM Flanigan, KA Williams, DF Mielewski and DQ Houston (2005), Hemp fibre reinforced sheet moulding compounds for automotive applications, 5th Annual SPE Automotive Composites Conference, Troy MI. http://speautomotive.com/SPEA_CD/SPEA2005/pdf/h/h2.pdf, accessed 12:30 on 14 August 2012.

T Lenau (2004a), CPLA – polylactide aliphatic copolymer, http://www.designinsite.dk/htmsider/m0953.htm, accessed 12:04 on Saturday 27 November 2004.

T Lenau (2004b), PCL – polycaprolactone, http://www.designinsite.dk/htmsider/m0954.htm, accessed Saturday 27 November 2004 12:07.

T Lenau (2004c), PHAs – polyhydroxyalkanoates, http://www.designinsite.dk/htmsider/m0955.htm, accessed Saturday 27 November 2004 12:11.

T Lenau (2004d), PLA – polylactide, http://www.designinsite.dk/htmsider/m0956.htm, accessed Saturday 27 November 2004 12:00.

X Li, HG Tabil and S Panigrahi (2007), Chemical treatments of natural fibre for use in natural fibre-reinforced composites: a review, *Journal of Polymers and the Environment*, **15**(1), 25–33.

L-T Lim, R Auras and M Rubino (2008), Processing technologies for poly(lactic acid), *Progress in Polymer Science*, **33**(8), 820–852.

H Liu, F Xie, L Yu, L Chen and L Li (2009), Thermal processing of starch-based polymers, *Progress in Polymer Science*, **34**(12), 1348–1368.

B Louis and P Ermanni (2012), Out-of-autoclave prepreg processing, *Encyclopedia of Composites* – second edition, John Wiley and Sons, 2052–2058.

TS Lundstrom, BR Gebart, and CY Lundemo (1992), Void formation in RTM, In Proceedings of the 47th Annual Conference, Composites Institute, The Society of the Plastics Industry, pp 1–5.

TS Lundstrom, BR Gebart and CY Lundemo (1993), Void formation in RTM, *Journal of Reinforced Plastics and Composites*, **12**, 1339–1349.

TS Lundström, R Stenberg, R Bergström, H Partanen and PA Birkeland (2000), In-plane permeability measurements: a nordic round-robin study, *Composites Part A: Applied Science and Technology*, **31**(1), 29–43.

T Maha and G Songa (2010), An investigation of the assessment of fabric drape using three-dimensional body scanning, *Journal of the Textile Institute*, **101**(4), 324–335.

T Mannermaa (2011), Bio based Envirez polyester resins – properties and applications, Ashland Performance Materials, 2011, accessed at 13:33 on 10 August 2012.

© Woodhead Publishing Limited, 2014

G Marsh (2002), Resin film infusion – composites cost reducer, Reinforced Plastics, 46(2), 44–49.

R Masoodi and KM Pillai (2011), Modeling the processing of natural fiber composites made using liquid composite molding, Chapter 3 in S Pilla (editor): *Handbook of Bioplastics and Biocomposites Engineering Applications*, Scrivener Publishing LLC/Wiley, 43–73. ISBN 978–0-470–62607–8.

PB Maurus and CC Kaeding (2004), Bioabsorbable implant material review, *Operative Techniques in Sports Medicine*, **12**(3), 158–160.

SK Mazumdar (2002), *Composites Manufacturing: Materials, Product and Process Engineering*, CRC Press, Boca Raton FL. ISBN 0–8493–0585–3.

S McBeath and B O'Rourke (2009), *Competition Car Composites: A Practical Handbook* – second edition, Haynes, Sparkford UK. ISBN 978–1-84425–701–0.

RW Meyer (1985), *Handbook of Pultrusion Technology*, Chapman & Hall, London. ISBN 0–412–00761–4.

N Le Moigne, M van den Oever and T Budtova (2011), A statistical analysis of fibre size and shape distribution after compounding in composites reinforced by natural fibres, *Composites Part A: Applied Science and Manufacturing*, **42**(10), 1542–1550

B Mutnuri, CJ Aktas, J Marriott, M Bilec and H GangaRao (2010), Natural fiber reinforced pultruded composites, Proceedings of Composites 2010, Las Vegas NV.

M Munro (1988), A review of manufacturing of fiber composite components by filament winding, *Polymer Composites*, **9**(5), 352–359.

GC Newell, RO Buckingham and K Khodabandehloo (1996), The automated manufacture of prepreg broadgoods components – a review of literature, *Composites Part A: Applied Science and Manufacturing*, **27**(3), 211–217.

K Noakes (2008), *Successful Composite Techniques: A Practical Introduction to the Use of Modern Composite Materials*, fourth edition, The Crowood Press, Marlborough UK. ISBN 978–1-84797–054–1.

MF Omar, H Md Akil, ZA Ahmad, AAM Mazukia and T Yokoyama (2010), Dynamic properties of pultruded natural fibre reinforced composites using Split Hopkinson Pressure Bar technique, *Materials & Design*, **31**(9), 4209–4218.

P Ouagne, L Bizet, C Baley and J Bréard (2010), Analysis of the film-stacking processing parameters for PLLA/flax fiber biocomposites, *Journal of Composite Materials*, **44**(10), 1201–1215.

R S Parnas (2000), *Liquid Composite Moulding*, Hanser Gardner Publications, Cincinnati OH, USA. ISBN 1–569–90287–9.

NRL Pearce, FJ Guild and J Summerscales (1998), An investigation into the effects of fabric architecture on the processing and properties of fibre reinforced composites produced by resin transfer moulding, *Composites Part A: Applied Science and Manufacturing*, **A29**(1), 19–27.

X Peng, M Fan, J Hartley and M Al-Zubaidy (2012), Properties of natural fibre composites made by pultrusion process, *Journal of Composite Materials*, **46**(2), 237–246.

ST Peters, WD Humphrey and RF Foral (1999), *Filament Winding Composite Structure Fabrication* – second edition, SAMPE, Covina CA. ISBN 0–938994–81–6.

ST Peters (editor) (2011), *Composite Filament Winding*, ASM International, Materials Park OH. ISBN 978–1–61503–852–7.

© Woodhead Publishing Limited, 2014

KL Pickering, Y Li, RL Farrell, M Lay (2007), Interfacial modification of hemp fibre reinforced composites using fungal and alkali treatment, *Journal of Biobased Materials and Bioenergy*, **1**(1), 109–117.

R Pinzelli (1990), Cutting and machining of composites based on aramid fibres, *Composites Plastiques Renforces Fibres de Verre*, **30**(4),17–23 (in French) and 23–25 (in English). ISSN 0754–0876.

R Pinzelli (1991), Cutting and machining of composite materials based on aramid fibres, DuPont report H-23157(1M).

K Potter (1997), *Resin Transfer Moulding*, Chapman & Hall, London. ISBN 0–412–72570–3.

C Quijano-Solis, N Yan and Y Zhang (2009), Effect of mixing conditions and initial fiber morphology on fiber dimensions after processing, *Composites Part A: Applied Science and Manufacturing*, **40**(4), 351–358.

M Revellino, L Saggese and E Gaiero (2000), Chapter 2.22: Compression molding of SMCs, In R Talreja and J-A Månson (editors): '*Comprehensive Composite Materials Encyclopædia, volume 2: Polymer Matrix Composites*', Elsevier Science, Oxford, pp 763–805. Set ISBN 0–08–043720–6. Volume ISBN 0–08–043725–7.

GM Robinson, MJ Jackson and MD Whitfield (2007), A review of machining theory and tool wear with a view to developing micro and nano machining processes, *Journal of Materials Science*, **42**(6), 2002–2015.

F Roig, E Dantras, J Dandurand and C Lacabanne (2011), Influence of hydrogen bonds on glass transition and dielectric relaxations of cellulose, *Journal of Physics D: Applied Physics*, **44**(4), 045403 (8 pp).

MB Roller (1975), Characterization of the time-temperature-viscosity behaviour of curing B-staged epoxy resin, *Polymer Engineering and Science*, **15**(6), 406–414.

C D Rudd, A C Long, K N Kendall and C G E Mangin (1997), *Liquid Moulding Technologies*, Woodhead Publishing, Cambridge. ISBN 1–85573–242–4.

AB Sadat (2012), Machining of composites, *Encyclopedia of Composites* – second edition, John Wiley and Sons, pp 1497–1505.

JC Seferis (2000), Chapter 2.20: Prepregging and autoclaving, in R Talreja and J-A Månson (editors): *Comprehensive Composite Materials Encyclopædia, volume 2: Polymer Matrix Composites*, Elsevier, Oxford, pp 701–736.

VS Sharma, M Dogra and NM Suri (2008), Advances in the turning process for productivity improvement – a review, *Proceedings of the Institution of Mechanical Engineers, Part B: Journal of Engineering Manufacture*, **222**(11), 1417–1442.

JY Sheikh-Ahmad and J Paulo Davim (2012), Cutting and machining of polymer composites, *Encyclopedia of Composites* – second edition, John Wiley and Sons, pp 648–657.

A Shojaei, F Trochu F, SR Ghaffarian, SMH Karimian and L Lessard (2004), An experimental study of saturated and unsaturated permeabilities in resin transfer molding based on unidirectional flow measurements. *Journal of Reinforced Plastics and Composites*, **23**(14), 1515–1536.

FC Smith (1999), The current status of resin infusion as an enabling technology for toughened aerospace structures, *Materials Technology*, **14**(2), 71–80.

TF Starr (2000), *Pultrusion for Engineers*, Woodhead, Cambridge. ISBN 1–85573–425–7.

LG Stringer (1989), Optimization of the wet lay-up/vacuum bag process for the fabrication of carbon fibre epoxy composites with high fibre fraction and low void content, *Composites*, **20**(5), 441–452.

© Woodhead Publishing Limited, 2014

AB Strong (2008), *Fundamentals of Composites Manufacturing: Materials, Methods and Applications*, Society of Manufacturing Engineers, Dearborn. ISBN 978–0–87263–854–9.

BC Suddell and WJ Evans (2005), Natural fiber composites in automotive applications, in AK Mohanty, M Misra and LT Drzal (editors): *Natural Fibers, Biopolymers and their BioComposites*, CRC Press, Boca Raton FL, USA, pp 231–259. ISBN 978–0-8493–1741–5.

J Summerscales (2003), Chapter 2: In-process monitoring for control of closed-mould techniques for the manufacture of thermosetting matrix composites, pages 57–101 in GO Shonaike and SG Advani (editors): *Advanced Polymeric Materials – Structure Property Relationships*, CRC Press LLC, Boca Raton FL. ISBN 1–58716–047–1.

J Summerscales (2004), The effect of permeant on the measured permeability of a reinforcement, 7th International Conference on Flow Processes in Composite Materials (FPCM-7), University of Delaware, Newark, pp 471–476.

J Summerscales (2012), Resin Infusion Under Flexible Tooling (RIFT), *Encyclopedia of Composites* – second edition, John Wiley and Sons, pp 2648–2658.

J Summerscales and TJ Searle (2005), Low pressure (vacuum infusion) techniques for moulding large composite structures, *Proc IMechE Part L – Journal of Materials: Design and Applications*, **L219**(1), 45–58.

J Summerscales, N Dissanayake, W Hall and AS Virk (2010a), A review of bast fibres and their composites. Part 1: fibres as reinforcements, *Composites Part A: Applied Science and Manufacturing*, **41**(10), 1329–1335.

J Summerscales, N Dissanayake, AS Virk and W Hall (2010b), A review of bast fibres and their composites. Part 2: composites, *Composites Part A: Applied Science and Manufacturing*, **41**(10), 1336–1344.

J Summerscales, AS Virk and W Hall (2013), A review of bast fibres and their composites. Part 3: modelling, *Composites Part A: Applied Science and Manufacturing*, **44**(1), 132–139.

MC Symington, OS David-West, WM Banks, JL Thomason and RA Pethrick (2008), Vacuum infusion of natural fibre composites for structural applications, 13th European Conference on Composite Materials (ECCM 13), Stockholm.

L Szcześniak, A Rachocki and J Tritt-Goc (2008), Glass transition temperature and thermal decomposition of cellulose powder, *Cellulose*, **15**(3), 445–451.

FG Torrres and ML Cubillas (2005), Test method: study of the interfacial properties of natural fibre reinforced polyethylene, *Polymer Testing*, **24**(6), 694–698.

K van Harten (1993), 'Production by resin transfer moulding', in R A Shenoi and J F Wellicome (editors): *Composite Materials in Maritime Structures*, Cambridge University Press, Cambridge, Chapter 4, 86–126.

B van Voorn, HHG Smit, RJ Sinke and B de Klerk (2001), Natural fibre reinforced sheet moulding compound, *Composites Part A: Applied Science and Manufacturing*, **32**(9), 1271–1279.

AW van Vuure, J Vanderbeke, L Osorio, E Trujillo, C Fuentes and I Verpoest (2009), Natural fibre composites: tough (silk) and strong (bamboo), Proceedings of ICCM17: The 17th International Conference on Composite Materials, Edinburgh – Scotland.

A Vázquez and M Escobar (2012), Pultrusion, *Encyclopedia of Composites* – second edition, John Wiley and Sons, pp 2545–2560.

© Woodhead Publishing Limited, 2014

AS Virk, W Hall and J Summerscales (2012), Modulus and strength prediction for natural fibre composites, *Materials Science and Technology*, **28**(7), 864–871.

MD Wakeman and CD Rudd (2000), Chapter 2.27: Compression molding of thermoplastic composites, In R Talreja and J-A Månson (editors): '*Comprehensive Composite Materials Encyclopædia, volume 2: Polymer Matrix Composites*', Elsevier Science, Oxford, pp 915–963. Set ISBN 0–08–043720–6. Volume ISBN 0–08–043725–7.

P Wambua, J Ivens and I Verpoest (2003), Natural fibres: can they replace glass in fibre reinforced plastics?, *Composites Science and Technology*, **63**(9), 1259–1264.

RP White (1974), Time-temperature superpositioning of viscosity-time profiles of three high temperature epoxy resins, *Polymer Engineering and Science*, **14**(1), 50–57.

CD Williams, J Summerscales and SM Grove (1996), Resin infusion under flexible tooling (RIFT): a review, *Composites Part A: Applied Science and Manufacturing*, **A27**(7), 517–524.

O Wolf, M Crank, M Patel, F Marscheider-Weidemann, J Schleich, B Hüsing and G Angere (2005), Techno-economic feasibility of large-scale production of bio-based polymers in Europe, European Commission Director-General Joint Research Centre Technical Report EUR 22103 EN. ISBN 92–79–01230–4. http://ftp.jrc.es/EURdoc/eur22103en.pdf accessed on 17 August 2011.

World Commission on Environment and Development (1987), *Our Common Future* (The Brundtland Report), Oxford Paperbacks, Oxford. ISBN 0–19–282080-X.

F Xie, PJ Halley and L Avérous (2012), Rheology to understand and optimize processibility, structures and properties of starch polymeric materials, *Progress in Polymer Science*, **37**(4), 595–623.

X Yuan, AFT Mak, KW Kwok, BKO Yung and K Yao (2001), Characterization of poly(L-lactic acid) fibers produced by melt spinning, *Journal of Applied Polymer Science*, **81**(1), 251–260.

NE Zafeiropoulos (editor) (2011), *Interface Engineering of Natural Fibre Composites for Maximum Performance*, Woodhead Publishing, Cambridge. ISBN 978–1–84569–742–6.

M Zampaloni, F Pourboghrat, SA Yankovich, BN Rodgers, J Moore, LT Drzal, AK Mohanty and M Misra (2007), Kenaf natural fiber reinforced polypropylene composites: A discussion on manufacturing problems and solutions, *Composites Part A: Applied Science and Manufacturing*, **38**(6), 1569–1580.

F Zhang, S Comas-Cardona and C Binetruy (2012a), Statistical modelling of in-plane permeability of non-woven random fibrous reinforcement, *Composites Science and Technology*, **72**(12), 1368–1379.

F Zhang, S Comas-Cardona and C Binetruy (2012b), Variability of fibrous materials: experimental and theoretical study, Proceedings 11th International Conference on Flow Processes in Composite Materials, Auckland NZ, July 2012, pp 521–528.

© Woodhead Publishing Limited, 2014

8

Compression and injection molding techniques for natural fiber composites

Y. W. LEONG, Institute of Materials Research and Engineering, Republic of Singapore and S. THITITHANASARN, K. YAMADA and H. HAMADA, Kyoto Institute of Technology, Japan

DOI: 10.1533/9780857099228.2.216

Abstract: The forming of a natural fiber composite part, particularly when it involves intricate geometries, is often one of most difficult challenges faced by manufacturers. The intrinsic properties of natural fibers, such as the hygroscopicity and heat sensitivity, further complicate this process. This chapter outlines the challenges faced during compression and injection molding, which are two of the most frequently used techniques for forming natural fiber composites. Several emerging technologies – such as micro-braiding, long fiber pellet and textile insert molding – that are tailored for natural fiber composite forming will be introduced. A strategy to enhance the thermal resistance of natural fibers so that they can be incorporated into high temperature engineering thermoplastics is also discussed.

Key words: micro-braiding, enhancing thermal resistance of natural fiber, textile insert molding, long fiber pellet.

8.1 Introduction

The molding of natural fiber composites can be a challenging task since the handling and intrinsic properties of natural fibers such as jute, hemp, and kenaf are very different from those of inorganic fibers, such as glass, aramid, or carbon fibers. The main considerations when processing natural fibers are their hygroscopic behavior and low resistance to high temperature, which has effectively limited the choices of resins that could be used as the matrix. Fortunately, the techniques and equipment for forming natural fiber composites are relatively similar to those used for conventional inorganic fiber composites, which makes it easier for industries to adopt natural fiber composites for various applications.

The method for processing natural fiber composites is mainly dependent on the type of matrix resins but, interestingly, the processing conditions usually depend on the type of natural fiber used. Low viscosity thermosetting resins

© Woodhead Publishing Limited, 2014

that can be cured at ambient temperatures are thought to be a preferable choice as the matrix since they can easily impregnate the natural fibers and do not cause any damage related to thermal degradation. Resin transfer molding (RTM), vacuum assisted resin transfer molding (VaRTM), and sheet molding compound (SMC) are some of the most common techniques used for impregnating and forming thermosetting resin-based natural fiber composites. The natural fibers used can be in the form of mats containing randomly oriented fibers, or of fabrics woven from continuous natural fiber strands. It should be noted, however, that these techniques are very time consuming and costly, since curing times can vary between 2 and 24 h. Furthermore, most molded parts would require post-molding processes, such as trimming and grinding of flash, which further contributes to the cost. Therefore, these processes are normally applied to fabricate large moldings, such as structural columns, wall panels, and some automotive components. The long cycle times and high cost in processing thermosetting composites may have driven much of the research effort to develop natural fiber composites from thermoplastic resins as matrices.

Thermoplastic resin-based composites can be produced at a much shorter cycle time (in the order of minutes), since the materials would become easily formable upon heating and quickly solidify upon rapid cooling. Natural fibers are typically infused with thermoplastic resins via the compounding process. During this process, short natural fibers and resins are fed through separate hoppers and conveyed into a heated barrel with a screw. The resin will melt to combine with the fibers before being extruded through a die to form a strand, which will then be cut into small pellets. These pellets are then used to form products via the injection or compression molding techniques. It is important to understand that these processes will involve heating of the material above the melting point of the resins, which is typically above 130°C. Since the degradation temperature of most natural fibers is in the range of 130–220°C, care should be taken to minimize the exposure of the natural fibers to the heat, i.e. reduce processing temperature or shorten residence time of the natural fibers in the barrel. The thermal decomposition of the fibers produces volatiles and the obtained composites exhibit low mechanical properties.[1–7] Another consideration that could substantially aggravate degradation is the moisture content in the fibers during processing. The moisture content of natural fibers is typically between 6% and 12% by weight, and this has to be reduced to less than 3% in order to obtain good quality moldings.

In spite of the shortcomings in terms of processability and compatibility with thermoplastic resins, natural fiber is still desirable as a key reinforcement component due to its abundance, low price, sustainability, biodegradability, and low density.[8–12] The aim of this chapter is to demonstrate the feasibility of compression and injection molding techniques in the fabrication of

© Woodhead Publishing Limited, 2014

thermoplastic natural fiber composites, while highlighting common as well as non-trivial problems affecting these processes. The contents of this chapter will revolve around the following topics:

1. Emerging compression and injection molding technologies in the production of natural fiber composites
2. Processing natural fiber composites at high temperatures

8.2 Emerging compression and injection molding technologies in the production of natural fiber composites

Compression and injection molding are two of the most common and preferred technologies for mass production of plastics and composites parts due to their high precision and fast cycle times. As part designs become more complex and added functionalities are desired in products, the molding technologies would need to be upgraded in order to also cater for high mix low volume productions. The usage of unique materials such as natural fiber composites would also need specialized processing and molding techniques in order to maximize the potential of these materials. The following are some examples of techniques that were customized to improve productivity and optimize performance of natural fiber composites.

8.2.1 Compression molding of thermoplastic natural fiber composites

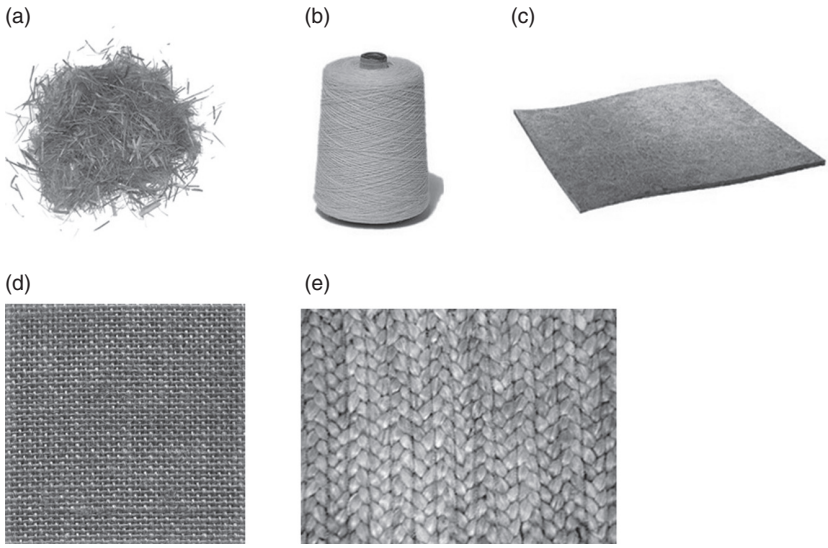
In recent years, many researchers, as well as industries, have shown interest in thermoplastic composites reinforced with natural fibers, such as jute, sisal, and hemp, as they can potentially serve as cheap reinforcement of polymers if compounded into polymers without decomposition. Natural fiber reinforced thermoplastic composites have been used widely, because the combination between natural fiber and thermoplastic resins can mass-produce high-performance, low-density composites. The main constraint of natural fiber reinforced thermoplastic composites has been the limitation of choice of polymer matrix. This is because natural fibers degrade at temperatures below the processing temperatures of most engineering thermoplastics such as polycarbonate (PC) and most polyamides (PA). As such, the polymers currently in use as matrices for natural fiber filled composites are those with low-to-moderate processing temperatures.[13–25] These comprise thermoplastic polymers such as polypropylene (PP), polyethylene (PE), poly(vinyl chloride) (PVC), and polystyrene (PS). There is also the problem of poor compatibility between the predominantly hydrophobic thermoplastic

© Woodhead Publishing Limited, 2014

polymers and the hydrophilic cellulosic natural fibers.[26] Due to the poor interfacial interaction leading to poor bonding between the hydrophobic thermoplastics and natural fibers, polymer-fiber bonding is often improved by the use of coupling agents and fiber surface treatments.[27,28]

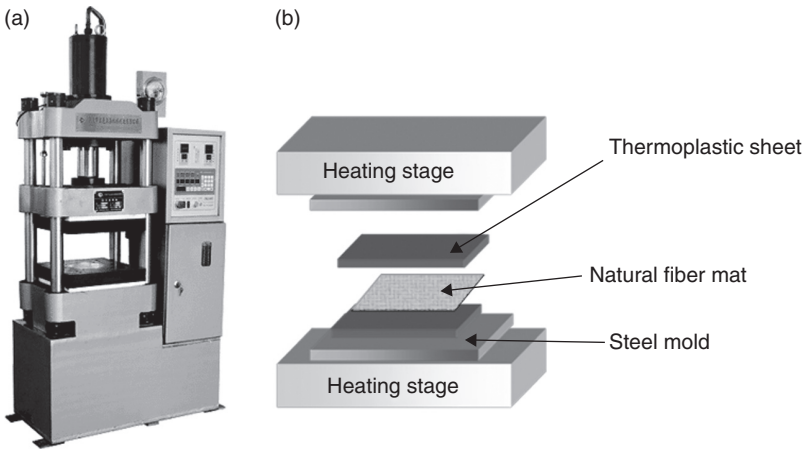
The molding technique for thermoplastic natural fiber composites is usually chosen based on the size of the molded part as well as on the form and orientation required of the natural fibers. Natural fibers can be obtained as short or long fibers that can be made into more advanced forms such as continuous strands, braidings, randomly oriented mats, woven textiles, and fabrics. The various forms of natural fibers are illustrated in Fig. 8.1. The injection molding process is typically limited to fabrication of parts containing short to intermediate length fibers, and these lengths will depend on the length of the pellets produced during the compounding process. The compression molding, on the other hand, is a more versatile technique that can be used for all forms of fibers, although the forming process would require longer cycle times when compared with injection molding. It is therefore reasonable that the industry has recently developed the injection–compression molding technology in order to exploit the benefits from both molding processes.

A typical compression molding machine comprises top and bottom heating stages that can be heated and cooled to a desired temperature, as shown in Fig. 8.2. Natural fiber mats can be sandwiched or laminated between thermoplastic sheets and pre-heated at a pre-determined temperature and time.



8.1 Various forms of natural fibers: (a) short fibers; (b) continuous fiber yarn; (c) randomly oriented fiber mat; (d) woven textile; (e) braided textile.

© Woodhead Publishing Limited, 2014

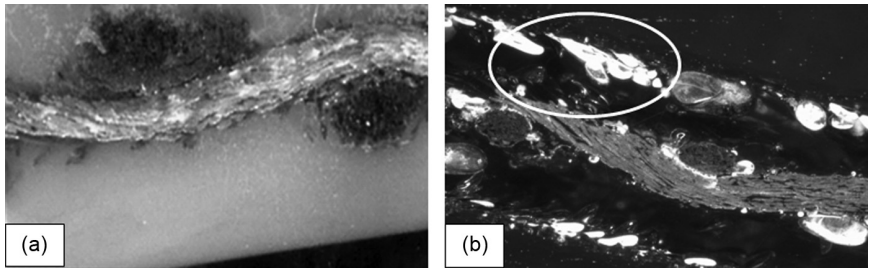


8.2 An example of a compression molding machine (a), and a schematic representative of the lamination process to fabricate natural fiber composites through compression molding (b).

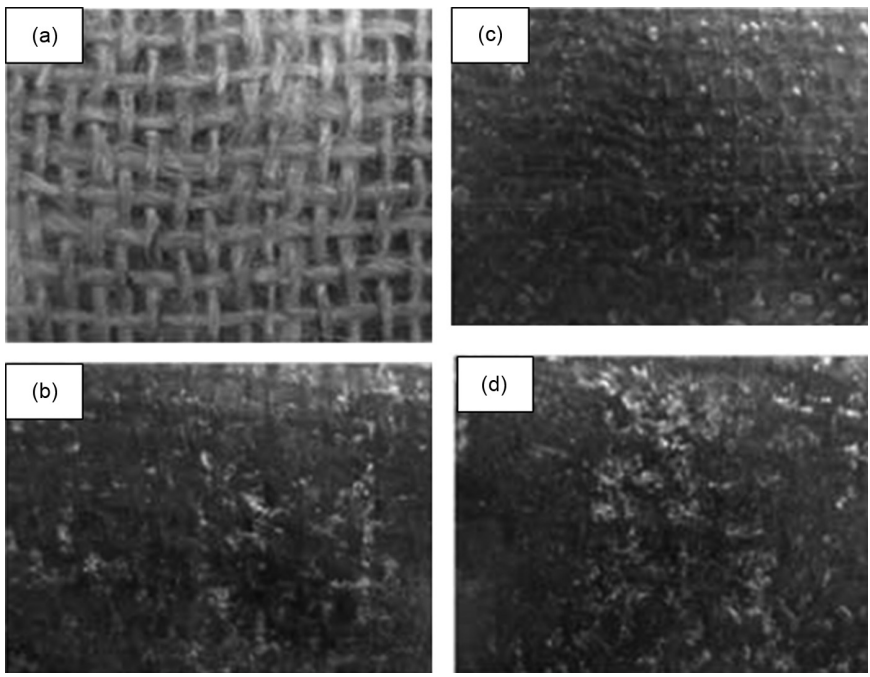
Pre-heating is an important step to sufficiently melt the thermoplastic sheet in order to prevent uneven resin flow or tearing of the natural fiber mat due to excessive shear forces during compression. The pre-heating is followed by compression of the materials at a certain pressure to allow the resin to infuse into the natural fiber mats. A balance between temperature, pressure, and molding time during the compression stage is essential to optimize impregnation of the resin into the fibers while reducing thermal degradation of both the fibers and resin. The mold is subsequently cooled by flowing chilled water into the heating stages while the pressure on the materials is maintained. Once the molded part has sufficiently cooled and solidified, it will be de-molded, and excess resin on the sides of the moldings can then be removed by grinding or trimming.

It is important that the natural fibers are thoroughly dried so that the moisture content is less than 3 wt.% prior to the pre-heating stage. Since the moisture absorption rate is very high in natural fibers, it is suggested that the fibers are directly transferred from the drying oven to the compression mold with minimal exposure to the ambient conditions (less than 10 min transfer time is preferable). The effects of moisture in the natural fibers on the appearance of the moldings can be observed in Fig. 8.3. Since the molding temperature is typically higher than 100°C, any residual moisture in the natural fibers will immediately evaporate to form bubbles and voids inside the composites while in some cases, blisters would appear on the surface of the moldings. Degradation of polar matrix resins such as polyesters is also possible since they are sensitive to hydrolytic degradation. In most cases, the degradation of the resins will cause the color to change into a yellowish

© Woodhead Publishing Limited, 2014



8.3 (a) Composites molded after removal of moisture from natural fibers; (b) formation of voids and bubbles (in circle) when composites are molded without prior drying of natural fibers.

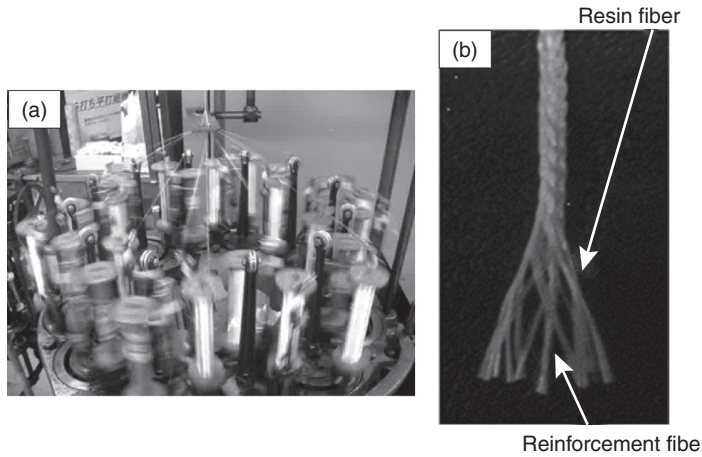


8.4 Effect of molding time when the jute/poly(ethylene terephthalate) (PET) composites were molded at 260°C: (a) 1.5 min., (b) 3 min., (c) 4.5 min., (d) 6 min.

tone, while the natural fibers turn dark due to the emission of furanoic compounds, as shown in Fig. 8.4.

The main advantage of compression molding is the ability to use any forms of natural fibers as reinforcements. An interesting advancement would be the use of braided natural fiber yarns produced by a process termed 'micro-braiding' for the fabrication of natural fiber composites. Micro-braided

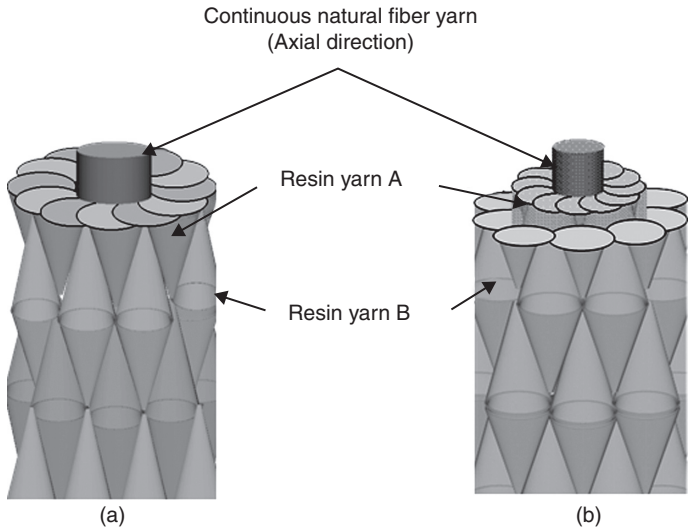
© Woodhead Publishing Limited, 2014



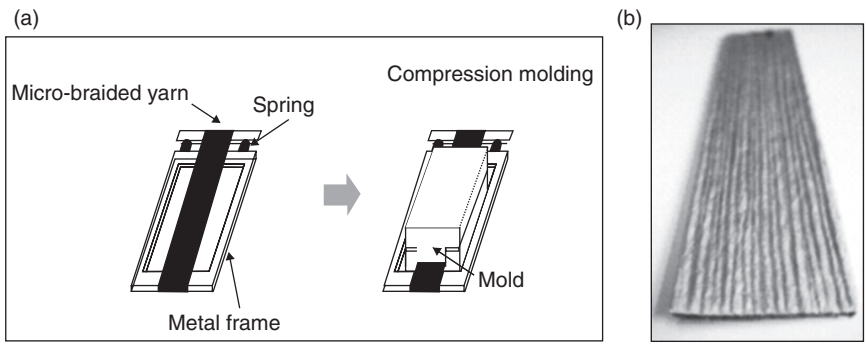
8.5 A typical braiding machine (a) that is used to produce MBYs (b).

yarns (MBY) were first developed at Kyoto Institute of Technology, Japan by Prof. Hiroyuki Hamada and Prof. Asami Nakai, who have tried to apply traditional kimono braiding techniques to advanced composite materials. A typical braiding machine and a photograph of an MBY are shown in Fig. 8.5. The idea is to braid thermoplastic resin yarns around the reinforcement fibers to form continuous MBY, which can then be aligned unidirectionally or made into woven mats. These materials will then be heated in a mold where the thermoplastic resin would melt and then diffuse into the core of the reinforcement fibers during compression molding. Since each reinforcement tow in the MBY is enveloped with the resin, the chances for the reinforcements to be fully impregnated by the resin are significantly higher. Impregnation is a problem typically associated with compression molded thermoplastic composites, due to the difficulty of high viscosity resins in diffusing to the core of the reinforcement fiber bundles. Apart from improving impregnation, the micro-braiding technique can also be useful to control the reinforcement fiber volume fraction by varying the number of resin tows used to wrap around the reinforcement, or by simply changing the braiding angle. Moreover, tows of different polymers can also be conveniently braided together to create *in situ* polymer blends. The advantage of micro-braiding in this case is that instead of having a homogeneous polymer blend as the matrix, functional polymers (e.g. that have better compatibility or have higher impregnation rates) can be preferentially deposited on the reinforcement fiber surface thus improving the overall fiber–matrix interaction. Examples of MBY containing multiple types of polymeric phases are illustrated in Fig. 8.6. An example of a composite molded from unidirectionally aligned MBY is shown in Fig. 8.7.

© Woodhead Publishing Limited, 2014



8.6 MBYs containing hybrid polymers: (a) MBY with alternating resin yarns; (b) MBY with two-layered stacking.



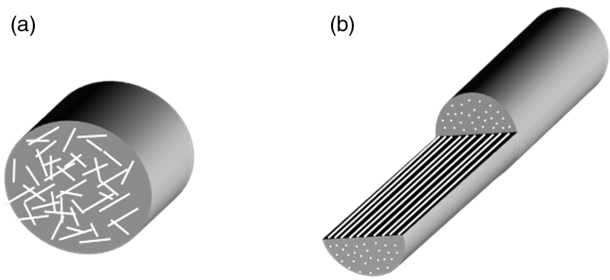
8.7 (a) Mold setup and alignment of MBY for fabricating unidirectional natural fiber composites; (b) an example of a molded unidirectional natural fiber composite profile.

8.2.2 Injection molding of thermoplastic natural fiber composites

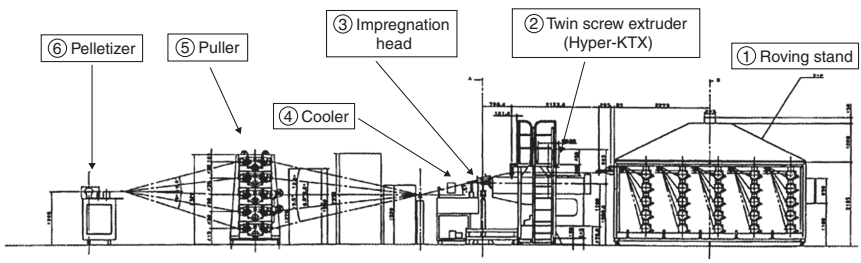
The injection molding technique is an indispensable tool for the composites manufacturing industries due to its ability to produce parts with very precise dimensions at very low cycle times. Injection molded parts require minimal post-processing, which reduces labor cost and ultimately the cost of the product itself. However, conventional injection moldings would be inferior in terms of mechanical performance when compared with compression

© Woodhead Publishing Limited, 2014

molded products, since the former can only contain short reinforcement fibers with low aspect ratios while it is possible to incorporate long or continuous fibers in the latter. Since the length of the extruded pellets generally limits the fiber lengths in injection moldings, various studies have been conducted on the viability of producing longer pellets. Apart from the dimensions, the method to produce long fiber pellets (LFP) is vastly different from that of short fiber pellets. As mentioned earlier, feeding both the resin and fibers through separate hoppers into the extruder produces short fiber pellets, where the resin is infused into the fibers through shear forces from the screw as well as pressure from the barrel. This would produce pellets with randomly oriented fibers, as shown in Fig. 8.8a. LFPs are produced through a pultrusion technology, whereby continuous fibers from rovings are pulled through the extruder where the resins are melted and infused into the fibers. As such, the fibers in the pellet are unidirectionally oriented and the fiber length is similar to the length of the pellets, as illustrated in Fig. 8.8b. The pultrusion setup for the production of LFPs is illustrated in Fig. 8.9. The length of short pellets is typically about 2–4 mm while the LFPs are about 10–12 mm. It should be noted that there should be a limit to the length of the pellets since it will be difficult to feed longer pellets through standard hoppers during the injection molding process. The LFP technology has been used since a decade ago in order to enhance the toughness and dimensional



8.8 (a) Conventional short pellets (typically 2–4 mm in length); (b) LFPs (typically 10–12 mm in length).

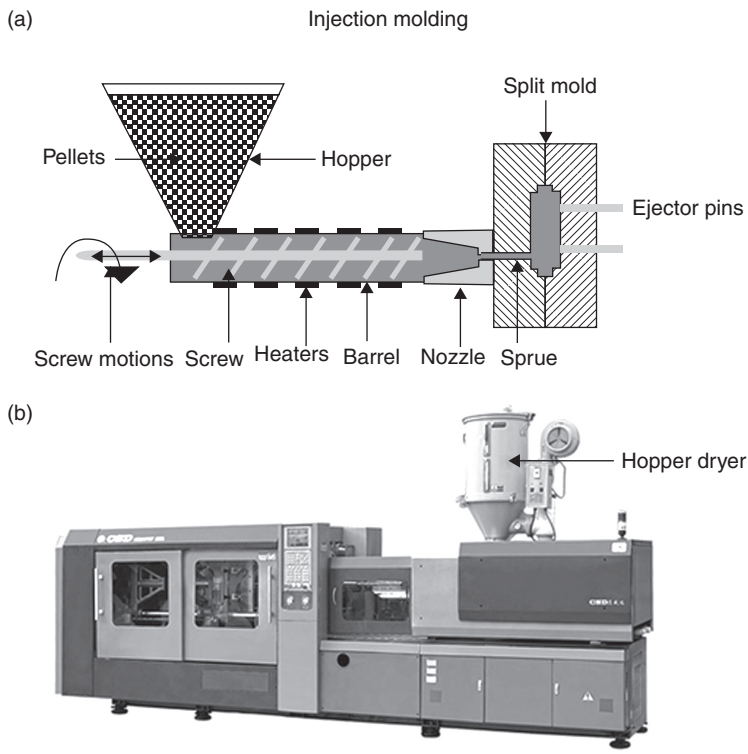


8.9 Schematic of a long fiber pellet pultrusion machine.

© Woodhead Publishing Limited, 2014

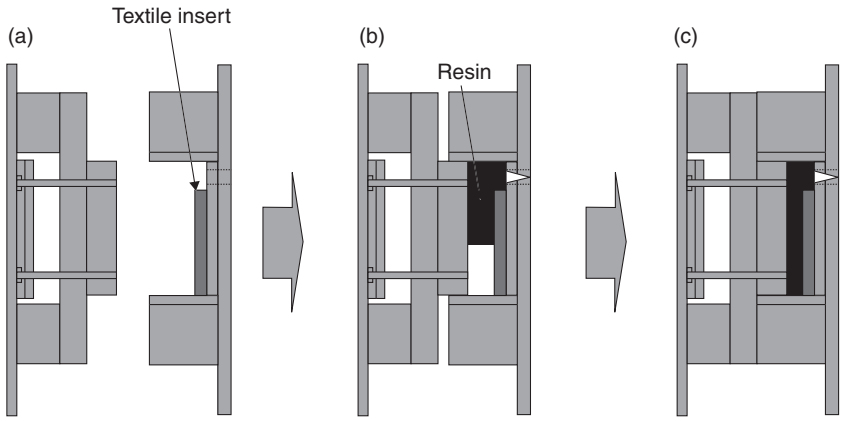
stability of glass and carbon fiber reinforced thermoplastic composites. However, researchers are still developing this technology so that it can be applicable to natural fibers. One of the major challenges is to significantly reduce the viscosity of the resins so that they can impregnate into the fibers while maintaining a low temperature to prevent thermal degradation.

A typical injection molding process involves the feeding of the material in the form of pellets through a hopper, as shown in the schematic in Fig. 8.10a. Note that for natural fiber composite pellets, it is recommended that the hopper is fitted with a hopper dryer, as shown in Fig. 8.10b, so that the pellets will remain dry throughout the injection process. The pellets are then conveyed by a screw to the heated barrel where the resin is melted. Once the desired amount of material is metered into the barrel, the same screw will then act as a plunger to inject the material through a nozzle into the mold where the material will take its shape and rapidly cool. The mold will then be opened and the molded part is ejected through ejector pins embedded in the mold. The size of the product determines the size of the mold, which in turn determines the size of the injection molding machine.

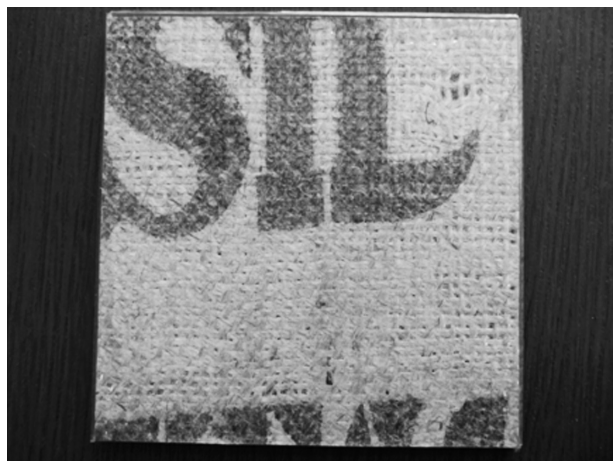


8.10 (a) Schematic showing a typical injection molding machine setup; (b) an injection molding machine equipped with a hopper dryer.

© Woodhead Publishing Limited, 2014



8.11 The textile insert injection–compression molding process: (a) insertion of textile; (b) partial mold closing and injection of resin; (c) full mold closing and compression of resin onto the textile insert.



8.12 An example of a textile insert injection molded sample. The textile is recycled jute fabric while the resin is poly(ethylene terephthalate) (PET).

Although the injection molding process is able to fabricate products within very good dimensional tolerances at a fast pace, it is not capable of producing continuous fiber reinforced composites. Therefore, the injection–compression molding technique was used to fabricate natural fiber textile insert moldings, with some degree of success. The textile insert molding process, as demonstrated in Fig. 8.11, involves firstly the insertion of a woven natural fiber fabric into the mold. The mold is initially partially closed prior to the injection of a thermoplastic resin. Upon injection of the resin, the mold will

© Woodhead Publishing Limited, 2014

be closed fully at a desired pressure and speed to compress the resin against the inserted fabric. In this case, the fabric will appear on the surface of the moldings as shown in Fig. 8.12. The textile insert molding process can be fully automated and useful for lining of textiles onto the inner or outer surfaces of moldings. Over-molding of another resin layer onto the surface of the textiles can also be done if the textiles are meant to be embedded inside the resin to form the core.

8.3 Processing natural fiber composites at high temperatures

Natural fibers, such as jute, sisal, and hemp have recently attracted the attention of scientists and technologists because of the advantages that these fibers provide over conventional reinforcement materials, such as low density, low cost, good recyclability and biodegradability. One of the main challenges of using natural fibers as reinforcement for thermoplastic resins is that natural fibers are inherently polar and hydrophilic, while the non-polar characteristic of most thermoplastic polymers create difficulties in compounding, which results in poor composite performance. Chemical and physical modifications to the fibers have been attempted to improve the interfacial adhesion between the fiber surfaces and the polymer matrix. Some of these treatments could even increase the strength of the fibers, as reported by some workers.[29,30]

Another challenge would be that the processing temperature of the natural fiber reinforced thermoplastics is limited due to the potential of fiber to degrade at high temperatures. Therefore, polymer matrices that can be used with natural fibers are also limited to low melting temperature commodity thermoplastics such as PP, PE, PVC, and PS. However, most of these thermoplastics are inherently weak in terms of mechanical performance when compared with engineering thermoplastics, as shown in Table 8.1. In order to expand the usage of natural fibers in composites, innovative techniques are required to reduce the gap between the processing temperatures of engineering polymers and the decomposition temperatures of natural fibers. Jana and Prieto[31,32] attempted this by using a reactive solvent as well as a low molecular weight epoxy to form a miscible blend with poly(phenylene ether) (PPE). This could significantly reduce the viscosity of the melt resin, which enabled them to process the composites at temperatures below the decomposition temperature of the natural fiber. They also noted the importance of compatibility between the polar wood flour and the epoxy component. The drawback of this system is that the matrix would become significantly weaker with increasing epoxy content.

Another alternative would be to enhance the thermal resistance of natural fibers in order to facilitate their usage with high temperature engineering

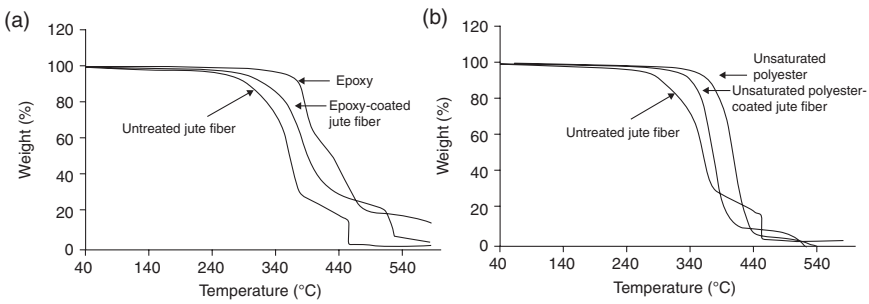
© Woodhead Publishing Limited, 2014

Table 8.1 Comparison of mechanical properties between commodity thermoplastics and engineering thermoplastics

Mechanical properties	Commodity thermoplastics*			Engineering thermoplastics†		
	PP	PE	PS	PC	ABS	PET
Tensile modulus (GPa)	1.3	0.2	2.8	2.4	2.1	3.0
Tensile strength (MPa)	22	11	45	72	65	82
Flexural modulus (GPa)	1.5	0.2	2.5	2.3	2.5	5.8
Flexural strength (MPa)	40	17	70	90	75	130
Un-notched Izod impact strength (kJ/m^2)	NB	NB	14.0	NB	39.2	170.0

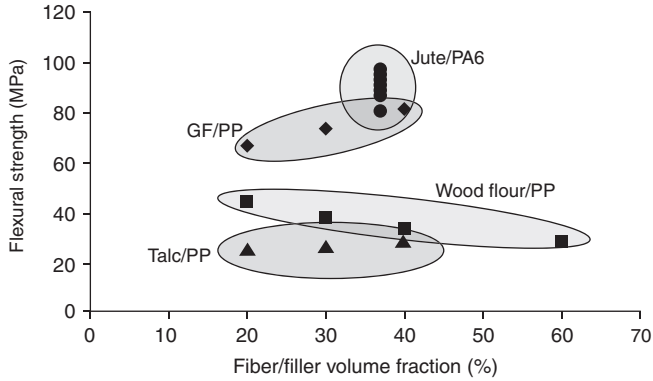
* Processing temperatures for commodity thermoplastics = 180–220°C.
† Processing temperatures for engineering thermoplastics = > 240°C.
NB = no break.

thermoplastics. Leong *et al.* [33] have shown that the thermal resistance of jute fabrics could be significantly improved when they were coated with thermosetting resins, which allowed them to be compression molded with engineering thermoplastics such as PC and PE terephthalate at temperatures of as high as 290°C. The thermal decomposition characteristics of the jute fibers as a function of time, as presented in Fig. 8.13, shows that the decomposition temperature of coated jute fibers can be increased by about 100°C as compared with uncoated jute. The advantage of using engineering thermoplastics as the matrix for natural fiber composites can be seen in Fig. 8.14, whereby the flexural strength of jute–polyamide-6 (jute–PA6) composites was superior to most composites with commodity thermoplastics (in this case PP) as matrices. It is interesting to note that the strength of the jute–PA6 composites was even comparable to that of glass fiber reinforced PP (GF–PP) at similar reinforcement loadings. When comparing the flexural strengths of PA6-based composites in Fig. 8.15, it can be shown that the

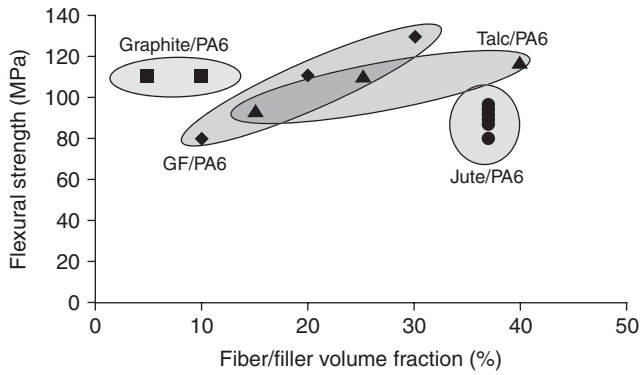


8.13 Thermal decomposition characteristics of jute fibers as a function of time: (a) comparison between uncoated jute and epoxy-coated jute; (b) comparison between uncoated jute and unsaturated polyester (UP)-coated jute.

© Woodhead Publishing Limited, 2014



8.14 Comparison of flexural strength between jute/PA6 composites and other composites with commodity thermoplastic matrices. Values obtained from MatWeb (www.matweb.com) except for those of jute/PA6 which are based on the authors' experiments.



8.15 Comparison of flexural strength between jute/PA6 composites and other PA6-based composites with different reinforcements. Values obtained from Matweb (www.matweb.com) except for those of jute/PA6 which are based on the authors' experiments.

performance of PA6–jute composites is quite comparable to other composites even when these were reinforced with inorganic fillers.

8.4 Conclusions

Compression and injection molding are two of the most versatile composites fabrication techniques, each having unique capabilities in forming composites of various shapes and sizes. Typically, large composite panels incorporated with either chopped fiber strands or continuous fibers can be

© Woodhead Publishing Limited, 2014

fabricated by using the compression molding technique and the molded article will usually require post-molding finishing. Injection moldings are typically more intricate in shape and have very tight dimensional tolerances. The length of the reinforcements will be shorter than the pellets, which is typically less than 3 mm. Due to the requirement for longer fiber lengths in injection moldings for certain applications, the long fiber pellet technology was developed whereby the pellet size (as well as the fiber length) could be as long as 12 mm. This technology can also be applied to obtain pellets incorporated with natural fiber strands, provided the thermoplastic resins can impregnate the fibers without thermal degradation. There has been continuous effort and attempts to incorporate natural fibers into high temperature engineering thermoplastics, mainly by reducing the melting point of the resin or improving the thermal resistance of natural fibers. The latter strategy seems to be more promising in enhancing the overall composite performance since the intrinsic properties of the matrix resin is not affected.

8.5 References

1. H. S. Kim, H. S. Yang, H. J. Kim, B. J. Lee and T. S. Hwang (2005). Thermal properties of ago-flour-field biodegradable polymer bio composites, *Journal of Thermal Analysis and Calorimetry*, **81**, 299–306.
2. J. Gassan and A. K. Bledzki (2001). Thermal degradation of flax and jute fibers, *Journal of Applied Polymer Science*, **82**, 1417–1422.
3. P. Ganna and I. Mondragon (2004). Thermal and degradation behavior of fique fiber reinforced thermoplastic matrix composites, *Journal of Thermal Analysis and Calorimetry*, **73**, 783–795.
4. S. Ouajai and R. A. Shanks (2005). Composition, structure and thermal degradation of hemp cellulose after chemical treatments, *Polymer Degradation and Stability*, **89**, 327–335.
5. P. Jundura, B. Riedi and B. V. Kokta (2000). Thermal degradation behavior of cellulose fiber partially esterified with some long chain organic acids, *Polymer Degradation and Stability*, **70**, 387–394.
6. K. G. Mansaray and A. E. Ghaly (1998). Thermal degradation of rick husks in nitrogen atmosphere, *Bioresource Technology*, **65**, 13–20.
7. A. J. Stamm (1956). Thermal degradation of wood and cellulose, *Industrial and Engineering Chemistry*, **48**, 413–417.
8. S. Shibata, Y. Cao and I. Fukumoto (2005). Effect of bagasse fiber on the flexural properties of biodegradable composites, *Polymer Composites*, **26**, 689–694.
9. S. S. Tripathy, G. Levita and L. D. Landro (2001). Interfacial adhesion in jute polyolefin composites, *Polymer Composites*, **22**, 815–822.
10. M. Miao and N. Finn (2008). Conversion of natural fibers into structural composites, *Journal of Textile Engineering*, **54**, 167–177.
11. K. S. Ahmed and S. Vijayarangan (2007). Experimental characterization of woven jute-fabric-reinforced isothatic polyester composites, *Journal of Applied Polymer Science*, **104**, 2650–2662.

© Woodhead Publishing Limited, 2014

12. J. George, M. S. Sreekala and S. Thomas (2001). A review on interface modification and characterization of natural fiber reinforced plastic composites, *Polymer Engineering and Science*, **41**, 1471–1485.
13. J. Gassan and A. K. Bledzki (2001). Thermal degradation of flax and jute fibers, *Journal of Applied Polymer Science*, **82**, 1417–1422.
14. A. K. Mohanty, M. Misra, and G. Hinrichsen (2000). Biofibres, biodegradable polymers and biocomposites: a review, *Macromolecular Materials and Engineering*, **276–277**, 1–24.
15. K. Goda and Y. Cao (2007). Research and development of fully green composite reinforced with natural fibers, *Journal of Solid Machines and Materials Engineering*, **1**, 1073–1084.
16. D. Maldas, B. V. Kokta, R. G. Raj and C. Daneault (1988). Improvement of the mechanical properties of sawdust wood fibre-polystylene composites by chemical treatment, *Polymer*, **29**, 1255–1265.
17. L. M. Matuana, C. B. Park and J. J. Balatinecz (1997). Processing and cell morphology relationships for microcellular foamed PVC/wood-fiber composites, *Polymer Engineering and Science*, **37**, 1137–1147.
18. R. G. Raj, B. V. Kokta, D. Maldas and C. Daneault (1988). Use of wood fibers in thermoplastic composites: VI isocyanate as a bonding agent for polyethylene –wood fiber composites, *Polymer Composites*, **9**, 404–411.
19. R. G. Raj and B. V. Kokta (1991). Improving the mechanical properties of HDPE-wood fiber composites with additive/coupling agents, *SPE ANTEC Proceeding*, **37**, 1883–1885.
20. R. G. Raj, B. V. Kokta and C. Daneault (1990). Wood flour as a low-cost reinforcing filler for polyethylene: studies on mechanical properties, *Journal of Materials Science*, **25**, 1851–1855.
21. G. E. Myers, I. S. Chahuadi, C. Gonzalez, C. A. Coberly and D. S. Ermer (1991). Wood floor and polypropylene or high density polyethylene composites: influence of maleated propylene concentration and extrusion temperature on properties, *International Journal of Polymeric Materials*, **15**, 171–186.
22. F. M. B. Coutinho, T. H. S. Costa and D. L. Carvalho (1997). Polypropylene-wood fiber composites: effect of treatment and mixing conditions on mechanical properties, *Journal of Applied Polymer Science*, **65**, 1227–1235.
23. M. Lu, J. R. Collier and B. J. Collier (1995). Improving mechanical properties of propylene-wood fiber composites by compounding and in-line maleation, *SPE ANTEC Proceeding*, **2**, 1433–1437.
24. C. B. Vick, K. Richter, B. H. River and A. R. Fried (1995). Hydroxy methylate resorcinlo coupling agent for enhanced durability of bisphenol-a epoxy bond to sitka spruce, *Wood and Fiber Science*, **27**, 2–12.
25. C. B. Vick and E. A. Okkonen (1997). Structurally durable epoxy bond to aircraft woods, *Forest Products Journal*, **47**, 71–77.
26. M. M. Sain and B. V. Kokta (1993). Toughened thermoplastic composite I crosslinkable phenol formaldehyde and epoxy resins coated cellulosic polypropylene, *Journal of Applied Polymer Science*, **48**, 2181–2196.
27. A. K. Bledzki, J. Gassan and W. Zhang (1999). Impact properties of natural fibre reinforced epoxy foams, *Journal of Cellular Plastic*, **35**, 550–562.
28. C. B. Vick (1997). More durable epoxy bonds to wood with hydroxymethylated resorcinol coupling agent, *Adhesive Age*, **40,** 24–29.

© Woodhead Publishing Limited, 2014

29. C. B. Vick, A. W. Christiansen and E. A. Okkonen (1998). Reactivity of hydroxymethylated resorcinol coupling agent as it affects durability of epoxy bonds to douglas-fir, *Wood and Fiber Science*, **30**, 312–322.
30. D. N. Saheb and J. P. Jog (1999). Natural fiber polymer composites: a review, *Advances in Polymer Technology*, **18**, 351–363.
31. K. Goda and Y. Cao (2007). Research and development of fully green composite reinforced with natural fibers, *Journal of Solid Machines and Materials Engineering*, **1**, 1073–1084.
32. S. C. Jana and A. Prieto (2002). On the development of natural fiber composites of high temperature thermoplastic polymers, *Journal of Applied Polymer Science*, **86**, 2159–2167.
33. S. C. Jana and A. Prieto (2002). Natural fiber composites of high-temperature thermoplastic polymers: effects of coupling agents, *Journal of Applied Polymer Science*, **86**, 2168–2173.

© Woodhead Publishing Limited, 2014

9

Thermoset matrix natural fibre-reinforced composites

A. CROSKY and N. SOATTHIYANON, University of New South Wales, Australia and Cooperative Research Centre for Advanced Composite Structures, Australia, D. RUYS, St Andrew's Cathedral School, Australia and S. MEATHERALL and S. POTTER, Composites Innovation Centre, Canada

DOI: 10.1533/9780857099228.2.233

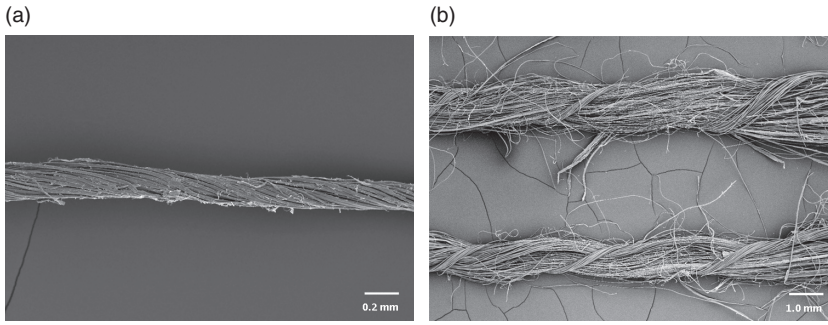
Abstract: Plant fibres have specific stiffnesses, similar to glass fibres, and this makes them attractive as renewable alternatives to glass fibres in glass-reinforced thermoset matrix composites, i.e. fibreglass. Thermoset matrix resins have traditionally been synthetic resins, but bioderived thermoset resins are now becoming available, creating the possibility for thermoset matrix composites in which both the fibres and the matrix are bioderived. This chapter reviews the common synthetic and bioderived thermoset matrix materials, the processes commonly used for fabricating thermoset matrix composites, and the mechanical properties of a wide range of plant fibre-reinforced composites made with both synthetic and bioderived thermoset matrix resins. Potential applications for plant fibre/thermoset matrix composites are also discussed. Due to the wide variation in the properties of plant fibres, even within a given species, it is considered that a rigorous system for grading incoming fibres will need to be developed if thermoset matrix plant fibre composites are to become a realistic alternative to fibreglass. Some insight might be provided from the textiles industry, which has already addressed this problem.

Key words: biocomposites, plant fibres, thermoset matrix composites, bioresins, mechanical properties.

9.1 Introduction

Thermoset matrix composites are composites made from resins which crosslink during curing. Crosslinking is induced either by addition of curing agents or by heating. As a result of crosslinking, thermoset plastics generally have better strength and stiffness than thermoplastics, which do not contain crosslinks, and this has made them attractive as the matrix resin in conventional fibre-reinforced plastic composites, such as fibreglass and carbon fibre composites. While natural fibres are inferior to high performance

© Woodhead Publishing Limited, 2014



9.1 (a) Twisted yarn, (b) straight yarn wrapped with spiral wrapping thread.

fibres, such as carbon fibres, they have a specific modulus which is similar to, or better than, that of glass fibres. This makes natural fibre thermoset matrix composites attractive as an alternative to fibreglass (glass fibre-reinforced thermoset matrix composites).

9.2 Natural fibres used in thermoset matrix composites

All types of natural fibres used generally in composites can be used in thermoset matrix composites. Where curing and/or post-curing (heating of the resin after initial curing) is carried out above room temperature, the temperatures used are generally well below those which cause heat-induced decomposition of natural fibres, so the full range of thermosetting resins can potentially be used in natural fibre composites.

Thermoset resins are usually obtained in liquid form permitting the use of fabrics and mats as the fibre reinforcement. To date, natural fibres have been used most commonly as needle punched mat; however, woven and unidirectional fabrics are now becoming available. The fabrics are made from either twisted yarns, Fig. 9.1a, or wrapped straight yarns, Fig. 9.1b. Surface treatments are often used to improve adhesion between the fibres and the matrix. Surface treatments are discussed in detail in Chapters 13 and 14.

9.3 Thermoset matrix types

9.3.1 Synthetic resins

Synthetic resins commonly used in fibre-reinforced plastic composites are unsaturated polyester (UPE), vinyl ester, phenolic and epoxy. Typical properties of these resins are given in Table 9.1 (Aranguren and Reboredo, 2007).

© Woodhead Publishing Limited, 2014

Table 9.1 Properties of common thermosetting matrix materials (Aranguren and Reboredo, 2007)

Property	Polyesters	Vinyl esters	Epoxies	Phenolics
Tensile strength (MPa)	34–105	73–81	55–130	50–60
Tensile modulus (GPa)	2.1–3.5	3–3.5	2.7–4.1	4–7
Flexural strength (MPa)	70–110	130–140	110–150	80–135
Flexural modulus (GPa)	2–4	3	3–4	2–4
Glass transition temperature (°C)	130–160		170–300	175
Specific gravity	1.1–1.4	1.1–1.3	1.2–1.3	1.2–1.3
Moisture uptake (wt.%)	0.5–2.5		2.5–6.0	
Cure shrinkage (%)	5–12	5–10	1–5	2–4

While epoxy resins have been widely used as a model matrix for research into natural fibre composites, they are unlikely to see widespread use in commercial natural fibre composites because of their relatively high cost. Cheaper resins, such as polyester and vinyl ester, are more commonly used. Phenolic resins have good fire resistance but are more difficult to process.

9.3.2 Bio-based resins

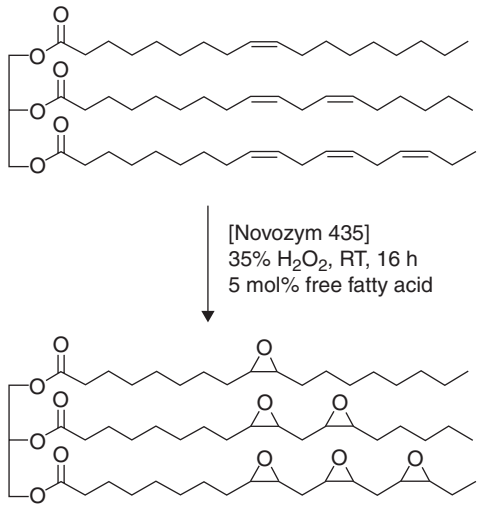
Particularly attractive for natural fibre/thermoset matrix composites is the use of plant-based resins and considerable development of these resins has taken place in recent years. Several different types have been developed – see for example Karak (2012). Those used in composites include epoxidized plant oil-based resins, protein-based resins, bio-based polyurethane (PU) resins, bio-based phenolic resins and lactic acid (LA)-based thermoset resin.

Epoxidized plant oil-based resins

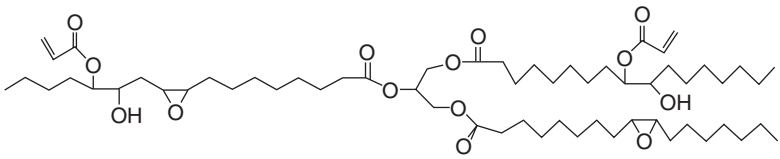
Plant oils are predominantly made up of triglycerides which are composed of three generally unsaturated fatty acids joined at a glycerol juncture. The fatty acids are typically 14–22 carbon atoms in length with 0–3 double bonds per fatty acid (Wool, 2005). The fatty acids can be epoxidized by a variety of methods (Biermann *et al.*, 2000) to convert the unsaturation to epoxy. Figure 9.2 shows an example for a triglyceride containing 1, 2 and 3 double bonds, respectively, in each of the three fatty acids.

Common plant oils used for epoxidation are soybean oil and linseed (flax seed) oil. The resulting products are referred to as epoxidized soybean oil (ESO) and epoxidized linseed oil (ELO). The flexural modulus and strength of ELO-based resin used as the matrix for natural fibre composites have been reported to be 1.8 GPa and 60 MPa, respectively (Boquillon, 2006), which is comparable to that of synthetic resins.

© Woodhead Publishing Limited, 2014



9.2 Chemo-enzymatic epoxidation of vegetable oil through conversion of the unsaturated bonds (top) to epoxy groups (bottom) (Biermann *et al.,* 2000).



9.3 Chemical structure of acrylated epoxidized soybean oil (AESO) resin (Ramamoorthy *et al.,* 2012).

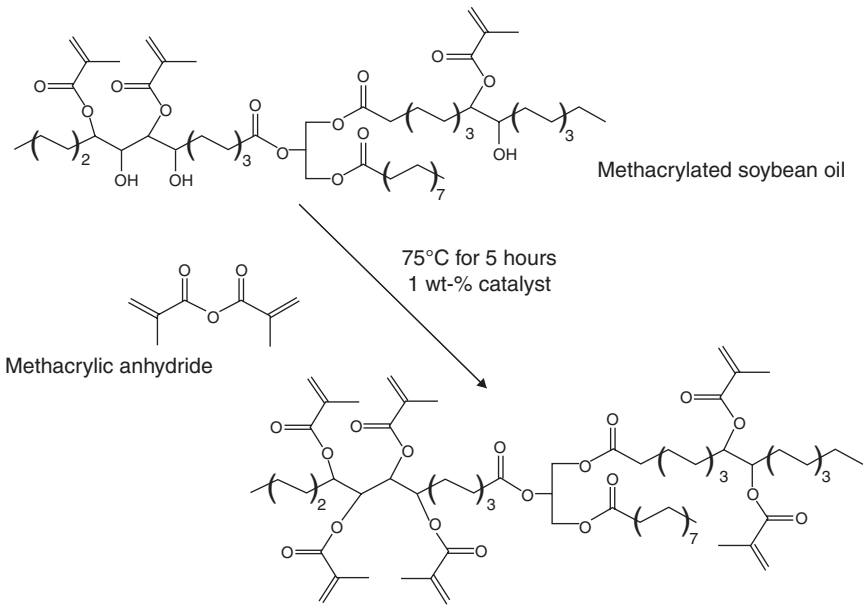
ESO has been modified using acrylic acid to become acrylated epoxidized soybean oil (AESO) (Åkesson *et al.*, 2009) and this has also been used as the matrix resin in natural fibre thermoset matrix composites. The chemical structure of the AESO resin is shown in Fig. 9.3.

Additionally, ESO can be modified to methacrylated soybean oil (MSO) (Ramamoorthy *et al.*, 2012) and the MSO then modified using methacrylic anhydride to produce methacrylic anhydride-modified soybean oil (MMSO) (Adekunle *et al.*, 2011) as shown in Fig. 9.4. Although bio-based epoxy resins are environmentally friendly, limitations of bio-based epoxy resins are their high water absorption and swelling, compared with traditional epoxy resins (Masoodi and Pillai, 2012).

Protein-based resins

Resins can also be made from soy protein. Soy protein products include soy protein isolate (SPI), soy protein concentrate (SPC) and soy flour (SF).

© Woodhead Publishing Limited, 2014



9.4 Synthesis of methacrylic anhydride-modified soybean oil (MMSO) (Adekunle *et al.*, 2011).

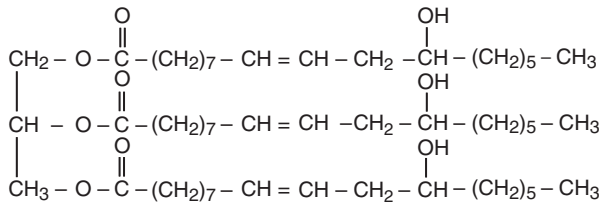
SPI contains more than 90% protein and is synthesized by precipitation at a pH of 4.5. Preparation of SPC is carried out by elutriation of soluble components from defatted SF. The SPC contains more than 70% protein and approximately 18% carbohydrate. The SF consists of approximately 56% protein and approximately 34% carbohydrate (Paetau *et al.*, 1994). These soy protein products have been used as the matrix material in natural fibre thermoset matrix composites.

SF can be modified to enhance the protein content to give an improvement in the tensile properties. The modified SF is known as modified soy flour (MSF). Another modification of SF is to crosslink the SF using glutaraldehyde (GA). This modified SF is called cross-linked soy flour (CSF). Additionally, a modification of the SPI can be done using stearic acid to improve the mechanical properties of the composites.

Bio-based PU resins

Vegetable oils, such as castor oil, can be used to make bio-based thermoset PU resins, and these have also been used in natural fibre composites. The castor oil triglyceride is characterized by the presence of ricinoleic fatty acid which, in addition to containing double bonds, contains hydroxyl groups on its backbone (Dwan'Isa *et al.*, 2005) (Fig. 9.5). The hydroxyl

© Woodhead Publishing Limited, 2014



9.5 Structure of castor oil (Mistri *et al.*, 2011).

groups can be reacted with isocyanates to form castor oil-based polyurethane (COPU). The tensile strength of a COPU matrix resin has been reported to be 2.5 MPa, which is very low compared with that of synthetic thermoset resins, but the elongation to break was 31%, which is extremely high (Milanese *et al.*, 2011).

Rubber seed oil (RSO) has also been used to make PU (Bakare *et al.*, 2010). Compared with synthetic thermoset resins, the mechanical properties of rubber seed oil polyurethane (RSOPU) are again very low, with the tensile modulus and strength being reported as 0.4 GPa and 4.8 MPa, respectively (Bakare *et al.*, 2010).

Bio-based phenolic resins

Cardanol can be obtained from cashew nut shell liquid (CNSL) and then modified and condensation polymerized to produce cross-linked phenol formaldehyde resins (Bisanda and Ansell 1992; Barreto *et al.*, 2010), commonly known as phenolic resins. This bio-based resin is known as cashew nut shell liquid (CSNL) resin and has also been used as the matrix resin in natural fibre composites.

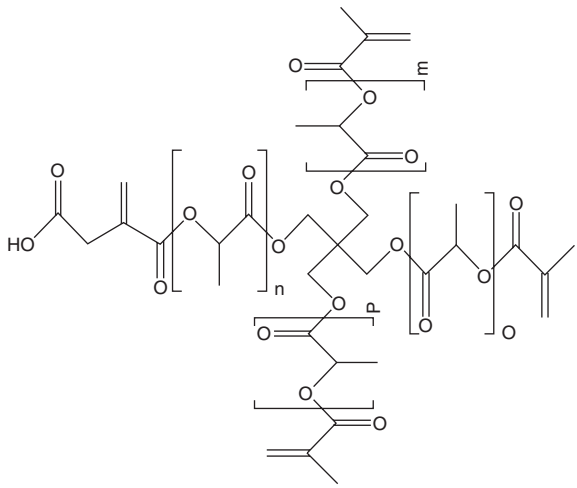
LA-based thermoset resin

LA-based thermoset resin has also been used as bio-based thermoset matrix resin in natural fibre composites. The structure of the LA-based resin is shown in Fig. 9.6. Synthesis of the LA-based resin is done in two steps. First, LA and itaconic acid are reacted with pentaerythritol. The star-shaped oligomers which result are then end-capped with methacrylic acid (Åkesson *et al.*, 2011).

9.4 Fabrication of thermoset matrix composites

A variety of techniques are used for fabrication of thermoset matrix composites. A detailed account of composite fabrication techniques is given in Strong (2008). The simplest of these is the hand lay-up (also known as wet lay-up) technique, where fibres in the form of mat or fabric are placed in an open mould and wetted-out with liquid resin. Curing may be carried out

© Woodhead Publishing Limited, 2014



9.6 Idealized structure of the LA-based resin (Åkesson *et al.*, 2011).

at room temperature or at elevated temperature. Additional elevated temperature post-curing may also be used. A modification of this technique is the spray-up technique where chopped fibres, mixed with resin, are sprayed onto the mould.

Another common technique is resin infusion, where resin is infused into a mat or fabric preform under the application of pressure and/or vacuum. Two different types of process are used. The first, known as resin transfer moulding (RTM), utilizes a two-piece closed mould into which the fibre preform is placed and the resin then infused. A simpler process is vacuum bag resin infusion. This uses a single mould into which the fibre preform is placed. A plastic film is then placed over the preform, sealed around the edges to form a vacuum bag, and vacuum then applied to the mould cavity, i.e., the space between the vacuum bag and the mould. The vacuum acts to draw resin into the mould cavity, thereby infusing the preform. These closed mould processes have the advantage over open mould processes of producing more consistent parts and avoiding emission of volatiles from the resin into the atmosphere.

Other processes use fibre preforms that have been preimpregnated with resin, which is then partially cured prior to fabrication of the composite. Two common products are prepreg and sheet moulding compound. Prepreg usually contains fibres in the form of unidirectional or bi-directional fabrics. The fabrics are cut, laid-up, and then cured at elevated temperature, usually under applied pressure. Sheet moulding compound consists of chopped fibres preimpregnated with resin. It is fabricated into parts by compression moulding at elevated temperature and pressure.

© Woodhead Publishing Limited, 2014

More automated fabrication is possible using pultrusion and filament winding. In pultrusion, fibres are passed through a resin bath, and then drawn through a heated die to produce long products of constant cross section. Filament winding involves passing fibres through a resin bath and then winding the wet-out fibres onto a rotating mandrel. Most commonly, resin infusion processes are used for producing parts from thermoset matrix natural fibre composites. However, in research, open mould hand lay-up, with or without applied pressure (e.g. through compression moulding), is often used.

9.5 Mechanical properties of synthetic resin composites

9.5.1 Epoxy resin composites

Epoxy resin has been used widely as a matrix resin in research into natural fibre composites, since it has been found to bond well to natural fibres because of its affinity for the hydroxyl groups attached to cellulose (O'Brien and Hartman, 1971). However, it is unlikely to be cost competitive in most of the applications currently envisaged for thermoset matrix natural fibre composites. None the less, in view of the large body of work, it is useful to review the research done using this matrix material.

Unidirectional composites

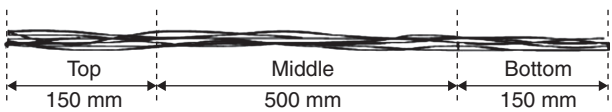
Unidirectional thermosetting composites have been used widely to evaluate the potential mechanical properties of natural fibre composites. Most of this work has been carried out using long technical fibres cut to the length of the laminate. Oksman (2001) determined the tensile properties of unidirectional untreated flax fibre/epoxy composites fabricated using RTM with fibre volume fractions of 21–47%. The tensile properties of the composites ranged from 15 to 39 GPa, for the tensile modulus, and from 132 to 280 MPa, for the tensile strength. The elongation at break of the composites ranged from 0.8% to 1.2%. Van de Weyenberg *et al*. (2003) obtained similar values for the stiffness and strength of 50 volume percent (vol.%) unmodified flax fibre/epoxy composites with values of 32 GPa and 268 MPa, respectively, being recorded. Hepworth *et al*. (2000) produced flax/epoxy composites with a volume fraction of 80% by hand lay-up and obtained values of 26 and 378 GPa, respectively. With such a high fibre volume fraction it is unlikely that the fibres were fully bonded to the matrix, and this might account for the low value of the measured modulus.

In more recent work, Charlet *et al*. (2007) determined the tensile properties of 20 vol.% unidirectional Hermès flax fibre/epoxy composites fabricated

© Woodhead Publishing Limited, 2014

using wet impregnation. The flax fibres were obtained from three different locations of the stems, namely the top, middle and bottom, as shown in Fig. 9.7. The highest values of the modulus and strength were obtained from the middle of the stems, where values of 17 GPa and 127 MPa, respectively, were recorded (Table 9.2). These values are consistent with those reported in the earlier study by Oksman (2001).

The present authors examined the tensile and flexural properties of pultruded unidirectional flax and hemp epoxy matrix composites containing 50 vol.% fibres in both the untreated and dewaxed conditions. A distinct knee was detected in the stress–strain curves (Fig. 9.8), as reported previously by Hughes *et al.* (2007), with the slope of the curve decreasing noticeably after the knee. The knee occurred at a strain ε of 0.13–0.15% for the flax composites and 0.17–0.20% for the hemp composites. The modulus values obtained before the knee were 27–30 GPa with reductions of 30–60% occurring after the knee, Table 9.3. The reduction in modulus was substantially higher for the hemp fibres (50–60%) than for the flax fibres (30–40%). For both types of fibre, the reduction in modulus was slightly lower when the fibres had been dewaxed. The ultimate strength of the hemp composites was 210–220 MPa, while for the flax composites it was 270–280 MPa. The strain to failure was 1.4–1.7% for the hemp composites and 1.3% for the flax composites. The flexural properties were also determined for both the flax and hemp composites, giving values of 23–26 GPa for the flexural modulus and 210–230 MPa for the flexural strength, Table 9.4. As for the tensile properties, the flexural properties were again generally better for the flax composites than for the hemp composites.

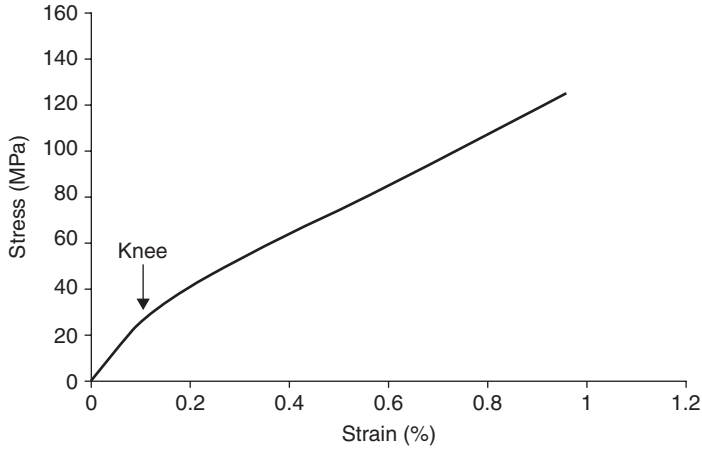


9.7 Locations in stem where flax fibres were examined (Charlet *et al.*, 2007).

Table 9.2 Tensile properties of unidirectional flax fibre/epoxy composites (values in brackets represent one standard deviation) (Charlet *et al.*, 2007)

Location of fibre stems	Tensile property		
	Young's modulus (GPa)	Strength (MPa)	Ultimate strain (%)
Top	12.4 (1.3)	126 (14)	1.3 (0.2)
Middle	16.7 (3.7)	127 (14)	0.9 (0.2)
Bottom	11.1 (1.4)	113 (11)	1.5 (0.1)

© Woodhead Publishing Limited, 2014



9.8 Typical stress–strain curve for 50 vol.% hemp epoxy composite showing distinct knee.

Table 9.3 Tensile properties of 50 vol.% flax and hemp epoxy matrix composites (values in brackets represent one standard deviation)

Fibre type	Modulus before knee (ε = 0–0.08%)	Modulus after knee (ε = 0.2–0.3%)	Ultimate tensile strength (MPa)	Strain to failure (%)
Flax, untreated	29.8 (3.2)	18.4 (1.5)	275 (19)	1.32 (0.12)
Flax, dewaxed	29.3 (1.8)	19.7 (1.6)	277 (23)	1.27 (0.07)
Hemp, untreated	26.5 (2.7)	11.7 (0.7)	211 (13)	1.67 (0.08)
Hemp, dewaxed	29.7 (2.2)	15.4 (2.0)	224 (15)	1.38 (0.18)

The impact properties of the composites are given in Table 9.5. The Charpy impact energy was also significantly higher for the flax composites than for the hemp composites (60–80 kJm^{-2} compared with 40 kJm^{-2}). It was also higher for the untreated fibres than for the dewaxed fibres for both the flax and hemp fibres.

Abdullah *et al*. (2011) determined the tensile properties of 15 and 45 vol.% unidirectional kenaf fibre/epoxy composites using hand lay-up compression moulding at room temperature. The modulus was 4.0 GPa for the 15% composite and 7.8 GPa for the 45% composite, while the strength was 58 and 101 MPa, respectively. The strain to failure was 2.1% and 1.9%, respectively.

Virk *et al*. (2011) determined the mechanical properties of 19 vol.% unidirectional jute/epoxy matrix composites fabricated by resin infusion. The composites had a tensile modulus of 8.2 GPa, a tensile strength of 100 MPa, and a strain to failure of 1.3%. Mishra *et al*. (2000) fabricated unbleached and bleached jute sliver/epoxy composites using impregnation. The fibre loading was 40, 50 and 57 wt.% for the unbleached jute slivers and 50 wt.%

© Woodhead Publishing Limited, 2014

Table 9.4 Flexural properties of 50 vol.% flax and hemp epoxy matrix composites (values in brackets represent one standard deviation)

Fibre type	Flexural modulus (GPa)	Flexural strength (MPa)	Strain to failure (%)
Flax, untreated	25.9 (0.7)	225 (5)	2.3 (0.2)
Flax, dewaxed	24.3 (2.2)	233 (13)	2.3 (0.2)
Hemp, untreated	22.6 (1.9)	209 (11)	2.7 (0.3)
Hemp, dewaxed	26.4 (2.2)	228 (18)	2.2 (0.2)

Table 9.5 Charpy impact energies for 50 vol.% flax and hemp epoxy matrix composites (values in brackets represent one standard deviation)

Fibre type	Impact toughness (kJm^{-2})
Flax, untreated	76 (12)
Flax, dewaxed	59 (8)
Hemp, untreated	44 (6)
Hemp, dewaxed	37 (8)

for the bleached jute slivers. The 50% unbleached jute composite had better tensile properties than either the 40% or 57% composites (Table 9.6). The tensile properties were also higher for the unbleached 50% composite than for the bleached 50% composite, although the reverse was true for the flexural properties (Table 9.7).

Van de Weyenberg *et al*. (2006) studied the effect of 1–3% sodium hydroxide (NaOH) treatment on the flexural properties of 40 vol.% unidirectional flax fibre/epoxy composites fabricated by autoclave curing of prepreg. Data for the transverse direction, as well as the longitudinal direction, was obtained. The flexural properties were improved by NaOH treatment in both directions, especially in the transverse direction (Table 9.8).

Padmavathi *et al*. (2012) studied the effect of fibre fraction and alkali treatment of the fibres on the mechanical properties of unidirectional sisal fibre/epoxy composites fabricated using the wet lay-up technique. The fibre fraction was varied between 15 wt% and 40 wt% for the treated fibre composites, while a 40 wt% fibre fraction was used for the untreated fibre composites. The untreated sisal fibre/epoxy composites had a tensile strength of 185 MPa and a tensile modulus of 7.1 GPa. The tensile strength and modulus of the treated sisal fibre/epoxy composites ranged from 161 to 235 MPa and from 5.6 to 6.4 GPa, respectively. While the tensile strength was substantially higher for the 40 wt% composite made using the treated fibres than for its counterpart made with untreated fibres, the reverse was true for the tensile modulus.

© Woodhead Publishing Limited, 2014

Table 9.6 Tensile properties of unbleached jute sliver/epoxy composites (Mishra *et al.*, 2000)

Tensile property	Unbleached jute sliver/epoxy		
	40% Fibre loading	50% Fibre loading	57% Fibre loading
Ultimate tensile strength (MPa)	140	148	143
Ultimate tensile strain (%)	7.3	6.3	6.0
Tensile modulus (MPa)	2826	3184	3060

Table 9.7 Mechanical properties of 50% unbleached and bleached jute sliver/epoxy composites (Mishra *et al.*, 2000)

Mechanical property	Unbleached jute sliver/epoxy	Bleached jute sliver/epoxy
Tensile property		
Ultimate tensile strength (MPa)	148	131
Ultimate tensile strain (%)	6.3	7.4
Tensile modulus (GPa)	3.2	2.3
Flexural property		
Flexural yield strength (MPa)	155.8	196.1
Flexural modulus (GPa)	14.2	20.4

Table 9.8 Flexural properties of untreated and treated flax fibre/epoxy composites (Van de Weyenberg *et al.*, 2006)

Flexural property	Fibre treatment			
	Untreated	1% NaOH	2% NaOH	3% NaOH
Longitudinal direction				
Strength (MPa)	218	237	261	283
Modulus (GPa)	18	23	20	22
Transverse direction				
Strength (MPa)	8	20	15	19
Modulus (GPa)	0.4	2.3	1.1	1.2

The compressive strength and impact strength were also determined. The compressive strength of the treated fibre composites ranged from 76 to 137 MPa while that for the untreated fibre composite was 116 MPa. The compressive strength was again substantially higher for the treated fibre composite than for the untreated fibre composite at the same fibre fraction. The treated fibre composites had impact energies ranging from 2.3 to 11.1 J, while the impact energy of the untreated fibre composite was 4.3 J. The impact energy

© Woodhead Publishing Limited, 2014

of the 40 wt% treated fibre composite was significantly higher than that of the 40 wt% untreated fibre composite (Padmavathi *et al*., 2012).

Yarn composites

Bledzki *et al*. (2004) examined the influence of mercerization on the flexural properties of hemp/epoxy composites made from yarn. The hemp yarns were treated with 22% NaOH for 60 min at 4°C, 10°C and 20°C and then fabricated into composites using filament winding. The flexural properties were enhanced by mercerization. The flexural modulus of the treated hemp yarn/epoxy composites ranged from 11.8 to 12.4 GPa compared with 5.9 GPa for the composites made with untreated yarn. Similarly, the flexural strength of the composites with treated yarns ranged from 219 to 228 MPa, compared with 148 MPa for the untreated yarns.

Knitted composites

Goutianos *et al*. (2006) fabricated 28 vol.% unidirectional warp knitted flax/epoxy composites using the hand lay-up technique. The mechanical properties of the composites were determined in both the longitudinal and transverse directions. The tensile modulus and strength of the composites in the longitudinal direction were 15 GPa and 160 MPa, respectively, while the values in the transverse direction were 3 GPa and 15 MPa, respectively. The flexural modulus and strength were 16 GPa and 190 MPa, respectively, in the longitudinal direction and 4 GPa and 40 MPa, respectively, in the transverse direction.

Mat composites

Kushwaha and Kumar (2010) examined untreated and acrylonitrile treated (cyanoethylation) bamboo mat/epoxy composites fabricated using the hand lay-up technique. The acrylonitrile treatment was carried out for 1 and 5 h. The tensile modulus and strength of the untreated bamboo mat composites were 6.7 GPa and 86 MPa, respectively, while the treated mat composites had moduli of 9.0–9.9 GPa and strengths of 102–125 MPa. The untreated bamboo mat/epoxy composites had a flexural modulus of 11.9 GPa and a flexural strength of 119 MPa. The flexural moduli of the treated bamboo mat composites were lower than in the untreated mat composites, being 5.8–6.6 GPa; however, the flexural strength was slightly higher, having values of 121–133 MPa. It was noted that cyanoethylation decreased water absorption of the bamboo mats in the epoxy composites.

Sastra *et al*. (2006) studied the effect of fibre loadings on the tensile properties of long random sugar palm fibre/epoxy composites fabricated using compression moulding. Fibre loadings of 10, 15 and 20 wt.% were used.

© Woodhead Publishing Limited, 2014

The 15% loading gave the best tensile strength and modulus. Bachtiar *et al*. (2008) examined the effect of 0.25 g/mol NaOH treatment for 1, 4 and 8 h on the tensile properties of long random sugar palm fibre/epoxy composites fabricated using the hand lay-up technique. The alkali treatment only marginally improved the tensile properties of the composites, with the effect being greatest for the modulus. The maximum tensile strength was obtained using the 1 h treatment, while the maximum tensile modulus was achieved with the 4 h treatment.

The same authors also studied the effect of 0.25 and 0.5 M NaOH treatments for 1, 4 and 8 h on the impact strength of sugar palm fibre/epoxy composites (Bachtiar *et al*., 2009). The highest impact strength was obtained with the 0.5 mol/L, 8 h treatment, with a value 30% higher than for the untreated fibres being achieved. However, for both NaOH concentrations, some of the shorter treatments substantially reduced the impact strength, Table 9.9.

Rassmann *et al*. (2010) examined the mechanical properties of non-woven kenaf fibre mat composites fabricated using RTM at 50–55°C. Epoxy resin, vinyl ester and orthophthalic UPE resin were used as the matrix resins. Fibre volume fractions of 15%, 22.5% and 30% were examined. For all three resins, the tensile and flexural properties increased with increased fibre loading. The effect of varying the resin type was more complex. The tensile modulus was generally highest for the polyester composites and lowest for the epoxy composites; however, the reverse was true of the tensile strength. The effect of resin type on flexural strength was less clear.

9.5.2 Epoxy-phenolic resins

Woven fabric composites

Patel and Parsania (2010) examined the mechanical properties of 50 wt.% untreated and treated woven jute fabric/epoxy-phenolic (25:25 wt.%) composites. The jute fabrics were treated with 5% NaOH, and then treated

Table 9.9 Impact strength of untreated and treated sugar palm fibre/epoxy composites (Bachtiar *et al.*, 2009)

Sugar palm fibre/epoxy composite	Izod impact strength (J/m)
Untreated	46.7
0.25 M NaOH treated for 1 h	35.2
0.25 M NaOH treated for 4 h	37.8
0.25 M NaOH treated for 8 h	50.0
0.5 M NaOH treated for 1 h	40.7
0.5 M NaOH treated for 4 h	49.3
0.5 M NaOH treated for 8 h	60.1

© Woodhead Publishing Limited, 2014

with 10 wt.% acrylic acid to clean the fibre surface and reduce hydrophilicity of the fibres. The composites were fabricated using hot pressing at 150°C for 2 h. The tensile and flexural strengths of the untreated jute fibre composite were 44.3 and 56.2 MPa, respectively, whereas the tensile and flexural strengths of the treated jute fibre composite were 63 and 65 MPa, respectively.

9.5.3 Epoxy vinyl ester resins

Woven fabric composites

Rodriguez *et al*. (2007) examined the influence of 5 wt.% NaOH treatment at room temperature for 24 h on the mechanical properties of 30 vol.% woven jute/epoxy vinyl ester composites fabricated using the vacuum infusion technique. The flexural modulus and strength were 6.6 GPa and 103 MPa, respectively, for the untreated jute fibre composites, with lower values of 5.5 GPa and 83 MPa, respectively, being obtained for the treated jute fibre composites. The impact strength was 57 J/m for the untreated fibre composite and 47 J/m for the treated fibre composite.

9.5.4 Vinyl ester resins

Unidirectional composites

The present authors determined the tensile, flexural, compression and in-plane shear properties in 25 vol.% untreated flax/vinyl ester composites fabricated from untwisted unidirectional flax fabric using vacuum-assisted RTM. As in the 50 vol.% unidirectional flax and hemp epoxy matrix composites examined by these authors, and also the flax/polyester composites examined by Hughes *et al*. (2007), a distinct knee was again observed in the tensile stress strain curves. The tensile modulus was 13 GPa before the knee (Table 9.10), with a 30% reduction after the knee. The tensile strength was 122 MPa. The flexural modulus and strength were 10 GPa and 170 MPa, respectively, the compression modulus and strength were 10 GPa and 131 MPa, respectively, while the in-plane shear modulus and strength were 2.1 GPa and 51 MPa, respectively (Table 9.10).

Woven fabric composites

The present authors also determined the tensile, flexural, compression and in-plane shear properties of 25 vol.% untreated flax/vinyl ester composites fabricated from woven untwisted flax yarn twill fabric using vacuum-assisted RTM. The properties are given in Table 9.11. The tensile modulus and strength were 7.9 GPa and 62 MPa, respectively, the flexural modulus

© Woodhead Publishing Limited, 2014

Table 9.10 Tensile, flexure, compression and in-plane shear properties of 25 vol.% unidirectional flax/vinyl ester composites (values in brackets represent one standard deviation)

Test type	Test specification	Modulus (GPa)	Strength (MPa)
Tension	ASTM D 638	13.2 (0.3)	122.4 (5.0)
Flexure	ASTM D 790	10.3 (0.3)	170.0 (5.8)
Compression	ASTM D 6641	9.8 (0.6)	131.4 (2.0)
In-plane shear	ASTM D 7078	2.1 (0.1)	51.3 (1.2)

Table 9.11 Tensile, flexure, compression and in-plane shear properties of 25 vol.% twill weave flax/vinyl ester composites (values in brackets represent one standard deviation)

Test type	Test specification	Modulus (GPa)	Strength (MPa)
Tension	ASTM D 638	7.9 (0.2)	62.0 (2.4)
Flexure	ASTM D 790	6.7 (0.6)	107.3 (4.6)
Compression	ASTM D 6641	5.2 (0.3)	102.6 (3.9)
In-plane shear	ASTM D 7078	1.7 (0.2)	41.1 (2.2)

and strength were 6.7 GPa and 107 MPa respectively, the compression modulus and strength were 5.2 GPa and 103 MPa, respectively, and the in-plane shear strength and modulus were 1.7 GPa and 41.1 MPa respectively.

Li *et al*. (2005) examined the tensile, flexural and impact properties of 32 vol.% plain weave sisal fabric/vinyl ester composites fabricated using RTM. The sisal fabric was used in the untreated condition, after treating with silane (γ-methacryloxypropyl trimethoxy silane) and with $KMnO_4$. Values of 4.4–5.1 GPa were obtained for the tensile modulus and 29–32 GPa for the tensile strength (Table 9.12). The flexural modulus was 3.1–4.0 GPa while the flexural strength was 62–73 MPa. The Charpy impact strength was 20–36 kJ/m^2. The tensile modulus, flexural modulus and flexural strength were all increased by the fibre treatments; however, no increase in the tensile strength was observed. The impact strength was decreased substantially by the fibre treatments.

Mat composites

Qi and Zhao (2011) determined the tensile and flexural properties of untreated and treated jute fibre mat/vinyl ester composites fabricated using vacuum-assisted RTM. The treatments used were 5% NaOH, 0.055% $KMnO_4$ and 2% silane. The tensile modulus, tensile strength and strain to failure were 1.6–2.0 GPa, 42–64 MPa and 2.0–3.2%, respectively, while the flexural modulus and strength were 3.8–6.0 GPa and 56–100 MPa, respectively (Table 9.13). All tensile and flexural properties were improved by the treatments.

© Woodhead Publishing Limited, 2014

Table 9.12 Mechanical properties of untreated and treated plain weave sisal fabric/vinyl ester (VE) composites (Li *et al.*, 2005)

Mechanical property	Composite		
	Untreated sisal/VE	Silane treated sisal/VE	Permanganate treated sisal/VE
Tensile property			
Strength (MPa)	31.3	31.8	29.2
Modulus (GPa)	4.4	5.1	5.1
Flexural property			
Strength (MPa)	62.1	72.7	72.4
Modulus (GPa)	3.1	4.0	4.0
Charpy impact strength			
Strength (kJ/m^2)	35.6	28.8	20.5

Table 9.13 Tensile and flexural properties of untreated and treated jute mat/vinyl ester (VE) composites (Qi and Zhao, 2011)

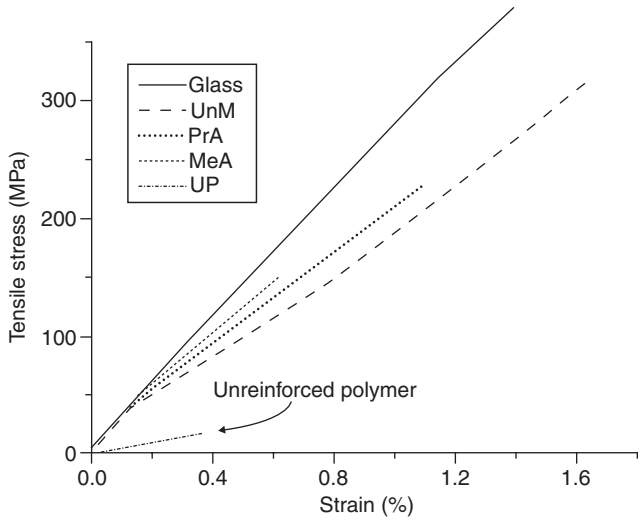
Mechanical property	Composite			
	Untreated jute/VE	Alkali treated jute/VE	Permanganate treated jute/VE	Silane treated jute/VE
Tensile property				
Strength (MPa)	42.0	47.3	56.1	63.5
Modulus (GPa)	1.61	1.72	1.84	1.97
Elongation at break (%)	2.0	2.6	2.4	3.2
Flexural property				
Strength (MPa)	56.2	92.6	86.3	99.7
Modulus (GPa)	3.78	5.51	5.34	5.97

9.5.5 Polyester resins

Unidirectional composites

Hughes *et al.* (2007) examined the tensile behaviour of compression moulded 60 vol.% treated and untreated flax fibre/polyester composites. As noted earlier, they found that the stress–strain curves exhibited a distinct knee at a strain of ~0.12%, after which the slope of the curve decreased markedly. The modulus determined before the knee ranged from 28 to 30 GPa with the tensile strength ranging from 165 to 304 MPa and the failure strain ranging from 0.8% to 1.7%. The untreated fibres had the highest tensile strengths and strain to failure. The modulus dropped by 30–50% after the knee. The decrease in modulus was less pronounced for the treated fibre composites than for the untreated fibre composites (Fig. 9.9), indicating that fibre treatment was beneficial to the post-knee performance of the composites.

© Woodhead Publishing Limited, 2014



9.9 Typical stress–strain curves for unreinforced (UP), glass fibre reinforced, unmodified (UnM), propionic anhydride modified (PrA) and methacrylic anhydride modified (MeA) flax fibre reinforced unsaturated polyester composites (Hughes *et al.*, 2007).

Ratna Prasad and Mohana Rao (2011) determined the tensile and flexural properties of 40 vol.% unidirectional jowar, sisal and bamboo fibre/polyester composites fabricated using the hand lay-up compression moulding technique. The tensile modulus and strength ranged from 1.9 to 2.8 GPa and from 66 to 126 MPa, respectively, while the flexural modulus and strength ranged from 2.5 to 7.9 GPa and from 100 to 134 MPa, respectively (Table 9.14). The properties of the sisal fibre composites were substantially poorer than those of the jowar or bamboo composites.

Laranjeira *et al.* (2006) determined the longitudinal and transverse mechanical properties (including impact strength) of long jute fibre/UPE composites fabricated using compression moulding. The fibre weight fraction was varied from 10% to 50%. In the longitudinal direction, all mechanical properties were highest for the 50% composite which had a tensile modulus of 5.6 GPa, a tensile strength of 162 MPa, a strain to failure of 5.3% and an impact strength of 1295 J/m (Table 9.15). The transverse properties decreased with increased fibre loading, except for the impact strength, which was highest for the highest fibre loading.

Brahim and Cheikh (2007) examined the tensile properties of unidirectional alfa fibre/UPE composites fabricated using the wet lay-up technique, having fibre volume fractions of 12–44%. The modulus and strength increased progressively with volume fraction from 6.6 to 12.3 GPa and from

© Woodhead Publishing Limited, 2014

Table 9.14 Mechanical properties of jowar, sisal and bamboo fibre/polyester composites (Ratna Prasad and Mohana Rao, 2011)

Composite	Tensile property		Flexural property	
	Strength (MPa)	Modulus (GPa)	Strength (MPa)	Modulus (GPa)
Cured polyester resin	31.5	0.63	55.1	1.54
Jowar/polyester	124	2.75	134	7.87
Sisal/polyester	65.5	1.90	99.5	2.49
Bamboo/polyester	126	2.48	128	3.70

Table 9.15 Tensile and impact properties of long jute fibre/unsaturated polyester composites (Laranjeira *et al.*, 2006)

Fibre content (% w/w)	Test direction	Mechanical property			
		Tensile strength (MPa)	Tensile modulus (GPa)	Elongation at break (%)	Izod impact strength (J/m)
0	–	34.8	1.36	2.1	22
10	Longitudinal	55.6	3.45	3.3	119
	Transverse	5.3	1.98	0.31	23
20	Longitudinal	110	3.45	3.3	339
	Transverse	8.1	1.96	0.36	21
30	Longitudinal	140	4.84	4.4	439.1
	Transverse	3.9	1.73	0.33	41
40	Longitudinal	142	5.61	4.3	1135
	Transverse	3.8	1.68	0.39	52
50	Longitudinal	162	5.58	5.3	1295
	Transverse	0.43	0.98	0.18	148

75 to 149 MPa, respectively (Table 9.16). The strain to failure also increased from 2.3% to 3.1%. A shear modulus of 2.5 GPa was reported for the 44% composite. The effect of off-axis loading was also examined for a 45 vol.% composite. The tensile modulus and strength in the 0° direction were 12 GPa and 150 MPa, respectively, decreasing progressively to 5 GPa and 18 MPa, respectively, for the 90° direction (Table 9.17).

Nosbi *et al*. (2010) studied the influence of water absorption on the compression properties of 70 wt.% unidirectional kenaf fibre/UPE composites fabricated using pultrusion. The composites were soaked in distilled water, seawater and acidic solution at room temperature. The compression properties of the composites are given in Table 9.18. The compression properties of the composites were marginally reduced after soaking in distilled water. However, the composites soaked in seawater and acidic solution had

© Woodhead Publishing Limited, 2014

Table 9.16 Longitudinal tensile properties of unidirectional alfa/unsaturated polyester composites with different fibre volume fractions (Brahim and Cheikh, 2007)

Fibre volume faction (%)	Modulus (GPa)	Stress (MPa)	Strain (%)
0	4.1	64	2.7
12	6.6	75	2.3
21	8.2	96	2.3
32	10.2	118	2.6
44	12.3	149	3.1

Table 9.17 Tensile properties of 45% unidirectional alfa/unsaturated polyester composites for different angles of loading (Brahim and Cheikh, 2007)

Angle between the fibres and tensile load (degree)	Modulus (GPa)	Strength (MPa)
0	12.3	150
10	11.5	104
30	8.1	43
45	6.4	33
90	5.0	18

significantly lower compression properties than the dry composites, except for the failure strain which was slightly higher than for the dry composite.

Knitted composites

Goutianos *et al*. (2006) examined the mechanical properties of unidirectional warp knitted flax/UPE composites fabricated using both the hand lay-up and RTM techniques. The fibre volume fraction of the composites was 28% for the hand lay-up technique and 31% for the RTM technique. The tensile and flexural properties of the composites are given in Table 9.19. The longitudinal (l) and transverse (t) modulus and strength for the hand laid-up composite were 14 GPa (l) and 2 GPa (t) and 140 MPa (l) and 12 MPa (t), respectively, while the flexural moduli and strength were 15 GPa (l) and 3 GPa (t) and 170 MPa (l) and 32 MPa (t), respectively. The RTM composites had a marginally higher longitudinal tensile strength of 143 MPa and a substantially higher flexural strength, in both the longitudinal and transverse directions, of 198 and 49 MPa, respectively. Only marginal increases in the flexural moduli were obtained.

Fabric composites

Thiruchitrambalam *et al*. (2009) examined the mechanical properties of 40% non-woven and woven banana-kenaf hybrid fibre/UPE composites.

© Woodhead Publishing Limited, 2014

Table 9.18 Compression properties of unidirectional kenaf fibre/unsaturated polyester composites (Nosbi *et al.*, 2010)

Condition	Strength (MPa)	Young's modulus (GPa)	Failure strain (%)
No soaking	45.3	2.32	31.4
Distilled water	40.7	1.57	28.3
Seawater	32.4	1.02	36.0
Acidic solution	32.7	1.02	35.3

Table 9.19 Mechanical properties of unidirectional warp knitted flax/unsaturated polyester composites (Goutianos *et al.*, 2006)

Mechanical property	Technique	
	Hand lay-up	RTM
Tensile property		
Longitudinal direction		
Strength (MPa)	140	143
Modulus (GPa)	14	14
Transverse direction		
Strength (MPa)	12	–
Modulus (GPa)	2	–
Flexural property		
Longitudinal direction		
Strength (MPa)	170	198
Modulus (GPa)	15	17
Transverse direction		
Strength (MPa)	32	49
Modulus (GPa)	3	4

The non-woven hybrid fibres and woven hybrid fabrics were chemically treated with 10% NaOH and 10% sodium lauryl sulphate ($NaC_{12}H_{25}SO_4$). The tensile strength, flexural strength and impact strength were higher for the woven composites than for their non-woven counterparts. The composites treated with sodium lauryl sulphate had higher mechanical properties than those treated with NaOH.

Munikenche Gowda *et al.* (1999) determined a wide range of mechanical properties for 45 vol.% woven jute fabric/polyester composites fabricated using the hand lay-up method (Table 9.20). The tensile modulus and strength in the longitudinal direction were 7.0 GPa and 60 MPa, respectively, with substantially lower values of 3.5 GPa and 35 MPa, respectively, being obtained for the transverse direction. The flexural modulus and strength were 5.1 GPa and 93 MPa, respectively, the compression modulus and strength were 2.1 GPa and 45 MPa, respectively, while the in-plane shear modulus

© Woodhead Publishing Limited, 2014

and strength were 2.2 GPa and 17 MPa, respectively. The short beam shear strength was 10 MPa, while the impact strength was 29 kJ/m^2.

Ahmed *et al*. (2006) determined a similar range of mechanical properties for 43 wt.% woven jute fabric/isophthalic polyester composites fabricated using hand lay-up. In this case, the tensile modulus and strength in the warp direction were 9.6 GPa and 80 MPa, respectively. Substantially lower values of 5.8 GPa and 41 MPa, respectively, were again obtained for the transverse (weft) direction. The flexural modulus and strength were 7.6 GPa and 122 MPa, respectively, while the in-plane shear modulus and strength were 1.7 GPa and 21 MPa, respectively. The interlaminar shear strength was 13.9 MPa. The impact strength was also determined for a similar composite, however, with a fibre weight fraction of 47%, with a value of 32 kJ/m^2 being obtained (Table 9.21).

De Carvalho *et al*. (2006) determined the impact strength of jute fabric/unsaturated orthophthalic polyester composites fabricated using compression moulding, in the warp and weft direction, as well as in the 45° direction.

Table 9.20 Mechanical properties of jute fabric/polyester composites (Munikenche Gowda *et al.,* 1999)

Property	Polyester resin		Jute fabric/polyester	
	Strength	Modulus	Strength	Modulus
Tensile in longitudinal direction	12.1 MPa	1.4 GPa	60 MPa	7.0 GPa
Tensile in transverse direction	–	–	35 MPa	3.5 GPa
Flexure	48.0 MPa	2.2 GPa	92.5 MPa	5.1 GPa
Compression	47.1 MPa	0.94 GPa	45 MPa	2.1 GPa
In-plane shear	–	–	16.5 MPa	2.2 GPa
Interlaminar shear	–	–	10 MPa	–
Impact strength	1.76 kJ/m^2		29 kJ/m^2	–

Table 9.21 Mechanical properties of jute fabric/polyester composites (Ahmed *et al*, 2006)

Property	Polyester resin		Jute fabric/polyester		
	Strength	Modulus	Strength	Modulus	Strain at failure
Tensile in warp direction	43.6 MPa	4.4 GPa	80.2 MPa	9.6 GPa	1.6%
Tensile in weft direction	–	–	40.5 MPa	5.8 GPa	1.5%
Flexure	92.4 MPa	2.5 GPa	121.8 MPa	7.6 GPa	–
In-plane shear	–	–	20.8 MPa	1.7 GPa	–
Interlaminar shear	–	–	13.9 MPa	–	
Impact strength	4.48 kJ/m^2		31.9 kJ/m^2	–	

© Woodhead Publishing Limited, 2014

Two types of the jute fabric were examined, these being plain weave (PWF) and plain weft knit (WKT) fabric, both at fibre weight fractions of approximately 25% and 40%. The impact strength in the warp direction only was also determined for a 46% WKT. The impact strengths were similar in the warp and weft directions for both types of fabric, but substantially lower in the 45° direction (Table 9.22). The impact strength increased with fibre fraction for both types of fabric.

Sever *et al.* (2010) determined the tensile, flexure and interlaminar shear properties of 35% woven jute fabric/polyester composites fabricated using hand lay-up compression moulding. Untreated, 2% NaOH treated, and 0.1%, 0.3% and 0.5% γ-methacryloxypropyltrimethoxysilane (γ-MPS) treated composites were examined. The 0.3% silane treated composites gave the highest tensile, flexure and interlaminar shear properties (Table 9.23).

Mat composites

Monteiro *et al.* (2008) determined the flexural strength of coir fibre/UPE composites fabricated by compression moulding. Two types of fibre preform were used, namely tangled fibres and pressed mats, both processed with moulding pressures of 2.6 and 5.2 MPa. Fibre weight fractions of 10–80% were examined. For both preforms, and both moulding pressures, the highest flexural strength was obtained at a weight fraction of 10%, with the strength then decreasing progressively with increased fibre weight fraction (Table 9.24). The flexural strength was higher for the tangled coir composites than for the pressed mat composites, particularly as the fibre weight fraction increased.

Kushwaha and Kumar (2010) examined the effect of acrylonitrile treatment (cyanoethylation) for 1–5 h on the mechanical properties of bamboo mat/UPE composites fabricated using the hand lay-up technique. The tensile properties were improved by the treatment, but the flexural properties were decreased. The tensile modulus was 4.2 GPa for the untreated bamboo composites and 5.8–8.4 GPa for the treated composites, while the corresponding

Table 9.22 Influence of fabric orientation on impact strength (%) of jute fabric/polyester composites (de Carvalho *et al.*, 2006)

Jute/polyester composite	Fabric orientation		
	0° (Weft direction)	45°	90° (Wrap or fill direction)
24.9% PWF	157	116	150
38.0% PWF	340	289	371
24.9% WKT	168	163	165
40.9% WKT	385	315	351
46.0% WKT	521	–	–

© Woodhead Publishing Limited, 2014

Table 9.23 Mechanical properties of the untreated and treated jute fabric/polyester composites (Sever *et al.*, 2010)

Jute/polyester composite	Tensile property			Flexural property		Shear property
	Strength (MPa)	Modulus (GPa)	Elongation at break (%)	Strength (MPa)	Modulus (GPa)	Interlaminar shear strength (MPa)
Untreated jute	47.6	4.4	1.2	63.7	3.5	8.9
NaOH treated jute	49.6	5.6	1.3	62.3	4.0	9.9
NaOH and 0.1% γ-MPS treated jute	65.6	6.3	1.8	74.8	5.1	14.7
NaOH and 0.3% γ-MPS treated jute	74.6	6.3	2.0	81.5	5.9	16.8
NaOH and 0.5% γ-MPS treated jute	54.7	6.1	1.4	68.8	4.6	11.5

Table 9.24 Flexural strength of coir fibre/unsaturated polyester composites (Monteiro *et al.*, 2008)

Fibre weight fraction (%)	Preform type			
	Tangled coir fibre/polyester		Pressed coir mat/polyester	
	Moulding pressure (MPa)		Moulding pressure (MPa)	
	2.6	5.2	2.6	5.2
	Strength (MPa)	Strength (MPa)	Strength (MPa)	Strength (MPa)
10	29.1	32.8	25.7	31.2
20	28.2	29.5	18.9	22.6
30	22.5	24.7	14.5	21.4
40	20.7	23.9	9.6	11.4
50	15.5	21.1	6.0	11.9
60	6.7	14.3	4.3	5.9
70	5.4	8.8	3.0	4.6
80	3.6	6.1	0.9	1.0

tensile strengths were 74 and 84 to 97 MPa, respectively. The flexural modulus was 4.4 GPa for the untreated bamboo composite, but only 2.5–4.2 GPa for the treated ones. The flexural strength was 107 MPa for the untreated composite, but only 78–79 MPa for the treated counterparts.

© Woodhead Publishing Limited, 2014

Non-woven felt composites

Hughes *et al*. (2002) determined the mechanical properties of 20 vol.% non-woven jute and hemp felt/UPE composites fabricated using vacuum infusion (Table 9.25). The tensile modulus was similar for both composites. However, the jute/polyester composites had better tensile strength than their hemp/polyester counterparts, while the hemp/polyester composites had higher fracture toughness than their jute/polyester counterparts.

Yarn composites

Akil *et al*. (2009) examined the effect of water absorption in various solutions on the mechanical properties of continuous twisted roving jute fibre/UPE composites fabricated using pultrusion. The solutions examined were distilled water, sea water (pH of 8) and an acidic solution (pH of 3). For all solutions, the flexural and compression properties of the composite decreased with increased immersion time.

9.5.6 Phenolic resins

Woven composites

Milanese *et al*. (2012a) examined the effect of thermal treatment on the tensile and flexural strength of 33 wt.% untreated and thermally treated woven sisal fabric/phenolic resin composites fabricated using compression moulding. The thermal treatment was carried out by heat treating the fabric at 60°C for 72 h which replicates drying of the fabric. It did not, however, produce any appreciable change in the tensile or flexural strength of the composites (Table 9.26).

9.5.7 Acrylic resins

Medina *et al*. (2009) examined the effect of processing pressure on the flexural and impact strength of 50:50 hemp-kenaf needle punched mat/acrylic resin composites. The mat was impregnated with 22 wt.% acrylic resin using

Table 9.25 Mechanical properties of 20 vol.% non-woven jute and hemp felt/unsaturated polyester composites (Hughes *et al.*, 2002)

Property	Unsaturated polyester	Non-woven jute/polyester	Non-woven hemp/polyester
Young's modulus (GPa)	3.80	6.79	6.70
Tensile strength (MPa)	49.10	47.35	37.82
Fracture toughness (MPa.m$^{1/2}$)	0.62	2.56	3.51

© Woodhead Publishing Limited, 2014

Table 9.26 Tensile and flexural strength of woven sisal fabric/phenolic composites (Milanese *et al.*, 2012a)

Property	Phenolic resin	Composite	
		Untreated sisal/phenolic	Thermally treated sisal/phenolic
Tensile strength at yield (MPa)	4.9	25.2	24.9
Flexural strength (MPa)	8.6	10.7	11.2

Table 9.27 Flexural and impact properties of 50:50 hemp-kenaf mat/acrylic resin composites in the machine direction (MD) and the cross direction (CD) (Medina *et al.*, 2009)

Pressure (bar)	Flexural modulus (MPa)		Flexural strength (MPa)		Elongation (%)		Impact strength (kJ/m^2)	
	MD	CD	MD	CD	MD	CD	MD	CD
15	2924	3500	46	48	2.7	2.3	8.8	9.7
20	3055	3302	51	51	2.9	2.7	9.2	10.7
30	3416	4141	57	63	2.6	2.4	9.9	11.8
60	4805	5301	79	85	2.5	2.5	11.0	12.4
80	3340	3681	73	66	3.8	3.2	12.5	12.7
100	2787	3435	64	70	3.8	3.2	13.2	12.6
150	2271	2138	44	57	3.2	5.4	12.8	12.4
200	1977	1870	52	46	4.2	4.5	13.1	13.6

a foulard system. The impregnated mats were then hot pressed using pressures of 15, 20, 30, 60, 80, 100, 150 and 200 bar and the mechanical properties measured in the machine direction (MD) and cross direction (CD) (Table 9.27). The flexural and impact strength were generally slightly higher in the CD than in the MD. The highest flexural modulus and strength were obtained using a pressure of 60 bar; however, the highest impact strength was obtained using a pressure of 200 bar.

9.6 Bioderived resin composites

9.6.1 Epoxidized plant oil-based resins

Boquillon (2006) examined 28 vol.% hemp fibre reinforced/ ELO-based resin composites fabricated using hot pressing. The length and diameter of the hemp fibres used were 6 mm and 40 μm, respectively. The flexural modulus and strength of the composites were 5.6 GPa and 91 MPa, respectively, compared with 1.8 GPa and 60 MPa, respectively, for the neat ELO-based resin. Good fibre matrix adhesion was reported.

© Woodhead Publishing Limited, 2014

Williams and Wool (2000) examined the tensile properties of 20 wt.% non-woven hemp fibre mat/AESO composites fabricated using RTM. The tensile modulus and strength of the composites were 4.4 GPa and 35 MPa, respectively.

The dynamic mechanical properties of hemp fibre mat/AESO composites fabricated using vacuum-assisted RTM were also examined by O'Donnell *et al*. (2004). The storage modulus and loss modulus of the composites were 2.16 and 0.27 GPa, respectively, compared with 1.11 and 0.068 GPa, respectively, for the neat resin.

Ramamoorthy *et al*. (2012) examined the mechanical properties of 40 wt.% unidirectional non-woven and biaxial-woven jute/AESO composites fabricated using compression moulding. The jute fibres were treated with 4 wt.% NaOH before composite fabrication. The unidirectional composites had better tensile properties than the cross-woven composites. The flexural strength was also slightly higher; however, the flexural modulus was marginally lower.

Åkesson *et al*. (2009) examined the mechanical properties of 70 wt.% flax mat/AESO composites fabricated using spray impregnation followed by compression moulding. The tensile modulus and strength of the composites were 9.7 GPa and 78 MPa, respectively, while the flexural modulus and strength were 6.9 GPa and 98 MPa, respectively.

Adekunle *et al*. (2011) prepared 60 wt.% biaxial-woven jute fabric/MMSO composites using impregnation followed by compression moulding. Three different areal weights of jute fabric were used, namely 100, 240 and 300 g/m^2. The jute fibres were treated with 4% NaOH. The mechanical properties of the jute/MMSO composites ranged from 14 to 19 GPa for the tensile modulus, from 65 to 84 MPa for the tensile strength, from 5 to 8.5 GPa for the flexural modulus, from 20 to 137 MPa for the flexural strength, and from 11 to 13 kJ/m^2 for the Charpy impact resistance.

9.6.2 Protein-based resins

Lodha and Netravali (2005) examined the mechanical properties of 45 wt.% unidirectional ramie fibre/SPI composites and unidirectional ramie fibre/stearic acid modified soy protein isolate (MSPI) composites. The tensile modulus and fracture stress were higher for the MSPI composites than for their SPI counterparts in both the longitudinal and transverse directions (Table 9.28). The flexural modulus and strength were also higher in both directions for the MSPI composites (Table 9.29).

The tensile properties of 54–58% sisal fibre/SPC composites were examined by Kim and Netravali (2010a). The fibres were pre-treated with 2 M NaOH. The tensile modulus and strength of the untreated fibre composites (58% fibre volume fraction) were 2.8 GPa and 168 MPa, respectively, while

© Woodhead Publishing Limited, 2014

Table 9.28 Tensile properties of ramie fibre/SPI and MSPI composites (Lodha and Netravali, 2005)

Composite	Test direction	Young's modulus (GPa)	Fracture stress (MPa)
Ramie fibre/SPI	Longitudinal	3.4	180
	Transverse	0.25	6.6
Ramie fibre/MSPI	Longitudinal	5.8	268
	Transverse	1.3	9.6

Table 9.29 Flexural properties of ramie fibre/SPI and MSPI composites (Lodha and Netravali, 2005)

Composite	Test direction	Chord modulus (GPa)	Flexural stress (MPa)
Ramie fibre/SPI	Lengthwise	7.3	107
	Crosswise	0.72	14.3
Ramie fibre/MSPI	Lengthwise	14.0	185
	Crosswise	2.7	22.7

Table 9.30 Tensile properties of ramie fibre/SF and MSF composites (Kim and Netravali, 2010a)

Composite	Test direction	Young's modulus (GPa)	Fracture stress (MPa)
Ramie fibre/SF	Longitudinal	2.9	88
	Transverse	0.27	2.8
Ramie fibre/MSF	Longitudinal	3.2	104
	Transverse	0.60	6.0

for the treated fibre composites (54–57 vol.%), they were 3.4–3.8 GPa and 170–189 MPa, respectively.

Kim and Netravali (2010b) also determined the tensile properties of 50 wt.% unidirectional ramie fibre/defatted SF and MSF composites in both the longitudinal and transverse directions. The tensile modulus and strength of the SF composites were 2.9 GPa and 88 MPa, respectively, in the longitudinal direction and 0.3 GPa and 2.8 MPa in the transverse direction (Table 9.30). Higher values were obtained for the MSF composites, with the tensile modulus and strength being 3.2 GPa and 104 MPa, respectively, in the longitudinal direction and 0.6 GPa and 6 MPa, respectively, in the transverse direction. The better properties of the MSF composites were attributed to the higher protein content. Chabba *et al*. (2005) determined the tensile and flexural behaviour of 60 wt.% unidirectional bleached flax yarn/CSF composites fabricated using hot pressing. The

© Woodhead Publishing Limited, 2014

tensile modulus and tensile strength were 3.7 GPa and 260 MPa, respectively, while the flexural modulus and strength were 10.4 GPa and 175 MPa, respectively.

9.6.3 Bio-based polyurethane resins

Bakare *et al.* (2010) determined the tensile and flexural properties of unidirectional sisal fibre/RSO-based PU composites containing 20, 25 and 30 wt.% fibres. The fibres were pre-treated with 5% w/v NaOH. The composites were fabricated by compression moulding using a closed mould. The best properties were generally obtained for the 25% fibre loading with values of 2.2 GPa and 78 MPa for the tensile modulus and strength, respectively, and 3.3 GPa and 103 MPa for the flexural modulus and strength (Table 9.31). The highest tensile strength of 119 MPa was, however, obtained for the 30% composite.

Silva *et al.* (2006) examined the fracture toughness of untreated and 10% NaOH treated woven sisal fabric/castor oil PU composites fabricated using compression moulding. The fibre volume fraction was varied from 18% to 30% and from 22% to 40% for the untreated and treated sisal fabric/castor oil PU composites, respectively. The fracture toughness was considerably higher for the untreated sisal fabric/castor oil PU composites than for the treated sisal fabric/castor oil PU composites. The fracture toughness also improved with increased fibre volume fraction.

Mistri *et al.* (2011) compared the flexural and impact properties of 60 wt.% non-woven jute/maleated castor oil (MACO) composites with those of 60 wt.% non-woven jute/UPE composites. The flexural modulus was 1.7 and 1.8 GPa for the jute/MACO composites and for the jute/UPE composites, respectively, whereas the flexural strength was 14 and 34 MPa for the jute/MACO composites and for the jute/UPE composites, respectively. In addition, the impact strength was substantially higher (42%) for the jute/MACO composite than for the jute/UPE counterpart.

Milanese, Cioffi and Voorwald examined the tensile (Milanese *et al.*, 2011) and flexural properties (Milanese *et al.*, 2012b) of 44 wt.% woven sisal fabric/COPU composites fabricated using compression moulding. The fabrics were used in the undried condition and after drying at 60°C for 72 h. The tensile strength was the same for both composites, with a value of 17 MPa; however, the flexural strength was substantially higher for the dried composite than for the undried composite, with values of 3.7 MPa and 1.6 MPa, respectively, being obtained (Table 9.32).

9.6.4 Bio-based phenolic resins

Maffezzoli *et al.* (2004) produced alkaline-catalyzed cashew nut shell (CNSL) bio-based phenolic resin composites with flax, hemp, ramie and jute

© Woodhead Publishing Limited, 2014

Table 9.31 Tensile and flexural properties of sisal fibre/rubber seed oil polyurethane (RSOPU) composites (Bakare *et al.*, 2010)

Fibre loading (wt.%)	Tensile property		Flexural property	
	Tensile modulus (GPa)	Tensile strength (MPa)	Flexural modulus (GPa)	Flexural strength (MPa)
0	0.43	4.8	0.92	53.2
20	1.85	60.8	2.89	76.7
25	2.16	78.0	3.25	102.8
30	1.81	118.6	3.09	96.1

Table 9.32 Tensile and flexural properties of undried and dried woven sisal fabric/castor oil-based polyurethane composites (Milanese *et al.*, 2011, 2012b)

Tensile property	Castor oil-based polyurethane	Composite	
		Undried sisal/castor oil-based polyurethane	Dried sisal/castor oil-based polyurethane
Tensile strength at yield (MPa)	2.5	17.0	16.9
Elongation at yield (%)	29.4	8.0	6.2
Elongation at break (%)	31.2	11.3	8.0
Flexural strength (MPa)	0.45	1.6	3.7

Table 9.33 Tensile properties of sisal/bio-based phenolic resin mixed with epoxy resin composites (Barreto *et al.*, 2010)

Condition	Yield stress (MPa)	Ultimate stress (MPa)
Untreated	13.5	18.3
5% NaOH	20.0	23.5
10% NaOH	5.7	6.5

fibres with fibre contents of 13–15 wt.%. The best properties were obtained for the hemp and ramie composites which both had a modulus of 1.8 GPa and a strength of 20 MPa. Aziz and Ansell (2004) also produced jute and hemp CNSL composites using hot pressing. These had significantly better tensile properties to equivalent composites with a conventional polyester matrix. However, a temperature of 180°C and a pressure of 6–8 MPa were required. Barreto *et al.* (2010) examined the tensile properties of composites made from jute fibre with a matrix of bio-based phenolic resin mixed with epoxy resin, fabricated using impregnation. The best properties were obtained using the 5% NaOH treatment, with values of 20 and 24 MPa

© Woodhead Publishing Limited, 2014

being obtained for the yield strength and ultimate strength, respectively (Table 9.33).

9.6.5 Lactic acid-based thermoset resins

Åkesson *et al*. (2011) examined the mechanical properties of non-woven flax mat/LA-based thermoset composites, with various fibre loadings, fabricated using spray impregnation followed by compression moulding. The optimum properties were obtained with 70 wt.% fibre for which the tensile modulus and strength were 9 GPa and 62 MPa, respectively. The storage modulus and loss modulus at 20°C were 9.3 and 0.3 GPa, respectively.

9.7 Applications of thermoset matrix natural fibre composites

The applications envisaged for thermoset matrix natural fibre composites are mostly as a replacement for fibreglass and include building and construction, automotive, leisure and sporting goods, and aircraft interiors. Some examples are shown Figs 9.10–9.12. In many applications, cost minimization is of prime importance, and mats have been considered as the most appropriate form for the fibre reinforcement. Recently, both unidirectional and cross-woven (0/90°) fabrics have become commercially available and these will allow higher performance products to be produced, although at a higher cost. The production of fabrics from natural fibres



9.10 Resin transfer moulded natural fibre composite hood. (Source: Courtesy Composites Innovation Centre.)

© Woodhead Publishing Limited, 2014



9.11 Natural fibre composite canoe. (*Source*: Courtesy Composites Evolution Ltd.)



9.12 Natural fibre composite sailboards. (*Source*: Courtesy Lineo.)

requires that the fibres, which have only limited length, be first formed into continuous yarns. This can be done by spinning, whereby the individual fibres are twisted together into a continuous length. However, this causes the fibres to have helical rather than linear trajectories as shown in Fig. 9.1a. As a result, the reinforcement efficiency of the yarn is reduced. Alternatively, the fibres can be held together without twisting by overwrapping them with a yarn as shown in Fig. 9.1b. This produces straighter fibres, which improves the reinforcement efficiency of the yarn, but the process is more laborious.

© Woodhead Publishing Limited, 2014

9.8 Future trends

Thermoset matrix natural fibre composites have a clear potential as a more environmentally friendly alternative to fibreglass. However, unlike glass fibres, the properties of natural fibres vary from species to species, from crop to crop, and even with location in the plant. This poses problems for the end users. In order to develop a successful industry it will be necessary to establish a rigorous system for grading incoming fibres. Some insight might be provided from the textiles industry, which has already addressed this problem.

Once the fibres are graded, a methodology will be required for predicting the performance of the resulting composite over a range of loading, environmental and other conditions. This will require knowledge of the strength limiting factors under different loading conditions, as well as the effect of different environmental and other conditions on the composite. It is considered that the Load and Resistance Factor Design methodology (also known as Limit State Design (Head, 1994)), which applies knock-down factors to the design allowables to account for different contingencies, may be useful in this respect.

9.9 Sources of further information and advice

Baillie, C., ed. (2004). *Green Composites: Polymer Composites and the Evironment*, Woodhead Publishing.

Fakirov, S., Bhattacharyya, D., Hanser (2007). *Handbook of Engineering Biopolymers: Homopolymers, Blends and Composites*.

Karak, N. (2012). *Vegetable Oil-based Polymers: Properties, Processing and Applications*, Woodhead Publishing.

Mohanty, A.K., Misra, M., Drzal, L.T., eds (2005). *Natural Fibers, Biopolymers and Biocomposites*, Taylor & Francis.

Pickering, K.L., ed. (2008). *Properties and Performance of Natural Fibre Composites*, Woodhead Publishing.

Summerscales J., Dissanayake, N., Virk A.S. and Hall W. (2010). A review of bast fibres and their composites. Part 2 – Composites, *Composites Part A*, **41**(10), 1336–1344.

Wool, R.P., Sun, X.S. (2005). *Bio-based Polymers and Composites*, Elsevier.

9.10 References

Abdullah, A, Khalina, A and Ali, A (2011), 'Effects of fiber volume fraction on unidirectional kenaf/epoxy composites: the transition region', *Polymer-Plastics Technology and Engineering,* vol. **50**, no. 13, pp. 1362–1366.

Adekunle, K, Patzelt, C, Kalantar, A and Skrifvars, M (2011), 'Mechanical and viscoelastic properties of soybean oil thermoset reinforced with jute fabrics and carded lyocell fiber', *Journal of Applied Polymer Science,* vol. **122**, no. 5, pp. 2855–2863.

© Woodhead Publishing Limited, 2014

Ahmed, KS, Vijayarangan, S and Rajput, C (2006), 'Mechanical behavior of isothalic polyester-based untreated woven jute and glass fabric hybrid composites', *Journal of Reinforced Plastics and Composites,* vol. **25**, no. 15, pp. 1549–1569.

Åkesson, D, Skrifvars, M, Seppälä, J and Turunen, M (2011), 'Thermoset lactic acid-based resin as a matrix for flax fibers', *Journal of Applied Polymer Science,* vol. **119**, no. 5, pp. 3004–3009.

Åkesson, D, Skrifvars, M and Walkenström, P (2009), 'Preparation of thermoset composites from natural fibres and acrylate modified soybean oil resins', *Journal of Applied Polymer Science,* vol. **114**, no. 4, pp. 2502–2508.

Akil, HM, Cheng, LW, Mohd Ishak, ZA, Abu Bakar, A and Abd Rahman, MA (2009), 'Water absorption study on pultruded jute fibre reinforced unsaturated polyester composites', *Composites Science and Technology,* vol. **69**, no. 11–12, pp. 1942–1948.

Aranguren, MI and Reboredo, MM (2007), 'Plant-based reinforcements for thermosets: matrices, processing, and properties', in S Fakirov and D Bhattacharyya (eds.), *Handbook of Engineering Biopolymers: Homopolymers, Blends and Composites*, Hanser Munich.

Aziz, SH and Ansell, MP (2004), 'The effect of alkalization and fibre alignment on the mechanical and thermal properties of kenaf and hemp bast fibre composites: Part 2 – cashew nut shell liquid matrix', *Composites Science and Technology,* vol. **64**, no. 9, pp. 1231–1238.

Bachtiar, D, Sapuan, SM and Hamdan, MM (2008), 'The effect of alkaline treatment on tensile properties of sugar palm fibre reinforced epoxy composites', *Materials & Design,* vol. **29**, no. 7, pp. 1285–1290.

Bachtiar, D, Sapuan, S and Hamdan, M (2009), 'The influence of alkaline surface fibre treatment on the impact properties of sugar palm fibre-reinforced epoxy composites', *Polymer-Plastics Technology and Engineering,* vol. **48**, no. 4, pp. 379–383.

Bakare, IO, Okieimen, FE, Pavithran, C, Abdul Khalil, HPS and Brahmakumar, M (2010), 'Mechanical and thermal properties of sisal fiber-reinforced rubber seed oil-based polyurethane composites', *Materials & Design,* vol. **31**, no. 9, pp. 4274–4280.

Barreto, A, Esmeraldo, M, Rosa, D, Fechine, P and Mazzetto, S (2010), 'Cardanol biocomposites reinforced with jute fiber: microstructure, biodegradability, and mechanical properties', *Polymer Composites,* vol. **31**, no. 11, pp. 1928–1937.

Biermann, U, Friedt, W, Lang, S, Lühs, W, Machmüller, G, Metzger, JO, Ruesch gen Klaas, M, Schaefer, HJ and Schneider, MP (2000), 'New syntheses with oils and fats as renewable raw materials for the chemical industry', *Angewandte Chemie International Edition,* vol. **39**, no. 13, pp. 2206–2224.

Bisanda, ETN and Ansell, MP (1992), 'Properties of sisal-CNSL composites', *Journal of Materials Science*, vol. **27**, no. 6, pp. 1690–1700.

Bledzki, A, Fink, HP and Specht, K (2004), 'Unidirectional hemp and flax EP-and PP-composites: influence of defined fiber treatments', *Journal of Applied Polymer Science,* vol. **93**, no. 5, pp. 2150–2156.

Boquillon, N (2006), 'Use of an epoxidized oil-based resin as matrix in vegetable fibers-reinforced composites', *Journal of Applied Polymer Science,* vol. **101**, no. 6, pp. 4037–4043.

© Woodhead Publishing Limited, 2014

Brahim, SB and Cheikh, RB (2007), 'Influence of fibre orientation and volume fraction on the tensile properties of unidirectional Alfa-polyester composite', *Composites Science and Technology,* vol. **67**, no. 1, pp. 140–147.

Chabba, S, Matthews, G and Netravali, A (2005), "'Green'composites using cross-linked soy flour and flax yarns', *Green Chemistry,* vol. **7**, no. 8, pp. 576–581.

Charlet, K, Baley, C, Morvan, C, Jernot, JP, Gomina, M and Bréard, J (2007), 'Characteristics of Hermès flax fibres as a function of their location in the stem and properties of the derived unidirectional composites', *Composites Part A: Applied Science and Manufacturing,* vol. **38**, no. 8, pp. 1912–1921.

De Carvalho, L, Cavalcante, J and d'Almeida, J (2006), 'Comparison of the mechanical behavior of plain weave and plain weft knit jute fabric-polyester-reinforced composites', *Polymer-Plastics Technology and Engineering,* vol. **45**, no. 7, pp. 791–797.

Dwan'Isa, JPL, Mohanty, AK, Misra, M and Drzal, T (2005), 'Biobased polyurethanes and their composites; present status and future perspectives', in AK Mohanty, M Misra and LT Drzal (eds.), *Natural Fibers, Biopolymers and Biocomposites*, Taylor & Francis Boca Raton.

Goutianos, S, Peijs, T, Nystrom, B and Skrifvars, M (2006), 'Development of flax fibre based textile reinforcements for composite applications', *Applied Composite Materials,* vol. **13**, no. 4, pp. 199–215.

Head, P (1994), Limit state design method, in L Hollaway (ed.), *Handbook of Polymer Composites for Engineers*, Woodhead Publishing Limited Cambridge.

Hepworth, DG, Bruce, DM, Vincent, JFV and Jeronimidis, G (2000), 'The manufacture and mechanical testing of thermosetting natural fibre composites', *Journal of Materials Science*, vol. **35**, no. 2, pp. 293–298.

Hughes, M, Carpenter, J and Hill, C (2007), 'Deformation and fracture behaviour of flax fibre reinforced thermosetting polymer matrix composites', *Journal of Materials Science,* vol. **42**, no. 7, pp. 2499–2511.

Hughes, M, Hill, C and Hague, J (2002), 'The fracture toughness of bast fibre reinforced polyester composites Part 1 Evaluation and analysis', *Journal of Materials Science,* vol. **37**, no. 21, pp. 4669–4676.

Karak, N (2012), *Vegetable Oil-Based Polymers: Properties, Processing and Applications*, Woodhead Publishing Limited, Cambridge.

Kim, JT and Netravali, AN (2010a), 'Mercerization of sisal fibers: effect of tension on mechanical properties of sisal fiber and fiber-reinforced composites', *Composites Part A: Applied Science and Manufacturing,* vol. **41**, no. 9, pp. 1245–1252.

Kim, JT and Netravali, AN (2010b), 'Mechanical, thermal, and interfacial properties of green composites with ramie fiber and soy resins', *Journal of Agricultural and Food Chemistry,* vol. **58**, no. 9, pp. 5400–5407.

Kushwaha, PK and Kumar, R (2010), 'Studies on performance of acrylonitrile-pretreated bamboo-reinforced thermosetting resin composites', *Journal of Reinforced Plastics and Composites,* vol. **29**, no. 9, pp. 1347–1352.

Laranjeira, E, De Carvalho, L, Silva, SML and D'almeida, J (2006), 'Influence of fiber orientation on the mechanical properties of polyester/jute composites', *Journal of Reinforced Plastics and Composites,* vol. **25**, no. 12, pp. 1269–1278.

Li, Y, Mai, YW and Ye, L (2005), 'Effects of fibre surface treatment on fracture-mechanical properties of sisal-fibre composites', *Composite Interfaces,* vol. **12**, no. 1, 141–163.

© Woodhead Publishing Limited, 2014

Lodha, P and Netravali, AN (2005), 'Characterization of stearic acid modified soy protein isolate resin and ramie fiber reinforced 'green' composites', *Composites Science and Technology,* vol. **65**, no. 7–8, pp. 1211–1225.

Maffezzoli, A, Calo, E, Zurlo, S, Mele, G, Tarzia, A and Stifani, C (2004), 'Cardanol based matrix biocomposites reinforced with natural fibres', *Composites Science and Technology*, vol. **64**, no. 6, pp. 839–845.

Masoodi, R and Pillai, KM (2012), 'A study on moisture absorption and swelling in bio-based jute-epoxy composites', *Journal of Reinforced Plastics and Composites,* vol. **31**, no. 5, pp. 285–294.

Medina, L, Schledjewski, R and Schlarb, AK (2009), 'Process related mechanical properties of press molded natural fiber reinforced polymers', *Composites Science and Technology,* vol. **69**, no. 9, pp. 1404–1411.

Milanese, AC, Cioffi, MOH and Voorwald, HJC (2011), 'Mechanical behavior of natural fiber composites', *Procedia Engineering,* vol. **10**, pp. 2022–2027.

Milanese, AC, Cioffi, MOH and Voorwald, HJC (2012a), 'Thermal and mechanical behaviour of sisal/phenolic composites', *Composites Part B: Engineering,* vol. **43**, no. 7, pp. 2843–2850.

Milanese, AC, Cioffi, MOH and Voorwald, HJC (2012b), 'Flexural behavior of sisal/castor oil-based polyurethane and sisal/phenolic composites', *Materials Research,* vol. **15**, no. 2, pp. 191–197.

Mishra, H, Dash, B, Tripathy, S and Padhi, B (2000), 'A study on mechanical performance of jute-epoxy composites', *Polymer-Plastics Technology and Engineering,* vol. **39**, no. 1, pp. 187–198.

Mistri, E, Routh, S, Ray, D, Sahoo, S and Misra, M (2011), 'Green composites from maleated castor oil and jute fibres', *Industrial Crops and Products,* vol. **34**, no. 1, pp. 900–906.

Monteiro, SN, Terrones, LAH and D'Almeida, JRM (2008), 'Mechanical performance of coir fiber/polyester composites', *Polymer Testing,* vol. **27**, no. 5, pp. 591–595.

Munikenche Gowda, T, Naidu, ACB and Chhaya, R (1999), 'Some mechanical properties of untreated jute fabric-reinforced polyester composites', *Composites Part A: Applied Science and Manufacturing,* vol. **30**, no. 3, pp. 277–284.

Nosbi, N, Akil, HM, Mohd Ishak, ZA and Abu Bakar, A (2010), 'Degradation of compressive properties of pultruded kenaf fiber reinforced composites after immersion in various solutions', *Materials & Design,* vol. **31**, no. 10, pp. 4960–4964.

O'Brien, RN and Hartman, K (1971), 'Air infrared spectroscopy study of epoxy-cellulose interface', *Journal of Polymer Science Part C: Polymer Symposia,* vol. **34**, no. 1, pp. 293–301.

O'Donnell, A, Dweib, MA and Wool, RP (2004), 'Natural fiber composites with plant oil-based resin', *Composites Science and Technology,* vol. **64**, no. 9, pp. 1135–1145.

Oksman, K (2001), 'High quality flax fibre composites manufactured by the resin transfer moulding process', *Journal of Reinforced Plastics and Composites,* vol. **20**, no. 7, pp. 621–627.

Padmavathi, T, Naidu, SV and Rao, R (2012), 'Studies on mechanical behavior of surface modified sisal fibre – epoxy composites', *Journal of Reinforced Plastics and Composites,* vol. **31**, no. 8, pp. 519–532.

© Woodhead Publishing Limited, 2014

Paetau, I, Chen, CZ and Jane, J (1994), 'Biodegradable plastic made from soybean products. 1. Effect of preparation and processing on mechanical properties and water absorption', *Industrial & Engineering Chemistry Research,* vol. **33**, no. 7, pp. 1821–1827.

Patel, V and Parsania, P (2010), 'Performance evaluation of alkali and acrylic acid treated–untreated jute composites of mixed epoxy-phenolic resins', *Journal of Reinforced Plastics and Composites,* vol. **29**, no. 5, pp. 725–730.

Qi, N and Zhao, L (2011), 'The mechanical properties of jute fiber mats reinforced vinyl ester resin composites', *Advanced Materials Research,* vol. **284–286**, pp. 277–283.

Rodriguez, ES, Stefani, PM and Vazquez, A (2007), 'Effects of fibers' alkali treatment on the resin transfer molding processing and mechanical properties of jute-vinylester composites', *Journal of Composite Materials,* vol. **41**, no. 14, pp. 1729–1741.

Ramamoorthy, SK, Di, Q, Adekunle, K and Skrifvars, M (2012), 'Effect of water absorption on mechanical properties of soybean oil thermosets reinforced with natural fibers', *Journal of Reinforced Plastics and Composites,* vol. **31**, no. 18, pp. 1191–1200.

Rassmann, S, Reid, RG and Paskaramoorthy, R (2010), 'Effects of processing conditions on the mechanical and water absorption properties of resin transfer moulded kenaf fibre reinforced polyester composite laminates', *Composites Part A: Applied Science and Manufacturing,* vol. **41**, no. 11, pp. 1612–1619.

Ratna Prasad, AV and Mohana Rao, K (2011), 'Mechanical properties of natural fibre reinforced polyester composites: Jowar, sisal and bamboo', *Materials & Design,* vol. **32**, no. 8–9, pp. 4658–4663.

Sastra, H, Siregar, J, Sapuan, S and Hamdan, M (2006), 'Tensile properties of Arenga pinnata fiber-reinforced epoxy composites', *Polymer-Plastics Technology and Engineering,* vol. **45**, no. 1, pp. 149–155.

Sever, K, Sarikanat, M, Seki, Y, Erkan, G and Erdoğan, ÜH (2010), 'The mechanical properties of γ-methacryloxypropyltrimethoxy silane-treated jute/polyester composites', *Journal of Composite Materials,* vol. **44**, no. 15, pp. 1913–1924.

Silva, RV, Spinelli, D, Bose Filho, WW, Claro Neto, S, Chierice, GO and Tarpani, JR (2006), 'Fracture toughness of natural fibers/castor oil polyurethane composites', *Composites Science and Technology,* vol. **66**, no. 10, pp. 1328–1335.

Strong, AB (2008), *Fundamentals of Composites Manufacturing: Materials, Methods and Applications*, 2nd edn, Society of Manufacturing Engineers, Dearborn, Michigan.

Thiruchitrambalam, M, Alavudeen, A, Athijayamani, A, Venkateshwaran, N and Perumal, AE (2009), 'Improving mechanical properties of banana/kenaf polyester hybrid composites using sodium laulryl sulfate treatment', *Materials Physics and Mechanics,* vol. **8**, no. 2, pp. 165–173.

Van de Weyenberg, I, Berghmans, B, Vangrimde, B and Verpoest, I (2003), 'The continuous production of UD flax composites', *Proceedings of ECOCOMP 2003,* London, UK.

Van de Weyenberg, I, Chi Truong, T, Vangrimde, B and Verpoest, I (2006), 'Improving the properties of UD flax fibre reinforced composites by applying an alkaline fibre treatment', *Composites Part A: Applied Science and Manufacturing,* vol. **37**, no. 9, pp. 1368–1376.

© Woodhead Publishing Limited, 2014

Virk, AS, Hall, W and Summerscales, J (2011), 'Modelling the tensile properties of jute fibres', *Materials Science and Technology,* vol. **27**, no. 1, pp. 458–460.

Williams, GI and Wool, RP (2000), 'Composites from natural fibers and soy oil resins', *Applied Composite Materials,* vol. **7**, no. 5, pp. 421–432.

Wool, RP (2005), 'Polymer and composite resin from plant oil', in RP Wool and XS Sun (eds.), *Bio-Based Polymers and Composites*, Elsevier Academic Press Amsterdam.

© Woodhead Publishing Limited, 2014

10

Non-destructive testing (NDT) of natural fibre composites: acoustic emission technique

F. SARASINI and C. SANTULLI,
University of Rome 'La Sapienza', Italy

DOI: 10.1533/9780857099228.3.273

Abstract: This chapter discusses the use of acoustic emission (AE) as a useful tool for mechanical behaviour monitoring and characterization of natural fibre composites. The chapter begins by providing a detailed overview of non-destructive techniques and the principles of the (AE) method. It then reviews the instrumentation and analysis of (AE) data, with particular emphasis on the field of composite materials, thus highlighting the potential of this technique in providing information about the failure of natural fibre composites. The chapter includes indications on future trends related to the analysis of (AE) data for the identification and discrimination of failure mechanisms in composite materials, along with a section devoted to sources of further and relevant information.

Key words: non-destructive testing (NDT), acoustic emission (AE), polymer matrix composites, natural fibres.

10.1 Introduction

This section reviews some fundamentals about the field of non-destructive testing (NDT) and acoustic emission (AE) (principles and sources, wave propagation and history) that are useful in analysing the concepts described in the following sections.

10.1.1 Non-destructive evaluation (NDE)

Non-destructive evaluation (NDE) is the examination of an object with technology that does not affect the object's future usefulness, as stated by the American Society of Non-destructive Testing (ASNT) (ASNT, 2012). The basic principle of NDE is simple. To determine the quality or integrity of an item non-destructively, simply find a physical phenomenon (the *interrogating parameter*) that will interact with and be influenced by the test specimen (*the interrogated parameter*) without altering the specimen's function (Shull, 2002).

© Woodhead Publishing Limited, 2014

The terms commonly used in the testing community are very similar but slight differences exist as described below (Shull, 2002):

- NDT usually denotes the actual test only;
- NDE implies not only the test but also its role in the process;
- NDE is used in areas other than process control;
- non-destructive Inspection (NDI) is similar to NDE;
- non-destructive characterization (NDC) refers to the specific characterization of materials properties;
- non-destructive sensing (NDS) refers to the use of sensors to obtain information in a non-destructive way, irrespective of whether the object will be returned to service or not.

In spite of these differences, most terms are used interchangeably. In particular, NDE, NDT and NDI are the most common and non-specific.

Modern non-destructive tests are used by manufacturers: (1) to ensure product integrity, and in turn, reliability; (2) to avoid failures, prevent accidents and save human life; (3) to make a profit for the user; (4) to ensure customer satisfaction and maintain the manufacturer's reputation; (5) to aid in better product design; (6) to control manufacturing processes; (7) to lower manufacturing costs; (8) to maintain uniform quality level; and (9) to ensure operational readiness. In addition, non-destructive tests are also used for research studies in the field of materials science (ASNT, 2012).

NDT methods for composite materials range from simple visual inspection and coin tapping to very sophisticated techniques such as acousto-ultrasonics and shearography. Many of these techniques were originally developed for metallic structures and, with some modifications, are also used with fibre reinforced composite materials. These alterations have been necessary to account for the different behaviour between metals and composites. In fact, metals are essentially isotropic and homogeneous materials, while composites are inherently anisotropic and heterogeneous. The quality in the context of NDT is defined in terms of flaws and defects. However, not all flaws severely affect the strength, stiffness or other performance criteria of the composite materials. Therefore, a good non-destructive test should be able not only to detect the presence of defects but also to discriminate between critical and non-critical defects in terms of their influence on the overall performance and reliability of the structure. Flaws in composite materials can be classified as process-induced or as service-related. The process-induced flaws are introduced during the moulding time due to lack of process control. They can also be caused by insufficient raw material quality, improper tool design and human error. Obviously, this kind of defect strongly depends on the manufacturing technique employed. Typical process-induced defects are, for instance: (1) contamination due to foreign particles, fibres and pieces

© Woodhead Publishing Limited, 2014

of release film (peel ply) not eliminated from the pre-preg surface; (2) broken filaments produced by scratches; (3) delamination of plies caused by poor consolidation and undercure in the moulding operation; (4) resin-rich or fibre-starved areas; (5) fibre misalignment and fibre swelling; (6) undercure due to a wrong choice of the cure cycle parameters and (7) voids due to air entrapment between layers, moisture and gases evolved during curing in the mould. On the other hand, service-related flaws are generated by unintentional overloading, low-velocity impacts, fatigue and environmental factors related to temperature and moisture.

10.1.2 Principles and sources of acoustic emission (AE)

The AE testing method is a unique NDT method where the material being inspected generates signals that warn of impending failure. Formally defined, AE is that class of phenomena in which transient elastic waves are generated by the rapid release of energy from localized sources within a material, or the transient elastic waves so generated (ASTM E 1316, 2011). A key aspect of AE, in comparison to other NDE techniques, is that the signals are produced within the material itself. An external stimulus, such as a change in load, pressure, strain, or temperature is necessary to induce the source to emit acoustic waves. Usually the source is a permanent and irreversible change within the material. The AE test method detects and locates flaw data for the stressed object the moment the flaw is active; therefore, flaws cannot be retested by the AE method. The basic concept of AE is very simple, but there are many factors that make its implementation for NDE not easy. First of all, acoustic wave propagation in solids is quite complex as multiple modes that propagate with different velocities, reflection, refraction, mode conversion, velocity dispersion, attenuation, can all occur and affect the measured signal. In addition, AE testing is complicated by the fact that the characteristics of the input are relatively unknown. In fact, different AE sources can generate completely different AE waveforms. In spite of these problems, AE monitoring has some unique advantages over other NDT techniques, which can be schematically summarized as follows (Moore, 2005):

- AE is a dynamic inspection method, in that it provides a response to discontinuity growth under imposed structural stresses – static discontinuities will not generate AE signals;
- AE is non-directional;
- AE method may be used to prevent catastrophic failure of systems with unknown discontinuities;
- AE can be used *in situ* to monitor a structure while it remains in service. This feature makes AE a suitable sensing technique for structural health monitoring (SHM).

© Woodhead Publishing Limited, 2014

Another advantage not mentioned before is related to the fact that AE can be virtually applied to all materials, since sources of AE include many different mechanisms of deformation and fracture. Materials in which AE has been measured include metals, ceramics, polymers, composites (including those with metal, ceramic and polymer matrices and a wide variety of reinforcement materials), wood, concrete, rocks and geological materials. Sources that have been identified in metals include crack growth, twinning, slip and dislocation movements. Other sources exist which are not related to damage mechanisms but are nevertheless important for industrial applications, such as leakage of fluids and gases, frictional noise from machinery, cavitation, realignment and growth of magnetic domains (Barkhausen effect), liquefaction and solidification, solid to solid phase transformations. These sources are often called secondary sources, or pseudo sources. As explained above, the interpretation of AE signals is complicated by the occurrence of signals generated by sources of noise. Noise signals may be continuous or intermittent and the source can be either internal or external to the test object. Typical noises are generated by fretting or rubbing of components in contact with the specimen, serrated wedge grips, rain, hail, windblown debris and electromagnetic interference. As regards the AE testing of composites, AE monitoring has proven effective when compared with other non-destructive test methods (Duesing, 1989; Hamstad, 1986a; Hamstad and Sendeckyj, 1993). The specific mechanisms that produce AE events in composite materials are numerous and include the following: (1) second phase or fibre cracking and failure; (2) second phase or fibre interfacial debonding; (3) second phase or fibre plastic deformation; (4) matrix plastic deformation and cracking; (5) delamination; and (6) rubbing of the second phase or fibre against the matrix. The situation is complicated by the fact that fibre composite structures fail as a result of the accumulation of damage within the composite, and three factors make this accumulation of damage a complex process:

- damage begins at relatively low load levels;
- damage grows as a result of time under load; and
- damage occurs due to load cycling to the same load level.

In general, fibre breaks are particularly important and represent critical events in the component failure process. The matrix damage affects the load under which the discontinuity propagates unstably, whereas impact damage and related delaminations are the most likely failure modes for in-service organic composite structures.

AE is an irreversible process. In practice, it is often found that once a given load has been applied and the AE from accommodating that stress has

© Woodhead Publishing Limited, 2014

ceased, additional AE will not occur until that stress level is exceeded, even if the load is completely removed and then reapplied. This behaviour has been named the *Kaiser effec*t in honour of the researcher who first reported it. However, in many non-metal materials, the Kaiser effect does not hold and significant AE is always detected at loads lower than the previous maximum. This is known as the *Felicity effect* (Hamstad, 1986b; Summerscales, 1986). The Felicity ratio is defined as the load at which significant AE reinitiates divided by the previous maximum load.

Composite materials are an example of a material that will consistently emit AE at loads below their previous maximum and thus have a Felicity ratio of less than one. Similar to the use of the Kaiser effect, repeated loading can be used with previously determined Felicity ratio values for a given material to obtain information about the previous maximum applied load. A change in the Felicity ratio over time has also been correlated with increased damage in some materials. The Felicity ratio has proved to be a valuable diagnostic tool in one of the most successful of all AE applications, the testing of fibreglass vessels. The Kaiser effect fails most noticeably in situations where time dependent mechanisms control the deformation, such as viscoelasticity and stress relaxation (e.g., polymeric matrix composite materials). Another is that some of the AE that occurs prior to previous maximum loads may be caused by friction of existing crack surfaces, rather than by the onset of new damage. Other cases where the Kaiser effect will fail are corrosion processes and hydrogen embrittlement, which are also time dependent.

10.1.3 History of AE

It has been said that the first practical use of AE occurred in about 6500 BC as pottery makers listened to the cracking sounds made by clay pots that had been allowed to cool too quickly. By experience the potters learned that cracked pots were structurally defective and would fail prematurely. In metals it is reasonable to assume that the first AE heard was tin cry, the audible sounds produced by mechanical twinning of pure tin during plastic deformation. Tin cry is commonly found in books on chemistry published in the last half of the nineteenth century. The transition from the incidental observation of audible tin cry to the deliberate study of AE phenomena consisted of three separate and unrelated experiments in which instrumentation was used to detect, amplify and record AE events taking place in the test specimens. The first experiment was conducted in Germany and the results were published in 1936 by Förster and Scheil (1936) who reported ‘noises’ caused by the formation of martensite in 29% nickel steel. The second instrumented AE experiment was performed by Mason

© Woodhead Publishing Limited, 2014

et al. (1948). The third experiment was performed by Millard (1950) with Rochelle salt transducer to detect twinning in single crystals of cadmium. However, the father of modern AE testing was the work of Kaiser (1950) at the Technische Hochschule München in Germany. His work demonstrated that AE is an irreversible phenomenon. These early AE studies were followed by considerable research during the late 1950s through to the 1970s. A published bibliography (Drouillard, 1996) of AE studies provides numerous references. Since the late 1970s, considerable advances have been made in waveform recording instrumentation. Transient recorders with multi-MHz digitization sampling frequencies necessary for high frequency AE signals were developed. Simultaneously, additional improvements in the capture and storage rate of digitizers have made full waveform capture and analysis possible for practical AE testing and, nowadays, increases in the speed and available memory of computers have significantly improved analysis capabilities making possible, through AE, the:

- periodic or continuous monitoring of pressure vessels to detect and locate active discontinuities;
- detection of incipient fatigue failures in aerospace and other engineering structures;
- monitoring materials behaviour tests to characterize several failure mechanisms;
- monitoring stress corrosion cracking and hydrogen embrittlement tests.

10.1.4 Wave propagation

After acoustic waves are generated by the source they propagate through the structure up to the detectors located on the surface. The most common AE modes of propagation are bulk modes, Rayleigh (surface) waves and Lamb (plate) waves. For a more detailed description, readers are referred to (Shull, 2002). Waves in real media change in amplitude as they propagate through the solid. The term used to describe the decrease in acoustic wave amplitude as a function of propagation distance is called *attenuation*. This is an aspect of remarkable concern, especially in composite materials. In fact, in polymeric composite materials, attenuation can be relatively high due to absorption of sound energy by the viscoelastic matrix. High frequency components may be selectively absorbed by the matrix and scattered by the fibres and other discontinuities. So AE monitoring of fibrous composites requires much closer transducer spacings than metal components. In addition, attenuation can also affect source location accuracy. Since it is also frequency dependent, it can influence not only the signal amplitude but also the wave shape, thus making the source identification analysis complicated.

© Woodhead Publishing Limited, 2014

The attenuation is often reported in units of dB/unit length of propagation. The amplitude (A) of an AE signal is expressed in decibels (dB) by

$$\mathrm{A(dB)} = 20\log\frac{V_{\mathrm{sig}}}{V_{\mathrm{ref}}} \qquad [10.1]$$

where V_{sig} is the voltage of the measured signal and V_{ref} is a reference voltage, often 1 μV. The four basic attenuation mechanisms for acoustic waves are absorption, scattering, beam spreading (divergence or geometric attenuation) and dispersion (Moore, 2005).

The aim of this chapter is to provide an overview of the AE method and to underline the potential of this technique in monitoring, identifying and discriminating the relevant damage mechanisms that lead to the final failure of natural fibre reinforced composites.

10.2 Using the acoustic emission (AE) technique in practice

AE testing can be thought of as a process chain consisting of the following steps (Mix, 2005):

- test object and application of load;
- source mechanisms: releasing elastic energy;
- wave propagation: from the source to the sensor;
- sensors: converting a mechanical wave into an electrical AE signal;
- acquisition of measurement data: converting the electrical AE signal into an electronic data set;
- display of measurement data: plotting the recorded data into diagrams;
- evaluation of the display: from diagrams to a safety-relevant interpretation.

10.2.1 Measurement

Once generated and propagated, AE signals must be detected, conditioned and recorded for analysis. Components common to all AE systems are transducers, preamplifiers, filters and amplifiers to make the signal measurable. Techniques used for measurement, display and storage vary widely according to the demands of the specific application. A transducer's function is the conversion of the mechanical energy of the elastic wave into usable electrical energy. Usually, piezoelectric sensors are used as electromechanical conversion devices because they provide the best combination of sensitivity, signal/noise and dynamic range. A classical definition of piezoelectricity, a Greek

© Woodhead Publishing Limited, 2014

term for pressure electricity, is the generation of electrical polarization in a material in response to a mechanical stress. This phenomenon, known as direct piezoelectric effect, was discovered by P. and J. Curie in 1880. Progress in finding practical piezoelectric materials for ultrasonic NDE applications became more significant with the discovery of barium titanate and the ability to activate it as a piezoelectric material by poling. This success was followed by the observation of the very strong effect in lead zirconate titanate (PZT) ceramics. Today, most of AE transducers are made of the various forms of PZT. The transducers can be resonant or broad-band. Nevertheless, the main considerations in transducer selection are (1) operating frequency, (2) sensitivity and (3) environmental and physical characteristics. The preamplifier must be located close to the transducer and it provides filtering and gain. Filtering in the preamplifier is the primary means of defining the monitoring frequency for the AE test. The practically used frequency range is about 50 kHz up to 1 MHz. The lower frequency limit is governed by background noise and it is therefore unusual to go below 10–20 kHz. The upper frequency limit is governed by wave attenuation, which is particularly significant in composite materials. It is unusual to go above 1 MHz. As a consequence, the most used frequency range for AE testing is 100–300 kHz.

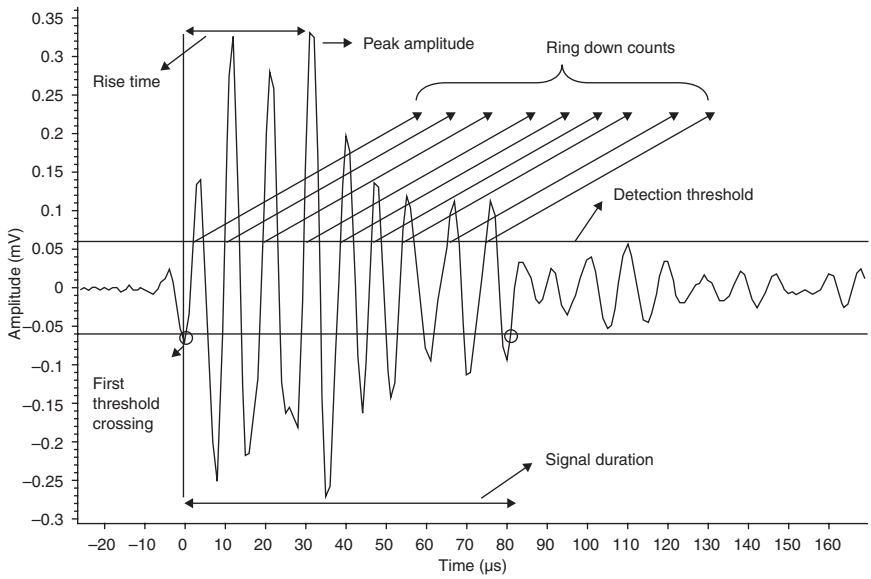
Crucial to a successful AE test is the coupling procedure that provides good acoustic contact between the sensor and the surface of the test object. A variety of silicone greases are available for industrial, aerospace and other applications. Generally, the coupling layer should be made as thin as possible by firmly pressing the sensor against the test object's surface.

10.2.2 Analysis of the AE data

AE sources and the resulting signals are often characterized as being either continuous or discrete. Individual damage mechanisms produce discrete signals that are characterized by a clear beginning and end. Sources such as leakage may produce continuous signals that are not characterized by a clear beginning and end. The most commonly reported AE from fibre reinforced composites is burst emission. AE data can be analysed in many ways, even though it is possible to refer to two main analyses, namely parameter-based analysis and waveform-based analysis. The former is the traditional one, while the latter is gaining increasing interest during recent years due to the improved capabilities of hardware components.

Parameter-based analysis deals with the extraction and measurement of features of individual discrete AE signals. Some of these features are illustrated in Fig. 10.1, which shows a single-burst waveform with highlighted AE parameters. Signal detection and feature extraction are based on a preset voltage threshold. The main terms used in AE are defined as listed in Table 10.1 (EN 1330–9, 1999).

© Woodhead Publishing Limited, 2014



10.1 Features of transient AE signals.

Table 10.1 Terms used in the AE method

Term	Explanation
AE event	Physical phenomenon giving rise to AE
AE source	Physical origin of one or more AE events
AE signal	Electrical signal from an AE sensor resulting from AE
AE activity	Occurrence of AE signals as a result of AE
AE detection threshold	Voltage level which has to be exceeded before an AE signal is detected and processed
Arrival time	Absolute time when a burst signal first crosses the detection threshold
Burst signal duration	Interval between the first and the last time the detection threshold was exceeded by a burst signal
Ring down count	Number of times a burst signal crosses the detection threshold
Burst signal peak amplitude	Maximum absolute amplitude within the duration of the burst signal
Burst signal rise time	Time interval between the first threshold crossing and the maximum peak amplitude of the burst signal
Burst signal energy	The area of the rectified envelope of the signal
Hit	Detection of one burst signal on a channel

© Woodhead Publishing Limited, 2014

Feature-based AE measurement systems are still widely used and there are numerous approaches for analysing such data. Approximate source locations can be obtained from the triangulation of arrival times for a signal detected by multiple sensors at different locations, provided that the average wave velocity in the material is known.

Bohse (2004) has recently summarized the currently used tools for the identification and location of AE sources, as well as for the evaluation of damage in composite materials. This overview is reported in Table 10.2.

10.2.3 AE in composite materials studies

AE data provide information that is unobtainable by any other technique. First, AE data give a real-time record of the progressive damage that occurs. Such information is valuable for developing damage and failure models for composite materials. Secondly, AE signals are very sensitive. Thirdly, AE technique is sensitive to energy releases within the entire test object, and finally has the potential to determine the integrity of composite parts and to locate growing discontinuities, which is particularly meaningful for composites materials which usually fail as a result of damage accumulation during loading.

Much research has been done to establish relationships between composite failure mechanisms and AE signals. The underlying assumption is that each type of failure releases stress-energy packets that differ in amplitude, frequency content or other waveform characteristics, and that the AE detection system can distinguish these differences. As a stress wave or AE signal travels through a material, its characteristics are constantly changing due to attenuation, damping, boundary surface interactions, etc. These signal changes are called propagation alterations. In addition, detection alterations occur to the stress wave due to the AE hardware receiving the signal (sensors, cables, amplifiers, etc.). Consequently, a stress wave recorded by the AE equipment is a transformed representation of the original source wave.

Of the many parameters used to describe AE data, the peak amplitude of the event waveform is one the most informative. Typically, the AE from a fibre reinforced composite material is of significantly higher amplitude than from a metal. AE signals from a transducer are often 2–50 mV for fibre reinforced composites, whereas signals from metal are typically 500 μV or less. Consequently, the event amplitude and its associated events versus amplitude plot (what is called amplitude distribution) have proven to be the key for assessing the integrity of composite structures (Barrè and Benzeggagh, 1994; Bennedakhene *et al.*, 1999; Huguet *et al.*, 2002; Jeng *et al.*, 1989; Kim and Lee, 1997; Mittelman and Roman, 1991; Zhuang and Yan, 2006). As shown in these studies, the AE technique offers a very effective method capable of locating and detecting non-visual damage and tracking its progression and

© Woodhead Publishing Limited, 2014

Table 10.2 Summary of the currently used tools for the identification and location of AE sources as well as for the evaluation of damage in composite materials

Changes in AE activity or intensity with time or external parameter	Location of AE sources	Identification of AE sources – tools
First AE hits/events Onset of damage processes	*Planar or zonal location of single events or event clusters* Location, size, shape and growth direction of AE active zones, which belong to individual type of damage (delamination, impact, etc.)	Conventional AE features (peak amplitude, counts, duration, energy; histograms and correlation plots of features) Waveform/wave mode analysis Frequency spectrum (FFT) Pattern recognition by means of neural networks Inverse moment tensor analysis Modelling of AE sources
Characteristic changes of AE hit/event/energy rate or cumulative sum Progressive increase – 'knee point' (progressive damage or occurrence of new failure mechanisms) Continued non-decreasing or increasing AE activity and intensity during hold periods of loading Increasing AE activity during unloading (rubbing of damaged areas)		
AE amplitude distribution Number of failure mechanisms		
Felicity ratio Ultimate failure warning if it falls below a certain value		

© Woodhead Publishing Limited, 2014

accumulation in real time. A detailed analysis of the AE event parameters could identify the actual type of damage. The correlations between event amplitude and source damage modes have been established through several approaches. Most of them used special specimens designed to fail under well-defined modes such as matrix cracking, debonding, fibre pull-out and fibre failure to find a correlation between these modes and amplitudes of the AE signal detected. Very often, these investigations have been performed using, besides AE, optical techniques and scanning electron microscopy (SEM) to relate the actual damage modes and progression to the amplitude ranges. Barrè and Benzeggagh (1994) while testing glass–polypropylene (PP) reported that the acoustic signal amplitude varies with the different modes of failure: AE amplitude range from 40 to 55 dB corresponds to matrix cracking, 60–65 dB to debonding, 65–85 dB to pull-out and 85–95 dB to fibre fracture. Ely and Hill (1995) showed that when fibre breaks and longitudinal splitting occur at the same location in graphite–epoxy specimens, the stronger signals (high amplitude, energy, counts and long duration) belonged to fibre breakage and the weaker ones to longitudinal splitting. Other researchers have attempted to model the amplitude distribution in order to produce ultimate strength prediction equations for unidirectional graphite–epoxy tensile specimens (Walker and Hill, 1992). Mittelman and Roman (1987) proposed a new approach for the analysis of the peak amplitude distribution (PAD) by employing the statistical moments of the PAD. In particular, the third moment, or skewness, allowed them to differentiate between matrix fracture and fibre failure modes of unidirectional Kevlar–epoxy composites. This method was also successfully used in graphite–epoxy composites. Several authors have attributed various other parameters of AE signals to different damage modes. For example, de Groot *et al*. (1995) analysed the frequency distribution to identify damage mechanisms in carbon–epoxy composites. The role of frequency for signal differentiation has been underlined by many authors (Giordano *et al*., 1998; Ramirez-Jimenez *et al*., 2004). However, these correlations are not universal due to the dependency of the AE parameters on the specimen geometry, materials properties and AE hardware. The AE technique has been successfully applied to impact studies. Ochiai *et al*. (1982) correlated characteristics of the impact load versus time curve with the corresponding AE during instrumented impact of plates of graphite–epoxy. They demonstrated that no AE is observed when no impact damage occurs and that AE is observed when damage occurs. This result led them to observe that with a fixed impact level, defective plates produce AE and non-defective plates do not produce AE. Kwon *et al*. (1995) monitored the progress of damage during post-impact tensile loading of carbon fibre–epoxy composites. They pointed out the importance of root-mean-square (RMS) voltage and signal duration data in evaluating the degree of impact damage. Santulli (2001, 2006) reported the ability of AE to perform reliable

© Woodhead Publishing Limited, 2014

measurement of the level of damage in natural fibre reinforced laminates, while Caprino and Teti (1995) used AE detection and analysis to attempt the prediction of residual tensile strength after impact of glass-reinforced plastic (GRP) laminates.

10.3 Assessing results

The production of polymer composites reinforced with natural fibres has substantially increased in the last few years, especially in sectors such as the automotive (see Chapter 7 for details), leisure and furniture industries, where their reduced cost and higher bio-degradability may represent important incentives for use (Wambua *et al.*, 2003). However, their applications are mainly as cosmetic, that is, non-load-bearing, materials (see Chapter 7). A significant difficulty is offered by the structure of reinforcement itself. In particular, plant fibres are not homogeneous, being cellular structures assembled in nature through a hierarchical procedure (see Chapters 1 and 2), so that the single filaments present a hollow of variable dimensions, defined as a lumen. In some types of leaf fibre, such as for example in pineapple fibre, a lacuna, of much larger dimension than the lumen, is also present at the centre of the whole natural structure (Santulli, 2008).

In addition, their introduction in a polymer matrix may generate compatibility issues, whose consequence may be a large scattering of properties in the final laminate, only partially addressed through fibre surface treatment (Tserki *et al.*, 2005) (see Chapters 7, 9 and 14 for details). This is the cause of persistent uncertainty as to the mechanical properties of the composite obtained, resulting in the difficulty of setting reliable stress limits for materials design, and assessing the effect of damage, whether induced by previous loading or impact, on the structure (Eichhorn *et al.,* 2001).

These limitations are inherent in the case of ligno-cellulosic fibres. A frequent procedure involves fabricating hybrids normally including glass fibres reinforced laminates in various combinations with vegetable fibre reinforced ones (Santulli, 2007). In this case, a significant parameter for the effectiveness of the AE analysis is the possibility to make comparative considerations about the mechanical behaviour of different hybrid configurations; this approach has been often followed. For example, in De Rosa *et al.* (2009a), the use of AE allowed establishing the relative merits of sandwich and intercalated E-glass–jute reinforced composites impacted at different energies during cyclic flexural tests. It was in particular suggested that sandwich hybrids performed better at lower impact energies, while, when approaching penetration, the possibility to provide further interfaces by intercalating jute and glass fibre reinforced layers offered an improved resistance, in terms of increased load when AE activity started during post-impact cyclic flexural loading.

© Woodhead Publishing Limited, 2014

Another significant difference from that obtained in the case of glass fibre reinforced laminates is that on natural fibre composites it is not yet easy to discern reliably between different damage modes detected in the material, for example, matrix cracks, delamination and fibre fracture. This is normally carried out on glass fibre laminates by a combination of frequency range and AE parameters (such as in particular amplitude and duration). A number of studies have been carried out using AE and mainly based on amplitude analysis, along the lines initially suggested by Berthelot and Rhazi (1990) on carbon fibre reinforced composites in the early nineties. However, studies carried out following this method on natural fibre composites did often lead to somewhat conflicting evidence. A difficulty is that the possibility of damage characterization using AE depends on the complexity of fibre architecture, so that the presence of multiple damaged zones can lead to difficult interpretation of AE data. This is very likely to happen on plant fibre composites, where the dimensional scattering and difficult compatibility often leads to an interface of very variable strength, with the consequence that a measurement of interface strength becomes even more crucial than in traditional composites to guarantee the durability of the material. This is particularly true considering that the hydrophilic nature of natural fibres adversely influences adhesion to the hydrophobic matrix (see Chapters 7, 9 and 14), whenever an oil-derived polymer is used, resulting in low compatibility and strength (Mohanty *et al.,* 2000).

An aspect, which is essential for the possible application in service of natural fibre composites, is the measurement of the level of stress at which substantial irreversible damage starts to take place. This can be measured with different methods, in particular using the AE cumulative counts curve versus applied stress. This curve can be divided into different stages, normally three, which give rise sometimes to a markedly visible 'AE knee', sometimes indicated as 'AE critical stress limit' (De Rosa *et al.,* 2009b). A different type of analysis is aimed in contrast at establishing the change in the characteristics (mainly amplitude and duration) of AE signals detected during the loading, for example by performing a full history of their evolution: this was carried out by De Rosa *et al.* (2012), on hemp fibre reinforced laminates and, combined with AE localization data, allowed establishing the presence of delaminations opening and closing during cyclical loading. In other instances, the loading period (or the stress) has been divided into a number of intervals, each corresponding to an equal percentage of the ultimate stress (De Rosa *et al.,* 2011). This allows understanding of how the mode of damage changes in the composite during the load application, which may also have a predictive quality in suggesting when the fracture of laminate approaches.

© Woodhead Publishing Limited, 2014

10.4 Applications of AE

This section covers the application of AE to the monitoring of damage development of both hybrid glass–natural fibre composites and pure natural fibre composites (NFC). In practice, three modes of loading have mainly been applied to these materials and monitored using AE: these are single fibre fragmentation tests (SFFT), crack propagation tests, and quasi-static loading (on as-received, already loaded, e.g., impacted, or artificially aged laminates).

10.4.1 AE during single fibre fragmentation tests

One of the factors that limits the application of plant fibre reinforced laminates is the difficulty to achieve a sufficient reinforcement/matrix interfacial shear strength (IFSS), which is required for an effective transfer of the applied load during service (see Chapters 7, 9 and 14). Conversely, the weakness of the interface is likely to lead to a premature failure of the composite. As described above, the IFSS is a critical factor affecting the toughness, transverse mechanical properties and interlaminar shear strength of composites, increasing the tensile and flexural strength of the composite while lowering the impact strength and toughness (Luo and Netravali, 1999). SFFT is often used to measure the IFSS, due to the simplicity of the test procedure, and it is the technique among those listed above which is most easily monitored using AE. SFFT is based on the application of an external stress to a single fibre embedded in a matrix, so that the tensile stress is transferred to the fibre by means of interfacial shear stress. As the tensile load increases, the tensile strain in the fibre will eventually exceed the failure strain of the fibre, and the fibre will start fracturing, and will continue to fracture into shorter lengths as the load increases, until the fragment length reaches a critical value. This situation is described as saturation in the fibre fragmentation process, while the shortest fragment length is defined as critical fibre length. It is therefore essential to know the exact number of fragments in order to estimate the average critical length, which in turn is needed to measure the IFSS. It has been demonstrated that almost all fibre breakages were detected and associated with a single AE event according to a one-to-one correspondence. Furthermore, the correspondence between the AE events detected and the microscopically observed fibre breakages (Clough and McDonough, 1996) was generally well established, allowing calculation of the IFSS by the Kelly-Tyson model (Kelly and Tyson, 1965) using, for average critical length, the total number of fibre fracture signals divided by the distance between two sensors (Narisawa and Oba, 1985).

© Woodhead Publishing Limited, 2014

In addition, interfacial bonding affects unambiguously the AE response, thus giving information about the characteristics of the interface, the level of adhesion and the interfacial failure modes (Okoroafor *et al.*, 1996).

Romhány *et al.* (2003a) used AE monitoring to track the failure modes in technical flax fibre during a single fibre fracture test. They showed that an AE range of amplitudes can be assigned to identify three failure mechanisms: longitudinal splitting of the pectin boundary layer among the elementary fibres (AE amplitude less than 35 dB); transverse cracking of the elementary fibre (35–60 dB); and fracture of elementary fibres and their microfibrils (over 60 dB). In contrast, no correlation has been found between AE signals characteristics and individual failure events. Park *et al.* (2006) carried out single fibre composite (SFC) tests using two bast fibres embedded in epoxy matrix, ramie and kenaf, respectively. The AE analysis was supported by optical microscopy, which allowed mutual interpretation of data. The AE parameters monitored were amplitude and energy along with the fast Fourier transform (FFT) analysis. The lower level of amplitude and energy signals occurred during the initial loading period, and was ascribed to the axial splitting along the boundaries of elementary fibres and fibrils. The breakages of the elementary fibrils and fibres occurred during the last loading period close to the failure of fibre bundles. These differences were reflected in the waveforms of the signals; in particular, breakages were characterized by high frequency peaks, whereas axial splitting was characterized by low frequency peaks. The following conclusions were drawn: for fibre breakage, AE energy and frequency were higher than those of fibrillation and matrix cracks. In particular, for kenaf fibres a greater number of higher AE energy and amplitude signal occurred than for ramie fibres. In addition, kenaf fibres were identified as more subject to fibrillation than ramie fibres. Park *et al.* (2006b) studied the correlation of the interfacial and mechanical properties of jute and hemp single fibre reinforced PP–MAPP (PP–maleic anhydride-*g*-PP) composites by micro-droplet test and AE. The AE and the FFT analysis revealed that jute fibres were characterized by events of higher energy and amplitude than hemp ones, due to micro-failure processes occurring through the crystalline material area (for jute) instead of through the amorphous one (for hemp), consistently with the observation that jute fibres showed a marked tendency to fibril splitting (inside the crystal areas), unlike hemp fibres.

In the previous papers, only AE descriptors such as amplitude and energy have been used to identify the micro-failure mechanisms. These studies were performed in the time domain together with the FFT analysis of the acquired waveforms, based on the consideration that each failure mechanism is characterized by a different frequency peak. In particular, three different micro-failure mechanisms were investigated and tracked down: fibre breakages, fibrillation and matrix cracking. As a general conclusion,

© Woodhead Publishing Limited, 2014

events of higher energy and frequency were ascribed to fibre breakages, while signals of lower energy and frequency were ascribed to fibrillation and matrix cracking (a clear distinction between these two mechanisms was not always achieved). It is also worth noting that differences in chemical composition between natural fibres are supposed to be responsible for the extent of fibrillation, which in turn affects the AE response, which is characterized by a larger number of AE signals coming from fibril splitting.

In most papers, the IFSS values were obtained from micro-droplet test, in which a single fibre is pulled out of a small droplet of resin. This procedure has a number of limitations: first, the complexity of failure mechanisms in NFCs may lead to difficult recognition between damage modes with overlapping feature modes, such as fibril splitting and matrix cracking. This can be solved if the measured AE features are coupled with supplementary information such as applied stress field or microstructural observations of the test specimen (Park *et al.,* 2008). Second, adhesion studies based on single fibre model methods can be subject to errors due to the simplified representation of the stress state existing at the fibre–matrix interface. Moreover, measuring the interface properties using real composites is further complicated by the interferences resulting from several mechanisms during composite testing. An approach used with traditional composites involves the use of simple multi-fibre composites to limit failure mechanisms to those recognized to be associated with interface failure (Okoroafor *et al.*, 1996). In this way, a sufficiently accurate evaluation of adhesion strength for several composite systems made of different natural fibres (treated and untreated) and matrices could be obtained. This represents an important issue in NFCs, considering the variety of physical and chemical treatments developed to enhance the fibre–matrix adhesion. Furthermore, since both time and frequency domains contain valuable information, a technique based on a joint time-frequency analysis could be useful with the aim of failure modes identification; one of the best candidates could be the wavelet analysis of AE signals. As a conclusion, these promising results should be also supported by further investigations on a larger number of natural fibres.

10.4.2 AE during crack propagation studies

AE can assist crack propagation studies in a two-fold sense – either enabling crack tip localization, or allowing the correlation of AE data with toughness measurements.

Localizing the crack tip encounters the typical difficulties of damage localization by AE in composite samples. These are especially due to the short distances involved, which require a high accuracy of stress wave velocity measurement, not always easy to obtain on non-uniform and anisotropic materials; as a result, the localization accuracy of AE systems does not

© Woodhead Publishing Limited, 2014

usually exceed 1 mm, so that in practice, on traditional composites, damage localization using AE has an accuracy in the order of the centimetre or lower. In particular, during monotonic tests it is possible to predict the area of the laminate where failure will finally occur (Godin *et al.,* 2005). Another more empirical possibility involves dividing the laminate into regions and quantifying the distribution of AE events in the different regions (Aicher *et al.,* 2001). A third and more mathematically rigorous possibility is the use of weighing algorithms based on a bell-shaped function, which account for the neighbourhood of the detected events. By achieving a smoothing of the events curve, weighting allows discerning between events representing a substantial amount of concentrated AE and isolated events (Benevolenski and Karger-Kocsis, 2001).

In principle, tests on notched specimens to assess the elasto-plastic fracture mechanics behaviour of composites would appear easier to be characterized using AE, since the progression of damage should approximately follow an oriented direction: such progression can be followed knowing AE sensors position. The weighing centre of AE amplitudes is supposed to correspond to the notch root, while the damaged area is supposed to be equivalent to the area in which 90% of AE events are detected, to account for occasional events unrelated with crack growth (Acha *et al.*, 2006).

The application of AE can be useful to detect the onset of fibre-related breakage events, assuming that events detected in the matrix have lower amplitude than those due to fibre pull-out, which have in turn lower amplitude than those due to fibre failure: this can be considered true as a first assumption, although the geometrical dimension of the respective damage may also have an influence. In this way, AE amplitude distributions plots from SENB tests allowed establishing that in hemp–basalt hybrid laminates crack propagation starts before the maximum load is reached (Czigany, 2006). A similar measurement was performed in flax-starch (MaterBi) composites, where data were compared, finding good agreement, with damage area measurement using IR thermography, suggesting that this material failed in a ductile way with pronounced crack growth and enabled the determination of the J-R integral (Romhany *et al.*, 2006). The same method, employed on jute cloth reinforced composites, clarified that the value of the J-integral is consistently higher in single edge notched tension (SENT) specimens with the introduction of a larger volume of reinforcement (40 wt.% against 20 wt.%) (Acha *et al.,* 2006). The presence of a quasi-linear relation between material toughness and AE activity, though dependent on the fibre length, was also clarified in plotting the values of K_{IC} against the number of detected AE events in flax–PP composites (Czigany, 2004).

It is noteworthy that it does not appear by any means general, as mentioned by Anuar *et al.* (2007), that AE events related with fibre pull-out have lower amplitudes than those related to fibre breakage. In any case,

© Woodhead Publishing Limited, 2014

the presence of shorter fibres, and hence a larger number of fibres in the composite, would lead to a higher proportion of AE high amplitude events.

To summarize, the analysis of toughness data with AE appears quite reliable and repeatable, when concentrating on localization data and on the use of bell-shaped amplitude distribution to follow crack growth progress. In contrast, any relationship established with toughness data using AE counts or number of events is probably of less general use in NFCs, although it may be useful in specific cases.

10.4.3 AE monitoring during quasi-static tests

When introducing natural fibres and fillers in a composite, it has been revealed in a number of circumstances that it is not necessarily certain that the introduction of a larger amount of fibre in the polymer matrix does lead to an increase in properties (see e.g., De Rosa *et al.*, 2011b). This may be due to an ineffective impregnation of the fibres, or to the fact that the fibres are very far from being oriented in the envisaged directions, whether unidirectional or randomly disposed in uniform quantities at all angles.

Identification of the different failure modes using AE was proposed by Anuar *et al.* (2007) on kenaf fibres reinforced composites. Their objective was evaluating the evolution of the damage zone in thermoplastic natural rubber reinforced with untreated and treated kenaf fibres. Double edge notched tensile (DENT) specimens at different ligament lengths (4, 6, 8, 10 and 12 mm) were tested. AE higher amplitude signals (55 dB) were emitted in the composites reinforced with untreated kenaf fibres compared with composites reinforced with treated ones (50 dB). Furthermore, a higher average number of AE event counts was measured for the composites with untreated fibres and for the samples having a higher ligament length. This was explained by a stick–slip mechanism caused by the rough surface of the kenaf fibre, which opposes the pull-out mechanism, resulting in higher amplitude signals for pull-out, while chemical treatment, improving fibre–matrix adhesion, resulted in lesser pull-out.

Acha *et al.* (2006) used the AE technique to study the fracture and failure behaviour of biodegradable jute fabric reinforced thermoplastic polyester composites. During the tensile test, they also observed that AE amplitude increased in accordance with the following ranking from lowest to highest: matrix deformation, debonding, fibre pull-out, fibre fracture, with some caveats suggested by the geometrical extension of the single damage occurrence.

In particular, in the longitudinal direction, the typical form of damage besides the matrix deformation were debonding and tearing of the matrix, while in the transverse direction the dominant forms of damage were fibre pull-out and debonding. The analysis of the AE cumulative counts during

© Woodhead Publishing Limited, 2014

tensile tests was divided in three stages, according to the increasing strain: in Stage I, values typically below 50 dB in the transverse direction were measured and ascribed to matrix deformation and small extent delamination; in Stage II, pull-out occurred, reaching AE amplitudes of 70 dB; in Stage III, besides the failure modes above mentioned, some amount of fibre breakage was highlighted (below 70 dB in the longitudinal direction, and between 70 and 80 dB in the transverse direction). Pull-out events appear to become more dominant with increasing jute content, suggesting a gradually less effective wetting of the jute cloth.

Finkenstadt *et al.* (2007) correlated AE hit rate versus time and cumulative AE hits versus the stress–strain curve in poly(lactic acid) (PLA)–milkweed composites, with different fibre content (8, 15, 30 and 45 wt.%). They discerned between three different stages of deformation: at first, debonding of the filler from PLA matrix occurs; during the second stage the yielding of matrix occurs; in the last stages, the ductile fracture of the matrix occurs. They also noted that as the oil seed content increased the fracture changed from ductile to brittle: this suggested that the defects in material integrity prevailed over any advantageous interaction between oil seed and matrix.

Romhány *et al.* (2003b) showed that AE monitoring can be used to identify the failure mode sequence of flax fibre reinforced composites during a tensile test. Furthermore, they found that it was possible to identify the AE amplitudes released by the flax fibres during the failure of the composite. The flax fibres were arranged both unidirectionally (UD) and crossed-ply (CP) at different content (20%, 40% and 60%). The failure modes were characterized by correlating AE amplitude/cumulative number of AE events/duration versus elongation and relative AE amplitude distribution. In the three ranges of increasing load, fibre–matrix debonding and axial splitting of the elementary fibres occurred (20–35 dB), fibre pull-out and transverse microcracks within the elementary flax fibres become significant (35–55 dB), and the previous failure mechanisms were accompanied by multiple fibre breakage (above 55 dB) respectively. In composite reinforced with CP oriented fibres the breakage of the technical flax fibres does not occur. This is due to the fibres laid perpendicular to the loading direction, which do not contribute to the reinforcement since they split easily along their longitudinal axis (fibre–matrix debonding and axial splitting at fibre–fibre interface).

Shin *et al.* (1989) used the AE cumulative counts during tensile and flexural loading test to predict and evaluate the onset of fracture and material failure of unidirectional bamboo fibre–epoxy composites. They showed that the onset of fracturing can be predicted with the occurrence of small AE events, while the onset of critical damage with the occurrence of higher AE activity (explosive AE), defines the maximum load value safety region for effective service of these composites.

© Woodhead Publishing Limited, 2014

Santulli (2006) used AE during three-point bend test on impacted specimens of jute fabric polyester laminates to investigate the residual properties, and to predict the occurrence of failure. The correlation between AE data and mechanical results suggested that impact damage and residual properties of the laminates are defects-driven characteristics. These results confirmed that there is no real dependence of the damage produced on the energy applied. Santulli (2001) also proved elsewhere the AE capacity of measuring the level of damage on natural fibre reinforced composites. In particular, AE has been applied, during tensile, flexural, staircase and continuous indentation testing, on jute fabric–polyester laminate. He showed a correspondence between the stress–strain curve and the onset of AE activity. Therefore, investigating the variation of slope of the AE curve against the applied stress, 'AE knee', he evaluated the elastic limit of the laminate. The author also showed that it was possible to measure the AE limit only for low impact energies, since at high impact energies the AE activity was continuous during loading. It was also shown during three-point bend testing that it is possible to clearly evaluate the damage development and the mode of failure of the composite.

De Rosa *et al.* (2009a) used AE monitoring to evaluate the effect of damage dissipation offered by the jute fibre core in glass–polyester laminates. Correlating the AE activity to the applied cyclic bend stress on impacted specimens at various energies, the level of impact loading and the residual strength of the laminates were evaluated. Furthermore, it was clarified that the failure in the hybrid laminates started on the compressive side close to the interface between the skins and the jute core.

While investigating the correlation between cumulative AE event counts and stress–strain curves in unidirectional flax reinforced composites, Hughes *et al.* (2007) found evidence of yielding at low values of stress and strain. This evidence indicated that microstructural damage occurred in the proximity of yield point.

Sreekala *et al.* (2003) used AE monitoring to investigate the failure modes of oil palm and pineapple reinforced phenol formaldehyde composites. They highlighted that a correlation between the cumulative AE events and average amplitude versus elapsed time exists during the application of loading. At the beginning of the loading, the distribution of events showed small amplitude signals due to matrix deformation and debonding. In contrast, in the proximity of the maximum load value, AE events distribution was characterized by the presence of higher amplitude signals due to pull-out and fibre fracture.

A study on phormium–epoxy (De Rosa *et al.*, 2010), comparing long and short fibre reinforcements, indicated that AE activity takes place only at a later stage in both flexural and tensile tests and for both fibre configurations. As a general result, more AE events were recorded during flexural loading

© Woodhead Publishing Limited, 2014

compared with tensile loading. This could be due to the complex state of stress that is present during a flexural test with tensile, compression and interlaminar stresses. Long fibre reinforced laminates show a more uniform distribution of signals over the four subsequent loading intervals, each corresponding to 25% of the ultimate strain, with a larger number of higher amplitude signals during the final stage. These signals originate from fibre breakages and suggest that fibre orientation also plays a minor role by flexure, by virtue of the more complex state of stress. It is clear therefore the negligible effect of the short fibres on flexural strength compared to the significant decrease reported for tensile strength. On similar composites, Newman *et al.* (2010) observed that phormium–epoxy composites showed Felicity ratios close to unity after loading to 75% of estimated maximum stress, demonstrating that they clearly retained sound load-bearing fibres, despite intense acoustic activity when loaded to 75% of estimated maximum stress.

AE provided useful information also in durability studies, involving quasi-static tests on aged laminates. Yang *et al.* (2011) studied injection-moulded jute–PP composites with different fibre contents (10–50 wt.%) to investigate the effect of hot water immersion on the tensile property and AE behaviour of the composites. In this case, it was observed that cumulative AE count decreased remarkably with increasing jute fibre content, becoming very low for composites with 40 and 50 wt.% of jute fibres. It was suggested that the composites were becoming brittle with the increase of jute content, since very few irreversible damage indications are detected before the ultimate failure, evidence that in practice deters from in-service application of these high-fibre content jute–PP composites. A measurement of the AE yield stress through the analysis of AE cumulative count curves showed an increased value of the yield stress with increasing jute fibre content up to 40 wt.%, while decreasing for a fibre content of 50 wt.%. This was attributed to variable fibre orientation, due to the larger amount of reinforcement introduced.

A study was carried out on the AE response of flax–epoxy laminates, compared with glass fibre–epoxy laminates, aged by different durations of water immersion (Assarar *et al.*, 2011). The analysis suggested that the response of the unaged specimens is mainly located around the amplitudes of 40–45 dB, during two-thirds of the tensile test while, after ageing, amplitude distribution becomes uniform between 40 and 70 dB. Moreover, proceeding with water ageing, the amplitude of the first signals increases, to reach a value of 65 dB after 20 d of immersion. When the saturation weight gain is reached, the acoustic activity started from the beginning of tensile test, a result that was not observed for glass fibre–epoxy laminates. Unsupervised pattern recognition analysis was also performed, according to the method followed by Marec *et al.* (2008), so as to allow the classification of the events. It was suggested that on flax–epoxy events associated to debonding and fibre fracture

© Woodhead Publishing Limited, 2014

are only revealed for high durations of water absorption (10 and 20 d), while the majority of events are always attributed to matrix cracking.

10.5 Future trends

In recent years, AE monitoring has been considered a very attractive NDT method, as it provides real-time information on damage progression within the material. Most studies so far have used AE descriptors, such as counts, amplitude and energy, to characterize the development of failure mechanisms. Usually each signal is associated with a pattern composed of multiple relevant descriptors. Then the patterns can be divided into clusters representative of damage mechanisms, according to their similarity, by the use of multivariable data analyses based on pattern recognition algorithms (Godin *et al*., 2004). Since it is not possible to know exactly the origin of an emitted event and then to provide a training set of patterns belonging to several composite damage mechanisms, unsupervised pattern recognition is sometimes used with the problem of labelling the clusters. In this regard, Godin *et al*. (2005) use this approach for clustering AE events with a Kohonen's neural network associated with the *k*-means algorithm. However, this approach seems to be less effective for complex composite materials, and in order to improve the classification process, fuzzy C-means clustering associated with a principal component analysis (PCA) have been proposed (Marec *et al*., 2008). This approach allows identifying the damage mechanisms and following the time development of each damage mechanism till the final fracture of the samples. However, descriptor-based AE techniques often focus on time features that cannot be completely suitable for characterizing the AE waveforms for complex materials. First, other studies performed in the frequency domain have suggested that each damage mechanism is characterized by a different frequency peak obtained by Fourier analysis (Giordano *et al*., 1998). Since both time and frequency domains contain valuable information for the source and the medium of propagation of AE waveforms, a technique of joint time-frequency analysis is needed. The first candidate tool for such an approach is short-time FFT. Though relatively easy to apply, its precision is limited by the size of the window and all frequencies are analysed with the same resolution. For this reason SFFT has not become popular in AE analysis. Wavelet transform (WT) is a more sophisticated joint time-frequency analysis method. Wavelets were developed the last 20 years and have become a quite powerful tool in signal analysis field (Serrano and Fabio, 1996). Thus, waveform processing of AE signals based on time-scale or time-frequency analysis appears as a very promising signal processing technique to discriminate fracture mechanisms. Many previous works have shown that both the continuous wavelet transform (CWT) and the discrete wavelet transform

© Woodhead Publishing Limited, 2014

(DWT) bring an AE signal discrimination tool on different materials and under different kinds of load (Loutas *et al*., 2006; Ni and Iwamoto, 2002; Qi, 2000). The DWT enables decomposing each signal into different continuous frequency bands that depend on the level of decomposition. Thus, it is possible to determine with the DWT the most energetic levels of decomposition and then identify the frequency bands representative of different damage mechanisms. The results of this approach are promising, and many indications confirm that wavelets are an extremely useful tool in AE analysis, although much work is still to be done.

10.6 Conclusions

The capabilities of AE testing in traditional composite materials research have been significantly improved by several recent advances. This chapter proves that some consideration of the particular structure and behaviour of NFCs has been also attempted in more recent studies involving AE monitoring. In particular, some critical aspects of NFCs, such as detection of damage initiation and measurement and characterization of damage area, have been addressed. In this regard, AE may represent a useful tool for mechanical behaviour monitoring of NFCs. In addition, more advanced waveform-based analyses of AE signals could be successfully used to evaluate and discriminate damage mechanisms in NFCs, thus allowing a better understanding of their behaviour in view of a transition towards fully biodegradable materials.

10.7 Sources of further information and advice

This section is intended to provide links to additional sources of information.

Major organizations concerned with codes, standards, practices and guidelines are:

- ISO – International Organization for Standardization – http://www.iso.org
- CEN – European Committee for Standardization – http://www.cen.eu
- ASTM – American Society for Testing and Materials – http://www.astm.org
- EWGAE – European Working Group on Acoustic Emission – http://ewgae.eu
- AEWG – Acoustic Emission Working Group – http://www.aewg.org
- DGZIP – German Society for Non-destructive Testing – http://www.dgzfp.de
- AIPnD – Italian Society for Non-destructive Testing – http://www.aipnd.it

© Woodhead Publishing Limited, 2014

- ASNT – The American Society for Non-destructive Testing, Inc. – http://www.asnt.org
- Links to websites of international journals dealing with NDT: NDT and evaluation – http://www.tandfonline.com/toc/gnte20/current
- *NDT & E International* – http://www.journals.elsevier.com/ndt-and-e-international
- *Journal of Testing and Evaluation* – http://www.astm.org/DIGITAL_LIBRARY/JOU4RNALS/TESTEVAL
- *Journal of Non-destructive Evaluation* – http://www.springer.com/materials/mechanics/journal/10921
- *Journal of Acoustic Emission* – http://www.aewg.org/jaeonline.htm
- Open access NDT database – http://www.ndt.net

Websites of AE equipment manufacturers:

- Vallen Systeme GmbH – http://www.vallen.de
- Physical Acoustics Corporation – http://www.pacndt.com
- Interunis – http://eng.interunis.ru

10.8 References

Acha B A, Marcovich N E and Karger-Kocsis J (2006), 'Biodegradable jute cloth reinforced thermoplastic copolyester composites: Fracture and failure behaviour', *Plast Rubber Compos,* **35**, 73–82. doi: 10.1179/174328906X79978.

Aicher S, Höfflin L and Dill-Langler G (2001), 'Damage evolution and acoustic emission of wood at tension perpendicular to fiber', *Holz als Roh- und Werkstoff,* **59**, 104–116. doi: 10.1007/s001070050482.

Anuar H, Ahmad S H, Rasid R, Surip S N, Czigany T and Romhany G (2007), 'Essential work of fracture and acoustic emission study on TPNR composites reinforced by kenaf fiber', *J Compos Mater,* **41**, 3035–3049. doi: 10.1177/0021998307082173.

Assarar M, Scida D, El Mahi A, Poilâne C and Ayad R (2011), 'Influence of water ageing on mechanical properties and damage events of two reinforced composite materials: Flax–fibres and glass–fibres', *Mater Des,* **32**, 788–795. doi: 10.1016/j.matdes.2010.07.024.

ASTM E 1316 (2011), Standard terminology for Non-destructive examinations.

Barrè S and Benzeggagh M L (1994), 'On the use of acoustic emission to investigate damage mechanisms in glass-fibre-reinforced polypropylene', *Compos Sci Technol*, **52**, 369–376. doi: 10.1016/0266–3538(94)90171–6.

Benevolenski O I and Karger-Kocsis J (2001), 'Comparative study of the fracture behavior of flow-molded GMT-PP with random and chopped-fiber mats', *Compos Sci Technol,* **61**, 2413–2423. doi: 10.1016/S0266–3538(01)00160–9.

Bennedakhene S, Kenane M and Benzeggagh M L (1999), 'Initiation and growth of delamination in glass/epoxy composites subjected to static and dynamic loading by acoustic emission monitoring', *Compos Sci Technol*, **59**, 201–208. doi: 10.1016/S0266–3538(98)00063–3.

© Woodhead Publishing Limited, 2014

Berthelot J M and Rhazi J (1990), 'Acoustic emission in carbon fibre composites', *Compos Sci Technol*, **37**, 411–428. doi: 10.1016/0266–3538(90)90012-T.

Bohse J (2004), 'Damage analysis of polymer matrix composites by acoustic emission testing', *Proceedings of the 26th European Conference on Acoustic Emission Testing*, Berlin, 15–17 September 2004, 339–348.

Caprino G and Teti R (1995), 'Residual strength evaluation of impacted GRP laminates with acoustic emission monitoring', *Compos Sci Technol*, **53**, 13–19. doi: 10.1016/0266–3538(94)00062-X.

Clough R B and McDonough W G (1996), 'The measurement of fiber strength parameters in fragmentation tests by using acoustic emission', *Compos Sci Technol,* **56**, 1119–1127. doi: 10.1016/S0266–3538(96)00076–0.

Czigany T (2004), An acoustic emission study of flax fibre-reinforced polypropylene composites, *J Compos Mater,* **38**, 769–778. doi: 10.1177/0021998304042481.

Czigany T (2006), 'Special manufacturing and characteristics of basalt fiber reinforced hybrid polypropylene composites: Mechanical properties and acoustic emission study', *Compos Sci Technol,* **66**, 3210–3220. doi: 10.1016/j.compscitech.2005.07.007.

de Groot P J, Wijnen P A M and Janssen R B F (1995), 'Real-time frequency determination of acoustic emission for different fracture mechanisms in carbon/epoxy composites', *Compos Sci Technol*, **55**, 405–412. doi: 10.1016/0266–3538(95)00121–2.

De Rosa I M, Santulli C, Sarasini F and Valente M (2009a), Effect of loading-unloading cycles on impact-damaged jute/glass hybrid laminates, *Polym Compos,* **30**, 1879–1887. doi: 10.1002/pc.20789.

De Rosa I M, Santulli C, Sarasini F and Valente M (2009b), Post-impact damage characterization of hybrid configurations of jute/glass polyester laminates using acoustic emission and IR thermography, *Compos Sci Technol*, **69**, 1142–1150. doi: 10.1016/j.compscitech.2009.02.011.

De Rosa I M, Santulli C and Sarasini F (2010), Mechanical and thermal characterization of epoxy composites reinforced with random and quasi-unidirectional untreated phormium tenax leaf fibers, *Mater Des,* **31**, 2397–2405. doi: 10.1016/j.matdes.2009.11.059.

De Rosa I M, Santulli C and Sarasini F (2011a), Mechanical characterization of untreated waste office paper/woven jute fabric hybrid reinforced epoxy composites, *J Appl Polym Sci,* **119**, 1366–1373. doi: 10.1002/app.32933.

De Rosa I M, Iannoni A, Kenny J M, Puglia D, Santulli C, Sarasini F and Terenzi A (2011b), Poly(lactic acid)/phormium tenax composites: Morphology and thermo-mechanical behaviour, *Polym Compos,* **32**, 1362–1368. doi: 10.1002/pc.21159.

De Rosa I M, Dhakal H N, Santulli C, Sarasini F and Zhang Z (2012), Post-impact static and cyclic flexural characterisation of hemp fibre reinforced laminates, *Compos Part B,* **43**, 1382–1396. doi: 10.1016/j.compositesb.2011.09.012.

Drouillard T F (1996), 'A history of acoustic emission', *J Acoustic Emission*, **14**, 1–34.

Duesing L A (1989), 'Acoustic emission testing of composite materials', *Proceedings Annual Reliability and Maintainability Symposium*, Atlanta, GA, 24–26 January 1989, 128–134.

Eichhorn S J, Baillie C A, Zafeiropoulos N, Mwaikambo L Y, Ansell M P, Dufresne A, Entwistle K M, Herrera-Franco P J, Escamilla G C, Groom L, Hughes M, Hill C, Rials T G and Wild P M (2001), 'Review. Current international

© Woodhead Publishing Limited, 2014

research into cellulosic fibres and composites', *J Mater Sci,* **36**, 2107–2131. doi: 10.1023/A:1017512029696.

Ely T M and v.k.Hill E (1995), 'Longitudinal splitting and fiber breakage characterization in graphite epoxy using acoustic emission data', *Mater Eval*, **53**, 288–294.

EN 1330–9, Non-destructive testing – Terminology – Part 9: Terms used in acoustic emission testing, 1999.

Finkenstadt V L, Liu C K, Evangelista R, Liu L S, Cermak S C, Hojilla-Evangelista M and Willett J L (2007), Poly(lactic acid) green composites using oilseed coproducts as fillers. *Ind Crops Prod,* **26**, 36–43. doi: 10.1016/j.indcrop.2007.01.003.

Förster F and Scheil E (1936), 'Akustische untersuchung der bildung von martensitnadeln', *Z Metallkd*, **29**, 245–247.

Giordano M, Calabrò A, Esposito C, D'Amore A and Nicolais L (1998), 'An acoustic emission characterization of the failure modes in polymer-composite materials', *Compos Sci Technol*, **58**, 1923–1928. doi: 10.1016/S0266–3538(98)00013-X.

Godin N, Huguet S, Gaertner R and Salmon L (2004), 'Clustering of acoustic emission signals collected during tensile tests on unidirectional glass/polyester composites using supervised and unsupervised classifiers', *NDT & E International*, **37**, 253–264. doi: 10.1016/j.ndteint.2003.09.010.

Godin N, Huguet S and Gaertner R (2005), 'Integration of the Kohonen's self-organising map and k-means algorithm for the segmentation of the AE data collected during tensile tests on cross-ply composites', *NDT & E International*, **38**, 299–309. doi: 10.1016/j.ndteint.2004.09.006.

Hamstad M A (1986a), 'A Review: Acoustic emission, a tool for composite-materials studies', *Exp Mech,* **26**, 7–13. doi: 10.1007/BF02319949.

Hamstad M A (1986b), 'A discussion of the basic understanding of the felicity effect in fiber composites', *J Acoustic Emission*, **5**, 95–102.

Hamstad M A and Sendeckyj G P (1993), 'Acoustic emission technology for smart structures', *J Acoustic Emission*, **11**, 33–41.

Hughes M, Carpenter J and Hill C (2007), 'Deformation and fracture behaviour of flax fiber reinforced thermosetting polymer matrix composites', *J Mater Sci*, **42**, 2499–2511. doi: 10.1007/s10853–006–1027–2.

Huguet S, Godin N, Gaertner R, Salmon L and Villard D (2002), 'Use of acoustic emission to identify damage modes in glass fibre reinforced polyester', *Compos Sci Technol*, **62**, 1433–1444. doi: 10.1016/S0266–3538(02)00087–8.

Jeng J S, Ono K and Yang J M (1989), 'Fracture mechanism studies of carbon/PMR-15 composites by acoustic emission', *J Acoustic Emission*, **8**, 268–271.

Kaiser J (1950), 'Untersuchungen über das Auftreten von Geräuschen beim Zugversuch', PhD Thesis, Munich, Germany.

Kelly A and Tyson W R, (1965) 'Tensile properties of fiber reinforced metals: Copper/tungsten and copper/molybdenum', *Mech and Phys Solids,* **13**(6), 329–350. doi: 10.1016/0022–5096(65)90035–9.

Kim S T and Lee Y T (1997), 'Characteristics of damage and fracture process of carbon fiber reinforced plastic under loading – unloading test by using AE method', *Mater Sci Eng A*, **234–236**, 322–326. doi: 10.1016/S0921–5093(97)00226–8.

Kwon O Y, Lee J H and Yoon D J (1995), 'Acoustic emission during tensile loading of low velocity impact-damaged CFRP laminates', *J. Acoustic Emission*, **13**, 83–88.

© Woodhead Publishing Limited, 2014

Loutas T H, Kostopoulos V, Ramirez-Jimenez C and Pharaoh M (2006), 'Damage evolution in center-holed glass/polyester composites under quasi-static loading using time/frequency analysis of acoustic emission monitored waveforms', *Compos Sci Technol*, **66**, 1366–1375. doi: 10.1016/j.compscitech.2005.09.011.

Luo S and Netravali AN (1999), Interfacial and mechanical properties of environment-friendly 'green' composites made from pineapple fibers and poly(hydroxybutyrate-co-valerate) resin, *J Mater Sci,* **34**, 3709–3719. doi: 10.1023/A:1004659507231.

Marec A, Thomas J H and El Guerjouma R (2008), 'Damage characterization of polymer-based composite materials: Multivariable analysis and wavelet transform for clustering acoustic emission data', *Mech Syst Signal Pr*, **22**, 1441–1464. doi: 10.1016/j.ymssp.2007.11.029.

Mason W P, McSkimin H J and Shockely W (1948), 'Ultrasonic observation of twinning in Tin', *Phys Rev*, **73**, 1213–1214. doi: 10.1103/PhysRev.73.1213.

Millard D J (1950), 'Twinning in single crystals of cadmium', PhD Thesis, University of Bristol, England.

Mittelman A and Roman I (1987), 'A new approach to the use of acoustic emission peak amplitude distribution as a tool of characterizing failure mechanisms in composite materials', *J Acoustic Emission*, **6**, 73–77.

Mittelman A and Roman I (1991), 'Monitoring the tensile deformation in real unidirectional Kevlar/epoxy composites', *NDT & E International*, **24**, 85–89. doi: 10.1016/0963–8695(91)90822-K.

Mix P E (2005), *Introduction to Non-Destructive Testing: A Training Guide*, 2nd edition, Hoboken, New Jersey, John Wiley & Sons, Inc.

Mohanty A K, Misra M and Hinrichsen G (2000), 'Biofibres, biodegradable polymers and biocomposites: An overview', *Macromol Mater Eng*, **276–277**(1), 1–24. doi: 10.1002/(SICI)1439–2054(20000301)276:1.

Moore P O (2005), *Non-Destructive Testing Handbook, Acoustic Emission Testing*, Volume 6, 3rd Edition, Columbus, American Society for Non-destructive Testing.

Narisawa I and Oba H (1985), An evaluation of acoustic emission from fibre-reinforced composites. Part 2: The application of acoustic emission techniques to aramid fibre-reinforced model composites, *J Mater Sci,* **20**, 4527–4531. doi: 10.1007/BF00559344.

Newman R H, Le Guen M J, Battley M A and Carpenter J E P (2010), Failure mechanisms in composites reinforced with unidirectional Phormium leaf fibre, *Composites Part A,* **41**, 353–359. doi: 10.1016/j.compositesa.2009.11.001.

Ni Q Q and Iwamoto M (2002), 'Wavelet transform of acoustic emission signals in failure of model composites', *Eng Fract Mech*, **69**, 717–728. doi: 10.1016/S0013–7944(01)00105–9.

Ochiai S I, Lew K Q and Green J E (1982), 'Instrumented impact testing of structural fiber-reinforced plastic sheet materials and the simultaneous AE measurements', *J Acoustic Emission*, **1**, 191–192.

Okoroafor E U, Priston A-M and Hill R (1996), 'Adhesion in fibre reinforced plastics investigated by means of acoustic emission', *Int J Adhes Adhes,* **16**, 141–146. doi: 10.1016/0143–7496(95)00010–0.

Park J-M, Quang S T, Hwang B-S and DeVries K L (2006a),'Interfacial evaluation of modified Jute and Hemp fibers/polypropylene (PP)-maleic anhydride

© Woodhead Publishing Limited, 2014

polypropylene copolymers (PP-MAPP) composites using micromechanical technique and non-destructive acoustic emission', *Compos Sci Technol,* **66**, 2686–2699. doi: 10.1016/j.compscitech.2006.03.014.

Park J-M, Son T Q, Jung J-G and Hwang B-S (2006b), 'Interfacial evaluation of single Ramie and Kenaf fiber/epoxy resin composites using micromechanical test and non-destructive acoustic emission', *Compos Inter,* **13**, 105–129. doi: 10.1163/156855406775997051.

Park J-M, Kim P-G, Jang J-H, Wang Z, Hwang B-S and DeVries K L (2008), 'Interfacial evaluation and durability of modified Jute fibers/polypropylene (PP) composites using micromechanical test and acoustic emission', *Compos Part B*, **39**, 1042–1061. doi: 10.1016/j.compositesb.2007.11.004.

Qi G (2000), 'Wavelet-based AE characterization of composite materials', *NDT & E International*, **33**, 133–144. doi: 10.1016/S0963–8695(99)00037–7.

Ramirez-Jimenez C R, Papadakis N, Reynolds N, Gan T H, Purnell P and Pharaoh M (2004), 'Identification of failure modes in glass/polypropylene composites by means of the primary frequency content of the acoustic emission event', *Compos Sci Technol*, **64**, 1819–1827. doi: 10.1016/j.compscitech.2004.01.008.

Romhany G, Karger-Kocsis J and Czigany T (2003a), 'Tensile fracture and failure behavior of technical flax fibers', *J Appl Polym Sci,* **90**, 3638–3645. doi: 10.1002/app.13110.

Romhany G, Karger-Kocsis J and Czigany T (2003b), 'Tensile fracture and failure behavior of thermoplastic starch with unidirectional and cross-ply flax fiber reinforcements', *Macromol Mater Eng,* **288**, 699–707. doi: 10.1002/mame.200300040.

Romhany G, Czigany T and Karger-Kocsis J (2006), 'Determination of J-R curves of thermoplastic starch composites containing crossed quasi-unidirectional flax fibre reinforcement', *Compos Sci Technol,* **66**, 3179–3187. doi: 10.1016/j.compscitech.2005.01.016.

Santulli C (2001), 'Post-impact damage characterization on natural fibre reinforced composites using acoustic emission', *NDT & E International*, **34**, 531–536. doi: 10.1016/S0963–8695(01)00013–5.

Santulli C (2006), 'Post-impact flexural tests on jute/polyester laminates monitored by acoustic emission', *J Mater Sci*, **41**, 1255–1260. doi: 10.1007/s10853–005–4235–2.

Santulli C (2007), 'Review. Impact properties of glass/plant fibre hybrid laminates', *J Mater Sci,* **42**, 3699–3707. doi: 10.1007/s10853–006–0662-y.

Santulli C (2008), 'A biomimetic approach to the production of sustainable structural composites using plant fibres', chap. 5 in '*Biologically Inspired Textiles*', Ellison MS and Abbott AG (eds), Cambridge, Woodhead Publishing Limited, ISBN 978–1-4200–7985–2.

Serrano E P and Fabio M A (1996), 'Application of the wavelet transform to acoustic emission signal processing', *IEEE Trans Signal Process*, **44**, 1270–1275. doi: 10.1109/78.502340.

Shin F G, Xian X J, Zheng W G and Yipp M W (1989), 'Analysis of the mechanical properties and microstructure of bamboo–epoxy composites', *J Mater Sci,* **24**, 3483–3490. doi: 10.1007/BF02385729.

Shull P J (2002), *Non-destructive Evaluation: Theory, Techniques, and Applications*, New York, Marcel Dekker Inc.

© Woodhead Publishing Limited, 2014

Sreekala M S, Czigany T, Romhany G and Thomas S (2003), 'Investigation of oil palm and pineapple fiber reinforced phenol formaldehyde composites by acoustic emission technique', *Polym Compos*, **11**, 9–18.

Summerscales J (1986), 'The Felicity Effect in Acoustic Emission from Composites', *International Symposium on Composite Materials and Structures*, Beijing, China.

The American Society for Non-destructive Testing, Inc. Available from: http://www.asnt.org/ndt/primer1.htm (Accessed 2 July 2012).

Tserki V, Zafeiropoulos N E, Simon F and Panayiotou C (2005), 'A study of the effect of acetylation and propionylation surface treatments on natural fibre', *Compos Part A,* **36**, 1110–1118. doi: 10.1016/j.compositesa.2005.01.004.

Walker J L and v.k.Hill E (1992), 'Amplitude distribution modelling and ultimate strength prediction of ASTM D-3039 graphite/epoxy tensile specimens', *Proceedings of AECM-4*, Seattle, 115–131.

Wambua P, Ivens J and Verpoest I (2003), 'Natural fibres: Can they replace glass in fibre reinforced plastics?', *Compos Sci Technol,* **63**, 1259–1264. doi: 10.1016/S0266–3538(03)00096–4.

Yang Y, Ota T and Morii T and Hamada H (2011) 'Mechanical property and hydrothermal aging of injection molded jute/polypropylene composites', *J Mater Sci,* **46**, 2678–2684. doi: 10.1007/s10853–010–5134–8.

Zhuang X and Yan X (2006), 'Investigation of damage mechanisms in self-reinforced polyethylene composites by acoustic emission', *Compos Sci Technol*, **66**, 444–449. doi: 10.1016/j.compscitech.2005.07.013.

© Woodhead Publishing Limited, 2014

11

High strain rate testing of natural fiber composites

W. KIM and A. ARGENTO,
University of Michigan-Dearborn, USA

DOI: 10.1533/9780857099228.3.303

Abstract: The constitutive behavior of composites of polymer resins reinforced by various natural fibers and containing microcellular voids is considered. Tensile and compressive tests are conducted at strain rates up to 2500/s to study the rate dependence and energy dissipation of the various material formulations. It is found that, in compression, the natural fiber composites with microcellular voids show reduced rate hardening of yield stress and possess enhanced energy dissipation, but these benefits are diminished in tension. In some cases of solid natural fiber composites, the fibers themselves play a role in reducing rate dependence.

Key words: rate dependence, energy dissipation, strain rate, microcellular voids, natural fibers.

11.1 Introduction

The focus of this work is the rate dependent constitutive behavior of composite materials containing natural fibers, as well as systems containing natural fibers and microcellular voids. Rate dependence refers to an increase in modulus and yield stress, and a decrease in failure strain, which occurs in many materials when they are loaded at rates beyond quasi-static. Polymers are particularly affected by rate dependence (Dean and Read, 2001) though all three features do not always occur, and the effect of loading rate on modulus is usually small in comparison to its effect on yield point. The phenomenon is problematic for impact safety applications mainly because of the increase in yield stress, which can be quite pronounced and results in increased contact stress on the impacting objects.

A broad overview of work on quasi-static stress–strain behavior, failure, and Charpy/Izod impact properties for various natural fibers and composite formulations can be found in Mishra *et al*. (2000), Gassan *et al*. (2001), Bledzki and Faruk (2004), Low *et al*. (2007), Santulli (2007), Summerscales *et al*. (2011), Zaman *et al*. (2011), Al-Zubaidy *et al*. (2012), and Chandra *et al*. (2012). The tailoring of mechanical properties of natural fiber composites

© Woodhead Publishing Limited, 2014

for structural applications has received much treatment. The primary focus has been on modulus and strength. In Keller (2003) and Mohanty *et al*. (2003) the effect of material processing on the impact strength and the other mechanical properties is studied, while in Santulli and Cantwell (2001), Lodha and Netravali (2002), Cabral *et al*. (2005), De Medeiros *et al*. (2005), and Rodriguez *et al*. (2005) the role of fiber type and arrangement are investigated. Also, numerous research is available (Mohanty *et al*., 2000; Mishra *et al*., 2000; Khan *et al*., 2001; Rana *et al*., 2003; Datta *et al*., 2004; Razera and Frollini, 2004; Rajulu *et al*., 2005) on mechanical property modifications due to various chemical compatibilizations and mechanical treatments of the resins and fibers.

Rate testing in which the material is subjected to dynamic loads resulting in general stress–strain diagrams at various rates are not as widely available for natural fiber-based composite materials. Tests at low strain rates, less than 1/s, have been conducted on various natural fiber materials in tension in George *et al*. (1999) and in compression in Song *et al*. (2011) and Ip *et al*. (1997). Increased yield and modulus were observed from the tests. Compressive tests at rates more indicative of impact (up to about 2500/s) were conducted in Omar *et al*. (2010), Argento *et al*. (2011), and Kim *et al*. (2012), resulting in pronouncedly increased yield stress and decreased failure strain. In some cases, natural fiber-based composites showed reduced rate-effects compared with conventional systems, likely because of particular failure properties and failure modes of the fibers as well as their interaction with the binding resin. The cellular structure of the specific cellulose of which the plant fiber is comprised is likely also an important factor in the resulting mechanical behavior (Bledzki and Gassan, 1999). In an effort to tailor the load-bearing characteristic of the glass composite and the energy dissipation characteristic of the hemp composite, various hemp/glass hybrid systems have been studied in Kim *et al*. (2012). The hybrid systems resulted in behavior intermediate between the glass and hemp cases. These had higher strength than the hemp case and lower rate dependence than the glass case.

Though natural fibers may be a factor in mitigating rate dependence in composites, the strong rate dependence of most polymeric resins used to bind the composites may play the dominant role in the phenomenon. When composites are to be used in an impact safety capacity, rate dependence is critical because it increases the stress that occurs during the impact. Microcellular plastics have been found to reduce the impact stress and enhance energy absorption characteristics in composites (Argento *et al*., 2011) by directly altering the mechanical response of the binding resin. These are composites consisting of a polymer resin infused with microcellular voids and a reinforcing material. Natural fibers have been found to be suitable reinforcements for these systems and the resulting composites are

© Woodhead Publishing Limited, 2014

lightweight and possess good, tunable properties (Matuana-Malanda *et al*., 1996; Bledzki *et al*., 1999a, 1999b; Faruk and Bledzki, 2006; Neagu *et al*., 2012; Xie *et al*., 2012).

In this work, rate dependent tests are conducted on natural fiber-reinforced polymeric composites with and without microcellular voids. Tension and compression curves are given at rates up to about 27/s and 2500/s, respectively. Energy absorption diagrams are determined from the tests for the systems that demonstrate the advantage of using microcellular-based composites for critical, compressive impact safety applications. A possible mechanical response mechanism leading to improved energy absorption in impact events is described using the finite element method incorporating measured data. The enhanced impact energy absorption characteristics found in compression for the microcellular systems are seen to be diminished in tension.

11.2 Materials

Various voided and solid composites of natural fibers embedded in a polymer base material have been studied. These are described in this section.

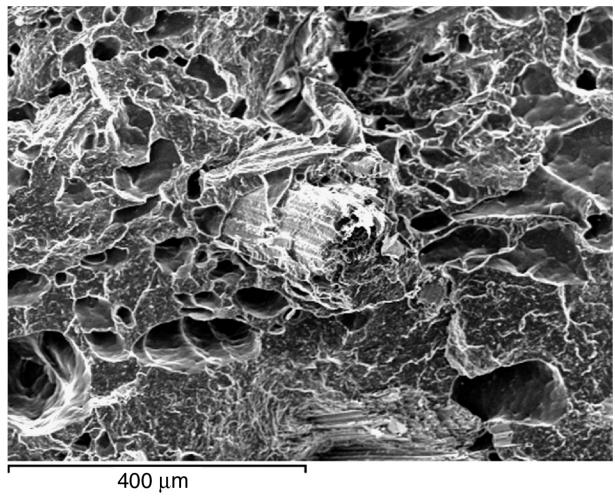
11.2.1 Natural fiber-reinforced polypropylene thermoplastic composites

Composites of polypropylene (PP) homopolymer reinforced with wheat straw fibers (WSF) and purified cellulose have been tested. Each composite has a 20% loading of natural fibers. (All fiber loading compositions given in this chapter are on a weight basis.) Unreinforced PP homopolymer specimens have also been tested to serve as a control for the evaluations.

11.2.2 Natural fiber-reinforced polypropylene thermoplastic composites containing microcellular voids

Polymer materials with micron sized voids can be manufactured by physical or chemical foaming (Bledzki *et al*., 2006a; Argento *et al*., 2011; Velasco *et al*., 2011). These methods were originally developed for creating stiff, lightweight materials, but of interest in the present work is the effect of microcellular structure on the constitutive behavior under loading over a range of strain rates. In order for the foaming process to yield materials with uniform microcellular structure, a reinforcing filler material is recommended. Here two separate natural fiber reinforcements are used: wheat straw and cellulose. A conventional talc (powder) reinforcement is also

© Woodhead Publishing Limited, 2014



11.1 Microscopic image of sisal fiber-reinforced polypropylene containing microcellular voids (Argento *et al.,* 2011).

used for comparison. Each PP specimen contains 20% reinforcing material and a 10% weight reduction has been achieved by microcellular voids. The microcellular structure, as well as the presence of fillers and reinforcements, has significant effects on the mechanical and dynamic performance of the molded component (Vanvuchelen *et al*., 2000; Bledzki *et al*., 2005, 2006a; Gunkel *et al*., 2008). Cell size, density, and uniformity are routinely characterized for microcellular composites. For example, Fig. 11.1 shows a portion of a typical untested specimen revealing sisal fibers surrounded by PP and microcellular voids. Overall, the specimen contains 30% sisal fibers and 10% microcellular voids. The average diameter of the voids is about 100 μm.

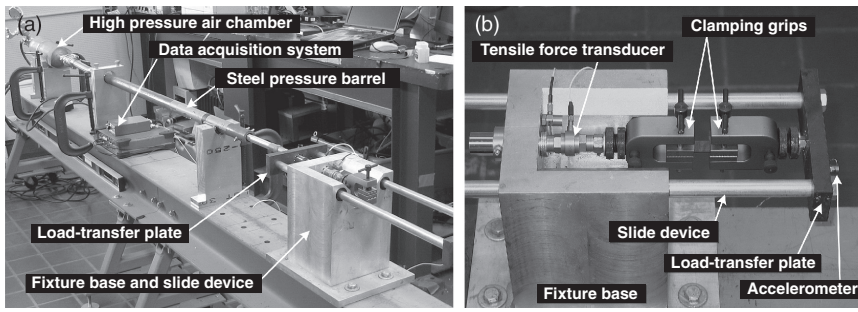
11.2.3 Natural fiber-reinforced vinyl ester thermoset composites

Sheet molded hemp fiber-reinforced vinyl ester and glass fiber-reinforced vinyl ester (as a control) (Kim *et al*., 2012) are studied. In both cases the materials consist of 40% fibers (25.4 mm length) compounded with 50% vinyl ester resin along with typical fillers and additives.

11.3 Test methods

Tensile tests have been conducted using the custom-made test system shown in Fig. 11.2. The major components of the test system are a pressure chamber, a steel pressure barrel, a heavy fixture base, a slide device, clamping

© Woodhead Publishing Limited, 2014

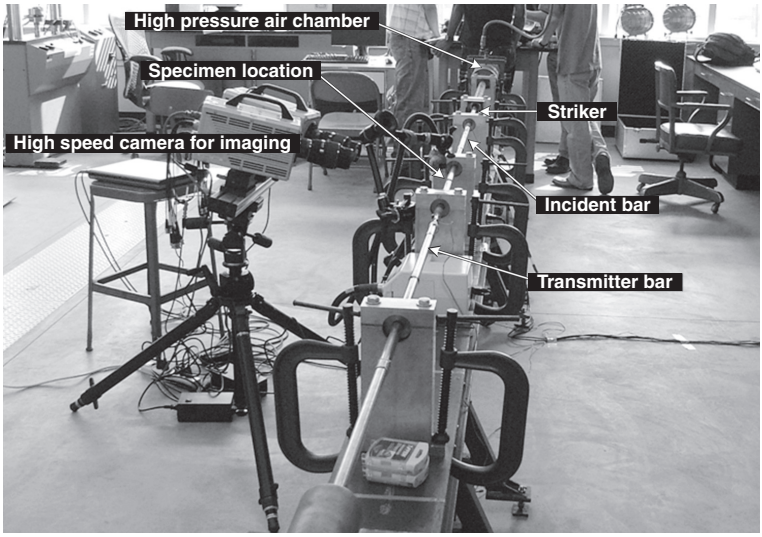


11.2 Custom-made test system: (a) overall system in dynamic test arrangement, and (b) fixture base and slide device in tensile test arrangement.

grips, sensors, and data acquisition systems. For tensile tests, dog bone-shaped specimens (162 mm overall length, 3.15 mm thickness, and 12.7 mm width in the gauge section) are installed in grips and the slide device loaded from the left end resulting in tension at the specimen location. The system uses a screw-driven mechanical actuator (TestResources Inc. Model 500, not shown in the figure) and a high pressure air chamber for low- and high-rate loadings, respectively. Loads are applied on the load-transfer plate by pushing and by impact for quasi-static and dynamic tests, respectively. Load is measured by a tensile force transducer placed between the heavy fixture base and the stationary grip. In quasi-static and low-rate tests, a low-rate transducer is used (TestResources Inc., SM-500–294). In moderate-rate tests, a high-rate sensor is used (PCB Piezotronics Inc., Model 223B). Specimen displacement, from which strain is determined, is measured in quasi-static tests using a motion encoder incorporated in the load actuator. In dynamic tests, displacement is determined by time integration of acceleration signals measured on the load-transfer plate to which the moving grip is attached. Acceleration of the heavy fixture base is also acquired to ensure its motion is negligible during the dynamic tests. Data is collected using an Oros data acquisition system.

High strain rate compressive tests are performed using the split Hopkinson pressure bar apparatus shown in Fig. 11.3 that transmits high-rate strain through a small disk-shaped specimen placed between long cylindrical incident and transmitter bars. All disk specimens tested have nominal dimensions of 13 mm in diameter and 3 mm in thickness. The Hopkinson method is fairly well established for materials of all but low stiffness; details of its measurement theory, techniques, and instrumentation are described in, for example, Al-Mousawi *et al*. (1997) and Kim *et al*. (2012). Here the device is used to produce stress–strain and energy dissipation curves of solid and microcellular composites at rates up to about 2500–/s.

© Woodhead Publishing Limited, 2014



11.3 Split Hopkinson pressure bar apparatus.

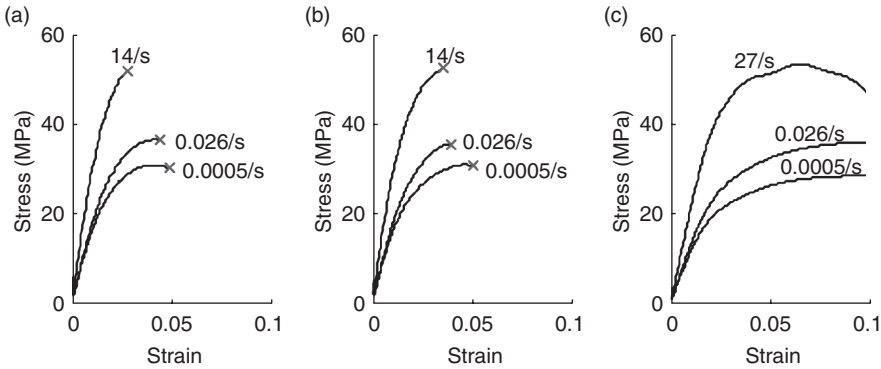
11.4 Results and discussion

Results of mechanical tests on the materials are described in this section. Tests were conducted in tension and compression up to strain rates of 2500/s.

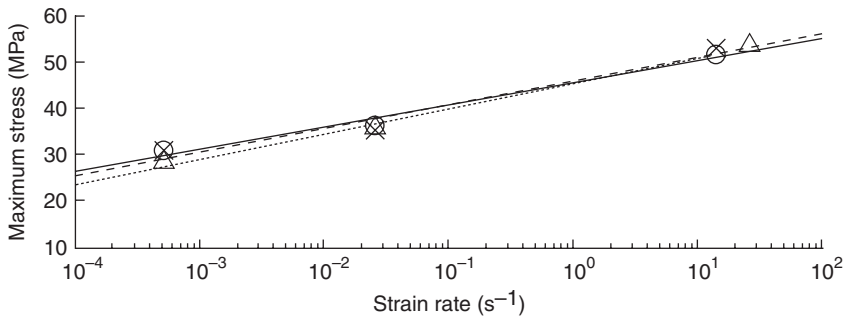
11.4.1 Tensile strain rate dependence of natural fiber-reinforced polypropylene thermoplastic composites

Figure 11.4 shows tensile stress–strain curves measured by the custom-made test system (Fig. 11.2) at various strain rates. Figure 11.4a and 11.4b are plots of the PP homopolymer composites reinforced by WSF(WSF–PP) and cellulose (cellulose–PP), respectively, while Fig. 11.4c shows curves of unreinforced pure PP. Each plot shows three stress–strain curves at quasi-static (0.0005/s), low (0.026/s), and moderate (14/s or 27/s) rates. In all three materials, strain rate dependence is observed. Strain rate dependence, or rate hardening, generally refers to the tendency of a material's yield stress to increase and failure strain to decrease when loaded at a higher rate. Since a clearly defined yield point is not discernible in the plots, the maximum stress induced during each test will be investigated instead of the yield stress. In Fig. 11.5, the maximum stress is plotted as a function of strain rate. Note that the horizontal axis scale is logarithmic. The solid, dashed, and dotted lines are obtained by linear curve fitting of the WSF–PP, cellulose–PP, and PP data, respectively, and their slopes indicate the degree of rate hardening. It is seen in Fig. 11.5 that the rate-induced increases in maximum stress

© Woodhead Publishing Limited, 2014



11.4 Tensile stress–strain curves at various strain rates of (a) WSF–PP, (b) cellulose–PP, and (c) PP.



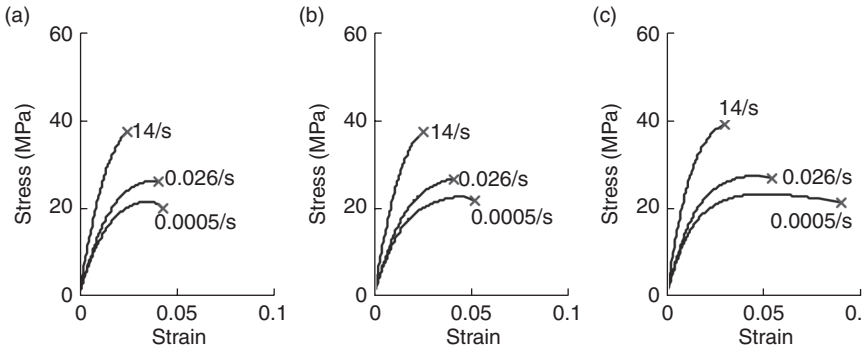
11.5 Maximum tensile stress of WSF–PP (circles, solid line), cellulose–PP (crosses, dashed line), and PP (triangles, dotted line) as functions of strain rate.

are significant and quite similar in these materials at the tested rates. The effect of dynamic loading on the failure strain can also be seen in Fig. 11.4 in which an x-mark at the end of a curve indicates specimen fracture. In general, specimens failed at lower strains when loaded at higher rates. Another important point is that the initial slope of a stress–strain curve (i.e., modulus) increases, compared with pure PP, due to natural fiber reinforcement. The failure strain, however, significantly decreases by using natural fibers. Note that PP specimens did not fracture in the strain range shown in Fig. 11.4c.

11.4.2 Tensile strain rate dependence of natural fiber-reinforced polypropylene thermoplastic composites containing microcellular voids

The measured tensile stress-strain curves of the microcellular voided specimens of wheat straw fiber-reinforced PP (microcellular WSF–PP),

© Woodhead Publishing Limited, 2014



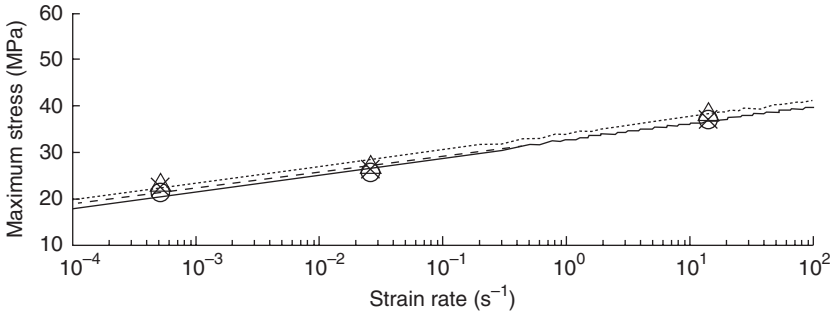
11.6 Tensile stress–strain curves at various strain rates of (a) microcellular WSF–PP, (b) microcellular cellulose–PP, and (c) microcellular talc–PP.

cellulose-reinforced PP (microcellular cellulose–PP), and conventional talc-reinforced PP (microcellular talc–PP) are plotted at various strain rates in Fig. 11.6. Similar to the strain rate dependence seen in the previous graphs, when loaded at higher rates, specimens fail at lower strains in all three materials in Fig. 11.6. The maximum stresses are plotted in Fig. 11.7 as functions of strain rate. The solid, dashed, and dotted lines are obtained by linear curve fitting of the microcellular WSF–PP, microcellular cellulose–PP, and microcellular talc–PP data, respectively. It is seen that the degree of rate hardening is essentially equal in the materials. It is also observed in Fig. 11.6 that the maximum stress (strength) and modulus (stiffness) are not degraded by using the wheat straw and cellulose fibers instead of talc as reinforcing agents. Note also that the weight of natural fiber specimens is slightly lower than that of talc specimens.

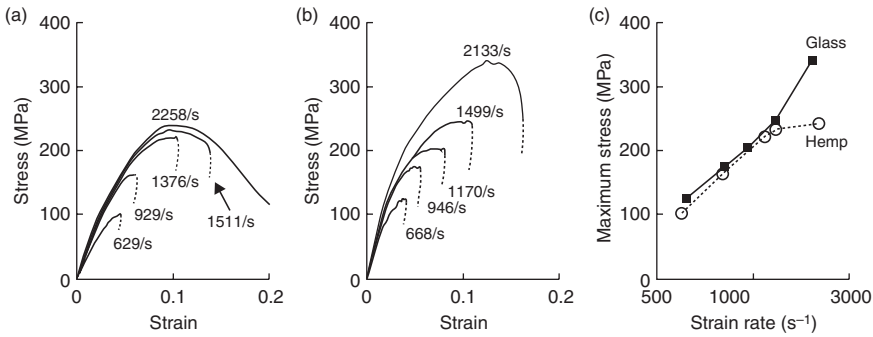
11.4.3 Compressive strain rate dependence of hemp fiber-reinforced vinyl ester thermoset composites

Compressive stress–strain curves of hemp fiber-reinforced vinyl ester thermoset composite specimens, measured by using the split Hopkinson pressure bar apparatus at high strain rates, are shown in Fig. 11.8a. Results for conventional glass fiber-reinforced vinyl ester are also presented in Fig. 11.8b for comparison. It should be noted in these tests that the reversing trend seen in the dotted end portion of the curves represents an unloading process, and so does not indicate material failure. Also, the elastic modulus from these tests should be regarded as approximate, since its precise measurement by the Hopkinson test method is not always reliable and should be confirmed by other measurements (Al-Mousawi *et al.*, 1997; Nicholas, 1981). Another

© Woodhead Publishing Limited, 2014



11.7 Maximum tensile stress versus strain rate of WSF–PP (circles, solid line), cellulose–PP (crosses, dashed line), and talc–PP (triangle, dotted line) containing microcellular voids.



11.8 Compressive stress–strain curves at various strain rates of (a) hemp and (b) glass composites, and (c) the maximum stresses of the two composite systems versus strain rates. (*Source*: Adapted from Kim *et al.*, 2012.)

point is that precise control of the strain rate induced in the specimens is difficult to achieve in the Hopkinson tests, so the strain rates are not exactly the same for both materials (Argento *et al.*, 2011). Moreover, the strain rate varies during a test. The strain rate values presented in Fig. 11.8 are the maximum strain rates induced during the tests.

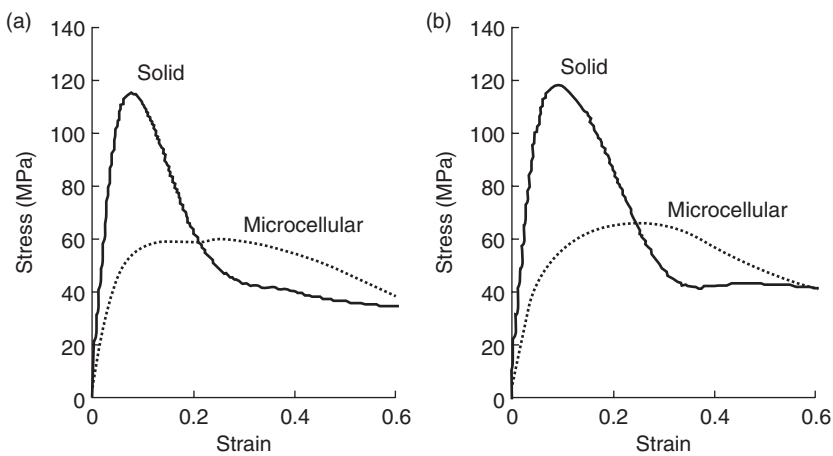
In Fig. 11.8c, the maximum stresses of the hemp and glass fiber-reinforced vinyl ester composites are plotted for comparison as functions of strain rate in which the horizontal axis scale is logarithmic. The solid and dotted lines (between approximately 600 and 1500 /s) are obtained by linear curve fitting of the glass and hemp data, respectively, and their slopes indicate the degree of strain rate dependence. Some observations reported in Kim *et al.* (2012) will be presented here. It is seen that up to 1376 /s, rate hardening in the glass and hemp composites are essentially equal. At higher rates, the maximum stress of the glass composite is much higher than that of the hemp

© Woodhead Publishing Limited, 2014

composite. In load-bearing applications, high yield stress is desirable for mechanical performance. On the other hand, the hemp curves (Fig. 11.8a) are seen to nearly coalesce at higher rates, and the corresponding rate hardening is seen to greatly lessen as depicted in Fig. 11.8c. This overall behavior indicates the material is appropriate for applications where the material is nominally low load bearing (since the hemp composite has lower stiffness than the glass composite), but must be able to dissipate impact energy at low stress for safety purposes.

11.4.4 Compressive energy dissipation of natural fiber-reinforced polypropylene thermoplastic composites containing microcellular voids

Figure 11.9a and 11.9b shows the compressive stress–strain curves of wheat straw fiber- and cellulose-reinforced PP homopolymers, respectively, measured by the Hopkinson test apparatus at a strain rate of approximately 2500/s. In each plot, a microcellular voided specimen (dotted line) is compared with a solid specimen (solid line). The compressive stress of the solid specimen reaches its maximum value at approximately 0.1 strain in both wheat straw fiber and cellulose homopolymers. However, the flow stress abruptly decreases when the material deforms further. The mechanism of this abrupt failure is not clear at this time and warrants further investigation. Note that the abrupt failure process seen in these composites is not

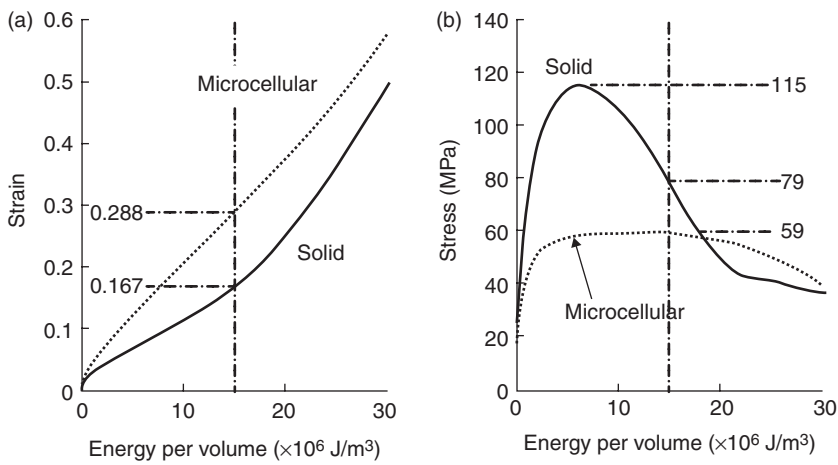


11.9 Compressive stress–strain curves at approximately 2500/s of (a) wheat straw fiber- and (b) cellulose-reinforced polypropylene homopolymers: microcellular (dotted line) versus solid (solid line) composites.

© Woodhead Publishing Limited, 2014

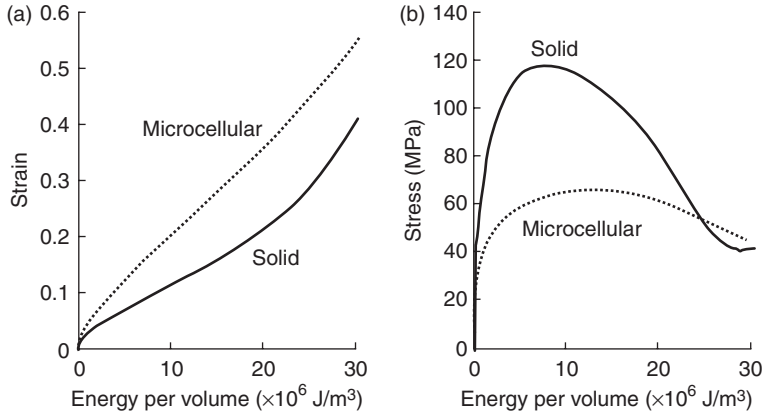
observed in the wheat straw fiber-reinforced PP copolymer case reported in Kim *et al*. (2012).

It is also observed in Fig. 11.9 that the microcellular specimens do not show the abrupt failure at low strain seen in the solid specimens and deform smoothly through their yield stress point into large deformation. These characteristics are very positive for impact safety applications since impact energy dissipation starts at low stress and proceeds continuously through high strain regions without catastrophic failure (Argento *et al*., 2011). In order to quantitatively investigate these behaviors further, the dissipated energy per unit volume during material deformation is calculated. Figure 11.10a and 11.10b show strain and stress, respectively, versus dissipated energy per unit volume, that is, the area under the stress–strain curves of the wheat straw fiber-reinforced PP composites in Fig. 11.9a. The curves show that energy is dissipated by the microcellular composite at greater strain and lower stress than the solid composite. For example, if the material is to absorb a specified amount of energy, 15 MJ/m^3, the microcellular composite needs to deform to 0.288 strain while the solid composite deforms to 0.167 strain as shown in Fig. 11.10a. However, in Fig. 11.10b, the stress induced during the deformation is only 59 MPa in the microcellular case, compared with 79 MPa in the solid case. Moreover, the solid specimen has already passed through its peak stress (115 MPa) to reach the energy dissipation level of 15 MJ/m^3. In Fig. 11.11, the cellulose reinforced PP homopolymer shows a similar trend. Therefore, for an impact situation, the microcellular composite has better



11.10 Compressive (a) strain and (b) stress versus energy dissipation per unit volume of wheat straw fiber-reinforced polypropylene homopolymers: microcellular (dotted line) versus solid (solid line) composites.

© Woodhead Publishing Limited, 2014



11.11 Compressive (a) strain and (b) stress versus energy dissipation per unit volume of cellulose-reinforced polypropylene homopolymers: microcellular (dotted line) versus solid (solid line) composites.

material characteristics than the solid, absorbing the necessary energy while maintaining low peak stress.

11.5 Applications and future trends

Possible applications taking advantage of the unique behaviors of these systems are described here. Modeling approaches are reviewed that capture the effects of voids and fiber reinforcements in polymer composites. Such an approach would be necessary to produce effective, optimized designs of material systems for specific applications.

11.5.1 Energy dissipation mechanisms due to natural fiber properties and microcellular voids

It has been determined that the natural fiber-reinforced polymeric composites studied possess unique energy dissipation characteristics and muted rate dependence in compression, compared with a glass reinforced composite system. In addition, microcellular foaming of the materials further enhances the effects. The reason for the muted rate dependence in the non-foamed case is not fully known at present, but is likely the result of internal failure processes occurring at lower stresses and in a more gradual manner (Kim *et al.*, 2012). These processes can be generally characterized by matrix cracking, fiber transverse fracture and axial splitting, fiber pull-out from the matrix, etc. Additionally, some microscopy has suggested that the vasculature of natural fiber materials could play an additional role in muting rate

© Woodhead Publishing Limited, 2014

dependence (Argento *et al*., 2011). Some of the basic knowledge on rate hardening mechanisms available for polymers can be extended to microcellular polymeric biocomposites, namely the role of the polymeric binding resin (Hamdan and Swallowe, 1996; Al-Maliky *et al*., 1998; Chen *et al*., 1999), but dynamic mechanisms functioning due to microcellular voids, the vascular anatomy of the natural fibers, and interactions of the various constituents, are unknown and much more study is needed.

Applications potentially suited to these systems are those that require a lightweight, semi-structural component or filler that provides good dynamic response, energy dissipation, low-rate hardening, high damping, or shock absorbance. For example, guard rails (Hargrave *et al*., 1997); energy absorbing flooring for elderly care facilities (Laing and Robinovitch, 2009), playgrounds (Huang and Chang, 2009), factories, and running tracks, all of which must dissipate energy without being too compliant; electronics protection, such as laptop casings; packaging and safety equipment, such as helmets (Edwards *et al*., 2004; Goldsberry, 2006; John and Thomas, 2008; Satyanarayana *et al*., 2009;). Hybridized versions of the natural material systems could enhance seismic infill panels (Jung and Aref, 2005) by adding to the overall dissipative property of the system. With further research, the materials might find use in composite slabs (da Silva *et al*., 2003) and concrete barriers (Atahan and Sevim, 2008).Transportation industries and systems have been identified as potential major users of natural fiber composites (Brouwer, 2000; Pervaiz and Sain, 2003; Wibowo *et al*., 2003; Joshi *et al*., 2004; Bledzki *et al*., 2006b; Ashori, 2008) due to the wide diversity of available applications and the magnitude of resource consumption and product turnover by the industries. Transportation related applications include exterior vehicle body panels for pedestrian impact protection, interior energy absorbing material in automobiles, aircraft and trains for head impact, bumper energy reinforcements, and energy dissipation rails to improve offset crash.

11.5.2 Biomedical applications

Current research is also leading to applications in the biomedical fields. Foamed, rigid polymers are being explored for biomedical scaffolds since they are naturally porous, and the porosity can be controlled by the processing parameters (Leicher *et al*., 2005; Chien and Shah, 2012). In the latter reference, the scaffolds are formed from soy protein. Soy protein has also been processed into fibers to form biomedical composite materials and structures. Membranes of nanofibers produced by electrospinning a soy protein isolate solution have potential applications as tissue scaffolds and wound dressings (Xu *et al*., 2012). Wet spinning has been used to produce larger soy protein fibers having mechanical properties suitable for biomedical substrates (Reddy and Yang, 2009). The same authors have also developed

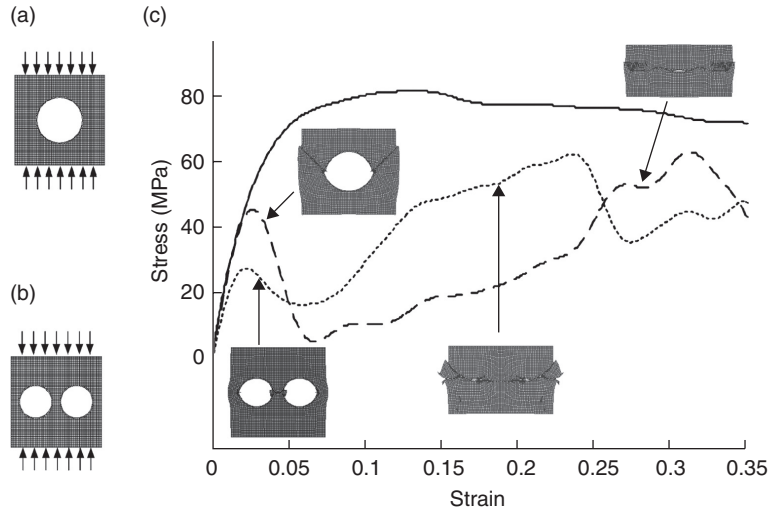
© Woodhead Publishing Limited, 2014

natural fibers from wheat gluten potentially suitable for implants, sutures and scaffolds (Reddy and Yang, 2007).

11.5.3 Modeling

Analytical and/or numerical models can be a good tool for the elucidation of micromechanical behavior and intrinsic dynamic characteristics of fiber-reinforced composite materials. In the case of composites with natural fibers and infused voids, deformation and failure modes associated with void collapse and the unique morphology of the fibers complicates matters. To capture some of these effects, a suitable approach may be one utilizing the unit cell method that proved efficient in Bonora and Ruggiero (2006a, 2006b) on the modeling and prediction of the progressive failure mechanisms of metal matrix composites. In such finite element analysis models, the effects of possible frictional contact/slip between fibers and matrix, which may occur in fiber pull-out and de-bonding processes, need to be included. In general, weaker interfacial adhesion causes fiber pull-out and increased energy absorption, while strong adhesion increases strength (Berglund, 2006). The frictional sliding of de-bonded fiber fragments within the matrix, fiber fracture, and the creation of new crack surfaces are also responsible for energy absorption (Fowler *et al*., 2006). Because plant fibers behave differently from conventional fibers, particularly in regards to their failure, a model of plant anatomy to a degree necessary to capture the operating physics, based on microscopy, should also be incorporated. In the microcellular voided composite, the enhanced energy dissipation characteristics seen in the compressive curves could partly be due to a mechanical process in which the voids carry the major response out of the material and into the void region, inhibiting, or delaying possible fundamental rate effect mechanisms (Hamdan and Swallowe, 1996; Al-Maliky *et al*., 1998; Chen *et al*., 1999) in the binding polymer. Some initial work demonstrating this is shown in Fig. 11.12. Results are given from preliminary two-dimensional finite element models of sisal–PP biocomposites (sisal–PP) with one and two voids. The size of the models is 1 mm × 1 mm and the voided area is about 20% in both cases. Compressive loading is applied at the rate of about 2300 /s and average load-deflection curves are plotted in Fig. 11.12c. In the simulations, measured stress–strain data at 2300/s of sisal–PP without microcellular voids shown as the solid line in Fig. 11.12c is adopted for the surrounding material. In the case of one void (dashed line in Fig. 11.12c), cracks are generated when the strain is about 0.03, and flow stress decreases due to cracking. However, in the region beyond 0.07 strain, stress increases while the void is collapsing and the material undergoes densification. Maximum stress is observed at around 0.3 strain. The case of two voids (dotted line in Fig. 11.12c) has a similar trend, but the progression from one to two voids offers clues of

© Woodhead Publishing Limited, 2014



11.12 Collapsing void models of sisal–PP: (a) one- and (b) two-void models, and (c) their stress–strain curves (solid line shows sisal–PP without microcelluler voids).

how the presence of voids enhances energy dissipation characteristics in a material. The initial stress peak in the material noted at about 0.03 strain in the one-void case again occurs, but is reduced from about 45 to 28 MPa. The two-void material also undergoes densification, and higher stresses are delayed to higher strain values. Comparing the one-void and two-void cases, one can see how increasing the number of voids will inhibit the negative response features seen in Fig. 11.9. Along these lines, other researchers have successfully predicted the large-strain mechanical response of heterogeneous polymer systems with voids using finite element models considering the irregularity of the void distribution (Smit *et al.*, 1998, 1999, 2000a, 2000b, 2000c; Meijer *et al.*, 2000; Meijer and Govaert, 2003), and showed that voids in polymer systems are responsible for the enhancement of toughness. Their approach could be extended to model microcellular biocomposite systems.

11.6 Acknowledgments

This chapter is based upon work supported by the National Science Foundation under grant numbers CMMI-0800254 and CMMI-1000307. The support is gratefully acknowledged. Any opinions, findings, and conclusions or recommendations expressed in this material are those of the authors and do not necessarily reflect the views of the National Science Foundation. All materials studied in this work have been manufactured by researchers at Ford Motor Company, as described in previous research

© Woodhead Publishing Limited, 2014

(Argento *et al*., 2011; Kim *et al*., 2012). Specifically, the work of Cynthia Flanigan, Angela Harris, Dan Houston, Ellen Lee and Deborah Mielewski is acknowledged.

11.7 References

Al-Maliky N, Fernandez J O, Parry D J and Swallowe G M (1998), 'Drops in the flow stress of semi-crystalline polymers at very high rates of strain', *Journal of Materials Science Letters,* **17**, 1141–1143.

Al-Mousawi M M, Reid S R and Deans W F (1997), 'Use of the split Hopkinson pressure bar techniques in high strain rate materials testing', *Proceedings of the Institution of Mechanical Engineers, Part C: Journal of Mechanical Engineering Science,* **211**, 273–292.

Al-Zubaidy M, Hartley J, Fan M and Peng X (2012), 'Properties of natural fiber composites made by pultrusion process', *Journal of Composite Materials,* **46**, 237–246.

Argento A, Kim W, Lee E C, Harris A M and Mielewski D F (2011), 'Rate dependencies and energy absorption characteristics of nanoreinforced, biofiber, and microcellular polymer composites', *Polymer Composites,* **32**, 1423–1429.

Ashori A (2008), 'Wood-plastic composites as promising green-composites for automotive industries!', *Bioresource Technology Exploring Horizons in Biotechnology: A Global Venture,* **99**, 4661–4667.

Atahan A O and Sevim U K (2008), 'Testing and comparison of concrete barriers containing shredded waste tire chips', *Materials Letters,* **62**, 3754–3757.

Berglund L (2006). New concepts in natural fibre composites. *In:* Lilholt, H., Madsen, B., Andersen, T. L., Mikkelsen, L. P. and Thygesen, A. (eds). 27th Riso International Symposium on Materials Science, Roskilde, Denmark.

Bledzki A K and Faruk O (2004), 'Creep and impact properties of wood fibre-polypropylene composites: influence of temperature and moisture content', *Composites Science and Technology,* **64**, 693–700.

Bledzki A K, Faruk O, Kirschling H, Kuhn J and Jaszkiewicz A (2006a), 'Microcellular polymers and composites. Part I. Types of foaming agents and technologies of microcellular processing', *Polimery/Polymers,* **51**, 697–703.

Bledzki A K, Faruk O and Sperber V E (2006b), 'Cars from bio-fibres', *Macromolecular Materials and Engineering,* **291**, 449–457.

Bledzki A K and Gassan J (1999), 'Composites reinforced with cellulose based fibres', *Progress in Polymer Science,* **24**, 221–274.

Bledzki A K, Gassan J and Kessler A (1999a), 'Loss energy of composite materials. Part II: impact loading', *Journal of Testing and Evaluation,* **27**, 36–41.

Bledzki A K, Gassan J and Zhang W (1999b), 'Impact properties of natural fiber-reinforced epoxy foams', *Journal of Cellular Plastics,* **35**, 550–562.

Bledzki A K, Kirschling H, Steinbichler G and Egger P (2005), Notched impact strengths of compact and microcellular polycarbonate. *In:* Society of Plastics Engineers Annual Technical Conference 2005, May 1–5 2005. Society of Plastics Engineers, 56–60.

Bonora N and Ruggiero A (2006a), 'Micromechanical modeling of composites with mechanical interface – Part 1: unit cell model development and manufacturing

© Woodhead Publishing Limited, 2014

process effects', *Composites Science and Technology: Experimental Techniques and Design in Composite Materials,* **66**, 314–322.

Bonora N and Ruggiero A (2006b), 'Micromechanical modeling of composites with mechanical interface – Part II: damage mechanics assessment', *Composites Science and Technology: Experimental Techniques and Design in Composite Materials,* **66**, 323–332.

Brouwer W D (2000), 'Natural fibre composites: where can flax compete with glass?', *SAMPE Journal,* **36**, 18–23.

Cabral H, Cisneros M, Kenny J M, Vazquez A and Bernal C R (2005), 'Structure-properties relationship of short jute fiber-reinforced polypropylene composites', *Journal of Composite Materials,* **39**, 51–65.

Chandra P R, Jalan A K, Shrivastava S and Nunna S (2012), 'A review on mechanical behavior of natural fiber based hybrid composites', *Journal of Reinforced Plastics and Composites,* **31**, 759–769.

Chen L P, Yee A F and Moskala E J (1999), 'The molecular basis for the relationship between the secondary relaxation and mechanical properties of a series of polyester copolymer glasses', *Macromolecules,* **32**, 5944–5955.

Chien K B and Shah R N (2012), 'Novel soy protein scaffolds for tissue regeneration: material characterization and interaction with human mesenchymal stem cells', *Acta Biomaterialia,* **8**, 694–703.

Da Silva J G S, Vellasco P C G D S, De Andrade S A L, Soeiro F J D C P and Werneck R N (2003), 'An evaluation of the dynamical performance of composite slabs', *Computers & Structures, Civil Comp Special Issue,* **81**, 1905–1913.

Datta C, Basu D, Roy A and Banerjee A (2004), 'Mechanical and dynamic mechanical studies of epoxy/VAc-EHA/HMMM IPN-jute composite systems', *Journal of Applied Polymer Science,* **91**, 958–963.

De Medeiros E S, Agnelli J A M, Joseph K, De Carvalho L H and Mattoso L H C (2005), 'Mechanical properties of phenolic composites reinforced with jute/cotton hybrid fabrics', *Polymer Composites,* **26**, 1–11.

Dean G and Read B (2001), 'Modelling the behaviour of plastics for design under impact', *Polymer Testing,* **20**, 677–683.

Edwards S A, Kennedy J, Nicholson J, Choudhury N R and Provatas M (2004). An investigation of microcellular injection moulding on the structure-property relationships of engineering thermoplastics used in exterior automotive applications. *In:* ANTEC 2004 – Annual Technical Conference Proceedings, May 16–20 2004. Society of Plastics Engineers, 2537–2541.

Faruk O and Bledzki A K (2006), 'Microcellular injection molded wood fiber-PP composites: Part I – effect of chemical foaming agent content on cell morphology and physico-mechanical properties', *Journal of Cellular Plastics,* **42**, 63–76.

Fowler P A, Hughes J M and Elias R M (2006), 'Biocomposites: technology, environmental credentials and market forces', *Journal of the Science of Food and Agriculture,* **86**, 1781–1789.

Gassan J, Chate A and Bledzki A K (2001), 'Calculation of elastic properties of natural fibers', *Journal of Materials Science,* **36**, 3715–3720.

George J, Thomas S and Bhagawan S S (1999), 'Effect of strain rate and temperature on the tensile failure of pineapple fiber reinforced polyethylene composites', *Journal of Thermoplastic Composite Materials,* **12**, 443–464.

Goldsberry C (2006), 'Packaging green', *Modern Plastics Worldwide,* **83**, 37–39.

© Woodhead Publishing Limited, 2014

Gunkel F, Sporrer A N J, Lim G T, Bangarusampath D S and Altstadt V (2008), 'Understanding melt rheology and foamability of polypropylene-based TPO blends', *Journal of Cellular Plastics,* **44**, 307–325.

Hamdan S and Swallowe G M (1996), 'Crystallinity in PEEK and PEK after mechanical testing and its dependence on strain rate and temperature', *Journal of Polymer Science, Part B: Polymer Physics,* **34**, 699–705.

Hargrave M W, Munley E and Pasko T (1997). 'FHWA's Applied Highway Infrastructure Program on Composite Materials', *Public Roads,* [Online]. Federal Highway Administration. Available: http://www.tfhrc.gov/pubrds/spring97/compos.htm (Accessed 31 July 2012).

Huang T J and Chang L T (2009), 'Design and evaluation of shock-absorbing rubber tile for playground safety', *Materials & Design,* **30**, 3819–3823.

Ip T D, Tobias B and He J (1997), Dynamic characterization of natural fiber-reinforced composite materials under impact tests. *In:* Proceedings of the 1997 42nd International SAMPE Symposium and Exhibition. Part 2 (of 2), 4–8 May 1997, Anaheim, CA, USA. SAMPE, Covina, CA, USA, 1102–1110.

John M J and Thomas S (2008), 'Biofibres and biocomposites', *Carbohydrate Polymers,* **71**, 343–364.

Joshi S V, Drzal L T, Mohanty A K and Arora S (2004), 'Are natural fiber composites environmentally superior to glass fiber reinforced composites?', *Composites Part A: Applied Science and Manufacturing,* **35**, 371–376.

Jung W-Y and Aref A J (2005), 'Analytical and numerical studies of polymer matrix composite sandwich infill panels', *Composite Structures,* **68**, 359–370.

Keller A (2003), 'Compounding and mechanical properties of biodegradable hemp fibre composites', *Composites Science and Technology,* **63**, 1307–1316.

Khan M A, Kopp C and Hinrichsen G (2001), 'Effect of vinyl and silicon monomers on mechanical and degradation properties of bio-degradable jute-Biopol (registered trademark) composite', *Journal of Reinforced Plastics and Composites,* **20**, 1414–1429.

Kim W, Argento A, Lee E, Flanigan C, Houston D, Harris A and Mielewski D F (2012), 'High strain-rate behavior of natural fiber-reinforced polymer composites', *Journal of Composite Materials,* **46**, 1051–1065.

Laing A C and Robinovitch S N (2009), 'Low stiffness floors can attenuate fall-related femoral impact forces by up to 50% without substantially impairing balance in older women', *Accident Analysis & Prevention,* **41**, 642–650.

Leicher S, Will J, Haugen H and Wintermantel E (2005), 'MuCell (registered trademark) technology for injection molding: a processing method for polyether-urethane scaffolds', *Journal of Materials Science,* **40**, 4613–4618.

Lodha P and Netravali A N (2002), 'Characterization of interfacial and mechanical properties of 'green' composites with soy protein isolate and ramie fiber', *Journal of Materials Science,* **37**, 3657–3665.

Low I M, Mcgrath M, Lawrence D, Schmidt P, Lane J, Latella B A and Sim K S (2007), 'Mechanical and fracture properties of cellulose-fibre-reinforced epoxy laminates', *Composites Part A: Applied Science and Manufacturing,* **38**, 963–974.

Matuana-Malanda L, Park C B and Balatinecz J J (1996), 'Characterization of microcellular foamed PVC/cellulosic-fibre composites', *Journal of Cellular Plastics,* **32**, 449–469.

© Woodhead Publishing Limited, 2014

Meijer H E H and Govaert L E (2003), 'Multi-scale analysis of mechanical properties of amorphous polymer systems', *Macromolecular Chemistry and Physics,* **204**, 274–288.

Meijer H E H, Govaert L E and Smit R J M (2000), 'A multi-level finite element method for modeling rubber-toughened amorphous polymers', *ACS Symposium Series,* **759**, 50–70.

Mishra H K, Dash B N, Tripathy S S and Padhi B N (2000), 'Study on mechanical performance of jute-epoxy composites', *Polymer-Plastics Technology and Engineering,* **39**, 187–198.

Mohanty A K, Khan M A and Hinrichsen G (2000), 'Surface modification of jute and its influence on performance of biodegradable jute-fabric/Biopol composites', *Composites Science and Technology,* **60**, 1115–1124.

Mohanty A K, Wibowo A, Misra M and Drzal L T (2003), 'Development of renewable resource-based cellulose acetate bioplastic: effect of process engineering on the performance of cellulosic plastics', *Polymer Engineering and Science,* **43**, 1151–1161.

Neagu R C, Cuénoud M, Berthold F, Bourban P-E, Gamstedt E K, Lindström M and Månson J-A E (2012), 'The potential of wood fibers as reinforcement in cellular biopolymers', *Journal of Cellular Plastics,* **48**, 71–103.

Nicholas T (1981), 'Tensile testing of materials at high rates of strain', *Experimental Mechanics,* **21**, 177–185.

Omar M F, Md Akil H, Ahmad Z A, Mazuki A A M and Yokoyama T (2010), 'Dynamic properties of pultruded natural fibre reinforced composites using Split Hopkinson Pressure Bar technique', *Materials & Design,* **31**, 4209–4218.

Pervaiz M and Sain M M (2003), 'Sheet-molded polyolefin natural fiber composites for automotive applications', *Macromolecular Materials and Engineering,* **288**, 553–557.

Rajulu A V, Rao G B, Devi L G, Ramaiah S, Prada D S, Bhat K S and Shylashree R (2005), 'Mechanical properties of short, natural fiber hildegardia populifolia-reinforced styrenated polyester composites', *Journal of Reinforced Plastics and Composites,* **24**, 423–428.

Rana A K, Mandal A and Bandyopadhyay S (2003), 'Short jute fiber reinforced polypropylene composites: effect of compatibiliser, impact modifier and fiber loading', *Composites Science and Technology,* **63**, 801–806.

Razera I A T and Frollini E (2004), 'Composites based on jute fibers and phenolic matrices: properties of fibers and composites', *Journal of Applied Polymer Science,* **91**, 1077–1085.

Reddy N and Yang Y (2007), 'Novel protein fibers from wheat gluten', *Biomacromolecules,* **8**, 638–643.

Reddy N and Yang Y (2009), 'Soyprotein fibers with high strength and water stability for potential medical applications', *Biotechnology Progress,* **25**, 1796–1802.

Rodriguez E, Petrucci R, Puglia D, Kenny J M and Vazquez A (2005), 'Characterization of composites based on natural and glass fibers obtained by vacuum infusion', *Journal of Composite Materials,* **39**, 265–282.

Santulli C (2007), 'Impact properties of glass/plant fibre hybrid laminates', *Journal of Materials Science,* **42**, 3699–3707.

Santulli C and Cantwell W J (2001), 'Impact damage characterization on jute reinforced composites', *Journal of Materials Science Letters,* **20**, 477–479.

© Woodhead Publishing Limited, 2014

Satyanarayana K G, Arizaga G G C and Wypych F (2009), 'Biodegradable composites based on lignocellulosic fibers – An overview', *Progress in Polymer Science,* **34**, 982–1021.

Smit R J M, Brekelmans W A M and Meijer H E H (1998), 'Prediction of the mechanical behavior of nonlinear heterogeneous systems by multi-level finite element modeling', *Computer Methods in Applied Mechanics and Engineering,* **155**, 181–192.

Smit R J M, Brekelmans W A M and Meijer H E H (1999), 'Prediction of the large-strain mechanical response of heterogeneous polymer systems: local and global deformation behaviour of a representative volume element of voided polycarbonate', *Journal of the Mechanics and Physics of Solids,* **47**, 201–221.

Smit R J M, Brekelmans W A M and Meijer H E H (2000a), 'Predictive modelling of the properties and toughness of polymeric materials. Part I. Why is polystyrene brittle and polycarbonate tough?', *Journal of Materials Science,* **35**, 2855–2867.

Smit R J M, Brekelmans W A M and Meijer H E H (2000b), 'Predictive modelling of the properties and toughness of polymeric materials. Part II. Effect of microstructural properties on the macroscopic response of rubber-modified polymers', *Journal of Materials Science,* **35**, 2869–2879.

Smit R J M, Brekelmans W A M and Meijer H E H (2000c), 'Predictive modelling of the properties and toughness of polymeric materials. Part III. Simultaneous prediction of micro- and macrostructural deformation of rubber-modified polymers', *Journal of Materials Science,* **35**, 2881–2892.

Song J H, Mun S D and Kim C S (2011), 'Mechanical properties of sisal natural fiber composites according to strain rate and absorption ratio', *Polymer Composites,* **32**, 1174–1180.

Summerscales J, Hall W and Virk A S (2011), 'A fibre diameter distribution factor (FDDF) for natural fibre composites', *Journal of Materials Science,* **46**, 5876–5880.

Vanvuchelen J, Perugini C, Deweerdt M, Chen L and Burnham T (2000), 'Microcellular PVC foam for thin wall profile', *Journal of Cellular Plastics,* **36**, 148–157.

Velasco J I, Antunes M, Realinho V and Ardanuy M (2011), 'Characterization of rigid polypropylene-based microcellular foams produced by batch foaming processes', *Polymer Engineering & Science,* **51**, 2120–2128.

Wibowo A, Mohanty A K, Misra M and Drzal L T (2003). Injection molded eco-friendly biocomposites from natural fiber and cellulosic bio-plastic. *In:* ICCM-14, 14–18 July 2003 San Diego, CA, United States. Society of Manufacturing Engineers, 79–84.

Xie B, Cui Y H, Xu J, Wang X X, Zhang H H and Zhang Z D (2012), 'Investigation on microstructure and properties of foamed (wood fiber)/(recycled polypropylene) composites', *Journal of Vinyl and Additive Technology,* **18**, 105–112.

Xu X, Jiang L, Zhou Z, Wu X and Wang Y (2012), 'Preparation and properties of electrospun soy protein isolate/polyethylene oxide nanofiber membranes', *ACS Applied Materials & Interfaces*.

Zaman H U, Khan M A and Khan R A (2011), 'A comparative study on the mechanical and degradation properties of plant fibers reinforced polyethylene composites', *Polymer Composites,* **32**, 1552–1560.

© Woodhead Publishing Limited, 2014

12

Performance of natural fiber composites under dynamic loading

H. MD AKIL and M. H. ZAMRI, Universiti Sains Malaysia (USM), Malaysia

DOI: 10.1533/9780857099228.3.323

Abstract: This chapter covers a number of studies of the dynamic mechanical properties of natural fiber reinforced composites. Due to the limited number of such studies, special emphasis has been given to kenaf fiber reinforced and jute fiber reinforced unsaturated polyester composites produced using the pultrusion method. In the past, the majority of dynamic mechanical tests were performed using dynamic mechanical analysis (DMA), although several other techniques are available such as the Split Hopkinson Pressure Bar Apparatus (SHPBA), the drop weight impact tester, and servo-hydraulic machines. In this chapter, two measurement techniques are considered; these are the DMA and the SHPBA approaches. Effects of loading frequency and strain rate are studied based on the fiber loading and water absorption behavior of the composites. A summary of the results obtained from experiments is compared with previously published data and the findings are presented.

Key words: natural fibers, composites, dynamic properties, dynamic mechanical analysis (DMA), Split Hopkinson Pressure Bar Apparatus (SHPBA), strain rates.

12.1 Introduction

Measuring the dynamic properties of composite materials at different temperatures and loading rates is useful when considering the use of composites in conditions involving cyclic loading and deformation. Dynamic properties are often required for composite applications, including automotive and civil engineering components.

Dynamic mechanical properties are usually related to the load applied to the sample over different times, temperatures, and strain rates. Due to their long molecular chains, polymers behave differently compared with traditional materials such as metals and ceramics. This is associated with the viscoelastic properties of the polymer matrix, due to the combined characteristics of elastic solids and Newtonian fluids. Considering these issues, several attempts have been made in the past to measure and study the dynamic

© Woodhead Publishing Limited, 2014

behavior of various composites, including natural fiber composites. For example, dynamic mechanical properties have been subjected to intensive research by several researchers (Mazuki *et al*., 2011; Omar *et al*., 2010; Pothan *et al*., 2003) especially concerning polymer matrix composite (PMC) materials. It has been suggested that the dynamic mechanical properties of composite materials are affected by their constituents and structures, as well as the temperature and the rate at which the stress is applied.

The dynamic behavior of polymers and composites is closely related to the phenomenon of mechanical relaxation. This in turn is attributed to molecular motions in the transition from the glass- to the rubber-like state, dependent on the components and structure of polymeric materials. Similar effects also manifest in the PMCs, including fiber reinforced polymer composites. Any advanced materials or composites based on polymeric materials should consider this effect with respect to design and long term application. For the case of heterogeneous materials such as polymer composites, the response is more complex and depends on a greater number of variables, including the reinforcement types, geometry and quantity of fiber, type of polymer, and related properties.

During dynamic mechanical testing, frequency and applied stress are two commonly used parameters. It has been reported that frequency is dependent on molecular relaxation in polymeric materials. For example, it was observed that the frequency decreased with increasing temperature for an epoxy resin (tetraglycidylmethylendianilin–diaminodiphenylsulfone). Below and in the transition temperature regions, the elastic behavior exhibited linear decrease and a dramatic fall. The deterioration of the frequency was caused by moisture absorption, which is very prominent in natural fiber reinforced composites. The dynamic mechanical properties were also affected by fiber type and orientation, as well as fiber or filler content and the level of microvoid presence in the sample.

In the past few decades, polymer composite technology has experienced active development in reinforcing the polymer matrix with particulate fillers or fibers, which has resulted in improved properties over those of pure polymer (Reynaud *et al*., 2001; Rothon, 2003). PMCs produced using polymeric materials as a matrix phase are usually reinforced with various filler or fibers acting as a dispersed phase.

Various particulate fillers, such as silica, alumina, mica, etc., have been used extensively in the past. Furthermore, the uses of particulate fillers such as silica, alumina, muscovite, etc. in the polymer matrix potentially reduce the production cost of the composites. From earlier findings, it has been reported that the sizes of the particles have a significant effect on the mechanical behavior of particulate reinforced composites. PMCs reinforced with fiber, more commonly known as fiber reinforced polymers (FRP), are also emerging in applications such as building and construction.

© Woodhead Publishing Limited, 2014

A wide variety of synthetic fibers such as glass fibers (GF), aramid fibers (AF), carbon fibers (CF), and polypropylene fibers (PPF) have been used in the past. As far as the FRPs are concerned, there is a strong tendency to switch from synthetic to natural fibers for improved sustainability.

12.2 Natural fibers and natural fiber composites

Natural fiber composite materials have been used increasingly over the last decade (Joshi *et al.*, 2004; Nosbi *et al.*, 2011; Satyanarayana *et al.*, 2009; Zamri *et al.*, 2012). Environmental concerns have led to replacement of synthetic composites and plastics with natural fiber composites. Many natural fiber composites are biodegradable and come from renewable sources. Other advantages are that they are lightweight and relatively inexpensive. The emerging 'green' economy is based on energy efficiency, renewable feed stocks in polymer products, industrial processes that reduce carbon emissions, and recyclable materials, and is in tandem with the development of NFRC. By way of comparison, growing 1 tonne of jute fiber requires less than 10% of the energy used for the production of polypropylene. Processing results in residues that can be used in biocomposites for various applications. Natural fibers are considered to be 100% biodegradable.

Each year, farmers harvest around 35 million tonnes of natural fibers from a wide range of plants and animals – from sheep, rabbits, goats, camels and alpacas, from cotton balls, abaca and sisal leaves and coconut husks, and from the stalks of jute, hemp, flax, and ramie plants.

The use of NFRCs has grown steadily in various sectors of engineering including the automotive sector. In Europe, car makers are using mats made from abaca, flax, and hemp in press-molded thermoplastic panels for door liners, parcel shelves, seat backs, engine shields, and headrests. For consumers, natural fiber composites in automobiles provide better thermal and acoustic insulation than fiberglass, and reduce irritation to the skin and respiratory system. The low density of plant fibers also reduces vehicle weight, which cuts fuel consumption. For car manufacturers, the molding process consumes less energy than that of fiberglass and produces less wear and tear on machinery, cutting production costs by up to 30%.

The use of natural fibers by Europe's car industry is projected to reach 100 000 tonnes by 2010. For example, Daimler-Chrysler has developed a flax reinforced polyester composite, and in 2005 produced an award-winning spare wheel well cover that incorporated abaca yarn from the Philippines. Vehicles in some BMW series contain up to 24 kg of flax and sisal fibers. Released in July 2008, the Lotus Eco Elise features body panels made with hemp, along with sisal carpets and seats upholstered with hemp fabric. Japan's carmakers are also 'going green'. In Indonesia, Toyota

© Woodhead Publishing Limited, 2014

manufactures door trims made from kenaf and polypropylene, and Mazda is using a bioplastic made with kenaf for car interiors.

Worldwide, the construction industry is moving to natural fibers for a range of products, including light structural walls, insulation materials, floor and wall coverings, and roofing. Recent innovations include cement blocks reinforced with sisal fiber now being manufactured in Tanzania and Brazil. In India, a growing shortage of timber for the construction industry has spurred development of a composite board made from jute veneer and coir ply – studies show that coir's high lignin content makes it both stronger and more resistant to rotting than teak.

Geotextiles are another promising new outlet for natural fiber producers. Originally developed in the Netherlands for the construction of dykes, geotextile nets made from hard natural fibers strengthen earthworks and encourage the growth of plants and trees, which later provide further reinforcement. Unlike plastic textiles used for the same purpose, natural fiber nets – particularly those made from coir – decay over time as the earthworks stabilize.

12.3 Dynamic properties of natural fiber composites

The dynamic mechanical properties of natural fiber reinforced composites depend on several factors, such as the fiber content, additive type and content, filler and fiber geometry, fiber orientation, and modes of loading. Important dynamic properties include storage modulus (a measure of the maximum energy stored in the composite during loading), loss modulus (the amount of energy that has been dissipated), and mechanical damping. Various studies have been reported on the dynamic properties of natural fiber reinforced composites. For example, it has been reported (Jacob *et al.*, 2006) that dynamic tests over a wide range of temperatures and frequencies are highly sensitive to transitions and relaxation processes of the matrix, as well as the morphology of the PMC.

Bledzki and Zhang (2001) reported on the dynamic mechanical properties of natural fiber reinforced epoxy foams and found that a 42 %v/v of fiber content significantly enhanced the shear modulus of the foam. It was observed that the temperature of the log decrement peak for the jute fiber-based composites was shifted by about 5°C in comparison with that of pure epoxy resin. Sreekala *et al*. (2005) reported on the dynamic mechanical properties of oil palm fiber–phenol formaldehyde composites using a DMA technique. It was found that the incorporation of oil palm fiber increases the dynamic modulus and damping characteristics of the neat sample, such that damping increases linearly with increasing fiber content. However, the loss modulus was reported to decrease with increasing fiber loading.

© Woodhead Publishing Limited, 2014

Idicula *et al.* (2005) reported on the DMA of randomly oriented mixed short banana–sisal hybrid fiber reinforced composites. The effects of test temperature and volume fraction of fiber were studied. It was found that the storage modulus increases with increasing fiber volume fraction in the region above the glass transition temperature (T_g).

Jacob *et al.* (2006) reported on the DMA of sisal–oil palm hybrid fiber reinforced natural rubber composites. The fiber was treated using an alkaline solution prior to testing and the volume fraction of fiber was varied. It was reported that the storage modulus was increased with increasing fiber loading due to the stiffness enhancement offered by the addition of the fiber. The loss modulus was reported to follow the same trend as the storage modulus. On the other hand, damping characteristic were found to decrease with increasing fiber content as the presence of the fiber restricted the movement of the macromolecular chain of polymer matrix during loading and unloading.

Wielage *et al.* (2003) studied the dynamic mechanical properties of flax and hemp fiber reinforced polypropylene composites. The authors found that increasing mobility of the macromolecules is counteracted by the fibers leading to an increase in the storage modulus with increasing fiber loading. The loss factor was found to increase less significantly with increasing fiber loading as compared to the storage modulus. It was found that the storage modulus values of an untreated system were higher than those of a treated system. This was due to the formation of much stiffer polymer interfaces around the fiber tip relating to the treatment process.

12.4 Dynamic mechanical testing of natural fiber composites

Dynamic mechanical tests are performed using various methods such as the drop weight tester (Lin *et al.*, 2006), servo-hydraulic machine (Othman *et al.*, 2009), and SHPBA (Evora and Shukla, 2003).

Lin *et al.* (2006) investigated the mechanical behavior of epoxy reinforced modified montmorillonite (Cloisite 30B) and titanium dioxide nanocomposites at dynamic loading using a falling mass impact tester and found significant improvements in impact strength with filler content.

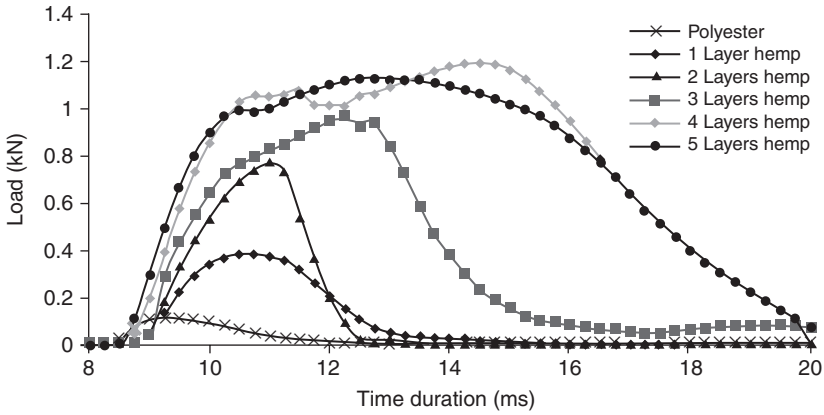
Although a falling mass impact test can give impressive results, the tests are limited by several factors, including sensitivity toward contact conditions between the impactor and specimen (Hsiao *et al.*, 1999). In addition, the system is also restricted to the lower strain rate loading condition (between 1 and 10 $m\,s^{-1}$) (Richardson and Wisheart, 1996).

Another common dynamic tester is the servo-hydraulic machine. However, this technique has a similar restriction, in that it is suitable only for intermediate strain rates loading (Othman *et al.*, 2009). Dhakal *et al.*

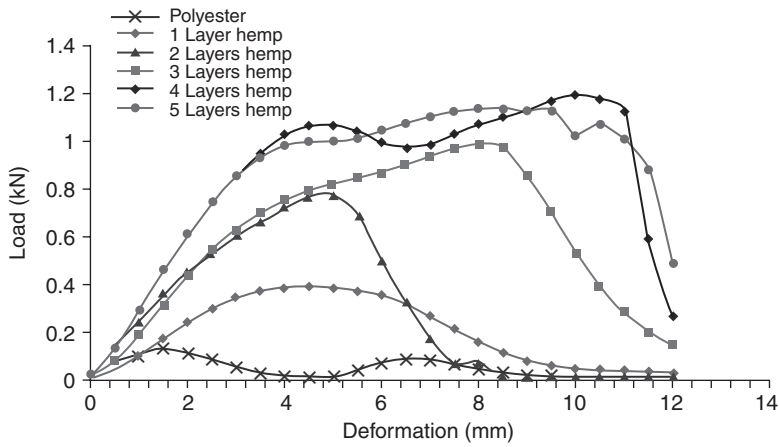
© Woodhead Publishing Limited, 2014

(2006, 2007) has shown that by using a drop weight tester, the dynamic mechanical properties of the non-woven hemp fiber reinforced polyester can be fully investigated. Their results indicate that increasing the volume fraction of hemp fibers resulted in a significant improvement of the peak load and energy absorption, as shown in Fig. 12.1. Increasing the fiber volume fractions induces a higher contact time, which directly relates to higher peak load.

Dhakal *et al.* (2006, 2007) showed that increasing the volume fraction of fibers may lead to an increase in the damage propagation phase, thus increasing the impact resistant properties of the hemp reinforced polyester composite as shown in Fig. 12.2. At lower volume fractions of fiber the composite exhibits brittle fracture behavior, while at higher volume fractions



12.1 Load–time traces of impact events (Dhakal *et al.,* 2007).



12.2 Load–deformation traces of impact events (Dhakal *et al.,* 2007).

© Woodhead Publishing Limited, 2014

it exhibits ductile fracture behavior with a correspondingly higher energy absorption.

The most promising technique for studying the behavior of materials at high strain rate is the Split Hopkinson Pressure Bar (SHPB) technique. The SHPB technique was developed by Kolsky (1949) and Houser and his co-workers (Daimaruya *et al.*, 1989). In this approach a stress pulse travels through an elastic input bar, through a short sample, and into an elastic output bar.

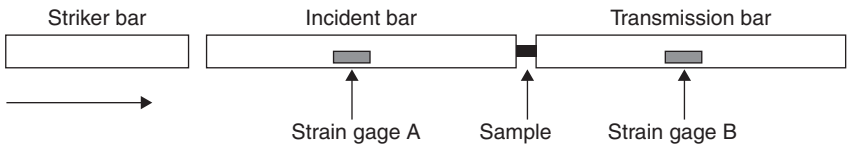
The SHPB technique has become the standard method of measuring material dynamic mechanical properties, including PMC, in the range of (10^2 to 10^4)s^{-1} strain rates (Evora and Shukla, 2003; Field *et al.*, 2004). However, it has been reported that the characterization of composite materials using SHPB may be problematic due to the anisotropic nature of composites, which can complicate the design of the specimen-loading bar interface (Hamouda and Hashmi, 1998). Optimized geometry specimens for particulate reinforced composites have been reported to address this issue (Evora and Shukla, 2003; Guo and Li, 2007).

Many techniques have been developed to study the dynamic properties of natural fiber composites; however, only a limited number of papers have reported on the dynamic properties of PMCs at strain rates higher than 10 $m{\cdot}s^{-1}$. Only the SHPB approach is capable of providing strain rate data higher than 10 $m{\cdot}s^{-1}$, allowing generation of a full stress–strain curve similar to those obtained during static mechanical testing.

In the SHPB approach, the elastic wave is both reflected and transmitted at the specimen. By measuring the reflected and transmitted waves in the incident and transmitted bar *via* strain gages, the specimen stress and strain can be calculated by calibrating the raw data with theoretical values. Figure 12.3 shows the schematic diagram for SHPB.

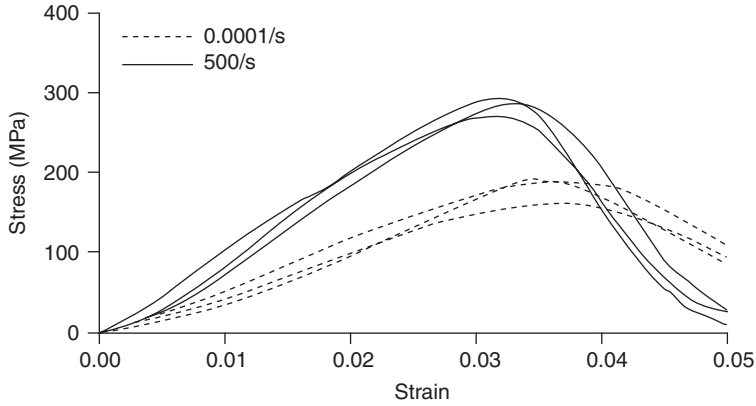
Few researchers have used the SHPB technique to investigate the dynamic mechanical properties of natural fiber composites. The approach has however been used to investigate the properties of conventional reinforcement and metal-based composites.

For example, Yulong and co-workers (2008) (Mingshuang *et al.*, 2008) had shown that by using the SHPB apparatus the dynamic compressive behavior of C/C composites at high strain rates can be successfully obtained. The stress–strain curve under dynamic loading (5.0×10^2 s^{-1}) for carbon/carbon



12.3 The schematic diagram for SHPB.

© Woodhead Publishing Limited, 2014



12.4 Compressive engineering stress–strain curves of the C/C composites at two strain rates (Mingshuang *et al.*, 2008).

(C/C) composites is shown in Fig. 12.4. These C/C composites can be easily characterized where the dynamic compressive properties such as compressive modulus, strength and stiffness are identified.

12.5 Testing in practice: the example of pultruded natural fiber reinforced composites

For the purpose of illustrating the effect of strain rate on NFRCs, pultruded kenaf fiber reinforced composites (PKRC) were used. The PKRCs were prepared using a pultrusion machine at the School of Materials and Mineral Resources Engineering, University Sains Malaysia, Malaysia. In this study, pultruded rod profiles were successfully manufactured using kenaf yarn with tex no 1400 and unsaturated polyester resin (UPR) as the reinforcement fiber and matrix respectively. These were used in a ratio of 70:30 by volume fraction (% v/v). During manufacture of the composites, kenaf fibers (roving) were placed on a creel of shelves and equipped with a roving guide to lead the strands to the resin bath.

The roving guide was used to ensure the strands did not scrape across one another, as this generates considerable static and causes 'fuzz balls' to build up in the resin bath, raising its viscosity (Meyer, 1985). The continuous kenaf fibers were first impregnated with UPR in a resin impregnation tank. The resin impregnated kenaf fiber was then pulled though a steel die to obtain the desired shape. The curing process was carried out in a curing die, which was precision machined to impart the final shape. Finally, the profile was cut into the desired length. The average diameter of the composites rods was 12.7 mm.

DMA was performed using the Mettler Toledo (Model 861) three-point bending configuration following ASTM D5023–7. The specimens were cut

© Woodhead Publishing Limited, 2014

to a size of 50 × 12 × 3 mm. The pultruded kenaf fiber reinforced composite (PKFRC) samples were tested in temperatures ranging from 0°C to 250°C, with a heating rate of 2°C per min, using several ranges of operating frequency (0.1, 1, 10 and 100 Hz) and a displacement amplitude of 10 μm.

For the SHBP analysis, cylindrical specimens of jute fiber reinforced composites (JFRC) and kenaf fiber reinforced composites (KFRC) were used. Selection of specimen geometry, especially length, has been reported to strongly influence the result obtained using SHPB (Song, 2004; Wu, 1997). Optimum specimen geometries have been investigated by previous researchers. For example, Davies and Hunter (1963) suggested that the optimum slenderness ratio (height/diameter) for metallic material is 0.5, and more recently, a study by Nakai and Yokoyama (2008) applied a similar slenderness ratio during SHPB testing. The length of the specimen chosen was based on the studies reported earlier, where the impact specimen length was fixed such that l/d (d = 12 mm) is equal to 0.5.

12.6 Dynamic testing of composites

The design or performance assessment of a component or structure requires accurate knowledge of the elastic and inelastic strength properties of the materials involved. These properties may vary with both temperature and time. Conventional mechanical test systems have been available for years to obtain strength data under long term conditions (hours to days) or static conditions (minutes) using screw or hydraulic loading systems. The maximum deformation or strain rate of these machines is about 0.1 per second (0.1 s^{-1}). Pendulum impact machines such as Charpy or Izod can produce strain rates of up to about 100 s^{-1}, thus yielding the energy absorbed till fracture, but not the complete stress–strain curve. SHPB is the only technique that allows a complete stress–strain curve to be probed.

12.6.1 Dynamic mechanical analysis (DMA)

Dynamic mechanical analysis, otherwise known as DMA, is a technique such that a small deformation is applied to a sample in a cyclic manner. This allows the material's response to stress, temperature, frequency and other parameters to be studied. The term is also used to refer to the analyzer that performs the test. DMA works by applying a sinusoidal deformation to a sample of known geometry. The sample can be subjected to a controlled stress or a controlled strain. A force motor is used to generate the sinusoidal wave and this is transmitted to the sample via a drive shaft. In a DMA test, the storage modulus (E') measures the energy stored in the specimen and the loss modulus (E'') measures the dissipation of energy. The ratio between the loss modulus and the storage modulus is called internal friction (tan δ).

© Woodhead Publishing Limited, 2014

DMA of materials can also be used to define the material's structure in terms of parameters such as molecular weight and crosslinking for polymers, or can be used to explain a material's response to environmental or external variables such as temperature, time or frequency, and relative humidity. DMA is widely used in research on materials such as polymers and metals, but applications of DMA on natural fiber composites have not been fully investigated. As the temperature varies, thermally induced transitions in material properties occur. Several inflections points can be noted in the internal friction (tan δ) versus temperature plot that coincide with those transitions. The transition related to the motion of the main backbone of the material is called the glass transition temperature (T_g). Time-dependent behavior is exhibited when materials are subjected to dynamic deformation at different frequencies. Characterization of the thermo-rheological properties of composites has been reported using mechanical analysis. Calleja *et al*. (1991), Geethamma *et al*. (2005), Hashmi *et al.* (2003).

Contrary to the established instruments for quasi-static determination of the elastic parameters from stress–strain testing, DMA only requires a sample with small mass or small size. In pultruded composites materials that are highly reinforced and hence have only a very low polymer content, that is, 70% v/v, the determination of the glass transition temperature T_g by means of a differential scanning calorimeter (DSC) becomes very difficult as the specific heat capacity of the sample changes the glass transition temperature very little (Ghosh *et al*., 1997). DMA has been proved to be an effective method to study relaxation in polymers and thereby the behavior of the materials under various conditions of stress, temperature, and phase composition of fiber composites and their respective roles in determining the mechanical properties.

12.6.2 Split Hopkinson Pressure Bar (SHPB) test

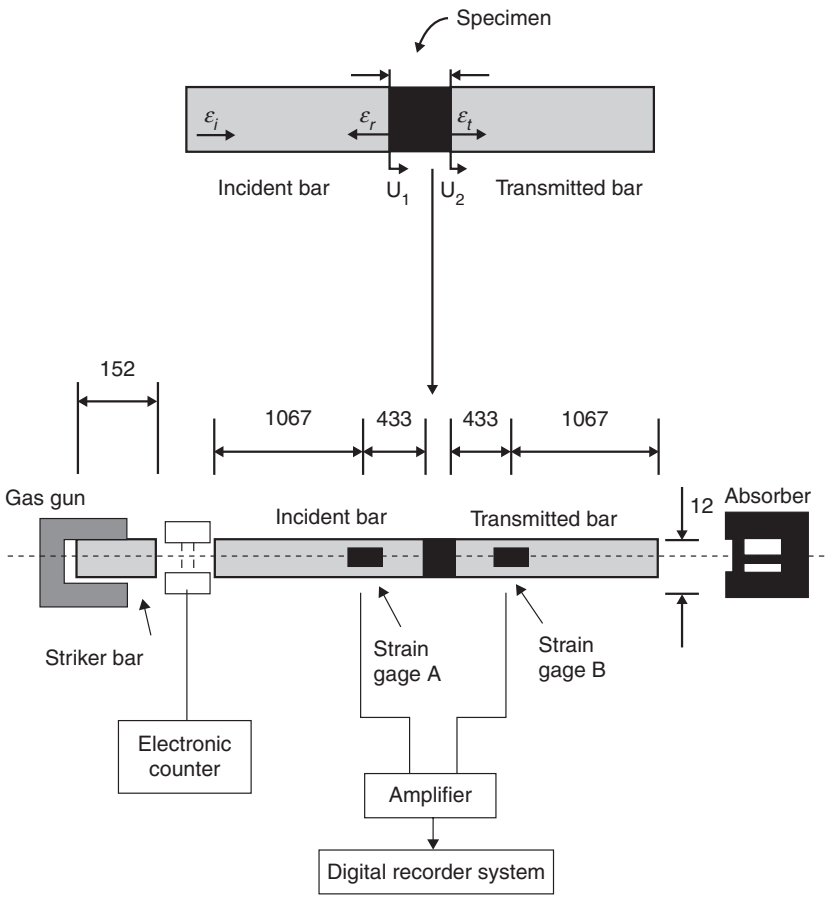
A technique to measure the shape of a stress pulse in a long elastic bar was first described in 1914 in England by Bertram Hopkinson. In 1949, Herbert Kolsky, also in England, improved on Hopkinson's device, adding displacement gages and oscillographic recording techniques to obtain complete pulse amplitude wave forms in elastic bars. Kolsky used a two-bar system, sandwiching a short compression specimen between them. The test specimen, being lower in strength than the bars, experienced plastic deformation. Both the stress and strain could be derived. This modification became known as the SHPB. Hopkinson and Kolsky used explosive pellets to generate the stress pulse that propagated along the bar.

A conventional SHPB apparatus normally has the same general components which include a striker bar that is usually propelled by a gas chamber, incident bar, transmitter bar, absorber, strain gages, strain transducer with signal conditioners, and a means of digital storage. In practice, a high strength

© Woodhead Publishing Limited, 2014

material is needed in order to reduce the drastic impedance mismatch between the specimen and bar, which results in a transmitted strain signal with very low S/N ratio (Nakai and Yokoyama, 2008). Thus, in current SHPB testing, a high strength silver steel bar is used.

A schematic diagram of compression the SHPB approach used in this study (KHT-52-CT) is shown in Fig. 12.5. The diameter of the striker bar, incident bar, and transmitter bar are 12 mm, and their lengths are 152, 1500, and 1500 mm, respectively. At the beginning stage of the SHPB test, the specimens are clamped between incident and transmitter bar. As with a static test, wax is applied to both ends of the specimen to minimize frictional effects. The striker bar is accelerated by the pressure from a helium tank and then launched through the gun barrel before colliding with the incident bar.



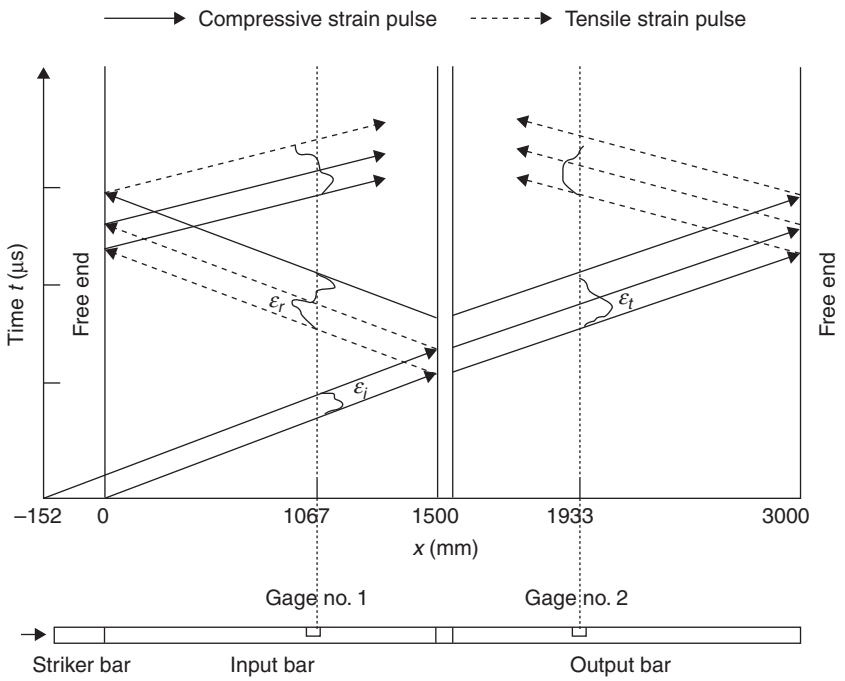
12.5 The schematic diagram of the SHPB set-up for high velocity impact test (units are mm).

© Woodhead Publishing Limited, 2014

During the collision, a compressive strain pulse (ε_i) is generated in the incident bar and travels toward the specimen. Due to the impedance mismatch at the surface between the bar and specimen, some amount of the generated pulse is reflected back (ε_r) to the incident bar and the remaining strain pulse is transmitted (ε_t) through the specimen into the transmitter bar.

The propagation of the strain pulse along the Hopkinson bars can be understood via the Lagrangian *x*–*t* diagram which is shown in Fig. 12.6. The generated incident, transmitted and reflected pulse are then captured by the piezoelectric strain gages (Kyowa: KFG-20–120-CI) mounted on the incident and transmitter bar using special adhesive (Kyowa: CC-33A). The output voltage of the Wheatstone circuit due to the change of resistance in the strain gage when deformation occurred in the Hopkinson bars is then transferred to the transducer amplifier (Fylde: HYLDE FE-H359-TA) to amplify the voltages produced by the strain gages. The signal is then captured using an oscilloscope (PICOSCOPE 3206) with a 100 μs/word sampling rate and saved in the computer for data processing.

The propagation of the elastic wave in a slender cylindrical bar during the SHPB test can be described by the one-dimensional elastic wave equation. One-dimensional elastic wave equations were also used to obtain the strain



12.6 Lagrangian diagram illustrating wave movement in silver steel Hopkinson bars.

© Woodhead Publishing Limited, 2014

and stress in the samples. The histories of stress, strain, and strain rate during compression SHPB testing were calculated based on the strain measured on the incident and transmitter bars. The equations are as follows:

$$\sigma_s(t) = E\frac{A_b}{A_s}\varepsilon_r(t) \quad [12.1]$$

$$\varepsilon_s(t) = -\frac{2Co}{L}\int_0^t \varepsilon_r(t)\mathrm{d}t \quad [12.2]$$

$$\varepsilon_s(t) = \frac{\mathrm{d}\varepsilon(t)}{\mathrm{d}t} = \frac{-2c}{L}\varepsilon_r(t) \quad [12.3]$$

where A, E and c ($=E/\rho^{½}$, ρ is mass density of the bar) are cross-sectional area, Young's modulus, and wave velocity of the bars, respectively. L and A_s refer to length and cross-sectional area of the sample, respectively. $\varepsilon_r(t)$ and $\varepsilon_t(t)$ are the recorded axial strains of the reflected pulse and transmitted pulse, respectively, measured from the reflected and transmitted bars as a function of time.

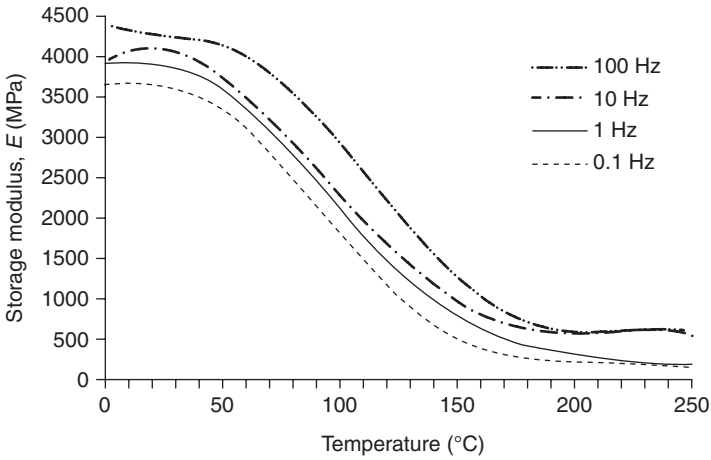
12.7 Performance of natural fiber reinforced composites under dynamic loading

Performance of natural fiber reinforced composites under dynamic loading is as important as under static loading, especially for applications involving high loading rate. To date, this part of the test has not been widely reported by researchers. Areas that have been studied include the effect of loading frequency on the dynamic moduli of the composites and the effect of strain rate on the dynamic moduli of the composites.

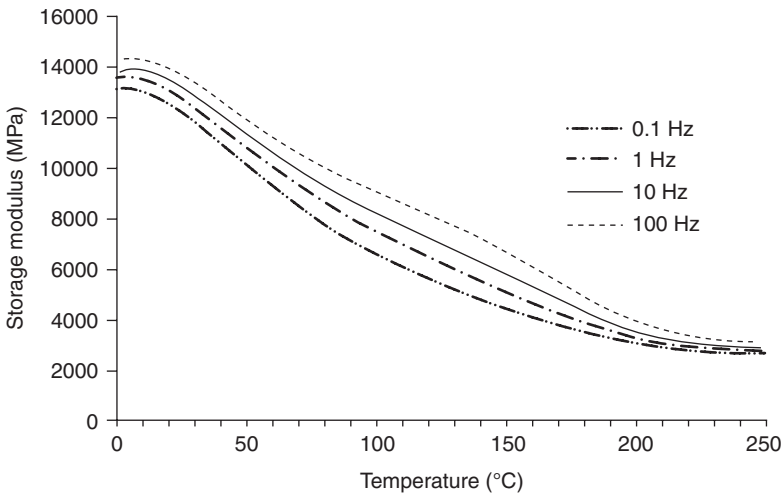
12.7.1 Effect of loading frequency on the dynamic moduli of the composites

The storage modulus, E' and damping peaks (tan δ) have been found to be affected by loading frequency (Li *et al.*, 2000; Menard, 2008). The variation of E' with frequency of neat polyester as a function of temperature is shown in Fig. 12.7. An increase in frequency has been found to increase the modulus values. Figure 12.8 shows the effect of frequency on the dynamic modulus of samples with 70% fiber loading. Frequency has a direct impact on the dynamic modulus, especially at high temperatures. The modulus values are found to drop at a temperature of around 45°C. This drop in modulus

© Woodhead Publishing Limited, 2014



12.7 The variation of storage modulus, E' of neat unsaturated polyester with different loading frequencies (Hz).



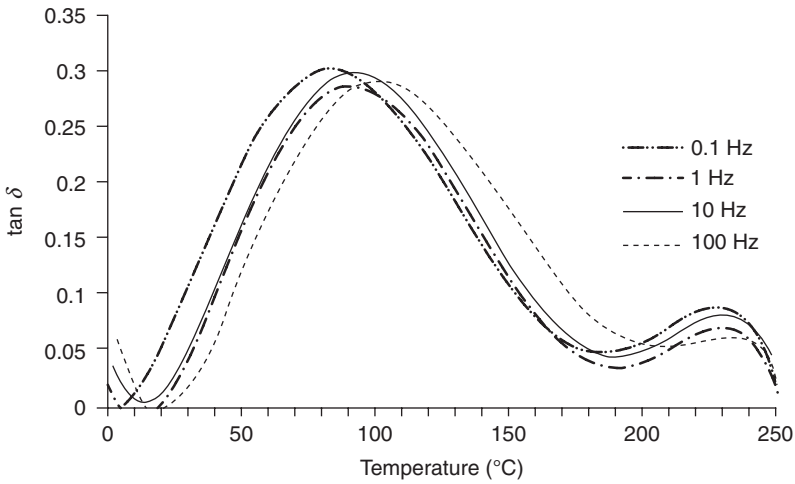
12.8 Effects of loading frequency on the storage modulus of samples with 70% v/v fiber loading.

value continues until a temperature of 140°C is reached. Molecular motion is believed to set in at 45°C. The change in dynamic properties is also associated with crazing and formation of microscopic cracks and voids. At high temperature, breaking up of the fiber agglomerates, and of the bond between the fiber and polymer phases, may also occur (Menard, 2008; Pothan *et al.*, 2003). Frequency is also observed to have a direct impact on the tanδ values.

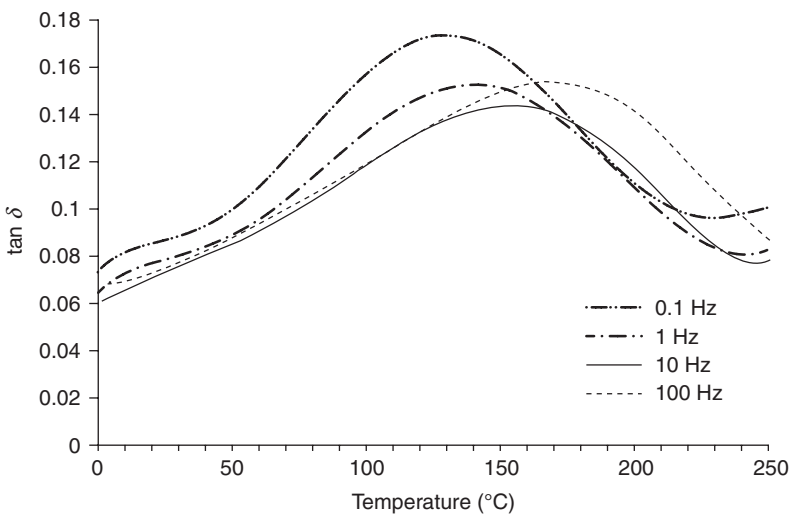
The viscoelastic properties of a material are dependent on temperature, time, and frequency. If a material is subjected to a constant stress, its elastic

© Woodhead Publishing Limited, 2014

modulus will decrease over a period of time. This is due to the fact that the material undergoes molecular rearrangement in an attempt to minimize the localized stresses. Modulus measurements performed over a short time (high frequency) result in higher values, whereas measurements taken over longer periods of time (low frequency) result in lower values (Menard, 2008; Pothan *et al.*, 2003). The tanδ values measured over a range of frequencies for the neat polyester samples are shown in Fig. 12.9. The tanδ peak is found to shift to higher temperature with an increase of frequency. The damping



12.9 Effect of frequency (Hz) on the tan δ of neat unsaturated polyester.



12.10 Effect of frequency (Hz) on the tanδ of composites with 70%·v/v fiber loading.

© Woodhead Publishing Limited, 2014

peak is associated with the partial loosening of the polymer structure so that groups and small chain segments can move. The tanδ curve peak, which is indicative of the glass transition temperature, is also indicative of the degree of crosslinking of the system.

Figure 12.10 shows the effect of frequency on the tanδ curve of samples with 70 %·v/v loading of treated PKRC. An increase in frequency is found to have a broadening effect on the tanδ curve. Broadening of the curve is due to heterogeneity in the network structure. This broadening is more prominent in composites with high fiber content. The addition of fiber increases the free volume between monomeric units, which in turn affects the curing reaction as well as molecular motions and diffusion (Pothan *et al.*, 2003).

Table 12.1 shows the tanδ max and the corresponding T_g values for the treated pultruded KFRC and untreated pultruded KFRC. The values of T_g underwent a positive shift due to plasticization resulting from the addition of fiber within the polyester matrix. With the increase in frequency the tanδ peak, which corresponds to the glass transition temperature, is also found to be shifted to higher temperature.

12.7.2 Effect of strain rate on the dynamic moduli of the composites

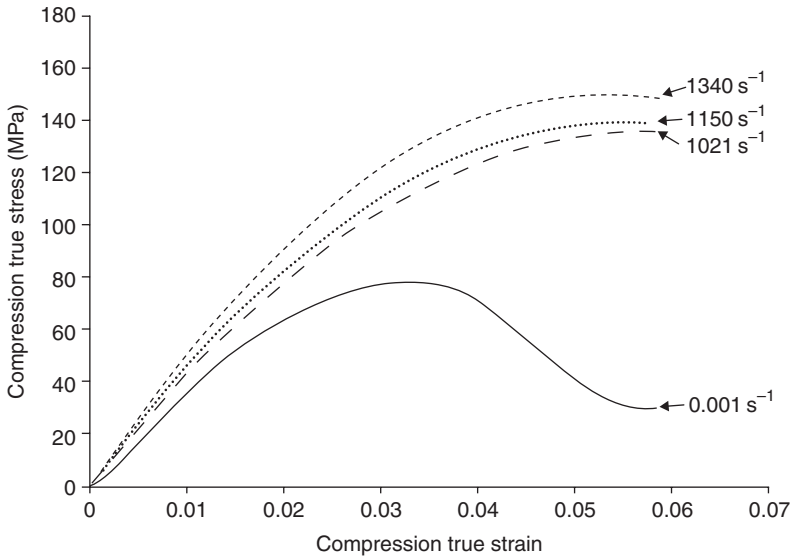
In order to understand the effect of strain rate on the dynamic mechanical properties of natural fiber reinforced composites, the dynamic results are compared to the static results. Figures 12.11 and 12.12 show typical stresses

Table 12.1 Values of tan δ maximum and T_g values of neat polyester and kenaf fiber reinforced polyester composites at different fiber loadings

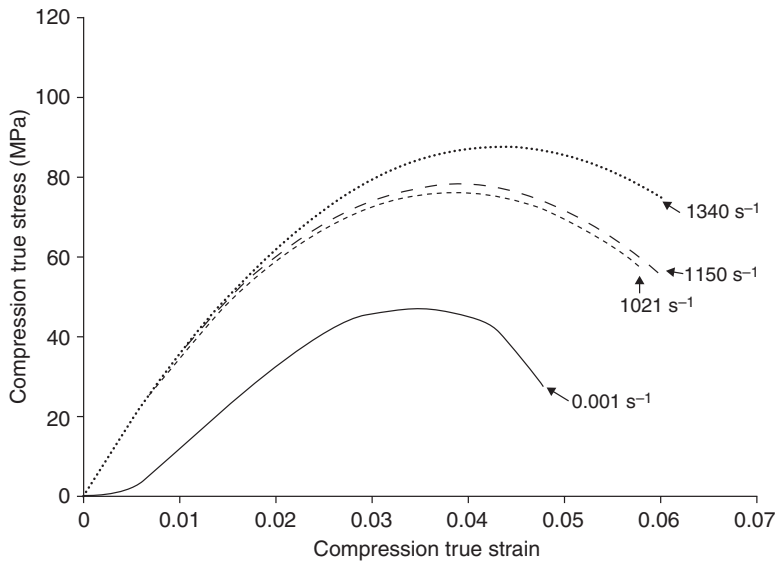
Fiber loading	tan δ max				T_g from tan δ max (°C)			
	Frequency (Hz)				Frequency (Hz)			
	0.1	1	10	100	0.1	1	10	100
Treated pultruded Kenaf reinforced composite								
UP	0.3	0.29	0.27	0.28	85.2	91.3	99.2	105.7
50%	0.24	0.23	0.21	0.22	110	115	121	127
60%	0.22	0.21	0.17	0.19	125	130	135	140
65%	0.19	0.16	0.15	0.16	130	134	138	143
70%	0.17	0.15	0.14	0.15	140.5	143.3	147	151.4
75%	0.23	0.225	0.22	0.21	114	120	125	130.5
Untreated pultruded kenaf reinforced composite								
50%	0.28	0.26	0.23	0.22	91.3	98	103.6	109.3
60%	0.25	0.247	0.21	0.21	97.2	101	106.2	112.2
65%	0.24	0.231	0.2	0.19	108.5	113	116.8	121.1
70%	0.23	0.219	0.18	0.16	118	121.1	125.4	128.6
75%	0.26	0.25	0.2	0.22	95	100.4	106.7	112.7

UP: unsaturated polyester.

© Woodhead Publishing Limited, 2014



12.11 The stress–strain curve of jute fiber reinforced composites (JFRC) at various strain rates.



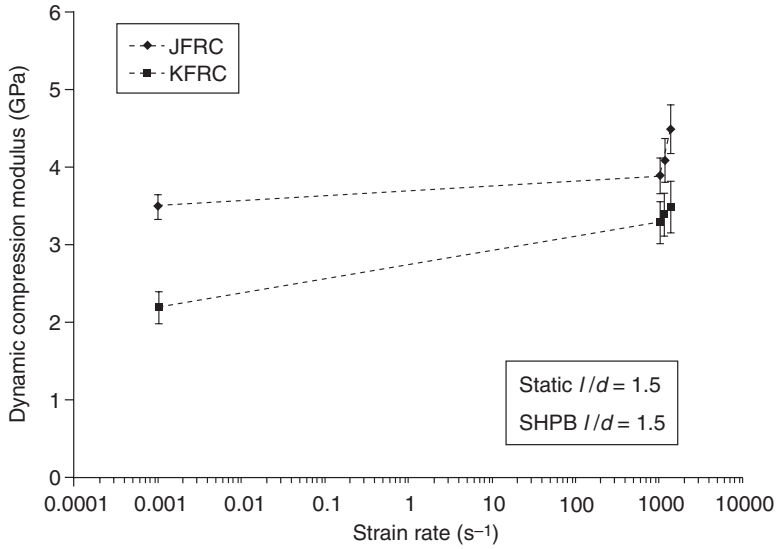
12.12 The stress–strain curve of kenaf fiber reinforced composites (KFRC) at various strain rates.

versus strain curves for both pultruded natural fiber reinforced composites at four different levels of average strain rates.

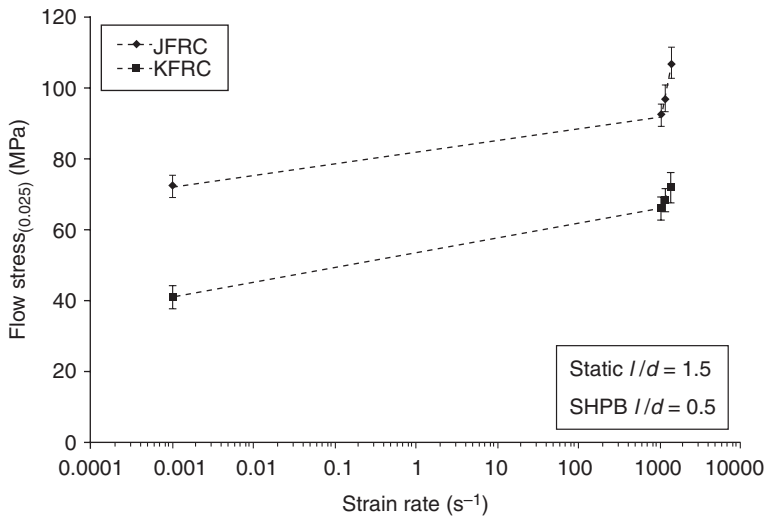
As can be seen in Figs 12.11 and 12.12, both pultruded natural fiber reinforced composites behaviors are strongly affected by the levels of strain

© Woodhead Publishing Limited, 2014

rate. The yield stress, as well as the flow stress, of the composites goes up dramatically as the strain rate increases. Chen *et al*. (1999) believe that the increase in stress can be directly related to the secondary molecular processes and this phenomenon has been clarified by Guo and Li (2007). In



12.13 Effect of strain rate on dynamic compression modulus for both pultruded natural fiber reinforced composites.



12.14 Effect of strain rate on flow stress (0.025) for both pultruded natural fiber reinforced composite.

© Woodhead Publishing Limited, 2014

addition, increasing strain rate decreases the molecular mobility of the polymer chains and thus makes the material stiffen (Guo and Li, 2007).

The values of the dynamic compression modulus and flow stress as a function of strain rate are plotted in Fig. 12.13. The flow stress is measured at 2.5% strains. Figure 12.14 shows that the JFRC recorded a higher dynamic compression modulus than that of KFRC over the range of tested strain rates. The JFRC also recorded higher values of 2.5% flow stress as compared to KFRC at all tested strain rates.

12.8 Future trends

Based on the results collected, it is clear that the dynamic behavior of natural fiber reinforced polymer composites is comparable with a range of polymer composites reinforced with various fibers and fillers. Their behaviors are predictable and can be measured using conventional techniques. DMA and SHPB analyses show that both techniques are capable of determining the dynamic properties of natural fiber reinforced composites and these results will be of interest to many scientific communities and industries. The trend toward use of natural fiber reinforced composites is emerging especially in automotive, infrastructure, and sport goods industries and their market share continues to grow. In this respect, the need to further characterize the NFRCs in terms of materials properties and design requirements will continue to grow. Determination of the influence of humidity, hygrothermal conditions, thermal cyclic, hazardous chemicals, as well as impact and shock loading, on the dynamic properties of natural fiber reinforced composites remains necessary in order to safely design natural fiber reinforced composites for various applications.

12.9 Acknowledgments

The author would like to acknowledge support from USM under the Polymer Composite Research Cluster Fund (1001/PKT/8640013) which has made this work possible.

12.10 References

Bledzki, A. K. and Zhang, W. (2004). Dynamic mechanical properties of natural fiber-reinforced epoxy foams. *Journal of Reinforced Plastics and Composites,* **20**, 1263–1274.

Calleja, R. D., Ribelles, J., Pradas, M. M., Greus, A. R. and Colomer, F. R. (1991). On the dynamic mechanical behavior of poly (methyl methacrylate) reinforced with Kevlar fibers. *Polymer Composites,* **12**, 428–435.

© Woodhead Publishing Limited, 2014

Chen L.P., Albert, Y. and Moskala, E.J. (1999). The molecular basis for the relationship between the secondary relaxation and mechanical properties of a series of polyester copolymer glasses. *Macromolecules,* **32**, 5944–5955.

Daimaruya, M., Naitoh, M., Kobayashi, H. and Tanimura, S. (1989). A sensing-plate method for measuring force and duration of impact in elastic-plastic impact of bodies. *Experimental Mechanics,* **29**, 268–273.

Davies, E. D. H and Hunter, S. (1963). The dynamic compression testing of solids by the method of the split Hopkinson pressure bar. *Journal of the Mechanics and Physics of Solids,* **11**, 155–179.

Dhakal, H., Zhang, Z., Richardson, M. and Errajhi, O. (2007). The low velocity impact response of non-woven hemp fibre reinforced unsaturated polyester composites. *Composite Structures,* **81**, 559–567.

Evora, V. M. F. and Shukla, A. (2003). Fabrication, characterization, and dynamic behavior of polyester/TiO_2 nanocomposites. *Materials Science and Engineering: A,* **361**, 358–366.

Field, J., Walley, S., Proud, W., Goldrein, H. and Siviour, C. (2004). Review of experimental techniques for high rate deformation and shock studies. *International Journal of Impact Engineering,* **30**, 725–775.

Geethamma, V., Kalaprasad, G., Groeninckx, G. and Thomas, S. (2005). Dynamic mechanical behavior of short coir fiber reinforced natural rubber composites. *Composites Part A: Applied Science and Manufacturing,* **36**, 1499–1506.

Ghosh, P., Bose, N., Mitra, B. and Das, S. (1997). Dynamic mechanical analysis of FRP composites based on different fiber reinforcements and epoxy resin as the matrix material. *Journal of Applied Polymer Science,* **64**, 2467–2472.

Guo, Y. and Li, Y. (2007). Quasi-static/dynamic response of SiO_2–epoxy nanocomposites. *Materials Science and Engineering: A,* **458**, 330–335.

Hamouda, A. and Hashmi, M. (1998). Testing of composite materials at high rates of strain: advances and challenges. *Journal of Materials Processing Technology,* **77**, 327–336.

Hashmi, S., Kitano, T. and Chand, N. (2003). Dynamic mechanical behavior of LLDPE composites reinforced with kevlar fibers/short glass fibers. *Polymer Composites,* **24**, 149–157.

Hsiao, H., Daniel, I. and Cordes, R. (1999). Strain rate effects on the transverse compressive and shear behavior of unidirectional composites. *Journal of Composite Materials,* **33**, 1620–1642.

Idicula, M., Malhotra S. K., Joseph, K. and Thomas, S. (2005). 'Dynamic mechanical analysis of randomly oriented intimately mixed short banana/sisal hybrid fibre reinforced polyester composites'. *Composites Science and Technology,* **65**(7–8), 1077–1087.

Idicula, M., S. K. Malhotra, *et al*. (2005). Dynamic mechanical analysis of randomly oriented intimately mixed short banana/sisal hybrid fibre reinforced polyester composites.' *Composites Science and Technology*, **65**(7–8): 1077–1087.

Jacob, M., Francis, B., Thomas, S. and Varughese, K. (2006). Dynamical mechanical analysis of sisal/oil palm hybrid fiber-reinforced natural rubber composites. *Polymer Composites,* **27**, 671–680.

Joshi, S., Drzal, L., Mohanty, A. and Arora, S. (2004). Are natural fiber composites environmentally superior to glass fiber reinforced composites? *Composites Part A: Applied Science and Manufacturing,* **35**, 371–376.

© Woodhead Publishing Limited, 2014

Kolsky, H. (1949). An investigation of the mechanical properties of materials at very high rates of loading. *Proceedings of the Physical Society. Section B,* **62**, 676.

Li, Y., Mai, Y.-W. and Ye, L. (2000). Sisal fibre and its composites: a review of recent developments. *Composites Science and Technology,* **60**, 2037–2055.

Lin, J. C., Chang, L., Nien, M. and Ho, H. (2006). Mechanical behavior of various nanoparticle filled composites at low-velocity impact. *Composite Structures,* **74**, 30–36.

Mazuki, A. A. M., Akil, H. M., Safiee, S., Ishak, Z. A. M. and Bakar, A. A. (2011). Degradation of dynamic mechanical properties of pultruded kenaf fiber reinforced composites after immersion in various solutions. *Composites Part B: Engineering,* **42**, 71–76.

Menard, K. P. (2008). *Dynamic Mechanical Analysis*, A Practical Introduction CRC, Wiley Online Library.

Meyer, R. (1985). *Handbook of Pultrusion Technology*. Methuen, Inc, 733 Third Ave, New York 10017, USA, 180.

Mingshuang, L., Yulong, L., Fei, X., Zejian, X. and Laifei, C. (2008). Dynamic compressive mechanical properties and a new constitutive model of 2D-C/SiC composites. *Materials Science and Engineering: A,* **489**, 120–126.

Nakai K and Yokoyama, T. (2008). Strain rate dependence of compressive stress–strain loops of several polymers. *Journal of Solid Mechanics and Materials Engineering,* **2**(4), 557–566.

Nosbi, N., Akil, H. M., Ishak, Z. A. M. and Bakar, A. A. (2011). Behavior of kenaf fibers after immersion in several water conditions. *BioResources,* **6**, 950–960.

Omar, M. F., Md Akil, H., Ahmad, Z. A., Mazuki, A. a. M. and Yokoyama, T. (2010). Dynamic properties of pultruded natural fibre reinforced composites using Split Hopkinson Pressure Bar technique. *Materials & Design,* **31**, 4209–4218.

Othman, R., Guégan, P., Challita, G., Pasco, F. and Lebreton, D. (2009). A modified servo-hydraulic machine for testing at intermediate strain rates. *International Journal of Impact Engineering,* **36**, 460–467.

Pothan, L. A., Oommen, Z. and Thomas, S. (2003). Dynamic mechanical analysis of banana fiber reinforced polyester composites. *Composites Science and Technology,* **63**, 283–293.

Reynaud, E., Jouen, T., Gauthier, C., Vigier, G. and Varlet, J. (2001). Nanofillers in polymeric matrix: a study on silica reinforced PA6. *Polymer,* **42**, 8759–8768.

Richardson, M. and Wisheart, M. (1996). Review of low-velocity impact properties of composite materials. *Composites Part A: Applied Science and Manufacturing,* **27**, 1123–1131.

Rothon, R. N. (2003). *Particulate-Filled Polymer Composites*, Smart Pubns.

Satyanarayana, K. G., Arizaga, G. G. C. and Wypych, F. (2009). Biodegradable composites based on lignocellulosic fibers – An overview. *Progress in Polymer Science,* **34**, 982–1021.

Song, B and Chen, W. (2004). Dynamic stress equilibrium in split Hopkinson pressure bar tests on soft materials. *Society of Experimantal Mechanics,* **44**, 12.

Sreekala, M., Thomas, S. and Groeninckx, G. (2005). Dynamic mechanical properties of oil palm fiber/phenol formaldehyde and oil palm fiber/glass hybrid phenol formaldehyde composites. *Polymer Composites,* **26**, 388–400.

© Woodhead Publishing Limited, 2014

Wielage, B., Lampke T., Utschick, H. and Soergel, F. (2003). 'Processing of natural-fibre reinforced polymers and the resulting dynamic–mechanical properties'. *Journal of Materials Processing Technology,* **139**(1–3): 140–146.

Wu, X.J. and Gorham, D. (1997). Stress equilibrium in the split Hopkinson pressure bar test. *Journal of Physics IV France,* **7**, 6.

Zamri, M. H., Akil, H. M., Bakar, A. A., Ishak, Z. A. M. and Cheng, L. W. (2012). Effect of water absorption on pultruded jute/glass fiber-reinforced unsaturated polyester hybrid composites. *Journal of Composite Materials,* **46**, 51–61.

© Woodhead Publishing Limited, 2014

13

The response of natural fibre composites to impact damage: a case study

H. GHASEMNEJAD and A. ABOUTORABI,
Kingston University London, UK

DOI: 10.1533/9780857099228.3.345

Abstract: This chapter describes an investigation into hybrid laminate lay-up in multi-delaminated and single lap joint composite beams where the Charpy impact test was chosen to measure the energy absorbing capability of the beam. It was shown that beams that are stitched through the thickness are able to arrest crack propagation and consequently absorb more energy in comparison with non-stitched beams. It was also shown that composite beams that were bonded by stitching were able to absorb more energy in comparison with adhesively bonded composite joints in the hybrid composite beams.

Key words: delamination, cellulose, impact, single lap joint, composite.

13.1 Introduction

The brittle nature of most fibre reinforced polymer (FRP) composites accompanying varying forms of energy absorption mechanisms, such as fibre breakage, matrix cracking, debonding at the fibre-matrix interface and particularly ply delamination, play important roles on progressive failure modes and energy absorption capability of composite structures. These failure modes under low-velocity impact loading conditions are strongly dependent on the fibre type, resin type, lay-up thickness, loading velocity and projectile type (see Chapter 10). For low-velocity impact events, the use of pendulums such as those present in Charpy test (Abrate, 1998), drop towers or drop weights (Richardson and Wisheart, 1996) has become standard. Delamination can occur during the manufacturing processes due to contaminated reinforcing fibres, insufficient wetting of fibres, machining and mechanical loading such as impact loading. Delamination can occur due to the lack of reinforcement in the thickness direction since interlaminar stresses exist in the boundary layer of laminates under transverse loading.

Adhesive joints are one of the most important joining techniques used for bonding composite structures. Joint design technology has become a main factor in structural integrity for design of composite sub-structures

© Woodhead Publishing Limited, 2014

in various engineering disciplines such as aerospace, marine engineering, automotive structural parts, micro-electro-mechanical systems, wind turbine blades and civil structures for strengthening.

Many researchers have investigated the impact behaviour of various composite material structures. Hufenbach *et al.* (2008) experimentally investigated the influence of key parameters, such as fibre-reinforcement type, hybrid materials, fibre type and architecture as well as core fibre orientation, on the impact damage resistance of composite structures. Using experimental data, they performed numerical studies on impacted specimens to obtain forces and failure modes (Khalili *et al.*, 2009). They experimentally studied the response to a Charpy impact test of edge-cracked aluminium plates repaired with one-sided composite patches. They found that carbon-fibre patches were more effective than glass-fibre patches in reinforcing the cracked plates. They showed that when a constant ratio between crack length and width of specimen exists, the carbon-fibre patches showed better characteristics than glass-fibre patches. Schubbe and Mall (1999a, 1999b) have studied patch geometry and stiffness ratio with respect to fatigue response of thick cracked plates repaired with single-sided patches. According to their results the stiffness ratio was close to 1 for thick plates while this ratio was around 1.4 for thin plates.

Hong and Liu (2004) found a linear relationship between the impact energy and the total delaminated area in glass–epoxy laminates. They showed that an efficient way to improve the energy absorption capacity of laminate composites in the through-thickness direction was to promote controlled delamination by weakening the interlaminar bond strength or interlaminar fracture toughness. Borg *et al.* (2004) developed a delamination model for use in transverse impact simulations. According to their model, the relative orientation of the delamination front with respect to the fibres above and below the interface can be determined. It was shown that the delamination model can be used for modelling delamination initiation and growth in transverse impact simulations.

Sohn and Hu (1996) investigated the delamination mechanisms and energy dissipation of carbon-fibre epoxy composites under impact and high strain rate conditions. In their work the failure modes were successfully separated and the toughness results showed the transition from mode-I to mode-II delamination when the mixed mode specimens were tested at the two extreme conditions. Kim and Sham (2000) studied the fracture response and failure mechanisms of composite laminates containing woven fabrics in mode-I and mode-II delamination and under impact loading. They established a correlation between resistance and tolerance of impact damage and the delamination resistance of composites. They showed that mode-I interlaminar fracture toughness of glass-woven-fabric composites could be controlled by fibre-surface treatment. Martinez *et al.* (2005) performed impact

© Woodhead Publishing Limited, 2014

tests over a carbon-fibre reinforced epoxy using low energy in the striker. In their work a non-conservative and non-linear spring-clashpot series model was proposed to reproduce the material behaviour. The model considered, simultaneously, both flexural and indentation phenomena accounting for energy losses by means of the restitution coefficient. Using this model the experimental force–time trace was predicted accurately. Pegoretti *et al.* (2008) investigated the correlation between interlaminar fracture toughness and impact energy absorption for the fracture of epoxy–carbon laminates. According to their results, the bending strength determined both under quasi-static and impact conditions markedly increase as the interlaminar fracture toughness increases and the interlaminar fracture toughness has an opposite effect on the initiation and propagation energies under impact conditions. Ghasemnejad *et al.* (2008, 2009, 2010a, 2010b) studied interlaminar crack propagation in mode-I, mode-II and mixed mode I–II on the progressive crushing modes and energy absorption capability of laminated FRP composite box structures. They showed that during progressive collapse from bending, following the growth of a main central interwall crack due to delamination in the side wall, caused a significant amount of energy absorption. The main central interwall cracks were mode-I interlaminar crack propagation. They concluded that using suitable laminate design for composite box improved interlaminar fracture toughness and consequently energy absorption capability. The variation of specific energy absorption (SEA) with interlaminar fracture toughness was non-linear for different lay-ups.

Grassi *et al*. (2006) proposed a simple and efficient computational approach for analysing the benefits of through-thickness pins for restricting debonding failure in joints. According to their experimental results increases in debonding resistance and ultimate strength depended on the material, size, density, location, and angle of deployment of the pins and the mechanisms of pin deformation, which are complex and strongly affected by the mode ratio of the debonding crack. Mouritz (2007) published a comprehensive review into polymer composite laminates reinforced in the through-thickness direction with Z-pins by describing research into the manufacture, microstructure, delamination resistance, damage tolerance, joint strength and mechanical properties of Z-pinned composites. Benefits of reinforcing composites with z-pins are assessed, including improvements to the delamination toughness, impact damage resistance, post-impact damage tolerance and through-thickness properties. Other experimental researchers (Childress and Freitas, 1992; Freitas *et al.*, 1994, 1996; Partridge *et al.*, 2003, 2004) have shown that Z-pinning reduced the amount of delamination damage caused by impact events from low energy objects, ballistic projectiles and high-speed hailstones.

Borsellino *et al.* (2007) studied rheological, static and impact tests on two adhesive resins usually employed in marine applications. Single lap joint tests

© Woodhead Publishing Limited, 2014

were conducted on composites joints evidencing the contribution of curing time of both resins on the mechanical properties of the joint. Furthermore, they developed a numerical model of the single lap joint test with software ANSYS in the elastic regime. Their model is suitable for designing and/or verifying the mechanical performances of composites joints, evaluating the shear, axial and peel stress trends on the joint overlap length.

Taib *et al*. (2006) investigated the end curvature effect, adhesive thickness and adherend stiffness in the single lap joint and its effect on shear and peel stresses in that region. They showed experimentally three more joint configurations namely: double lap joints, joggle lap joints and L-section joints. The single lap joints were found to be stronger than the joggle lap joints. Their results showed that for joggle lap joints the spew fillet effect depended on both the adherend stiffness and adhesive ductility. The spew fillet was more effective when the adhesive was relatively ductile compared with the adherends.

Most of above previous researchers have investigated the impact response of adhesive as well as Z-pinned and stitched bonded joints using synthetic fibres. Natural fibres may demonstrate a different characteristic when used to reinforce polymers. Natural fibres consist of a wide range of materials such as cotton, bark, wood, pulp, nut shells, bagasse, corncobs, bamboo, cereal straw, and vegetable (e.g., flax, jute, hemp, sisal, and ramie) (Li *et al.*, 2000; Xiao *et al.*, 2003; Sabu and Pothan 2009). These fibres are mainly made of cellulose, hemicelluloses, lignin and pectins, with a small quantity of extractives. The fibre constituents vary depending on their origin. Compared with conventional inorganic fillers such as glass and carbon fibres, natural fibres provide many advantages including: (1) abundance and therefore low cost, (2) biodegradability, (3) flexibility during processing resulting in low machine wear, (4) minimal health hazards, (5) low density, (6) desirable fibre aspect ratio, and (7) relatively high tensile and flexural modulus. Incorporating the tough and light-weight natural fibres into polymer matrices (thermoplastic and thermoset) produces composites with a high specific stiffness and strength (Xie *et al.*, 2010).

As discussed before, FRP composite structures are likely to experience delamination during their service life. It is therefore important to investigate the response of stitched single lap joints and delaminated composite structures under impact loading.

13.2 Mechanical characterization

In this work the Charpy impact response of hybrid composite beams were studied experimentally. The hybrid composite beams were fabricated from combination of glass–epoxy and carbon–epoxy of $[G_0/C_0]_3$, $[G_{90}/C_{90}]_3$, $[G_0/C_{90}]_3$ and $[G_{90}/C_0]_3$.

© Woodhead Publishing Limited, 2014

Table 13.1 Material properties of the unidirectional CFRP and GFRP

	E_1 (GPa)	E_2 (GPa)	G_{12} (GPa)	υ_{12}	σ_μ 0° (MPa)	σ_μ 90° (MPa)	τ_s (MPa)	V_f (%)	μ
CFRP	138 ± 12	10.5 ± 1	6.3 ± 0.4	0.2	330 ± 14	32 ± 4	147 ± 14	42	0.41
GFRP	35.1 ± 4	9.6 ± 1	4 ± 0.5	0.32	807 ± 10	21.3 ± 2	97.9 ± 4	40.3	0.35

CFRP: carbon fibre reinforce plastic. GFRP: glass fibre reinforced plastic. E = Young's modulus, G = shear modulus, σ = strength, μ = coefficient of friction, τ = shear stress, V_f = Volume fraction.

The mechanical characteristics of carbon–epoxy and glass–epoxy were obtained in accordance with the relevant standards (ASTM, 2002; BS-ENISO 1998a,b, 2002) using tensile, shear, fibre volume fraction and coefficient of friction tests. All specimens were manufactured from carbon-fibre reinforced plastic (CFRP) and glass-fibre reinforced plastic (GFRP) materials of density 1.8 and 1.6 g/cm^3 respectively with epoxy resin. The findings for tensile, shear and fibre volume fraction are summarized in Table 13.1.

13.3 Specimen preparation

13.3.1 Delaminated composite beams

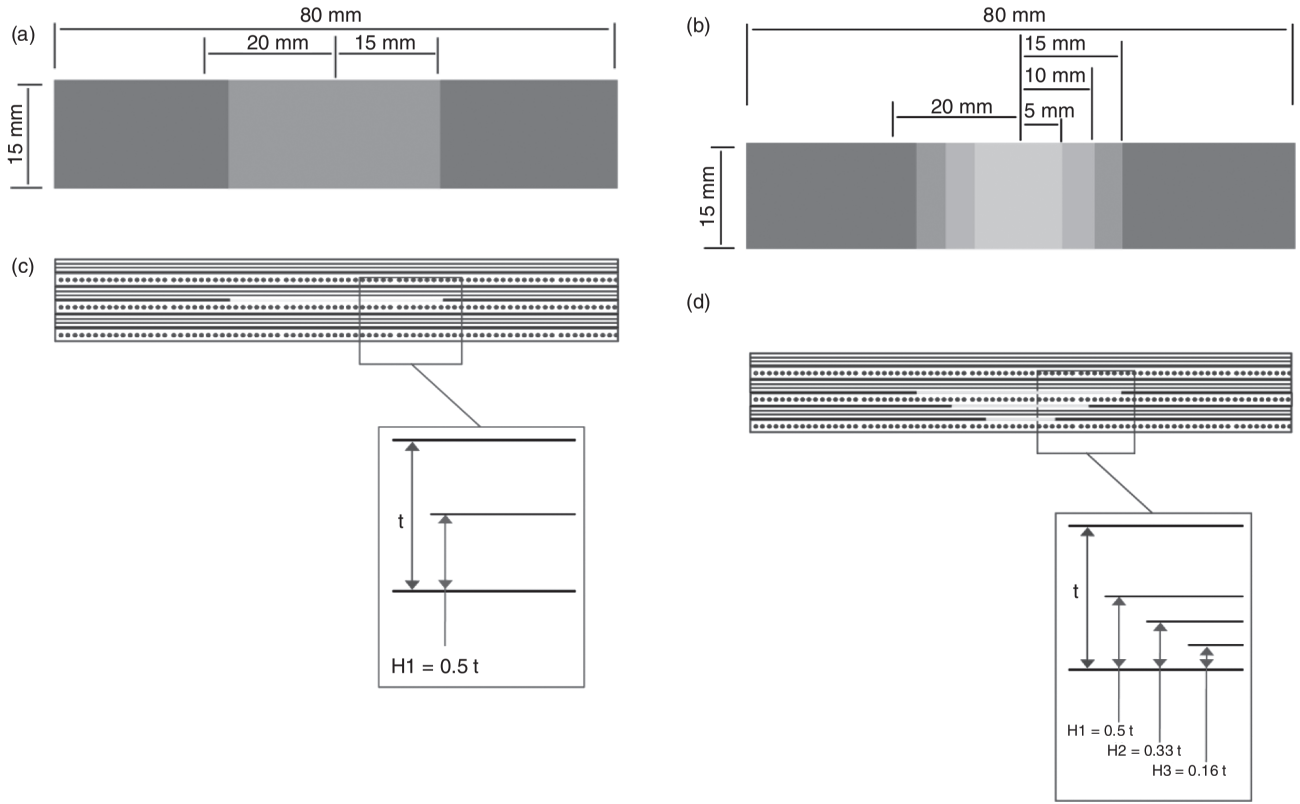
The recommended specimen size for the Charpy impact test is at least 80 mm long and 15 mm wide. The hybrid laminates were laid-up from GFRP and CFRP composites with laminate design of $[C_0/G_{90}]_3$ and $[C_{90}/G_0]_3$. A fibre orientation of 0 was aligned with the longitudinal direction of beam. The variation of lay-ups was to reach a constant thickness for all specimens. To aid in introducing multi-delaminated beams, three positions of $H/t = 0.5$, 0.33 and 0.166 were chosen and polytetrafluoroethylene (PTFE) film of 13 μm was placed at these particular positions (see Fig. 13.1). To cure the specimens the temperature was initially raised to 80°C and held for 60 min, then increased to 140°C and held for 4 h. This stepped heat-up meant the heat was raised gradually to 140°C, rather than quickly, allowing the epoxy matrix to fully infuse the reinforcement before hardening. After curing, the specimen was left in an oven to cool to room temperature. Each specimen was labelled with the specimen lay-up and specimen number prior to testing. The laminates were then machined into 15 × 80 mm^2 beams.

13.3.2 Single lap joint beams

The hybrid laminates were laid-up from GFRP and CFRP composites with laminate design of $[C_0/G_0]_3$ and $[C_{90}/G_{90}]_3$. After the curing process, the

© Woodhead Publishing Limited, 2014

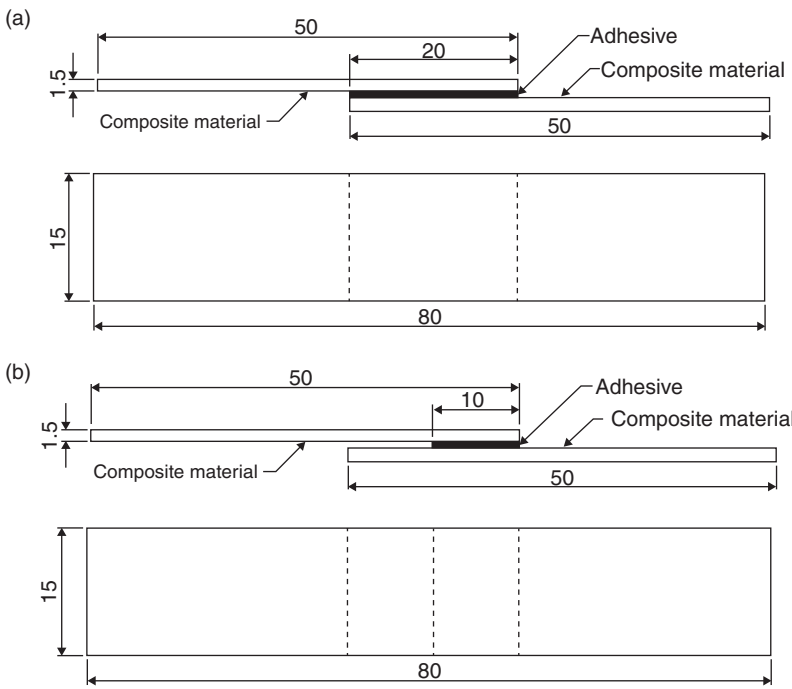
© Woodhead Publishing Limited, 2014



13.1 Schematic representation of single (a) and multi (b) delaminated composite specimens, with the view through the thickness for single (c) and multi (d) delamination.

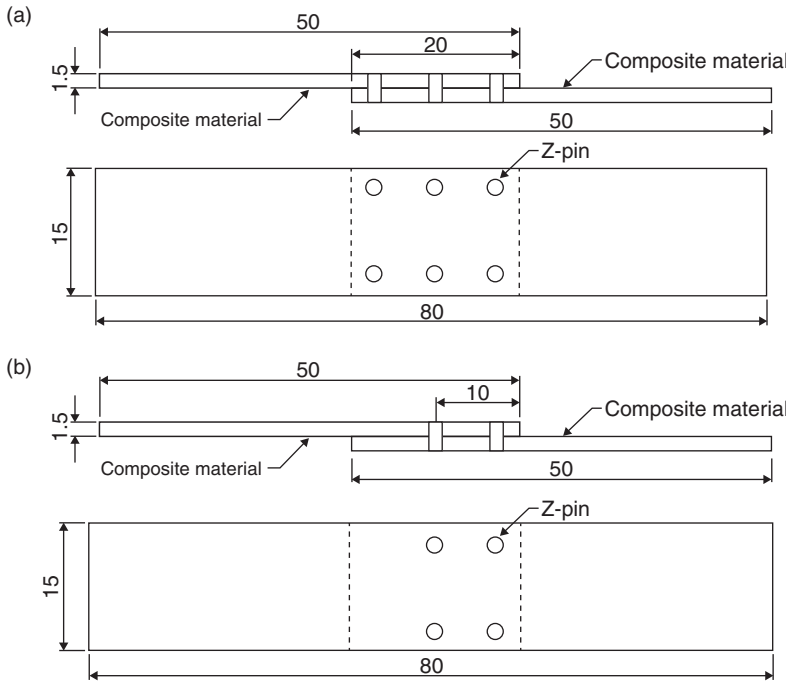
laminates were then machined into 15 × 50 mm^2 beams. To ensure a good bonding of adherend surfaces, the bonding surfaces was cleaned with acetone, and then sanded with 1000 grit silicon carbide paper. They were then immersed in potassium dichromate solution in sulphuric acid for 60 min at 25°C and cleaned with acetone again, then wiped in dry air at 40°C. The composite beams (adherends) were bonded using Loctite ESP110 adhesive to make two types of single lap joint specimens. A bead of adhesive was applied along the centre line of the bond area and the adherends were joined. A gentle pressure was applied to squeeze out any extra adhesive. The thickness of the adhesive was controlled as 0.75 mm. Metal spacers were used to maintain the required bond-line thickness. The potential stress concentration was assumed negligible compared with applied kinetic energy. The first specimen was completely bonded (CB). The second specimen was partially bonded, that is, de-bonded (DB), to introduce debonding in a single lap joint specimen (see Fig. 13.2).

Many novel techniques have been developed to reinforce laminated polymer composites in the through-thickness direction as a solution to problems of poor impact damage tolerance, low through-thickness mechanical properties,

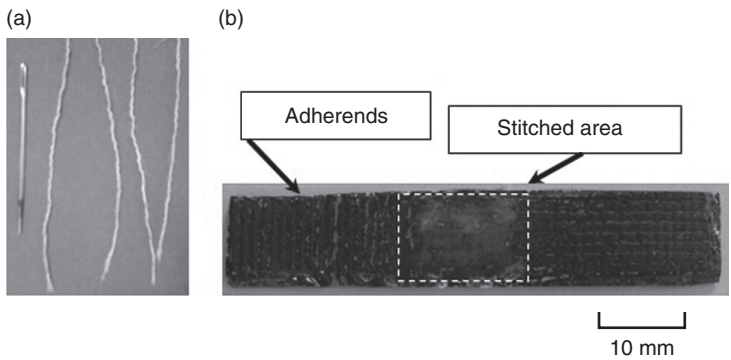


13.2 Composite material $[C_0/G_0]_3$ and $[C_{90}/G_{90}]_3$ (a) CB with adhesive and (b) de-bonded DBS specimen (all dimensions in mm).

© Woodhead Publishing Limited, 2014



13.3 Composite material $[C_0/G_0]_3$ and $[C_{90}/G_{90}]_3$ (a) completely bonded with stitching (CBS) and (b) de-bonded with stitching (DBS) (all dimensions in mm).



13.4 (a) Needle and flax yarn for stitching and (b) CBS single lap joint, 6 pines (natural flax fibres).

© Woodhead Publishing Limited, 2014

and weak strength of bonded joints. The most common through-thickness reinforcement techniques are 3D weaving, stitching and braiding. More advanced techniques include embroidery, tufting, stitching and Z-anchoring, hereafter known as Z-pinning. These techniques are effective at increasing the delamination resistance and impact damage tolerance. The manufacturing of stitched hybrid composite specimens in the current investigation is similar to the normal hybrid composite specimens, except that the composite was stitched with natural flax yarn (Tong *et al.*, 2002) before curing process (see Fig. 13.3).

Flax yarns (with diameter of 1.1 mm) were stitched onto the test specimens in the z-direction using a needle. Six pins were stitched to make a complete bonding, that is, completely bonded z-stitched (CBZ), such that there were two rows in total and three pins in each row. For DB, that is, de-bonded Z-stitched (DBZ), specimens, four pins were stitched at the lap joint area. For each specimen, two rows of stitches, each row containing two pins, were stitched (see Fig. 13.4). The two stitched adherends were then cured and a bond was established via the composite matrix.

13.4 Charpy impact test

All specimens were tested using a Zwick Roell instrument consisting of a free supported specimen stand and a pendulum with a defined mass attached to a rotating arm pinned at the machine body (Hufenbach *et al.,* 2008). The material absorbed energy (AE) was measured in joules. For a single- and multi-delaminated beam, the PTFE film was placed between the plies (as described before). The applied energy for impact test was set as 2 J with a pendulum of 0.5 kg mass and an arm length of 200 mm leading to a speed at impact of around 2.83 m/s. Three specimens were tested for each laminate design. The AE for each laminate design with different delamination positions and single lap joint specimens is presented in Table 13.2.

Table 13.2 The AE of the simple and stitched single- and multi-delaminated hybrid composite beams

Laminate design	AE (J)	
	Single-delaminated	Multi-delaminated
$[C_0/G_{90}]_3$	0.80 ± 0.27	0.45 ± 0.02
$[C_{90}/G_0]_3$	0.90 ± 0.01	0.90 ± 0.25
2Stitched-$[C_0/G_{90}]_3$	0.80 ± 0.16	0.60 ± 0.12
2Stitched-$[C_{90}/G_0]_3$	0.90 ± 0.13	1.20 ± 0.20
4Stitched-$[C_{90}/G_0]_3$	1.20 ± 0.13	1.50 ± 0.14

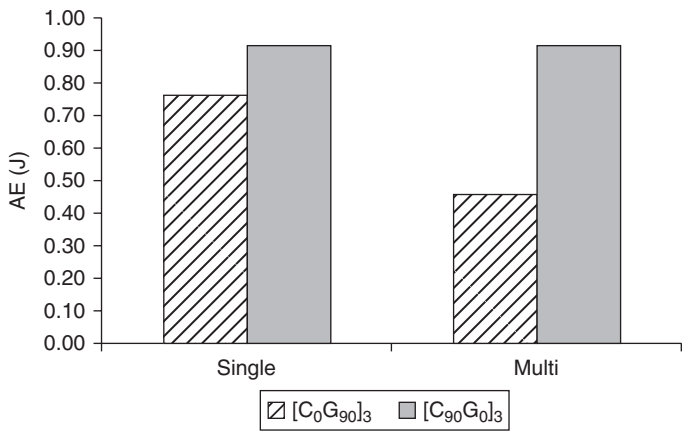
© Woodhead Publishing Limited, 2014

13.5 Experimental results

13.5.1 Response of single- and multi-delaminated composite beams

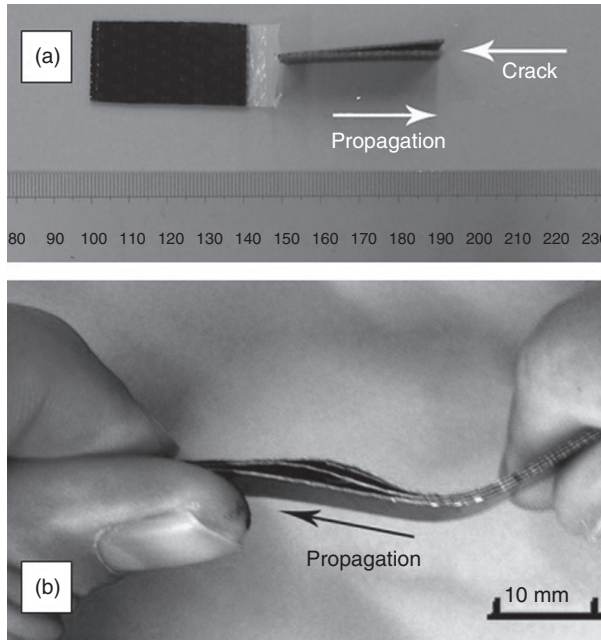
For the first part of the experiment, hybrid composite beams of $[C_0/G_{90}]_3$ and $[C_{90}/G_0]_3$ were manufactured of six plies with the defect position between layers 3||4. The experimental results obtained are shown in Fig. 13.5. It was observed that the laminate design of $[C_0/G_{90}]_3$ offered lower AE in comparison with the laminate design of $[C_{90}/G_0]_3$. During the test, all of the $[C_0/G_{90}]_3$ specimens failed in the middle and the delamination crack propagated from one side of the specimens (see Fig. 13.6a). However, even though the crack propagation was similar in $[C_{90}/G_0]_3$ specimens, they did not fracture and no failure was recorded. As the results indicate, the $[C_{90}/G_0]_3$ specimens showed better respond in terms of energy absorption and failure of the specimens.

In the next step of the experiment, the hybrid composite beams of $[C_0/G_{90}]_3$ and $[C_{90}/G_0]_3$ were manufactured of six plies with the multi-defects positioned between layers 3||4, 4||5 and 5||6 (see Fig. 13.5). The outcomes for this step of the experiment are shown in Fig. 13.7. The results indicate that the laminate design of $[C_{90}/G_0]_3$ laminate has produced the highest amount of energy absorption. The amount of AE by this laminate design was around 77% higher than the laminate design of $[C_0/G_{90}]_3$. The $[C_0/G_{90}]_3$ specimens failed during the test, but little crack propagation was observed in the specimens. In the $[C_{90}/G_0]_3$ specimens, the defect cracks propagated from one side but failure of specimens did not occur (see Fig. 13.6b).

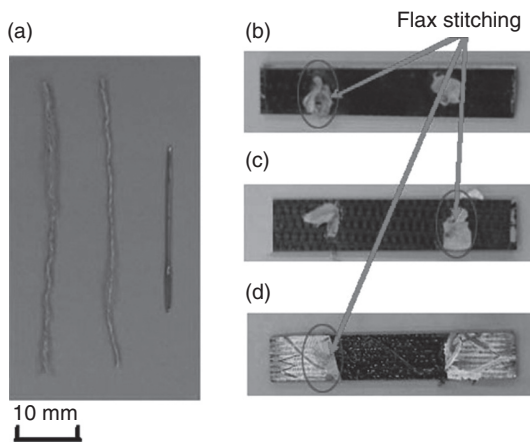


13.5 Comparison of AE for single-delaminated and multi-delaminated hybrid composite beams of $[C_0/G_{90}]_3$ and $[C_{90}/G_0]_3$.

© Woodhead Publishing Limited, 2014



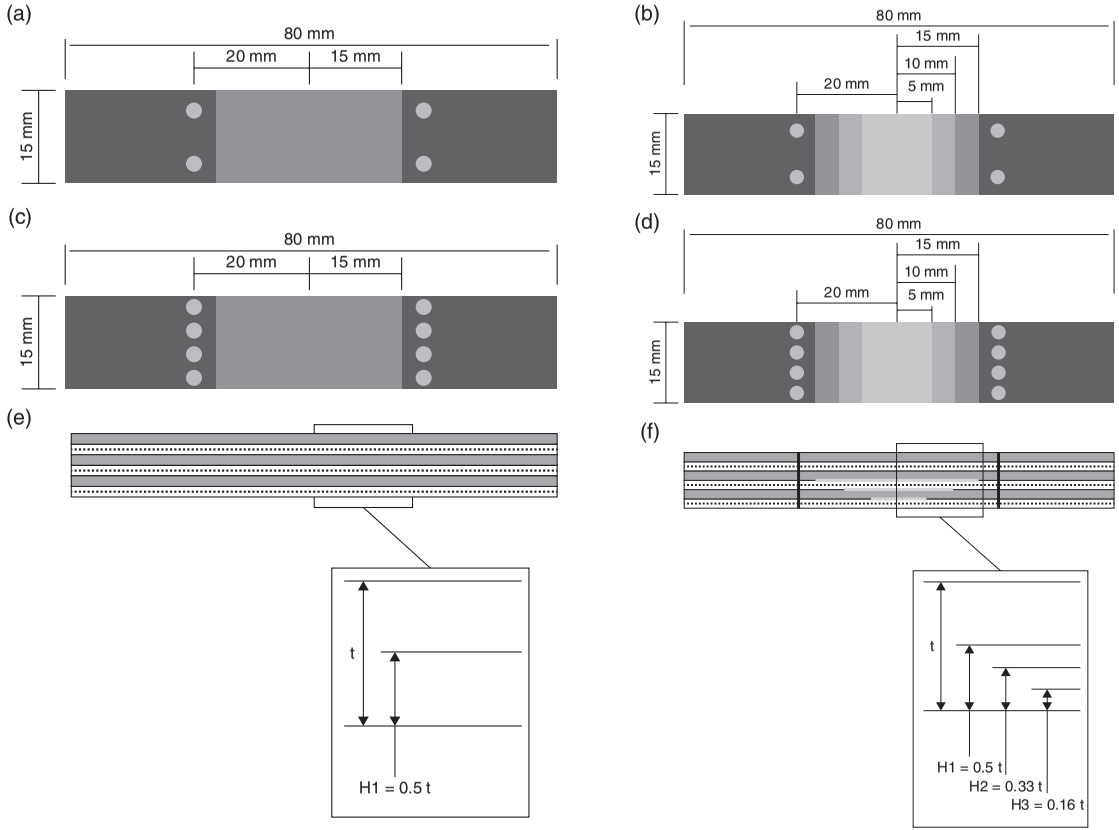
13.6 Crack propagation and fracture of (a) $[C_0/G_{90}]_3$ specimens with defect position between layers 3||4 and (b) $[C_{90}/G_0]_3$ specimen with multi-defects at 3||4, 4||5 and 5||6.



13.7 (a) Needle and flax yarn for stitching, (b) two stitched single-delaminated, (c) two stitched multi-delaminated and (d) four stitched multi-delaminated composite beams.

© Woodhead Publishing Limited, 2014

© Woodhead Publishing Limited, 2014



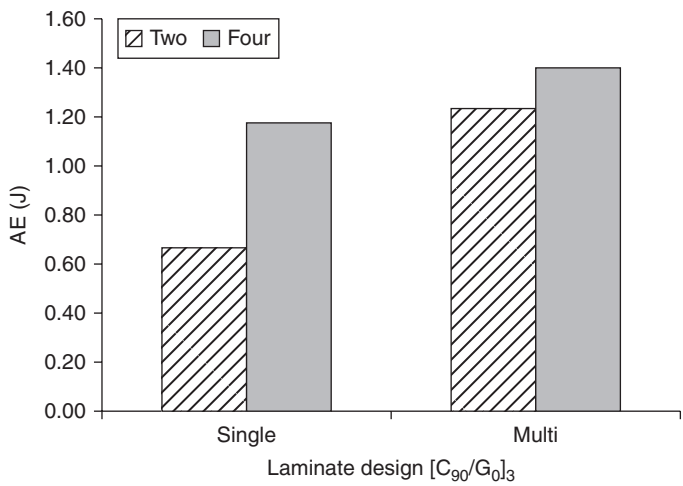
13.8 Schematic representation of delaminated composite specimens with (a) two stitched single-delaminated, (b) two stitched multi-delaminated, (c) four stitched single-delaminated, (d) four stitched multi-delaminated composite beams and layout of (e) single and (f) multi-delaminated specimen through the thickness.

13.5.2 Effect of stitching on impact damage response

A stitching method using natural flax yarns were carried out to improve the energy absorbing capability of delaminated composite beams. Similar sets of specimens with laminate design of $[C_{90}/G_0]_3$ that showed the highest amount of energy absorption in Section 13.3 were manufactured. However, these specimens were pinned at two points in through the thickness at 20 mm on either side of the longitudinal centre line using flax yarn as illustrated in Fig. 13.8.

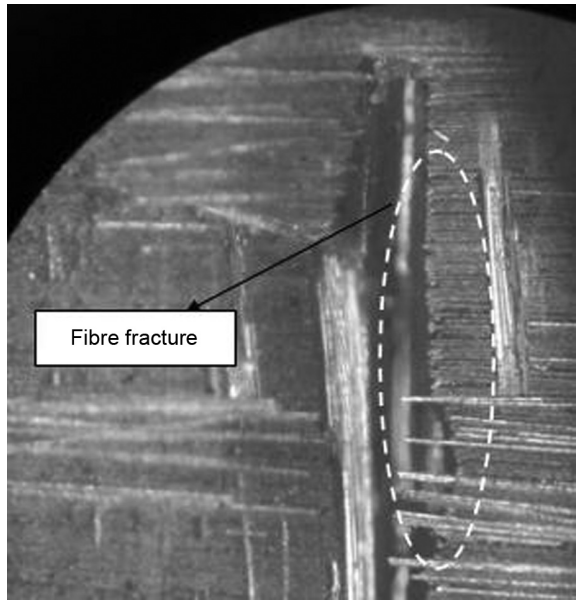
Introducing the natural flax yarns through the thickness in all specimens gave an improvement in AE. In order to better understand the effects of flax stitching, these sets of specimens were pinned four times 20 mm on either side of the longitudinal centre line. The comparison of the results for the specimens before and after introduction of stitching, and the difference achieved by changing the number of pins from two to four, are found in Fig. 13.9. The average AE was improved by 76% for single-defect design and by 14% for the multi-defect design when the number of Z-pin points was increased from two to four.

As was observed in an early stage of this study, during impact process the longest delamination in multi-delaminated composite beams propagates on one side of specimen. In this case the impact energy was absorbed by two failure mechanisms of intralaminar and interlaminar (delamination). The intralaminar failure that is related to failure through the lamina consisted of some fibre breakage and matrix cracking (see Fig. 13.10). In addition



13.9 Comparison for the amount of AE in simple and stitched composite beams with laminate design of $[C_{90}/G_0]_3$.

© Woodhead Publishing Limited, 2014



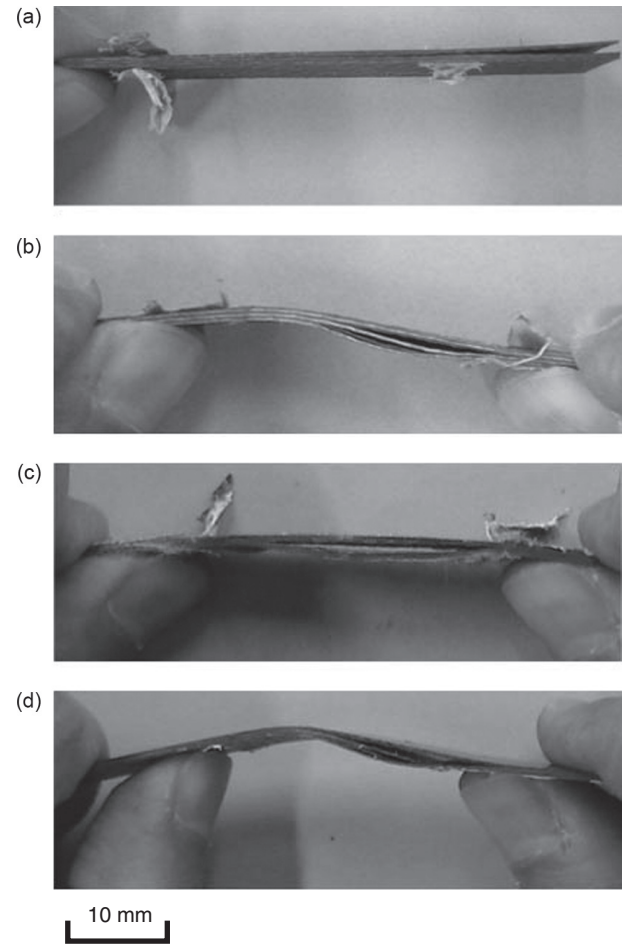
13.10 Optical micrograph from fracture surface of impacted specimens showing fibre breakage combination of intralaminar $C_{90}//G_0$ interface.

delamination propagation is an interlaminar failure mode that occurred in the specimens during an impact event. In this regard, natural flax yarns that were pinned through the thickness of multi-delaminated specimens significantly arrested crack propagation in the specimens. In this case there was more resistance within the specimens that as a consequence absorbed more energy. It is worth mentioning that increasing the number of flax yarns affected the energy absorption capability of multi-delaminated specimens and by increasing the flax yarns there was more resistance against crack propagation and failure in the multi-delaminated composite beams (see Fig. 13.11).

13.5.3 Impact damage response of adhesive bonded single lap joint

Adhesive bonded hybrid composite beams of $[C_0/G_0]_3$ and $[C_{90}/G_{90}]_3$ were manufactured of six plies to make comparative strength analysis. Two types of adhesive bonding conditions were used: CB joints for a bonding length of 20 mm (overlap length = 20 mm) and DB joints for a bonding length of 10 mm (overlap length = 20 mm). Three specimens were tested for each design and the average results are presented in Table 13.3. It was observed that the AE of DB joints with laminate design of $[C_0/G_0]_3$ was 0.42 J, while

© Woodhead Publishing Limited, 2014



13.11 Stitched single- and multi-delaminated hybrid composite beams with laminate design of $[C_{90}/G_0]_3$ after impact: (a) two stitched single-delaminated composite beam, (b) two stitched multi-delaminated composite beam, (c) four stitched single-delaminated composite beam, and (d) four stitched multi-delaminated composite beam.

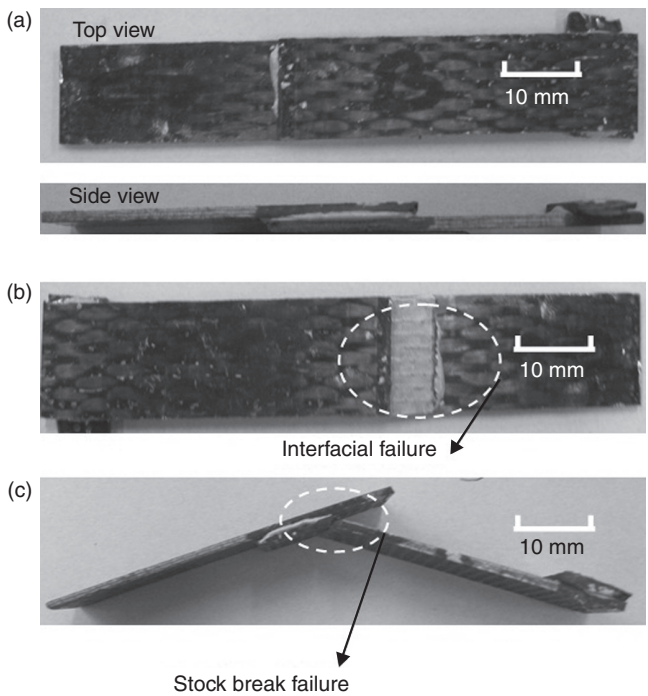
Table 13.3 Comparison of energy absorption of adhesive CB and DB composite joints

Bonding type	Laminate design	AE E_A (J)
Adhesive CB	$[C_0/G_0]_3$	0.43 ± 0.07
Adhesive DB	$[C_0/G_0]_3$	0.42 ± 0.03
Adhesive CB	$[C_{90}/G_{90}]_3$	0.43 ± 0.04
Adhesive DB	$[C_{90}/G_{90}]_3$	0.47 ± 0.04

© Woodhead Publishing Limited, 2014

for the laminate design of $[C_{90}/G_{90}]_3$ it was 0.47 J. However, the energy absorbed according to both laminate design of $[C_0/G_0]_3$ and $[C_{90}/G_{90}]_3$ in the CB joint were 0.43 J (see Table 13.3).

These hybrid composite beams showed various modes of failure during the impact testing process. The laminate design of $[C_0/G_0]_3$ with the CB joint showed adhesive failure (or interfacial failure) where the separation appeared to be at the adhesive-adherend interface. The laminate design of $[C_0/G_0]_3$ with the DB joint showed thin layer cohesive failure (or interphase failure) where the failure was close to the adhesive–adherend interface, characterized by a light dusting of adhesive on one adherend surface and a thick layer of adhesive left on the other. The laminate design of the $[C_{90}/G_{90}]_3$ CB showed a mixed failure including both adhesive failure and fracture in the middle of the specimen. Similarly the laminate design of the $[C_{90}/G_{90}]_3$ DB showed a mixed failure including both adhesive failure and stock break failure. The stock break failure occurred when the separation was within the adherend but outside the bonded region (see Fig. 13.12). The energy absorption capacity for the laminate designs of the $[C_0/G_0]_3$ CB, $[C_0/$



13.12 (a) Completely bonded joint specimen before impact, (b) CB joint $[C_0/G_0]_3$ and (c) DB joint specimen after impact with laminate design of $[C_{90}/G_{90}]_3$.

© Woodhead Publishing Limited, 2014

$G_0]_3$ DB and $[C_{90}/G_{90}]_3$ CB were close to each other and showed similar characteristic modes of failure. The laminate design of the $[C_{90}/G_{90}]_3$ DB resulted in maximum energy absorption with the least damage behaviour in comparison with other laminate designs.

13.5.4 Impact damage response of stitched single lap joint

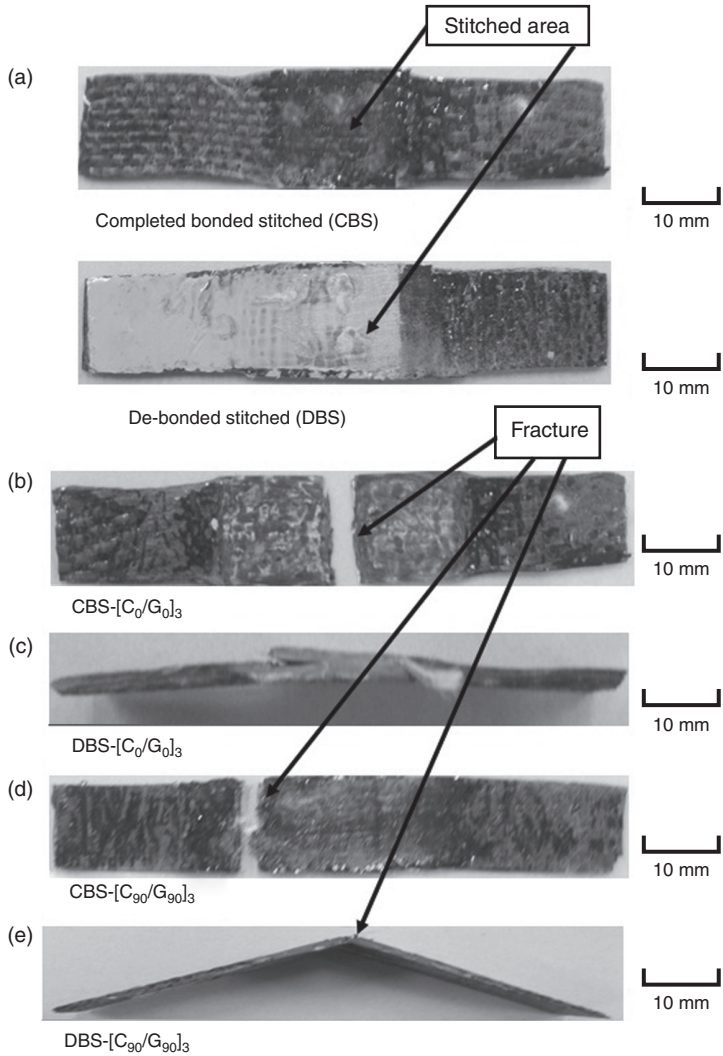
The single lap joint specimens of $[C_0/G_0]_3$ and $[C_{90}/G_{90}]_3$ were manufactured using six plies with two types of stitched joints, that is, completely bonded stitched (CBS) joint for a bonding length of 20 mm (overlap length = 20 mm) and de-bonded stitched (DBS) joint for a bonding length of 10 mm (overlap length = 20 mm). The results showed that the AE of the DBS joint with laminate design of $[C_0/G_0]_3$ was 0.72 J, while the AE for the laminate design of $[C_{90}/G_{90}]_3$ was 0.64 J for the DBS joint. The energy absorbed by the laminate of design $[C_0/G_0]_3$ and $[C_{90}/G_{90}]_3$ in the CBS joint were 1.06 and 0.86 J respectively (see Table 13.4).

The impact test process resulted in various modes of failure for these stitched single lap joint specimens. The single lap joint of CBS with lay-up of $[C_0/G_0]_3$ showed shear-out failure mode, where the stitching was sheared out and the adherends were separated from the bonded area. This delivered minimum damage behaviour to the composite beam and significantly absorbed more energy during impact. The laminate design of the $[C_0/G_0]_3$ DBS showed a failure in the form of fracture. Fracture occurred outside the stitched region, that is, DB area. In the laminate design of the $[C_{90}/G_{90}]_3$ CBS, fracture occurred outside the stitched area, that is, the edge of the overlap joint and the adherends were separated at that juncture. The laminate design of the $[C_{90}/G_{90}]_3$ DBS showed a mixed failure mode that included fracture in the middle of the specimen and fracture at the edge of the overlap joint. This laminate design showed high damage behaviour and low energy absorption. This clarifies that the laminate design of the $[C_0/G_0]_3$ CBS joint absorbed maximum energy and showed the least damage compared with other types of stitched laminate designs (see Fig. 13.13).

Table 13.4 Comparison of energy absorption of CBS and DBS composite joints

Bonding type	Laminate design	AE E_A (J)
CBS	$[C_0/G_0]_3$	1.06 ± 0.03
DBS	$[C_0/G_0]_3$	0.72 ± 0.06
CBS	$[C_{90}/G_{90}]_3$	0.86 ± 0.06
DBS	$[C_{90}/G_{90}]_3$	0.64 ± 0.04

© Woodhead Publishing Limited, 2014



13.13 (a) Completely bonded stitched and de-bonded stitched joint specimens before impact, (b) CBS joint $[C_0/G_0]_3$, (c) DBS joint $[C_0/G_0]_3$, (d) CBS joint $[C_{90}/G_{90}]_3$ and (e) CBS joint $[C_{90}/G_{90}]_3$ specimens after impact.

13.6 Conclusion

The results of this investigation show that hybrid composite beams stitched with natural flax yarn exhibit higher impact resistance capacity compared with adhesive bonded joints by modifying and retarding the failure mode. This technique will therefore make a major contribution to the application

© Woodhead Publishing Limited, 2014

of composite structures under dynamic service conditions. Sustainable utilization of natural resources in strengthening of advanced composite structures explained in this work will also contribute to the concept of green composite engineering.

13.7 References

Abrate S (1998). *Impact on Composites Structures*. Cambridge University Press.

ASTM D 3171–99 (2002). Standard test method for constituent content of composite materials. Annual book of ASTM standards, West Conshohocken, PA.

Borg R, Nilsson L and Simonsson K (2004). Simulation of low velocity impact on fibre laminates using a cohesive zone based delamination model. *Compos Sci Technol*, **64**, 279–288.

Borsellino B, Calabrese L, Di Bella G and Valenza A (2007). Comparisons of processing and strength properties of two adhesive systems for composite joints. *Int J Adhes Adhes,* **27**(6), September 2007, 446–457.

BS EN ISO 2747 (1998a). Glass Fibre Reinforced Plastics-Tensile Test, British Standard Institute, London.

BS EN ISO 14129 (1998b). Fibre Reinforced Plastics Composite-Determination of the In-plane Shear Stress/Shear Strain Response, Including the In-plane Shear Modulus and Strength by the ±45 Tension Test Method, British Standard Institute, London.

BS EN ISO 15024 (2002). Fibre-reinforced plastic composites. Determination of mode I interlaminar fracture toughness, G_{IC}, for unidirectional reinforced materials. BSI.

Childress JJ and Freitas G (1992). Z-Direction pinning of composite laminates for increased survivability. In: Proceedings of the AIAA aerospace design conference, Irvine, California, February 92–109.

Freitas G, Magee C, Dardzinski P and Fusco T (1994). Fibre insertion process for improved damage tolerance in aircraft laminates. *J Adv Mater*, **25**, 36–43.

Freitas G, Fusco T, Campbell T, Harris J and Rosenberg S (1996). Z-Fibre technology and products for enhancing composite design. In: Proceedings of the 83rd meeting of the AGARD SMP conference on bolted/bonded joints in polymeric composites, Paper 17, Florence Italy; 2–3 September.

Ghasemnejad H, Blackman BRK, Hadavinia H and Sudall B (2008). Experimental studies on fracture characterisation and energy absorption of GFRP composite box structure. *Compos Struct,* **88**(2), 253–261.

Ghasemnejad H and Hadavinia H (2009). Off-axis crashworthiness characteristic of woven glass/epoxy composite box structures. *J Reinf Plast Comp*, **29**(15), 2306–2330.

Ghasemnejad H, Hadavinia H and Aboutorabi A (2010a). Effect of delamination failure on the crashworthiness of hybrid composite box structures. *Mater Design,* **31**, 1105–1116.

Ghasemnejad H, Furquan ASM and Mason PJ (2010b). Charpy impact damage behaviour of single and multi-delaminated hybrid composite beam structures. *Mater Design*, **31**(8), 3653–3660.

Grassi M, Cox B and Zhang X (2006). Simulation of pin-reinforced single-lap composite joints. *Compos Sci Technol*, **66**, 1623–1638.

© Woodhead Publishing Limited, 2014

Hufenbach W, Marques Ibraim F, Langkamp A, Bohm R and Hornig A (2008). Charpy impact tests on composite structures – An experimental and numerical investigation. *Compos Sci Technol*, **68**, 2391–2400.

Khalili SMR, Ghajar R, Sadeghinia M and Mittal RK (2009). An experimental study on the Charpy impact response of cracked aluminium plates repaired with GFRP or CFRP composite patches. *Compos Struct*, **89**, 270–274.

Kim J and Sham M (2000). Impact and delamination failure of woven-fabric composite. *Compos Sci Technol*, **60**, 745–761.

Li Y, Mai YW and Ye L (2000). Sisal fibre and its composites: a review of recent developments. *Compos Sci Technol,* **60**, 2037–2055.

Martinez AB, Sanchez-Soto M, Velasco JI, Maspoch MLI, Santana OO and Gordillo A (2005). Impact characterization of a carbon fiber-epoxy laminate using a non-conservative model. *J Appl Polym Sci*, **97**, 2256–2263.

Mouritz AP (2007). Review of z-pinned composite laminates. *Compos: Part A*, **38**, 2383–2397.

Partridge IK, Cartie DDR and Bonnington T (2003). Manufacture and performance of z-pinned composites. In: *Advanced Polymeric Composites*, Shonaike G, Advani S (eds) FL: CRC Press.

Partridge IK, Cartie´ DDR, Troulis M, Grassi M and Zhang, X (2004). Evaluating the mechanical effectiveness of z-pinning. In: Proceedings of the SAMPE technical conference, September.

Pegoretti A, Cristelli i and Migliaresi C (2008). Experimental optimization of the impact energy absorption of epoxy-carbon laminates through controlled delamination. *Compos Sci Technol*, **68**(13), 2653–2662.

Richardson MOW and Wisheart MJ (1996). Review of low-velocity impact properties of composite materials, *Composites Part A*, **27A**, 1123–1131.

Schubbe JJ and Mall S (1999a). Investigation of cracked thick aluminum panel repaired with bonded composite patch. *Eng Fract Mech*, **63**(4), 305–323.

Schubbe JJ and Mall S (1999b). Modeling of cracked thick metallic structure with bonded composite repair using three-layer technique. *Compos Struct*, **45**, 185–193.

Sohn MS and Hu XZ (1996). Impact and high strain rate delamination characteristics of carbon fibre epoxy composites. *Theor Appl Fract Mec*, **25**, 17–29.

Taib AA, Boukhili R, Achiou S, Gordon S and Boukehili H (2006). Bonded joints with composite adherends. Part I. Effect of specimen configuration, adhesive thickness, spew fillet and adherend stiffness on fracture. *Int J Adhes Adhes*, **26**(4), July 2006, 226–236

Tong L, Mouritz AP and Bannister M (2002). *3D Fibre Reinforced Polymer Composites*. Elsevier, ISBN-13: 978–0-08–043938–9.

Xiao Z, Zhao LB, Xie Y and Wang QW (2003). Review for development of wood plastic composites. *J Northeast Forest Univ*, **31**, 89–93.

Xie Y, Hill CAS, Xiao Z, Militz H and Mai C (2010). Silane coupling agents used for natural fiber/polymer composites: a review. *Compos: Part A*, **41**, 806–819.

© Woodhead Publishing Limited, 2014

14

Natural fibre composites in a marine environment

M. P. ANSELL, University of Bath, UK

DOI: 10.1533/9780857099228.3.365

Abstract: Natural fibres have been employed in maritime applications since ancient times in the form of ropes, lashings and sails. More recently, natural fibre composites (NFCs) have provided a solution for the manufacture of fibre composite boats and surfboards with enhanced eco-profiles, but they suffer from questionable environmental stability. This chapter considers the history of natural fibres in marine applications and compares their mechanical properties and eco-profile with synthetic fibres. The hygroscopic performance of NFCs is briefly reviewed and methods for reducing moisture uptake are explained. Marine applications for NFCs are restricted to water craft including yachts, canoes and surfboards, and recent examples are described. Key web links and references are listed at the end of the chapter.

Key words: marine applications, history, physical properties, moisture uptake, fibre geometry.

14.1 Introduction

Natural fibres have played a key role in traditional maritime technology in the form of ropes, lashings, hulls and sails. Primitive timber rafts were lashed together with ropes and twine using locally available fibre resources. In Thor Heyerdahl's (1950) classic account of the Kon-Tiki expedition (crossing the Pacific by raft), the raft was constructed from balsa logs lashed together with inch and a quarter hemp rope, firmly knotted. The deck was formed from split bamboos plaited with bamboo reeds and the open cabin was made from bamboo canes, plaited bamboo reeds and bamboo slats with roof tiles comprising overlapping banana leaves. The masts and rudder were crafted from mangrove wood and the sails were plain-woven canvas, probably using hemp yarn. The design was largely based on ancient sea-craft built in Peru and Ecuador from around AD 500. In the account of the later Ra expeditions Heyerdahl (1972) describes the building of Ra I and Ra II papyrus rafts, which sailed the Atlantic from Africa. Worries associated with moisture uptake and waterlogging of the cellulose-based materials of construction

© Woodhead Publishing Limited, 2014

were common to both the Kon-Tiki and Ra expeditions and represent a challenge to modern sea-craft which employ natural fibres as reinforcement for composite materials. However, the Kon-Tiki raft and Ra II completed their voyages.

The weaving of canvas sails from flax (linen), cotton and hemp dates back to ancient times (e.g. Anderson, 1924; Turner, 1983). Flax is stronger but denser than cotton so until natural fibre sails were replaced by synthetic fibres such as polyester, aramid and carbon from the mid-twentieth century, cotton was increasingly favoured over flax. In addition, the waterproofing of sails was achieved by applying linseed oil or paraffin wax to cotton or flax sailcloth. The selection of indigenous natural fibres for traditional marine applications was historically a matter of necessity in the absence of synthetic materials. The present day selection of natural fibres for marine applications is driven by cost, sustainability and reduction in carbon footprint in competition with synthetic fibres. The selection of natural fibres in preference to synthetic fibres generally results in a lower composite stiffness, which is a key factor in mechanical design. It is therefore worthwhile examining the mechanical properties and eco-profiles of natural and synthetic fibres.

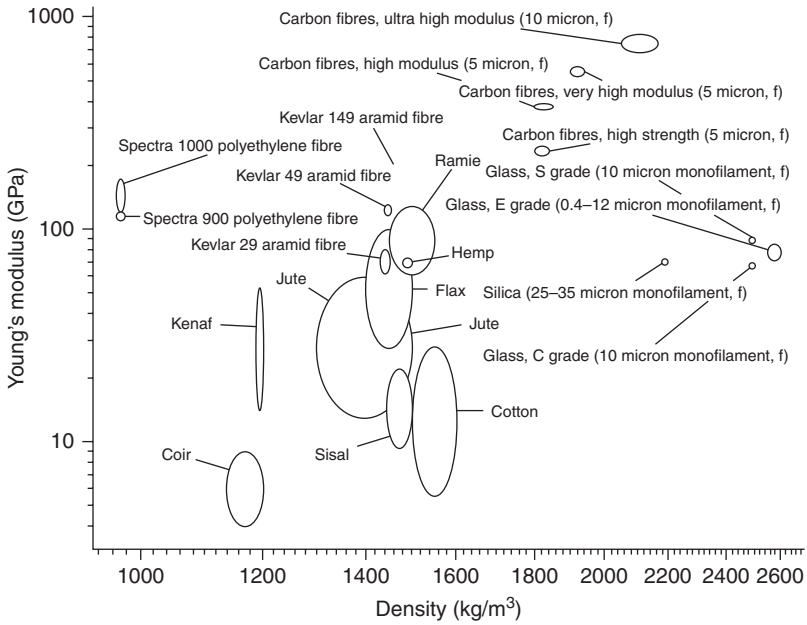
14.2 Properties and environmental impact of natural versus synthetic fibres

The Young's modulus versus density of natural and synthetic fibres is plotted in Fig. 14.1 using materials selection software marketed by Granta Design (CES 2013 EduPak, 2013). Bearing in mind that the y-axis is logarithmic, the high elastic moduli of carbon and aramid fibres offer a clear advantage when designing stiff marine structures such as composite boat hulls and laminated sails. Of the plant fibres, jute, ramie and flax possess the highest stiffness of the natural fibres included within the database. The range of values of Young's modulus and density are represented by the height and width of the ovals, and variability in these properties is also reviewed by Ansell and Mwaikambo (2009).

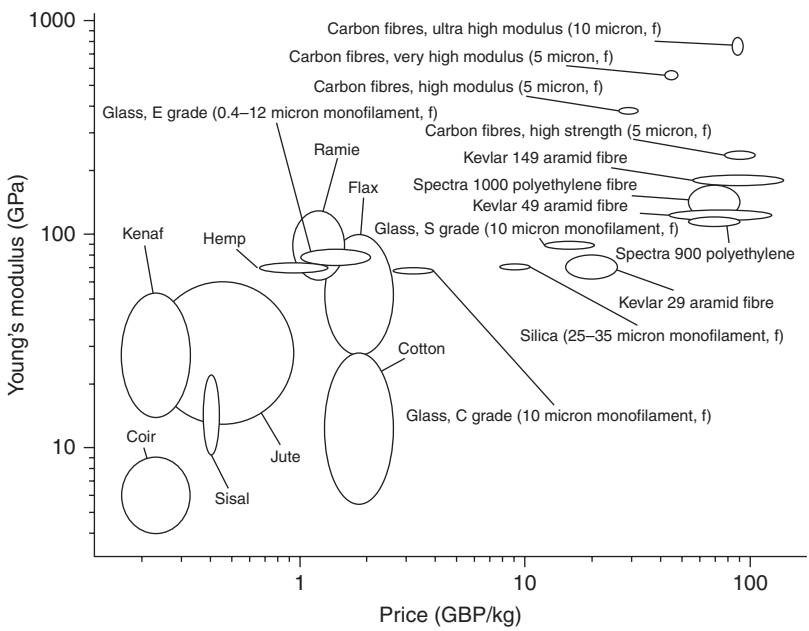
When the elastic modulus of these fibres is compared as a function of price (Fig. 14.2), natural fibres such as ramie, kenaf and jute have a clear financial advantage, with comparable elastic properties to glass fibres. Embodied energy in primary production of plant and synthetic fibres is ranked in Fig. 14.3, and the CO_2 footprint versus price compared in Fig. 14.4.

In terms of environmental impact and price, plant fibres offer a clear advantage. The selection of natural fibres for marine applications and the construction of engineered marine products are ideally linked to the country of origin, for example, flax and hemp in Europe, sisal and henequen in Tanzania and Mexico, and kenaf in Indonesia.

© Woodhead Publishing Limited, 2014

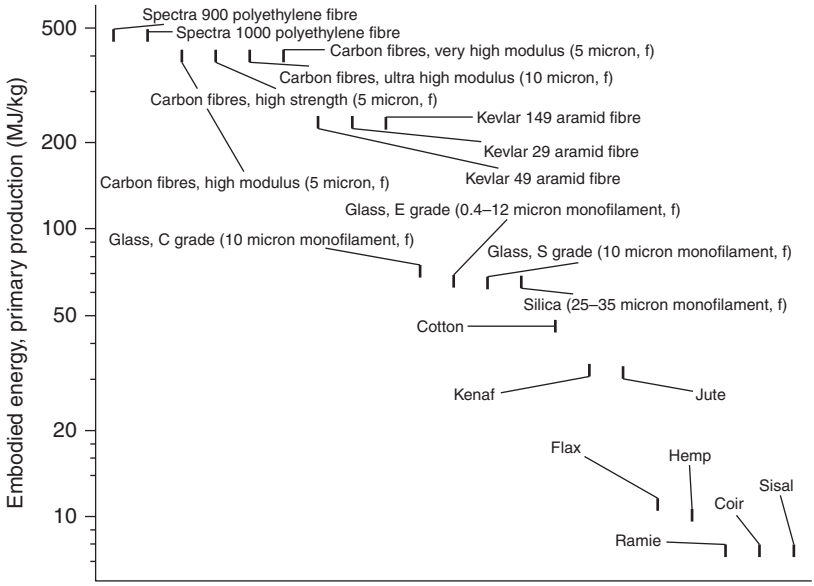


14.1 Young's modulus versus density for plant and synthetic fibres (f, fibre).

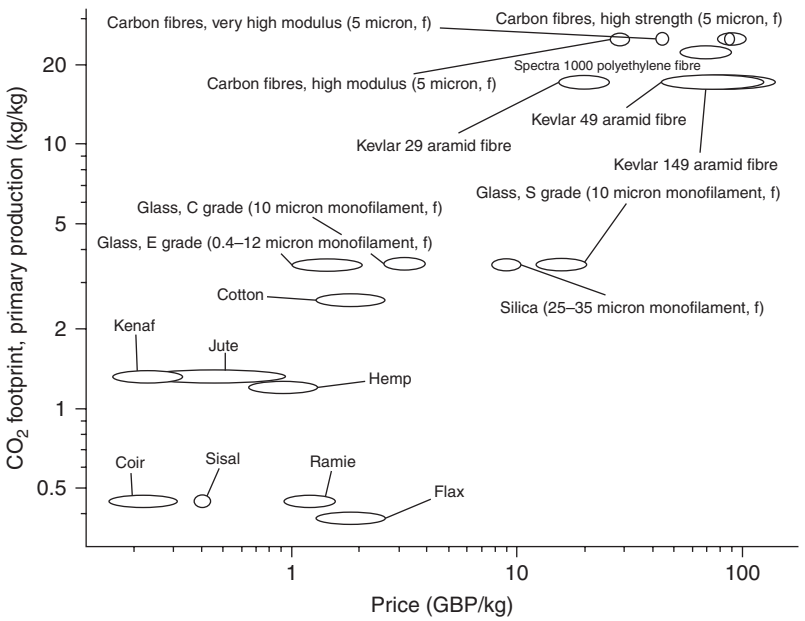


14.2 Young's modulus versus price for plant and synthetic fibres.

© Woodhead Publishing Limited, 2014



14.3 Embodied energy in primary production for plant and synthetic fibres.



14.4 CO_2 footprint versus price for plant and synthetic fibres.

© Woodhead Publishing Limited, 2014

14.3 Natural fibre composites (NFCs) and moisture uptake

Assuming that the elastic stiffness and strength of plant fibres is adequate for the reinforcement of natural fibre composites (NFCs), the problem of moisture uptake in marine applications must be addressed. Numerous papers examine the moisture uptake of NFCs. For example, Wambua *et al.* (2003) stress the importance of coherent fibre-to-matrix adhesion in NFCs. The detrimental effect of water absorption on the mechanical properties of hemp-reinforced composites was investigated by Dhakal *et al.* (2007) and exposure to high temperatures accelerated degradation in properties significantly. In a study of injection moulded thermoplastics containing short sisal fibres (Chow *et al.,* 2007), moisture uptake initially improved impact resistance at the expense of tensile modulus and strength due to the modification of the fibre-to-matrix interface. Le Duigou *et al.* (2009) evaluated the hygrothermal degradation of flax–poly(lactic acid) (PLA) composites in sea water. The strength and stiffness of the composites were reduced following exposure to seawater at 40°C.
Several strategies may be adopted to reduce moisture absorption:

(i) Chemically treating or resin coating the plant fibres to optimise adhesion with the polymer matrix to reduce diffusion of moisture by wicking at the fibre–matrix interface.
(ii) Improving the compatibility of the polymer matrix with the plant fibre to reduce diffusion of moisture by wicking at the fibre–matrix interface.
(iii) Laminating an inner layer of NFC with an outer layer of conventional synthetic fibre composites to form hybrid composites which minimise ingress of water by protecting the NFC.

In the case of (i), Bisanda and Ansell (1991) observed a significant decrease in moisture uptake and improvement in mechanical properties of sisal–epoxy composites following the treatment of sisal fibres with bi-functional silanes. In the case of (ii), Aziz *et al*. (2005) evaluated modified polyester resins for application in the boat-building industry, which had been formulated by making them more polar in character to offer improved adhesion to plant fibres. Kenaf–polyester composites absorbed significantly less moisture than kenaf composites manufactured with standard polyester resins, but the performance of standard glass–polyester composites formulated for marine applications was still superior.

In the case of (iii), the properties of hybrid plant fibre composites was investigated in an early paper by Clark and Ansell (1986), where jute and glass fibre laminates were arranged in different configurations to optimise

© Woodhead Publishing Limited, 2014

static and impact properties. In review papers by Bledzki and Gassan (1999) and Li *et al.* (2000) the use of hybrid composites is recommended for special performance requirements. This strategy is also adopted in the design of laminated wood wind turbine blades located off-shore where an outer glass fibre-reinforced plastic (GFRP) skin protects the inner laminated wood structure (Bond and Ansell, 1993).

The polymer matrix for an NFC may also be bio-sourced and, in the case of resins based on the polymerisation of modified cashew nut shell liquid (CNSL), may offer reasonable resistance to moisture uptake (Bisanda and Ansell, 1992; Mwaikambo and Ansell, 2003). However, curing temperatures are of the order of 190°C and an alkaline catalyst must be used to prevent the fibre being chemically degraded, so these adhesives are unsuitable for the manufacture of boats, which are generally cured at temperatures up to about 40°C.

14.4 Geometrical considerations for plant fibres in NFCs

In common with all engineering applications for NFCs, fibre alignment and placement should be optimised (Aziz and Ansell, 2004) to suit the application. Bader (2000) considered the stiffness index of fibres (Table 14.1) as a function of their geometry, for example, aligned unidirectional (UD), woven, cross-laminated (orthogonal), random. The stiffness index is the product of the fibre volume fraction and orientation factor. There are clear

Table 14.1 Implications of the choice of reinforcement format for fibre composites (Bader, 2000)

Reinforcement format	Maximum fibre volume fraction	Orientation factor	Stiffness index	Manufacturing processes
UD tow	0.80	1.00	0.80	Filament wind, pultrusion, hot press
UD prepreg	0.65	1.00	0.65	Autoclave, RFI
Multi-axial prepreg*	0.60	0.31	0.19	Autoclave, RFI
2D non-crimp fabric	0.55	0.30	0.17	RFI, RTM
Woven 2D fabric*†	0.50	0.27	0.14	RTM, wet lay-up
Orthogonal 3D fabric	0.40	0.30	0.12	RTM
Random planar	0.30	0.30	0.09	SMC, RTM, wet lay-up
Random 3D short fibre	0.20	0.12	0.02	BMC, IM (thermoplastic)

* Quasi-isotropic lay-up; †allows for the effect of crimp.
UD = unidirectional, RFI = resin film infusion, RTM = resin transfer moulding, SMC = sheet moulding compound, BMC = bulk moulding compound, IM = injection moulding.

© Woodhead Publishing Limited, 2014

advantages in maximising the elastic properties of plant fibres in surfboards or boat hulls by packing them closely in a unidirectional configuration and using untwisted yarns.

However the handling of plant fibre arrays is more easily achieved in the form of a woven fabric, which generally comprises twisted yarns reducing stiffness. Weager (2013) describes the microstructure and properties of jute and explains the twistless technology developed by Composites Evolution to optimise yarn stiffness. The jute yarns are co-mingled with thermoplastic PLA filaments, derived from corn starch, which are then woven to produce Biotex fabrics. The production of plant fibre composite components can be achieved by hot pressing Biotex fabrics to produce net shape components. In a second venture, Composites Evolution have supplied Biotex flax fabric to Amber Composites to produce a prepreg impregnated with Multipreg 8020 epoxy resin.

14.5 Marine applications of plant fibre composites

A canoe comprising flax skins on a marine plywood and solid pine frame was manufactured by Flaxland (Stewart, 2011). A Biotex flax hopsack weave reinforced a matrix of UV-cured EcoComp UV-L resin (95% vegetable oil) manufactured by Sustainable Composites. Joint ventures between Sustainable Composites and Movevirgo Ltd. have led to the manufacture of an Eco Boat and surfboards moulded from EcoComp UV-L resin.

Huntsman Advanced Materials were responsible for providing epoxy resin for the manufacture of a lightweight Mini Transat 6.5 composite racing boat prototype named the 'Araldite' (Fig. 14.5), which contains a fibre content of 50% flax and 50% carbon fibre. The flax fibres were supplied by Lineo, who pre-impregnate flax fibres with epoxy resin to prevent moisture



14.5 'Araldite' Mini Transat 6.5 (www.classemini.com).

© Woodhead Publishing Limited, 2014

uptake. Lineo's FlaxPly and FlaxPreg (epoxy–flax pre-preg) products have been used to manufacture canoes, surfboards, windsurfers, kite surfers and yachts. As well as boosting the eco-profile of the 'Araldite', the flax fibres endow the composite structure with good damping characteristics. The external hull was constructed from sandwich laminates comprising flax fabrics and structural foam. The sandwich laminates were impregnated with epoxy resin by vacuum infusion and cured at 50°C. Internal framing and reinforcement were fabricated from carbon fibre composite. Niels Haarbosch from Holland has also constructed a flax–epoxy catamaran based on an Aero Skimmer design.

In a study of the performance of plant fibre composites and bio-foams versus conventional materials for the fabrication of surfboards, Johnstone (2010) evaluated hemp fibre as a substitute for glass fibre with matrices of polyester or epoxy resin. He concluded that plant fibre composites were inferior to industry standard composites. However, bamboo fibre, which is stronger and stiffer than plant fibres, has been used to produce biocomposite structures including surfboards (Abdul Khalil *et al.*, 2012).

14.6 Conclusions and future trends

In terms of durability in saline environments, adhesive matrices for fibre composites are dominated by epoxy and polyester resins reinforced by glass and carbon fibres. In future it may be possible to adapt natural protein-based marine adhesives, which allow organisms such as barnacles and oysters to attach themselves to rocks under water (Waite, 1990), to function as the matrix for NFCs. Pre-treatment of natural fibres with resin or adhesion promoters such as silanes improves resistance to moisture uptake although long-term exposure to saline environments is necessary to determine stability. A historical perspective demonstrates that natural fibres have been utilised for ropes and bindings in marine applications to the limit of their performance since the earliest times. Advances in fibre processing and adhesive technology have opened the door to new developments in the application of sustainable composites in severe saline environments.

14.7 Sources of further information and advice

- Advanced Composites Manufacturing Centre, University of Plymouth, Composite materials and structures for the marine environment (compiled by Dr John Summerscales): http://www.tech.plym.ac.uk/sme/composites/marine.htm
- Amber Composites: http://www.ambercomposites.com/
- 'Araldite' video: http://vimeo.com/21878671

© Woodhead Publishing Limited, 2014

- Composites Evolution: http://www.compositesevolution.com
- Flaxcat: http://cat.inist.fr/?aModele=afficheN&cpsidt=24336207
- Flaxland: http://www.flaxland.co.uk/
- Hemp and bio-foam surfboard: https://studentjournals.plymouth.ac.uk/index.php/pss/article/viewFile/151/195
- Huntsman: http://www.huntsman.com/
- Huntsman Araldite Mini Transat 6.50 video: http://vimeo.com/21878671
- Lineo flax fibre impregnation: http://www.lineo.eu/
- Movevirgo Ltd: http://www.movevirgo.co.uk/
- NFCs – recent developments: http://xa.yimg.com/kq/groups/1853519/203368237/name/Natural%20fibres%20composites%20Leuven.pdf
- Sustainable Composites Ltd: http://www.suscomp.com/resins.htm

14.8 References

Abdul Khalil, HPS, Bhat, IUH, Jawaid, M, Zaidon, A, Hermawan, D and Hadi, YS (2012), 'Bamboo fibre reinforced biocomposites: A review', *Materials and Design,* **42**, 353–368.

Anderson, F (1924), 'Some aspects of linen weaving, ancient and modern', *Journal of the Textile Institute Proceedings*, **15(8)**, 348–373.

Ansell, MP and Mwaikambo, LY (2009), 'The structure of cotton and other plant fibres', chapter in '*Handbook of Textile Fibre Structure, Volume 2: Natural, Regenerated, Inorganic and Specialist Fibres*', S.J. Eichhorn, J.W.S. Hearle, M. Jaffe and T. Kikutani (Eds), Cambridge, UK, Woodhead Publishing Limited, ISBN 978–1-84569–730–3.

Aziz, SH and Ansell, MP (2004), 'Optimizing the properties of green composites', Chapter 8 of '*Green Composites –Polymer Composites and the Environment*', Caroline Baillie (Ed.), Cambridge, UK: Woodhead Publishing Limited, ISBN 1 85573 739 6.

Aziz, S, Ansell, MP, Clarke, SJ and Panteney, SR (2005), 'Modified polyester resins for kenaf natural fibre composites', *Composites Science and Technology*, **65(3–4)**, 525–535.

Bader, MG (2000), 'Polymer composites in: structure, performance, cost and compromise', presented at *Microstructure of Composite Materials – V*, St Johns College, Oxford, 3rd and 4th April 2000, Royal Microscopical Society.

Bisanda, ET and Ansell, MP (1991), 'The effect of silane treatment on the mechanical and physical properties of sisal-epoxy composites', *Composites Science and Technology*, **41(2)**, 163–176.

Bisanda, ETN and Ansell, MP (1992), 'The properties of sisal-CNSL composites', *Journal of Materials Science*, **27**, 1690–1700.

Bledzki, AK and Gassan, J (1999), 'Composites reinforced with cellulose based fibers', *Progress in Polymer Science*, **24**, 221–274.

Bond, IP and Ansell, MP (1993), 'Effect of marine environment on the fatigue life of wind turbine blade materials', *Wind Engineering*, **17(2)**, 100–107.

CES 2013 EduPak (2013), 'Cambridge Engineering Selector engineering materials database, Granta Design Ltd., Cambridge. http://www.grantadesign.com/education/.

© Woodhead Publishing Limited, 2014

Chow, CPL, Xing, XS and Li, RKY (2007), Moisture absorption studies in sisal fibre reinforced polypropylene composites', *Composite Science and Technology*, **67**, 306–313.

Clark, RA and Ansell, MP 'Jute and glass fibre hybrid laminates', *Journal of Materials Science*, **21**, 269–276, 1986.

Dhakal, HN, Zhang, ZY, Richardson, MOW (2007), 'Effect of water absorption on the mechanical properties of hemp fibre reinforced unsaturated polyester composites', *Composites Science and Technology*, **67**, 1674–1683.

Heyerdahl, T (1950), '*The Kon-Tiki Expedition by Raft Across the South Seas*', George Allen and Unwin Ltd., London.

Heyerdahl, T (1972), '*The Ra Expeditions*', Penguin Books, Harmondsworth, England.

Johnstone, JM (2010), 'Flexural testing of sustainable and alternative materials for surfboard construction, in comparison to current industry standard materials', *The Plymouth Student Scientist*, **4(1)**, 109–142.

Le Duigou, A, Davies, P and Baley, C (2009), 'Seawater ageing of flax/poly(lactic acid) biocomposites', *Polymer Degradation and Stability*, **94(7)**, 1151–1162.

Li, Y, Mai, Y-W and Ye, L (2000), 'Sisal fibre and its composites: a review of recent developments', *Composites Science and Technology*, **60**, 2037–2055.

Mwaikambo, LY and Ansell, MP (2003), 'Hemp fibre reinforced cashew nut shell liquid composites', *Composites Science and Technology*, **63(9)**, 1297–1305.

Stewart, R (2011), 'Better boat building – trend to closed-mould processing continues', *Reinforced Plastics*, **55(6)**, 30–32, 34–36.

Turner, WHK (1983), 'Flax weaving in Scotland in the early 19th Century', *Scottish Geographical Magazine*, **99(1)**, 16–30.

Waite, JH (1990), 'Marine adhesive proteins: natural composite thermosets', *International Journal of Biological Macromolecules*, **12(2)**, 139–144.

Wambua, P, Ivens, J and Verpoest, I (2003), ' Natural fibres: can they replace glass in fibre reinforced plastics? ', *Composites Science and Technology*, **63**, 1259–1264.

Weager, B (2013), 'Growing for gold', *Materials World*, **21(1)**, 24–25.

© Woodhead Publishing Limited, 2014

Index

acetic acid, 127
acetone, 127
acetylation, 86, 179
acoustic emission (AE), 275
acoustic emission technique, 273–96
  applications, 287–95
    crack propagation studies, 289–91
    monitoring during quasi-static tests, 291–5
    single fibre fragmentation tests, 287–9
  assessing results, 285–6
  future trends, 295–6
  history of AE, 277–8
  principles and sources of acoustic emission (AE), 275–7
  using the technique in practice, 279–85
    AE in composite materials studies, 282–5
    analysis of AE data, 280–2
    currently used tools for the identification and location of AE sources as well as damage in composite materials, 283
    features of transient AE signals, 281
    measurement, 279–80
    terms used in AE method, 281
  wave propagation, 278
acrylated epoxidised soybean oil (AESO), 98–9
acrylic resins, 257–8
AE critical stress limit, 286
AE knee, 286, 293
aloe vera, 136
American Society of Non-destructive Testing (ASNT), 273
amine oxides, 118
Araldite, 371
Aropol, 187
Arrhenius equation, 194
ASTM D1388–08, 181
ASTM D4032–08, 182
ASTM D5023–7, 330
ASTM D15732–01, 181
atomic force microscopy (AFM), 10–11, 146
attenuation, 278
automated processes, 203
  composite systems reported to be manufactured by pultrusion, 203
automotive application, 204

bacterial cellulose, 91–9
  coating surface of natural fibres using slurry dipping method, 95–9
    SEM of sisal fibres coated with dense layer of BC and hairy sisal fibres, 95
    tensile properties of sisal fibre reinforced PLLA composites, 96
    tensile strength of neat and BC-coated sisal fibre reinforced PLLA, 97
    tensile strength of neat polyAESO and sisal fibre preform reinforced composites, 98
  culturing in presence of natural fibres, 91–5
    images of natural fibres immersed in culture medium before culturing and after 2 days, 92

© Woodhead Publishing Limited, 2014

bacterial cellulose (*cont.*)
interfacial shear strengths between modified CAB or PLLA, 94
mechanical properties modified with BC nanofibrils, 93
mechanical properties of BC modified hemp and sisal fibres reinforced CAB and PLLA, 94
SEM images of neat sisal fibre and sisal fibre coated with bacterial cellulose, 92
benzoylation, 86
binary solvent system, 130
bio-based phenolic resins, 238
bio-based polymer matrices, 183–7
bio-based thermoplastics, 183, 186
bio-based thermoset resin systems, 187
key properties for some bio-based resins and thermoplastics, 184–5
bio-based PU resins, 237–8
bio-based resins, 235–8
bio-based phenolic resins, 238
bio-based PU resins, 237–8
epoxidised plant oil-based resins, 235–6
LA-based thermoset resin, 238
protein-based resins, 236–7
bio-based thermoplastics, 183, 186
Bio-Composites Centre, 187
Bio-PDO, 186
Biocidal Products Regulations (BPR), 22
biological treatments, 179
BioRez, 187
Biotex fabrics, 371
bleaching, 179
BMW, 325
bonding, 204
Breton NavEcoMat, 205
BS 5058:2007, 182
BS 3356:1990, 181
bulk moulding compound (BMC), 28, 188

Cantilever Test Option, 181
Carboform, 189
carding, 178
Cargill Dilulin, 187
cashew nut shell liquid (CNSL), 370
cellulose, 108, 178–9
polymorphism, 77
purification, 76–7
cellulose-2,5-acetate, 77
cellulose acetate butyrate (CAB), 93
cellulose acetate (CA), 126–7
cellulose chains assembly, 72–3
cellulose derivatives, 130
cellulose fibres, 112
chemistry and structure as reinforcements in natural fibre composites, 66–81
applications, 80–1
cellulose polymorphism, 77
chemical and solubility properties of cellulose, 73–5
chemical modification, 78–9
glucose biopolymerisation, 70–1
glucose monomer, 67–70
nano-cellulose preparation, 79
processing, 79–80
purification, 76–7
separation, 75–6
sources of cellulose, 75
structure, 71–3
anti-parallel cellulose chain segments, 73
cellulose chain segment showing intramolecular hydrogen bonding, 72
cellulose chain segment showing relatively planar structure, 72
parallel cellulose chain segments showing intra- and inter-molecular hydrogen, 72
cellulose nanofibre-reinforced polymer composites, 147–9
cellulosic fibre reinforced polymer composites
hierarchical structures for advanced performance, 84–100
coating with bacterial cellulose, 91–9
future trends, 99–100
ligno(cellulosic) fibres, 86–7
renewable composites by incorporating MFC into matrix, 90–1
surface microfibrillation, 87–90

© Woodhead Publishing Limited, 2014

chemical coupling, 110
chemical modification, 18–21
  coupling, 21
  crosslinking, 20
  grafting, 21
  mercerisation, 18–20
    main chemical treatments and modification mechanism of natural fibre, 19
  oxidation, 20
chemical treatments, 86–7
  techniques, 13
chemimechanical pulps (CMP), 13
chemithermomechanical pulps (CTMP), 13
composite manufacturing methods, 187–9
Composites Evolution, 371
compounding, 27
compression, 28
compression and injection moulding techniques, 216–30
  emerging technologies in the production of natural fibre composites, 218–27
    composites moulded after removal of moisture, 221
    compression moulding machine, 220
    compression moulding of thermoplastic natural fibre composites, 218–23
    conventional short pellets, 224
    effect of moulding time on jute/polyethylene terephthalate composites, 221
    injection moulding machine set-up, 225
    injection moulding of thermoplastic natural fibre composites, 223
    long fibre pellet pultrusion machine, 224
    MBYs containing hybrid polymers, 223
    mould set-up and alignment of MBY for fabricating unidirectional natural fibre composites, 223
    textile insert injection-compression moulding process, 226
    typical braiding machine, 222
    various forms of natural fibres, 219
  processing natural fibre composites at high temperature, 227–9
    commodity thermoplastics vs engineering thermoplastics mechanical properties, 228
    flexural strength of jute/PA6 composites and other composites with commodity thermoplastic matrices, 229
    flexural strength of jute/PA6 composites with other PA6-based composites with different reinforcements, 229
    thermal decomposition characteristics of jute fibres, 228
compression moulding, 108, 109, 188, 202–3
continuous wavelet transform (CWT), 295
copolymers, 70
corona discharge, 179
coupling, 21
crosslinking, 20, 233

3D body scanning, 182
Daimler-Chrysler, 325
Darcy equation, 196–7
decortication, 75–6, 178
derivatised cellulose, 126–35
  binary and ternary systems used to electrospin CA, 128–9
  cellulose derivative electrospun nanofibres, 131–2
desiccation, 177
designer solvents, 124–5
differential scanning calorimetry (DSC), 74, 332
diffuse coplanar surface barrier discharge (DCSBD), 17
direct piezoelectric effect, 280
discharge treatment, 16
discrete wavelet transform (DWT), 295–6
double edge notched tensile (DENT), 291

© Woodhead Publishing Limited, 2014

drape, 181
drilling, 177
dry cellulose, 191
dry-jet wet-electrospinning, 125
DuPont, 186
dynamic loading, 323–41
  dynamic mechanical testing of natural fibre composites, 327–30
    compressive engineering stress-strain curves at two strain rates, 330
    load-deformation traces of impact events, 328
    load-time traces of impact events, 328
    schematic diagram for SHPB, 329
  dynamic properties of natural fibre composites, 326–7
  dynamic testing of composites, 331–5
    dynamic mechanical analysis (DMA), 331–2
    Lagrangian diagram of wave movement in silver steel Hopkinson bars, 334
    schematic diagram of SHPB set-up for high velocity impact test, 333
    Split Hopkinson Pressure Bar (SHPB) test, 332–5
  future trends, 341
  natural fibres and natural fibre composites, 325–6
  performance of natural fibre reinforced composites under dynamic loading, 335–41
    effect of loading frequency on dynamic moduli, 335–8
    frequency effect on the dynamic modulus of samples with 70% v/v fibre loading, 336
    frequency effect on the tanδ of composites with 70% v/v fibre loading, 337
    frequency effect on the tanδ of neat unsaturated polyester, 337
    strain rate effect on dynamic compression modulus for both pultruded natural fibre reinforced composites, 340
    strain rate effect on flow stress for both pultruded natural fibre reinforced composite, 340
    strain rate effect on the dynamic moduli, 338–41
    stress-strain curve of JFRC at various strain rates, 339
    stress-strain curve of KFRC at various strain rates, 339
    values of tanδ maximum and T_g values of neat polyester and kenaf fibre reinforced polyester composites, 338
    variation of storage modulus of neat unsaturated polyester, 336
  testing in practice, 330–1
dynamic mechanical analysis (DMA), 149, 323
dynamic viscosity, 193

Eco Boat, 371
EcoComp, 187, 371
electrospinning, 124
electrospraying, 124
electrospun cellulosic fibre-reinforced composite materials, 115–50
  cellulose nanofibre-reinforced polymer composites, 147–9
    mechanical properties, 148
  electrospinning of non-derivatised and derivatised cellulosic fibres, 118–35
    derivatised cellulose, 126–35
    non-derivatised cellulose, 118–26
  future trends, 149–50
  mechanical properties of electrospun fibres and mats, 146–7
  nanocomposite fibres, 138–46
  polymer blends, 135–8
    fibre blending, 137
    hybrid fibres, 137–8
    solution blending, 135–7
electrospun nanocomposite fibres, 138–46
  carbon nanotube-reinforced cellulose fibres, 138, 142
  cellulose nanocrystal-reinforced biopolymer fibres, 142–6

© Woodhead Publishing Limited, 2014

mechanical properties, 143–5
nanocomposite fibres, 139–41
Envirez 500, 187
enzymatic hydrolysis, 70–1
epoxidised linseed oil (ELO), 235
epoxidised plant oil-based resins, 235–6
epoxidised soybean oil (ESO), 235
epoxy-phenolic resins
mechanical properties, 246–7
impact strength of untreated and treated sugar palm fibre/epoxy composites, 246
epoxy resin, 195
mechanical properties, 240–6
Charpy impact energies for 50 vol.% flax and hemp epoxy matrix composites, 243
flexural properties of 50 vol.% flax and hemp epoxy matrix composites, 243
flexural properties of untreated flax fibre/epoxy composites, 244
knitted composites, 245
locations in stem where flax fibres were examined, 241
mat composites, 245–6
mechanical properties of 50% unbleached and bleached jute silver/epoxy composites, 244
stress-strain curve for 50 vol.% hemp epoxy composite, 242
tensile properties of 50 vol.% flax and hemp epoxy matrix composites, 242
tensile properties of unbleached jute sliver/epoxy composites, 244
tensile properties of unidirectional flax fibre/epoxy composites, 241
unidirectional composites, 240–5
yarn composites, 245
epoxy-vinyl ester resins, 247
ethical framework, 163
ethical practices
green composites processing, 161–73
case study of Waste for Life waste management model, 164–72
social impact, 162–4
ethics of care, 162–3
European End of Life Vehicle (ELV), 204
exotherm, 192
extrusion, 28–9, 108

Felicity effect, 277
fibre blending, 137
fibre cultivation, 177–8
fibre production, 177–8
fibre reinforced polymer (FRP), 324
fibre reinforcements, 177–80
fibre cultivation and production, 177–8
improving the fibre matrix interface, 179–80
plant fibres structures, 178–9
filament winding, 240
filler size, 108–9
film stacking, 202–3
Flax, 80
Flaxland, 371
FlaxPly, 372
FlaxPreg, 372
Forest Product Laboratory (FPL), 43
Forest Products Industry-Vision and Technology Roadmap, 43
Fourier transform infrared (FTIR) spectroscopy, 78–9
fractography analysis, 97
freeze drying, 79

geotextiles, 326
gilling, 178
glass fibre-reinforced plastic (GFRP), 370
glucose biopolymerisation, 70–1
celluobiose in stereochemical repeat unit of cellulose, 71
glucose monomer, 67–70
β-glucopyranose chemical structure, 68
β-glucopyranose showing out of plane hydrogen atoms; chemical structure, 68
glucuronic acid, cyclic form of β-glucuronic acid, gluconic acid and glutaric acid structure, 69
grafting, 21, 179

© Woodhead Publishing Limited, 2014

Granta Design, 366
green composites
  processing and ethical practices, 161–73
    case study of Waste for Life waste management model, 164–72
    social impact, 162–4

hackling, 178
hairy fibres, 87
hand lamination, 201
harvest, 177
Heart Loop Test Option, 181
hemicellulose, 108
heteronuclear single quantum coherence spectroscopy, 17
HexFIT, 189
hierarchical composites, 204
hierarchical structures
  cellulosic fibre reinforced polymer composites for advanced performance, 84–100
    coating ligno (cellulose) with bacterial cellulose, 91–9
    design strategies for biological vs engineering materials, 85
    future trends, 99–100
    ligno (cellulose), 86–7
    surface microfibrillation, 87–90
  renewable composites by incorporating microfibrillated cellulose (MFC) into matrix, 90–1
    interfacial shear strength and fracture toughness of bamboo fibres, 91
high-energy ionising radiation, 21
high performance composites, 188
high strain rate testing, 303–17
  applications and future trends, 314–17
    biomedical applications, 315–16
    collapsing void models of sisal/PP, 317
    energy dissipation mechanisms due to natural fibre properties and microcellular voids, 314–15
    modelling, 316–17
  materials, 305–6
    microscopic image of sisal fibre-reinforced polypropylene containing microcellular voids, 306
    natural fibre-reinforced polypropylene thermoplastic composites, 305
    natural fibre-reinforced polypropylene thermoplastic composites containing microcellular voids, 305–6
    natural fibre-reinforced vinyl ester thermoset composites, 306
  mechanical tests results, 308–14
    compressive energy dissipation of natural fibre-reinforced PP thermoplastic composites containing microcellular voids, 312–14
    compressive strain and stress vs energy dissipation per unit volume of reinforced PP homopolymers, 313, 314
    compressive strain rate dependence of hemp fibre-reinforced vinyl ester thermoset composites, 310–12
    compressive stress-strain curves at various strain rates of hemp and glass composites, 311
    compressive stress-strain curves of wheat straw fibre and cellulose reinforced PP homopolymers, 312
    maximum tensile stress of WSF/PP, cellulose/PP and PP, 309
    maximum tensile stress vs strain rate of WSF/PP, cellulose/PP and talc/PP containing microcellular voids, 311
    tensile strain rate dependence of natural fibre-reinforced polypropylene thermoplastic composites, 308–9
    tensile strain rate dependence of natural fibre-reinforced PP thermoplastic composites containing microcellular voids, 309–10

© Woodhead Publishing Limited, 2014

test methods, 306–8
custom-made test system, 307
split Hopkinson pressure bar apparatus, 308
Hopkinson test apparatus, 312
hot press, 168–70
Kingston hotpress computer aided design (CAD), 170
Kingston hotpress-Rhode Island School of Design (RIS) and UWA prototype, 170
Huntsman Advanced Materials, 371
hybrid fibres, 137–8
hydrothermal treatment, 16
hydroxyl groups, 70

impact damage
Charpy impact test, 353
AE of simple and stitched single and multi-delaminated hybrid composite beams, 353
experimental results, 354–62
comparison of AE in simple and stitched composite beams with laminate design of $[C_{90}/G_0]_3$, 357
comparison of AE for single delaminated and multi-delaminated hybrid composite beams, 354
comparison of energy absorption of adhesive CB and DB composite joints, 359
completely bonded joint specimen before impact, 360
completely bonded stitched and de-bonded stitched joint specimens before impact, 362
crack propagation and fracture of $[C_0/G_{90}]_3$ specimens, 355
effect of stitching on impact damage response, 357–8
energy absorption of CBS vs DBS composite joints, 361
impact damage response of adhesive bonded single lap joint, 358–61
impact damage response of stitched single lap joint, 361–2
impacted specimens showing fibre breakage combination of intralaminar C_{90}/G_0 interface, 358
needle and flax yarn for stitching, 355
response of single and multi-delaminated composite beams, 354–6
schematic representation of delaminated composite specimens, 356
stitched single and multi-delaminated hybrid composite beams with laminate design of $[C_{90}/G_0]_3$ after impact, 359
mechanical characterisation, 348–9
material properties of the unidirectional CFRP and GFRP, 349
natural fibre composites response, 345–63
specimen preparation, 349–53
composite material $[C_0/G_0]_3$ and $[C_{90}/G_{90}]_3$ completely bonded CBS with stitching and de-bonded DBS with stitching, 352
composite material $[C_0/G_0]_3$ and $[C_{90}/G_{90}]_3$ with adhesive and de-bonded DBS specimen, 351
delaminated composite beams, 349
single and multi delaminated composite specimens, 350
single lap joint beams, 349–53
infrastructure applications, 204–5
injection moulding, 29–30, 108, 109, 201
inorganic compounds, 23
interdisciplinary support network, 164–5
interfacial shear strength (IFSS), 287
internal friction, 331
interrogated parameter, 273
interrogating parameter, 273
intramolecular hydrogen bonds, 72
ionic liquids (IL), 124–5
island in the sea structures, 136–7
ISO 14040, 177
isocyanate treatment, 86

jute fibre reinforced composites (JFRC), 331

© Woodhead Publishing Limited, 2014

Kaiser effect, 277
Kantian ethics, 162–3
Kelly-Tyson model, 287
kenaf fibre reinforced composites (KFRC), 331
kinematic viscosity, 193
Kingston hotpress, 169–70
Kohonen's neural network, 295
Kraft, 13
Krozeny-Carman equation, 199
Krozeny constant, 197

LA-based thermoset resin, 238
Lagrangian *x–t* diagram, 334
layer-by-layer deposition, 22
lignin, 108
lignin-carbohydrate complex (LCC), 8
ligno cellulosic fibres, 86–7
  coating with bacterial cellulose, 91–9
    culturing in presence of natural fibres, 91–5
    slurry dipping method, 95–9
  surface microfibrillation, 87–90
    critical length and apparent interfacial shear strength of neat Lyocell fibres, 90
    SEM of Lyocell fibres at x1000 magnification, 90
    SEM of neat and surface microfibrillated sisal fibres, 88
    tensile properties of hybrid phenolic resin composites reinforced with sisal and neat aramid fibres, 89
    tensile properties of sisal fibre reinforced phenolic resin composites, 89
Limit State Design, 265
linear low density polyethylene (LLDPE), 166
linear thermal coefficient of expansion (LTCE), 86–7
Lineo, 371
liquid composite moulding (LCM), 199–200, 202
  examples of composite systems reported to be manufactured by LCM process, 202
lithium chloride–dimethylacetamide (LiCl/DMAc), 119–20
Load and Resistance Factor Design methodology, 265
Loctite ESP110 adhesive, 351
long fibre pellets (LFP), 224
Lotus Eco Elise, 325
lower critical solution temperature (LCST), 74
Lyocell, 74–5, 79, 118

machining, 204
macroscopic level, 5
maleated coupling agents, 86
manufacturing methods
  natural fibre composites, 176–205
    bio-based polymer matrices, 183–7
    case studies, 204–5
    composite manufacturing methods, 187–9
    fibre reinforcements, 177–80
    key parameters for successful processing, 189–201
    reinforcements forms, 180–3
    techniques for natural fibre-reinforced polymer matrix composites, 201–4
marine application, 205
marine environment
  geometrical considerations for plant fibres in NFCs, 370–1
    implications of the choice of reinforcement format for fibre composites, 370
  marine applications of plant fibre composites, 371–2
    'Araldite' Mini Transat 6.5, 371
  natural fibre composites, 365–72
    future trends, 372
  natural fibre composites and moisture uptake, 369–70
  properties and environmental impact of natural vs synthetic fibres, 366–8
    CO_2 footprint vs price, 368
    embodied energy in primary production, 368

© Woodhead Publishing Limited, 2014

Young's modulus, 367
materials production process, 166–8
different stages of processing by different filters in lab, 168
strength data comparison for various paper/plastic composites, 169
Mazda, 326
mechanical relaxation, 324
medium density fibreboard (MDF), 16
mercerisation, 18–20, 77, 110, 179
methacrylated soybean oil (MSO), 236
methacrylic anhydride-modified soybean oil (MMSO), 236
Mettler Toledo three-point bending configuration, 330
microbraided yarns (MBY), 222
microbraiding, 221
microfibrillated cellulose (MFC), 90–1
microfibrillation, 87–90
microscopic level, 5–6
modelling, 181
modified soy flour (MSF), 237
modulus of elasticity (MOE), 21
moisture, 189–90
control, 27
Movevirgo Ltd, 371
multi-jet electrospinning, 137
multiwalled carbon nanotubes (MWCNT), 138

N-methylmorpholine oxide (NMMO), 118–19
NANOFOREST, 43
nanotechnology (NT) modification, 21–2
natural fibre composites
case studies, 204–5
cellulosic fibres chemistry and structure as reinforcements, 66–81
applications, 80–1
cellulose polymorphism, 77
chemical and solubility properties of cellulose, 73–5
chemical modification, 78–9
glucose biopolymerisation, 70–1
glucose monomer, 67–70
nano-cellulose preparation, 79
processing, 79–80
purification, 76–7
separation, 75–6
sources of cellulose, 75
structure, 71–3
compression and injection moulding techniques, 216–30
emerging compression and injection moulding technologies, 218–27
processing natural fibre composites at high temperature, 227–9
high strain rate testing, 303–17
applications and future trends, 314–17
materials, 305–6
mechanical tests results, 308–14
test methods, 306–8
key parameters for successful processing, 189–201
exotherm, 192
moisture, 189–90
permeability, 196–200
rheology, 193–6
shrinkage, 200–1
thermal transition temperatures, 190–2
volatile components, 192–3
manufacturing methods, 176–205
bio-based polymer matrices, 183–7
composite manufacturing methods, 187–9
fibre reinforcements, 177–80
reinforcements forms, 180–3
techniques for natural fibre-reinforced polymer matrix composites, 201–4
marine environment, 365–72
future trends, 372
geometrical considerations for plant fibres in NFCs, 370–1
marine applications of plant fibre composites, 371–2
natural fibre composites and moisture uptake, 369–70
properties and environmental impact of natural vs synthetic fibres, 366–8

© Woodhead Publishing Limited, 2014

natural fibre composites (*cont.*)
non-destructive testing, 273–96
applications of AE, 287–95
assessing results, 285–6
future trends, 295–6
using the acoustic emission technique in practice, 279–85
performance under dynamic loading, 323–41
dynamic mechanical testing, 327–30
dynamic properties of natural fibre composites, 326–7
dynamic testing of composites, 331–5
future trends, 341
natural fibres and natural fibre composites, 325–6
performance of natural fibre reinforced composites under dynamic loading, 335–41
testing in practice, 330–1
products, 164–5
response to impact damage, 345–63
Charpy impact test, 353
experimental results, 354–62
mechanical characterisation, 348–9
specimen preparation, 349–53
natural fibre composites reinforcements
wood fibres structure, properties, processing and applications, 3–43
applications, 34–41
future trends, 41–3
matrices or binders, 22–7
modifications, 15–22
nature and behaviour, 5–15
process techniques, 27–32
properties, 32–4
natural fibre-reinforced polymer composites
recycled polymers, 103–12
applications, 111–12
different types of matrices used to made composites, 104
future trends, 112
mechanical properties improvement, 109–11
process, 108–9
usage, 104–8
natural polymers, 23–4
net polymer matrix, 149
neutral sulfite semi-chemical (NSSC), 13
Nomex, 190
non-derivatised cellulose, 118–26
electrospinning, 120–2
phase diagram of cellulose-NMMO-water, 123
typical electrospinning apparatus, 116
non-destructive characterisation (NDC), 274
non-destructive evaluation (NDE), 273
non-destructive inspection (NDI), 274
non-destructive sensing (NDS), 274
non-destructive testing
acoustic emission technique, 273–96
applications, 287–95
assessing results, 285–6
future trends, 295–6
using the technique in practice, 279–85
nuclear magnetic resonance spectroscopy of carbon (1^3C-NMR), 17

open mould process, 201
organic solvent extraction, 76
Oros data acquisition system, 307
oxidation, 20, 179
oxidative alkaline extraction, 76–7
oxidised cellulose (OC), 130

peak amplitude distribution (PAD), 284
permeability, 196–200
saturated and unsaturated permeability values as function of porosity, 198
transverse continuous saturated permeabilities of flax and glass mat preforms, 199
phenolic resins
mechanical properties, 257, 258
tensile and flexural strength of woven sisal fabric/phenolic composites, 258
woven composites, 257

© Woodhead Publishing Limited, 2014

photo degradation, 111–12
physical modification, 16–18
  schematic of plasma treatment, 17
PICOSCOPE 3206, 334
piezoelectricity, 279
plant extracts, 127, 130
plant fibres, 111
  structures, 178–9
plant growth, 177
plasma technology, 16
plasma treatment, 179
plastic, 165–6
polycaprolactone (PCL), 18, 183
polyester resins
  mechanical properties, 248–57
    compression properties of unidirectional kenaf fibre/unsaturated polyester composites, 253
    fabric composites, 252–5
    flexural strength of coir fibre/unsaturated polyester composites, 256
    influence of fabric orientation on impact strength of jute fabric/polyester composites, 255
    jowar, sisal and bamboo fibre/polyester composites, 251
    jute fabric/polyester composites, 254
    knitted composites, 252
    longitudinal tensile properties of unidirectional alfa/unsaturated polyester composites, 252
    mat composites, 255–6
    non-woven felt composites, 257
    non-woven jute and hemp felt/unsaturated polyester composites, 257
    stress-strain curves for unreinforced, glass fibre reinforced, unmodified, propionic andydride modified and methacrylic anhydride modified flax fibre reinforced unsaturated polyester composites, 250
    tensile and impact properties of long jute fibre/unsaturated polyester composites, 251
    tensile properties of 45% unidirectional alfa/unsaturated polyester composites, 252
    unidirectional composites, 249–52
    unidirectional warp knitted flax/unsaturated polyester composites, 253
    untreated and treated jute fabric/polyester composites, 256
    yarn composites, 257
poly(glycolic acid) (PGA), 186
polyhydroxyalkanoate (PHA), 186
polylactide aliphatic copolymer (CPLA), 183
polylactide (PLA), 90–1, 186
polymer blends, 135–8
poor solubility, 134–5
press core, 169
pressure groundwood (PGW), 13
process techniques
  compression, 28
    schematic of compression moulding, 28
  extrusion, 28–9
    schematic of extrusion moulding, 29
  injection moulding, 29–30
    schematics of injection moulded wood fibre composites, 30
  resin transfer moulding (RTM), 31–2
    schematics, 32
  sheet moulding compound (SMC), 30–1
    schematics of SMC and SMC moulded wood fibre composite products, 31
product designs, 170–2
  examples of composite plastics products, wallets, 171
  Nueva Mente group constructing Eco-Park Trashbin, 171
protein-based resins, 236–7
pulping, 12–13
pultruded kenaf fibre reinforced composites (PKRC), 330
pultrusion, 240
pulverising, 12–13

© Woodhead Publishing Limited, 2014

Quantitative Life Cycle Analysis (QLCA), 177

Raman spectroscopy, 10–11
rate dependence, 303
rate hardening, 308
rate testing, 304
Rayon, 79
recycled polymers
  natural fibre-reinforced polymer composites, 103–12
    applications, 111–12
    future trends, 112
    mechanical properties improvement, 109–11
    process, 108–9
  natural fibre reinforcements usage in composites, 104–8
    classifications, 105
    date palm leaf waste and palm leaf fibres, 106
    mechanical properties of natural and industrial fibres, 107
refiner mechanical pulps (RMP), 13
reinforcements
  cellulosic fibres chemistry and structure in natural fibre composites, 66–81
    applications, 80–1
    cellulose polymorphism, 77
    chemical and solubility properties of cellulose, 73–5
    chemical modification, 78–9
    glucose biopolymerisation, 70–1
    glucose monomer, 67–70
    nano-cellulose preparation, 79
    processing, 79–80
    purification, 76–7
    separation, 75–6
    sources of cellulose, 75
    structure, 71–3
reinforcements forms, 180–3
  fabrics, 180–3
    coefficients of variation in principal permeabilities and anisotropy ratios, 183
    proposed definition for drape and conformability, 181
  roving, tows and yarns, 180
renewable resources, 106
repair, 204
resin infusion, 239
resin infusion under flexible tooling (RIFT), 188–9
resin systems, 195
resin transfer moulding (RTM), 27, 31–2, 108, 109, 187, 239
retting, 75, 178
rheology, 193–6
  effect of cure on viscosity, 194–6
  effect of temperature on viscosity, 193–4
  indicative viscosities for various materials or conditions, 194
rippling, 178
room temperature ionic liquids (RTIL), 124–5

scanning electron microscopy (SEM), 203
Schopper-Reigler (SR) values, 87
scouring, 179
Seeman Composites Resin Infusion Moulding Process (SCRIMP), 188–9
self-reinforcing cellulose, 204
semi-chemical techniques, 13
semi-empirical equation, 110
servo-hydraulic machine, 327
shake test, 87–9
sheet moulding compound (SMC), 27, 30–1, 188
short fibre-reinforced thermoplastics, 201
shrinkage, 200–1
  cure shrinkage of typical commercial resins systems, 200
silylation, 86
single-angle X-ray scattering (SAXS), 77
single edge notched tension (SENT), 290
single fragmentation tests (SFFT), 287
single lap joint tests, 347
single walled carbon nanotubes (SWCNT), 138
slurry dipping method, 95–9
social impact, 162–4

© Woodhead Publishing Limited, 2014

sol-gel process, 22
solution blending, 135–7
Sorona, 186
soy flour (SF), 236
soy protein concentrate (SPC), 236
soy protein isolate (SPI), 236
specific mechanical energy (SME), 27
spinning, 178
split Hopkinson pressure bar apparatus (SHPBA), 307, 323
Split Hopkinson Pressure Bar (SHPB)
  technique, 329
  test, 332–5
spray lamination, 201
spray-up technique, 239
SPRINT, 189
spun fibres, 179
starch, 23–4
steam explosion, 76
stiffness index, 370
stone groundwood (SGW), 13
strain rate dependence, 308
sulfate, 13
surface property, 9
sustainable composites, 371
synthetic polymer, 24–7
  advantages and disadvantages, 26
  chemical structure of thermoplastic and thermoset matrices, 25

Teflon, 167
TEMPO oxidation system, 20
Tencel, 74–5, 79
tensile modulus, 21
tensile properties, 96–7
ternary system, 127
textile process, 178
thermal degradation, 73–4
thermal transition temperatures, 190–2
thermal treatment, 16
thermoforming, 108, 109
thermogravimetry, 73–4
thermomechanical pulps (TMP), 13
thermoplastic composites, 188
thermoset matrix natural fibre-reinforced composites, 233–65
  applications, 263–4
    natural fibre composite canoe, 264
    natural fibre composite sailboards, 264
    resin transfer moulded natural fibre composite hood, 263
  bioderived resin composites, 258–63
    bio-based phenolic resins, 261–2
    bio-based polyurethane resins, 260–1
    epoxidised plant oil-based resins, 258–9
    flexural and impact properties of 50:50 hemp-kenaf mat/acrylic resin composites in the MD and the CD, 259
    flexural properties of ramie fibre/SPI and MSPI composites, 260
    lactic acid-based thermoset resins, 262–3
    protein-based resins, 259–60
    ramie fibre/SF and MSF composites tensile properties, 261
    ramie fibre/SPI and MSPI composites tensile properties, 260
    sisal/bio-based phenolic resin mixed with epoxy resin composites tensile properties, 263
    sisal fibre/RSOPU composites tensile and flexural properties, 262
    undried and dried woven sisal fabric/castor oil-based polyurethane composites tensile and flexural properties, 262
  fabrication of thermoset matrix composites, 238–40
  future trends, 265
  mechanical properties of synthetic resin composites, 240–58
    acrylic resins, 257–8
    epoxy-phenolic resins, 246–7
    epoxy resin composites, 240–6
    epoxy vinyl ester resins, 247
    phenolic resins, 257
    polyester resins, 249–57
    vinyl ester resins, 247–8

© Woodhead Publishing Limited, 2014

thermoset matrix natural fibre-reinforced composites (*cont.*)
natural fibres used in thermoset matrix composites, 234
thermoset matrix types, 234–8
bio-based resins, 235–8
chemical structure of acrylated epoxidised soybean oil resin, 236
chemo-enzymatic epoxidation of vegetable oil through conversion of unsaturated bonds to epoxy groups, 236
idealised structure of LA-based resin, 239
properties of common thermosetting matrix materials, 235
structure of castor oil, 238
synthesis of methacrylic anhydride-modified soybean oil (MMSO), 237
synthetic resins, 234–5
twisted yarn and straight yarn wrapped with spiral wrapping thread, 234
tillage, 177
transmission electron microscopy (TEM), 146
trifluoroacetic acid (TFA), 123–4

ultrastructural level, 7–8
ultraviolet (UV), 111–12
utilitarianism, 162–3

Vacuum-Assisted Resin Transfer Moulding (VARTM), 189
vinyl ester resins
mechanical properties, 247–8
mat composites, 248
mechanical properties of untreated and treated plain weave sisal fabric/vinyl ester composites, 249
tensile, flexure, compression and in-plane shear properties of 25 vol.% twill weave flax/vinyl ester composites, 248
tensile, flexure, compression and in-plane shear properties of 25 vol.% unidirectional flax/vinyl ester composites, 248
tensile and flexural properties of untreated and treated jute mat/vinyl ester composites, 249
unidirectional composites, 247
woven fabrics, 247–8
virtue theory, 162–3
Vlassak model, 11
volatile components, 192–3

Waste for Life waste management model
case study, 164–72
making the hot press, 168–70
material, 165–6
materials production process, 166–8
product designs, 170–2
social context, 165
waste paper, 165–6
water absorption, 111
water evaporation, 79
wavelet transform (WT), 295
weed control, 177
Weibull modulus, 10
wet lay-up technique, 250
wide-angle X-ray scattering (WAXS), 77
wood fibre-cement composites, 38
wood fibre-clay composites, 35, 37–8
wood fibre insulation board, 39
wood fibre-plastic composites, 38
wood fibres
applications, 13
production of commercially important fibre sources during 2002–2011, 15
natural fibre composites reinforcements structure, properties, processing and applications, 3–43
future trends, 41–3
matrices or binders, 22–7
modifications, 15–22
nature and behaviour, 5–15
number of publications on wood fibres and products, 4
process techniques, 27–32
properties, 32–41

© Woodhead Publishing Limited, 2014

Yuchang Lou in Fuijan, China, 4
physical and mechanical properties, 9–12
effect of wood species of wood fibres, 11
mechanical properties of natural fibres, 10
surface properties of natural fibres, 9
Weibull modulus of natural fibres, 11
processing, 12–13
process and application, 12
pulp yield and relative strength using various pulping methods, 14
structure, 5–9
chemical composition of softwood and softwood fibres, 8
dimension of typical softwood and hardwood fibres, 7
macroscopic to molecular level, 6
wood fibres composites
aerospace applications, 41
applications, 34–41
natural composite market vs synthetic composites, 35
natural fibre composites, 35
products, 36
automotive applications, 39–41
hemp car and wood car, 40
vehicle manufacturers and use of natural fibres composites, 42
building applications, 35, 37–40
MDF in building construction, 39
steps, trellies, wood flooring and cladding wood fibre-plastic composites, 38
Tulou and SEM morphology of wood fibre-clay composite in building, 37
wall, sound wall, cladding and house wood fibre-cement composites, 37
wood fibre board as insulation, 40
matrices or binders, 22–7
inorganic compounds, 23
natural polymers, 23–4
synthetic polymer, 24–7
mechanical properties, 32
factors affecting properties of natural fibre reinforced concretes, 33
physical properties, 32–4
embodied energy and carbon of fibreglass timber and wood fibre-based board, 34
natural fibre-based materials thermal insulativity vs cement based concrete, 34
process techniques, 27–32
compression, 28
extrusion, 28–9
injection moulding, 29–30
resin transfer moulding (RTM), 31–2
sheet moulding compound (SMC), 30–1
properties, 32–4
wood flour, 24

X-ray diffraction (XRD), 10–11

Young's modulus, 10, 127, 146

Z-pinning, 353
ZPREG, 189
Zwick Roell instrument, 353
zwitterionic solvent, 74–5

© Woodhead Publishing Limited, 2014